Asia Oceania Journal of Nuclear Medicine & Biology
Official Journal of Asia Oceania Federation of Nuclear Medicine & Biology (AOFNMB)

Volume 3 Supplement 1 October 2015

Abstracts of

11th Asia Oceania Congress of Nuclear Medicine and Biology

54th Annual Autumn Meeting of the Korean Society of Nuclear Medicine

14th Annual General Meeting of Asian Regional Cooperative Council for Nuclear Medicine

October 31-November 4, 2015

Jeju, Korea

The abstracts published in this Supplement were not subject to the standard peer reviewing process of *Asia Oceania Journal of Nuclear Medicine & Biology*

Asia Oceania Journal of Nuclear Medicine & Biology

Official Journal of Asia Oceania Federation of Nuclear Medicine & Biology (AOFNMB)

ISSN (print edition) 2322-5718
ISSN (electronic edition) 2322-5726

Abstracted and indexed in: DOAJ, EBSCO, Index Copernicus, ISC, IMEMR, Magiran

Editorial Office
Asia Oceania Journal of Nuclear Medicine & Biology
Nuclear Medicine Research Center
Ghaem Hospital, Ahmadabad Ave, Mashhad, Iran
Postal Code: 91766-99199
Tel: ++98-51-38400494
Fax: ++98-51-38419521
E-mail: aojnmb@mums.ac.ir

Welcome Address

Dear Colleagues

Nuclear Medicine and Molecular Imaging (NMMI) is confronted with both challenges and chances. It is particularly true in Asia and Oceania which has become a hot spot in the recent development of NMMI. The Asia Oceania Federation of Nuclear Medicine and Biology (AOFNMB) and the Asian Regional Cooperative Council for Nuclear Medicine (ARCCNM) are working together to promote nuclear medicine in the region, and this time, the AOCNMB 2015 will be held in conjunction with the Korean Society of Nuclear Medicine (KSNM) to enhance the exchange and cooperation of NMMI. We believe that AOCNMB 2015, the 11th Asia Oceania Congress of Nuclear Medicine and Biology in conjunction with 54th Annual Autumn Meeting of the Korean Society of Nuclear Medicine will give you a vivid overview of challenges and chances of NMMI, and that you will be able to realize the momentum of a big change of NMMI in the Region.

Moreover, you will have the opportunity to enjoy one of the seven natural wonders in the world, Jeju Island. Jeju Island is also triple crowned by UNESCO for its biosphere reserve, world natural heritage as well as its global giopark networks. We expect highly beneficial exchanges of knowledge and experience of science, technology, education/training, and most importantly friendship among attendants. We cordially invite you to the meeting filled with attractive programs surrounded by splendid nature.

We look forward to seeing you in Jeju, 2015.
Thank you.

Henry Hee Seung Bom, President of AOFNMB
Jaetae Lee, President of KSNM
Jun Hatazawa, Chairman of ARCCNM

[Organizing Committee]

Jaetae Lee	President of KSNM (Kyungbuk National University Hospital, Korea)
Jun Hatazawa	Chairman of ARCCNM (Osaka University, Japan)
Henry HeeSeung Bom	President of AOFNMB (Chonnam National University Hwasun Hospital,Korea)
Gang Huang	Dean of ASNM (Shanghai Jiaotong University, China)
June-Key Chung	Chair of Financial Committee (Seoul National University Hospital, Korea)
Dong Soo Lee	Chair of International Committee (Seoul National University Hospital, Korea)
Jae Seung Kim	Secretary General of KSNM (Asan Medical Center, Korea)
Kyung-Han Lee	Treasurer of KSNM (Samsung Medical Center, Korea)
Byeong-Cheol Ahn	Chair of Scientific Committeeof KSNM (Kyungpook National University Hospital, Korea)
Raihan Hussain	Secretary General of AOFNMB (Institute of Nuclear Medicine and Ultrasound BSM Medical University Campus Dhaka, Bangladesh)
Ho Young Lee	Treasurer of AOFNMB (Seoul National University Bundang Hospital, Korea)

[Scientific Committee]

Do-Young Kang	Dong-A University Hospital, Korea
Joo Hyun Kang	Korea Institute of Radiological & Medical Sciences, Korea
Seong-Young Kwon	Chonnam National University Hwasun Hospital,Korea
Kyeong Min Kim	Korea Institute of Radiological & Medical Sciences, Korea
Byung Il Kim	Korea Cancer Center Hospital, KIRAMSKorea Institute of Radiological & Medical Sciences, Korea
Sungeun Kim	Korea University Anam Hospital, Korea
Ji Young Kim	Hanyang University Seoul Hospital, Korea
Seungjun Oh	Asan Medical Center, Korea
Tae JooJeon	Gangnam Severance Hospital, Korea
Shin Young Jeong	Kyungpook National University Hospital, Korea
Yong-An Chung	The Catholic University of Korea, Korea
Hwan-Jeong Jeong	Chonbuk National UniversityMedical School & Hospital, Korea
Joon Young Choi	Samsung Medical Center, Korea
Jin Chul Paeng	Seoul National University Hospital, Korea

General Information

[Reception & Ceremony]

Exhibition Opening
- Date & Time: 08:30 – 09:00, Saturday, October 31, 2015
- Place: Exhibition Hall(1F), Jeju ICC

Opening Ceremony & Welcome Reception
- Date & Time: 19:00 – 20:30, Saturday, October 31, 2015
- Place: Tamna Hall(5F), Jeju ICC

Presidential Dinner (Invited Only)
- Date & Time: 19:00 – 20:30, Sunday, November 1, 2015
- Place: Ocean view(5F), Jeju ICC

ANMB Dinner (Invited Only)
- Date & Time: 19:00 – 20:30 , Monday, November 2, 2015
- Place: Ocean view(5F), Jeju ICC

RCA Dinner (Invited Only)
- Date & Time: 19:30 – 21:00, Tuesday, November 3, 2015
- Place: Deomjang, Jeju Jungmun

[AOFNMB Meeting]

AOFNMB Governing Council Meeting
- Date & Time: 07:30 – 08:30, Tuesday, November 3, 2015
- Place: 401(4F), Jeju ICC

National Delegate Assembly of AOFNMB/ARCCNM
- Date & Time: 12:45 – 14:00, Tuesday, November 3, 2015
- Place: 401(4F), Jeju ICC

[KSNM Program]

KSNM Council Meeting (대한핵의학회 평의원회)
- Date & Time: 12:45 – 14:15, Sunday, November 1, 2015
- Place: 303(3F), Jeju ICC

KSNM General Assembly (대한핵의학회 총회)
- Date & Time: 12:45 – 13:45, Monday, November 2, 2015
- Place: Tamna B(5F), Jeju ICC

Program at a Glance

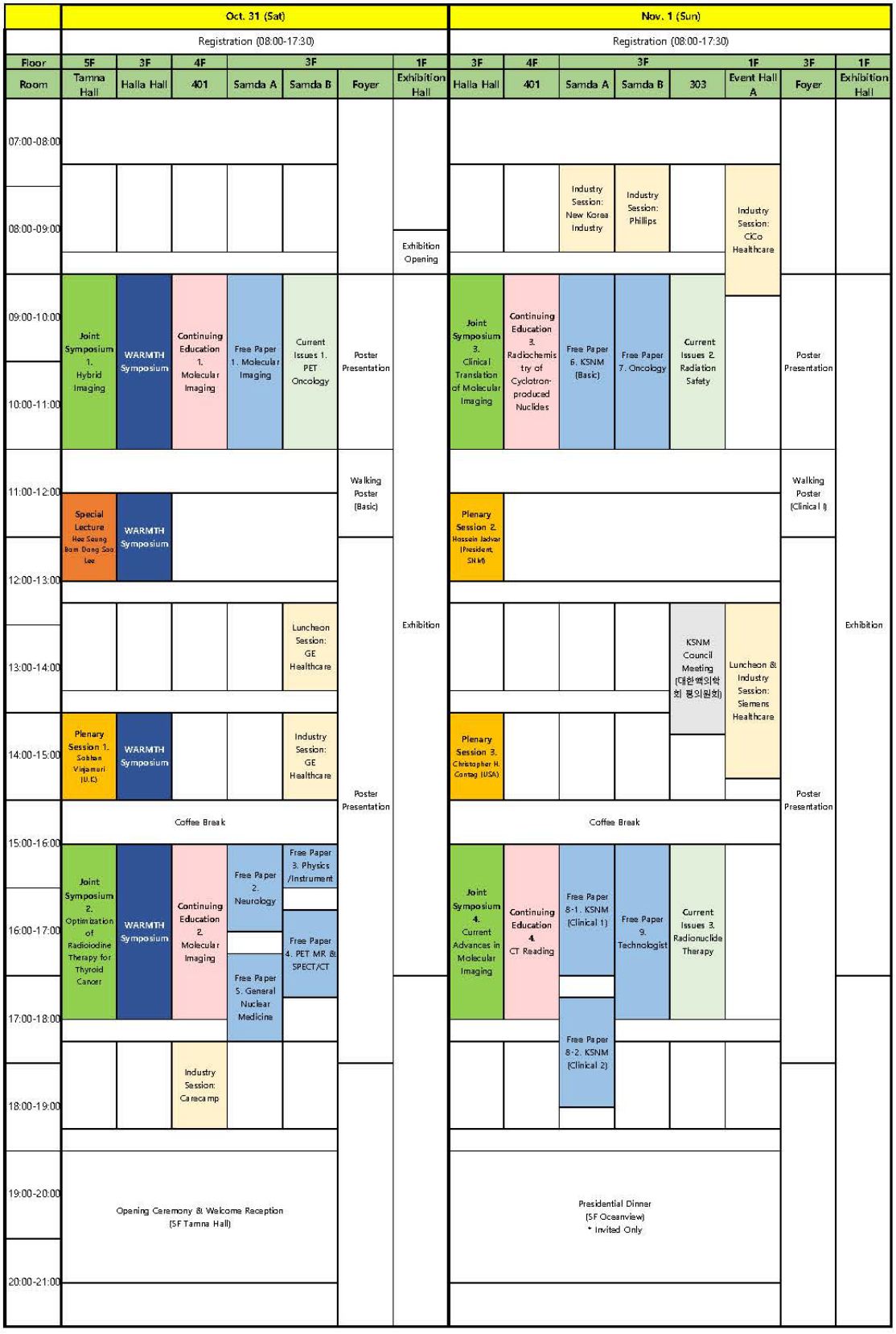


Nov. 2 (Mon)
Nov. 3 (Tue)
Nov. 4 (Wed)
Registration (08:00-17:30)
Registration (08:00-17:30)
3F
4F
5F
3F
1F
3F
4F
3F
4F
3F
4F
Floor
Halla Hall
401
Tamna B
Samda A
Samda B
303
Foyer
Exhibition Hall
300
402 A, B
Halla Hall
401
Samda A
Samda B
303
Foyer
300
401
Room
07:00-08:00
08:00-09:00
AOFNMB GC (07:30-08:30)
Joint Symposium 5. Future of Targeted Radionuclide Therapy
Continuing Education 5. Pediatric Nuclear Medicine
Young Investigator Session for KSNM
Free Paper 10. Cardiology
Current Issues 4. Current Nuclear Medicine Activities in Arabic Region
Poster Presentation
Joint Symposium 7. Future of Cardiovascular Imaging
ARCCNM Session
Free Paper 14. Molecular Imaging
Free Paper 15. Oncology
Current Issues 6. General Nuclear Medicine
Poster Presentation
FANMB Session
09:00-10:00
10:00-11:00
Walking Poster (Clinical II)
Coffee Break
Walking Poster (FANMB)
11:00-12:00
Plenary Session 4. Richard Baum (President, WARMTH)
Plenary Session 6 Nagara Tamaki (Hokkaido University, Japan)
12:00-13:00
KSNM General Assembly (대한핵의학회 총회)
Exhibition
AOFNMB/ ARCCNM NDA
Poster Presentation
IAEA Workshop
13:00-14:00
Plenary Session 5. Andrew Scott (President, WFNMB)
Honorary Fellow Lecture Yong-Whee Bahk
14:00-15:00
Poster Presentation
Coffee Break
Coffee Break
Walking Poster (FANMB)
15:00-16:00
Joint Symposium 6. PET GMP
Continuing Education 6. CT Reading
Free Paper 11. Endocrinology
Free Paper 12. General Nuclear Medicine
Current Issues 5. Translational Research
Free Paper 13. Radiochemistry
Joint Symposium 8. Imaging for non-coronary Heart Disease
Young Investigator Competition for AOFNMB (Basic)
Young Investigator Competition for AOFNMB (Clinical)
Poster Presentation
16:00-17:00
17:00-18:00
Highlight Session
Closing Ceremony
18:00-19:00
ANMB Dinner (SF Oceanview) * Invited Only
RCA Dinner (Daemjang, Jeju Jungmun) * Invited Only
19:00-20:00
20:00-21:00

Scientific Program

Day 1. Oct. 31 (Sat)

[Tamna Hall (5F)]

09:00 - 11:00	Joint Symposium 1. Hybrid Imaging *Co-organized by IEEE NPSS Seoul Chapter*
11:30 - 12:30	Special Lecturer
14:00 - 15:00	Plenary Session 1. Sobhan Vinjamuri
15:30 - 17:30	Joint Symposium 2. Optimization of Radioiodine Therapy for Thyroid Cancer

[Halla Hall (3F)]

09:15 - 10:55	WARMTH Symposium Session 1. Established Radionuclide Therapies: Practical Aspects and New Development (I)
11:15 - 12:55	WARMTH Symposium Session 2. Established Radionuclide Therapies: Practical Aspects and New Developments (II)
14:00 - 15:40	WARMTH Symposium Session 3. Novel Radionuclide Therapies: Practical Aspects and New Development
15:40	WARMTH Symposium International Round Table Discussion

[401 (4F)]

09:00 - 11:00	Continuing Education 1. Molecular Imaging
15:30 - 17:30	Continuing Education 2. Molecular Imaging *Co-organized by Korean Society of Molecular Imaging*

[Samda A (3F)]

09:00 - 11:00	Free Paper 1. Molecular Imaging
15:30 - 16:30	Free Paper 2. Neurology
16:45 - 17:45	Free Paper 5. General Nuclear Medicine

[Samda B (3F)]

09:00 - 11:00	Current Issues 1. PET Oncology
15:30 - 16:00	Free Paper 3. Physics / Instrument
16:15 - 17:15	Free Paper 4. Clinical applications of PET/MR and SPECT/CT

[Foyer (3F)]

09:00 - 18:00	Poster Presentation
11:00 - 12:00	Walking Poster Session 1. Basic

Day 2. Nov. 1 (Sun)

[Halla Hall (3F)]

09:00 - 11:00	Joint Symposium 3. Clinical Translation of Molecular Imaging *Co-organized by Biomedical Polymers Division, The Polymer Society of Korea*
11:30 - 12:30	Plenary Session 2. Hossein Jadvar
14:00 - 15:00	Plenary Session 3. Christopher H. Contag
15:30 - 17:50	Joint Symposium 4. Current Advances in Molecular Imaging *Co-organized by Federation of Asian Societies for Molecular Imaging*

[401 (4F)]

09:00 - 11:00	Continuing Education 3. Radiochemistry of Cyclotron-produced Nuclides
15:30 - 17:30	Continuing Education 4. CT Reading

[Samda A (3F)]

09:00 - 11:00	Free Paper 6. KSNM (Basic)
15:30 - 17:00	Free Paper 8-1. KSNM (Clinical I)
17:15 - 18:30	Free Paper 8-2. KSNM (Clinical II)

[Samgda B (3F)]

09:00 - 11:00	Free Paper 7. Oncology
15:30 - 17:30	Free Paper 9. Technologist

[303 (3F)]

09:00 - 11:00	Current Issues 2. Radiation Safety
15:30 - 17:30	Current Issues 3. Radionuclide Therapy

[Foyer (3F)]

09:00 - 18:00	Poster Presentation
11:00 - 12:00	Walking Poster Session 1. Basic

Day 3. Nov. 2 (Mon)

[Halla Hall (3F)]

09:00 - 11:00	Joint Symposium 5. Future of Targeted Radionuclide Therapy
11:30 - 12:30	Plenary Session 4. Richard P. Baum
14:00 - 15:00	Plenary Session 5. Andrew Mark Scott
15:30 - 17:30	Joint Symposium 6. PET GMP

[401 (4F)]

09:00 - 11:00	Continuing Education 5. Pediatric Nuclear Medicine
15:30 - 17:30	Continuing Education 6. CT Reading

[Samda A (3F)]

09:00 - 11:00	Young Investigator Award for KSNM
15:30 - 16:30	Free Paper 11. Endocrinology
16:45 - 17:45	Free Paper 13. Radiochemistry

[Samgda B (3F)]

09:00 - 10:30	Free Paper 10. Cardiology
15:30 - 17:30	Free Paper 12. General Nuclear Medicine

[303 (3F)]

09:00 - 11:00	Current Issues 4. Current Nuclear Medicine Activities in Arabic Region
15:30 - 17:30	Current Issues 5. Translational Research

[Foyer (3F)]

09:00 - 18:00	Poster Presentation
11:00 - 12:00	Walking Poster Session 3. Clinical (II)

Day 4. Nov. 3 (Tue)

[Halla Hall (3F)]

09:00 - 11:00	Joint Symposium 7. Future of Cardiovascular Imaging
11:30 - 12:30	Plenary Session 6. Nagara Tamaki
14:00 - 15:00	Honorary Fellow Session
15:30 - 17:30	Joint Symposium 8. Imaging for Non-coronary Heart Disease
17:45 - 18:45	Highlight Session

[Halla Hall (3F)]

09:00 - 11:00	ARCCNM Session

[Samda A (3F)]

09:00 - 10:00	Free Paper 14. Molecular Imaging
15:30 - 17:30	Young Investigator Competition for AOFNMB (Basic)

[Samda B (3F)]

09:00 - 10:00	Free Paper 15. Oncology
15:30 - 17:30	Young Investigator Competition for AOFNMB (Clinical)

[303 (3F)]

09:00 - 11:00	Current Issues 6. General Nuclear Medicine

[Foyer (3F)]

09:00 - 18:00	Poster Presentation
11:00 - 11:30	Walking Poster Session 4. FANMB (I) (II)
15:00 - 15:30	Walking Poster Session 4. FANMB (III) (IV)

Day 5. Nov. 4 (Wed)

[401 (4F)]

09:00 - 12:00	FANMB Session

Plenary Session 1

Code of Ethics for Nuclear Medicine: Why and How?

Sobhan Vinjamuri

Royal Liverpool University Hospital

Like other specialities, Nuclear Medicine is not immune to ethical dilemmas. The specialty of nuclear medicine has gone through rapid change in the recent past. Cutting edge technology, new radiopharmaceuticals, new concept for metabolic changes in disease prevalence as well as progression and new imaging equipment have given the nuclear medicine physicians numerous challenges where a wide range of ethical issues are being tested. Diagnostic pitfalls can be at many levels which include issues related to documenting specific information on medical records, inappropriate justification of requested diagnostic tests, prescribing the wrong radioisotope, accepting sub-optimal images and incompetence in interpretation of images. A strategic and robust system of working pattern should be designed and implemented at every level (Referrer, Practitioner, Operator and Medical physics) to avoid legal implications. The working pattern needs to be reviewed periodically to find whether there is any room for improvement and necessary changes should be put into practice to improve the service and minimise the errors. This plenary lecture will explore some of the common ethical dilemmas facing NM practitioners and will also explore some ways forward.

Plenary Session 2

Molecular Imaging and Targeted Radionuclide Therapy of Prostate Cancer

Hossein Jadvar, MD, PhD, MPH, MBA, FACNM

Associate Professor of Radiology and Biomedical Engineering
University of Southern California, Los Angeles, CA USA

Prostate cancer is a prevalent public health problem worldwide. While imaging has played a major role in this disease, there still remain many challenges and opportunities. Positron emission tomography with various physiologically-based radiotracers is fundamentally suited to interrogate this biologically and clinically heterogeneous disease along the course of its natural history. There have also been great strides in targeted radionuclide therapy of prostate cancer. In this presentation, I review briefly the evidence for the use of positron emission tomography with a number of radiotracers including but not limited to ^{18}F-fluorodeoxyglucose, ^{11}C-acetate, and ^{18}F- or ^{11}C-choline, and those radiotracers that are targeted to the androgen receptor, amino acid metabolism, and prostate specific member antigen. I will also review 223Ra dichloride alpha therapy in castrate resistant metastatic prostate cancer and the exciting novel prospects for the use of therapeutic-diagnostic (theranostic) pairs in the management of patients with prostate cancer.

Plenary Session 3

Solving Big Problems with Small Devices

Christopher H. Contag, Ph.D

Stanford University

Current technologies for the detection of cancer lack the sensitivity for early detection at times when therapy would be most effective, and cannot detect minimal residual disease that persists after conventional therapies. Therefore, it will be necessary to develop image-guided approaches for multiplexed molecular characterization of cancer and methods to visualize small numbers of cancer initiating cells. Imaging and sensing will need to move from detection limits of 1 cm to 1 mm, or even 100 μm diameter masses, and new technologies with this sensitivity need to be developed. Optical imaging has the sensitivity for this level of detection and there are a number of recent advances that will enable the use of optics in the clinic for cancer detection. New instruments based on micro-optical designs can be used to reach in the body to reveal microanatomic and molecular detail that are indicators of early cancers. We are advancing the technologies that enable miniaturization of 3-D scanning confocal microscopes and Raman endoscopes to examine tissue in situ for early anatomic and molecular indicators of disease, in real time, and at cellular resolution. These new devices will lead to a shift from the current diagnostic paradigm of biopsy followed by histopathology and recommended therapy, to one of non-invasive point-of-care diagnosis with the possibility of treatment in the same session. By creating the tools for point-of-care pathology we are reducing the time and distance between the patient and the diagnostic event, and changing the practice of medicine. The emerging combinations of instruments and molecular probe strategies will reveal disease states in finer detail and provide greater information to clinicians for more informed, and directed therapies. Personalized medicine is really molecular medicine and

the new imaging and diagnostic tools that characterize molecular basis of disease are driving personalized care and early intervention.

Plenary Session 4

Targeted Molecular Imaging and Radiotherapy of Cancer Using Ga-68 and Lutetium-177 Labeled Peptides: From Bench to Precision Medicine at Bedside

Richard P. Baum

THERANOSTICS Center for Molecular Radiotherapy and Molecular Imaging, ENETS Center of Excellence, Zentralklinik Bad Berka, Germany

1. Theranostics of Neuroendocrine Tumors
The strong expression of SSTR2 by neuroendocrine tumors (NETs) enables peptide receptor radionuclide therapy (PRRT), the molecular internal radiation therapy of NETs. The most important points to consider for PRRT are: Patient selection
Appropriate choice of peptide and radionuclide
Kidney protection
Tumor and organ dosimetry (post-treatment scans) and Monitoring of toxicity (follow-up)
In our hospital, which was certified as ENETS Center of Excellence in March 2011 and re-certified in March 2014, a dedicated multidisciplinary team of experienced NET specialists is responsible for the management of NET patients (over 1,200 patient visits per year).
Patient selection for PRRT is based on the Bad Berka Score (BBS) which takes into account clinical aspects and molecular features. The therapy plan for each patient is individualized.
Frequent therapy cycles (4-6 and up to 10), applying low or intermediate doses of radioactivity are suitable for these relatively slow-growing tumors ("long term low dose, not short term high dose concept").
For kidney protection, patients are well hydrated and receive an amino acid infusion containing lysine and arginine given intravenously for 4 hours beginning 30 minutes before PRRT. Renal function is serially determined by Tc-99m MAG3 scan (TER) and by Tc-99m DTPA (GFR) measurements.
After each 2 treatment cycles, restaging is performed by morphologic (CT/MRI) and molecular imaging (Ga-68 SSTR PET/CT), metabolic imaging (at least one F-18 FDG PET/CT before start of treatment), and in selected cases also F-18 fluoride PET/CT, blood chemistry and tumor markers.
All data are entered in a prospective structured database (<250 items per patient).
Another very important aspect is dosimetry. Estimation of tumor and normal organ doses performed after PRRT (using Lu-177 labeled somatostatin analogues DOTATATE or DOTATOC) is important to ensure that maximum dose is delivered to the metastases, therefore optimizing an individualized treatment protocol.

NET Center Bad Berka - Overall Results
Retrospective analysis was performed using our database in 1000 patients (age 4 - 85 years) with metastatic and / or progressive NETs, undergoing 1 - 9 cycles of PRRT at our center using Lu-177 (n=331), Y-90 (n=170) or both (n=499). Median total administered activity was 17.5 GBq. Patients were followed up for up to 132 months after the 1st cycle of PRRT. Well-differentiated NETs (G1-2) accounted for 54 %. Most patients (95.6 %) had undergone at least 1 previous therapy (surgery 86.8 %, medical therapy 55 %, ablative therapy 14.2 % and radiotherapy 3.4 %).
The median overall survival (OS) of all patients from the start of PRRT was 52 months (mo). Median OS according to radionuclide used: Y-90 24 mo, Lu-177 55 mo, both (TANDEM or DUO PRRT) 64 mo; according to the grade of tumor: G1 87 mo, G2 55 mo, G3 28 mo, unknown 50 mo; and according to origin of primary tumors: pancreas 45 mo, small intestine 77 mo, unknown primary 55 mo, lung 36 mo. Median progression-free survival (PFS) measured from the last therapy cycle was 22 mo, comparable for pancreatic (23 mo) and small intestinal (25 mo) NETs.
We have also treated patients with progressive metastases of NETs and with a single functional kidney (24 patients). None of these patients showed grade 3 or 4 nephrotoxicity. PRRT resulted in partial remission in 36% and stable disease in 36% of the patients, 28% had PD. In 2009, we have given fractionated low dose PRRT to 3 patients on hemodialysis (to the best of our knowledge, this was the first ever worldwide experience).
The Bad Berka neuroendocrine tumor center was the first also to use Y-90 DOTATATE. In a large patient group (>350 patients), Lu-177 DOTATOC was administered for PRRT of progressive NETs, non-responsive to octreotide/interferon treatment or chemotherapy. Historical comparison to established treatment modalities showed a significant benefit in progression free survival (PFS) or time to progression (TTP), e.g. compared to Octreotide LAR (PROMID study) PFS vs. TTP was 16 months longer, and compared to Sunitinib and Everolimus, respectively, PFS there was an improvement of PFS by 19 months.
An important influence on the decision of the choice of radionuclide is the size of tumors. More commonly, patients present with tumors of various sizes and inhomogeneous distribution of somatostatin receptors.

The use of a **combination of Lu-177 and Y-90** takes this heterogeneity into account. Sequential administration of Y-90 and Lu-177 labeled analogues is useful for the treatment of larger tumors, followed by treatment of smaller metastases, respectively in further treatment cycles. The BBNETC group pioneered the systematic use of Y-90 and Lu-177 DOTATATE **(DUO PRRT)** in sequence and concurrently, as well as the intra-arterial use of Y-90 DOTATATE and DOTATOC.

Lu-177 DOTATATE or Lu-177 DOTATOC is predominantly used for small metastases or in patients with impaired renal or haematological function. Long term follow-up of up to 10 years after DUO PRRT showed no significant grade 3 or grade 4 nephrotoxicity attributed to concurrent or sequential DUO PRRT. The median fall in tubular extraction rate (TER) was lesser in patients undergoing DUO PRRT than in those undergoing PRRT with Y-90 alone. The results of a study by Kunikowska et al. also indicated that TANDEM PRRT (concurrent PRRT with Y-90/Lu-177 DOTATATE) provided longer overall survival than with a single radioisotope (Y-90 DOTATATE); the safety of both methods was comparable.

Results of a German Multi-institutional Registry Study

A German multi-institutional registry study with prospective follow up in 450 patients indicates that PRRT is an effective therapy for patients with G1-2 neuroendocrine tumors, irrespective of previous therapies, with a survival advantage of several years compared to other therapies and only minor side effects. **Median overall survival (OS) of all patients from the start of treatment was 59 months. Median progression-free survival (PFS) measured from last cycle of therapy accounted to 41 mo**. Median PFS of pancreatic NET was 39 mo. Similar results were obtained for NET of unknown primary (median PFS: 38 mo) whereas NET of small bowel had a median PFS of 51 months. Side effects like °3-4 nephro- or hematotoxicity were observed in only 0.2% and 2% of patients respectively.

A randomized prospective international multi-center clinical trial (the NETTER-1 Study) has been performed in patients with progressive midgut NET comparing Lu-177 DOTATATE PRRT (4 cycles at 7.4 GBq each plus 30 mg Octreotide LAR per month) with high dose (60 mg) Octreotide LAR per month and first results will be presented.

Conclusions

PRRT lends a significant benefit in progression free survival as well as in overall survival in metastasized and / or progressive G1-2 NETs as compared to other treatment modalities and regardless of previous therapies. Combination of Lu-177 and Y-90 (DUO) based PRRT may be more effective than either radionuclide alone. Thus, in patients with progressive NETs, fractionated, personalized PRRT with lower doses of radioactivity given over a longer period of time (Bad Berka Protocol) is effective even in advanced cases and results in excellent therapeutic responses. Up to 10 cycles of PRRT, given over several years were tolerated very well by most patients. Severe renal toxicity can be completely avoided or reduced by nephroprotection applying aminoacids; haematological toxicity is usually mildto moderate (except for some cases of MDS which occurs in 2-3%). Quality of life can be significantly improved. Though cure is rarely possible, excellent palliation with significant improvement of symptoms can be achieved by PRRT. In addition, neoadjuvant PRRT could be administered in cases of inoperable NET so as to render the tumor operable by inducing radiation induced necrosis and decrease in tumor size. Use of intra-arterial PRRT (>100 treatments were already performed up to now at our center) is more effective for selectively targeting liver metastases and large, inoperable primary tumors.

PRRT should only be performed at specialized centers as NET patients need highly individualized interdisciplinary treatment and long term care. PRRT can be effectively combined with transarterial chemoembolization (TACE), radiofrequency ablation (RFA), chemotherapy (e.g. using Capecitabine/5-FU, Temozolomide or Doxorubicin), and kinase inhibitors (e.g. Everolimus).

2. Theranostics of Prostate Cancer

The significant overexpression of the prostate specific membrane antigen (PSMA) on tumor cells makes this enzyme an ideal target for the diagnosis as well as for therapy (THERANOSTICS) of prostate cancer. Ga-68 PSMA is a sensitive and specific tracer for the detection of primary prostate cancer, recurrent tumors and metastases. We have performed over 1,000 Ga-68 PSMA PET/CT studies until to date, using Ga-68 HBED PSMA and also applying DOTAGA PSMA I&T. Based on our experience, the potential indications for PET/CT in prostate cancer are:

Elevated PSA without tumor detection by conventional imaging, or patients with negative biopsies and high serum PSA (in well differentiated tumors also bombesin antagonists may be useful)

Initial staging in patients with intermediate or high risk (detection of lymph node and distant metastases), especially in case of strongly elevated PSA levels (suspicious distant metastases)

Detection of recurrence after initial therapy - in our experience, Ga-68 PSMA is far superior to choline due to detection of recurrence at very low PSA levels (<0.5 ng/ml), especially in undifferentiated tumors with high

Gleason grade.
Therapy monitoring (depending on the clinical question which needs to be answered)
Molecular radiation therapy planning (MRTP), e.g., for dose painting
THERANOSTICS before planned PRLT for selection of the most appropriate radiopharmaceutical for therapy as well as for follow-up and assessment of therapy response after radionuclide therapy (this indication holds great future potential).

PSMA Radioligand Therapy (PRLT)
Based on the principles of targeted radionuclide therapy, Lu-177 labeled ligands binding specific to PSMA were developed by the Pharmaceutical Radiochemistry at the Technical University Munich using DOTAGA as chelator. PSMA radioligand therapy (PRLT) with Lu-177 DOTAGA PSMA ligands was performed in 53 progressive, metastasized, castrate-resistant prostate cancer patients. Ga-68 PSMA PET/CT was used for patient selection and follow-up. 34 patients received multiple cycles (range 2 to 5, in total 106 administrations). The mean injected activity of Lu-177 PSMA per cycle was 5.7±0.8 GBq (median 5.8 GBq). Post-therapy response could be assessed until now in 27 patients. Patient-specific dosimetry was carried out according to MIRD scheme.
The metastases exhibited intense PSMA expression, demonstrated by baseline Ga-68 PET/CT, high Lu-177 PSMA uptake on post-therapy planar scans and on SPECT/CT.
Molecular treatment response (partial remission) was observed in 11 patients, and morphological response (according to RECIST) was seen in 6 patients. Stable disease was noted in 5 and 13 patients, according to molecular and morphological response criteria, respectively, whereas disease progressed in 8 patients. All symptomatic patients reported significant improvement in pain and in quality of life after therapy. The treatment was very well tolerated by all patients, no acute (vomiting, emesis) or long term side effects were reported (especially there was no evidence of significant salivary or lacrimal gland toxicity). There were no significant alterations in any of the laboratory parameters (blood, renal, hepatic panel and chemistry), especially no hematotoxicity was observed (despite extensive bone metastases in many of the patients) or any change in renal function (as determined by creatinine, GFR clearance and Tc-99m MAG3/TER scintigraphy). Organ- and tumor doses were as follows: whole body 0.02+/-0.01 mGy/MBq; kidneys 0.35+/-0.14 mGy/MBq; tumor lesions 0.14-19.8 mGy/MBq. In bone metastases, the maximum dose reached by a single cycle was up to 300 Gy in some cases; complete remissions of lymph node metastases were observed in some patients. The median for progression free survival (PFS) and overall survival (OS) has not yet been reached.

Conclusions
Lu-177 DOTAGA PSMA small molecules exhibit very high tumor uptake, rapid blood clearance and fast renal washout. PRLT using Lu-177 PSMA is effective in end-stage disease after failure of all conventional/approved therapies (killing tumor and not only improving symptoms). There was excellent tolerability in all patients treated, i.e., no hematological, renal or salivary gland toxicity was observed. Selection of suitable patients as well as follow-up after PRLT by Ga-68 PSMA PET/CT is feasible and successful (THERANOSTICS concept). Improving the treatment potency and safety by means of hyperfractionation, increase of treatment activity, new methods for kidney protection (e.g. by using PMPA), application of radiosensitizers, different radionuclides and combination of various therapies must be considered in future.

Plenary Session 5

Imaging Metabolic and Signalling Pathways in Cancer

Andrew M. Scott

Department of Molecular Imaging and Therapy, Austin Hospital
Department of Medicine, University of Melbourne
and Olivia Newton-John Cancer Research Institute, La Trobe University, Melbourne, Australia

Molecular imaging can make a significant contribution to understanding the causes and biology of disease, as well as the development of new therapeutics. This can involve high resolution microscopy and cell-based imaging approaches, animal model imaging, and human studies with a broad range of molecular imaging approaches. The gene mutation changes responsible for many cancers are frequently associated with phenotype changes that involve changes in cell surface receptors and intracellular signalling processes, and metabolic pathways, which can be abrogated by therapeutics for clinical benefit. Examples include Epidermal Growth Factor Receptor (EGFR), HER2, and Le^y expression in colon, breast, lung, head and neck cancer and glioma; somatostatin receptor expression in neuroendocrine tumours; androgen and estrogen receptor expression in breast and prostate cancer; and receptor kinase mutations in leukemias, GIST and lung cancers. Molecular imaging approaches allow the non-invasive identification of cancer cell phenotype through receptor expression and metabolic signatures, and can also assist with prediction of response to targeted therapeutics and

hormonal treatments. We have explored the biology and therapeutic approaches targeting EGFR in glioma, colon, head and neck and lung cancer using a novel antibody which binds to a conformationally exposed epitope of EGFR (mAb806). Validation of targeting of humanised 806 in preclinical models has been extended to human trials, where imaging of biodistribution and tumour uptake has been used to identify patient populations suitable for therapy. This approach is currently being explored in Phase II trials. We have also explored TRAIL receptor expression and targeting with a humanised antibody (CS-1008) against Death Receptor 5 (DR5) in preclinical models, and shown a direct correlation of receptor occupancy and therapeutic effect. This has been extended into a clinical trial in colorectal cancer patients, where ^{111}In-CS-1008 uptake in tumour was found to be highly predictive of clinical benefit, and superior to any other biomarker analysed. The use of molecular imaging "Theranostics" is a powerful approach to developing new therapeutics for cancer patients, and is increasingly being utilised in oncology trials.

Plenary Session 6

New Applications of FDG-PET for Cardiovascular Medicine

Nagara Tamaki, MD, PhD

Department of Nuclear Medicine, Graduate School of Medicine, Hokkaido University, Sapporo, Japan

PET plays an important role to probe a variety of molecular and cellular dysfunctions in vivo in cardiovascular diseases. FDG has long been used for assessing myocardial viability and selecting candidates for revascularization treatment, particularly in patients with poor left ventricular dysfunction. Based on the experimental data suggesting high FDG accumulation of macrophage infiltration, FDG has recently been used for active inflammation in various cardiovascular diseases.

FDG imaging has a promise for identifying intraplaque inflammation. In our atherosclerotic mouse models, FDG uptake correlated with the degrees of macrophage infiltration. FDG uptake in the aorta was highest in atheromatous stage among various AHA stages. In addition, serial analysis in vascular FDG uptake is valuable for treatment monitoring in atherosclerotic lesions. Clinical studies confirmed the value of FDG imaging for identifying active inflammation in aortitis and aortic aneurysm, and also in active atheromatous lesions with carotid arteries. In order to identify active lesion as an area of increased FDG uptake, physiological FDG uptake in the normal myocardium should be suppressed. For this purpose, FDG is administrated under a long (>18 hours) fasting with low carbohydrate diet. Premedication of heparin may often be used to increase plasma free fatty acid.

One exciting application of FDG in the myocardium is for detecting cardiac sarcoidosis. We have reported that cardiac involvement is often seen as areas with focal or focal on diffuse FDG uptake in the myocardium. Cardiac involvement is nicely observed on both gadolinium (Gd) enhanced MRI and FDG-PET. Gd-MRI may identify myocardial fibrosis, whereas FDG may detect active inflammation. Therefore, FDG-PET seems to be more valuable for treatment monitoring. In addition, recent multicenter study suggested FDG-PET may enhance prognostic assessment in patients suspected with cardiac sarcoidosis.

We conclude that FDG-PET may hold a new role for identifying active lesions in the assessment of atherosclerosis and various myocardial disorders.

Special Lecture

Themes of AOCNMB 2015: From Globalization to Localization & Young Leadership Development

Henry Hee-Seung Bom, MD, PhD, FANMB

President, AOFNMB

Confronting challenges are common in every corners of the world. It is also true in the nuclear medicine (NM) as medical environments are ever changing. There are differences in NM practice and research among different regions. This heterogeneity of NM practice and research is particularly challenging in Asia. NM is rapidly expanding in East Asia and Southeast Asia. There is a big need for education and training in these regions. Considering the huge geographic area in Asia and Oceania communication is a big challenge. Adoption of electronic communication is urgently needed. Shortage of human resources is the utmost challenge in many countries in the region. Therefore local issues should be identified and strategies to solve the local issues need to be separately developed in the region.

As the future is the time for the next generation development of young leadership is important. It is particularly true in Asia and Oceania where needs for NM is relatively larger than other continents. A systematic approach is needed to develop young leadership. Asia NM Board examination started last year and continues this year. New fellows organize their own program. Communication and networking through the congress will be a concrete platform for young leadership in AOFNMB.

Special Lecture

Radionanomedicine: Combined Nuclear and Nanomedicine

Dong Soo Lee

Seoul National University Hospital, Korea

Nuclear medicine has used small molecules and biomacromolecules but without much success for radionuclide/pharmaceutical therapy yet. The advent of nanotechnology foresaw the renaissance of therapy in because nanomaterials supply huge areas of multiplex labeling. Combined Lu-177/Y-90 therapy and combined Lu-188/Cu-64 imaging were enabled and thus theranostics to monitor therapy effect or to predict the therapeutic efficacy using radiolabeled nanomaterials became possible. Inorganic molecules such as upconverting nanoparticles (UCNP), iron oxide, mesoporous silica or SERS dots (surface-enhanced Raman scattering dots) were used with surface-labeling with radionuclides as well as core-labeled ones. Surface encapsulation was one of the breakthroughs to make it easy to label multiple ligands and radionuclides. Jeong's method is one example which successfully labeled simultaneously polyethylene glycols (PEGs), small peptides and chelators. On the surface of nanomaterials, well-adopted click chemistry also allowed labeling huge molecules such as monoclonal antibodies or peptides and their analogues setting the functional residues exposed to the exterior of labeled nanomaterials.
Another sub-discipline of radionanomedicine is 'endogenous nanomedicine' using exosomes (extracellular vesicles). If exosomes are to be used as therapeutic carrier, they need to be labeled with radionuclides, in which case Tc-99m HMPAO and Cu-64 were used. Radiolabeled exosomes were examined for their biodistribution using SPECT and PET. In vitro monitoring of GFP-labeled exosomes also opened the possibility of companion diagnostics. Radionanomedicine, combined nuclear and nanomedicine is sure to encourage nanomedicine to enter more easily into preclinical and clinical translation with use of trace amount and applying tracer kinetics. I propose that the use of trace amount of radio-nanomaterials for in vivo diagnostic/theranostic and tracer-kinetic interpretation of in vivo behavior of these materials shall facilitate the in vivo use and finally clinical translation of radionanomedicine.

Honorary Fellow Lecture

Gamma Correction Pinhole Bone Scan as an Identify of Nuclear Imaging in the Era of Hybridization: Development and Maturation

Yong- Whee Bahk

Sungae Hospital, Korea

Joint Symposium 1

Research Trends in Positron Emission Tomography Instrumentation

Jung Yeol Yeom, Ph.D

Korea University, Korea

Positron emission tomography (PET) is a nuclear medicine imaging technique that uses radioactive tracers attached to biologically active molecules to produce three-dimensional images of functional processes in the body. In this presentation, recent research trends in PET instrumentation, including but not limited to, techniques such as ultrahigh resolution scanners, Time-of-Flight PET (ToF-PET), depth-of-interaction (DOI), multi-modality imaging and image reconstruction/processing are covered.

Brief Biosketch
Prof. Yeom acquired his B.Sc. from Department of Nuclear Engineering, Seoul National University and his M.Eng./Ph.D. from the Department of Quantum Engineering and Systems Science, University of Tokyo. He has had prior work/training experiences at Seoul National University Hospital, LG Electronics, Stanford University and Kumoh National Institute of Technology before joining Korea University.

Joint Symposium 1

A Multi-Modality Imaging System for Laparoscopic Sentinel Lymph Node Detection

Seong Jong Hong

Department of Senior Healthcare, Graduate School, Eulji University, Daejeon, Korea
Department of Radiological Science, Eulji University, Gyeonggi-do, Korea

Minimally invasive laparoscopic and robot-assisted

surgeries which use single- or multi-ports for surgical lights and tools have become preferred approaches for prostatectomy, and gynecological and many other surgeries. A radio tracer, a NIR dye or both have been used for the SLN mapping procedure of prostate cancer. A NIR fluorescence imaging has played an important role in the SLN mapping. Particularly, indocyanine green (ICG), a NIR fluorophore approved by the Food and Drug Administration, has been used widely in clinical environments to visualize the SLN during the surgery. Most commercially available NIR imaging systems have employed simultaneous NIR/visible imaging techniques to offer a new vision to surgeons by visualizing either NIR fluorophore distributions or bright field anatomical images. However the tissue penetration depth of NIR is still limited to less than 10 mm, which can lead to false negative results in the SLN mapping.

Even though radionuclide guided mapping can detect the SLN inside the deep tissue, it still suffers from high backgrounds in normal tissues. Radionuclide guided SLN mapping usually uses ^{99m}Tc-based radiopharmaceuticals such as ^{99m}Tc-HSA (human serum albumin), ^{99m}Tc-antimony (Sb), and ^{99m}Tc-sulfur colloid. SPECT/CT also has been used for the SLN mapping. Several groups attempted to improve the SLN identification by combining a NIR-guided mapping with radionuclides. These studies employed a sequential study of the NIR-guided mapping and gamma probes/images due to lack of a combined system of NIR and gamma imaging. A multi-modal imaging system to study the feasibility of NIR/visible/gamma imaging for the SLN mapping in the laparoscopic or robot-assisted surgery will be presented.

Joint Symposium 1

Oncologic Application of Parallel PET-MRI

Ilhan Lim MD, Ph.D

Department of Nuclear Medicine, Korea Cancer Center Hospital, Korea Institute of Radiological & Medical Sciences
75 Nowongil, Nowon-Gu, Seoul, 139-706, Korea

PET-CT has proved its excellence in that it facilitates the attenuation correction and accomplishes the combination of anatomical and molecular information. Stimulated by the enormous prosperity of PET-CT, the combination of PET and MRI was expected as a coming new world to the clinicians and researchers. Although integrated PET-MRI is available nowadays, the development of PET-MRI was limited because of the interferences between PET and MRI technologies, for example the adverse effect among photomultiplier tubes, field gradients, and MR radio frequency.

Therefore, previous model of PET-MRI was parallel type. Parallel PET-MRI system was installed in our institute in the year of 2009. After the installation of parallel PET-MRI, we performed various clinical trials with regards to breast cancer patients undergoing neoadjuvant chemotherapy, osteosarcoma cancer patients with neoadjuvant chemotherapy, hepatocellular carcinoma patients treated with sorafenib.

It has been tried to achieve an early assessment of response to anti-cancer treatment because early prediction assist to make a right decision for further treatment. When the inefficacy of treatment is discovered, the medication or the modality should be modified to prolong the patients' survival. Information from interim treatment assessment can provide significant suggestion to predict the patients' prognosis. Also, proper assessment of cancer treatment enables the society to allocate the medical property in a right way.

FDG-PET has demonstrated the excellent capability to distinguish between treatment responder and non responder in many malignant diseases. Functional imaging shows better outcome than anatomical imaging because anatomical imaging cannot differentiate between fibrotic tissue and viable tumor. As the MRI technologies are developed, diverse functional parameters can be obtained from MRI. There are many functional imaging techniques such as dynamic contrast enhancement (DCE) MRI, diffusion weighted (DW) MRI, ^{1}H-MR spectroscopy (MRS), and blood oxygenation level-dependent (BOLD) MRI. They are expected to detect the biological changes early and to supply complementary information other than PET. Many researchers have applied these functional parameters in the clinical situation. However, the Effectiveness is controversial, and depends on each researcher.

This presentation will summarize studies which have suggested the usefulness of parallel PET-MRI in the field of oncology in terms of assessing treatment response and predicting prognosis. These results strongly indicate that the integration of functional parameters from PET-MRI may improve the prediction of treatment response and prognosis in various oncologic situations.

Joint Symposium 1

Multimodal Image Fusion

Hiroshi Watabe

Cyclotron and Radioisotope Center, Tohoku University, Sendai, Japan

There are several medical imaging modalities such as

X-ray CT, MRI, PET, and SPECT, and each modality has different aspect for visualizing inside of human body. Morphological information can be archived by X-ray CT and MRI, while PET and SPECT offer functional or physiological information. Diagnostic power will be significantly improved by combining these images, including better differentiation between lesion and normal regions. The integrated system such as PET/CT, SPECT/CT and PET/MRI scanner is one solution to provide fusion image between two different modalities. By the integrated system, the images from two different modalities are simultaneously acquired and the both images share same image coordinates and no image registration is required. Disadvantages of the integrated system are the cost of installation, and restricted usages due to limitation of hardware specification such as limited field-of-view.

Alternatively, multimodal image fusion can be performed with several individual imaging modalities. By this strategy, more applications can be expected than the integrated system. For example, fused image of the cutting edge X-ray CT and PET images is expected to outperform the image from the integrated PET/CT scanner. One drawback of the image fusion of two different individual system is requirement of image registration because images from one modality to other are different in terms of position of patient, and time when data are acquired. Many investigators have developed software based image registration methods in which two images are coregistered for fusion. If the target region is brain, it is relatively easy because rigid body transformation is enough for the image registration. If the target region is thorax or abdomen, it may be necessary to perform non-rigid transformation, which is sometimes problematic to get well-matched registered images.

In my talk, I will discuss topics related to the multimodal image fusion including theories and techniques and introduce our recent works for the image fusion.

Joint Symposium 2

Prognostic Evaluation of Therapeutic Response to Radioiodine Therapy In Differentiated Thyroid Cancer

Dong Jun Lim MD, Ph.D

Seoul St. Mary's Hospital, The Catholic University of Korea, Korea

Remnant ablation or adjuvant therapy using radioactive iodine (RI) after total thyroidectomy has been the standard of care in patients with differentiated thyroid cancer (DTC) for several decades. However, recent clinical trends in DTC management emphasize the importance of more conservative care and lower dose RI, highlighting subdivision of DTC patients, not to over-treat low-risk patients.

Conventional methods to evaluate therapeutic response to RI therapy were measurement of serum thyroglobulin levels and diagnostic RI whole-body scan but ultrasonography with thyroglobulin levels has become the mainstay of surveillance in most DTC patients. Besides more aggressive thyroid cancer suspicious of metastasis can also be evaluated using FDG-PET scan so all response variables to RI therapy should be comprehensively considered in decision-making of further treatment.

Recent clinical guidelines suggest risk stratification using risk-adapted evaluation and ongoing risk assessment, especially after RI therapy. However, practical application of this policy is not easy due to variable clinical situations and less standardized evaluation. Several clinical studies including ours reflect dynamic risk assessment with serum thyroglobulin levels and imaging after RI therapy. Herein clinical parameters and prognostic factors from various diagnostic modalities around RI therapy will be discussed to readily detect persistence/recurrence and to facilitate optimal surveillances in DTC patients.

Joint Symposium 2

Role of Surgery in RAI Avid and Non-avid Thyroid Cancer

Hang-Seok Chang MD, Ph.D, F.A.C.S

Department of Surgery, Director of Thyroid Cancer Center, Gangnam Severance Hospital, Yonsei University College of Medicine, Seoul, Korea

The best therapeutic effect can be achieved by complete surgical removal in majority of well differentiated thyroid cancer(WDTC), and the combination with radio-active iodine(RAI) ablation enhance the effect. However, small portion of patients may develop recurrence or distant metastasis. Now it is well known that the differentiation can be worse in about 1/3 of recurrent or metastatic WDTC, so RAI therapy is often ineffective. And the patients with bone metastasis, even in the cases without dedifferentiation of thyroid cancer cells, RAI therapy may not be successful due to low penetration of energy. For the treatment of loco-regional disease, regardless the avidity for RAI, the choice should be complete surgical resection of all foci. However, only 1/3

of such patients will become biochemical cure status. So, surgical treatment should be carefully planned to avoid severe complication. The goal of surgical treatments is achieving the long-term remission rate and also leaving minimal morbidity.

Joint Symposium 2

Current Guidelines for Radioiodine Therapy of Differentiated Thyroid Cancer

Sang Kyun Bae

Department of Nuclear Medicine, Inje University Haeundae Paik Hospital, Busan, Korea

Thyroid cancer is the most common malignancy in Korea and increasing all over the world. The reason of this increase is not exactly known. This is mainly due to an increase in papillary microcarcinoma. The use of high-resolution ultrasonography and fine needle aspiration cytology is suspected as one of this increased detection. But other factors also exist for this increasing trend of thyroid cancers.

Radioiodine therapy after surgery is aimed to ablate any remnant thyroid tissue and microscopic residual tumor to decrease the risk of locoregional recurrence and make easier the long-term follow-up based on serum Tg and diagnostic radioiodine scan.

Even though differentiated thyroid cancer has a good prognosis, there are still problematic cases with recurrence or metastasis that have few options for treatment. There were quite few randomized clinical trials to evaluate the efficacy of treatment modality including radioiodine therapy. Therefore, there are still many controversies about surgical extent, indication and dose of radioactive iodine ablation and follow-up strategy. Traditionally, radioactive iodine dose recommendation was 30 - 100 mCi for remnant ablation, 150 - 175 mCi for nodal metastasis, and 200 mCi for distant metastasis. Recent prospective trials (ESTIMABL, HiLo) concluded that a low-dose is not inferior to high-dose to achieve successful ablation for differentiated thyroid cancer patients with low- to intermediate-risk and a recent meta-analysis data showed there was no significant difference between the low and high dose therapy. However, these studies do not have sufficient long-term follow-up to compare recurrence or survival rate.

There are several guidelines for management of thyroid cancer from many expert groups over the world such as the American Thyroid Association (ATA), the European Thyroid Association (ETA), the American Association of Clinical Endocrinologists, the National Comprehensive Cancer Network (NCCN), the British Thyroid Association/Royal College of Physician, the European Society for Medical Oncology (ESMO), the Korean Thyroid Association (KTA), the Japanese Society of Thyroid Surgeons and Japanese Association of Endocrine Surgeons, etc.

ATA suggests that the objective of guideline is intended to inform about the best available evidence and its limitations, relating to the diagnosis and treatment of differentiated thyroid cancer and to inform clinical decision-making. The guideline should not be interpreted as a replacement for clinical judgement and should be used to complement informed, shared patient-healthcare provider deliberation on complex issues.

The draft version of 2014 American Thyroid Association management guidelines for patients with thyroid nodules and differentiated thyroid cancer was introduced last year but the final version is not published yet.

In this symposium I would like to discuss about current guidelines for radioiodine therapy of differentiated thyroid cancer.

Joint Symposium 2

Iodine Refractory Thyroid Cancer and the Use of Tyrosine Kinase Inhibitors

Haluk B. Sayman

Istanbul University Cerrahpasa Tıp Faculty, Turkey

ifferentiated thyroid cancer (DTC) subtypes (papillary, follicular, Hurthle cell) make up ~96% of all thyroid cancers, with medullary and anaplastic subtypes making up 3% and 1%, respectively.

Management of DTC typically consists of surgery followed by radioactive iodine (RAI) ablation of the thyroid remnant, followed by TSH suppression.

But, there is still a considerable debate on methods to follow to treat thyroid cancer patients. Treatment options change with continuing improvements and new justifications. Nevertheless, near total thyroidectomy is a milestone in the well-differentiated thyroid tumors less than 1cm. in diameter.

There are similar algorithms or guidelines defined for the treatment of DTC by authorities such as NCCN, ATA or ESMO.

Inevitably, during the course of follow-up, some of the cases may have increased thyroglobulin levels without any evidence of radioiodine uptake. This poses a real problem in the treatment algorithm.

Since a relationship exists between the amount of radioactive iodine administered and the risk of second primary malignancies or other adverse effects, it has been suggested that repeated RAI courses could be administered safely to a cumulative dose of 600 mCi, after which further RAI should be administered only on an individual basis with careful consideration of risks and benefits.

This condition, radioiodine refractory (RAIR) thyroid cancer is defined as:

Local disease or distant metastasis unable to take up RAI: negative TxWBS (all lesions or some of them),

Local disease or distant metastasis able to take up RAI but with progression during 12-18 months after the last RAI treatment,

Persistence of disease after administration of cumulative activity of 600 mCi RAI without any evidence of clinical benefit.

There are many treatment modalities leading to new horizons for these patients. Among them tyrosine kinase inhibitors (TKI) propose favorable results. Receptor tyrosine kinases have important role on a cell membrane signalling pathways regulated by RET proto-oncogene, RAS or BRAF mutations. TKIs, blocking these pathways, stop angiogenesis, differentiation and tumor growth.

Early results of the use of Sorafenib in DTC patients suggested that considerable partial response rates might be reached by this drug. DECISION, a pase III trial performed in 417 pts with progressive DTC, showed that daily use of sorafenib (2x400 mg) vs. placebo resulted in a PR rate of 12.2%, extended PFS for 5 mths with a SD condition of more than 6mths. vs. placebo. In 73% of patients the lesion size is reduced according to RECIST criteria. It has adverse effects such as hand-foot reaction, alopecia, diarrhea, rash, etc. which do not essentially impair the quality of life and most of them are treatable and rarely lead to drug withdrawal.

The combination of two TKIs, sorafenib and everolimus also showed promising results, especially in the Hurthle cell and medullary subgroups when sorafenib was used alone. The results of this new combination therapy were better as compared with the results of DECISION trial.

In another study named SELECT, the authors announced that PFS was significantly extended by lenvatinib, another TKI that mainly targets vascular endotelial growth factor receptors.

In thyroid cancer PBF (pituitary-tumor transforming-gene binding factor) is significantly upregulated and higher PBF expression is detected which binds to NIS and reduces iodide uptake. Targeting PBF phosphorylation via TKI thought to be a novel therapeutic strategy to enhance the efficacy of ablative radioiodine treatment in thyroid cancer.

In a study by AL Ho, et al the use selumetinib enhanced the RAI uptake in 12 out of 20 patients and 8 of them further receieved radioactive iodine therapy. In 5/8 pts PR and 3/8 pts SD is reached.

Although most patients with DTC can be successfully treated by surgery and adjuvant RAI, some thyroid cancers develop resistance to RAI. In these patients, therapeutic options have been limited, are relatively ineffective and associated with significant and treatment-limiting toxicities and impaired quality of life. Therefore, patients with RAIR DTC are candidates for TKIs therapy, which may improve outcomes.

Joint Symposium 3

Multimodal Molecular Imaging with Polymer Nanoparticles: Dynamic Imaging of Targeted Versus Passive Diffusion of Nanomedicines Into Tumours

Kristofer J Thurecht

The University of Queensland, Australia

Objectives: Nanomedicines are typically designed to have long residence times in the body as a result of the enhanced permeation and retention effect (EPR). Most nanomedicines in clinical use utilise the EPR effect to passively target tumours.[1] Despite the observation that active-targeting of nanoparticles with ligands such as antibodies enhances uptake and efficacy in pre-clinical models, nanomaterial formulations that have progressed to clinical use typically do not utilise active targeting.[2] Thus, there is a real need for new imaging models that provide a mechanism for assessing directly the advantages of active targeting.

Method: The aim of this study was to develop new nanomedicines that directly target prostate cancer cells by way of prostate specific membrane antigen (PSMA) and measure the relative uptake of Cu-64 labelled nanomedicine into two tumours (one that overexpressed PSMA (PC3-PIP) and one that didn't (PC3-FLU)[3]) using PET. The relative advantages of different imaging modalities will also be discussed.

Results. Pegylated nanoparticles were labelled with Cu-64 and a fluorophore for imaging. The small molecule inhibitor of PSMA (glutamate urea) was attached to the periphery of the nanomedicine for targeting the antigen.[4] This chemistry utilized well-established polymerization techniques for ensuring stoichiometric addition of targeting ligand to all PEG end-groups.

The mouse model utilised separate growth of two tumours per mouse, with PC3-PIP on the left flank and PC3-FLU on the right flank. Dynamic imaging of the animals following injection of ~10 MBq nanomedicine

via catheter was achieved over the first two hours, followed by longitudinal scanning over 2 days. The PC3-PIP tumour showed far higher uptake of the nanomedicine compared to the PC3-FLU during the first hour following injection, and we used a two compartment model with reference tissue uptake in order to quantify enhanced accumulation due to receptor binding. This trend of enhanced uptake of targeted nanomedicine continued over the whole imaging period out to 24 hr.

Summary. Targeted therapies not only provide a means of rapidly accumulating nanomedicines into tumours (compared to non-targeted materials), but they also show much less wash-out during the lifetime of the imaging. Multiple imaging modalities, including Gd^{3+} contrast enhanced PET-MR, offers a powerful methodology for investigating the distribution of nanomedicines throughout a tumour volume in vivo. This informs on depth of penetration away from primary blood vessels and can lead to development of more efficacious delivery vehicles.

Joint Symposium 3

Design of Nanobiomaterials for Gene/ Drug Delivery

Won Jong Kim

Center for Self-assembly and Complexicity, Institute for Basic Science and Department of Chemistry, Pohang University of Science and Technology (POSTECH), Pohang, Korea

Keywords: Photothermal; i-motif; pH-responsive; Cyclodextrin; Nitric Oxide

For the synergistic gene therapy, gold nanoparticles were employed as photothermal agents or the templates for drug loading. The pH-responsive i-motif DNA was utilized for the effective intracellular performance of photothermal therapy and chemotherapy. The developed systems exhibited synergistic anticancer effects via combination of siRNA and photothermal/ chemo therapy. In addition to gene delivery systems, self-assembled nanoparticles via multivalent host-guest chemistry between PTX and β-cyclodextrin (β-CD) were reported as a novel paclitaxel (PTX) delivery platform. CD and PTX were polymerized into the pCD and pPTX which provide the chance to produce the stable inclusion complex in blood circulation and release drug in intracellular regions. Furthermore, we also developed novel nitric oxide (NO) delivery system using catecholamine and diazeniumdiolates. Simple two-step reactions comprising catecholamine and diazeniumdiolates enable virtually any material surfaces to release NO with appreciable storage.

In the case of photothermal gene therapy, the i-motif DNA formed interstrand tetraplex in endosomal acidic pH, which could induce the formation of Au nanoclusters, resulting in endosomal escape of AuNP clusters and release of siRNA in the cytosol. As a result, when irradiated with laser, the synergistic anticancer effects was established by combination of photothermal ablation and gene silencing. For the synergistic gene and chemotherapy, the pH-responsive i-motif DNA facilitated the disassembly of the gold nanoclusters and dehybridization of i-motif/RNAi duplex, resulting in the release of therapeutic antisense RNA and Dox. Therefore, drug-mediated apoptosis was significantly accelerated by sensitizing the cancer cells to the drug. For the PTX delivery, the nano-assembly showed the high stability in blood and intracellular esterase-responsive drug release properties owing to the strong multivalent host-guest interactions and the ester bond linkages. This well-designed polymeric nano-carrier demonstrated a long-term suppression of tumor growth in vivo. Finally, in the case of surface NO delivery, the developed methods could offer a versatile platform which could be applied to surfaces of various materials and resulting surfaces could efficiently inhibit the bacterial adhesion, and kill adhered bacteria cells and yet demonstrate excellent biocompatibility.

Joint Symposium 3

Experience on Development of Radioembolization Device for Treatment of Hepatic Cancer

Hwan-Jeong Jeong MD, PhD

Department of Nuclear Medicine, Molecular Imaging & Therapeutic Medicine Research Center, Institute for Medical Sciences, Resarch Institute of Clinical Medicine, Chonbuk National University Medical School & Hospital, Korea

Introduction of biomaterial to the molecular imaging gives us the opportunity of opening the new field that contributes to expand the usefulness of biomaterials such as chitosan in the process of developing imaging agents. Nowadays molecular imaging advance therapeutic field as well as early diagnosis. Sensitive detection and bioengineering technologies make it possible. As development of interventional technology for treatment of disease, direct delivery of therapeutic materials such as radionuclide, chemotherapeutic drug and embolic particles to block the arterial supply to cancer cells has also been established.

I want to present some data here to introduce biomaterial to be used in the field of its validation

as well as treatment. My study focuses on the development of a new therapeutic agent for selective internal radiochemotherapy (SIRCT). The agent been developing in my laboratory is a biodegradable and biocompatible chitosan hydrogel that has been modified with a chelator to label a radioisotope. Until now the therapeutic effectiveness studies have been finished and PK/PD results acquired as well. Biologic and product characterization studies are nearly finished. We are going to submit the information on biological data and safety to KFDA for approval of a clinical trial.

Joint Symposium 3

Biodegradable Nanocarriers for Ddlivery of Rnai Therapeutics in Cancer

In-Kyu Park

Department of Biomedical Sciences, Chonnam National University Medical School, Gwangju 501-746, South Korea

Gene therapy to treat the genetic disease like cancer, restenosis has lot of importance in the field of biomedical science. Successful delivery of gene to the target site without side effects has been the aim to many researchers for more than a decade. Delivered gene has to be expressed efficiently in the target site, which is another area of concern. In order to overcome the drawbacks, cationic polymers have been employed to aid in the delivery of genes. But the cationic polymers were not degradable and its toxicity was an issue. In order to solve the issue, we employed the cationic polymer with modifications to deliver the genes. Modifications include polyethylene glycol attachment, introduction of disulfide bond and sorbitol group to the cationic polymer along with the degradable esters. Once these modifications were done the gene delivery was efficient without compromising the bio-compatibility. Imaging the delivery of the gene will help in visualizing the target place accumulation and distribution, so we have loaded the imaging agents like quantum dots, superparamagnetic ironoxides, indocyanin green etc to the modified polymeric carriers. Replacement of the missing genes or suppression of the overexpressed gene can be done through plasmid DNA, siRNA and microRNA delivery. Initial study we have loaded the quantum dots in to the polysuccinimide, Polyethylenimine (PEI) and polyethylene glycol polymersome to deliver the killer red plasmid DNA. In the next study disulfide modified PEI was employed to deliver the anti-proliferative siRNA. Finally the sorbitol modified PEI was used to deliver the microRNA which can suppress the cancer cell proliferation.

Joint Symposium 4

Opportunity and Challenge of Molecular Imaging in Asia and Oceania

Ren-Shyan Liu MD

National Yang-Ming University, Taiwan

Molecular imaging investigates molecular signature of the disease through measurement and characterization of biological processes in molecular or cellular compartment and thus enables opportunities to replace population-based treatment methods by personalized genotype/phenotype-adapted concepts. Molecular imaging with appropriate biomarkers/probes would initiate a concept of individualized imaging and hence individualized diagnosis as well as treatment. The future of imaging appears to skew toward molecular imaging and hybrid imaging and to get integrated into the therapeutic protocols of evidence-based personalized medicine. The opportunities and challenges of molecular imaging in Asia are:

Opportunities

- Basic science and pre-clinical researches
- Innovation through in vivo molecular imaging
- Drug efficacy evaluation: pre-clinical and clinical
- Opportunity to participate multi-center clinical trials

Challenges

- Personalized medicine
- Nanomedicine
- Precision medicine

Joint Symposium 4

Selection of Molecular Signature-targeted Peptide Probes using Phage Display and their Applications to Molecular Imaging

Byung-Heon Lee

Department of Biochemistry and Cell Biology, School of Medicine, Kyungpook National University, Daegu, Korea

A growing number of evidence shows that individual tissues and even their vessels are biochemically distinct, and pathological lesions put their own molecular signatures on the tissue and vasculature. These molecular signature-targeted peptides have been isolated by phage display in our laboratory. Such peptides can be used in targeted delivery of imaging

agents or therapeutic drugs to the diseased tissues. For example, IL4RPep-1 (IL-4 receptor-binding peptide-1), with the sequence of CRKRLDRNC homologous with IL-4, bound to H226 lung tumor cells that over-express IL-4 receptor. When injected intravenously into nude mice bearing a subcutaneous tumor, near-infrared fluorescence (NIRF) dye and IL4RPep-1-labeled liposomes selectively homed to H226 tumor and more efficiently inhibited tumor growth than untargeted liposomes. As another example, ApoPep-1 (apoptosis-targeting peptide-1), with the sequence of CQRPPR that binds to histone H1 exposed on the surface of apoptotic cells, homed to apoptotic areas at tumor tissue. ApoPep-1 bound to apoptotic tumor cells on culture at higher levels than that to healthy cells. In vivo imaging of apoptosis using NIRF-labeled ApoPep-1 could enable early monitoring of tumor response to chemotherapy. We also selected a peptide that homes to lung tumor in K-ras transgenic mouse model. In vivo detection of lung tumor by the accumulation of the NIRF-labeled peptide was achieved using fluorescence imaging and photoacoustic tomography. Taken together, molecular signature-targeted peptide probes will be a useful tool for imaging and diagnosis of diverse pathologic lesions.

Joint Symposium 4

Molecular Imaging in Drug Development

Mei TIan MD, Ph.D

Hangzhou BInjiang Hospital, Zhejiang University School of Medicine, The Second Hospital of Zhejiang University School of Medicine, Hangzhou, Zhejiang 310009, CHINA

Molecular imaging technology offer high-sensitivity and high-resolution visualization of imaging probes. In the past years, in vivo imaging has been gradually growing in importance as an aid for the development of new drug, which allow rapid repetitive (and thus potentially high throughput) assessment of the drug deposition in various tissues in the body, which can vastly facilitated the eventual translation into clinic. This lecture will provide brief review of the in vivo imaging techniques, including PET. SPECT, and optical imaging; focus on the importance, current status and future perspectives on molecular imaging in drug development.

Joint Symposium 4

Molecular Imaging Study of Acute Ischemic Stroke

Jun Hatazawa MD, PhD

PET Molecular Imaging Center, Department of Nuclear Medicine and Tracer Kinetics, Osaka University Graduate School of Medicine

Molecular, cellular, and tissue pathology after cerebral ischemia has been extensively studied over the last decades in experimental animals and in patients. Recently, the development of imaging modalities for small animals combined with new biological probes made it possible to study molecular basis of ischemic penumbra. Here, I review the important clinical works regarding cerebral energy failure following acute embolic occlusion of carotid/cerebral arteries by 15O-PET and Diffusion-Perfusion MR. I also provide a testable hypothesis that astrocytic TCA (Tricarboxylic acid) cycle activity has a critical role for protection of cerebral tissue damages induced by acute ischemia.

In patients with acute embolic occlusion of carotid/cerebral arteries, the initial 3-day infarct volume expansion was associated with disturbed CMRO2 but not with cytotoxic edema (defined as “Metabolic penumbra”) as early as 6 hours of onset (Shimosegawa E, et al. Ann Neurol 2005).

The next question was a role of astrocytes in ischemic brain and how astrocytes relate to the expansion of infarct volume. Acetate is preferentially taken up and metabolized by astrocytes. We demonstrated that 14C-acetate is a sensitive marker of TCA cycle activity in astrocytes (Hosoi R, et al. 2004 JCBFM). After short-term ischemia, 14C-acetate uptake in the brain was reduced but not immediately recovered after reperfusion (Hosoi R, et al. JSCD, 2007). Astrocytic metabolic dysfunction caused cerebral infarction even after short-term ischemia in rats (Hosoi R, et al. Ann Nucl Med, 2006). These findings indicated that recovery of astrocytic TCA cycle activity is a key issue to protect infarct volume expansion.

It is well known that the astrocytic TCA cycle is coupled with glutamate-glutamine cycle. Extracellular glutamate concentration was increased after astrocytic TCA cycle inhibition by fluoro-citrate (Largo P, et al. J Neurosci, 1996; Rodriguez Diaz, et al., Glia, 2005). These studies indicated that astrocytic TCA cycle dysfunction during ischemia and initial reperfusion period may induce an elevation of extracellular glutamate concentration. Hirose et al. revealed in rat brain that astrocytic TCA cycle inhibition induced enhanced glucose consumption, which was protected by pretreatment of NMDA receptor antagonists (Neuroscience Letters, 2007).

The hypothesis that astrocytic TCA cycle dysfunction

may occur in ischemic or metabolic penumbra is now testable by the PET with ^{11}C-acetate.

Joint Symposium 4

Tips of Quantitative Mouse Brain PET Studies using Small Animal Scanner

Hiroshi Toyama, MD, PhD

Professor & Chairman, Department of Radiology, Fujita, Health University, Toyoake, Aichi, Japan

Recent technical advances have made it possible to use PET for small animals such as transgenic mice. A major advantage of small animal PET studies compared to necropsy studies is that the former allows longitudinal within-subject design and reduces the cost and overall time needed to obtain a result. Also, comparative studies with in-vitro measurements and histological and pharmacokinetic studies for radiotracer development are possible. Fully quantitative PET studies require information on the time course of tracer delivery to the tissue. This "input function" is best obtained from direct frequent arterial blood sampling during PET study[1]. Due to the small mice (20-30g) body weight, arterial blood sampling volume should be very small amount (0.015 – 0.023mL).

We developed Microfluidic Micro Plasma radioactivity Counting system (μFmPC) [2] with the micro-liter ordered automatic blood sampling system. In this presentation, I talk about tips of quantitative metabolic brain imaging with small animal PET in mice.

Joint Symposium 5

Improved Internal Dosimetry for Targeted Radionuclide Therapy Using Nonrigid Registration on Sequential SPECT/CT

Greta S. P. Mok

Biomedical Imaging Laboratory, Department of Electrical and Computer Engineering, Faculty of Science and Technology, University of Macau, Macau

Voxel-level and patient-specific 3D dosimetry for targeted radionuclide therapy (TRT) typically involves serial SPECT/CT scans. Misalignment of the images can result in reduced dosimetric accuracy. Since the scans are typically performed over a period of several days, there will be patient movement between scans and possible nonrigid organ deformation. Previously researchers proposed using rigid registration on sequential quantitative SPECT (QSPECT) or nonrigid registration on sequential CT images. However, sequential CT scans are usually not performed in the standard protocols due to the radiation concern. This presentation aims to discuss the current methods, especially nonrigid registration on sequential SPECT or CT images, for reducing misalignments among scans and their effects on dosimetric results. Simulation and sample In-111 Octreo and Re-188 liposome patient studies are presented.

Joint Symposium 5

Bone Metastasis Treatment: From Palliation to Survival Gain

Gi Jeong Cheon, MD, PhD

Department of Nuclear Medicine, Seoul National University Hospital

Bone metastases occur frequently in many kinds of malignant tumors, especially in advanced stage of breast cancer, prostate cancer, lung cancer, and so on. Bone metastases contribute to a significant degree of morbidity and mortality in oncologic patients through the development of skeletal related events (SRE) such as bone pain and pathological fracture. The main therapy has been applied loco-regional managements as well as systemic therapy, such as surgical removal, radiotherapy, chemotherapy, osteoclast inhibiting agents, and combination of those therapies. Although these therapeutic combinations can achieve a degree of local control, they only provide palliation and rarely cure in most cases with bone metastatic disease. Radionuclide therapy for palliation of pain from bone metastases is one of systemic targeted therapies, based on the use of therapeutic radionuclides. The goal of targeted therapy is to enhance the therapeutic efficacy and to reduce the systemic toxicity as disease-specific targeting with coverage of whole system as well as loco-regional disease. Bone-seeking radiopharmaceuticals for the treatment of painful bone metastases are Phosphorus-32, Strontium-89, Rhenium-186, Rhenium-188, Samarium-153, and Radium-223) and the combination therapy with biphosphonates and chemotherapy. Recently, an alpha emitter, radium-223 dichloride, has been approved in patients with castration-resistant prostate cancer and bone metastases. It has been reported that radium-223 shows benefits of survival gain as well as palliative purpose in the phase III clinical trials in metastatic prostate cancer. In addition, radium-223 was associated with

low myelosuppression and fewer adverse events. Given the potent and desirable properties of alpha particles with regard to the induction of DNA strand breaks, the application of targeted alphas may be helpful in many diseases of refractory or incurable disease in case of existence of suitable disease targets. Although targeted radiopharmaceuticals such as I-131 tositumomab and Y-90 ibritumomab have been commercial failures, they are scientific successes. More work in the targeted delivery of isotopes needs to be performed for additional therapeutic advances.

Joint Symposium 5

Estimation of 10B Concentration in BNCT: Potential of Image-guided Therapy by ^{18}FBPA-PET

Eku Shimosegawa[1,2], Kayako Isohashi[2], and Jun Hatazawa[2]

1. Department of Molecular Imaging in Medicine, Osaka University Graduate School of Medicine, Suita, Osaka, Japan
2. Department of Nuclear Medicine and Tracer Kinetics, Osaka University Graduate School of Medicine, Suita, Osaka, Japan

The boron neutron capture therapy (BNCT) is expected as one of the effective treatment for the intractable malignant tumor. The heavy charged particles from the $^{10}B(n, \alpha)^{7}Li$ reaction have a range of approximately 10 μm in tissue and are known to have a high relative biological effectiveness. ^{10}BPA is one of the representative drugs for the delivery of ^{10}B to the tumor tissue. ^{18}FBPA-PET is used for the decision of the BNCT because the chemical structure of ^{18}FBPA is similar to ^{10}BPA.

Although the effectiveness of treatment in BNCT and the occurrence of complications depend on the ^{10}B concentrations in a tumor or the normal tissue, the correct method for measurement of ^{10}B concentrations has not been established. Therefore, we investigated a quantitative method to estimate ^{10}B concentrations of the tissue by ^{18}FBPA-PET. In a tumor rat model, good correlation between the ^{18}FBPA accumulation of the tracer dose and the ^{10}B quantity after the ^{10}BPA administration of pharmacologic dose was observed both in the normal organs and tumor tissue. Dynamic measurements of ^{18}FBPA-PET in healthy volunteers showed that suggested ^{10}B concentrations in normal brain after therapeutic ^{10}BPA administration were low enough (14.0 ± 2.7 ppm) compared with the previous data of glioblastoma ^{10}B concentration (21.0 – 61.8 ppm). These results indicated that quantitative evaluation of ^{18}FBPA-PET contributes to the estimation of the tissue ^{10}B concentrations before BNCT. On the other hand, the treatment protocol of BNCT and the method of ^{18}FBPA-PET analysis in clinical studies have not been standardized so far. Practically, using FBPA radioactivity of the blood as a reference would be a better index in evaluating the degree of tumor ^{10}B concentration.

Joint Symposium 5

Radionuclide Theranostics for Differentiated Thyroid Cancer

Byeong-Cheol Ahn, MD, PhD

Department of Nuclear Medicine, Kyungpook National University School of Medicine and Hospital, Daegu, Republic of Korea

Theranostics is portmanteau word of therapeutics and diagnostics, which is coined by PharmaNetics president and CEO John Funkhouser in 2002 to describe his company's business model in developing diagnostic tests directly linked to the application of a specific therapies. As a valuable tool in personalized medicine, the theranostics can be defined as diagnostic methodology for personalizing therapeutic intervention and it customizes healthcare practices to an individual patient by eliminating unnecessary treatments for patients whom a standard therapy is not appropriate and/or by optimizing therapeutic plan for a particular patient. Although the theranostics, which integrates diagnostic testing to detecting the molecular target for certain therapeutic modality, just started to be used after second millennium, however, the basic principle of theranostics had been started to be applied long ago in the arena of thyroidology with radioiodine.

Differentiated thyroid cancer, which arises from follicular cell of the thyroid, is the most common endocrine malignancy and theranostic radionuclide has been successfully applied to diagnose or treat the differentiated thyroid cancer and the applications were included in guidelines published by various thyroid or nuclear medicine societies. Through the advancements of bioengineering, electrical engineering and radiochemical technologies, theranostic radionuclide strategies extensively contribute to modern tailored personalized management by providing high therapeutic effect and by avoiding significant adverse effects in the differentiated thyroid cancer.

The presentation will covers basics to recent update of theranostic radionuclide applications for the differentiated thyroid cancer.

Joint Symposium 6

Challenges Faced for PET GMP in an Industrial Setting

Chih-Hao K. Kao

Buddhist Tzu Chi Foundation Hualien Tzu Chi Hospital, TAIWAN
PET Pharm Biotech Co., Ltd., Taiwan

In Taiwan, an industrial PET radiopharmaceutical manufacturer, as opposed to one of hospitals or universities, follows guidelines laid out in "PIC/S guide to GMP for Medicinal Products (PIC/S GMP)." Though PIC/S GMP does offer a few exemptions for radiopharmaceuticals as described in its Annex 3 ("Manufacture of Radiopharmaceuticals"), aseptically processed PET radiopharmaceuticals (such as FDG) must also comply with its Annex 1, "Manufacture of Sterile Medicinal Products." This creates huge challenge for routine production of PET radiopharmaceuticals, not least is the skyrocketing cost. We in PET Pharm Biotech had built a plant which became one of the very first of its kind in Asia to be certified. Experiences of some specific issues are emphasized and discussed here.

One of the most notables is hydrogen peroxide fumigation before each and every batch of FDG productions. Not only does this daily (even twice daily) disinfection causing decomposition in some most corrosive-resistant equipment surface, but also make production scheduling difficult. Another is bioburden assay on each batch before aseptic filling of FDG. The once familiar continuous flow of FDG production that we all considered as an efficient method of production is no longer possible due to this need of bioburden monitoring.

The combination of a grade "A" aseptic filling compartment (ours is an isolator hot cell) situated in a grade "B" room is a nonnegotiable requirement. That says a continuous particle counting and air sampling among others is a mandate to guarantee the cleanliness status. Gadgets thus need modifications to fit in the isolator hot cell.

Bothersome as all these may be, we nevertheless have developed a "hard" system that meets all terms. This short report, however, still has not covered "soft" part of challenges. Personnel training, risk assessments, validations and qualifications, are all just parts of the whole band concerted to perform a great practice of PET radiopharmaceutical manufacturing.

Joint Symposium 6

The GMP of ^{18}F-FDG Production in Singapore

Sidney Wing Kwong Yu

Singapore General Hospital, Singapore

The objective of Good Manufacturing Practice(GMP) is to ensure that the manufactured products are of correct identity, correct formulation , correct strength , free of contamination, free of manufacturing errors and safe for patient use . It is more than a set of rules applied to the manufacturing process, but a "culture" that dwells into the mind of every person involved.

While GMP regulations varies in different countries, it generally looks deep into issues such as management , personnel, premises and equipment, documentation, production and process controls, quality control, contract manufacture and analysis, complaints and product recall, as well as internal inspections.

The impact of complying to GMP on health sciences Industry is very significant. It involves very strict regulatory control, huge additional cost / time / resources and immerse paperwork. However, the price of non-compliance could be high.

Joint Symposium 6

Standardized PET-drug Production in Japan

Yasuhisa Fujibayashi, Ph.D., D.Med.Sci.

Molecular Imaging Center, National Institute of Radiological Sciences Chiba, Japan

Japan has a long history of PET research, and developed its own regulation for PET-drug production. In 2010, Japanese Society of Nuclear Medicine (JSNM) established a strategic committee for promoting molecular imaging (JSNM-MI Strategic Committee). The committee intended to harmonize PET drug regulations in Japan and those in US or Europe, and published JSNM-GMP Guideline. To assure the compliance of each hospital, National Institute of Radiological Sciences has been appointed as an audit organization under the supervision of JSNM.

Pharmaceutical and Medical Device Agency (PMDA) approved this process, and a certificate of compliance issued by JSNM has become essential when a newly approved PET drug synthesizer is installed and used for clinical practice.

This process is also useful for use of new PET drug in advanced clinical care, and "brain cancer diagnosis

using C-11-methionine" is now in progress under this regulation.
Also, in Micro-dose study, this regulation is considered to be in accordance with CGMPs for IND, which is essential for Micro-dose study under GCP.

Joint Symposium 6

Radiopharmaceuticals GMP Status at Korea

Boeun Lee

Seoul National University Hospital

In Korea, GMP (Good Manufacturing Practice) regulations were revised on August 2014 because Korea Ministry of Food and Drug Safety (MFDS) joined to PIC/S on July 2014. Due to the revised GMP regulations contain radiopharmaceuticals GMP, the new facilities to be obtained radiopharmaceutical company from MFDS are enforced to have GMP system from 1st July 2015 and already established companies include several hospitals those have MFDS approved products should prepare GMP system until 30th June 2017 (a 2 years grace period).
The Korea radiopharmaceuticals GMP regulations were under the Pharmaceutical Affairs Act, Enforcement Rule of Medicinal Product Safety and its attached table. It contains most of PIC/S GMP guide, but the articles are implicative and simpler than PIC/S regulations. The details were described in Notifications and Guidance on GMP for radiopharmaceuticals issued by MFDS. The guidance gives some examples of other country such as USA, Canada, Australia and WHO (World Health Organization). It means Korea radiopharmaceutical GMP can accept other countries regulation if it is reasonable for GMP system.
In here, I try to review Korea radiopharmaceuticals GMP regulation and give the most important issues for radiopharmaceutical GMP in Korea.

Joint Symposium 7

Current and Future of Cardiac CT and MRI

Yeon Hyeon Choe, MD, PhD

Department of Radiology and HVSI Imaging Center, Samsung Medical Center, Sungkyunkwan University School of Medicine, Seoul, Korea

CT techniques are evolving very fast. However, diagnostic capability of coronary CTA is still hampered by motion and blooming artifacts. Recently manufacturing companies and radiologists have been interested in radiation dose reduction with CT scanning and substantial improvement has been achieved by adoption of new iterative reconstruction techniques and new detectors. Dual-energy/spectral CT and dynamic CT technologies for cardiac applications are improving. Myocardial blood flow and flow reserve can be measured with dynamic perfusion CT due to recent technological developments. Stress myocardial perfusion CT may serve as a surrogate for lesions to be treated. New developments in software would improve detection of myocardial perfusion abnormalities with color-coding/quantification in the resting state. Supercomputers are now being used for model-based iterative reconstruction and calculation of flow dynamics of coronary arteries. Degrees of contrast enhancement in the coronary arteries may give insight on functional significance of the stenotic lesions (Transarterial Contrast Gradient). 4D assessment of coronary flow would be available with recent CT scanners. In the future, Smart CT for comprehensive cardiac evaluation with minimal radiation would be available for cardiac radiologists and patients.
MRI is being utilized and applied for cardiac diagnosis in Asian countries more frequently than before. Just recently 3-T systems have been prepared to provide adequate image quality for cardiac imaging. Quantitative approach in myocardial perfusion imaging enables more accurate diagnosis of ischemic heart disease. T1 mapping provides insight on previously unrecognized changes in the myocardium such as diffuse fibrosis. 4D flow shows promise in the comprehensive analysis of flow patterns and shear stress in the heart and vessels.
In summary, new CT and MRI techniques enable functional and anatomical assessment of the heart including coronary flow, myocardial perfusion, valvular function, and myocardial fibrosis.

Joint Symposium 7

Extended Application of Echocardiography in Cardiac Diseases

Jun-Bean Park

Division of Cardiology, Department of Internal Medicine, Seoul National University Hospital, Korea

In the era of multimodality imaging, echocardiography still remains the most commonly performed cardiac imaging tool and is an invaluable technique for the assessment of cardiac structure and function in various cardiac diseases. Recent advances in imaging technology permit an increasingly more detailed and accurate

evaluation of patients with a wide variety of cardiac disease, such as coronary heart disease, valvular heart diseases, heart failure, and congenital heart disease.

Despite these unprecedented advances, echocardiography has strengths and weaknesses, like other imaging modalities including nuclear imaging, computed tomography, and magnetic resonance imaging. Comparing to other imaging tools, echocardiography has advantages in terms of 1) hemodynamic evaluation, 2) portability, 3) versatility, 4) high temporal and spatial resolution, 5) assessment of exercise physiology, and 6) low cost. Disadvantages of echocardiography include suboptimal image quality in certain patients and clinical circumstances and large variability. Many of these limitations of conventional echocardiography can be overcome to some extent by using state-of-the-art modern echocardiography, such as contrast echocardiography, deformation imaging (ie, strain), 3-dimensional echocardiography.

Joint Symposium 7

Nuclear Medicine in Assessment of Cardiac Dyssynchron

Chetan D. Patel

All India Institute of Medical Sciences, India

Dyssynchrony indices derived from Phase analysis of Gated myocardial perfusion SPECT (GMPS) and Equilibrium radionuclide angiography (ERNA) are used for quantitative assessment of cardiac mechanical dyssynchrony. On GMPS, phase standard deviation (PSD) and phase histogram band (PHB) are used to measure left ventricular dyssynchrony (LVD) while in ERNA standard deviation of the mean phase angle (SDmPA) of LV blood pool measures LVD and the difference between the mean phase angles of the two ventricles i.e. LVmPA-RVmPA is used to quantify interventricular dyssynchrony (IVD). In a prospective study, at our centre, we evaluated role of ^{99m}Tc-MIBI GMPS in the prediction of response to cardiac resynchronization therapy (CRT) in non-ischemic dilated cardiomyopathy (DCM) patients. Thirty-two patients with severe heart failure, submitted for CRT implantation, were included in this study. Receiver-operating characteristic curve analysis demonstrated 86% sensitivity and 80% specificity at a cutoff value of 43° for PSD and 86% sensitivity and 80% specificity at a cutoff value of 128° for PHB in the prediction of response to CRT. In another study, we evaluated the relationship between perfusion pattern and stress-induced changes in LVD in 194 patients on stress-rest Tl-201 GMPS. We observed that LVD parameters are smaller in post-exercise stress as compared to rest on Tl-201 GMPS, regardless of perfusion pattern. Stress-induced worsening of LVD was observed only in patients with perfusion abnormalities, but this is not related to the type of perfusion abnormality. There is a relatively limited data on use of ERNA in the assessment of dyssynchrony. At our center we established normal values of mechanical synchrony (both LVD and IVD) in our population on ERNA. We further used these normal cut-off values to evaluate ERNA in prediction of response to CRT in patients with DCM. The study showed that baseline LVD & IVD are both useful for prediction of response to CRT in non-ischemic DCM patients. We have also used ERNA to compare LV systolic function and LVD in patients with right ventricular outflow tract (RVOT) versus right ventricular apical (RVA) pacing. Fifty one patients who underwent permanent pacemaker implantation (29 RVOT, 22 RVA) and had normal LV function were prospectively included. All patients underwent ERNA within 5 days post-pacemaker implantation and follow-up ERNA studies at 6 and 12 months. The study showed no significant difference between RVOT and RVA groups with regard to LV function and synchrony over a 12-month follow-up. In conclusion cardiac dyssynchrony can be reliably assessed by nuclear medicine techniques which can play an important role in various clinical settings

Joint Symposium 7

Coronary Flow Reserve Determination Using SPECT

Jerry M. Obaldo, Chetan D. Patel

Philippine Heart Center, Philippines

Coronary flow reserve (CFR) refers to the ratio of increased myocardial blood flow (MBF), from vasodilation of coronary arteries, to baseline MBF.

CFR determination may be useful in cases of balanced multivessel CAD or dilated cardiomyopathy, which may show a homogeneous perfusion pattern on SPECT. CFR can help assess microvascular dysfunction in patients with normal epicardial coronary arteries. In patients with multivessel disease where the best-perfused regions in conventional SPECT is usually assumed to have normal perfusion, CFR may potentially increase diagnostic sensitivity, and more accurately demonstrate the extent of CAD.

PET is able to measure absolute MBF, but the technique is complex and expensive, and is therefore not routinely performed in most centers. Conventional SPECT is unable to accurately measure absolute MBF due to factors such as attenuation, scatter, and the partial

volume effect; therefore calculation of CFR from MBF is not feasible with this modality.

A technique for estimating CFR with SPECT has been reported and validated. This technique is similar to the microsphere method where the amount of retained tracer is assumed to be proportional to MBF. First pass analysis of the tracer bolus injection is made by taking the integral of the time activity curve over the pulmonary artery, and using this as the input function. By calibrating the myocardial tissue counts to the time integral of the first-pass tracer counts over the pulmonary artery, the SPECT errors are cancelled out, obviating the need to measure absolute blood flow.

Various studies have shown that CFR has incremental prognostic value over SPECT perfusion data alone. Low CFR, obtained with SPECT techniques, predict major adverse cardiac events, similar to MBF reserve calculated with PET.

(edit. Verbatim from Cuocolo).

Coronary flow reserve (CFR) indicates the amount of additional blood flow that can be supplied to the heart over baseline blood flow. The absence of CFR implies maximal vasodilatation of the resistance vessels at rest and an inability to further increase MBF The procedure utilized for the estimation of CFR by SPECT is based on the microsphere method, considering that ^{99m}Tc-labelled tracers are taken up by the myocardium according to blood flow.

Low resolution-related factors, such as scatter, attenuation and partial volume effect, hamper the absolute quantitation of both arterial and tissue counts, but they may be cancelled out by computing the ratio of tissue and arterial counts.

(verbatim from de Kemp editorial)

Conventional MPI identifies local reductions in perfusion relative to the best ventricular wall, where the maximum value is presumed to be normal. However, this technique is known to underestimate the extent or severity of multi-vessel coronary disease, when the maximum value does not represent normally perfused myocardium.

The authors use first-pass planar imaging followed by conventional SPECT MPI to estimate a retention index of MBF and corresponding global flow reserve.

(verbatim from Storto)

For first-pass analysis, serial images of the first transit study were evaluated frame by frame, and on the summed image (3-5 s duration), 3 × 2-pixel regions of interest (ROI) were assigned at the main right PA and at LV chamber. After algorithm smoothing over a mean of 3 points, the area under the time-activity curve was calculated to obtain the time integral of the first-pass tracer counts for both PA and LV

Sestamibi activity was measured on two representative short-axis tomograms (at mediobasal and medioapical levels). For each short-axis tomogram, a global ROI including the whole myocardial thickness was assigned.

PET is not routinely performed for MPS in most institutions.

CFR has been shown to have incremental value over conventional SPECT imaging alone.

Possible clinical utility (from Cuocolo): Balanced multivessel CAD

Improve sensitivity of determining extent of CAD (e.g. diabetics)

Assess microvascular dysfunction in normal coronary arteries

Joint Symposium 7

Recent Development in Cardiac Nuclear Imaging

Won Jun Kang

Department of Nuclear Medicine, Yonsei University College of Medicine

Ischemic heart disease remains the major leading cause of death in most developed countries. For the evaluation of ischemic heart disease, cardiac nuclear imaging can provide useful information about myocardial perfusion and its response to stress. Myocardial perfusion SPECT and perfusion PET are two well-established nuclear cardiology imaging. They evaluate heart's ability to respond to stress using either exercise or pharmacologic vasodilator drug. Common indications of myocardial perfusion SPECT or PET include evaluation of chest pain, reevaluation of known coronary artery disease, heart failure or preoperative testing.

For stress perfusion imaging, exercise, adenosine or dipyridamole have been widely used. Regadenoson is a newly developed A2A adenosine receptor agonist, and can be used by bolus injection. Recently, heart dedicated SPECT cameras have been installed in many centers. The main advantages of hear-dedicated SPECT are short scan time, low radiation, high resolution, high sensitivity, and possibility of blood flow quantification. These cameras adopt CZT detector.

For myocardial perfusion PET, positron-emitting radioisotope such as Rb-82, N-13 ammonia, and O-15 water could be used. Rb-82 is easily available because it can be produced by generator, while N-13 ammonia requires on-site cyclotron. As stress method, pharmacologic drug is generally used because the half-lives are brief. Compared with myocardial SPECT, myocardial perfusion PET has advantages including short acquisition time, low radiation exposure, higher diagnostic accuracy, effective attenuation correction,

and calculation of absolute blood flow of myocardium. With these well-known advantages, PET is expected to have wider clinical usage.

With recent advancement coronary CT angiography, myocardial SPECT and PET can be hybridized with coronary CT angiography. Hybrid technique illustrates the anatomical abnormality and functional information simultaneously. In addition, it is possible to evaluate functional significance of the lesion detected by coronary CT. Although hybrid technique has pitfall of higher cost and higher radiation exposure, new technologies are being introduced to reduce the radiation exposure in hybrid imaging.

Joint Symposium 8

Clinical Needs for Imaging in Nonischemic Cardiomyopathy

Seung-Pyo Lee MD, PhD

Cardiovascular Center, Department of Internal Medicine, Seoul National University Hospital

With the advent of imaging technologies, clinicians have a wide array of choice for imaging not only the motion/structure of the heart but also, the process that is ongoing in the myocardium. Many of the cardiac imaging studies have stemmed from lessons learned by studies in coronary artery disease (CAD). Although CAD accounts for a majority of heart disease nowadays, perhaps lessons from the non-coronary artery disease or nonischemic cardiomyopathy are the ones that maximizes the usefulness of various imaging studies.

From a clinical point of view, the reasons why cardiac imaging should be developed are based on the next three essential necessities.

1) To assess the cardiac structure and function accurately

2) To assess the disease process that underlies the alteration of structure or impairment of function

3) To stratify the risk and predict future outcome/ prognosis of the disease and the patient

Although conventional imaging studies, such as two-dimensional/Doppler echocardiography, provide essential information to clinicians (for example, the ventricular function and (clues to) the ultimate diagnosis), the wide implementation of cardiac computed tomography angiography (CCTA), cardiac magnetic resonance (CMR) and positron emission tomography (PET) has enabled the clinicians to view cardiac disease in a different and a more sophisticated way.

1. Accurate assessment of cardiac structure and function using cardiac imaging

It is well known that CMR has a high signal-to-noise ratio and therefore, CMR has enabled the clinicians to view the parts of the heart that are insufficiently visualized by other modalities. For example, a significant proportion of the ventricle that are classified as 'normal' on echocardiography are in fact 'hypertrophic' on CMR in patients with hypertrophic cardiomyopathy (HCM). Three-dimensional echocardiography or CCTA has also been able to visualize the presence of 'small' pannus under the prosthetic valve that have 'big' impact on the ventricle. These pannus have not been accurately seen on conventional two-dimensional echocardiography.

2. Understanding the disease process that underlies the alteration of structure or impairment of function With the use of specific MR sequence and the gadolinium contrast, CMR has been able to visualize the extent of and also to accurately quantify the myocardial scar. The myocardial scar are or paramount importance clinically because of their potential to provoke significant malignant arrhythmia. Although the probability of having significant myocardial scar increases with the increase of myocardial thickness in HCM, this is not always true. This is also true in patients with aortic stenosis and the degree of myocardial fibrosis and the adaptation of the myocardium does not follow a uniform pathway. In addition, the development of novel tracers for PET and its clinical application has demonstrated its clinical usefulness in certain infiltrative cardiac disease, such as amyloidosis. These cases demonstrate the clinical utility of novel cardiac imaging tools for understanding the disease process that underlies the alteration of structure or impairment of ventricular function.

3. Stratification of the risk and prediction of the future outcome/prognosis of the disease

Ultimately, the real clinical aim of these imaging studies are in the prediction of the prognosis of the disease and the patient, him/herself. Gathering from large-scale human data, the presence/amount of myocardial scar is a robust prognostic indicator in various nonischemic cardiomyopathy. Likewise, information gathered from PET also provides clinical prognostic benefits that cannot be gained using other modalities.

In my talk, I will discuss the above mentioned clinical necessities of cardiac imaging in nonischemic cardiomyopathy with the relevant examples from real-world cases.

Joint Symposium 8

MRI for Cardiomyopathy

Sang-Chol Lee

Samsung Medical Center, Korea

Joint Symposium 8

Hybrid Imaging with PET/MRI in Cardiac Diseases

Ihnho Cho

Department of Nuclear Medicine, Yeungnam University hospital, Korea

PET/MR scanner has been expected to play a key role in research and clinical applications because of superior tissue contrast and multiparametric functional imaging of MR in conjunction with PET like PET/CT gained wide approval for oncologic imaging in recent years. In cardiology, hybrid imaging of PET/CT allows quantification of myocardial perfusion in combination with assessment to coronary anatomy by providing complementary information in patients who are being evaluated for coronary artery disease. On the other hand, PET/MRI has been used to demonstrate significant pathologies such as myocardial infarction, myocarditis or cardiac sarcoidosis, even though the additional value and potential clinical role of these new systems have not been established yet. In the future, it seems to be used routine application in clinics or studies. I will summarize the major advantages and disadvantages, technical requirements and workflow considerations for cardiac PET/MR imaging and present clinical experience and potential applications for hybrid PET/MRI imaging in the field of cardiology.

Joint Symposium 8

Dynamic Myocardial NH3 PET/CTA Image Fusion for Noninvasive Absolute Myocardial Flow Quantification Along Specific Coronary Vessels

Ernest V Garcia[1], Hee-Seung Bom[2], Marina Piccinelli[1], John R Votaw[1], C D Cooke[1], Russel D Folks[1], Daya Manatunga[1], Habib Samady[3]

1. Department of Radiology and Imaging Sciences, Emory University, Atlanta, US
2. Department of Nuclear Medicine, Chonnam National University, Gwangju, South Korea
3. Division of Cardiology, Emory University School of Medicine, Atlanta, US

Background. PET-derived myocardial blood flow (MBF) and flow reserve (MFR) quantification have been shown to have incremental clinical value in detecting CAD. Currently these measurements are not vessel-specific (VS), but calculated either globally for the entire LV or regionally to predefined vascular or segmental territories. Recently we reported (JACC 2015; 65,10S, A1079) the use of 10 normal (NL) patients that underwent NH_3 dynamic PET (dPET) for the estimation of absolute MBF along specific coronary vessels and particularly for the development of normality ranges (mean ± SD) for MBF, MFR and FFR along the LAD. Our aim is to noninvasively measure MBF, MFR and FFR proximal to distal (PtoD) along patient-specific coronary trajectories in patients with known CAD by means of image fusion of coronary CT and dPET and to compare it to our previously computed normality ranges.

Methods. Five patients with CAD >50% that underwent both dPET and CTA were selected. At cath the stenoses were at mid vessel level for 3 cases (DS: 99%, 95% and 80%) and at proximal level for 2 cases (DS: 99% and 80%). The myocardium and the centerlines of the main coronary vessels were extracted from the CTA and fused by means of our 2nd Generation HeartFusion algorithm to the dPET. Sampling volumes of interest (VOIs) were created within the myocardium following vessels path. Rest (r) and stress (s) absolute flow PtoD along the vessel length was calculated with established compartmental modeling. Vessel-specific MFR was computed as the point-wise ratio of stress over rest flows; vessel-specific FFR was computed as the point-wise ratio of each case's stress flow over mean normal stress flow from the NL patients NOT the contralateral sites of the CAD patients.

Results. When the individual PtoD flow measurements from each CAD vessel were compared to normal limits, abnormalities were detected in 5/5 by sMBF, 1/5 by rMBF, 5/5 by MFR and 5/5 by FFR.

Conclusions. These preliminary results show promise for the non-invasive quantification of MBF, MFR and FFR along patient-specific vessel trajectories by means of dPET/CTA image fusion.

Joint Symposium 8

Joon-Won Kang

Asan Medical Center, Korea

Joint Symposium 8

Sang Il Choi

Seoul National University Bundang Hospital, Korea

Joint Symposium 8

Jin Cheol Paeng, MD., Ph.D

Seoul National University Hospital, Korea

Highlight Session

June-Key Chung

Seoul National Univeristy Hospital, Korea

ARCCNM Session

Current Activities and Plans of ARCCNM

Jun Hatazawa MD, PhD

Asian Regional Cooperative Council for Nuclear Medicine (ARCCNM)

The ARCCNM consisted of Asian Nuclear Medicine Board (ANMB) for Annual General Meeting (AGM) every year and accreditation of nuclear medicine specialist and Asian School of Nuclear Medicine (ASNM) for education and training. The ASNM activity is summarized by Prof. Huang Gang, Dean of ASNM.

In 2014, the 13th ARCCNM AGM was held in Osaka, Japan in conjunction with the Japanese Society of Nuclear Medicine, Japanese Society of Nuclear Medicine Technology, and Asian Society of Nuclear Medicine Technology (Main Office in Osaka). The number of total registered participants was 2500 including nuclear medicine physicians, nurses, technologists, radio-pharmacist, nuclear physicist, medical engineers, computer scientist from 26 Asian and Middle East countries/regions, USA, Germany, France, and Italy. The total budget was US$1.2M by the support of the RCA Office/IAEA, JSNM, JSNMT, industries of Japan and China, Japan Isotope Association, and Osaka University. The Exhibition of the most advanced scanners by major industries was held. The site-visit of the PET/CT Center was organized with 50 attendees. The numbers of invited lectures and scientific abstracts were 12 and 150, respectively. The 13th ARCCNM AGM in Osaka is followed by the 14th in Jeju Island, the 15th in Shenyang, and the 16th in Yokohama.

The third organization in ARCCNM is Asian Nuclear Medicine Research Network now proposed for research activities within the ARCCNM countries. The first project under this organization (tentative at this moment) is scheduled for standardization of brain perfusion imaging with SPECT. The scientists of China, Taiwan, and Japan headed by Prof. Hiroshi Matsuda are working with the computer-software providers of Japanese and Chinese industries under the supervision of ARCCNM. The Asian Nuclear Medicine Research Network is similar to the EARL (EANM Research Limited.) and Clinical Trial Network in SNMMI, which strengthen collaboration of research institute/hospital in our area, academic/research outcome to patients with industries /companies, and financial background of the ARCCNM.

ARCCNM Session
Current Activities and Plans of AOFNMB and WFNMB

Henry Hee-Seung Bom MD, PhD, FANMB

President, AOFNMB

AOFNMB is making innovations in administration and congresses last three years. A new office in Seoul, Korea is running by a specialized association management company, Trinity Co. This change brought faster and more professional management of AOFNMB. Inputs from member states were more efficiently collected which consequently brought wider communications among leadership in the region. Congress is a good change to communicate face to face and to learn new knowledge. AOFNMB is planning to have more congresses in Asia and Oceania. Annual congress of AOFNMB is the final goal which will be realized from 2021.

WFNMB is making a huge change. The bylaws was amended this year. The new bylaws separated congress and administration. The office bearers which include president, secretary general and treasurer are concentrate their activities to more strategic issues. Congress of the world federation continues every four years. Election of new president and new congress site is scheduled during the next EANM congress in Barcelona. Summit of world NM leaders is going to be organized by the WFNMB office every year to discuss the current issues of NM.

ARCCNM Session

Current Activities and Plans of ASNM

Gang Huang MD., Ph.D

Dean, ASNM

ARCCNM Session

Current Activities and Plans of AOJNMB

S.R.Zakavi MD,IBNM, FANMB

Asia Oceania Journal of Nuclear Medicine & Biology

Asia Oceania Journal of Nuclear Medicine and Biology (AOJNMB) is a free journal published biannually and serves as the official journal of Asia Oceania Federation of Nuclear Medicine & Biology (AOFNMB). This young journal tries to provide a

platform for free publication of the research works from the physicians and scientists in the region and all over the world. AOJNMB also serves as a forum for discussion of scientific and professional issues in the field of Nuclear Medicine and Biology.

The first issue of AOJNMB published in May 2013 and we published 6 issues and 1 supplement up to now including 61 articles. The published articles were from 13 different countries and included original articles (in clinical, radiopharmacy and physics), technical notes, case reports, review articles, meeting reports and editorials. Also a section on "History and perspectives" were developed that introduce the history of nuclear medicine in different countries as well as their current status and facilities and their future plans. All articles have been peer reviewed by at least 2 reviewers who were blind to the authors and their affiliations. Our commitment in AOJNMB is to publish high quality of articles and that resulted in a mean rejection rate of 36% in last 2 years. We used an efficient website for article submission and we have been continuously improving its functionality.

Visibility is the main road to success in publication. We distributed hard copies of AOJNMB in different meetings, congresses and training courses throughout the world including ARCCNM, WARMTH and EANM. Also after publication of each issue, more than 200 journals were sent by air- mail to authors, editorial board and reviewers throughout the world. We have been applied for indexing in many indexing banks and successfully indexed in IMEMR (Index Medicus for Eastern Mediterranean Region), DOAJ(Directory for Open Access Journals), EBSCO, Index Copernicus, Google Scholar, SID and Magiran. And recently we are accepted in Pubmed Central (PMC) that significantly will increase visibility of AOJNMB.

The future plans of AOJNMB can be described in three different groups. The first plan focuses on improving performance and includes optimizing the website, obtaining DOI for all articles, standardization of the review forms and recruiting more reviewers. The second program targets authors and readers of the journal and focus on providing language edit service and improving the content of the articles by inviting top scientists for writing systematic reviews for AOJNMB as well as by critical review of the submitted articles. We noted that many of our colleagues in the AOFNMB countries would benefit from a training course on scientific writing and we are planning to provide seminars on scientific writing for physicians and scientists in the region. Publishing high quality articles will result in improving impact of AOJNMB in nuclear medicine and facilitate our indexing in major indexing centers. The third program is mainly related to visibility and includes indexing in different indexing centers that will be maximized by indexing in the web of science (ISI).

ARCCNM Session
IAEA Activities in Asia and Oceania

Thomas Neil B. Pascual M.D., M.H.P.ED

International Atomic Energy Agency (IAEA)

ARCCNM Session
Experience of IAEA Activities in India

Prof.G.P.Bandopadhyaya

President,Society of Nuclear Medicine India

The role of IAEA is to accelerate and enlarge the peaceful contribution of atomic energy in health and prosperity throughout the world. The disease prevention, based on diagnosis for treatment of health related problems /management, using nuclear techniques, with perfection without compromising in quality assurance. India is very much associated in its health care program using nuclear resources peacefully. Our main aim is to use our Atomic energy resources for constructive work only .Nuclear medicine in is advancing day by day india. The main role of IAEA in Nuclear medicine as of today are as follows:

1. coordinated research projects: at least 6 on going.
2. Support as experts: lecturer for regional training courses, experts missions for guidance and review, IMPACT missions,
3. Contributions in Technical meeting eg. future of imaging, Hybrid Imaging.
4. Contributions in publications of IAEA
5. lead country in regional projects (RAS)
6. particpation in IAEA conferences: eg IPET, IMIC
7. Host for IAEA fellows for continuous professional development and academic training
8. Implementation of DAT (distance assisted training program for nuclear medicine professionals.
9. Contribution to developing resources on human health campus

WARMTH Symposium 1

Radioactiveiodine Treatment for Hyperthyroidism-A Review

Emerita Andres-Barrenechea, MD, FPCP, FPSNM

Nuclear Medicine Dept Veterans Memorial Medical Center and St. Luke's Medical Center

The use of I-131 in 1946 for the treatment of hyperthyroidism marked a historic event. It ushered in a new era of radionuclides in medicine and led to the birth of nuclear medicine. Today I- 131 has become one of the most commonly used agents and best option for the treatment of hyperthyroidism.

Hyperthyroidism is a hypermetabolic state induced by excess of thyroid hormone. It can develop secondary to thyroid hormone released from an overactive or inflamed thyroid gland or from extraglandular sources. It is also a clinical syndrome or group of syndromes due to high levels of unbound or "free" thyroid hormone in the circulation. The prevalence is: The female-to-male ratio among patients with Graves' disease is between 5:1 and 10:1. The peak incidence is between 40 and 60 years of age, although the disease can occur at any age. The predisposing factors are: autoimmunity, genetic susceptibility to the disease stressful life events, infection and recent childbirth (postpartum-2 to 6 months). Causes: Graves Disease – Diffuse Toxic Goiter, Plummer's Disease – Toxic MNG, Toxic phase of Sub Acute Thyroiditis – SAT, Toxic Single Adenoma – STA, Pituitary Tumors – excess TSH, molar pregnancy/choriocarcinoma, metastatic thyroid cancer, iatrogenic intake of thyroid hormone, Struma ovary, INF, Amiodarone, SSRIs intake.

Evaluation is by: Clinical assessment and scoring, Serum TSH, T3, T4 BY RIA, Determine volume by ultrasound or uptake by nuclear scans.

Once the diagnosis of Graves' disease with hyperthyroidism has been established, the patient should be given a complete explanation of the illness and options for treatment. The goal is to involve the patient as a partner in the medical decision-making process and care, rather than dictate the choice of therapy

Management consists of three options: Antithyroids-for children and young adults; pregnant and lactating mothers; mild hyperthyroidism & small goiters; as pretreatment for elderly prior to RAI I-131- is for older patients, for recurrent hyperthyroidism and relapse after surgery; those with accompanying serious illness and those allergic to drugs. We resort to surgery for big bulky goiters causing obstruction and those with co-existent cancers

Propylthiouracil, Thiamazole (Strumazole), Carbimazole and Methimazole, both inhibit thyroid peroxidase, PTU also inhibits T4 to T3 conversion and believed to have immunomodulatory action.

When to advise surgery: Very large or toxic nodular goiters, suspicion of thyroid cancers, pregnancy/ lactation and intolerant to drugs (third trimester), failed medical therapy but refuses RAI and patient preference.

Main indications for RAI according to the latest ATA guidelines are: Graves' disease, toxic multinodular goiter, toxic autonomously functioning thyroid nodule(s), and nontoxic multinodular goiter.

Important considerations are: diagnosis must be confirmed clinically and biochemically, nature of thyrotoxicosis must be determined; it is ideal to treat patients first with antithyroids (2 weeks at least) prior to therapy. Discontinue antithyroids and no iodine rich foods at least five days prior to therapy. Dosing and choice of treatment must be individualized; Pregnancy and lactation are absolute contraindication to radioactive ablation.

The mechanism of I-131-90% is due to beta radiation producing radiation thyroiditis and chronic gland atrophy. Maximal amount of I-131 taken by gland, size and amount of tissue to be irradiated, effective half-life of the isotope in the thyroid and relative sensitivity of the thyroid to I-131 are important considerations prior to therapy.

Dosimetry includes: Delivering a dose of 5,000-15,000 rads to shrink the gland by using a preferred dose-160 uCi of I-131 per gram of gland or the usual dose; a calculated dose based on a formula of Quimby and Marinelli and an arbitrary empirical dose ranging from 2-10mCi.

Four basic approaches are: Administer same dose in mCi to every one (rarely used), vary dose in mCi according to gland size and severity of hyperthyroidism, administer a dose calculated to deliver a predetermined number of microcuries per gram based on RAIU, estimate dose in terms of rads delivered based on half-life of I-131 in the gland, thyroid weight and 24 hour uptake.

Logically the higher the dose, the more rapid the control but with a high incidence of hypothyroidism, intermediate dose-most commonly used approach, low dose rationale-less hypothyroidism, more re-treatments, and more costly and longer duration of morbidity. Studies have found no effect on fertility, no increased incidence of congenital malformations, and no increased risk of cancer in patients treated with radioactive iodine or in their off-spring

Advantages of RAI: Safe- no complications other than hypothyroidism although we aim for euthyroidism, no hospitalization, low cost, rapid elimination of goiter and symptoms It is highly effective-higher dose increases success rate but higher chance of hypothyroidism. Some studies have shown increase of hypothyroidism irrespective of dose. Conclusions: Treatment should be

individualized and tailored to each patient, they should be told of the various modalities of treatment giving them options, and they must be advised that there is a need for continued follow-up thru the years.

WARMTH Symposium 1

Radio Iodine Treatment of Thyroid Cancer : What has Changed in the Past Decade ?

Partha Choudhury

Rajiv Gandhi Cancer Institute & Research Centre Delhi, India

Thyroid cancer represents a spectrum of diseases. At one end of the spectrum this is considered to be one of the best human cancers like the classical papillary carcinoma of the thyroid, while at the other end there is anaplastic thyroid cancer which is a rapidly growing & a potentially fatal disease. The incidence of thyroid cancer has shown an upward trend but the mortality has essentially remained unchanged over the last two decades. This could be the result of improved detection of incidentalomas. An approach to a thyroid cancer patient has also undergone modification due to the recognition of various other new factors and guidelines. Risk stratification post-surgery is an important initial step which is based on the review of available parameters like USG neck, detailed HP report, completeness of surgical resection and serum thyroglobulin. One of the major advances is the use of thyroglobulin which gives an indication of the presence of residual disease post-surgery and directs an appropriate additional imaging strategy thereby changing the risk stratification. If the patient has undergone total thyroidectomy and radioactive iodine ablation, the rising thyroglobulin invariably indicates the presence of recurrent or metastatic disease based on the trend seen over time. The recurrent disease in the thyroid bed can be very well documented with appropriate imaging studies including an ultrasound and or PET-CT with ultrasound-guided needle biopsy for confirmation. The ultrasound has become an important tool in the follow-up of patients with thyroid cancer both for identification of the local recurrence in the thyroid bed and metastatic disease in the lymph nodes. Availability of Recombinant TSH has facilitated the radioiodine treatment both in terms of patient preparation & quality of life without compromising the outcome and this can be used for radioactive iodine dosimetry, ablation and treatment of metastasis. Clearly it has changed the quality of life of patients who are undergoing radioactive iodine treatment as they need not become hypothyroid anymore prior to treatment. Recombinant TSH can also be used for ablation within 7-10 days post-surgery with comparable outcome and this is of great help in saving many man hours and money. In this presentation I will be sharing our approach to a differentiated thyroid cancer patient in terms of risk stratification, post- surgery for planning radioactive iodine treatment and the utility of recombinant TSH in the whole paradigm. The utility of ^{18}F- FDG PET CT in the management of differentiated thyroid carcinoma refractory to radioactive iodine will also be discussed.

WARMTH Symposium 1

Radionuclide Skeletal Pain Palliation : an Overview

Ajit Shinto

Kovai Medical Center and Hospital, India

Systemic therapy using bone-seeking radiopharmaceuticals has clear advantages for the treatment of multisite metastatic pain. Evidence supporting the use of alfa particle, electron, and beta particle– emitting radiopharmaceuticals is reviewed here. Appropriate patient selection relies on correlating clinical symptoms with focal abnormalities on conventional bone scintigraphy.

Time to symptom relief and response duration vary with the physical half-life and dose rate of the radionuclide used, offering the opportunity to tailor radiopharmaceutical choice to individual patient circumstances. Toxicity is limited to temporary myelosuppression, governed by the administered activity and underlying bone marrow reserve. Optimal responses are achieved in patients with a modest skeletal tumor burden, suggesting that targeted therapy should be considered early in the management of bone metastases. The development of reliable dosimetric models will facilitate patient-specific prescribing to deliver enhanced symptom response within acceptable toxicity limits. It is likely that targeted therapy will be most effective in the context of multimodality tumor management. Further research is required to examine the potential of radionuclides in combination with external-beam irradiation, bisphosphonates, or chemotherapy.

This approach might allow targeted therapy to progress beyond symptom palliation to early intervention for survival gain.

Key Words: bone pain palliation; metastasis; targeted radionuclide; therapy; dosimetry

WARMTH Symposium 1

Radioembolization of Hepatocellular Carcinoma using Y-90 Labeled Microspheres

Jae Gol Choe, MD, PhD

Department of Nuclear Medicine, Korea University Anam Hospital, 126-1 Anam-dong 5-ga, Seongbuk-gu, Seoul, 136-705, South Korea

Although surgical resection or liver transplantation is the recommended curative therapies of the malignant hepatic tumors, many of them cannot be surgically resected because they are advanced at the time of diagnosis. Trans-arterial chemoembolization (TACE) is the major treatment option for the unresectable primary or secondary liver malignancies. Transarterial radioembolization (TARE) is an alternative trans-arterial embolization option, and might be a safe and effective treatment modality in intermediate-stage to advanced stage HCC and for colorectal liver metastasis. The TARE produces response rate of 26-52% and this method of treatment is usually very well tolerated.

Trans-arterial radioembolization using Y-90 labeled microspheres includes infusion of beta ray-emitting Y-90 labeled microspheres into the hepatic arteries so that the microspheres are delivered to the hepatic tumors where the embolized radiolabeled microspheres serve as sources for internal radiation. Until now, two kinds of microspheres are clinically available: glass-microspheres (TheraSpheres; MDS Nordion, Ottawa, Canada) and resin microspheres (SIR-spheres; SIRTEX, Sydney, Australia).

In addition to preparation angiography for evaluation of vascular anatomy, a Tc-99m albumin macroaggregate (MAA) hepatic angiography scan is performed to evaluate the microsphere distribution within the liver, to determine the tumor vascularity, to detect any possible radioactivity spillage through the collateral circulation to calculate the degree of shunting to the lung, and to use for the injection dose calculation. Several methods of calculation of administration dose of Y-90 microspheres is proposed.

It is necessary to know the actual distribution of Y-90 microspheres after administration, because intrahepatic distribution of radioactivity can predict the therapeutic effect, and unexpected adverse effects can be caused by extrahepatic regurgitation of microspheres. A bremsstrahlung image can be used for evaluation of post-administration distribution. Some recent studies have postulated the feasibility of positron emission tomography/computed tomography (PET/CT) imaging with Y-90 in the evaluation of post-administration distribution of radioactivity.

This presentation will discuss the usefulness of Y-90 microsphere treatment, practical guide of preparation and administration of microsphere and recent experience in Korea.

WARMTH Symposium 2

Radionuclide Therapy for Bleeding Joints: an Update

Emerita A. Barrenechea, MD, FPCP, FPSNM

Nuclear Medicine Dept. -St. Luke's Medical Center & Veterans Memorial Medical Center, Philippines

Radiosynovectomy is the radionuclide therapy of joint synovitis (inflammation) or synovial processes by intra-articular injection of radionuclides (90-Yttrium silicate/citrate, 186-Rhenium sulphide, 169- Erbium citrate)-EANM guidelines 2003. It is the intra-articular administration of radioactive particles, which are absorbed by the superficial cells of the synovium. The beta radiation leads to coagulation necrosis and sloughing of these cells. The indications are: rheumatoid arthritis, spondylarthropathy (e.g. reactive or psoriatic arthritis), other inflammatory joint diseases e.g. Lyme disease, Behcet´s disease, persistent synovial effusion and hemophilic arthritis. Absolute contraindications are pregnancy, breastfeeding, local skin infection and ruptured popliteal cyst [knee]. Relative:

"if the benefit of treatment is likely to outweigh the potential hazards", extensive joint instability with bone destruction and evidence of significant cartilage loss within the joint. The scope of the problem is that Approx 1 in 10, 000 births-Hemophilia A, 1 in 50,000 births for Hemophilia B, Annual incidence of about 400 babies (NHLBI), Around 400,000 worldwide, 28,000 in the US and 25 % are our potential patients (WFH), and the impact of the disease-when you know it is treatable. Hemophilia is an x-linked recessive disorder affecting males, causes coagulation defects because of lack of clotting Factor VIII for hemophilia A (85%) and Factor IX for Hemophilia B (15%). Bleeding is usually at the musculoskeletal level-joint bleeds (61.96%) in an Asian study.

Hemarthroses (or joint bleeds) are the most frequent bleeding episode arising from the subsynovial venous plexus where a lack of thromboplastic activity has been demonstrated. When intra-articular bleeding occurs, the blood breakdown products act as a potent stimulus for inflammatory response & when this occurs repeatedly it cause synovial hypertrophy. Current treatment consist of the following: Antihemophillic Factor (AHF) which is temporary, repeated and expensive; chemical synovectomy using Rifamficin, osmic acid, easily available but painful and irritating and requires

repeated intraarticular injections (weekly.) and surgery: although both open and arthroscopic synovectomy may treat hemophilic arthropathy, they can result in joint stiffness & prolonged rehabilitation, it is also invasive, bloody, costly, and does not prevent progression of arthropathy-success rate of over 80%. The best option seems to be Radiosynovectomy.

Yttrium-90 seems to be the ideal isotope as it has pure beta-emissions, a shallow depth penetration (focused on the synovium and not the surrounding tissues), rate of energy deposition, moderate half-life, carriers should have sufficient particle size (about 10 microns) so as not to produce leakage, non-toxic, easy to use and would degrade at the same rate of the isotope. This is good for the knee, which is considered a big joint. Established cases of hemophilia from the National Hemophilic Center in Manila were included if: they have a history of 3 bleeding episodes for the last 6 months and with at least 30% coagulopathy at the time of the procedure. They are willing to follow-up for one year. They should receive both verbal and written information about the procedure: initial flare, risks and potential complications, inform patient that 60-80% may benefit from RS, follow-up care after 1, 3, 6 and 12 months, bone scan, radiation exposure (therapy, fluoroscopy), need for immobilization by splinting (48 hours) (thrombosis, lymph edema, loss of motion). Baseline radiography of the knees in the AP and lateral views were obtained (presently an ultrasound scan can evaluate joint space, thickness & structure of the synovium, even effusion). Two phase bone scintigraphy within 5-25 mins then 2 hours scan were taken at baseline, 6, and 12 months and post-therapeutic whole body scan for leakage was done. Results or outcome was considered good if hemarthroses decreased by 50-100%, moderate when the decrease was 25-49% and failure when the reduction was less than 25%. Of the 21 patients, ten patients had 70-100% improvement, 9 had 50-70% and 1 patient barely improved, 1 was stable disease. Therapeutic results showed 86% had decrease of pain and swelling, 86% improvement from bleeding, bone scan improved in 62% giving an overall improvement of 90%.

Discussion: The key to the successful prevention of HA is an aggressive containment of the initial hemarthroses before chronic synovitis develops. Regular clotting factor replacement, physiotherapy and close ff-up are necessary. If chronic synovitis develops (arthropathy) RS should be done to prevent end-stage arthropathy. The most important element in this mode of treatment is that the effects are localized in the knees and there are no systemic effects. Radiosynovectomy likewise prevents joint deformities by preventing future bleeds or reducing bleeding episodes.

Conclusion: Radiosynovectomy is a minimally invasive, well-tolerated procedure that can be done on an outpatient basis; it is cost-effective requiring only 30% coagulopathy during the procedure. It is effective in those refractory to medical therapy and those not suitable for surgery as the hemophilics. RS prevents the deformation and deterioration of the joint by destroying the pathological synovium. Radiosynovectomy is an established and efficacious therapy for the treatment of bleeding joints in hemophilia.

WARMTH Symposium 2

Targeted Radionuclide Therapy with ^{131}I-MIBG: Experience in Japan

Seigo Kinuya

Kanazawa University School of Medicine, Japan

Targeted radionuclide therapy (TRT) with ^{131}I-MIBG has been a therapeutic choice for malignant neuroendocrine tumors for 15 years in Japan. In Kanazawa University Hospital, this therapy was initiated in 2001.

We experienced approximately 200 treatments in pheochromocytoma/paragangrioma, medullary thyroid cancer and neuroblastoma. It is hard to obtain remission in malignant pheochromocytoma/paragangrioma with our standard dose of 200 mCi. However, prognosis of patients is likely improved by multiple treatments (Ann Nucl Med 2013). In addition, hormonal and objective response to the first treatment would be prognostic factors. A high dose therapy with 400 mCi apparently has benefit without serious toxicity. We are currently considering even higher doses in confirmation of maximum tolerated dose of 2 Gy to the bone marrow.

In neuroblastoma, we have two therapeutic options. One is the use of modest dose of ^{131}I-MIBG, e.g. 100 mCi. Another is high-dose therapy at 15-18 mCi/kg combined with bone marrow rescue such as peripheral blood stem cell transplantation, autologous umbilical cord blood transfusion, and autologous bone marrow transplantation. With the latter strategy, we can attain complete remission in a number of children (Pediatr Blood Cancer 2008; Italian J Pediatr 2012).

The nationwide results as well as the institutional results will be demonstrated in the symposium.

WARMTH Symposium 2

Radioimmunotherapy of Lymphoma

Sang Moo Lim

Korea Institute of Radiological and Medical Sciences, Korea

WARMTH Symposium 2

PRRT of Somatostatin Receptor Positive Tumors (NEN)

Richard P. Baum

THERANOSTICS Center for Molecular Radiotherapy and Molecular Imaging, ENETS Center of Excellence, Zentralklinik Bad Berka, Germany

The strong expression of SSTR2 by neuroendocrine tumors (NETs) enables peptide receptor radionuclide therapy (PRRT), the molecular internal radiation therapy of NETs. The most important points to consider for PRRT are:
Patient selection
Appropriate choice of peptide and radionuclide
Kidney protection
Tumor and organ dosimetry (post-treatment scans) and
Monitoring of toxicity (follow-up).
In our hospital, which was certified as ENETS Center of Excellence in March 2011 and re-certified in March 2014, a dedicated multidisciplinary team of experienced NET specialists is responsible for the management of NET patients (over 1,200 patient visits per year).
Patient selection for PRRT is based on the Bad Berka Score (BBS) which takes into account clinical aspects and molecular features. The therapy plan for each patient is individualized.
Frequent therapy cycles (4-6 and up to 10), applying low or intermediate doses of radioactivity are suitable for these relatively slow-growing tumors ("long term low dose, not short term high dose concept").
For kidney protection, patients are well hydrated and receive an amino acid infusion containing lysine and arginine given intravenously for 4 hours beginning 30 minutes before PRRT. Renal function is serially determined by Tc-99m MAG3 scan (TER) and by Tc-99m DTPA (GFR) measurements.
After each 2 treatment cycles, restaging is performed by morphologic (CT/MRI) and molecular imaging (Ga-68 SSTR PET/CT), metabolic imaging (at least one F-18 FDG PET/CT before start of treatment), and in selected cases also F-18 fluoride PET/CT, blood chemistry and tumor markers.
All data are entered in a prospective structured database (<250 items per patient).
Another very important aspect is dosimetry. Estimation of tumor and normal organ doses performed after PRRT (using Lu-177 labeled somatostatin analogues DOTATATE or DOTATOC) is important to ensure that maximum dose is delivered to the metastases, therefore optimizing an individualized treatment protocol.

NET Center Bad Berka - Overall Results

Retrospective analysis was performed using our database in 1000 patients (age 4 - 85 years) with metastatic and / or progressive NETs, undergoing 1 - 9 cycles of PRRT at our center using Lu-177 (n=331), Y-90 (n=170) or both (n=499). Median total administered activity was 17.5 GBq. Patients were followed up for up to 132 months after the 1st cycle of PRRT. Well-differentiated NETs (G1-2) accounted for 54 %. Most patients (95.6 %) had undergone at least 1 previous therapy (surgery 86.8 %, medical therapy 55 %, ablative therapy 14.2 % and radiotherapy 3.4 %).
The median overall survival (OS) of all patients from the start of PRRT was 52 months (mo). Median OS according to radionuclide used: Y-90 24 mo, Lu-177 55 mo, both (TANDEM or DUO PRRT) 64 mo; according to the grade of tumor: G1 87 mo, G2 55 mo, G3 28 mo, unknown 50 mo; and according to origin of primary tumors: pancreas 45 mo, small intestine 77 mo, unknown primary 55 mo, lung 36 mo. Median progression-free survival (PFS) measured from the last therapy cycle was 22 mo, comparable for pancreatic (23 mo) and small intestinal (25 mo) NETs.
We have also treated patients with progressive metastases of NETs and with a single functional kidney (24 patients). None of these patients showed grade 3 or 4 nephrotoxicity. PRRT resulted in partial remission in 36% and stable disease in 36% of the patients, 28% had PD. In 2009, we have given fractionated low dose PRRT to 3 patients on hemodialysis (to the best of our knowledge, this was the first ever worldwide experience).
The Bad Berka neuroendocrine tumor center was the first also to use Y-90 DOTATATE. In a large patient group (>350 patients), Lu-177 DOTATOC was administered for PRRT of progressive NETs, non-responsive to octreotide/interferon treatment or chemotherapy. Historical comparison to established treatment modalities showed a significant benefit in progression free survival (PFS) or time to progression (TTP), e.g. compared to Octreotide LAR (PROMID study) PFS vs. TTP was 16 months longer, and compared to Sunitinib and Everolimus, respectively, PFS there was an improvement of PFS by 19 months.
An important influence on the decision of the choice of radionuclide is the size of tumors. More commonly, patients present with tumors of various sizes and inhomogeneous distribution of somatostatin receptors. The use of a combination of Lu-177 and Y-90 takes this heterogeneity into account. Sequential administration of Y-90 and Lu-177 labeled analogues is useful for the treatment of larger tumors, followed by treatment of smaller metastases, respectively in further treatment cycles. The BBNETC group pioneered the systematic use of Y-90 and Lu-177 DOTATATE (DUO PRRT) in sequence and concurrently, as well as the intra-arterial use of Y-90 DOTATATE and DOTATOC.
Lu-177 DOTATATE or Lu-177 DOTATOC is predominantly

used for small metastases or in patients with impaired renal or haematological function. Long term follow-up of up to 10 years after DUO PRRT showed no significant grade 3 or grade 4 nephrotoxicity attributed to concurrent or sequential DUO PRRT. The median fall in tubular extraction rate (TER) was lesser in patients undergoing DUO PRRT than in those undergoing PRRT with Y-90 alone. The results of a study by Kunikowska et al. also indicated that TANDEM PRRT (concurrent PRRT with Y-90/Lu-177 DOTATATE) provided longer overall survival than with a single radioisotope (Y-90 DOTATATE); the safety of both methods was comparable.

Results of a German Multi-institutional Registry Study

A German multi-institutional registry study with prospective follow up in 450 patients indicates that PRRT is an effective therapy for patients with G1-2 neuroendocrine tumors, irrespective of previous therapies, with a survival advantage of several years compared to other therapies and only minor side effects. Median overall survival (OS) of all patients from the start of treatment was 59 months. Median progression-free survival (PFS) measured from last cycle of therapy accounted to 41 mo. Median PFS of pancreatic NET was 39 mo. Similar results were obtained for NET of unknown primary (median PFS: 38 mo) whereas NET of small bowel had a median PFS of 51 months. Side effects like °3-4 nephro- or hematotoxicity were observed in only 0.2% and 2% of patients respectively.

A randomized prospective international multi-center clinical trial (the NETTER-1 Study) has been performed in patients with progressive midgut NET comparing Lu-177 DOTATATE PRRT (4 cycles at 7.4 GBq each plus 30 mg Octreotide LAR per month) with high dose (60 mg) Octreotide LAR per month and first results will be presented.

Conclusions

PRRT lends a significant benefit in progression free survival as well as in overall survival in metastasized and / or progressive G1-2 NETs as compared to other treatment modalities and regardless of previous therapies. Combination of Lu-177 and Y-90 (DUO) based PRRT may be more effective than either radionuclide alone. Thus, in patients with progressive NETs, fractionated, personalized PRRT with lower doses of radioactivity given over a longer period of time (Bad Berka Protocol) is effective even in advanced cases and results in excellent therapeutic responses. Up to 10 cycles of PRRT, given over several years

were tolerated very well by most patients. Severe renal toxicity can be completely avoided or reduced by nephroprotection applying aminoacids; haematological toxicity is usually mildto moderate (except for some cases of MDS which occurs in 2-3%). Quality of life can be significantly improved. Though cure is rarely possible, excellent palliation with significant improvement of symptoms can be achieved by PRRT. In addition, neoadjuvant PRRT could be administered in cases of inoperable NET so as to render the tumor operable by inducing radiation induced necrosis and decrease in tumor size. Use of intra-arterial PRRT (>100 treatments were already performed up to now at our center) is more effective for selectively targeting liver metastases and large, inoperable primary tumors.

PRRT should only be performed at specialized centers as NET patients need highly individualized interdisciplinary treatment and long term care. PRRT can be effectively combined with transarterial chemoembolization (TACE), radiofrequency ablation (RFA), chemotherapy (e.g. using Capecitabine/5-FU, Temozolomide or Doxorubicin), and kinase inhibitors (e.g. Everolimus).

WARMTH Symposium 3

Greater Effectiveness of High LET Electron Emitters for Theragnostic Applications

Suresh Srivastava, Ph.D

Collider-Accelerator Department, Brookhaven National Laboratory, Upton, NY, USA

Nuclear medicine has recently experienced a resurgence of interest in radiotherapeutic procedures. Using unsealed sources for radionuclide therapy is not new; it has been around for over five decades starting with the development of the treatment of thyroid disorders with radioiodine. However, recent advances in molecular biology have led to a better understanding of cancer. Parallel research has shown promise for monoclonal antibodies, peptides, and other biological vehicles to serve as specific carriers to deliver cell-killing radiation into tumors in a highly localized fashion. These developments have led to a renewed interest in the exciting possibility of treating human malignancies with the systemic administration of radionuclides. A number of other relatively new techniques such as the treatment of metastatic bone pain, radiation synovectomy, bone marrow ablation, and others, have given additional impetus to need for research on new and application-tailored therapeutic radionuclides. A major advantage of radionuclides is that they emit radiation of different radiobiological effectiveness and range of action. This offers the possibility of choosing a nuclide the physical and nuclear characteristics of

which are matched with a particular tumor type, or the disease under treatment.

The choice of a radionuclide best suited for a particular application depends on a number of factors. These include: half-life, type of emissions (α, β, γ, Auger or conversion electrons), specific activity, route of administration, internal dosimetry, radiation safety and environmental concerns, vehicles used as the carrier, bio-pharmacokinetics of the labeled carrier and the free nuclide, and very importantly, the cost of production and availability. Until very recently, a majority of clinical trials have used only a handful of radionuclides, which have less than ideal therapeutic properties but are available at reasonable cost with some degree of regularity. A number of other isotopes seem to offer much better properties for specific applications. These include: Auger and CE emitters Ga-67, Br-77, Tl-201, Sn-117m, I-123, Hg-195m, and Pt-195m; α-emitters At-211, Bi-212, Bi-213, Ac-225..

Out of the above list, Tin-117m has many advantages over other commonly used therapeutic radionuclides, in particular for application to systemic radionuclide therapy of cancer and of cardiovascular diseases. The production of ^{117m}Sn labeled molecules is relatively simple and they have high chemical and in-vivo stability. Tin-117m is much less toxic to bone marrow compared to other treatments including chemotherapy or radiation-induced bone marrow suppression., as well as therapy using common beta emitters. This paper presents the results of our initial work on the stable electroplating of commonly used stainless steel stents (BMS) with ^{117m}Sn, and their use in experimental animal models to evaluate therapeutic effectiveness.

Tin-117m has a half-life of 14 days and it emits three major short-range monoenergetic conversion electrons with discrete energies (and discrete ranges in tissue) of 127, 129, and 152 KeV with high linear energy transfer. These conversion electrons deposit their intense energy in discrete ranges in tissue within a distance of between 0.22 mm and 0.29 mm, which closely corresponds with the average thickness of the human coronary arteries and is thus optimum for the imaging and treatment of vulnerable plaques and other inflammatory disorders., with minimal collateral damage to adjacent, tissue because of its low-energy conversion electron emission and short penetration in tissue. In addition, ^{117m}Sn also emits a gamma photon of 159 KeV (86%) that is ideal for SPECT imaging.

This work was supported by the U.S. Department of Energy (DOE) under Contract # DE-AC02-98CH10886, at Brookhaven National Laboratory.

WARMTH Symposium 3

PRRT/Chemo-biotherapy of NETs and Radio-immunotherapy of Lymphoma

J Harvey Turner

The University of Western Australia, Australia

WARMTH Symposium 3

Re 188 Based Multipronged Therapy Project at KMCH, Coimbatore, India

Ajit S Shinto

Kovai Medical Center and Hospital, India

This is a summary prepared by Dr Ajit Shinto

Studies have proven the safety and efficacy of trans-arterial rhenium-188 HDD conjugated lipiodol (radio-conjugate) in the treatment of patients with inoperable hepatocellular carcinoma (HCC).

The radio-conjugate was prepared by using an HDD (4-hexadecyl 1-2,9,9-tetramethyl-4,7-diaza-1,10-decanethiol) kit developed in Seoul National University Korea, and lipiodol. A WARMTH team headed by Dr Ajit Padhy were in Coimbatore,India to help us set up the protocol and radio-chemistry in the month of August 2013.

Over a period of 24 months, 46 patients with inoperable HCC or metastatic liver lesions received at least one treatment of radio-conjugate. Only 4 patients were re-treated for residual active lesion or new lesions. The level of radio-conjugate administered was empiric with a range of doses between 30 to 300 mCi. Patients were followed for at least 12 weeks after therapy, until recovery from all toxicity. The clinical parameters evaluated included toxicity, response as determined by contrast-enhanced computed tomography, palliation of symptoms, overall survival, performance status (Karnofsky) and hepatic function (Child's classification). Liver function tests, serum alfa-fetoprotein (AFP) levels and complete blood counts were done at each follow-up visit. Side-effects were minimal and usually presented as loss of appetite, right hypochondrial discomfort and low-grade fever, even at high levels of administered radioactivity. The symptoms resolved with simple supportive therapy within 3 days of onset. Liver function tests done at 48 and 96 hours showed normalization by 4 days post therapy in all cases and complete blood counts at 1 week, 4 weeks and 12 weeks showed no changes (no bone marrow suppression). Survival at 6 months was 100 %. We could achieve biochemical or imaging stability of disease in almost 50 % and partial or complete regression in another 35 %

patients approximately.
Of the 46 patients treated so far, 41 are still alive and do come for regular follow up. All of them report good quality of life. The results of this study show that 188Re-lipiodol is a safe and cost-effective method to treat primary HCC or metastatic liver lesions via the trans arterial route. In terms of efficacy, it is potentially a new therapeutic approach for further evaluation by treatment of larger numbers of patients.
In addition we have developed in house labeling procedures for Re 188 HEDP/V DMSA and SN colloid for radiosynovectomy to make the Re generator more commercially viable. We have also implemented endovascular brachytherapy with Re 188 filled balloons to prevent instent restenosis in patients undergoing femoral/iliac artery stenting.

WARMTH Symposium 3

THERANOSTICS of Prostate Cancer

Richard P. Baum

THERANOSTICS Center for Molecular Radiotherapy and Molecular Imaging, ENETS Center of Excellence, Zentralklinik Bad Berka, Germany

Molecular Imaging of Prostate Cancer using Gallium-68 PSMA

The significant overexpression of the prostate specific membrane antigen (PSMA) on tumor cells makes this enzyme an ideal target for the diagnosis as well as for therapy (THERANOSTICS) of prostate cancer. Ga-68 PSMA is a sensitive and specific tracer for the detection of primary prostate cancer, recurrent tumors and metastases. We have performed over 1,000 Ga-68 PSMA PET/CT studies until to date, using Ga-68 HBED PSMA and also applying DOTAGA PSMA I&T. Based on our experience, the potential indications for PET/CT in prostate cancer are:
Elevated PSA without tumor detection by conventional imaging, or patients with negative biopsies and high serum PSA (in well differentiated tumors also bombesin antagonists may be useful)
Initial staging in patients with intermediate or high risk (detection of lymph node and distant metastases), especially in case of strongly elevated PSA levels (suspicious distant metastases)
Detection of recurrence after initial therapy - in our experience, Ga-68 PSMA is far superior to choline due to detection of recurrence at very low PSA levels (<0.5 ng/ml), especially in undifferentiated tumors with high Gleason grade.
Therapy monitoring (depending on the clinical question which needs to be answered)
Molecular radiation therapy planning (MRTP), e.g., for dose painting
THERANOSTICS before planned PRLT for selection of the most appropriate radiopharmaceutical for therapy as well as for follow-up and assessment of therapy response after adionuclide therapy (this indication holds great future potential).

PSMA Radioligand Therapy (PRLT)

Based on the principles of targeted radionuclide therapy, Lu-177 labeled ligands binding specific to PSMA were developed by the Pharmaceutical Radiochemistry at the Technical University Munich using DOTAGA as chelator. PSMA radioligand therapy (PRLT) with Lu-177 DOTAGA PSMA ligands was performed in 53 progressive, metastasized, castrate-resistant prostate cancer patients. Ga-68 PSMA PET/CT was used for patient selection and follow-up. 34 patients received multiple cycles (range 2 to 5, in total 106 administrations). The mean injected activity of Lu-177 PSMA per cycle was 5.7±0.8 GBq (median 5.8 GBq). Post-therapy response could be assessed until now in 27 patients. Patient-specific dosimetry was carried out according to MIRD scheme.
The metastases exhibited intense PSMA expression, demonstrated by baseline Ga-68 PET/CT, high Lu-177 PSMA uptake on post-therapy planar scans and on SPECT/CT.
Molecular treatment response (partial remission) was observed in 11 patients, and morphological response (according to RECIST) was seen in 6 patients. Stable disease was noted in 5 and 13 patients, according to molecular and morphological response criteria, respectively, whereas disease progressed in 8 patients. All symptomatic patients reported significant improvement in pain and in quality of life after therapy. The treatment was very well tolerated by all patients, no acute (vomiting, emesis) or long term side effects were reported (especially there was no evidence of significant salivary or lacrimal gland toxicity). There were no significant alterations in any of the laboratory parameters (blood, renal, hepatic panel and chemistry), especially no hematotoxicity was observed (despite extensive bone metastases in many of the patients) or any change in renal function (as determined by creatinine, GFR clearance and Tc-99m MAG3/TER scintigraphy). Organ- and tumor doses were as follows: whole body 0.02+/-0.01 mGy/MBq; kidneys 0.35+/-0.14 mGy/MBq; tumor lesions 0.14-19.8 mGy/MBq. In bone metastases, the maximum dose reached by a single cycle was up to 300 Gy in some cases; complete remissions of lymph node metastases were observed in some patients. The median for progression free survival (PFS) and overall survival (OS) has not yet been reached.

Conclusions

Lu-177 DOTAGA PSMA small molecules exhibit very high tumor uptake, rapid blood clearance and fast renal washout. PRLT using Lu-177 PSMA is effective in end-stage disease after failure of all conventional/approved therapies (killing tumor and not only improving symptoms). There was excellent tolerability in all patients treated, i.e., no hematological, renal or salivary gland toxicity was observed. Selection of suitable patients as well as follow-up after PRLT by Ga-68 PSMA PET/CT is feasible and successful (THERANOSTICS concept). Improving the treatment potency and safety by means of hyperfractionation, increase of treatment activity, new methods for kidney protection (e.g. by using PMPA), application of radiosensitizers, different radionuclides and combination of various therapies must be considered in future.

International Round Table Discussion

Richard P. Baum

President, WARMTH

International Round Table Discussion

Suresh Srivastava

Brookhaven National Laboratory, USA

International Round Table Discussion

J Harvey Turner

The University of Western Australia, Australia

International Round Table Discussion

Andrew Mark Scott, MD., FRACP, DDU, FAICD, FAANMS

Austin Health, Melbourne, Australia

International Round Table Discussion

Thomas Neil B. Pascual, M.D., M.H.P.ED.

International Atomic Energy Agency (IAEA)

International Round Table Discussion

June-Key Chung

Seoul National Univeristy Hospital, Korea

International Round Table Discussion

Tae-You Kim

Seoul National University Hospital, Korea

International Round Table Discussion

Vijay Kumar

Westmead Hospital, Australia

International Round Table Discussion

Ajit S Shinto

Kovai Medical Center and Hospital, India

Continuing Education 1

Basic Concepts for Molecular Biology

Hyewon Youn

Department of Nuclear Medicine, Seoul National University Hospital, Korea

Clinical and preclinical in vivo molecular imaging approaches have been used to study biological responses at the microscopic (intra-vital imaging) and macroscopic (whole-body imaging) level. A series of imaging techniques ranging from non-radiation based techniques such as optical imaging, MRI, and ultrasound to radiation based CT/nuclear imaging can be used for visualizing molecular events of living organisms. These imaging modalities highlight the intrinsic behavior of different cell populations in physiological context, which can be explained by molecular biology. In this session, I will briefly summarize basic concepts of molecular biology for molecular imaging.

Continuing Education 1

Molecular Imaging with Reporter Gene Expression

Young Hyun Jeon, Ph.D

Department of Nuclear Medicine, Kyungpook National University, Daegu, Korea
Leading-edge Research Center for Drug Discovery and Development for Diabetes and Metabolic Disease, Kyungpook National University Hospital, Daegu, Korea

Molecular imaging with various reporter genes has been extensively investigated in oncology, immunology, and neurology and so on. Reporter gene-based molecular imaging allows for real time monitoring of gene expression, signal transduction, cell tracking, and therapeutic response in living mice. In this CME section, we briefly overviewed several types of applicable reporter genes and possible bio-imaging application in current bio-medical research areas including pre-clinical and clinical setting.

Continuing Education 1

Molecular Imaging for Cell Tracking

Yong Jin Lee

Molecular Imaging Research Center, Korea Institute of Radiological & Medical Sciences, Korea

The molecular imaging techniques allow monitoring of the transplanted cells in the same individuals over time, from early localization to the survival, migration, and differentiation. Generally, there are two methods of stem cell labeling: direct and indirect labeling methods. Direct labeling method introduces a labeling agent into the cell, which is stably incorporated or attached to the cells prior to transplantation. Direct labeling of cell with radionuclide is a simple method with relatively less adverse events related to genetic responses. However, it can only allow short-term distribution of transplanted cells due to decreasing imaging signal with radio-decay, according to physical half-lives, or the signal becomes more diffused with cell division and dispersion. Indirect labeling method is based on the expression of reporter gene transduced into the cell before transplantation, which is then visualized upon the injection of appropriate probe or substrate. In this review, various imaging strategies to monitor the survival and behavior change of transplanted stem cells are covered. Taking these new approaches together, the direct and indirect labeling methods may provide new insights on the roles of in vivo stem cell monitoring, from bench to bed-side.

Continuing Education 1

Molecular Imaging for Biomolecules

Kwang Il Kim

Molecular Imaging Research Center, Korea Institute of Radiological & Medical Sciences, Korea

Biomolecules are the complex organic molecules which build up living organisms and are required for their growth and maintenance. Proteins, carbohydrates, lipids, and nucleic acids are the most abundant biomolecules. Monitoring the behavior of these biomolecules is very important to understand various biological phenomena including disease. Especially, antibody and peptide of protein molecules are steadily been studied as promising targeted molecular imaging agents in preclinical models and in patients. In this session, current approaches to radiolabeled antibodies and peptides will be presented, and key factors (target expression, radioisotopes, radiolabeling, and etc.) in selection of molecular imaging agents for clinical translation will be discussed.

Continuing Education 1

Overview of Multimodal Imaging

Jin Su Kim[1,2,3]

1. Molecular Imaging Research Center, Korea Institute of Radiological and Medical Sciences(KIRAMS)
2. Korea Drug Development Platform using Radio-Isotope(KDePRI)
3. Radiologcial and Medico-Oncological Sciences, University of science and technology (UST), Seoul,Korea

Non-invasive technologies that image different aspect of disease should really be viewed, in almost cases, as complementary rather than competing. When the sensitivity and specificity of one imaging technique for diagnosing or staging a specific disease is compared to that of another technique, it is usually to establish the superiority of one of the two techniques. A typical example is a primarily anatomical imaging modality such as Computed tomography (CT) or Magnetic Resonance Imaging (MRI) compared to a functional imaging modality such as Single Photon Emission Computed Tomography (SPECT). In practice, however, such comparisons are of little value because anatomical and functional imaging techniques have different physical specifications of spatial, temporal, and contrast resolution, and the images even reflect

different aspect of the disease process. CT and MRI are used primarily for imaging anatomical changes associated with an underlying pathology, whereas the molecular imaging techniques of PET and SPECT capture functional or metabolic changes associated with that pathology. Histologically, CT has been the anatomical imaging modality of choice for the diagnosis and staging of malignant disease and monitoring the effect of therapy. However, more recently, functional imaging with whole-body PET has begun assuming an increasingly important role in the detection and treatment of cancer.

A PET study is generally read in conjunction with the corresponding CT or MR scan, acquired on a different scanner and usually on a different day. PET/CT or PET/MR could provide the functional and anatomical images which were scanned on the same day and same scanner. These PET/MR or PET/CT images provide powerful information for us. For pediatric oncology applications PET/MRI has potential to reduce overall radiation exposure to the patient. In tumors with need for repetitive follow up studies PET/CT can lead to a significant radiation burden. If with PET/MR the radiation dose from CT omitted, the actual radiation exposure is limited to the radiation dose from the PET component only which is substantially minor in comparison to the radiation dose from CT. A recently published study in pediatric patients shows a triple risk of leukemia after a cumulative CT dose of 50 milligray (mGy) and a nearly triple risk of brain tumors after a cumulative CT dose of 60 mGy. This study emphasized the need to reduce the CT dose in this vulnerable population to the lowest dose possible and to try to establish alternative diagnostic procedures without ionizing radiation. PET/MRI has the potential to represent this diagnostic alternative solution. A recent study evaluating co-registration of PET and MRI datasets for staging and re-staging of pediatric cancers yielded very promising results. Not only pediatric patients but also the pregnant population may benefit from PET/MRI. For certain cancers during pregnancy an imaging modality including PET can be crucial for further treatment decisions. As MRI is not associated with any radiation burden a PET/MRI exam should be preferred vs. PET/CT.

In this talk, I will review the importance and feasibility of multimodal imaging such as PET/CT and PET/MR. In addition, I also briefly introduce the multiscale imaging strategy for the monitoring the therapeutic effect.

Continuing Education 2

Near-Infrared Fluorophores for Imaging, Targeting and Therapy

Hoon Hyun, Ph.D

Department of Biomedical Sciences, Chonnam National University Medical School, Gwangju, Korea

Surgery is one of the main treatments for primary tumors and operations for limb amputation or limb sparing surgery aiming to remove the tumor completely. Presently, however, there isn't a single optical contrast agent that binds to tumors or specific tissues after intravenous injection and highlights its location and quantity. The technique of near-infrared (NIR) fluorescence imaging provides extremely low background since living tissue has minimal absorption and autofluorescence in the NIR range of 700-900 nm. Introducing an exogenous NIR fluorophore can produce a signal adequate for imaging.

NIR fluorescence has the potential to revolutionize image-guided surgery. Especially, the FLARETM has already developed a surgical imaging system that simultaneously, and in real-time, acquires two independent wavelengths of NIR fluorescence emission images along with color video images. The imaging system has already been translated to the clinic, and is being formally evaluated in clinical trials. Nevertheless, the fundamental limitation to the future success of this technology is the development of NIR fluorophores that perform optimally in the body, and which can be made widely available to other academic researchers.

To be clinically viable, the ideal NIR fluorophore requires certain optical properties, including excitation and emission ≈800 nm, and a high extinction coefficient and quantum yield in serum. However, the reason why existing NIR fluorophores perform so poorly in vivo has to do with biodistribution and clearance. After intravenous injection, the ideal NIR fluorophore would rapidly equilibrate between the intravascular and extravascular spaces and would be cleared efficiently via renal filtration. To date, every NIR fluorophore described in the literature suffers from two fundamental flaws: 1) hepatic clearance, which results in NIR fluorescence signal throughout the GI tract that persists for hours, and/or 2) non-specific background uptake in normal tissues, which typically persists for hours and results in a low signal-to-background ratio (SBR).

The goal of this work is to develop a new class of ideal NIR fluorophores that can be injected into the bloodstream. These fluorophores would "stick" to tumors and other diseased tissue, but not to normal tissue. Currently, we are developing on the synthesis of optimized NIR fluorophores for in vivo and surgical

imaging, on validating their use as targeted diagnostic agents for various diseases including cancer. Completion of these aims will lay the foundation for future clinical testing during image-guided surgery.

Continuing Education 2

MR-based Molecular Imaging and Therapy

Woo Kyung Moon, MD, PhD

Department of Radiology, Seoul National University Hospital, Seoul, Korea

In molecular imaging science, MR imaging has emerged as a leading technique because it provides high-resolution three-dimension maps of the living subject. Differential contrast in soft tissues depends on endogenous differences in water content, relaxation times, and diffusion characteristics of the tissue of interest. To increase the intrinsic contrast generated in an MR image, paramagnetic or superparamagnetic complexes are used to develop new contrast agents that can target the specific molecular marker of the cells or can be activated to report on the physiological status or metabolic activity of biological systems.

Here, we report the MR reporter gene, ferritin, induced tumor-initiating cells and show their potential for tumor initiating cells in vivo studies. Heavy chain subunit of human ferritin (hFTH) and EGFP for the MR and fluorescent images were induced by lenti-viral vector. No significant changes between control tumor-initiating cells and ferritin induced cells were observed in cell growth assay and mammosphere forming abilities. Also, analysis of cell surface markers (CD44+/CD24-/CD133-/CD49f+) and ALDH expression showed that ferritin induced cells retained the markers of breast tumor-initiating cells. MR evaluations of ferritin gene on cellular level study (TR/TE=43/10ms) and animal level study (TR/TE=34/4.4ms) were performed with a 9.4 T MR scanner. Cells were cultured with 20 uM ferric ammonium sulfate for 5 days and hFTH induced cells (10.98±0.21ms) showed decreased T2* relaxation times compared to control cells(14.73±0.34ms). In animal study, cells were subcutaneously injected in immune compromised mice and MRI scans were performed after 3 weeks of transplantation. Similar results were obtained with cell study and decreased T2* relaxation times in hFTH induced tumors were observed (10.44±0.28ms) compared to control (13.73±0.58ms).

In addition, we will show in vivo theranostics strategy for targeting breast cancer stem cells responsible for drug resistance and metastasis.

The future of molecular MR imaging is promising as advancements in hardware, contrast agents, and image acquisition methods coalesce to bring high resolution in vivo imaging to the biochemical sciences and to patient care.

Continuing Education 2

Polysaccharide-Based Theranostic Nanomedicine for Cancer Treatment

Jae Hyung Park

School of Chemical Engineering, Sungkyunkwan University, Suwon 440-746, Republic of Korea

Self-assembled polymeric micelles have received attention as nanocarriers for cancer theranostics because they can circulate in blood for long periods of time, followed by selective accumulation into tumor tissue via the enhanced permeation and retention (EPR) effect. However, delivery of the therapeutic and/or diagnostic agents into the intracellular compartments of the cancer cell is often insufficient due to their slow release from nanoparticles. For example, aliphatic polyester-based micelles, extensively studied as drug carriers, have shown sustained drug release over a period of days to weeks[6-8], although dumping the drug to the intracellular compartments of the cell in tumor tissue can enhance therapeutic efficacy. In this regard, it is necessary to develop polymeric micelles that exhibit the rapid release of the drug, triggered by intracellular stimuli such as mildly acidic pH, reductive agents, and enzymes. After reaching the tumor sites via the EPR effect, such micelles can be internalized into tumor cells by endocytosis, followed by exposure to intracellular stimuli causing burst release of the drug.

In our group, various polysaccharide-based nanoparticles, responsive to cancer-specific stimuli, have been investigated as the carrier for cancer theranostics, including hyaluronic acid, glycol chitosan, and carboxymethyl dextran. When such nanoparticles are administered into tumor-bearing mice, they selectively accumulated into the tumor site. Their *in vivo* tumor targetability were achieved via passive or active targeting mechanism. Once they reach the tumor site, the therapeutic and/or diagnostic agents were rapidly released, primarily owing to the characteristic stimuli of tumor such as the low pH, reductive envionmnent, and hypoxic condition. Overall, the stimuli-sensitive polysaccharide nanoparticles might have promising potential as the carrier for cancer therapy and imaging.

Continuing Education 2

A Novel CT-based Direct Imaging of In Situ Carotid Thrombosis and Cerebral Thromboembolism in Mice: Translational Nanomedicine

Dong-Eog Kim MD, PhD

Molecular Imaging & Neurovascular Research Laboratory
Department of Neurology, Dongguk University Ilsan Hospital

Objective: Advancing the understanding and management of thromboembolic stroke requires simple and robust new methods that would be useful for the in vivo assessment of thrombus burden/distribution and for characterizing its evolution in a prompt and quantitative manner. Animals (n5127) with experimental models of thrombosis were imaged with microcomputed tomography 5 minutes (and/or 3 weeks) after intravenous injection of glycol chitosan (GC) gold nanoparticles (AuNPs). Nanoparticles accumulated in the thrombus, allowing computed tomography visualization of both the presence and extent of primary and recurrent thrombi in mouse carotid arteries without a single failure of detection. Nanoparticle thrombus imaging was also effective in monitoring the therapeutic efficacy of thrombolysis (n=118 tissue plasminogen activator [tPA] therapies). Thrombus evolution (either spontaneous or post-tPA) could be mapped at high resolution in both space and time. Due to a long circulating half-life, GC-AuNPs remain available for entrapment into fibrin matrix for an extended period of time (up to 3 weeks), allowing repetition or ongoing monitoring of thrombogenesis and thrombolysis. This is the first report on a hyperacute direct thrombus imaging technique using thrombus-seeking AuNPs and computed tomography. When translated into stroke practice, the thrombus imaging may allow us to advance to personalized thrombolytic therapy by demonstrating thrombus burden, distribution, and character in a prompt and quantitative manner. In addition to the above data, further study results on the direct 'cerebral' thrombus imaging will also be presented.

Continuing Education 3

Development of Ga-68 labelled Radiopharmaceuticals in the Management of Neuroendocrine Tumour Imaging.

Vijay Kumar

Clinical Professor, Sydney Medical School, Sydney University & Department of Nuclear Medicine & PET, Westmead Hospital and The Children's Hospital at Westmead, Sydney, Australia

Radiolabeled tracers provide a functional imaging technique to identify neuroendocrine tumors, usually with greater sensitivity and specificity than anatomic imaging techniques such as computed tomography (CT) and magnetic resonance imaging (MRI). In the early stages of development, there were several single-photon radiopharmaceuticals have been used for the diagnostic imaging of neuroendocrine tumours: eg. ^{123}I-MIBG, 111In-DTPA-pentetreotide (Octreoscan) or ^{99m}Tc-EDDA/HYNIC-tyr3-octreotate. In particular good results were obtained with 111In-pentetreotide scanning, which visualized more than 70% of all neuroendocrine tumours and in some indications, as in gastro-entero-pancreatic (GEP) tumours, has a diagnostic sensitivity superior to that of conventional radiological imaging. Later on ^{99m}Tc-labelled hydrazinonicotinamide-Tyr3-octreotide (^{99m}Tc-HYNIC-TOC) was extensively used for the diagnosis of pathologic lesions overexpressing somatostatin receptors. ^{18}F-deoxy-glucose (FDG)-PET has also been used to diagnose tumours of neuroendocrine origin. Although ^{18}F-FDG has been successfully and widely employed in oncology, it has not demonstrated a significant uptake in well differentiated neuroendocrine tissues. Another radiopharmaceutical in development for PET was ^{11}C L-DOPA, which was shown to be useful in visualizing endocrine pancreatic tumours.

^{68}Ga labelled somatostatin analogs have emerged as the most promising agents in the past decade and have revolutionized the targeting of somatostatin receptors and in the diagnosis and treatment of neuroendocrine tumours. Clinical studies were performed with ^{68}Ga-DOTA,Tyr3-octreotide, localizing neuroendocrine tumors with higher sensitivity than 111In-diethylenetriaminepentaacetic acid-octreotide. As a result a large spectrum of analogs of sst receptors have emerged.

Among these, ^{68}Ga deserves special attention, because it is available from an inexpensive generator rendering ^{68}Ga PET-tracer, without the need for an onsite cyclotron. ^{68}Ga has a half-life of 68 min and decays by 89% through positron emission. The parent, ^{68}Ge, is accelerator produced and decays with a half-life of 270.8 d by electron capture. ^{68}Ge is strongly absorbed on metal oxides or organic material, which minimized ^{68}Ge-breakthrough in the post-processed generator eluate. Further developments are in place towards making GMP grade generators for commercial supply. Several bifunctional chelators based on 1,4,7-triazacyclononane-N,N′,N″-triacetic acid and 1,4,7,10-tetraazacyclododecane-N,N′,N″,N‴-tetraacetic acid (DOTA) macrocycles are available for coupling to peptides and other biomolecules. Recently promising reports were available on the potential of sst-antagonists compared to sst-analogs, which may generate important data in the near future.

This review summarizes the potential of several nuclear medicine techniques and radiopharmaceuticals in the diagnosis of neuroendocrine tumours and stresses the renewed role of nuclear -medicine in the management of this disease.

Continuing Education 3

Understanding and Practical Aspects of F-18 Labeling Chemistry

Dae Yoon Chi

Department of Chemistry, Sogang University, 35 Baekbeomro Mapogu, Seoul 04107, Korea

Objectives:The labeling methods of fluorine-18 to organic compounds have become more important after commercialization of FDG for PET-CT imaging. Recently, many new labeling methods have been developed both nucleophilic and electrophilic ways. Although some radiopharmaceuticals does not require high specific activities, but it is very important to prepare radiopharmaceuticals with high specific activities for the imaging the protein targets.
Methods: In this lecture of Continuing Education, F-18 labeling chemistry will be summarized to understand labeling principles as well as review in practical aspects.
Results: Production of fluorine-18 from cyclotron, characteristics of fluorine-18, nucleophilic and electrophilic fluorinations, aliphatic and aromatic fluorination, bioconjugation using prosthetic groups, and click chemistry will be reviewed.
Conclusions: Most of practical fluorine-18 labeling method will be discussed. This overview is expected to be useful for the radiochemist, nuclear medicine doctors, and nuclear medicine scientists who want to develop new F-18 labeled radiopharmaceuticals.

Continuing Education 3

Cyclotron-Produced Radiopharmaceutical for Theranostics

Yasuhisa Fujibayashi, Ph.D., D.Med.Sci

Molecular Imaging Center, National Institute of Radiological Sciences, Chiba, Japan

Growing application of positron emission tomography (PET) has induced new installation of medical cyclotrons in regional hospitals/pharmacies. In general, these cyclotrons are dedicated for the bombardment of liquid or gas target materials. However, recent advances in research on production and application of non-standard radionuclides for solid target material have realized solid target system for ultra-small cyclotron system. At present, metal target systems are provided as a optional equipment for ordinary cyclotron system, although they are considered to be still under research basis. Using such system, Cu-64, Cu-60, Cu-61, Br-77, Br-76, and so on, have been produced and used for basic as well as clinical research. Among them, Cu-64 and Br-77 are considered to be useful for targeted radionuclide therapy(TRT) with in-vivo drug monitoring using PET. In vivo drug monitoring does not limited to drug monitoring during therapy, but prognostic evaluation of therapeutic as well as adverse effect before treatment.
Recently, an a particle-emitting Ra-223 has been approved as a therapeutic radiopharmaceutical for bone metastasis of cancer, and is rapidly distributed to all over the world. a particle has very short range with high LET, and more effective than Sr-89. However, Ra-223 is a daughter of Ac-227, a part of Actinium series started from U-235 to Th-227. Elements in Actinium series are strictly regulated as “nuclear fuel” and its handling is not easy for private pharmaceutical companies. Another plausible a particle-emitting radionuclide is At-211. At-211 can be produced by Bi-209(a,2n) At-211 using a medium energy cyclotron, and binds to organic carbon as halogen. Various At-211 labeled radiopharmaceuticals can be designed.
In this talk, some examples of Cu-64, Br-76 and At-211 labeled radiopharmaceuticals will be introduced.

Continuing Education 3

Carbon-11 Labeled Radiopharmaceuticals

Jae Min Jeong

Department of Nuclear Medicine, Seoul National University College of Medicine

C-11 is an excellent radionuclide for PET, because, unlike F-18, C-11 labeled compounds are the same compounds with cold compounds. However, it requires very rapid preparation because of short half-life of 20 min. The most important and widely used C-11 labeling method is a methylation by using [C-11]methyl iodide or [C-11] methyl triflate. [C-11]methyl triflate can be synthesized from [C-11]methyl iodide by passing through a heated silver triflate column straightforwardly. Thus the synthesis of [C-11]methyl iodide is the most important procedure of C-11 radiopharmaceutical synthesis. There are two synthetic methods of [C-11]methyl iodide. One is a liquid phase and the other is a gas phase method.

Both of these methods use [C-11]CO2 as a source of C-11, which is produced by N-14 (p, a) C-11 reaction in a gas target by cyclotron. Liquid phase method use LiAlH4 solution in tetrahydrofuran to capture the [C-11]CO2. LiAlH4 is extremely sensitive to moisture and actively absorb CO2 from air. So, great attention should be paid for synthesizing [C-11]methyl iodide by a liquid phase method to prevent contact with air. The captured [C-11] CO2 is reduced to [C-11]methanol and is converted to [C-11]methy iodide by heating in HI solution. The produced [C-11]methyliodide is collected by distillation. In case of gas phase synthesis, [C-11]CO2 is reduced to [C-11]CH4 by H2 gas in the presence of metal catalyzer. Sometimes, [C-11]CH4 is produced directly in the gas target using H2 containing N2 gas. [C-11]CH4 is converted to [C-11]methyl iodide by heating in a circulating chamber containing iodine vapor. The produced [C-11]methyl iodide is collected by a condenser. Generally, gas phase synthesis is preferred to liquid, because it is easier to use and produces higher specific activity radiopharmaceuticals. The produced [C-11]methyl iodide is used to methylate various compounds and thus produce [C-11]methionine, [C-11]raclopride, [C-11]PIB, [C-11]PK11195, [C-11]flumazenil, [C-11]NMSP, and so on. On the other hand, [C-11]acetic acid is produced by using Grignard reagent, which is different from [C-11] methyl iodide. And there are many other C-11 labeled radiopharmaceuticals labeled by Suzuki reaction or by using [C-11]CO.

Continuing Education 4

Course Introduction and Basic GI Embryology

Tae Joo Jeon, MD., Ph.D

Gangnam Severance Hospital, Yonsei University College of Medicine, Korea

Objectives: Knowledge of CT anatomy is currently essential part in interpretation of PET/CT findings. However, this Knowledge is not just confined to cross sectional anatomy itself but includes embryology, histology, compartment and space related to development. In daily practice, many of these are not seen and only appear after the progression of disease. Therefore, the understanding of spatial and compartmental anatomy based on embryology and histology is obviously helpful in prediction and localization of disease extent. This CME course will extend your perspective for the differentiation, localization as well as depiction of diseases involving brain, head and neck, chest and abdomino-pelvic areas.

Check points in basic GI Embryology.

- Three layers of zygote; endoderm, mesoderm and ectoderm.
- Originl location of ventral and dorsal mesentery, celiac artery, SMA and IMA
- Rotation of mesentery and forming lesser sac and peritoneal cavity.
- Ligaments: falciform, gastrohepatic, gastrosplenic, gastrocolic and splenorenal ligaments
- Peritoneal reflection, bare area, Morison's pouch, rectal shelf, cul de sac, paracolic gutters
- Formation of greater omentum and relation to transverse mesocolon.

Continuing Education 4

Neuroanatomy for PET/CT

Hyun Seok Choi

The Catholic University of Korea

PET/CT opened new era for functional and metabolic imaging of brain. New tracers have been developed and used in clinical field. As for the brain parenchyma, PET can tell much about functional and metabolic information. However, PET/CT has innate limitation in spatial resolution and soft tissue contrast. PET/MR is recently introduced and prevalent world widely. Experts in nuclear medicine should be aware of anatomy of brain as well as sellar, pineal, cerebellopontine regions, skull base, and etc. This short lecture will cover locoregional neuroanatomy.

Continuing Education 4

CT Anatomy for Parenchymal and Interstitial Lung Disease

Chul Whan Park

Yonsei University, Korea

I. Basic terminology

Mass vs. nodule

- Mass : A localized, space-occupying lesion, solid or partially solid, ≥ 3 cm in diameter
- Nodule: A focal, rounded opacity of varying size < 3cm in diameter, which can be well or ill defined.

Consolidation vs. Ground glass opacity

- Consolidation : An increase in lung opacity, which obscures underlying vessel

- Ground glass opacity : A hazy increase in lung opacity on HRCT that is not associated with obscuration of underlying vessels (minimal interstitial thickening, partial air-space filling, a combination of both interstitial and air-space abnormality, partial collapse of alveoli, increased capillary blood volume)

Bronchiectasis
Localized or diffuse, irreversible bronchial dilatation
A result of airway disease or in the presence of lung fibrosis

Bronchiolitis
Bronchiolar inflammation, either infectious or noninfectious
It may be associated with centrilobular nodules, tree-in-bud, obstruction with mosaic perfusion and air trapping

Tree in-Bud sign
Centrilobular bronchiolar dilatation, with impaction by mucus, pus, or fluid
On HRCT, a branching or budding tree , usually visible in the lung periphery,
Indicative of airways disease (common in endobronchial spread of infection (e.g., tuberculosis), cystic fibrosis, diffuse panbronchiolitis, and chronic airways infection)

Atelectasis
A reduction in lung volume or inflation
Increase in lung opacity
Because of resorption of gas distal to an obstructing lesion, lung compression, deficiency of surfactant, fibrosis.

Mosaic Attenuation
- Differing density being visible on HRCT
- Less specific than either mosaic perfusion or mosaic oligemia,
- Used if the cause is unclear.

Reticulation
Innumerable, interlacing line shadow suggesting a mesh or net.
A descriptive term usually associated with interstitial lung disease.
interlobular septal thickening, intralobular interstitial thickening or intralobular lines, honeycombing, or resulting from parenchymal bands or irregular linear opacities

Crazy Paving
- The superimposition of GGO and a reticular pattern
- Pulmonary alveolar proteinosis (PAP), Lipoid pneumonia, ARDS, Acute interstitial pneumonia etc.

Honeycombing
- A process characterized by the presence of cystic air spaces (several mm ~ cm) with thick, clearly definable fibrous walls lined by bronchiolar epithelium.
- Pulmonary fibrosis with lung destruction, dissolution of alveoli, and the loss of acinar architecture
- Commonly clustered and share walls, are predominantly subpleural, and occur in several layers at the pleural surface

Ⅱ. Basic anatomy
Lung interstitium
- Network of connective tissue fibers : form a continuous fiber skeleton for the lung
- Generally not visible on HRCT in normal patients
- Interstitial thickening - often recognizable
- Several components : peribronchovascular interstitium, centrilobular interstitium, subpleural interstitium, interlobular septa and intralobular interstitium

Secondary Pulmonary Lobule
- Smallest HRCT unit of lung surrounded by the connective tissue septa
- Contain variable number of acini
- Irregularly polygonal in shape
- Varies in size from 10 to 25 mm in diameter
- Core structure :
  * Bronchioles : 0.15mm of wall
  * Pulmonary arteriole : 0.5-1.0 mm
  * Lymphatic vessels

Continuing Education 4

Anterior and Middle Extracranial Skull Base Anatomy

You Mie Han MD

Hallym University Dongtan Sacred Heart Hospital, Korea

The skull base is an important area since it separates the brain from the remainder of the anatomic structures in the head, including the pharynx, sinuses, eyes and ears. In addition, the skull base also contains many openings connecting the intra- and extracranial spaces. Nerves and blood vessels travel through these openings. Many different types of head and neck disease occur in this area and can directly or indirectly (perineural extension through foramina) spread to adjacent structures including bones, other spaces, and the brain. So, it is important to have a good knowledge of these structures and their

anatomical relationship for the imaging interpretation and accurate disease staging.

The sphenoid bone is an unpaired bone of the skull and consists of a central part or body, two greater and lesser wings extending outward from the sides of the body, and two pterygoid processes which projects from it below. Instead of protection of the brain like the other bones of the skull, it has a number of functions, particularly in creating tunnels through with various nerves pass. The body of the sphenoid containing sinus makes up the central portion of the middle fossa and houses the sella turcica. The lesser wing forms the roor of the orbit and has the optical canal. The greater wing forms the anterior limit of the middle skull base. The foramen rotundum, foramen ovale, and foramen spinosum lie in the greater sphenoid wing with an anteroposterior and mediolateral plane. The superior orbital fissure (SOF) is lying between the lesser and greater wings and transmits the oculomotor nerve (CNIII), the trochlear nerve (CNIV) and the abducent nerve (CNIV), the ophthalmic division of the trigeminal nerve (CNV1) and the ophthalmic vein. The foramen rotundum is located posteroinferior to the SOF and transmits the maxillary division of the trigeminal nerve (CNV2) into the pterygopalatine fossa. The foramen ovale is transmits the mandibular division of the trigeminal nerve (CNV3) and the foramen spinosum transmits the middle meningeal artery. The foramen lacerum is a triangular hole located between the sphenoid, apex of petrous temporal and occipital, posteromedial to the foramen ovale and anteromedial to the carotid canal. The posterior limit is the clivus, which is formed from the sphenoid and occipital bones. The sphenoid sinus can serve as an access route to the pituitary and the clivus.

The nasopharynx lies posteriorinferior to the sphenoid sinus and anteroinferior to the clivus along the midline. Directly superior to the nasopharynx is the foramen lacerum and the ICA, just before its entry point into the cavernous sinus. The sinus of Morgagni is a weak point in the superolateral nasopharyngeal wall. This is a region for infections or tumor to potentially invade the skull base. Behind the orifice of the auditory tube is a deep recess, the pharyngeal recess (fossa of Rosenmmüller). This is clinically significant in that it is most common site of nasopharyngeal cancer.

The pterygopalatine fossa is cone-shaped paired areas deep to the infratemporal fossa and posterior to the maxilla, located between the pterygoid process and the maxillary tuberosity, close to the apex of the orbit. It communicates with the nasal cavity, the oral cavity, the infratemporal fossa, the orbit, the nasopharynx, and the middle cranial fossa through eight foramina.

The most important anatomic structures below the anterior cranial fossa are the orbits and the paranasal sinuses. The bony orbit is often a route for intracranial spread of infection or tumors because of its direct proximity to the anterior cranial fossa. The posterior aspect includes the optic canal, SOF, and the inferior orbital fissure (IOF). They convey cranial nerves and ophthalmic vessels and communicate with the middle cranial fossa, the infratemporal fossa and the pterygopalatine fossa.

Continuing Education 5

What's Different at the Pediatric NM Department? (Setting up a pediatric nuclear medicine department)

Zvi Bar-Sever

Schneider Children's Medical Center, Israel

Nuclear medicine provides important diagnostic information in the management of pediatric diseases. Children are not "small adults". Adequate performance of pediatric nuclear medicine scans is technically challenging and requires both technical skills and expertise in the interpretation. Pediatric studies are best performed within dedicated pediatric nuclear medicine departments or in a dedicated pediatric nuclear medicine service/unit within a general NM department. The facility hosting pediatric NM studies should create a relaxed and child friendly atmosphere. This could be achieved by wall and ceiling decorations and entertainment devices (games, audiovisual entertainment) in waiting room and in the imaging rooms. Imaging young children is especially challenging due to lack of cooperation which may cause motion artifacts, limited views, improper patient positioning and avoidance of SPECT leading to a major degradation in the diagnostic utility of the scan. Motion during the study could be significantly reduced by employing distraction techniques. Audiovisual entertainment in the form of over-head TV screens is one of the best distraction techniques. Proper immobilization techniques can be effective in reducing motion artifacts during imaging. Sedation carries a small risk and may require complex logistics. It should be reserved to hybrid studies involving a CT scan and to a few selected cases of extremely uncooperative children, for example older children with mental retardation.

Technologists involved in pediatric nuclear medicine studies should have dominant personal traits of patience, and empathy which are just as important as their technical skills. Familiarity with pediatric nuclear medicine study protocols and pediatric radiopharmaceutical doses is essential. Many children and parents experience anxiety when entering the nuclear medicine department. All NM staff should be supportive and the procedure should be thoroughly explained. Reducing anxiety is effective in

achieving optimal cooperation and results in improved diagnostic quality of the scans. Physicians interpreting pediatric NM studies must be familiar with the spectrum of pediatric diseases to offer useful consultations to the referring physicians. They should be familiar with normal growth and development findings that are unique to pediatric studies at certain ages (e.g. growth centers of irregular bones). The pediatric nuclear medicine department needs to be equipped with modern cameras that with optimal sensitivity and resolution. A pinhole collimator is important especially for neonatal thyroid scans for selected indications in skeletal scintigraphy and may also be useful in DMSA scans of young infants. A pediatric nuclear medicine practice should adhere to the international guidelines on pediatric radiopharmaceutical doses. Familiarity with CT dose reduction protocols is important for pediatric PET/CT and SPECT/CT. The nuclear medicine department/unit should have access to auxiliary services such as nursing support, IV teams and anesthesia services.

Continuing Education 5

Meeting/ Workshop on Paediatric Nuclear Medicine and the Role of PET/CT in Paediatric Oncology

Hamda Saleh

Australia

Illustrative case review of few inflammatory and infective conditions in paediatrics with conventional radioisotopes and FDG-PET incorporating hybrid fusion imaging with SPECT-CT and PET-CT performed at The Children's hospital at Westmead.

These cases highlight the role of nuclear medicine imaging in detection and evaluation of pathological condition earlier, and in sites which are clinically unsuspected. With use of fusion imaging the accuracy in detection of lesion increasing significantly.

Continuing Education 5

Multimodality Imaging in Pediatric Oncology (Which Modality? Why? How?)

T. Pfluger (Munich)

University München, Germany

MRI, bone scintigraphy, MIBG scintigraphy and FDG-PET are diagnostic imaging modalities that allow visualization of morphological as well as functional features of different diseases in childhood. MRI and nuclear medicine methods are often used separately or even in competition. Some of the most important indications for both PET and MRI lie in the field of pediatric oncology. The malignant diseases in children are leukemia, brain tumors, lymphomas, neuroblastoma, soft tissue sarcomas, Wilms' tumor, and bone sarcomas. Apart from leukemia, correct assessment of tumor expansion with modern imaging techniques, mainly consisting of ultrasonography, computed tomography (CT), magnetic resonance imaging (MRI), and positron emission tomography (PET), is essential for cancer staging, for the choice of the best therapeutic approach, and for restaging after therapy or in recurrence. MRI is an excellent tool for noninvasive evaluation of tumor extent and has become the study of choice for evaluating therapy-induced regression in size of musculoskeletal sarcomas. It directly demonstrates the lesion in relationship to surrounding normal structures with exquisite anatomical detail.

Especially in children, MRI offers several fundamental advantages compared to computed tomography (CT) examinations and other whole-body imaging modalities, such as the absence of radiation exposure, non-use of iodinated, potential nephrotoxic contrast agents, a high intrinsic contrast for soft tissue and bone marrow, and accurate morphological visualization of internal structure, all of which are decisive factors in tumor staging. Due to its much higher intrinsic soft tissue contrast compared to CT, MRI has been shown advantageous in neuroradiological, musculoskeletal, cardiac, and oncologic diseases. On the other hand, CT plays a major role in the assessment of thoracic lesions and masses due to a lower frequency of movement artifacts.

Because structural abnormalities are detected with high accuracy, MRI generally has a high sensitivity for detecting structural alterations, but a low specificity for further characterization of these abnormalities. Frequently, these structural abnormalities are not reliable indicators of viable tumor tissue, especially after treatment.

It is important to emphasize that MRI and nuclear medicine methods are not competing modalities. Instead, these methods in combination can produce a synergy between function and morphology. For planning of biopsies and resective surgery the knowledge of function (i.e. tumor viability) provided by PET and MIBG scintigraphy, and of the exact morphology of the tumor provided by MRI is often crucial.

Simultaneous evaluation of both modalities is to be emphasized.

Because of MRI's low specificity in oncological staging and especially at follow-up monitoring, the application of PET and/or MIBG scintigraphy for evaluating tumor vitality is essential.

Continuing Education 5
The Role of Nuclear Medicine in Pediatric Urinary Tract Infections

Maria Lourdes B. Mania-Taylan

University of St. Tomas Hospital Espana, Manila, Philippines

Urinary tract infections are one of the most common infections in the pediatric age group. Although mortality associated with UTI are very rare, the long-term consequences of pyelonephritis (i.e. scarring leading to hypertension, diminished renal function and end-stage urinary disease) are the more common causes of morbidity later on in life. Renal imaging using ^{99m}Tc Dimercaptosuccinic acid (DMSA) is still widely considered as the gold standard for detecting scars. However, there are still issues regarding the clinical utility of ^{99m}Tc DMSA versus other imaging modalities (ultrasound, CT scan, MRI, voiding cystourethrogram) in the investigation of pediatric UTIs.

This lecture aims to review the clinical value of ^{99m}Tc DMSA, as well other renal nuclear imaging studies, which are useful in the diagnosis and management of pediatric urinary tract infection

Continuing Education 5
PET/CT Clinical Application in Children Tumors to Understand the Difference between Children and Adult Tumors in PET/CT

Hui Wang

Shanghai Jiao Tong University

Section I

Characteristic of PET/CT examination of children with tumors

1. Poor Cooperation
- Familiar problem
  1. Children can hardly express their illness clearly
  2. Children are usually full of fear and anxiety, especially of injection of radiopharmaceutical
  3. Children can hardly stay still during the examination
- Countermeasure
  1. Proper mental adjustment
  2. Detailed preparation
  3. Sedative to be administered when necessary

2. radiation dosage
- Children with tumors undergo many examinations such as PET/CT,CT, X-ray, etc. in the progress of diagnosis and therapy, which lasts about three to five years.
- Organs of children receive more radiation dosage than adults.
- The risk is higher for children's survival is longer, and the radiation dose received by the unit cell is more.
- Radiation-induced cancer risk of children is higher than adults.

3.Malignant tumor spectrum of children

4. Common physiological uptake of FDG of children
- Lymphatic tissue of pharynx
- Thymus gland
- Brown fat
- Muscle
- Epiphyses

Section II

PET/CT Application in the Diagnosis of Children Tumors

Continuing Education 6
Hepatopancreatobiliary & Gastrointestinal Anatomy

Eun-Suk Cho

Radiology, Yonsei University College of Medicine, Gangnam Severance Hospital, Korea

Computed tomography and Magnetic resonance imaging are noninvasive diagnostic imaging procedures to produce axial and orthogonal images of the body. These show detailed images of any part of the body, including the bones, muscles, fat, and organs. CT or MR scans of the liver, gallbladder, bile ducts, and gastrointestinal tracts can provide more detailed information about the organ anatomy and related structures, thus providing more information related to injuries and/or diseases of the hepatobiliary and gastrointestinal tract.

In this lecture, I will review in detail the normal anatomy of the hepatobiliary and gastrointestinal tract using cross-sectional imaging.

Continuing Education 6
Genitourinary & Retroperitoneum Anatomy

Eun-Suk Cho

Radiology, Yonsei University College of Medicine, Gangnam Severance Hospital, Korea

Computed tomography and Magnetic resonance imaging

are noninvasive diagnostic imaging procedures to produce axial and orthogonal images of the body. These show detailed images of any part of the body, including the bones, muscles, fat, and organs. CT or MR scans of the genitourinary system can provide more detailed information about the organ anatomy and related structures, thus providing more information related to diseases of the genitourinary system. It has become essential to understand the anatomy of the peritoneal and retroperitoneal spaces in order to localize disease to a particular peritoneal space and formulate a differential diagnosis on the basis of that location.
In this lecture, I will review in detail the normal anatomy of the genitourinary system and peritoneal and retroperitoneal space.

Continuing Education 6

Lung Cancer Staging by CT

Sung Ho Hwang,MD

Korea University Anam Hospital, Korea

Lung cancer staging is important for determination of effective treatment strategy and prognosis of lung cancer. Staging of non-small cell lung cancer is based on the TNM classification for describing the anatomical extent of disease consisting of the three components: T (Tumor): size and degree of regional invasion by the primary tumor N (Node): extent of regional lymph node involvement.
M (Metastasis): presence or absence of intrathoracic or distant metastases
TX: Primary tumor cannot be assessed
TO: No evidence of primary tumor
Tis: Carcinoma in situ
T1 , T2, T3, T4: Increasing size and/or local extent of the primary tumor
NX: Regional lymph nodes cannot be assessed.
NO: No regional lymph node metastasis
N1, N2, N3 Increasing involvement of regional lymph nodes
MO: Absence of metastasis
Ml : Presence of metastasis
Recent TNM staging classification is based on evidence obtained from large global database with extensive validation. Several important concepts have been included, such as subdivision of tumor categories on the basis of size, differentiation between local intrathoracic (lung, pleura and pericardium) and extrathoracic distant metastatic disease, and reclassification of separate nodules. These concepts are better correlated with prognosis and current trends in lung cancer treatment.

Continuing Education 6

Neck Node and Compartment Anatomy

Ie Ryung Yoo

Seoul St. Mary's Hospital, The Catholic University of Korea, Korea

The goal of this session is to comprehend the definitions of cervical lymph node levels on CT images, and to understand the various space anatomies and their spatial relationship in neck.
Definition of cervical LN groups (Imaging-based nodal classification)
Level IA: Lymph nodes within the triangular boundary of the anterior belly of the digastrics muscle and the hyoid bone.
Level IB: Lymph nodes lateral to the level IA nodes and anterior to the back of each submandibular gland
Level II: Lymph nodes extend from the skull base to the level of the bottom of the body of the hyoid bone. They are posterior to the back of the submandibular glands and anterior to the back of the sternocleidomastoid muscle
Level III: Lymph nodes from the level of the bottom of the body of the hyoid bone to the level of the bottom of the cricoids arch. They lie anterior to the back of SCM muscle
Level IV: Lymph nodes from the level of the bottom of the cricoids arch to the level of the clavicle. They lie anterior to a line connecting the back of the SCM muscle and the posterior-lateral margin of the anterior scalene muscle. (lateral to the carotid arteries)
Level VA: Lymph nodes from the skull base to the level of the bottom of the cricoid arch. They are posterior to the back of the SCM muscle
Level VB: Lymph nodes from the level of the bottom of the cricoid arch to the level of the clavicles. They lie posterior to the line connecting the back of the SCM muscle and the posterior-lateral margin of the anterior scalene muscle.
Level VI: Lymph nodes between carotid arteries from the level of bottom of the body of the hyoid bone to the level of the top of the manubrium
Level VII: Lymph nodes between carotid arteries below the level of the top of the manubrium and above the level of the innominate vein
Supraclavicular nodes: Lymph nodes lie at or caudal to the level of the clavicles and lateral to the carotid artery. They are also above and medial to the ribs
Retropharyngeal nodes: Lymph nodes lie within 2 cm of the skull base and medial to the internal carotid arteries
Other superficial nodes are referred to by their anatomic names (e.g. occipital nodes)
Space anatomy of the neck
Suprahyoid neck (SHN): Spaces from skull base to hyoid

bone (excluding orbit, sinuses & oral cavity) including parapharyngeal (PPS), pharyngeal mucosal (PMS), masticator (MS), parotid (PS), carotid (CS), buccal (BS), retropharyngeal (RPS) and perivertebral (PVS) spaces.
Infrahyoid neck (IHN): Spaces below hyoid bone with some continuing into mediastinum including visceral (VS), posterior cervical (PCS), anterior cervical (ACS), CS, RPS and PVS.

Three layers of deep cervical fascia cleave neck into spaces

1.Superficial layer, deep cervical fascia (SL-DCF)

- SHN: Around MS and PS; part of carotid sheath
- IHN: Invests neck by surrounding strap, SCM and trapezius muscles

2. Middle layer, deep cervical fascia (ML-DCF)

- SHN: ML-DCF defines PMS deep margin; contributes to carotid sheath
- IHN: Circumscribes VS; part of carotid sheath

3. Deep layer, deep cervical fascia (DL-DCF)

- SHN & IHN: Surrounds PVS; contributes to carotid sheath
- SHN & IHN: Ala fascia is slip of DC-DCF

Providing lateral wall of RPS & DS; also posterior wall to RPS separating RPS from DS
Key spatial relationships
SHN spaces surrounding PPS

- Medial is PMS: PMS mass displaces PPS laterally
- Anterior is MS: MS mass displaces PPS posteriorly
- Lateral is PS: PS mass displaces PPS medially
- Posterior is CS: CS mass displaces PPS anteriorly
- Posteromedial is lateral RPS: Lateral RPS nodal mass displaces PPS anterolaterally

Current Issues 1

Clinical PET Beyond ^{18}F-FDG in Taiwan

Ruoh-Fang Yen, MD, PhD

Department of Nuclear Medicine, National Taiwan University Hospital

Department of Radiology, National Taiwan University College of Medicine ^{18}F-FDG, a glucose analog, which substitutes a fluorine atom for the hydroxyl group at C-2 on glucose, is a useful radiopharmaceutical for measuring in vivo biodistribution of glucose metabolism. It has been widely used in diagnosis, staging and follow-up of several malignancies. In addition, there are several other PET probes, such as ^{18}F-NaF for bone metastases, ^{18}F-fluorothymidine and ^{18}F-fluorocholine for cell proliferation, ^{18}F-fluordopa for dopaminergic neuron integrity and neuroendocrine tumors, etc. In addition, there are brain imaging tracers, including ^{11}C-PIB for β-amyloid, T-807 for tau protein, ^{18}F-fallypride for D2 receptor, etc. I would give an introduction on the PET tracers available at present in NTUH PET and Cyclotron center.

Current Issues 1

Applications of PET/CT in External Beam Radiation Therapy Dose Planning

Kalevi Kairemo

Visiting Professor, The University of Texas MD Anderson Cancer Center, Houston, TX. Chief Physician, Molecular Radiotherapy & Nuclear Medicine, Docrates Cancer Center, Helsinki, Finland

FDG-PET and PET/CT add information to the staging of patients with many solid cancers, such as lung cancer, head & neck cancer, GI cancers, lymphomas, melanoma, sarcomas etc. Other PET tracers can be used e.g. for staging of brain, prostate & breast cancers. External beam radiation therapy (EBRT) is an essential treatment modality in many of these malignancies.
In practice, molecular imaging based on PET/(SPECT) is the only modality in defining biological target volume (BTV) for EBRT. However, it is not yet widely used and there are no prospective randomized studies available.
Retrospectively, the EBRT response has been analyzed in a preliminary when dose planning was based on BTV target definition by comparing clinical and biochemical results of dose planning modulated therapy in group of 14 prostate cancer patients with PET/CT and conventional dose planning VMAT (RapidArc) (Kairemo et al., Curr Radiopharm, 2015; 8: 2-8). Patients with PET/CT dose planning VMAT had less incidence of biochemical relapse, clinical manifestation of diseases and longer statistically significant duration of disease free period and biochemical stability as compared to patients treated conventional dose planning VMAT.
Now, we apply this routinely in the daily praxis: besides FCH, we have experience of using ^{18}F-FACBC-PET and combinations with Na^{18}F-PET. PET based EBRT applications to dominant intraprostatic lesions require still further development.
Hypoxia is a key player in the resistance to EBRT in many cancers. Dose definition and planning should be based on combined information from FDG and hypoxia tracer PET/CT studies.
PET/CT should be part of EBRT development, because existing preliminary results are very
encouraging.

Current Issues 1

PET-CT for Lung Cancer Patients

Chiu Ming Lok

Hong Kong Baptist Hospital, Hong Kong

^{18}F-fluorodeoxyglucose (^{18}F-FDG) positron emission tomography (PET) has been widely used in the management of lung cancer. ^{18}F-FDG PET-CT can offer information on the diagnosis, the extent of disease, the treatment response and the likely prognosis when the best management option has been decided.

It would be a great challenge in PET-CT imaging of solitary pulmonary nodule (SPN). The sensitivity and specificity of PET-CT imaging will be affected by the size of the pulmonary nodule, its metabolic activity and the prevalence of benign causes of SPNs in a given population. There are many reported causes of false positive findings such as tuberculosis, cryptococcus & aspergillus infection, neurofibroma and Wegener's granulomatosis. On the other hand, malignancy such as bronchioloalveolar carcinoma may have low FDG avidity. There is promising performance of PET-CT in staging of non-small cell lung cancer (NSCLC), especially for the nodal staging in mediastinum and the assessment of distant metastases.

Correct staging is the most essential in planning for subsequent appropriate treatment. PET-CT may detect nodal lesions with FDG hypermetabolism even that they appear normal in size. PET-CT is demonstrated superior to CT alone on evaluation of mediastinal nodal status and detecting unexpected distant metastasis. These factors decide whether a patient would be a suitable candidate for surgery.

PET-CT also helps in radiotherapy planning. The extent of FDG-avid tumour can be better defined especially when it is located within a collapsed or consolidated lung zone. More accurate radiation portals may save normal tissue and improve treatment outcome. The change in FDG avidity of tumour is a good indicator of treatment response, which often occurs in advance of anatomical alternation. The fractional change in tumour glucose metabolism after initial cycles of chemotherapy also shows high predictive information on treatment outcome. PET-CT is also a powerful tool in the detection of tumour recurrence.

Molecular genotyping of lung cancer and the use of various tyrosine kinase inhibitors are hot topics in the management of lung cancer. The role of PET-CT imaging, with the use of new radiopharmaceuticals not limited to F18-FDG, needs to be explored.

Current Issues 1

Application of PET/CT in China

Yaming Li

The 1st Affiliated Hospital, China Medical University, China

By the end of 2013, there are 838 units related to nuclear medicine practice in China, 615 departments of nuclear medicine, 13 isotope departments, 10 RIA centers, 12 ECT units. 57.8% of departments of nuclear medicine with outpatient, 22.9% with therapy wards, 65.0% with SPECT(including SPECT/CT), 45.9% with RIA lab.

With 201 sets of PET or PET/CT and 87 medical cyclotrons, a total of 446,183 patients were examined in 2013, 45.3% increased compared with 2011, with 81% tumor, 14% tumor screening, 1% cardiovascular disease, 2% nervous system disease, 2% others.

Challenge faced are 1) The examination is effective but price high, and has a low reimbursement ratio. 2) The training of the working team need to be strengthened in order to adapt to the rapid developments.

Current Issues 2

ICRP Activities on Radiological Protection in Medicine

Keon Wook Kang, MD, PhD

Department of Nuclear Medicine, Seoul National University College of Medicine

The International Commission on Radiological Protection (ICRP) is an independent, international organization for developing, maintaining, and elaborating radiological protection standards, legislation, guidelines, programmes, and practice since 1928. ICRP is comprised of a Main Commission, five standing Committees, Task Groups and Working Parties. Committee 3 is concerned with protection of persons and unborn children when ionising radiation is used for medical diagnosis, therapy, and biomedical research. Until now, ICRP has published 129 publications on all aspects of radiological protection including fundamental recommendations, each describe the overall system of radiological protection. The basic principles of justification, optimisation and dose limitation are introduced by ICRP Publication 26 at 1977. Committee 3 published Protection of the Patient in Nuclear Medicine, Radiation Dose to Patients from Radiopharmaceuticals (jointly with Committee 4), Radiological Protection in Medicine, Pregnancy and Medical Radiation, Release of Patients after Therapy with Unsealed Radionuclides for issues relating nuclear medicine. Currently Task Group 36

is preparing an update of Radiation Dose to Patients from Radiopharmaceuticals, and Working Parties are preparing drafts for Diagnostic Reference Levels for Diagnostic and Interventional Imaging, and Radiological Protection in Therapy with Radiopharmaceuticals. In October 2015, the 3rd ICRP symposium and meeting was held and current progresses was discussed and updated in Seoul, Korea.

Current Issues 2

Diagnostic Reference Levels in Nuclear Medicine Imaging

Ho-Chun Song, M.D., Ph.D

Department of Nuclear Medicine, Chonnam National University Hospital, Medical Radiation Safety Research Center

Medical exposure remained by far the largest artificial sources of exposure and continues to grow significantly. The basic principle of radiological protection of patients in diagnostic and interventional x-ray procedures and nuclear medicine imaging is that necessary diagnostic information of a clinically satisfactory quality should be obtained at the expense of a dose as low as reasonably achievable, taking account of social and economic factors. The basic principles of radiation protection recommended by the International Commission on Radiological Protection (ICRP) are justification, optimisation and dose limitation. The basic aim of this optimisation of protection is to adjust the protection measures for a source of radiation in such a way that the net benefit is maximised. In the case of exposure from diagnostic and interventional medical procedures, the diagnostic reference levels (DRLs) has as its objective the optimisation of protection. The concept of DRLs was introduced by ICRP Publication 60 in 1990 as a form of investigation level used to identify situations where optimisation of protection may be required in the medical exposure of patients, and the use of DRLs was recommended in ICRP Publication 73 with further guidance in Supporting Guidance 2. The most recent ICRP publications 103 and 105 summarise previous definitions and recommendations about DRLs. The objective of DRLs is to help avoid radiation dose to the patient that does not contribute to the clinical purpose of a medical imaging task. DRLs can be used to improve a regional, national, or local distribution of observed results for a general medical imaging task, by reducing the frequency of unjustified high or low values, and to promote attainment of a narrower range of values that represent good practice for a more specific medical imaging task and to promote attainment of an optimum range of values for a specified medical imaging protocol. DRLs are not intended for individual patients and are not dose limits. DRLs should be based on clinical practice. Image quality must not be neglected. For nuclear medicine, DRLs are established in terms of the administered activity per kg body weight of a specific radionuclide for a specific clinical task and, if relevant, the radiopharmaceutical used, and the administered activity should be adjusted for patient weight for examinations where the radiopharmaceutical is distributed throughout the body. DRLs for nuclear medicine imaging procedures may include both minimum and maximum activities. DRLs have proven to be an effective tool for optimisation of radiological protection in the medical exposure of patients. Professional medical bodies in conjunction with national health and radiological protection authorities are encouraged to set DRLs that best meet their specific needs and that are consistent for the national area to which they apply.

Current Issues 2

Estimation of External Radiation Dose to Caregivers during Radionuclide Therapy

Jae Won Jung

East Carolina University, USA

Due to the remarkable increase in thyroid cancer cases, the number of patients treated with radioiodine (I-131) shows a sharply increasing trend in recent years. Accordingly, radiation exposure of other people, particularly caregivers or comforters, after release of patients from hospitals is getting more attention than ever. In the talk estimation of doses to caregivers and appropriate quarantine periods will be discussed. To reflect the degree of engagement between the caregiver and the patient, considering the duration and distance between two during exposure, the engagement factor has been introduced. The speaker will discuss how to estimate the engagement factor. The pattern of patient care and timing of exposure will also be discussed for a few patient cases.

Current Issues 2

Education and Training for the Radiation Safety Related to the Radiopharmaceutical

Emilija Janevik-Ivanovska[1], Uday Bhonsle [2], Marina Zdraveska-Kocovska[5], Zdenka Stojanovska[1], Adriano Duatti [3], Zoran Zdravev [4], Meri Angeleska[5], Osso Júnior João Alberto[2], Meera Venkatesh[2]

1. Faculty of Medical Sciences, Goce Delcev University, Stip,

Republic of Macedonia
2. Radioisotope Products and Radiation Technology Section, Division of Physical and Chemical Sciences, IAEA, Vienna, Austria
3. Laboratory of Radiopharmaceutical Chemistry, Department of Chemical and Pharmaceutical Sciences, University of Ferrara, Italy
4. Faculty of Medical Sciences, Goce Delcev University, Stip, Republic of Macedonia,
5. Institute of Pathophysiology and Nuclear Medicine, Faculty of Medicine,University Ss Cyril and Methodius, Skopje, Republic of Macedonia

Objectives: The importance of education and training for the radiation safety related to the radiopharmaceuticals became a need in all area of production and application of radiopharmaceuticals, for clinical and research purpose. To create the educational program and training that include application of International Basic Safety Standards for Protection against Ionizing Radiation and for the Safety of Radiation Sources (BSS) together with Good Radiopharmaceutical Practice is one of general starting point to cover all the aspect of the application of radiopharmaceuticals for diagnostic, both SPECT and PET and therapeutical purpose for all practices and interventions.

Methods: To establish the program of education and training for Good Radiation Safety Practice related to the usage of radiopharmaceuticals is important tool for all individuals working with radiopharmaceuticals. They have a responsibility to take all reasonable precautions to protect patients; to protect members of the general public; to protect their colleagues; and most importantly to protect themselves from unnecessary exposure to ionizing radiation.

Education and suitable training that include regular and continuing education as an formal and not formal approach in: Design and construction of facilitieas of production and application of radiopharmaceuticals;

Local radiation safety rules and procedures for quality control;Preparedness;Equipment;

Monitoring of the personnel and environment.

Results: All types of education and training in national and international level must to ensure that all radiopharmaceutical preparations and administration procedures should be carried under well-defined and controlled conditions. Good housekeeping is important and all work areas should be kept clean and tidy, all radionuclide containers must be safely stored and readily available, adequate supplies of consumables must be available within easy reach of staff performing radiopharmacy work, unnecessary visits to the radiopharmacy should be discouraged and contaminated sharp items such as needles must be safely stored behind shielding.

Regular obligatory records should be kept of: Receipt and disposal of radioactive materials;

All individual preparations for patient administration, including the patient's name, radiopharmaceutical used, activity and date; Quality control testing of the radionuclide calibrator and other instruments

Regular surveys (preferably weekly) of contamination must be performed. A decontamination kit should be held in or near the radiopharmacy.

A sensitive radiation monitor must be available at all times in the radiopharmacy for contamination checking, not only of surfaces, but also ofhands, clothing and disposables.

Conclusions: To have well trained competent staff who have the necessary skills and knowledge to deal with radioactive pharmaceutical products must be the goal of each institution involved in production and application of radiopharmaceuticals including its own quality assurance programme to ensure that the products administered to patients are of the desired quality.

This requires to develop an appropriate education and training for the radiation safety related to the radiopharmaceuticals as one of the vital component in the assurance of quality of administrated radiopharmaceuticals.

Current Issues 2

Nuclear Medicine Leadership in Radiation Accidents

Sobhan Vinjamuri

Sobhan Vinjamuri, Royal Liverpool University Hospital

Radiation Accidents are becoming an important matter for hospitals and health care service planners. Preparedness for possible accidents is very important, roles and responsibilities of key personnel within health care settings needs to be clearly defined.

In this plenary lecture, I will cover the various roles and responsibilities required for the preparation for radiation accidents and explore the possible role for Nuclear Medicine Professionals to contribute in a leadership capacity.

Current Issues 3

Developing a Personalized Model of PRRT Based Upon Molecular Imaging: Will it be a Realistic Approach?

Sandip Basu

Radiation Medicine Centre, Bhabha Atomic Research Centre, Tata Memorial Centre Annexe, Parel, Mumbai, India

Neuroendocrine tumor (NET) is a widely heterogeneous

group of tumors demonstrating varying tumor biology. Molecular functional imaging has the potential to explore and probe this varying biology which can be translated to development of a personalized model in the management of this group of tumors [1]. It is important in the coming years to examine the molecular imaging features vis-à-vis the histopathological parameters such as the Ki-67 or MiB1 index, which would aid in better understanding of the disease biology and prognosis and thereby select the most appropriate treatment approach on an individualized basis.

Current Issues 3

Ten Years Experiences Of Radioactive Iodine Therapy In Myanmar Thyrotoxicosis Patients

Kyin Myint

Department of Nuclear Medicine, Yangon General Hospital, Yangon, Myanmar

Objectives: Department of Nuclear Medicine, Yangon General Hospital, Yangon was the first center in MYANMAR, using radioactive sources for diagnostic and therapeutic applications since 1963. The centre performs routine planar and SPECT imaging and Radioimmunoassay of thyroid hormonal profile with kind guidance and assistance of Government of Myanmar and IAEA.1 Thyrotoxicosis and Papillary Carcinoma of Thyroid become the most common cause of morbidity in MYANMAR after the IDD project in 1989. Number of cases has been increasing year by year since then, because of dietary habit of the people (Salted fish and fish paste). Thyroiditis and Iodine induced thyrotoxisis have to be differentiated from Thyrotoxicosis by ^{99m}Tc thyroid scan. ^{131}I therapy for thyrotoxicosis had been initiated in MYANMAR since 1967, because of awareness of the referring Physicians as a simple and cost-effective remedy in the management of Thyrotoxicosis.

Method: This is the retrospective study of the Department of Nuclear Medicine, Yangon General Hospital. Radioactive Iodine-131 and ^{99m}Tc have been imported from ANSTO, Australia. As it is very costly, only 11,100 MBq per month is imported from year 2005 to 2010. It is insufficient for increasing number of cases. The individualized dose range is 148-370 MBq, only on the basis of thyroid hormonal profile. The new Government took in action in 2011 and increased Health budget 4 folds year by year. We can use up to 37 GBq per month, free of charge to the patients. The dose range is 296–555 MBq, after screening with ^{99m}Tc thyroid scan and uptake, Ultrasound, thyroid hormonal profile, and clinical manifestations. But, it is still insufficient and we are looking forward to using high dose therapy with ^{131}I capsule.

Results: We treated 1164 patients during 5 years (2005-2009) and 929 patients in next 5 years (2010-2014). Female to male ratio is 20:1. The low dose therapy without screening leads to early Hypothyroid even at the dose as low as 148 MBq (40%). Because, Thyroiditis and Iodine induced thyrotoxicosis are misdiagnosed as Thyrotoxicosis. Regarding the screening protocol and complete blood picture, number of ^{131}I therapy patients reduced as well as the incidence of early Hypothyroid (25%). The second most common complication of ^{131}I therapy is exophthalmos (Proptosis).

Conclusion: ^{131}I therapy in Myanmar Thyrotoxicosis patients is a safe, simple, non-invasive, and cost-effective remedy. The incidence of early hypothyroid was reduced by the available screening method prior to ^{131}I therapy. Government's interest plays a vital role in effective use of high-costly imported radiopharmaceuticals for the management of thyrotoxicosis patients.

Key words: Thyrotoxicosis, Iodine-131 therapy, ^{99m}Tc thyroid scan, exophthalmos

Current Issues 3

Management of Radioiodine Refractory Thyroid Cancer

Pradhan PK

Department of Nuclear medicine,Sanjay Gandhi Postgraduate Institute of Medical sciences (SGPGIMS),Lucknow, India

Objectives: Differentiated thyroid cancer accounts for 95% of all thyroid cancers worldwide. The general management is by surgery, radioiodine and levothyroxine suppression therapy. About 7-23% of these patients manifest metastasis. And out of these, 2/3rd become refractory to radioiodine eventually.

ATA 2014 guidelines have defined radioiodine-refractory cases as structurally-evident DTC in patients with appropriate TSH stimulation and iodine preparation in four basic ways: the malignant/metastatic tissue does not ever concentrate radioiodine (no uptake outside the thyroid bed at the first diagnostic or therapeutic WBS), the tumor tissue loses the ability to concentrate radioiodine after previous evidence of RAI-avid disease, radioiodine is concentrated in some lesions but not in others; metastatic disease progresses despite significant concentration of radioiodine.

Several genetic alteration have been known (RET/PTC, BRAF600E etc).In most of these radioiodine negative patients, ^{18}F-FDG PET/CT was performed to localise the

disease for planning further treatment.

Methods: Redifferentiation therapy, kinase inhibitors and lutetium DOTATATE therapy will be dicussed in this brief lecture. Patients were administered 13cis retinoic acid (RA) in 24 patients which were having persistent disease and were radioiodine negative on diagnostic I 131 scan in follow up. All patients received RA in dose of 1.5 mg/kg/bw for 6-12 weeks. Then,S.thyroglobulin, diagnostic I-131 scan were performed following 4 weeks stoppage of levothyroxine /rhTSH. Patients who showed good response to the therapy indicated by a positive I 131 scan and were further continued on the radioiodine therapy repeatedly.

Results: We evaluated total 24 patients (12 male and 12 female). Out of these 20 were diagnosed papillary carcinoma thyroid (recurrence, pulmonary or cervical lymph nodal metstasis), 01 follicular carcinoma thyroid and 01 poorly differentiated carcinoma thyroid and 02 were hurthle cell variants. Among them ,04 patients treated with RA showed increased tracer uptake, rest 20 patients were radioiodine negative. The patients which turned positive on iodine scan were treated with 100-150 mCi of radioodine depending on the disease burden . Post radioiodine changes in serum thyroglobulin level was noted in addition to enhanced radioiodide transport and clinical improvement.

Conclusion: These data suggest that RA redifferentiation therapy, considering especially its comparatively mild side effects (mucositis), 6 weeks intervention and reasonable cost may represent an alternative therapeutic approach to watchful anxious follow up.Our findings suggest that 13 cis retinoic acid therapy especially 06 weeks protocol is safe and effective ,may induce radioiodine uptake and reduce serum thyroglobulin levels in some patients with DTC, but whether this results in clinically significant response can only be ascertained on long-term follow-up.

Current Issues 3

Outcome of Well-Differentiated Thyroid Carcinoma Patients Receiving a umulative Doses of ≥600mci (22GBq) of I-131

Faria Nasreen

Associate Professor, National Institute of Nuclear Medicine & Allied Sciences, Dhaka

There is no maximum limit for cumulative dose of I-131 for persistent disease in well differentiated thyroid carcinoma (DTC) patients. However, most remissions are obtained with cumulative activity equal to or lower than 600mCi (22GBq). On the other hand a significantly increased risk of leukemia and secondary cancers has been reported with high cumulative dose of I-131 (≥600mCi). Several studies regarding factors related to refractory therapy has been done. DTC patients with follicular variant, ≥45 years of age having bone metastasis and significant thyroid remnant do not have a favourable outcome in spite of high cumulative doses of radioiodine. DTC patients with higher TNM stage and bone metastasis require higher and more radioiodine doses. However, above 22GBq cumulative activity further radioiodine therapy should be taken on an individualized basis.

Key Words: Well differentiated thyroid carcinoma, Cumulative Dose, 600mCi (22GBq) I-131

Current Issues 4

Enforcing Nuclear Medicine in Modern Oncology Practice & Updates on Arab Society of Nuclear Medicine (ARSNM)

Akram Naif Al-ibraheem

King Hussein Cancer Center, Jordan

Enforcing nuclear medicine in oncology practice can be achieved through multiple approaches including; Investing in human resources, Integrating into multidisciplinary fashion & Speaking the oncology language, Standardization & focusing on quality and Introducing new technologies. Implementation of personalized medicine and targeted medicine is new benchmark inn oncology practice; a niche where nuclear medicine can play a major role. In this regard, Establishing nuclear medicine therapeutic clinic is considered essential. In the era of hybrid modality, highlighting strengths & realizing limitations to other imaging modalities are important for nuclear medicine staff. Collaboration at national and international levels as well as participating in multicentric research and utilizing IAEA activity would have significant influence in enforcing nuclear oncology practice.

Arab Society of nuclear medicine which was established during the recent meeting of the IAEA –run regional ARASIA project (strengthening Nuclear Medicine Applications through Education and Training to Help Fighting Non-Communicable Diseases in the Arab Asian member states) ; held in Vienna 17 - 21 November 2015. This establishment was achieved by the national representative of the participating Arab countries in this project and it was agreed that Amman-Jordan will be the base for this society in the commencement phase. The goal of this society is to establish co-operation between

Nuclear Medicine & Molecular Imaging professionals, groups, societies active in the field of nuclear medicine in the Arab world and to cooperate and affiliate with the regional and international established nuclear medicine societies and to establish technical standards, to aid in the diffusion of knowledge and exchange of scientific and technical information by means of conferences, colloquia, symposia and course on regional and international levels.

Current Issues 4

Role of ^{18}F-FDG-PET/CT in the Evaluation of Head and Neck Squamous Cell Carcinoma

Mohamad Haidar

American Hospital Of Beirut

Since its implementation in the evaluation and monitoring of squamous cell carcinoma of the head and neck, PET/CT has become the imaging modality of choice for this category providing anatomical and metabolic information at once. ^{18}F-FDG-PET/CT is useful in identifying a cancer of unknown primary, extension of the primary tumor, detection of regional lymph node involvement even with infracentimetric lymph node, detecting a metastatic lesion and in few instances identifying a synchronous primitive tumor. It provides a vital role in assessing the response to treatment, monitoring the long-term recurrence and recently in planning radiotherapy.

Current Issues 4

Education/Training and Nuclear Cardiology

Batool Al Balooshi

Dubi Health Authority-Dubai Hospital, UAE

In Recent years, there has been a growing demand in nuclear medicine Technology and science worldwide, particularly in some Asian countries where limited infrastructure presently exists, based on cancer and cardiovascular disease management projects. The strengthening of national nuclear medicine capacities among Member States across different regions has enabled stronger regional cooperation among developing countries.

This type of support has been essential for the development and expansion of nuclear medicine especially in low-and middle-Income countries. The need for basic as well as specialized clinical training in was identified as apriority for health care providers in many countries. Since few years, IAEA introduced an educational program through its technical cooperation for Asian Arab countries under ARASIA project, which include trainings, workshops and scientific visits for participants. Also this project support conduction of national projects by providing expert visits and an overall assessment of nuclear medicine facilities prior to IAEA accreditation.

So far, two course for basics and advanced nuclear cardiology using PET and SPECT/CT was conducted In Dubai and Amman and there was great contribution not only among nuclear medicine physicians but also among also other medical professionals.

The increasing demand by nuclear medicine institutions to achieve high quality standards in the clinical applications has greatly affected IAEA programs and rapidly generated a remarkable number of activities and training courses especially in the Asian Arab countries.

Current Issues 4

First Nuclear Medicine in Yemen: A woman Behind

Fairoz Mohammed

Head Of the Nuclear Medicine Center , Yemen

First Idea: 2001 –Opened the first NMC in 2008 (Long Story in Between).

-Became IAEA coordinator for the NM project 2005

-Personnel trained, equipment arrived and installed. First patient July 2008.

Unexpected Difficulties of Local Type1:

- National Regulator has created radiation phobia over the year among government officials.
- Had to get clearances every two weeks from 5 different official governments entities (MoE, MoD, Intelligence, National Security, Nuclear Regulator, and Civil Aviation Authority).

How to Address:

- Made presentations to all to educate them on the subject.
- Had separate meetings with each .
- Final convinced to give one year permit.
- Problem solved (took one year).

Supply of reagents: New Challenges:

- Only two in the region: Syria and Turkey. Difficulties from ,currently only Turkey source.

Unexpected Difficulties of Local Type2:

- Trained 5 physicians -males, all left the country for better pay.
- One remained behind "The Speaker".(Run both the private and the public (morning in public and afternoon in private).
- There are many fresh GP doctors under training to be able to support NM field.

Future:

- Finished the planning for the new Nuclear Medicine Facility in Aden city.
- Will introduce PET/CT (more advance technique and costly) into my center (Korea is the donating country!!!).
- Promote the establishment of new centers in other cities.

Current Issues 5

Molecular Imaging for Infection using Radiolabelled Nanoprobes: from Bench to Bedside

G.P.Bandopadhyaya [1], Jaya Shukla[2]

1. Ex Professor, Department of Nuclear Medicine & PET-CT,AIIMS,New Delhi
2. Associate Professor, Department of Nuclear Medicine & PET-CT,PGI Chandigarh

Imaging infection remains a major challenge. The infection and inflammation have overlapping characteristics. The prime importances of our goal oriented bench to bed studies were to differentiate between aseptic and septic pathologies for the patient management. This suggests that the best way to identify infection and to image the organism responsible for infection.

It is well known that the incidents of infection are lower in infants on only breast feed.The reason being is the oligosaccharides present in the breast milk act as soluble receptors for different pathogens which protect the infantsfrom infection. The Maltose is an oligosaccharides and the monomeric periplasmic Maltose binding proteins (MBP) are present on bacterial cell membrane. MBP plays an important role in the transport and chemotaxis of bacteria.Besides binding to oligosaccharides, MBP can also bind to cyclic maltodextrins like cyclodextrins without inducing any chemotactic response. Additionally, the binding proteins of ABC-transporter of gram positive bacteria also exhibit high similarity with MBPs of gram negative bacteria also possess a cyclodextrin-binding site.

We have exploited MBP of bacteria to image active infections. Hydroxypropyl-β-cyclodextrin, a FDA approved cyclodextrin derivative, has been labelledwith technetium-99m (^{99m}Tc-HPβCD) using stannous chloride reduction method. The quality control of ^{99m}Tc-HPβCD was performed by ITLC. The cyclodextrin has the property of self-aggregation and therefore present as ^{99m}Tc-HPβCD nanoprobes in the solution. The formulation was characterized by electron microscopy and 1H-nuclear magnetic resonance. The MBP –HPβCD interaction was studied by docking studies using Autodock software. The ^{99m}Tc-HPβCD demonstrated good labelling efficiency (>98%)and was stable. The route of excretion of ^{99m}Tc-HPβCD nanoprobes was assessed in rats. These radiolabelled nanoprobes were injected in human subjects with clinically confirmed infected knee joints and other prosthesis.

The size of ^{99m}Tc HPβCD nanoprobes was between 60-180µm. The 1H NMR studies revealed the binding of ^{99m}Tc at C-8/H-8 position of HPβCD. The excretion of ^{99m}Tc HPβCD was via renal route. Docking studies demonstrated the interaction between HPβCD and bacterial maltose binding protein. The single photon emission tomography (SPET) was done to differentiate septic and aseptic infection. However, low density of bacterial population is difficult to image.

The data indicated that ^{99m}Tc HPβCD nanoprobes can be used for molecularimaging of infection.

Current Issues 5

Preclinical and Translational Researches of Novel PET and SPECT Tracers: [^{18}F]DiFA and [^{123}I]IIMU for Hypoxia and Thymidine Phosphorylase Imaging

Songji Zhao[1], Ken-ichi Nishijima[1], Hiroki Matsumoto[2], Hiromichi Akizawa[3], Kazue Ohkura[4],Nagara Tamaki[1], Yuji Kuge[1]

1. Hokkaido University
2. Nihon Medi-Physics Co. Ltd.
3. Showa Pharmacetical University
4. Health Sciences University of Hokkaido

Translational research bridges basic science and clinical applications, which in turn provides meaningful health-related outcomes. Molecular imaging is a rapidly developing discipline and forms many imaging modalities, providing us effective tools for visualizing, characterizing, and measuring molecular and cellular mechanisms in complex biological processes in living organisms, thereby deepening our understanding of biology and accelerating

preclinical research including cancer study and medicine discovery. It bridges the gap between in vitro exploratory and in vivo clinical research, facilitating the direct and rapid transfer of preclinical studies using animal models to clinical investigation in humans. Recently, we have developed novel PET and SPECT tracers, a hypoxia tracer, 1-(2,2-Dihydroxy-methyl-3-[^{18}F]Fluoropropyl Azomycin ([^{18}F]DiFA), and a radiolabeled uracil derivative, ^{125}I or ^{123}I-labeled 5-iodo-6-[(2-iminoimidazolidinyl) methyl]uracil ([^{125}I] or [^{123}I]IIMU) for hypoxia and thymidine phosphorylase imaging, respectively. In this lecture, I would like to introduce our experiences in the preclinical and translational research on both novel PET and SPECT tracers at Hokkaido University.

1. Preclinical and translational research on novel PET tracer, [^{18}F]DiFA, for hypoxia imaging

Hypoxia generated in solid tumors is associated with poor prognosis and has been implicated as a major factor in the resistance of tumors to both irradiation and chemotherapy. The detection of hypoxic regions in tumors provides much broader insights into the responses of targeted therapies and the selection of the therapeutic strategy. The PET tracer [^{18}F]FMISO has been widely used for imaging hypoxic regions in clinical studies. However, owing its high lipophilicity, [^{18}F]FMISO has slow clearance from nonhypoxic regions and a substantially low signal-to-background ratio. The limitation of [^{18}F]FMISO is its long waiting time; 4 h is required to acquire reproducible images. To image tumor hypoxia with higher contrast and shorter waiting time in comparison with a common hypoxia tracer [^{18}F]FMISO, we have recently designed and synthesized a new hypoxia tracer, [^{18}F]DiFA. In a biodistribution study, [^{18}F]DiFA displayed significantly higher tumor-to-muscle and tumor-to-blood ratios than [^{18}F]FMISO at 1 h postinjection. Ex vivo autoradiography showed a significant positive correlation between [^{18}F] DiFA uptake and regions of pimonidazole distribution, indicating that [^{18}F]DiFA selectively accumulated in tumor hypoxic regions. A PET imaging study showed a time-dependent increase in the tumor-to-normal tissue ratio of [^{18}F]DiFA levels. These findings suggest that our new tracer, [^{18}F]DiFA, may provide a better contrast image of tumor hypoxia with shorter waiting time for imaging than [^{18}F]FMISO. The manufacture and quality control of [^{18}F]DiFA were established under the quality control standards for clinical studies at Hokkaido University. [^{18}F]DiFA injection was shown to be safe and useful in preclinical studies. These findings support the feasibility of clinical studies of [^{18}F]DiFA in the near future.

2. Preclinical and translational research on novel SPECT tracer, [^{123}I]IIMU, for thymidine phosphorylase imaging

Thymidine phosphorylase (TP) regulates intracellular pyrimidine metabolism through the reversible deoxyribosylation of thymidine to thymine. TP expression correlates well with tumor malignancy, including infiltration, and metastasis, and overall poor survival. Moreover, TP is essential for the bioactivation of 5-fluorouracil and its prodrugs, including doxifluridine and capecitabine. Accordingly, in vivo imaging of TP activity will contribute not only to the estimation of tumor malignancy but also to the prediction of prognosis after treatment with the fluoropyrimidine-based anticancer drugs. To develop a radio-tracrer for in vivo TP imaging, a radiolabeled uracil-based TP inhibitor, [^{123}I]IIMU), was designed and synthesized by our group. In *in vitro* and *in vivo* studies using ^{125}I-labeled IIMU, high accumulation levels of radioactivity were observed in the tumor cells/tissues with high TP expression levels (A431, a human epidermoid carcinoma), and low accumulation levels were observed in the tumor cells/tissues with low TP expression levels (AZ521, a human gastric cancer). In blocking studies, levels of radioiodinated IIMU in the tumor cells and tumor tissues were markedly decreased by a co-injection of nonlabeled IIMU with radiolabeled IIMU. In SPECT/CT imaging studies, A431 tumors were clearly visualized 3 h after the injection of [^{123}I]IIMU. These results showed high and specific accumulation of radioiodinated IIMU in TP-expressing tumors. Thus, [^{123}I]IIMU has potentials as a novel SPECT tracer for imaging TP-expression in tumors. Furthermore, to assess whether [^{123}I]IIMU imaging could predict the efficacy of capecitabine, we examined the correlation among TP expression levels, sensitivity to capecitabine, and accumulation levels of [^{123}I]IIMU in human colorectal cancer cell lines that have different TP expression levels. In vitro and in vivo studies showed that the accumulation levels of [^{123}I]IIMU in the tumor cells/ tissues were correlated with TP expression levels, and effects of capecitabine were higher in the tumor with a high TP-expression than that with a low TP-expression. These findings indicate that ^{123}I-IIMU could be used not only as a SPECT tracer estimating tumor malignancy, but also an *in vivo* companion diagnostic agent for predicting the efficacy of capecitabine treatment. Recently, a first-in-man study in healthy adults has been started.

Current Issues 5
Molecular Imaging in Drug Development-Bench to Bed Approach

Baljinder Singh

Indian College of Nuclear Medicine, India

Current Issues 5

Hypoxia PET Imaging in Oncology

Sze Ting LEE MD, FRACP, FAANMS

Austin Health, Australia

Malignant tumours have been shown to have an increased glucose metabolism, poor perfusion and areas of hypoxia. The pathophysiologic consequence of structurally and functionally disturbed angiogenenesis resulting in inability of oxygen to diffuse through tissues is associated with propogation and progression of disease, as well as increased resistance to radiotherapy and even some types of chemotherapy. Hypoxia has an important role in tumour angiogenesis, via activation of hypoxia response genes such as HIF-1 α, VEGF and VEGFR1. The degree of angiogenesis is also inversely correlated with survival in many cancers.

PET offers a non-invasive modality of assessing the grading, staging and therapeutic monitoring of tumours, as well as the ability to differentiate different tumour biology, to allow modification of treatment accordingly. The development of PET tracers to target tissue hypoxia, cellular proliferation, tumour receptors and gene product expression provides further non-invasive method to assess tumour biology. More importantly, the indication that hypoxia may also induce the expression of specific genes and promote more aggressive tumour phenotype and worse prognosis in many tumour types, makes its diagnosis even more important, and there is increasing body of evidence that PET is able to do that non-invasively. The presentation with encompass a range of PET radiopharmaceuticals which have been used in the oncology field for these purposes, and the evidence supporting the use of these radiotracers as a non-invasive tool to evaluate hypoxia in tumour and as a prognostic indicators.

Current Issues 5

Clinical translation of serial ^{68}Gallium-labeled tracers

Zhaohui Zhu

Department of Nuclear Medicine, Peking Union Medical College Hospital, Beijing, China

Applications of ^{68}Ga-based radiopharmaceuticals grow rapidly in recent years in both pre-clinical image researches and clinical positron emission tomography (PET). ^{68}Ga has been used for the labeling of peptides targeted to specific receptors, enzymes, and antigens, as well as various compounds for imaging of biologic properties or pathological processes, such as blood pool, lymphatic drainage, and inflammation. In the past 3 years, our group underwent clinical translation of serial ^{68}Ga-labelled tracers, including ^{68}Ga-NOTA-PRGD2, ^{68}Ga-NOTA-Evan's blue, and ^{68}Ga-NOTA-Exendin-4. Using ^{68}Ga-NOTA-PRGD2, a novel PEGlated cyclic RGD dimer targeting integrin $\alpha_v\beta_3$, we underwent serial clinical translational studies for PET/CT diagnosis and evaluation of lung cancer, glioma, myocardial infarction, stroke, rheumatic arthritis, and idiopathic pulmonary fibrosis. ^{68}Ga-NOTA-Evan's blue was translated into clinical use and found useful for imaging of blood pool and lymphatic drainage. ^{68}Ga-NOTA-Exendin-4 PET/CT was used for detection of the insulinoma. ^{68}Ga-NOTA-Bombesin seemed useful for evaluation of Glioma. We also extended the use of ^{68}Ga-DOTATATE PET/CT to evaluate tumor-induce osteomalacia, germ cell tumor, and pituitary tumor. Several other ^{68}Ga-labeled tracers were also on the way of translation. According our experience, ^{68}Gallium-labeled tracers hold advantages of convenient generator production, robust labeling chemistry, and potential for precise and personalized theranostics.

Current Issues 6

Radionuclide imaging in Urinary Tract Infection in Children

D. K. K. Nanayakkara, S.I.Nawaz

Nuclear Medicine Unit, Faculty of Medicine, University of Peradeniya

Advance ultrasound scan (USS) technology has replaced the necessity of carrying out the Dimercaptosuccinic acid (DMSA) renal scan in the management of urinary tract infection in young children. We have noted that the number of requests for DMSA scans is getting less in the recent past. Performing renal USS at the first urinary tract infection (UTI) in a young child is very important to detect structural abnormalities which might need surgical intervention. It was a common practice that even the initial USS scan was normal, all febrile UTI children under 5 years should undergo a DMSA scan in 3-6 months to assess the renal cortex for scarring. However, there remains a widely held belief that USS is good at detecting renal scarring in children and also a little concern about radiation associated with DMSA scan. Due to widely available US facilities

clinicians tend to rely on USS than doing DMSA scan especially when the initial USS is normal. We carried out a prospective study to compare the efficacy of DMSA renal scan and renal USS in detecting cortical scars in children who had febrile UTI.

This study was conducted only on children aged less than 5years as they are the most liable age group for renal scarring. Children who were booked for DMSA scan in 3-6 months after the febrile UTI were enrolled. Data was collected between January 2012 and December 2014. Information was obtained from the Nuclear Medicine DMSA records. Children with US evidence of gross congenital renal anomalies were excluded. Chi-square test was used to compare the 2 imaging methods and p value <0.001was considered as significant. The sensitivity and specificity of DMSA and US scan for the detection of renal abnormalities were compared. Positive predictive value (PPV) and negative predictive values (NPV) of USS were also calculated considering DMSA scan as the reference imaging method.

Out of a total of 1014 DMSA scans done for children less than 5y complete USS information was available for 378 children. There were 216 females and 162 males (Mean age was 23.09±15.5 months).Total 756 kidneys were studied. Detection of renal cortical scaring by DMSA scan was significantly higher than using USS (p value < 0.001). USS showed high sensitivity (89.0%) and low specificity (30.0%). It was also noted that the positive predictive value (PPV) of detecting renal scars using USS was 84.0% and negative predictive value (NPV) of 53.0%. Same parameters were compared between the right and left kidney and showed no difference. It shows that the anatomical location of the kidney is not a predictive factor in detecting scars. Several other studies also have shown that USS does not have sufficient specificity to be used as a reliable imaging modality for the detection of renal scarring in children following UTI. On the other hand USS technique is operator-dependent which highly relies on the radiologist's skills whereas DMSA scan is a functional image which will not depend on the operator. Researchers also have shown that the agreement and inter-observer reliability on diagnosing renal scarring using USS was very low even between experienced radiologists. Results of this study also showed that USS should not be used as the sole imaging modality to find renal scars. Detecting a renal scar in a child is very important for long-term management of children who had febrile UTI.

We suggested that children with recurrent febrile UTI and age less than 5y should have DMSA scan irrespective of the initial USS finding.

Current Issues 6
Dementia Diagnosis using Nuclear Medicine

Tomohiro Kaneta MD, PhD

Associate Professor, Department of Radiology, Yokohama City University, Yokohama, Japan

Japan is now the most aging society in the world. The population aging rate reached 24.1% in 2012. The prevalence rate of dementia for the people aged 65+ years reached 15%, and that of mild cognitive impairment (MCI) reached 13%. About 30% of the people aged 65+ years will suffer from cognitive impairment. The diseases strongly associated with aging including dementia increase rapidly. We need to cope with problems caused by dementia.

As diagnostic radiologists and nuclear medicine physicians, our most important job for the dementia provision is the differentiation of dementing diseases. Dementia is a syndrome linked to a large number of underlying brain pathologies. The most common disease is Alzheimer's disease (AD), followed by vascular dementia (VaD), dementia with Lewy bodies and frontotemporal dementia. There are different strategies of support and treatment for the patient with each disease. Thus, it is very important to differentiate such dementing diseases. Clinical information is most important to make a diagnosis of dementia. However, medical images, such as SPECT, MRI, CT, etc. sometimes can be of great help to make a clinical diagnosis. MRI and CT can detect small infarctions which may cause VaD, and SPECT can be a powerful tool to differentiate AD and DLB, or AD and FTD. In addition, voxel-base analysis of SPECT is spreading and commonly used for the individual diagnosis of dementia in Japan. In this session, I would to talk about the basic strategy to read SPECT images for the differentiation of dementing diseases with providing some clues.

Current Issues 6
Clinical Applications of SPECT/CT in Orthopaedics

Gopinath Gnanasegaran

Dept of Nuclear Medicine, Guy's & St Thomas' Hospital, London

Early and accurate diagnosis of bone pain is achieved through the appropriate use of the many imaging modalities available to clinicians. The choice of investigation is determined by several factors including cost, radiation burden and availability, but most importantly, diagnostic accuracy. Each modality has strengths and weaknesses and the emergence of hybrid imaging challenges the dogma that MRI is the best second-line investigation, after plain imaging, for

evaluation many orthopaediac pathologies. Dedicated multislice SPECT/CT is combined to enhance localisation and characterisation of bone pathology. Multi-slice SPECT/CT scanners were introduced in 1999, with the advantage of having both the modalities fused into one machine (hardware fusion) simplifying the whole procedure This presentation discusses the benefits and weaknesses of radionuclide SPECT/CT imaging in orthopaedics, outlines potential clinical applications.

Current Issues 6

Update in Parathyroid Imaging:

Yuthana Saengsuda

Rajavithi Hospital, Rangsit University College of Medicine, Thailand

Primary hyperparathyroidism (HPT) is appeared by an inappropriate excess of parathyroid hormone(PTH) secretion which results in hypercalcemia and hypophostamia , with associated damaging effects to the patient. It is caused by a single parathyroid adenoma about 85% of patients and multiglandular disease about 10%. Surgical removal of the hyperfunctioning tissue should be considered to cure the disease. Surgeons use two surgical techniques to remove the overactive gland or glands , bilateral four- gland parathyroid exploration and minimally invasive surgery (MIS) .With the growing of acceptance of MIS , preoperative localization (PL) studies are predominantly used to determine whether or not a patient is a candidate for MIS. PL reduces operative time in unilateral parathyroid surgery. PL studies are also mandatory in patients with prior neck surgery or recurrent or persistent disease. Several noninvasive and invasive studies are obtainable in most medical center. Noninvasive studies include nuclear scintigraphy, ultrasonography (US), computed tomography scanning , magnetic resonance imaging and positron emission tomography. The invasive studies such as parathyroid selective venous sampling and parathyroid selective arteriography are rarely performed at present. Imaging studies are obtained only after biochemical confirmation of primary HPT to help plan the operative approach. However , a single focus positive imaging result does not reliably exclude the presence of multiglandular PT disease. Most experts rely on both US and sestamibi scan for PL as a first line studies but this varies by geography and institutional expertise. Two or more concordant preoperative imaging studies should localize hyperfunctional parathyroid tissue to the same region before exploration. Combining sestamibi scan and ultrasound provides high sensitivity 79-95% for predicting the location of a single parathyroid adenoma. Sestamibi scan with SPECT / SPECT-CT has the highest PPV techniques and some prefer this as the localizing procedure of choice for initial surgery . US is the most cost- effective imaging modality in cost analysis studies. The best imaging study or combination of studies for persistent disease or reoperation has not been determined. Recently, four- dimensional CT (4D-CT) increasingly offers advantages as an alternative primary investigation and is a useful second-line study in patients with primary HPT. It is also useful in the reoperating setting when initial imaging sestamibi scan and/or US is negative or discordant. Patients with negative imaging studies require bilateral neck exploration by an experienced parathyroid surgeon. For all patients undergoing reoperation, performing PL is recommended. Reoperation with negative imaging is associated with high failure rate up to 50%.

In conclusion, The diagnosis of primary HPT should be based upon the biochemical evaluation. Preoperative parathyroid localization studies are useful for identifying patients who are candidates for MIS approach. Localization studies do not reliably exclude multiglandular parathyroid disease. For initial MIS, the perferred localized imaging studies in primary HPT include sestamibi SPECT /SPECT-CT and US . 4D-CT is a useful second-line study.

Current Issues 6

Diagnosis of Tuberculosis Using ^{99m}Tc-Ethambutol

A. Hussein S. Kartamihardja

Universitas Padjadjaran, Dr. Hasan Sadikin General Hospital, Indonesia

Tuberculosis infection (TB) is still one of the major health problems in the world. It is affecting almost every organ of the body. Various sophisticated researches have been conducted to develop drug and various diagnostic modalities. Rapid and accurate diagnosis of TB is a important part of tuberculosis control strategies. Various diagnostic modalities have played important roles in diagnosis of TB, but despite several advantages, these modalities also have some limitations.

Nuclear medicine modality has been use to detect and locate the lesion at early stage of the disease. A wide variety of radiopharmaceuticals, such as 67Ga-citrate, FDG-PET, ^{99m}Tc-Ciprofloxacin are used, but they had limitation of being nonspecific and incapable of differentiating between infection and inflammation.

Ethambutol (EMB) is specific to the mycobacteria, and thus, all other bacteria, fungi, and yeasts are

insusceptible to the drug. The primary mode of action of ethambutol was inhibition of arabinan synthesis in the cell wall.

Ethambutol can be successfully labeled with ^{99m}Tc with high labeling efficiency more 85% and stable. ^{99m}Tc-EMB is stable in vitro as well as in vivo. The biodistribution and pharmacokinetic parameters were consistent with the original drug.

Several studies were done to evaluate the efficacy of ^{99m}Tc-EMB scintigraphy to detect and localize the site of pulmonary and extra pulmonary tuberculosis.

FANMB Session

Current Status of Nuclear Medicine In the Philippines

Eduardo Erasto Ongkeko, MD

St. Luke's Medical Center, Philippines

Nuclear medicine in the Philippines started in 1956 when the first rectilinear scanner became available at the Philippine General Hospital. There was slow progress through the decades due to limited resources and awareness in the field, however in the last 25 years, moreso the last 15 years, development and interest in Nuclear Medicine (NM) have grown exponentially. In 2003, there were only 20 nuclear medicine facilities, 80% of which are located in Metro Manila. Presently, the number of nuclear medicine facilities has increased to 54 with a favorable growth in facilities outside Metro Manila (now comprising 44% of total). This translates to about 1 NM facility per 1.8 million population, a mid-range figure when compared to the neighboring Southeast Asian countries. There are NM residency/ fellowship training programs in seven medical centers and currently 10 physician trainees, one of which is an international physician who will be the first nuclear medicine specialist once he returns to Cambodia. There is no research-only facility but few clinical/ academic centers have allowed their nuclear medicine departments to be research sites, for both local and international studies. St. Luke's Medical Center, a private institution, introduced the first PET scanner and medical cyclotron in 2002, followed by SPECT/ CT in 2004 and PET/CT scanner in 2008. Currently, the National Kidney and Transplant Institute has established a new cyclotron and PET-CT scanner this year through a public-private partnership.

Human resources in this field also have undergone reassuring growth. The number of physicians in 2003 were only 30 while today we have a total of 104 nuclear medicine physicians in active practice. Technologists, who play a vital role in our specialty, have tripled in number since 2003, to a total of 250 at present. There are 15 medical physicists and 5 radiochemists, which are considered quite insufficient. A constant challenge we face are in the areas of workforce retention, training and quality / skills improvement. The presentation will also touch on the barriers and potential solutions to these problems. Technologists have participated in distance-assisted training courses to supplement their knowledge and skills. The national society has come up with the first national certification board exam for nuclear medical technologists starting February 2016.

The Philippines actively participates in regional cooperation through the national society and our partners such as the IAEA, ARCCNM and AOFNMB, to name a few. We have hosted the Asia-Oceania Congress in Nuclear Medicine in 1980 and the International Conference on Radiopharmaceutical Therapy (ICRT-WARMTH) in 2013, both of which were well-attended, successful events. These are exciting times indeed. Come February 2016, we invite you to attend the Philippine Society of Nuclear Medicine's annual convention entitled "Golden Links: 50 Years of Connecting Nuclear Medicine with Clinical Specialties."

FANMB Session

Current Status of Nuclear Medicine in Saudi Arabia

Hamid Amer

Department of Medical Imaging, King Abdulaziz Hospital for National Guards , Al ahasa, Saudi Arabia

Nuclear Medicine has evolved in Saudi Arabia parallel to the development in other medical disciplines in general. Its development is considered as a part of a dedicated process to achieve the highest levels of medical and scientific competence. Nuclear Medicine in Saudi Arabia is well established and acts as a reliable support system for colleagues in the country. The roots of Nuclear Medicine in Saudi Arabia can be traced to the import of the first cyclotron for medical use in 1977. Currently most of the country's teaching hospitals have a department of Nuclear Medicine with state of the art SPECT gamma cameras, some of them with co-incidence capability in anticipation of the routine production of PET isotopes. The total number of nuclear medicine departments nowadays crossing 45 covering almost all of the country with newer ones under construction with even advanced modalities in this field. Private Nuclear Medicine facilities with modern equipment can also be found in most private hospitals

in the larger centers some of them with their individual cyclotrons. Most of the tertiary academic institutions in Saudi Arabia provide ongoing post-graduate training in Nuclear Medicine. The King Faisal Specialist Hospital and Research Centre Cyclotron is being used to produce radionuclides for nuclear medicine, short-lived positron emitters for positron emission tomography (PET) studies, neutrons for therapy and biological research. Radiopharmaceuticals for planar imaging at King Faisal Specialist Hospital and other hospitals in Saudi Arabia include thallous-201 chloride, gallium-67 citrate, sodium iodide ^{123}I capsules, ^{123}I orthoiodohippurate and 81mKr generators. Products from short-lived positron emitters such as ^{18}F fluordeoxyglucose, ^{11}C methionine, 15O water and others that prepared and used on site for physiological studies in a PET program. Several patients have been treated with neutron therapy and a program for studying neutron radiation effects on cells is underway. December 4, 2007 -- Belgian radiopharmaceutical firm Ion Beam Applications (IBA) has sold a Cyclone 30 cyclotron to King Faisal Specialist Hospital and Research Centre in Riyadh, Saudi Arabia. The cyclotron used to produce SPECT radioisotopes such as thallium-201 and iodine-123 as well as PET radioisotopes such as fluorine-18, according to the Louvain-la-Neuve-based firm. It is planned to supply Saudi Arabia as well as neighboring countries in the Middle East. Nuclear Medicine in Saudi Arabia is looking forward to a bright future.

FANMB Session

Current Status of Nuclear Medicine in Indonesia

Hendra Budiawan[1], Erwin Affandi[2], A Hussein S Kartamihardja[2], Johan S Masjhur[2]

1. Department of Nuclear Medicine, Mochtar Riady Comprehensive Cancer Centre, Jakarta, Indonesia
2. Department of Nuclear Medicine and Molecular Imaging, Hasan Sadikin Hospital, Bandung, Indonesia

Objectives: Nuclear medicine is still in growing phase in Indonesia. To cover the needs of nuclear medicine services, the status of human resources, equipments, and the contraints faced should be identified.

Methods: Survey methodology by questionnaire to 11 nuclear medicine department was performed. Items that were asked in questionnaire included number of human resources in each sub-field, number and type of cameras, area coverage of services, and the constraints faced.

Results: Number of nuclear medicine physicians has been increased in the last 5 years. Number of PET/CT and SPECT/CT has also grown with the need of some new radiopharmaceuticals to fullfil the needs of clinicians. However, the coverage of services still mainly covered big cities in some big islands and the radioisotope distribution to remote area was still a main problem. In general, nuclear medicine was still not regarded as the important and priority field. Nuclear phobia was also a classical constraint to be addressed. Most of the potential referring physicians were still not sufficiently aware of the use of nuclear medicine.

Conclusions: Although number of human resources and major equipments have increased in the recent years, continous efforts are still needed to provide more comprehensive and various nuclear medicine services covering more area in Indonesia.

FANMB Session

New Trend of PET Study in India

Amitabh Arya

Sanjay Gandhi Post Graduate Institute Of Medical Sciences, India

FANMB Session

New Trend of PET Tracer in Korea

Seong Young Kwon

Department of Nuclear Medicine, Chonnam National University Hwasun Hospital, Hwasun-gun, Republic of Korea

For several years, radiotracers for PET imaging have been actively studied and applied for clinical use. Especially, clinical interests in new tracers are continuously growing with the developments of PET technology, the success of F-18 FDG in oncology and the rapid supply of PET/CT worldwide. However, the development and approval of new PET tracers are related to considerable costs for development process, because their production and application are regulated with principles similar to the general rules used for other drugs. Furthermore, the dual regulation by several institutions is another major hurdle for the expansion of clinical applications of new tracers in Korea. Nevertheless, several kinds of F-18, C-11 or Ga-68 labeled compounds have been continuously introduced and approved in Korea. Especially, new PET tracer for amyloid imaging was developed first in Asia and has been under clinical trial.

Because the market for PET tracers are relatively small in comparison with the drug market, the success of new tracers will be dependent on the demand of clinical

situations, the investment of the radiopharmaceutical industry, the willingness of the regulatory and public funding institutions or authorities. In this presentation, I will discuss a current trend about the development of PET tracer in Korea and strategies for accelerating the clinical application and approval of PET tracer.

FANMB Session

Leadership for FANMB

Ho-Young Lee

Seoul National University Bundang Hospital, Korea

Nuclear Medicine is complex of medicine, basic science and high technique. Nuclear Medicine physician should have knowledge of medicine, basic-biology, chemistry and also physics. Compared to other medical doctors, Nuclear Medicine physician has typically different situation. In general, the most important relationship doctors should keep is said to be patient-doctor relationship. However, nuclear medicine doctors should consider more complicated relationship with many directions. Also, considering the number of NM physician, we are minority. Therefore, we should have leadership for constant advance and survive.

In hospital, NM Physician should be an expert of medicine not only interpreting the images but also treating patients. In addition, they should be expert of radiation safety. For the constant progress of Nuclear Medicine, NM physician should have leadership in many directions.

Nuclear Medicine is not familiar to the other medical doctors. Therefore, we should educate and show the way to use nuclear medicine in diagnosis and treatment to other doctors.

Nuclear Medicine physicians do not work alone in hospital. We work together with radiological technologists, radiopharmacists, nurses et al. We also should have leadership in the department and build up the best teamwork.

Out side of hospital, most of people feel hatred for radiation. But Nuclear Medicine could not be existed without radiation. Due to hatred for radiation, there are regulations dealing with radiation safety from government. We should communicate with government for reasonable regulation. Therefore, communication with government and general society is crucial for NM physician. Educating the patient and their family about radiation safety and the usefulness of radiation.

In last, there is relationship with industry. Most of the progresses in nuclear medicine are achieved with industry. However, the relationship between industry and doctors should be based on ethics due to conflict of interest.

There are several types of leadership.

Authoritarian (dictators), Participative, Laissez-faire, Narcissistic, Toxic, Task-oriented, relationship-oriented. There couldn't be one answer for the question; " Which leadership is best?" However, there could be appropriate leadership for each situation. The most important key is we could not achieve constant progress without colleague. All the fellows of FANMB have a potential for leadership. I hope all of you use your leadership for constant progress of nuclear medicine. If we do together, the dreams will come true soon.

FANMB Session

New Trend of PET Study in Bangladesh

SK Biswas[1], Zakir Hossain[2], Sanowar Hossain[1]

1. Institute of Nuclear Medicine & Allied Sciences, Dhaka
2. Medinova Medical Services Ltd. Dhaka

Objectives: The use molecular imaging, specially PET-CT, in the developing countries has developed the guidelines elaborated by the most developed countries in the world. So essentially, the concept of using molecular imaging in the evaluation of distinct disorders in oncology, cardiology and neuropsychiatry, however directly dependent on the availability of the proper instrumentation and infrastructure. PET has a positive impact on human health in the areas of cancer, heart disease, and brain disorders. PET affects medical decision making and there is growing evidence that PET is cost effective. PET-CT Scan change management in more than one-third of cancer patients. In Bangladesh 2 private centres continuing PET scan since 2011 & 2 will be started soon in government section. Medinova Medical Services Limited, Dhaka is one of the private centres where I have been working from the very beginning. One thousand six hundred & fifty patients already underwent PET-CT imaging in my centre, and day by day the number of patients are increasing.

Method: Whole body FDG PET scan was acquired from vertex to mid thigh in a whole-body PET-CT scanner, one hour after intravenous injection of ^{18}F-FDG. Plain CT scan and then high resolution 128 slice contrast CT scan were obtained. Oral contrast was administered for bowel opacification over 90 min. before the scan. A table dose of oral contrast was given just before the scan. Images were reconstructed using HD VUE point algorithm and slices were reformatted into transaxial, coronal and sagittal views. Semi-quantitative estimation of FDG uptake was performed by calculating

SUV_{max} value, corrected for dose administered and body weight (g/ml).

Results: There were diverse group of patients. Maximum patients came with lung cancer, followed by breast cancer, lymphoma, carcinoma of the urinary bladder, intestinal cancer, hepatobiliary & pancreatic cancer, head & neck cancer, cervical and ovarian cancer, malignant fibrous histocytoma (MFH), rest of the patients were with different neurological problems, and cancer of unknown primary.

Conclusions: PET played pivotal role for disease detection and management of different cancer patients. However we need more PET scanner to support the huge number of cancer patients in such a developing country.

FANMB Session

Present Status of Gamma Camera and Radionuclide Therapy in Bangladesh

Zeenat Jabin

PhD Student of Molecular Medicine, National Institute of Nuclear Medicine and Allied Sciences, Chonnam National University (CNU) Medical School, Department of Nuclear Medicine, Bangladesh

Bangladesh is a small Asian country but has a long and rich history of Nuclear medicine practice for more than sixty years. The first Nuclear Medicine facility was started in Dhaka, back in 1958 with only a rectilinear scan, two probe renograms and a radioactive iodine uptake system. Since then the journey and development in this field is significant. First single headed SPECT was installed in 1994 and first dual headed SPECT in 2003. There are 20 Nuclear Medicine establishments at present with a number of about 42 gamma camera / SPECTs. First SPECT-CT was installed in 2008 and first PET-CT in 2010. Current working employees consist of 95 physicians, 20 physicists, 10 radio-chemists and 150 technologists

In Bangladesh, Radioiodine therapy (RIT) was introduced in 1961, since then the use of RIT has tremendously increased in last few decades. Now it is about 30 times more than the number of patients treated with RIT than that was in early 1980s. Increased number of patients represents proven safety and cost effectiveness as well as dependable modality to the clinicians. Society of Nuclear Medicine, Bangladesh (SNM,B) had a long established guidelines for RIT in hyperthyroidism and Differentiated Thyroid Cancer (DTC) which was revised in 2015 with common agreements of experts in Nuclear Medicine, medicine specialists, endocrinologists and consultant surgeons through National Workshop on Management of differentiated thyroid cancer and thyrotoxicosis.

Beta (β) irradiation by Strontium (Sr-90) has been in use for a long time in Bangladesh for the therapy of postoperative cases of conjunctival squamous cell carcinoma (SCC) and pterygium from a Strontium-90 (Sr-90) applicator.

Besides our limitations we are maximizing the utilization of the Gamma Cameras we have and also providing radionuclide therapies to the highest number of patients referred to us. We are hoping to start Yttrium-90 radiation synovectomy in few more months.

Physics/Instrument_15

Striatum and Midbrain Specific F-18 FP-CIT Analysis in Parkinson Disease

Hyojeong Moon, Injoo Lee, Jungmin Kim, Minyoung Oh, Jae Seung Kim, Jungsu S. Oh

Department of Nuclear Medicine, Asan Medical Center, University of Ulsan College of Medicine, Korea

Conventional volume of interests (VOIs) analysis of F-18 FP-CIT PET using whole brain spatial normalization (SN) suffered from VOI mismatch caused by SN error. Thus, we needed to manually modify the VOIs for more accurate analysis, leading to labor intensiveness and inter-observer reliability issue. Especially in midbrain of Parkinson disease (PD) patients, we had more difficulties due to small VOI size and atrophies. Thus, we suggest a striatum and midbrain-specific mask-based SN (SMSN). We evaluated the SMSN performance for FP-CIT PET analysis in Raphe and Sustantia Nigra of PD patients, compared with conventional whole brain method.

140 subjects (23 normal controls (NC), 117 PD patients) underwent F-18 FP-CIT PET. PET acquisition was started 3 h after i.v. injection of ^{18}F-FP-CIT (185 MBq). Spatial normalization and VOI analysis were conducted using SPM8 and in-house FP-CIT PET and VOI templates. We applied 5.6cm-radius spherical mask to exclude regions other than midbrain/striatum on both template and individual FP-CIT images. An iterative SN using the masked template and individual images was conducted. Finally, mean uptake values of Raphe and Sustantia Nigra were estimated using our in house software. For the ground-truth (GT) of VOI uptake/location, one of us (IL) manually adjusted the SST/Convention VOIs under supervision of nuclear medicine physician (JK). We compared SMSN and conventional method in terms of VOI uptake % error and dice index.

The uptake % error of SMSN from GT was smaller (Raphe: 6.6%, Substantia Nigra: 6.8%) than that of conventional whole brain method (Raphe: 14.5%, Substantia Nigra: 16.1%, $P<0.05$ for both) in PD group. In both group, all VOIs exhibited significantly increased VOI dice index (0.6~0.8) by our devised method (0.3~0.6, $P<0.05$ for all) than conventional method.

Our devised SMSN outperformed than conventional spatial normalization-based approach in terms of significantly less % error and more accurate VOI location. We suggest our SSPM may serve as a new automatic VOI analysis method for midbrain and striatum analysis of FP-CIT PET.

Molecular Imaging_53

Discrepancy between tumor antigen distribution and antibody binding in nude mouse xenograft model of human melanoma

Yong-il Kim, Jin Chul Paeng, Gi Jeong Cheon, Keon Wook Kang, Dong Soo Lee, June-Key Chung

Seoul National University Hospital, Department of Nuclear Medicine, Korea

Biodistribution of antibodies is critical for successful immunoscintigraphy and immunotherapy and is assumed to be similar to antigen distribution. We measured and compared radiolabeled antibody binding patterns to tissue antigen distribution in a nude mouse human melanoma xenograft model.

A total of 107 FEM-XII human melanoma cells were transplanted in the right flank of 5 nude mice. As a control, 5×106 LS174T human colon cancer cells were transplanted in the left flank. After 2 weeks, 10 μCi of I-131 labeled melanoma-associated monoclonal antibody 96.5 (targeting p97 antigen) was intravenously injected. After mice were sacrificed, 96.5 antibody binding patterns in the tumors were evaluated using ex vivo quantitative autoradiography (QAR). Adjacent tissue slices were incubated in various concentrations of I-125 labeled 96.5 MoAb. After 2 months, distribution and concentration of p97 antigen was studied using in vitro QAR.

Radiolabeled 96.5 antibody binding varied between mice and location within the tumor (estimated bound antigen concentration = 0.7 – 6.6 pmol/g). In contrast, p97 antigen distribution was generally homogeneous in the tumors [total antigen concentration (Bmax) = 17.36 – 38.36 pmol/g). We did not identify any quantifiable parameters related to radiolabeled 96.5 antibody binding patterns and p97 antigen distribution. Antibody bound antigen to total antigen ratios ranged between 0.02 - 0.38.

We did not identify any correlations between 96.5 antibody binding and p97 antigen distribution and concentrations in melanoma tissue. Heterogeneous features of target antibody binding were observed. Antibody binding patterns within tumors cannot be predicted based on antigen distribution in the tumor.

Molecular Imaging_50

[^{18}F]Mefway is a Promising PET Radiotracer for Imaging Serotonin 1A Receptors

Jae Yong Choi, Minkyung Lee, Jin Sook Song, Chul Hyoung Lyoo, Kyochul Lee, Young Hoon Ryu

Department of Nuclear Medicine, Yonsei University College of Medicine, Gangnam Severance Hospital, Seoul, Korea

Dysfunction of the serotonin 1A (5-HT1A) receptors is closely related to the neuropsychiatric disorders such as depression, Schizophrenia and anxiety. Although many radiotracers have been developed to quantify the 5-HT1A receptors, there are few available PET radiotracers. In this presentation, we would like to introduce the of [^{18}F]Mefway as a candidate for clinical studies.

First of all, we have optimized synthetic method for reliable production. After biological characteristics for [^{18}F]Mefway were confirmed in the rodents, its the utility was evaluated in the animal disease models (i.e. Parkinsons model and depression model). Finally, the prospects for the human subject were assessed in comparison to [^{18}F]FCWAY. Dynamic PET scans were performed for 120 min. Non-displaceable binding potential (BPND) was used as an indication of receptor density and the cerebellum was used as the reference region.

We established an efficient synthetic method for [^{18}F]Mefway. [^{18}F]Mefway was underwent the in vivo defluorination in the rodents and this phenomena was inhibited by the pretreatment of fluconazole. [^{18}F] Mefway was identified a substrate for P-glycoprotein in the rodent. BPND values in the Parkinsons disease and depression animal model were significantly reduced compared with those of the sham operated groups. Although [^{18}F]Mefway showed relatively lower brain uptake and binding values compared to [^{18}F]FCWAY with disulfiram in human subjects, [^{18}F] Mefway has reasonable binding value with little skull uptake.

[^{18}F]Mefway may be a promising PET radiotracer for 5-HT1A receptor imaging in human.

Cardiology_29

Left ventricular mechanical dyssynchrony measured using myocardial SPECT predicts cardiac events in acute myocardial infarction with multi-vessel disease

Sang-Geon Cho, Ki Seong Park, Sae-Ryung Kang, Jong Sang Kim, Seran Min, Jahae Kim, Ho-Chun Song, Jae Yeong Cho, Kye Hun Kim, Minchul Song, Geum-Cheol Jeong, Hee Jeong Park, Young Jae Kim, Seong Young Kwon, Jung-Joon Min, Hee-Seung Bom

Chonnam National University Hwasun Hospital, Korea

We evaluated the prognostic value of left ventricular mechanical dyssynchrony (LVMD) measured using myocardial SPECT in patients with acute myocardial infarction (MI) with multi-vessel disease.

The 109 acute MI patients who underwent myocardial SPECT for decision of therapeutic strategy either after primary percutaneous coronary intervention (PCI) or hemodynamic stabilization without primary PCI were enrolled (79 non-ST elevation and 30 ST-elevation MI's). Phase standard deviation (PSD) and phase histogram bandwidth (PBW) were obtained for assessment of LVMD using Emory Cardiac Toolbox SyncTool® software. The patients were followed up for composite major adverse cardiac events (MACE) including death of any cause, unplanned rehospitalization due to heart failure (HF), and lethal arrhythmias (median follow-up: 26 months). We compared the LVMD parameters along with other risk factors between patients with and without MACE. Kaplan-Meier survival analysis was performed to compare the survival according to LVMD and overt HF at the time of acute MI. Multivariate Cox regression analysis was performed to differentiate the factors predictive of MACE after adjustment of other risk factors.

MACE occurred in 27 patients (24.8%). PSD (50.5 ± 18.3 vs. 35.1 ± 19.0 degrees; *P*< 0.001) and PBW (141.6 ± 59.7 vs. 95.6 ± 58.2 degrees; *P* = 0.001) were significantly higher in patients with MACE as compared to those without. Kaplan-Meier survival analysis revealed significantly poorer survival with PSD ≥ 35.8 (*P* = 0.001) and PBW ≥ 97.0 (*P* = 0.001). However, the difference in survival according to LVMD was not evident in patients with overt HF at the time of acute MI, neither for PSD (*P* = 0.255) nor PBW (*P* = 0.349). Multivariate analysis revealed that both PSD ≥ 35.8 (HR 6.681, 95%CI 1.638-27.244, *P* = 0.008) and PBW ≥ 97.0 (HR 6.477, 95%CI 1.237-33.927, *P* = 0.027) were predictive of MACE, as well as suboptimal revascularization, high right ventricular systolic pressure and no renin-angiotensin system blockade treatment.

LVMD measured with myocardial SPECT was significantly associated with future cardiac events in acute MI with multi-vessel disease without overt HF.

Oncology_90

F-18 FDG-PET/CT findings help to estimate recurrence risks based on a genomic assay

Seunggyun Ha, Suhyun Lee, Woo Kyung Moon, Wonshik Han, Gi Jeong Cheon

Seoul National University Hospital, Department of Nuclear Medicine

The purpose of this study was to evaluate association between molecular imaging parameters from F-18 FDG PET/CT and a recurrence risk index from a genomic assay.

In this retrospective study, total 57 cases were included by following inclusion criteria: 1) early breast cancer, 2) F-18 FDG PET/CT for preoperative work-up, 3) surgical removal of tumors, 4) ER/PR-positive and HER2-negative, and 5) Scoring of Oncotype Dx RS. Immunohistochemical features that Ki-67, p53, androgen receptor, nuclear grades, and histologic grades were involved in this analysis. PET analysis with SUV_{max}, SUV_{avg}, metabolic tumor volume (MTV) and total legion glycolysis (TLG) was restricted in the cases of the relatively large tumor (n = 26, MTV ≥ 2 cm3). Univariate and multivariate analysis among clinical, IHC and PET parmeters was performed to find out indicators for low and high recurrence risk cases which were defined based on Oncotype Dx RS less than 18.

There were 22 cases of low and 35 cases of high Oncotype Dx RS (Table 1). Among the 26 cases of available PET analysis, 17 cases had low Oncotype Dx RS (Table 1). Correlation analyses with Oncotype Dx RS showed significant correlations of Ki67 (r 0.421, *P*<0.001), SUV_{max} (rs 0.406, *P* = 0.040) and SUV_{avg} (rs 0.455, *P* = 0.020) (Figure 1). Nuclear grades and histologic grades showed association to Oncotype Dx RS (*P*<0.001 and *P*= 0.003, respectively) (Figure 2). Univariate analysis for low and high Oncotye Dx RS showed significance of factors of nuclear grades, SUV_{max} and SUV_{avg} (*P* = 0.031, 0.006, and 0.007, respectively) (Table 2). Each $SUV_{max}$and SUV_{avg} was revealed as independent indicators for high and low recurrence cases regardless of nuclear grades by multivariate analysis (*P* = 0.048 and 0.037, respectively) (Table 3). Area-under-curves of receiver operating characteristic for SUV_{max} and SUV_{avg} were 0.830 and 0.827, respectively (*P* = 0.006 and *P* = 0.007, respectively) (Figure 3).

PET/CT parameters, SUV_{max} and SUV_{avg}, showed possibility of imaging indicators for a recurrence risk index based on a genomic assay.

Radionuclide Therapy_28

Factors for ablation success of thyroid remnant in iodine-replete region

Seung Hyun Son, Chang-Hee Lee, Ji-hoon Jung, Choon-Young Kim, Ju Hye Jeong, Shin Young Jeong, Sang-Woo Lee, Jaetae Lee, Byeong-Cheol Ahn

Department of Nuclear Medicine, Kyungpook National university, School of Medicine and Hospital, Korea

Several studies reported that the ablation success rate was not different among the different radioiodine doses, especially between low (1100 MBq) and high (3700 MBq) doses in western countries. And, because of the side effect of thyroid hormone withdrawal (THW), recombinant human thyrotropin (rhTSH) stimulation has been recommended for the ablation. However, the results were not varied in iodine-replete regions. The aim of the study was to assess the effects of two different high doses (3700 MBq vs. 5550 MBq) for thyroid remnant ablation in Korea, known as an iodine-replete region.

The ablation success rate between 137 patients who treated with 3700 MBq I-131 were compared with 271 patients with 5550 MBq I-131; each group of patients were prepared with THW and rhTSH, respectively. End points were the rate of success of ablation at 6 to 12 months. Ablation success was defined as the TSH stimulated thyroglobulin of under 2 ng/mL and/or positive diagnostic radioiodine whole body scan (DxWBS).

Ablation success rates were 61.6% in the group receiving 3700 MBq I-131 with rhTSH versus 82.5% in the group receiving 5550 MBq with THW. There was significant difference of ablation success rates between 3700 MBq and 5550 MBq groups in high T category (T3 and T4) patients (62.0% vs. 84.3%), whereas there was no difference in low T category patients. In patients with N0 or N1a category, the ablation success rates were also significantly different between 3700 MBq and 5550 MBq groups: 61.1% vs. 92.7% in N0 patients and 63.5% vs. 77.9% in N1a patients, respectively.

The ablation success rate was lower in a group receiving 3700 MBq I-131 with rhTSH, compared to a group receiving 5550 MBq I-131 with THW in the study group. Low dose of radioiodine might not be sufficient for the ablation in an iodine-replete regions.

Physics/Instrument_7

Preliminary results of endoscopic NIR/gamma/visible fusion imaging for intra-operative surgery

Han Gyu Kang[1], Kyeong Min Kim[2], Ho-Young Lee[3], Seong Jong Hong[1,4]

1. Department of Senior Healthcare, Eulji University, South Korea
2. Korea Insitute of Radiological and Medical Science, South Korea
3. Department of Nuclear Medicine, Seoul National University, College of Medicine, South Korea
4. Department of Radiological Science, Eulji University, South Korea

Objectives: Intra-operative endoscopic NIR/gamma/visible fusion imaging for the sentinel lymph node mapping

Methods: An endoscopic NIR/gamma/visible fusion imaging system has been developed to show the feasibility of multi-modal intra-operative imaging. The imaging system consists of a tungsten pinhole collimator, a plastic focusing lens, a 2 mm thick BGO crystal, a fiber optic taper, a 122 cm long endoscopic fiber bundle, a relay lens and a CCD camera. A Derenzo-like phantom filled with indocyanine green (ICG) and ^{99m}Tc (12MBq) was used for NIR/gamma imaging. The NIR and gamma images were obtained with different intralipid gelatin phantom depths (0, 5, 10, 15 and 20 mm) and intralipid concentrations (1% and 2%) to investigate the penetration depth of the NIR and gamma. For the sentinel lymph node mapping of a mouse, a mixture of ^{99m}Tc-Sb (12 MBq) and ICG (0.1 mL) was injected into the right paw of the mouse (C57/B6) subcutaneously. After 1 hour, the NIR, gamma, and visible images of the Sentinel lymph node (SLN) were obtained. Subsequently, dissected SLN was imaged by the endoscopic NIR/gamma/visible imaging system.

Results: The NIR penetration depth in the intralipid gelatin phantom was less than 10 mm while the gamma (140 keV) penetration depth was not limited by the phantom depth. The NIR/gamma/visible fusion image of the SLN showed a good correlation between NIR, gamma, and visible images either for in-vivo or ex-vivo.

Conclusions: We demonstrated the feasibility of the intra-operative SLN mapping using the proposed endoscopic NIR/gamma/visible imaging. In the future study, simultaneous NIR/gamma/visible imaging will be investigated with dichroic mirrors and three CCD cameras.

Molecular Imaging_3

Evaluation of the Degree and Distribution of Sodium Fluoride-18 Uptake in the Normal Skeleton, and Relationship with CT-based Hounsfield Unit

Shintaro Nawata, Tomohiro Kaneta, Tsuyoshi Kawano, and Tomio Inoue

Department of Radiology, Yokohama City University, Yokohama, Japan

Purpose: Sodium fluoride (NaF) reacts with hydroxyapatite to give fluorapatite according to the chemical reaction. Previous studies have reported that ^{18}F-NaF PET is an important tool for the detection and evaluation of bone metastases from various malignancies. However, only a few studies have reported the degree and distribution of ^{18}F-NaF in the normal skeleton. In this study, we evaluated the uptake of NaF and CT-based Hounsfield Unit (HU) of normal skeleton using ^{18}F-NaF PET/CT.

Methods: We retrospectively reviewed ^{18}F-NaF PET/CT images of 30 patients with hip joint disorders. PET/CT scans were performed 40 min after the intravenous administration of approximately 185 MBq of ^{18}F-NaF using Celesteion PET/CT scanner (Toshiba, Tochigi, Japan). In order to evaluate a difference between NaF distribution and HU, we measured and compared the maximum standardized uptake value (SUV_{max}) and HU of lumber vertebra, ilium, proximal and distal femur, especially in cancellous bone. In this study, we did not focus on joint disorders.

Results: The distribution of ^{18}F-NaF was different among various skeletal sites. In particular, the lumber vertebra had the highest SUV_{max} and distal femur had the lowest SUV_{max}. The uptake of the lumber vertebra looked higher in the inside, suggesting cancellous bone. Additionally, a significant correlation between SUV_{max} and HU values of vertebra was seen.

Conclusions: Our results revealed some characteristics of the ^{18}F-NaF distribution in the normal skeleton. These characteristics might be useful for the further evaluation of bone metabolism and the detection of bone diseases.

Neurology_10

Synthesis of ^{18}F-Labeled 2-phenyl-imidazo[1,2-a]pyridine Analog, ^{18}F-CB251, and Its Biological Evaluation for Neuroinflammation PET Imaing

Byung Chul Lee[1], Byung Seok Moon[1], Mara Perrone[2], Hyun Soo Park[1,3], Jae Ho Jung[1], Valentino Laquintana[2], Annalisa Cutrignelli[2], Angela Lopedota[2], Massimo Franco[2], Nunzio Denora[2], Sang Eun Kim[1,3]

1. Seoul National University Bundang Hospital, Republic of Korea
2. University of Bari "A. Moro", Italy
3. Seoul National University, Republic of Korea

Purpose: The translocator protein (TSPO, 18 kDa) has become an extremely attractive biomarker for activated microglial cells occurring in inflammatory neurodegenerative disease. In this work, we report the synthesis, characterization, and *in vivo* evaluation of a new TSPO PET imaging agent, [^{18}F]CB251 (2-(6,8-dichloro-2-(4-[^{18}F]fluoroethoxyphenyl)imidazole[1,2-a]pyridine-3-yl)-*N*,*N*-dipropylacetamide), in a rat model of neuroinflammation.

Methods: [^{18}F]**1** was prepared by incorporating of fluorine-18 into the tosylate precursor in a single-step radiolabeling procedure. The affinity toward TSPO of **1** was measured on membrane extracts of C6 glioma cells. Tissue distribution was performed in normal ICR mice. Comparison of neuroinflammation imaging with [^{18}F]**1** versus [^{11}C]PBR28 was performed in the same lipopolysaccharide (LPS)-induced neuroinflammatory rat model including IC_{50}, Log D and in vitro stability.

Results: [^{18}F]**1** has been efficiently synthesized in 8.2 ± 2.5% of radiochemical yield (non-decay-corrected) with >99% of radiochemical purity and 129 ± 25 GBq/μmol of specific activity. The binding affinity (IC_{50}) of the **1** had 0.27 nM. [^{18}F]**1** was highly accumulated in the TSPO-enriched tissues such as the lung, heart and kidney, whereas it exhibited comparatively low uptake in liver and brain. In PET imaging studies in neuroinflammatory rat model, [^{18}F]**1** rapidly approached the highest target-to-background ratio (2.7 times) at early imaging time and was selectively accumulated in the ipsilateral striatum. The ratio of AUC in the ipsilateral and contralateral striatum of [^{18}F]**1** was comparable to that of [^{11}C]PBR28. In blocking experiment using flumazenil and PBR28, flumazenil did not intercept the uptake of [^{18}F]**1**, whereas the uptake of the ipsilateral area significantly decreased after injection with PBR28.

Conclusions: Taken together, [^{18}F]**1** hold promise as a neuroinflammation PET imaging agent in the field of brain degenerative disease.

Molecular Imaging_10

Synthesis and In Vivo Evaluation of ^{99m}Tc-Hynic Labeled Tumor Homing Cyclic NGR Peptide

Kusum Vats[1], Drishty Satpati[1], Haladhar Deb Sarma[2], Sharmila Banerjee[1]

1. Radiopharmaceuticals Chemistry Section, Radiation Biology and Health Sciences Division
2. Bhabha Atomic Research Centre, Trombay, Mumbai, India

Purpose: The peptide sequence asparagine-glycine-arginine (NGR) discovered by phage display technology binds specifically to aminopeptidase receptor (APN/CD13) upregulated in angiogenic blood vessels and various human solid tumors, including melanoma, prostate, lung and ovarian cancer. The aim of this study was to develop an angiogenesis imaging marker specifically targeting CD13 receptors.

Methods: The peptide c(CNGRC) was manually synthesized by standard Fmoc solid phase synthesis on Novasyn TGR resin and subsequently conjugated with indigenously synthesized HYNIC-Boc at the N-terminus. Acetamidomethyl thiol protected cysteines were cyclized on solid support with thallium (III) trifluoroacetate and the peptide chain was cleaved from the resin using 90% trifluoroacetic acid (TFA) and 10% triisopropylsilane (TIPS). The peptide conjugate, HYNIC-c(CNGRC) was radiolabeled with ^{99m}Tc (185 MBq) by incubation with EDDA, tricine and stannous chloride (100^{o}C, 20 min). In vitro stability (human serum, 37^{o}C, 24 h) and biodistribution studies (fibrosarcoma tumor bearing Swiss mice; 30 min, 1 h, 4 h; n = 4) were carried out.

Results: The peptide HYNIC-c(CNGRC) (>99% pure) was radiolabeled with ^{99m}Tc (>95% radiochemical yield, log *P* = -2.33). ^{99m}Tc-Hynic-c(CNGRC) was observed to be stable in vitro in human serum (>95% radiochemical yield). Biodistribution studies revealed rapid urinary excretion for ^{99m}Tc-Hynic-c(CNGRC) and fast clearance from other non-target organs (lungs, liver, intestine). Tumor uptake was observed to be maximum at 30 min p.i. (2.3 ± 0.1% ID/g) which decreased with time (1.5 ± 0.2, 0.6 ± 0.07% ID/g at 1 and 4 h p.i.), however tumor/blood ratio improved with time (0.75:1, 1.06:1, 1.62:1 at 30 min, 1 and 4 h p.i.). Blocking studies resulted in nearly 20% reduction in the tumor uptake at 1 h p.i. (1.2 ± 0.04% ID/g).

Conclusions: Biodistribution studies suggest that the radiotracer need to be tested in other CD13 specific animal tumor models and future studies will also be carried out by introducing different spacers between the peptide and the chelator.

Molecular Imaging_21

Molecular Imaging of EGFR-Expressing Tumors with Novel Targeted Protein Scaffold, anti-EGFR Repebody

Jung-Joon Min, Misun Yun, AYoung Pyo, Hyeon-Sik Kim, Zheng Jinhai, Dong-Yeon Kim, Hee-Seung Bom

Chonnam National University Medical School and Hwasun Hospital, Department of Nuclear Medicine, Korea

Repebody is a binding scaffold based on variable lymphocyte receptors, which are nonimmunoglobulin antibodies composed of leucine-rich repeat modules in jawless vertebrates (1). Repebody can be developed against variety of epitopes by module engineering. The epidermal growth factor receptor (EGFR, HER1) pathway contributes to a number of highly relevant processes in cancer development and progression. In this study, EGFR-specific repebody was developed to visualize the status of receptor expression in cancer.

We developed anti-EGFR repebody by phage display. We selected human non-small cell lung cancer (H1650) and human colon cancer (HT29) highly expressing EGFR for in vitro and in vivo experiments. Human melanoma (MDA-MB-435) was selected as a negative control. Specific binding of anti-EGFR repebody to cells and cancer tissue was determined by immunoflourescence (IF) staining and/or FACS analysis. In vivo imaging was done by i.v. injection of Cy5.5 labeled anti-EGFR repebody (30 μg/mouse) or ^{64}Cu-NOTA-repebody (7.4 MBq/mouse) in H1650- and HT29-bearing mouse models using cooled CCD camera or microPET, respectively.

In vitro and in vivo IF staining demonstrated that strong binding of anti-EGFR repebody to H1650 and HT29, but not to MDA-MB-435. In vivo near infrared (NIR) imaging demonstrated specific targeting of Cy5.5-labeled anti-EGFR repebody to grafted H1650 and HT20 tumor in mice. A strong fluorescence signals were detected at the grafted tumors from day 1, and continuously to day 10 after injection. The ^{64}Cu-NOTA-repebody was detected at the implanted tumor from 1 h (SUV_{max}: 1.34±0.12) after the injection, peaked at 6 h (1.75±0.18), maintained to 24 h (1.33±0.17), and declined at 48 h (1.11±0.05).

In conclusion, the anti-EGFR repebody could be developed for imaging of cancer overexpressing EGFR. Our work provides a basis to develop potential strategy of targeted imaging for early detection and imaging-based companion diagnostics of EGFR-expressing cancer, which may replace monoclonal antibodies.

Molecular Imaging_13

Biodistribution of tumor derived extracellular vesicle in mice after intravenous injection by using bioluminescent reporter system

Prakash Gangadaran[1], Xiu Juan Li[1], Senthilkumar Kalimuthu[1], Ji Min Oh[1], Shin Young Jeong[1], Sang-Woo Lee[1], Jaetae Lee[1, 2] and Byeong-Cheol Ahn[1]*

1. Department of Nuclear Medicine, Kyungpook National University School of Medicine, Hospital, Daegu-700-721, Republic of Korea
2. Daegu-Gyeongbuk Medical Innovation Foundation (DGMIF), 80 Cheombok-ro, Dong-Gu, Daegu, 701-310, Republic of Korea

Purpose: Extracellular vesicles (EVs) are released from cells into extracellular space, and are capable of carrying protein, mRNA and miRNA. Numerous studies have found that tumor-derived EVs (tEVs) transferring oncogenic activity and promoting tumor progression. Biodistribution of thyroid cancer EVs has not been investigated yet. Despite intense research in the field, there have been only few studies on EV distribution in vivo animal model with bioluminescence imaging (BLI) reporter. The current investigation explored the visualization of tEVs in a mouse using generated bioluminescent EVs in vivo and biodistribution of tEVs in a mice after intravenous (I.V) injection.

Methods: Human anaplastic thyroid cancer cells (CAL62) were transduced with a lentivirus expressing Rennila luciferase (Rluc). CAL62 cell culture media was harvested and EVs were isolated by ultracentrifugation. EVs were analyzed by TEM and ELS. Rluc expression in EVs determined by WB and BLI. To visualize and track the distribution of EVs in vivo, EVs or PBS was I.V injected into mice. The coelenterazine was injected over different time points and organ distribution of EVs was determined, imaged under IVIS imaging system.

Results: CAL62 cells were stably transfected with Rluc. BLI and WB confirmed Rluc reporter. EVs structure, size and protein markers were confirmed by TEM, ELS and WB respectively. In vitro, WB and BLI revealed the EV exhibits reporter. EV or PBS was injected into mice by I.V. BLI revealed a significant amount of Rluc signal in the region of lung, liver and spleen in EV injected mice, but not the controls. To confirm findings from in vivo, further organs were collected at two time points post-EV injection, resulted in agreement with results from in vivo imaging experiments. The highest EV signal was in the lung, liver and spleen and interestingly kidney also showed Rluc activity.

Conclusions: Here we designed a highly sensitive EV reporter system that enables in vivo imaging. In vivo and ex vivo imaging revealed that the tEVs distributed to organs. These results indicate that Rluc labeling is useful for tracing EVs In vivo. This is the first distribution study of EVs of thyroid cancer cells having Rluc reporter gene.

Musculoskeletal System_3

Is Intermittent Pneumatic Compression (IPC) a Good Method for Increasing Radiotracer Bone Uptake?

Shafiei S, Ayati N, Sadra H, Zare S, Zakavi R

Nuclear Medicine Research Center, Mashhad University of Medical Sciences, Mashhad, Iran

Purpose: Currently, Intermittent Pneumatic Compression (IPC) is a standard method of lymphedema treatment. Recently, the effect of this modality in patients with limb arterial insufficiency has been researched. It has been suggested that arterial inflow to the long bones is also increased by IPC. The purpose of this manuscript is to assess the effect of lower limb IPC on the blood flow as well as delayed bone uptake.

Methods: In this prospective study, we evaluated 30 patients who were referred for whole body bone scan to our nuclear medicine department. All patients had been examined by a vascular surgeon for ruling out any peripheral neuropathy, vasculopathy or ulcer in the lower limbs. Also all patients were questioned about HTN, DM and other chronic diseases with peripheral complications. Following 925MBq of ^{99m}Tc-MDP injection, perfusion and blood pool images of both legs as well as static delayed images were done after completion of IPC.

Results: 30 patients (10 male) with the age range of 30 to 84 years (mean=53.4) were included. Radiotracer uptake in flow and blood pool images in the compressed limb was significantly more than the contra-lateral limb, however, on delayed images; no significant difference was noted between two limbs.

Conclusions: Although IPC can significantly increase blood flow of the compressed limb, MDP uptake on delayed images was not increased. According to this study, IPC may not be useful as a technique to increase releasing chemotherapic drugs or other substances to the bone and promoting bone growth.

Oncology_2

Prognostic Value of Pre-treatment ^{68}Ga-RGD PET/CT in Predicting Disease Free Survival in Patients with Breast Cancer : A Comparison study with Dynamic Contrast Enhanced MRI

Yong-il Kim[1], Hai-Jeon Yoon[2], Jin Chul Paeng[1], Gi Jeong Cheon[1], Dong Soo Lee[1], June-Key Chung[1], E. Edmund Kim[1], Woo Kyung Moon[3], Keon Wook Kang[1]

1. Department of Nuclear Medicine, Seoul National University Hospital, Seoul, Korea
2. Department of Nuclear Medicine, Ewha Womans University, Seoul, Korea
3. Department of Radiology, Seoul National University College of Medicine, Seoul, Korea

Purpose: Angiogenesis, the process of new blood vessel formation, is a fundamental step of tumor growth and metastasis in breast cancer. We performed pre-treatment angiogenesis imaging (^{68}Ga-RGD PET/CT) to identify the prognostic value of breast cancer in comparison with dynamic contrast enhanced (DCE)-MRI.
Methods: Forty-four female patients of stage II or III breast cancer (age=47.3 ± 8.1 yr) were prospectively enrolled and performed ^{68}Ga-RGD PET/CT and DCE-MRI imaging before treatment. All of the patients received neoadjuvant chemotherapy and underwent surgery. Patients were followed up for 40.3 ± 7.2 mo by laboratory test, ultrasonography, contrast-enhanced MRI and/or ^{18}F-FDG PET/CT. On pre-treatment ^{68}Ga-RGD PET/CT, maximum and peak standardized uptake values (SUV_{max} and SUV_{peak}) of tumor on torso (-T) and regional (-R) images were measured. On pre-treatment DCE-MRI, largest diameter of tumor and LN, maximum enhancement index [maxEI; maxEI = (highest signal/baseline signal) – 1] and at 30 sec EI [EI30; EI30 = (signal at 30 sec/baseline signal) – 1] of tumor were assessed. Included immunohistochemical (IHC) parameters were estrogen receptor (ER), progesterone receptor (PR), human epidermal growth factor receptor-2 (Her-2), and Ki-67 (%).
Results: Ten patients (22.7%) exhibited breast cancer recurrence after 17.9 ± 11.2 mo. Among several parameters, SUV_{max}-R of Ga-68-RGD PET/CT, largest diameter of tumor and LN, maxEI and EI30 of DCE-MRI showed significant results by Log-rank test. The 3-yr disease-free survival (DFS) of SUV_{max}-R (cut-off > 2.79) was 91.7% vs. 59.1% by Kaplan-Meier analysis. Cox regression analysis demonstrated that SUV_{max}-R (P = 0.027, hazard ratio = 5.863) and maxEI (P = 0.026, hazard ratio = 10.394) is the significant parameters. Combined parameter (SUV_{max}-R and maxEI) revealed better specificity (91.18%), positive predictive value (72.73%), accuracy (88.64%) and weighed kappa (0.688) than each parameters.
Conclusions: Increased angiogenic activity of regional ^{68}Ga-RGD PET/CT can be an early prognostic marker for the prediction of breast cancer recurrence, and ^{68}Ga-RGD PET/CT (SUV_{max}-R) and DCE-MRI (maxEI) have complementary value.

Neurology_5

Role of PET / MRI Co-registration in Intractable Epilepsy

Anuj Jain, Pritam Patil

Vijaya Diagnostic centre Pvt Ltd, Hyderabad, India

Purpose: Routine pre-surgical evaluation of intractable epilepsy to localize epileptogenic focus includes clinical evaluation, EEG and MRI. In case of non-contributory MRI or discordance of clinical & EEG findings with MRI, further evaluation with interictal FDG PET scan or ictal SPECT scan is required. Few recommend routine inclusion of interictal FDG PET scan in pre-surgical evaluation, as it changes management in significant number of cases. Till date only a few articles have discussed impact of PET/MRI co-registration studies on management of intractable epilepsy patient.
Methods: We analyzed data of 34 patients of intractable epilepsy with age ranging between 5 to 55 years, had either non-contributory, discordant or multiple findings on MRI. If available MRI data did not have volumetric T1W or T2W sequence of 1.5T or 3T MRI scanner, it was acquired same day on a 3T MRI scanner, after PET scan. Later PET data and three-dimensional MRI data were fused with the help of dedicated integrated registration software on ADW 4.6 workstation of GE healthcare and PET, MRI and fused images were analyzed side by side.
Results: PET scan showed positive findings in 21 cases while no abnormalities in 13 cases. Out of 30 cases with normal or discordant MRI findings PET MR fusion study helped in finding subtle lesions on MRI images in 13 cases (43%), which could not be picked up in first read. In another 4 cases with hypometabolism on PET, no abnormality could be detected on MRI. In 4 cases of multiple findings (2 cases of tuberous sclerosis, one of multiple heterotopias and one of bilateral perirolandic atrophy) epileptogenic focus could be localized in 3 of the cases with the help of PET/ MR Co-registration.
Conclusions: PET MRI Co-registration studies could not improve overall sensitivity of FDG PET in evaluation of intractable epilepsy, but it certainly increases level of confidence of PET reporting. As it helped in localizing subtle anatomical lesion in a significant number of

cases, surgical planning can be done in a better way and therefore, better acceptance of PET findings amongst clinician. PET MRI Co-registration was of great help in cases with multiple lesions on MRI in establishing epileptogenic focus.

Oncology_74

Preoperative parallel PET/MR improves the prediction of the disease free survival in patients with breast cancer

Sang Moo Lim, Jihyun Park, Ilhan Lim, Woo Chul Noh, Hyun-Ah Kim, Ko Woon Park, Seung Sook Lee, In Ok Ko, Kyeong Min Kim, Byung Hyun Byun, Byung Il Kim, Chang Woon Choi

Department of Nuclear Medicine, Korea Cancer Center Hospital, Korea

The aim of this study was to determine whether PET/MR could predict disease-free survival (DFS) in patients with operable breast cancer.

Eighty-one patients with operable breast cancer were enrolled. All patients underwent preoperative parallel PET/MR: whole body PET/CT at 1 h after ^{18}F-FDG injection, breast dynamic contrast enhanced MR, and breast PET/CT at 2h after ^{18}F-FDG injection sequentially in prone position. All patients were analyzed by diverse parameters (maximum SUV at 1 h [$SUV_{max}1$], maximum SUV at 2 h [$SUV_{max}2$], retention index of SUV_{max} [RI], metabolic tumor volume [MTV], total lesion glycolysis [TLG], initial slope of the enhancement curve [IS], transfer constant [Ktrans], reflux constant [Kep], extravascular extracellular space volume fraction [Ve], and initial area under the curve [iAUC]). A relationship between covariates and DFS after operation was analyzed using Kaplan-Meier method and multivariate Cox proportional-hazard regression method.

The median follow-up of 81 patients was 55 months (31-67 months), and 9 (11%) patients developed recurrence or metastasis. Among parameters, higher RI (P = 0.0007), lower Ktrans (P = 0.0033), and lower Ve (P = 0.0044) were significantly associated with poorer DFS. In contrast, $SUV_{max}1$, $SUV_{max}2$, MTV, TLG, IS, Kep, and iAUC were not. On multivariate analysis, RI (P = 0.024; HR = 4.82; CI 1.2-18.7), and Ktrans (P = 0.017; HR = 0.17; CI 0.04-0.7) were found as independent predictors of DFS. Patients with higher RI and lower Ktrans revealed a significantly higher recurrence rate (66.7 %) than the rest of patients (6.7 %, P<0.0001).

RI and Ktrans measured by preoperative parallel PET/MR can predict DFS in patients with operable breast cancer. The combination of these parameters could make improvement of patients care because tailored surveillance would be applied for high risk group.

Neurology_7

Evaluating the Effectiveness of a Treatment for Codeine-containing Cough Syrups Dependent Patients using Single-photon Emission Computed Tomography

Shaowei Jia, Zhengqin Zhao

Department of Nuclear Medicine, Children's Hospital of Zhengzhou, China

To explore the effectiveness of new comprehensive methods in the treatment of codeine-containing cough syrups (CCS) dependent patients and evaluate the effectiveness of these methods using single photon emission computed tomography (SPECT).

Participants were 29 CCS dependent patients and 31 matched controls. The SPECT examination was used in this study and the imaging agent is ^{99m}Tc-TRODAT-1. All the controls received the SPECT examination. All the CCS dependent patients received the comprehensive methods as the treatment. Before and after treatments, the CCS dependent patients received the SPECT examination respectively. The striatal dopamine transporter (DAT) levels were measured by SPECT. The volume (V), weight (W) of bilateral corpus striatum and the ^{99m}Tc-TRODAT-1 uptake ratio of corpus striatum/the whole brain (Ra) were calculated by mathematical models.

In the CCS-dependent patients before the therapy, the DAT availability of striatum were decreased significantly and the V, W, Ra were reduced significantly compared to the controls. After the therapy, the clinical symptoms of the CCS-dependent patients relieved to varying degrees. The DAT availability of striatum were increased significantly and the V, W, Ra were enhanced significantly compared to those of the patients before the therapy. However, after the therapy, the DAT availability of striatum were still decreased significantly and the V, W, Ra were still reduced significantly compared to the controls.

The comprehensive methods used in this study were effective as the treatment to the CCS-dependent patients. This comprehensive methods can't cure these patients completely. SPECT can be used to evaluate the effectiveness of this comprehensive methods.

Radionuclide Therapy_2

^{177}Lu-labeled Carbon Nanoparticles Conjugated with cRGDfK Peptide for Efficient Tumor Targeted Therapy

Drishty Satpati, Ashis Satpati, Yugandhara Pamale, Haladhar Deb Sarma, Sharmila Banerjee

Radiopharmaceuticals Chemistry Section, Bhabha Atomic Research Centre, India

Carbon nanoparticles (CNP) are composed of non-toxic carbon materials and have particle size <20 nm. In this study carboxyl group containing CNPs were synthesized and conjugated with integrin αvβ3 targeting peptide c (RGDfK) / chelator for radiolabeling with ^{177}Lu. The aim of this work was to determine the potential of ^{177}Lu-CNP-c (RGDfK) for targeted radiotherapy of tumors expressing integrin αvβ3.

Carboxyl functionalized nanoparticles were synthesized by hydrothermal method and characterized by SEM and IR. Aqueous suspension of N-hydroxysuccinimidyl ester of CNP was conjugated with the peptide, cRGDfK and the chelator, p-NH2-Bz-DOTA (molar ratio 1:5, room temperature 6 h) and characterized by UV-Vis spectroscopy. ^{177}Lu labeling was carried out by addition of sodium acetate buffer (150 µL, 0.1 M, pH 4) to CNP conjugated with DOTA and cRGDfK peptide (25 µL), followed by addition of ^{177}LuCl3 (10 µL, 37 MBq) and incubation at 80°C for 20 min. In vitro stability studies (human serum, 37°C, 24 h) and in vivo biodistribution studies (C57BL6 mice bearing melanoma tumor; 3, 24, 48 and 72 h) were carried out..

Radiochemical purity of ^{177}Lu-CNP-c (RGDfK) was found to be >98% even without purification as determined by thin layer chromatography (TLC) and size exclusion chromatography using a PD-10 column. ^{177}Lu-CNP-c (RGDfK) was observed to be stable in human serum. There was rapid uptake of ^{177}Lu-CNP-c (RGDfK) in melanoma tumor within 3 h p.i. and it remained nearly constant with time (7.6 ± 0.7, 9.0 ± 0.7, 6.0 ± 1.7, 5.8 ± 1.2% ID/g at 3, 24, 48 and 72 h p.i.; n = 4). Blocking studies with c (RGDfK) led to >75% reduction (2.1 ± 0.3% ID/g) in tumor uptake at 24 h p.i. Fast urinary excretion and low uptake in reticuloendothelial system (RES) was observed for ^{177}Lu-CNP-c(RGDfK).

Simple preparation, high stability, tumor specificity and favorable pharmacokinetics of carbon nanoparticles conjugated with integrin αvβ3 targeting peptide, encourages further development of these nanoprobes for targeted radiotherapy.

Radionuclide Therapy_6

BRG1-Bromodomain Overexpression Sensitizes Both External and Internal Radiation Therapy

Juri Na[1,2,3], Hyewon Youn[1,3,4,5*], Keon Wook Kang[1,3], June-Key Chung[1,2,3*]

1. Department of Nuclear Medicine and
2. Biomedical Sciences, College of Medicine
3. Laboratory of Molecular Imaging and Therapy, Cancer Research Institute
4. Tumor Microenvironment Global Core Research Center
5. Cancer Imaging Center, Seoul National University Cancer Hospital

Purpose: For increasing therapeutic effect and reducing side effect of radiation treatment, radiation sensitization is required. Brahma-related gene 1 (BRG1), the catalytic subunit of SWI/SNF chromatin-remodeling complex, involves in DNA double strand breaks (DSB) repair. The strategy of this study is increasing therapeutic effect of radiation by overexpressing BRG1 bromodomain (BRD) as a competitor resulting inefficient DSB repair.

Methods: T*umor size* was measured with caliper and optical images were acquired by IVIS imaging system. To monitoring the therapeutic effect of BRD overexpression on external radiation, human colon cancer, HT29 cells were used. Retroviral pMX-BRG1-BRD vectors were transfected to HT29 resulting BRD over-expressing cell lines with low and high (1.48 times higher) copy number. Cells were irradiated using ^{137}Cs irradiator (IBL 437C) with 9 Gy. To test the radiosensitizing effect of BRD overexpression on internal radiation, FRO anaplastic thyroid cancer cells containing a human sodium iodide symporter gene (pMSCV-oNIS) were used for radioiodine therapy.

Results: Survival rates of irradiated HT29 cells expressing lower and higher level of BRD were 51.4% and 2.2%, respectively. Tumor growth of HT29 was reduced according to the higher BRD expression level *in vivo.* At 28 days after ionizing radiation, bioluminescence signals from low and high BRD overexpressed HT29 tumors were 40.77 % (P=0.048) and 7.37% (P=0.018), respectively. After 500 µCi of I-131 treatment on FRO mouse xenografts, luciferase signal of the FRO tumors having BRD showed 4.9 times lower than the FRO tumors at 10 days. Similarly, 60 µCi of I-131 treated mice bearing FRO with BRD tumors have shown slower proliferation (1.97 times) than mice bearing FRO tumors at day 10.

Conclusions: Radiation-sensitizing effect of BRD overexpression in human colon cancer and human thyroid cancer were successfully demonstrated using molecular imaging. From this result, we expect that

BRD overexpression could help to improve the efficacy of both external and internal radiation therapies with reducing the possible side effects by decreasing dose of radiation.

Oncology_56

Inverse agonist of estrogen-related receptor gamma (ERRγ) enhances sodium iodide symporter function in anaplastic thyroid cancer cells

Thoudam Debraj Singh[1], Shin Young Jeong[1], Sang-Woo Lee[1], Jeoung-Hee Ha[2], In-Kyu Lee[3,5], Byeong-Cheol Ahn[1], Young Hyun Jeon[1,5], Jaetae Lee[1,4]

1. Department of Nuclear Medicine
2. Department of Pharmacology
3. Department of Internal Medicine, School of Medicine, Kyungpook National University, Daegu, Korea
4. New Drug Development Center, Daegu-Gyeongbuk Medical Innovation Foundation, Daegu
5. Leading-edge Research Center for Drug Discovery and Development for Diabetes and Metabolic Disease, Kyungpook National University Hospital, Daegu, Korea

Purpose: Anaplastic thyroid cancer (ATC), a rare thyroid cancer with poor prognosis, is associated with insufficient function of the sodium iodide symporter (NIS). Estrogen-related receptor gamma (ERRγ) is a member of the orphan nuclear receptors, with important functions in cell development and homeostasis. However, there are no reports that demonstrate whether ERRγ is related with NIS function. Here, we evaluated the role of ERRγ on the regulation of NIS function in ATC cells by using GSK5182, an inverse agonist of ERRγ.

Methods: Two ATC cell lines, BHT-101 and CAL62, were incubated with the GSK5182 at various time points and dosages. Serial assessment of the NIS function was performed in the ATC cells by their uptake of radioiodine. The effects of GSK5182 on ERRγ and the mitogen-activated protein (MAP) kinase pathway as well as on NIS protein were evaluated by immunoblot assay. To examine whether the GSK5182-induced NIS functional activity can be affected by inhibition of the MAP kinase pathway, the MAP kinase activity and levels of radioiodine uptake were determined following treatment of an MEK inhibitor to GSK5182-treated cells. Finally, the cytotoxic effect of ^{131}I was determined by clonogenic assay.

Results: Treatment with GSK5182 resulted in dose- and time-dependent increases in iodide uptake in ATC cells, which were accompanied by both the down-regulation of ERRγ protein and the activation of extracellular signal-regulated kinase (ERK)-1/2. Both the increased radioiodine uptake and ERK-1/2 activation of ATC cells were completely inhibited by the specific MEK inhibitor. GSK5182 treatment enhanced the membrane localization of NIS in both ATC cells. Accordingly, pre-exposure to GSK5182 resulted in enhanced cytotoxic effects of ^{131}I treatment in ATC cells.

Conclusions: These findings suggest that the inverse agonist of ERRγ enhances the responsiveness of radioiodine therapy by modulating NIS function in ATC cells via the regulation of ERRγ and the MAP kinase signaling pathway.

Molecular Imaging_17

Radionuclide embedded Gold Nanoparticles (RIe-AuNPs) as a high sensitive and stable nuclear medicine imaging platform for *in vivo* DCs tracking

Sang Bong Lee[1,2], Su Bi Ahn[1], Ho Won Lee[1], Seul-Gi Oh[1], Thoudam Debraj Singh[1], Sang-Woo Lee[1,2], Byeong-Cheol Ahn[1], Dong-Kwon Lim[3],Young Hyun Jeon[1,2] , Jaetae Lee[1,2,4]

1. Department of Nuclear Medicine, School of Medicine, Kyungpook National University, Daegu, Korea
2. Leading-edge Research Center for Drug Discovery and Development for Diabetes and Metabolic Disease, Kyungpook National University Hospital, Daegu, Korea
3. KU-KIST Graduate School of Converging Science and Technology, Korea University, Korea
4. Daegu-Gyeongbuk Medical Innovation Foundation (DGMIF), Daegu, Korea

Purpose: The aim of this study is to develop a novel nuclear medicine imaging probe with combination of gold nanoparticles and radionuclides which have high sensitivity and long-term stability, and to demonstrate its feasibility as an imaging platform for DC tracking in living subjects.

Methods: Radionuclide embedded gold nanoparticles (RIe-AuNPs) was developed as illustrated in Supporting Fig. 1. The stability of RIe-AuNPs was evaluated in human serum and various pHs for 24h. A bone marrow derived dendritic cells (BMDCs) prepared from C57BL/6 mice was labeled with RIe-AuNPs to determine the efficiency of cell uptake in a dose- and time-dependent manner. The effects of RIe-AuNPs on DC function was examined in BMDCs by cell viability, phenotype marker, antigen uptake ability. For in vivo imaging, RIe-AuNPs labeled BMDCs was injected to footpad of mice and animal PET/CT imaging was done once a day for 4 days. Draining popliteal lymph nodes (DPLN) were excised at

day 4 post-transfer of labeled cells, followed by *ex vivo* imaging.

Results: RIe-AuNPs exhibited high stability in human serum and various pHs for 24h. Dose- and time-dependent increase of RIe-AuNPs uptake was shown in BMDC, revealing the saturation of its cellular uptake within as early as 3h and at 2 nM. Cellular labeling with RIe-AuNPs did not affect cell proliferation, phenotype marker and antigen uptake ability. The intense radioactive signals were detected in DPLN of mice injected with RIe-AuNPs labeled DCs at as early as 1 day, and the radioactivity at DPLN reached peak at day 3 with slight decrease of radioactivity at day 4 (Supporting Fig. 2). Consistently, ex vivo PET/CT imaging showed distinct radioactivity signal in excised DPLN.

Conclusions: We successfullytracked the BMDC migration to draining lymph nodes with newly developed RIe-AuNPs and PET/CT imaging, and these data support the feasibility of RIe-AuNPs as a potential imaging probe for cell tracking such as immune cells and stem cells

Molecular Imaging_20

Identification of the Role of Autophagy in *Salmonellae*-Mediated Cancer Imaging and Therapy

Mai Thi- Quynh Duong[1], Vu H. Nguyen[1], Thuy X. Phan[1], Eun-Kyeong Jo[2], Jung-Joon Min[1]

1. Department of Nuclear Medicine, Chonnam National University Medical School Gwangju, Republic of Korea
2. Department of Microbiology, Chungnam National University School of Medicine, Daejeon, Republic of Korea

Purpose: The aim of this project is to identify whether our non-invasive *Samonellae*- deffective ppGpp (SLDppGpp) strain could induce autophagy in cancer cell line *in vitro,* as well as we would like to figure out the impact of autophagy pathway in *Salmonellae*-mediated cancer imaging and therapy *in vivo*.

Methods: In brief, MC38 mouse colon carcinoma cells were infected with SLDppGpp or treated with lipopolysacchardies (LPS) in different time points. The autophagy flux was analyzed by western blot analysis (p62 and LC3-II protein levels) and LC3 puntuate staining. In order to obtain the autophagy deficient cell lines, we knocked down seperately two autophagy-related genes by using the pre-designed commercial shRNAs specific for murine Atg5 and Atg7. *In vivo* study was performed by analyzing the therapeutic effect of SLDppGpp on autophagy-knock down or autophagy competent MC38 tumor graft. The bacterial distribution in tumor was visualized and quantified by employing bioluminescence imaging system with SLΔppGpp-lux bacterial strain. To identify the relation between autophagy and immunogenic signals, we analyzes the translocation of Calreticulin and the release of high-mobility group box 1 (HMGB1) in cancer cells after treating with SLDppGpp.

Results: We demonstrated that non-invasive *Salmonella* could induce autophagy in cancer cells in a dose and time-point dependent manner. Lipopolysaccharides derived from *Salmonella* treatment also triggered autophagy through TLR4 expression on cellular membrane. This finding suggested a possible pathway that non-invasive *Salmonella* induced autophagic signaling pathway in cancer cells via the up-regulation of LPS/TLR4 pathway. Moreover, in response to bacteria-mediated cancer therapy, autophagy–competent, not autophagy-deficient cancer cell model, showed better tumor suppression effect. The exposure of calreticulin (CRT) and the release of high-mobility group box 1 protein (HMGB1), which required for immunogenicity, were significantly decreased in autophagy-deficient cancer cells as compared to autophagy-competent cells after bacterial infection. Thus, the release of HMGB1 and exposure of CRT from autophagic dying tumor cells are important factors that determines the therapeutic efficacy in bacteria-mediated cancer therapy.

Conclusions: Our findings proposed a model of how autophagic cancer cell death plays an important role in determining therapeutic efficacy after bacterial treatment via the regulation of immunogenic signals release in tumor microenvironment, suggesting more promising approaches for bacteria-mediated cancer therapy.

Oncology_59

Investigations of SP94 Peptide as a Specific Probe for Hepatocellular Carcinomas Imaging and Therapy

Yanli Li[1,2], Yanzhao Zhao[2], Lanfang Meng[2], Xiao Li[2], Guobing Liu[2], Dengfeng Cheng,[2*] Hongcheng Shi[1,2]

1. Shanghai Institute of Medical Imaging, Shanghai 200032, China
2. Department of Nuclear Medicine, Zhongshan Hospital, Fudan University, Shanghai 200032, China

Purpose: SP94 (SFSIIHTPILPL), a novel peptide, showed specifically binding to hepatocellular carcinomas (HCC) cells. Therefore, we are aiming to investigate the capability of SP94 peptide as a specific probe for HCC imaging and therapy after labeling by ^{99m}Tc and ^{188}Re.

Methods: Firstly, the HYNIC-SP94 peptide was prepared by solid phase synthesis and followed by ^{99m}Tc labeling

in citric-acid buffer for 30 min at room temperature. While glucohepatonate (10 mg) and $SnCl_2$ (0.4~1.0mg) were reacted with ^{188}Re perrhenate solution (37 MBq) for 1 h, then HYNIC-SP94 (200μg) was added to the solution and reacted for 1 h to yield ^{188}Re-HYNIC-SP94. The radiochemical purity and stability were investigated by radio-TLC. Cell competitive binding assay was performed by incubating ^{99m}Tc-HYNIC-SP94 and Huh-7 cells with increasing concentrations of SP94 peptide. Biodistribution and micro-SPECT/CT imaging studies were performed in Huh-7 and Hela cells tumor-bearing mice. In order to evaluate the potential of ^{188}Re-HYNIC-SP94 as a therapeutic agent, cell apoptosis, micro-SPECT/CT imaging and immunohistochemistry were performed.

Results: The labeling of HYNIC-SP94 was done with 98% yield for ^{99m}Tc and 89% for ^{188}Re. The specific activity of ^{99m}Tc and ^{188}Re tracers was 0.3~4 GBq/μmol. ^{99m}Tc/^{188}Re-HYNIC-SP94 were stable in PBS, saline and FBS up to 12 and 48h respectively. IC50 of ^{99m}Tc-HYNIC-SP94 was 4.49±0.20 nM when inhibited by HYNIC-SP94 to Huh-7 cells. In biodistribution studies, 1.02±0.26 %ID/g of the ^{99m}Tc labeled tracer was accumulated in Huh-7 tumors at 30 min postinjection. Huh-7 tumor was clearly visualized by micro-SPECT/CT and displayed significant difference with control tumor. Initial tumor targeting results inspired therapy evaluation when labeled by therapeutic isotope, such as ^{188}Re. After 15 h of ^{188}Re-HYNIC-SP94 treatment, Huh-7 cells exhibited typical apoptotic changes. From micro-SPECT/CT imaging, the uptake of ^{99m}Tc-HYNIC-SP94 was significantly decreased compared to prior treatment. The immunohistochemistry displayed that obvious necrosis and apoptosis can be seen in the ^{188}Re-HYNIC-SP94 group and no abnormal histopathology was noted in major organs.

Conclusions: *In vitro* and *in vivo* results supported that ^{99m}Tc-HYNIC-SP94 can be targeted to HCC cells. Furthermore, TUNEL assay, SPECT/CT imaging and immunohistochemistry results revealed that ^{188}Re-HYNIC-SP94 has the potential as a therapeutic radiopharmaceutical agent for HCC. As so far what we achieved, HYNIC-SP94 is a promising targeted carrier for HCC imaging and therapy.

Oncology_62

Preclinical Evaluation of ^{18}F-CB251 in Prostate Cancer Xenograft Model by PET

Byung Chul Lee[1], Byung Seok Moon[1], Tae Sup Lee[2], Jae Ho Jung[1], In Ho Song[2], Hyun Soo Park[3], Nunzio Denora[4], Sang Eun Kim[1,3]

1. Seoul National University Bundang Hospital, Republic of Korea
2. Korea Institute of Radiological and Medical Sciences, Republic of Korea
3. Seoul National University, Republic of Korea;
4. University of Bari "A. Moro", Italy

Purpose: Cerebral TSPO expression is dramatically increased after glial cell activation and well characterized marker for neuinflammation. Also, TSPO levels are elevated in a number of cancer such as breast and prostate, provides an opportunity of extended application of the TSPO selective radiotracers. In present study, we evaluated ^{18}F-CB251 ([^{18}F]**1**, 2-(6,8-dichloro-2-(4-[^{18}F]fluoroethoxyphenyl)imidazole[1,2-a]pyridine-3-yl)-*N,N*-dipropylacetamide) for tumor imaging in orthotopic tumor xenograft model by PET.

Methods: Affinity of [^{18}F]**1** was measured by displacement of [^{3}H]PK 11195 from rat cereberocortical samples. Time dependant cell binding uptake performed in several prostate cancer cells (PC3, LNCap and Du-145). Ex vivo biodistribution was performed in PC3 xenograft mice. Preclinical PET imaging was acquired post injected of [^{18}F]**1** at 30, 60, and 120 min static scan in PC3 orthotopic mice.

Results: In vitro binding affinity (IC_{50}) was 0.27 ± 0.09 nM. The cell binding uptake showed similar patterns in PC3 for 3.84, LNCap for 3.87, and Du-145 for 3.72 %ID at 60 min, respectively. In ex vivo biodistribution, the tumor uptake was 1.5 ± 0.7 %ID/g at 10 min and 1.4 ± 0.5 %ID/g at 60 min. The PET image of [^{18}F] CB251 visually reflected the ex vivo biodistribution and showed high uptake in the TSPO-rich organs such as lung, heart, and kidney cortex after injection, and the minor radioactivity was excreted in the urine. In orthotopic PC3 xenograft mice, the uptake of [^{18}F]**1** from PET imaging had 1.80 ± 0.28 %ID/g at 30 min, and 1.95 ± 0.21 %ID/g at 120 min, respectively, with high tumor to prostate uptake ratio (11.0 ± 5.5 at 10 min and 12.8 ± 5.4 times at 60 min, respectively).

Conclusions: Our data showed the potential of ^{18}F-CB251 to serve as a novel PET radiotracer for TSPO PET imaging of prostate cancer.

Molecular Imaging_27

PET Imaging Evaluation for Induced Pluripotent Stem Cell Transplantation in a Rat Model of Myocardial Infarction: a Pilot Study

Shuang Wu[1-4], Hao Liu[1-4], Yehua Shen[1-4], Fahuan Song[1-4], Hong Zhang[1-4], Mei Tian[1-4*]

1. Department of Nuclear Medicine, The Second Affiliated Hospital of Zhejiang University School of Medicine; Hangzhou, China

2. Zhejiang University Medical PET Center, Hangzhou, China
3. Institute of Nuclear Medicine and Molecular Imaging, Zhejiang University, Hangzhou, China
4. Key Laboratory of Medical Molecular Imaging of Zhejiang Province, Hangzhou, China
5. Department of Pathology, The Children's Hospital of Zhejiang University School of Medicine, Hangzhou, China

Purpose: The purpose of this study was to use small animal positron emission tomography (micro-PET) combined with echocardiography to evaluate and compare the therapeutic responses after pluripotent stem cells (iPSCs) and embryonic stem cells (ESCs) transplantation in a rat model of myocardial infarction (MI).
Methods: Twenty-one rats were randomly assigned to one of the three groups: iPSCs treatment, ESCs treatment, and the control phosphate-buffered saline (PBS) injection groups. Cells were administrated by intramyocardial injection into the border area of infarction at 30 min-post-MI. The treatment response was evaluated weekly by ^{18}F-FDG micro-PET and ECG studies. Imaging data were analyzed by using Lesion-to-normal (L/N) ratio for micro-PET and ejection fraction (EF) for ECG. At 4 weeks after stem cell transplantation, postmortem immunohistochemical staining and autoradiograpnic imaging were performed.
Results: Compared to the PBS control group, significantly higher left ventricular ejection fraction (LVEF) and increased ^{18}F-FDG accumulation in the peri-infarct area were observed in the stem cell (both iPSCs and ESCs) transplanted groups over the 4-week study period ($P < 0.05$ and $P < 0.001$, respectively). From Week 3 to 4, significantly intensive ^{18}F-FDG accumulations were found in iPSCs group compared to those of ESCs group ($P < 0.05$). Immunohistochemical staining demonstrated that transplanted stem cells survived in the injected sites and migrated to the peri-infact area.
Conclusions: ^{18}F-FDG PET imaging and echocardiography demonstrated metabolic and functional recovery after iPSCs and ESCs transplantation in the rat model of MI. Compared to ESCs, iPSCs seemed to be a better source of regenerative therapy for myocardial repair.

Radionuclide Therapy_23

Biodistribution and Evaluation of 131-I Labeled Neuropilin-binding Peptide for Tumor Imaging

Ping Dong, Hua Wei Cai, Lin Li*

West China Hospital of Sichuan University China

Purpose : In the present study, we describe a ^{131}I-labeled C-end rule motif peptide conjugate, Tyr-tLyp-1, for neuropilin-1 positive tumor targeting and imaging properties.
Methods: Truncated Lyp-1 was designed to expose its C-end motif (R/K)XX(R/K), and conjugated to Tyrosine for radiolabeling. In vitro targeted binding of the Tyr-tLyp-1 peptide was evaluated by fluorescent cellular analysis. Radiolabeling of the conjugate with ^{131}I produced ^{131}I-Tyr-tLyp-1 in high radiochemical yield (≥95%). In vivo behavior of the radiolabeled peptide conjugate was investigated in normal Balb/c mice and in A549 human NSCLC cancer experimental model.
Results: Tyr-tLyp-1 displayed specific binding affinity to cancer cells under micromole concentration, whereas this binding was depend on surface NRP-1 in cells and could be inhibited by NRP-1 antibodies. The subcutaneous NSCLC A549 tumor could be visualized and the tumor uptake of ^{131}I-Tyr-tLyp-1 was 4.77 times ($P<0.05$) higher than uptake in muscles in vivo by SPECT quantification at 6 h post injection.
Conclusion: Truncated Lyp-1 peptide specifically localized in NRP-1 positive tumors, indicating its potential use as a targeted imaging probe for radionuclide detection of NRP-1 positive tumors.

Molecular Imaging_36

The Labeling of ^{99m}Tc-HER2 Affibody and Its Imaging in Breast Cancer-xenografted nude mice

Xin Li, Jiong Cai

Department of Nuclear Medicine, Peking Union Medical College Hospital (PUMCH), Chinese
Academy of Medical Sciences & Peking Union Medical College (CAMS & PUMC), Beijing, China

Purpose: To prepare 99Tcm-human epidermal growth factor receptor 2 (HER2) affibody and explore its feasibility as an imaging agent in HER2-positive breast cancer.
Methods: Sodium glucoheptonate and SnCl2·2H2O were used to label HER2 AFFIBODY with 99Tcm. The labeling yield and radiochemical purity of 99Tcm-HER2 AFFIBODY were determined. The stability of 99Tcm-HER2 AFFIBODY was tested in PBS and serum. The equilibrium disassociation constant (Kd) of 99Tcm-HER2 AFFIBODY was measured with MBA-MD-361 breast cancer cells expressing HER2. SPECT/CT imaging was carried at 1.0 h and 4.5 h after injection of 37 MBq 99Tcm-HER2 AFFIBODY through tail vein of four nude mice xenografted with MBA-MD-361 breast cancer. The T/NT (liver, brain, lung, heart, bone and muscle) were deduced from

SPECT/CT acquired data. For blocking experiment, 200 μg HER2 AFFIBODY was injected intravenously before 99Tcm-HER2 AFFIBODY injection. SPECT/CT imaging was carried in the same way. The T/NT ratios were compared between non-blocked and blocked groups by analysis of viariance.

Results: The labeling of 99Tcm-HER2 AFFIBODY was finished with above 99% yield within 20 minutes. 99Tcm-HER2 AFFIBODY was substantial stable in PBS and serum; the radiochemical purity was (95.0±1.0)% after incubating 99Tcm-HER2 AFFIBODY with serum at 37 °C for 6.0 h. The Kd of 99Tcm-HER2 AFFIBODY was 1.7 nmol/L. The radioactive uptake in cancer was visualized at 1.0 h and 4.5 h after injection of 99Tcm-HER2 AFFIBODY in HER2 positive MDA-MB-361 breast cancer. 99Tcm-HER2 AFFIBODY was cleared out mainly through urinary system. The ratios of tumor to liver, lung, brain, heart, muscle, bone were 1.81±0.60, 8.95±1.13, 20.08±6.12, 7.61±0.56, 10.62±1.78, 11.42±2.07 respectively at 4.5 h after 99Tcm-HER2 AFFIBODY injection. After HER2 AFFIBODY blocking, the corre-sponding T/NT ratios were 0.60±0.23, 3.05±1.38, 5.24±2.17, 2.42±1.02, 8.16±2.66, 2.76±0.48 (F=29.38, t=3.162, both P<0.05) respectively.

Conclusions: 99Tcm-HER2 AFFIBODY can be synthezided with high purity and this new agent can be used to image HER2-positive breast cancer specifically.

Neurology_4

Predictive Factors of F-18 FDG PET/CT for Ischemic Stroke in Oncologic Patients

Jahae Kim[1], Kang-Ho Choi[2], Seran Min[1], Minchul Song[1], Ki Seong Park[1], Geum-Cheol Jeong[1], Hee Jeong Park[1], Sang-Geon Cho[1], Sae-Ryung Kang[1], Seong Young Kwon[1], Jung-Joon Min[1], Henry Hee-Seung Bom[1], Ho-Chun Song[1]

1. Department of Nuclear Medicine (Chonnam National University Hospital, Korea)
2. Department of Neurology (Chonnam National University Hwasun Hospital, Korea)

Purpose: The purpose of this study was to evaluate predictive factors of F-18 FDG PET/CT for ischemic stroke in patients with malignancy.

Methods: Total 134 oncologic patients were examined by F-18 FDG PET/CT. Vascular inflammation on PET imaging and visceral adipose tissue (VAT) area at the level of the umbilicus on CT imaging were evaluated. Vascular inflammation was evaluated using the target-to-background ratios (TBR) of large arteries on PET imaging. VAT area was measured from a single CT slice at the level of the umbilicus. Logistic regression analysis was used to determine the predictive factors of FDG PET/CT for ischemic stroke.

Results: Among 134 patients, the evidence of stroke was confirmed in 30 patients by brain MRI. Stroke group showed high TBR of both carotid arteries and abdominal aorta (P<0.001), VAT area (P=0.536) and abdominal circumference (P=0.011). TBR of right carotid artery (OR: 4330.344, P<0.001), left carotid artery (OR: 58.703, P=0.001) and abdominal aorta (OR: 23.479, P=0.006), and VAT area (OR: 1.038, P<0.001) were significantly associated with stroke after adjustment for risk factors and malignancy.

Conclusions: Severe vascular inflammation on PET and central obesity on CT are associated with ischemic stroke in oncologic patients. Oncologic FDG PET/CT can give prognostic information for ischemic stroke.

Neurology_12

Characteristics of Longitudinal Decline of Striatal F-18 FP-CIT Uptake in Parkinson's Disease: Retrospective Subregional Quantitative Analysis

Chang-Hwan Sung[1], Yin-Joo Lee[1], Jung-Soo Oh[1], Min-Young Oh[1], Sang-Ju Lee[1], Seung-Jun Oh[1], Sun-Ju Chung[2], Chong-Sik Lee[2], Jae-Seung Kim[1]

1. Department of Nuclear Medicine, Asan Medical Center, University of Ulsan College of Medicine, Seoul, Republic of Korea
2. Department of Neurology, Asan Medical Center, University of Ulsan College of Medicine, Seoul, Republic of Korea

Purpose: Dopamine transporter (DAT) imaging such as F-18 FP-CIT PET has been suggested to a useful imaging biomarker for the progression of Parkinson's disease (PD). The progression of striatal DAT loss in PD is known to be significantly greater than the normal aging effect. We evaluated the characteristics of the longitudinal decline of striatal F-18 FP-CIT uptake in PD.

Methods: We reviewed retrospectively 24 patients with PD (58±14 yr, M/F: 12/12, H&Y stage: 1.3±0.5) and 7 Non-PD (69±7 yr, M/F: 1/6, 4 essential tremor, 3 drug induced Parkinsonism). All patients underwent two F-18 FP-CIT PET scans at the initial diagnosis and follow-up (43±15 mo). PET images were spatially normalized and analyzed with 8 striatal subregional volume-of-interest (VOI) and 1 occipital VOI templates. We measured the specific to non-specific binding ratio (SNBR) of subregional VOIs and calculated the annual

decline rate (%/yr) of FP-CIT uptake.
Results: Striatal SNBRs (3.9±1.4) in patients with PD were significantly lower than those (6.6±0.9) in non-PD (P<0.001), and the difference was most significant in posterior putamen. Annual rate of decline in overall striatal uptake was significantly greater in PD (-7.6±4.2 %/yr) than in non-PD (-1.0±3.1 %/yr) (P<0.001), without relation with age, initial SNBR and follow-up period (P>0.05). Annual rate of decline in affected posterior putamen (-11.3±5.1 %/yr) was greatest among all subregions, followed by anterior putamen, caudate, ventral striatum (-4.7±4.3 %/yr) in PD, although there was no significant subregional difference in non-PD.
Conclusions: The decline of striatal F-18 FP-CIT uptake in PD was about eight times faster than those of non-PD, with difference among striatal subregions, where posterior putamen showed the fastest progression as well as the initial lowest uptake.

Neurology_14

Brain perfusion patterns in schizophrenia -An evaluation by ^{99m}Tc-HMPAO SPECT-CT

Amburanjan Santra, Rajarshi Neogi, Ramesh K Thukral

N R S Medical College & Hospital, Kolkata, India

Study aimed to evaluate the perfusion pattern in chronic medicated schizophrenics of different types.
Thirty two (20 male, 12 female) patients of schizophrenia with median age of 32 years undergone brain SPECT-CT study. All images are reviewed and processed in 'Neurogam' for further quantification. 'Medcalc' statistical software was used to analyze data. Kruskal-wallis test was applied to see any dependency of the regional perfusion defect to schizophrenia types.
There were 21 patients of disorganised type, 5 paranoid, 3 each in undifferentiated and residual type. All of them have low prefrontal cortex (PFC) activity and temporal hypoperfusion. Bilaterality noted in 82% of PFC defect and 94% of temporal lobe defect. Half of the patients had hypoperfusion in premotor area. Parietal lobe, mainly inferior parietal lobule was involved in 62.5%. Cingulate cortex, basal ganglia and cerebellum were hypoactive in one third cases. No significant dependency on type of schizophrenia noted in case of prefrontal (unilateral/bilateral), temporal, parietal, cingulate, basal ganglia or cerebellar hypoperfusion. Premotor cortex involvement is significantly higher in case of disorganized type than other groups (P=0.06). Dorsolateral prefrontal cortex (DLPFC) was involved in every patient, even with milder defect, 9 of all prefrontal hypoperfusion have only DLPFC defect. Other common areas are orbitofrontal cortex, temporopolar area and medial temporal lobe.
Hypoperfusion in prefrontal cortex and temporal lobe is a constant finding in all chronic medicated schizophrenic patients. There may also be involvement of premotor cortex, inferior parietal, cingulate, basal ganglia and cerebellum. Premotor cortex involvement seems higher in disorganized type. DLPFC is likely earliest area of involvement in most of schizophrenia type.

Molecular Imaging_39

Resting-State Glucose Metabolism and Functional MRI Multi-Modal Study in Healthy subjects

Jiao Fang-yang[1], Zang Yu-feng[2],Ge Jing-jie[1], Zhang Hui-wei[1], Jiang Cheng-feng[1],Guan Yi-hui[1], Zuo Chuan-tao[1], Wu Ping[1]

1. PET Center, Huashan Hospital, Fudan University, Shanghai 200235
2. Center for Cognition and Brain Disorders, Hangzhou Normal University, Hangzhou 311121, China

Purpose: To quantify and investigate the relationship between resting-state regional cerebral glucose metabolism and functional MRI in healthy subjects.
Methods: Eighteen healthy subjects were selected based on availability of data. Regional homogeneity (ReHo), amplitude of low frequency fluctuations (ALFF), fractional amplitude of low frequency fluctuations (fALFF), and degree of centrality (DC) maps were generated from the rs-fMRI data, and voxel-wise comparison to glucose uptake distribution provided by non-simultaneously acquired FDG-PET was performed. The mutual relationships among each couple of these five metrics were explored in terms of similarity, both of spatial distribution across the brain and the whole group, and voxel-wise across subjects, taking into account partial volume effects by adjusting for grey matter (GM) volume. Moreover, the correlation between PET and rs-fMRI derived metrics in several resting-state networks (RSNs) are also exploited.
Results: Figure 1 shows PET and rs-fMRI metrics maps calculated over the whole intracranial volume averaged across all 18 subjects.
Spatial distribution analysis: a significant correlation between the spatial distribution of glucose uptake and rs-fMRI derived metrics was present in Table 1, Figure 2 and 3. The full and partial correlation coefficients between ReHo, ALFF and PET achieve the best at a GM threshold of 0.6,and fALFF contrast positively and significantly correlated with

PET contrast, also achieving the best partial correlation coefficients at a GM threshold of 0.6 In brain networks, the highest correlation coefficients between PET and FC maps were achieved for all the rs-fMRI maps in the executive control network (ECN)(Figure 4), followed by default-mode network (DMN)(Table 2). Overall, ReHo provided significantly higher correlation coefficients with PET, compared to other metrics.

Across-subjects analysis: In general only a limited percentage (up to 5.8% when comparing PET vs. ReHo) of voxels showed a significant correlation across subjects between PET and the four modalities, with higher percentages for ALFF and ReHo, while fALFF don't showed any correlation with PET (Figure 5, Table 3) While the correlations between the three MRI derived measures showed significantly higher correlations with each other, with highest values (74.9%) when comparing ALFF with ReHo. The ranking of the correlations of the four rs-fMRI metrics with FDG obtained on the main RSNs was consistent across whole brain grey matter (Table 4).

Conclusion Our quantitative results of five MRI and PET imaging metrics are overall in line with the previous work that has directly correlated rs-fMRI metrics and PET across the whole brain in normal subjects. The positive correlations were significantly stronger for ReHo, ALFF and fALFF than for DC, although the strength of this correlation substantially varied across functional networks. Despite the similar spatial distributions of rs-fMRI metrics and PET, only a small percentage of GM voxels showed a significant correlation across subjects in normal conditions, unrelated to the similarities in the spatial distributions of these metrics, possibly also due to the limited inter-subject variability present in normal subjects.

Physics/Instrument_8

Motion Reduction in Respiratory Gated SPECT/CT Using Non-rigid Registration

Greta S. P. Mok, Duo Zhang

Biomedical Imaging Laboratory, Department of Electrical and Computer Engineering, Faculty of Science and Technology, University of Macau, Macau

Purpose: Respiratory gating reduces motion blur in cardiac SPECT. However, the reduced count level in each respiratory gate leads to higher image noise. This study aims to apply non-rigid registration on the gated reconstructed SPECT images to reduce motion blur while utilizing all detected counts at the same time.

Methods: We modeled a male patient with Tc-99m-MIBI activity distribution using the digital 4D XCAT phantom with respiratory motion of 2 cm. Normal cardiac uptake as well as a heart with 2 defects with 60% of the normal uptake placed at the mid-inferolateral and mid-anterolateral were modeled. The respiratory cycle was 6 s and divided into 96 frames which were grouped to simulate 6 respiratory gates. The average attenuation and activity maps in each phase represented gated CT and SPECT respectively. Realistic noisy projections with attenuation modeling were generated using an analytical projector. Projections in each gate were reconstructed with attenuation correction using the phase-matched gated CT using OS-EM method with up to 30 updates. We used affine plus b-spline registration method to register the reconstructed images of each gate to end-expiration phase. The unregistered (Unreg_recon) and registered (Reg_recon) images were then averaged to generate the polar plots separately. The polar plot of the reconstructed image at end-expiration (Ex_recon) was used as a baseline. Relative difference (RD) of the average intensity was computed for each segment using the original phantom of end-expiration as the reference in the 17-segment analysis. Normalized standard deviation (SD) of a normal uniform septal region with 420 pixels was calculated to assess the noise.

Results: For the normal heart, the RDmean for Unreg_recon, Reg_recon and Ex_recon were 22.70%, 6.53% and 3.73%, while the NSD were 0.076, 0.070 and 0.108 respectively. From visual assessment, the defect delineation substantially improves for Reg_recon and approaches to Ex_recon with reduction of noise of 35.19%.

Conclusions: Non-rigid registration on respiratory gated SPECT is feasible and substantially improves the image quality and quantitative accuracy as compared to gated SPECT without registration.

Physics/Instrument_9

Development of Network Based Scalable Data Acquisition System for Time-Of-Flight PET Scanner

Hyun Suk Yoon, Jeong-Whan Son, Jun Yeon Won, Jae Sung Lee

Department of Nuclear Medicine (Seoul National University, Korea)

Purpose: Improvement of detector technology in positron emission tomography (PET) imaging made possible to achieve under 350 ps system timing resolution for time-of-flight (TOF) PET scanner. Such TOF PET scanner is consists of a large number of detector elements. Therefore data acquisition (DAQ) system for high performance TOF PET scanner requires

high data processing capability, high precision timing measurement capability and sufficient number of readout channels. However, it is inefficient to acquire and process all the PET signals with single centralized DAQ system. In this paper, we propose a network based scalable DAQ system for a prototype TOF PET Scanner.

Methods: The Prototype TOF PET scanner has 40 block detectors based on high QE multi-anode PMTs and arrays of LGSO scintillators. The scanner has trans-axial and axial FOV of 51.8 cm and 4.64 cm, respectively. The system performance of 340 ps coincidence resolving time, 11.5 % energy resolution and 2 mm spatial resolution were achieved.

The DAQ system is composed of a set of 3 modules, ADC, TDC and DAQ processing modules. The ADC modules has 40 readout channels and sends digitized signal to DAQ processing modules. The TDC module has 40 dual-phase tapped-delayed-line TDCs with 14 ps measurement precision are implemented on a FPGA and sends fine timestamp of each event's trigger signal. The DAQ processing module is implemented on a separate FPGA and receives digitized signal and timestamp of each event from ADC and TDC module, respectively. It has real-time signal processing capability and sends processed data via 1-Gbps Ethernet. A set of ADC, TDC and DAQ processing modules is used for every 40 block detectors, and multiple set of modules are connected to a 10-Gbps network switch for scalability of DAQ system.

Results: TOF PET images of NEMA IEC body phantom were successfully and showed better image quality compare to non-TOF images. Maximum of 57.6 Mcps count rate performance and linear count rate scalability up to 5 DAQ modules was achieved with 10-Gbps Ethernet network based DAQ system.

Conclusions: A network based DAQ system for TOF PET scanner with high system count rate performance and scalability upto 400 block detectors was developed.

Clinical Applications of PET/MR and SPECT/CT_2

Detection of Recurrent Gliomas: a Prospective Comparison between ^{99m}Tc-GHA SPECT/CT and ^{13}N-NH3 PET/CT

Bangkim Chandra Khangembam[1], Varun Singh Dhull[2], Abhinav Singhal[3], Chandrasekhar Bal[4]

1. Department of Nuclear Medicine and Molecular Imaging, Dr. Bhubaneswar Borooah Cancer Institute, Guwahati, India
2. Delhi Institute of Functional Imaging, New Delhi, India
3. Department of Nuclear Medicine, Fortis Memorial Research Institute, New Delhi, India
4. Department of Nuclear Medicine and PET, All India Institute of Medical Sciences, New Delhi

Purpose: To assess the efficacies of ^{99m}Tc-GHA SPECT/CT (GHA) and 13N-NH3 PET/CT (NH3) in detecting recurrent gliomas.

Methods: 55 consecutive, histologically proven and previously treated glioma patients (age, 38.9±12.2 years) presenting with clinical suspicion of recurrence were evaluated with GHA and NH3. A combination of clinico-radiological follow-up, repeat imaging and/or biopsy (when available) was considered as the reference standard.

Results: 28 patients had recurrence. Sensitivity, specificity, positive predictive value, negative predictive value, accuracy of GHA and NH3 were 85.7, 85.2, 85.7, 85.2, 85.4% and 78.6, 88.9, 88.0, 80.0, 83.6% respectively (concordant findings in 46 patients). The performances of the two modalities were not significantly different (P=0.508, overall; P=0.687, low-grade; P=1.000, high-grade).

Conclusions: ^{99m}Tc-GHA SPECT/CT is a cost-effective modality equally efficacious as 13N-NH3 PET/CT in detecting recurrent gliomas.

Clinical Applications of PET/MR and SPECT/CT_6

Glioma Recurrence Evaluation Using Multiparametric Simultaneous O-(2-^{18}F-Fluoroethyl)-L-Tyrosine (^{18}F-FET) Positron Emission Tomography Magnetic Resonance Imaging (PET/MRI)

Amarnath Jena[1], Sangeeta Taneja[1], Aashish Gambhir[1], Anil Kumar Mishra[2], Rajnish Sharma[2], Maria M D'Souza[2], Sapna Manocha Verma[3], Puja Panwar Hazari[2], Pradeep Negi[1], Ganesh Krishna Rao Jadhav[3], Shanti Kumar Sogani[4]

1. PET SUITE, Department of Molecular Imaging and Nuclear Medicine
2. Indraprastha Apollo Hospitals, Sarita Vihar, New Delhi, Pin 110076
3. Institute of Radiation Oncology
4. Institute of Neuro Sciences

Purpose: To investigate the potential of hybrid gadolinium (Gd) enhanced 18Ffluoroethyl-L-tyrosine (^{18}F FET) PET/MRI in distinguishing recurrence from radiation necrosis using simultaneously acquired multiple structural and functional parameters.

Methods: 26 patients (5 females, 21 males; mean age ±SD: 51.58±15.97) with contrast enhancing lesions (n=32)

post surgery and radiation therapy were evaluated with simultaneously acquired ^{18}F FET PET/MRI. They were then followed up with re-surgery and histopathological diagnosis (n=9) and/or clinical /MRI or PET/MRI based imaging follow up (n=17). Using manually drawn regions of interest (ROI) over areas of maximal contrast enhancement and/or FET uptake TBRmax, TBRmean, and Cho: Cr ratios, normalized rCBVmean and ADCmean were determined. Accuracy of each parameter individually and in various combinations was evaluated using two tailed independent samples student t -test, receiver-operating-characteristic analysis and multivariate logistic regression analysis. Positive histopathology and long term imaging/clinical follow up suggestive of disease progression served as gold standard.

Results: Of 26 patients, 19 had recurrence and 7 patients showing radiation necrosis. Individually, TBRmax, TBRmean, ADCmean, and Cho: Cr ratios and normalized rCBVmean were significant in differentiating recurrence from radiation necrosis with an accuracy of 93.8%, 87.5%, 81.3%, 96.9% and 90.6% respectively. The accuracy of both normalized rCBVmean and ADCmean was improved in combination with TBRmax or Cho: Cr ratio. TBRmax with Cho: Cr ratio yielded highest accuracy approaching 97 %.

Conclusions: Our findings suggest that FET TBRmax with Cho: Cr ratio could be most useful to distinguish recurrence of primary glioma from radiation necrosis. Hybrid simultaneous ^{18}F-FET PET/MRI might play a significant role in the evaluation of patients with suspected glioma recurrence.

Clinical Applications of PET/MR and SPECT/CT_9

Integrated simultaneous PET MR in a tertiary healthcare setup: Initial experience of 1690 case studies

Amarnath Jena[1], Sangeeta Taneja[1], Aashish Gambhir[1], Sapna Manocha Verma[3], Pradeep Negi[1], Ganesh Krishna Rao Jadhav[3], Shanti Kumar Sogani[2]

1. PET SUITE, Department of Molecular Imaging and Nuclear Medicine
2. Institute of Neuro Sciences
3. Institute of Radiation Oncology, Indraprastha Apollo Hospitals, Sarita Vihar, New Delhi, Pin 110076

Purpose: (1) To discuss the use of PET/MRI in a prominent tertiary healthcare setup. (2) To provide examples of cases where PET/MRI added significantly to diagnostic value.

Methods: PET MR, introduced recently for imaging of clinical patients, combines the high soft-tissue contrast and biological sequences of MRI with metabolic imaging and high sensitivity of PET. Dedicated protocols for whole body and brain PET MRI were employed over a range of radiopharmaceuticals such as FDG (1584 cases), DOTATATE (55 cases), FET (42 cases), F-choline (7 cases) and PSMA (2 cases).

Results: A total of 1690 cases (790 females: 900 males; with age ranging from 1-94; mean age ±SD: 53.54 ± 15.437) underwent simultaneous PET MRI in our institute from 1/3/2013 to 30/4/2015. 17.2% of cases were dedicated brain and CNS studies while remaining 82.8% whole body studies. The whole body studies were mostly for oncological indications comprising of 325 breast, 302 genito-urinary, 155 head and neck, 108 gastrointestinal, 91 hematological, 82 musculoskeletal, 76 chest and lung, and others including FUO, MUO, neurodegenerative and infection imaging.

Conclusions: our experience demonstrates that whole body or brain PET MRI for various oncological and non-oncological indications is clinically feasible without any impairment of PET and MR image quality. Furthermore, it scores significantly specifically in pediatric population by reduction of radiation dose incurred, neuro-oncology using simultaneous multiparametric evaluation and single session evaluation of breast, head & neck and pelvic malignancies.

Clinical Applications of PET/MR and SPECT/CT_10

Additional Value of Post Therapy ^{131}I SPECT/CT in Patients with Differentiated Thyroid Cancer

Satyawati Deswal [1], Vibhor Mahendru[2], Dhananjay Kumar Singh[1], Gaurav Sinha[1], Arun Malhotra[1]

1. Department of Nuclear Medicine, Dr.Ram Manohar Lohia Institute of Medical Sciences, Lucknow, India
2. Department of Surgery, Eras' Lucknow Medical College, Lucknow, India

Radioiodine uptake in numerous physiologic and pathologic variants may lead to misinterpretations of planar scans. The specificity of planar imaging can be increased by detailed clinical history of patient, avoiding misinterpretation of the normal variants, by consideration of pattern of uptake.

Objective: We analysed the impact of addition of SPECT/CT which generates coregistered SPECT and CT images acquired with a single device during a single imaging session on the characterisation of lesions / Specificity and accuracy of whole body post therapy radioiodine scintigraphy.

Materials and Methods: A whole body post therapy scan was performed in both anterior and posterior projection

on a 16 slice SPECT CT (Discovery NM 670). In 15 patients with thyroid cancer, whole-body scintigraphy (WBS), SPECT, and SPECT/CT were prospectively performed 2-10 days after administration of 1110-6475 MBq (30-175 mCi) of I-131. SPECT/CT of the head and neck / other site if required, was performed in all patients. Incremental value of SPECT/CT in localisation and characterisation and its impact on management of patients was assessed.

Results: Planar imaging and SPECT/CT were performed in 15 consecutive patients with thyroid cancer (10 Papillary, 4 Follicular and 1 Hurthle cell) 2- 10 days post administration of 1110-6475 MBq of I-131. The indication for therapy was post surgical ablation or recurrent /metastatic disease with rising thyroglobulin levels. SPECT/CT accurately characterised the I 131 uptake in post surgical patients with metastatic disease in neck. In one patient multiple focal uptake in chest and abdomen localised on SPECT/CT. CT portion of SPECT/CT demonstrated non-iodine concentrating lesions in 2 out of 15 patients.

Conclusions: SPECT/CT significantly improved the specificity of post therapy whole body planar imaging. It better defined the extent and sites of metastases and is a valuable adjunct to standard techniques.

Endocrinology_18

Gain-value of ^{99m}Tc-MIBI SPECT/CT fusion imaging for the diagnosis of secondary hyperparathyroidism

Ye Peng, Guixia Pan, Chao Cheng, Changjing Zuo*

The department of Nuclear Medicine, Changhai Hospital of Second Military Medical University

Purpose: To investigate the value of SPECT/CT ^{99m}Tc-MIBI imaging in the diagnosis of secondary hyperthyroidism.

Methods: A retrospective analysis of 16 patients with secondary hyperparathyroidism caused by chronic renal failure from January 2013 to December 2014 in our department,with routine ^{99m}Tc-MIBI dual phase imaging firstly, and then got SPECT/CT fusion imaging, and compared with pathological results or follow up, to explore the value of SPECT/CT fusion imaging.

Results: 16 cases of patients with 46 hyperplasia of the parathyroid tissue, including 6 cases with 4 parathyroid-tissues cut, 2 cases with 3 parathyroid-tissues cut, and 8 cases with 2 parathyroid-tissues cut. The sensitivity of ^{99m}Tc-MIBI two-phase image is 71.7% ,36 (33 true-positive, and 3 false-positive) ,and false positive were all thyroid nodules. The sensitivity of SPECT/CT ^{99m}Tc-MIBI fusion imaging was 91.3%, which was corrected by 3 false-positive and 9 false-negative, and 4 false negative lesions were not detected.

Conclusion: The sensitivity of SPECT/CT ^{99m}Tc-MIBI fusion imaging was significantly higher than that of ^{99m}Tc-MIBI dual phase imaging, and it has a high gain value in the diagnosis of secondary parathyroid glands.

General Nuclear Medicine_16

Feasibility of glomerular filtration measurment in Tc-99m DTPA renal scan based on geographic mean of renal uptake and renal to background ratio

Sun Young Oh, Yuun Kwon Kim, Geun Woo Kim

Department of nuclear medicine National Police Hospital, Korea

In DTPA renal scan, quantification of renal function using geographic mean of anterior and posterior images might reduce the error caused by kidney depth correction. Hypothetically, %renal uptake in Gates' GFR might be over or underestimated depending on the volume of distribution of each patient. Considering the distribution of DTPA in ECF space, background activity of DTPA renal scan may represent the serum DTPA concentration. Therefore we propose the new parameter, renal to background ratio calculated from geographic mean of anterior and posterior image, and assess the feasibility and possibility to improve the accuracy in measuring camera based GFR.

Fourteen patients who underwent DTPA renal scan for evaluation of their renal function were included in this study. GFR were measured by dual plasma sample method as reference (rGFR). In DTPA renal scan, anterior image was obtained as well as posterior image with dual head gamma camera. The net renal uptake was determined by subtraction of the perirenal background activity from the renal activity. Geographic mean of renal uptake was calculated. For Renal to background ratio (RTB), background ROI was drawn at LLQ abdomen. RTB was determined from geographic mean of net renal uptake divided by LLQ background activity. RTB was compared with rGFR. Correlation between rGFR and estimated GFR (eGFR) from serum creatinine level using MDRD equation, Gates GFR (gGFR) were also analyzed.

Mean rGFR, eGFR, gGFR was 67.1±25.7 ml/mim (Range: 16.2-99.4 ml/min), 62.0±1.82 (Range: 38.9-100.08) and 63.4±20.6 (Range: 36.86-93.66), respectively. The eGFR , gGFR and RTB correlated well with rGFR .(r=0.70, r=0.71, r=0.94, P<0.005). Regression equation of RTB and rGFR was Y= 0.1126X-5.66. Mean Revised GFR from RTB was 67.1 ± 29.1 (Range: 11.1-93.1). Revised GFR

results in significantly better correlation with rGFR than eGFR or gGFR (P=0.041, P=0.046).
In Tc-99m DTPA renal scan, GFR measurement based on geographic mean of renal uptake and renal to background ratio could give more precise information in assessing the renal function than conventional camera based Gates GFR or estimated GFR from serum creatinine level.

Clinical Applications of PET/MR and SPECT/CT_21

Assessment of co-transplanted bone allograft viability and function in Living Related Kidney recipients Using SPECT-CT and Contrast-Enhanced Ultrasound (CEUS)

Si-juan Zou[1], Xian-zhang Luo[2], Nian-qiao Gong[2], Xiao-hua Zhu[1]

1. Huazhong University of Science and Technology
2. Department of Nuclear Medicine, Tongji Hospital, Tongji Medical College, Wuhan, China
3. Huazhong University of Science and Technology
4. Institute of Organ Transplantation, Tongji Hospital, Tongji Medical College, Wuhan, China

Purpose: The aim of the study was to monitor the viability and function of co-transplanted bone allograft in patients after kidney transplantation using bone SPECT-CT and Contrast-enhanced Ultrasonography (CEUS).
Methods: ^{99m}Tc-MDP SPECT/CT and CEUS were carried out in a series of 27 patients who underwent living-related kidney transplantation and bone fragments co-transplantation. The imaging of bone SPECT-CT and CEUS were analyzed separately and quantitative-based analysis were performed. The radioactivity ratio between the Max VOI counts of allogeneic bone fragments (B) to contralateral region (N) was calculated (B/N). And on CEUS, the parameters of time to enhancement (TTE), time to peak (TTP) and the maximum blood flow of the peri-bone area (MBF) were recorded when the peri-fragment showed enhancement.
Results: 41 scans of ^{99m}Tc-MDP SPECT/CT and 60 times of US/CEUS on 27 patients were performed. The value of B/N was declined with time from six months post-transplantation. And, in 14 of patients who experienced twice SPECT/CT examination, the B/N value on the second scan was significantly lower than the first one. On CEUS, the blood supply for bone fragments (TTP=17.2±6.4s) was lower than kidney allograft (TTP=14.9±6.3s) and higher than normal parenchyma (TTP=19.5±5.8s) during the first six months after transplantation, however, later on, it became lower than normal parenchyma. Meanwhile, the TTE and MBF showed the same tendency as TTP.
Conclusions: SPECT/CT and CEUS is reliable tool for monitoring viability and dynamic change of the co-transplanted bone allograft in Living Related Kidney recipients, especially in the first six months after transplantation.

Molecular Imaging_41

^{68}Ga-NOTA-PRGD$_2$ PET/CT in Evaluation of Active Idiopathic Pulmonary Fibrosis: A Pilot Proof-of-Concept Clinical Study

Shaobo Yao[1], Hui Huang[2], Peilin Wu[1], Wei Zhang[1], Zuojun Xu[2], Zhaohui Zhu[1*]

1. Department of Nuclear Medicine
2. Department of Respiratory Disease, Peking Union Medical College Hospital, Chinese Academy of Medical Science & Peking Union Medical College, Beijing, 100730, China

Purpose: Idiopathic Pulmonary Fibrosis (IPF) is a progressive, fatal lung disease with limited method to evaluate the disease activation. To prove the hypothesis that active IPF may be correlated with integrin $\alpha_v\beta_3$ over-expression, a pilot clinical study was performed to non-invasively image active IPF with PET/CT, using ^{68}Ga-labelled PEGlated cyclic arginine-glycine-aspartic acid (RGD) dimer peptide as the tracer. This study had been proved by the Institute Review Board of Peking Union Medical College Hospital. Written informed consent was obtained from each patient.
Methods: ^{68}Ga-NOTA-PRGD$_2$ was prepared by incubation of 10 μL NOTA-PRGD$_2$ (1 mM in H_2O) with 10-14 mCi of $^{68}GaCl_3$ elution, pH was adjusted to 4.5 with sodium acetate (1.25 M), and the mixture was incubated at 100 ºC for 10 minutes. The product was further purified by SPE (solid phase extraction) using Light C18 cartridge and the injection saline was analyzed by RP-HPLC. For clinical evaluation, two patients diagnosed with IPF and characterized as bilateral ground-glass opacities on CT were underwent ^{68}Ga-NOTA-PRGD$_2$ PET/CT. Whole-body images were acquired at 0.5 h after intravenous injection of 74-111 MBq ^{68}Ga-NOTA-PRGD$_2$. The standardized uptake values (SUVs) was measured for semi-quantitative evaluation.
Results: The decay-corrected yield of ^{68}Ga-NOTA-PRGD$_2$ was over 85% with the purity greater than 99%. The human studies, ^{68}Ga-NOTA-PRGD$_2$ PET/CT images demonstrated predominantly increased accumulation in regions of fibrosis in the lungs of the two patients with IPF, in compare to no significant increase accumulation relative to the normal lungs. The SUV_{max} of the lung

lesions were 2.08 and 2.38 at 0.5 h, and the lesion-to-normal lung ratios were 3.9 and 3.2, respectively for the two patients. ^{68}Ga-NOTA-PRGD$_2$ was excreted mainly through the urinary system. No adverse effect was reported related to the intravenous tracer injection.

Conclusions: This pilot clinical study preliminarily indicates that ^{68}Ga-NOTA-PRGD$_2$ PET/CT is a useful method for non-invasive imaging of active IPF in the patients, which merit further evaluation of disease status and response to treatments.

General Nuclear Medicine_36

Bone scintigraphy in trauma patients: Characteristics according to trauma type and involved site

Minjung Seo, Seol Hoon Park

Ulsan University Hospital, Korea

The purpose of this study is to evaluate the characteristics of uptake on bone scintigraphy in trauma patients.

Among trauma patients who underwent bone scans between January to March of 2014, 94 patients who had scans within 15 days (mean: 6, range 1-15 days) of trauma were retrospectively reviewed. Old lesions, surgically fixated lesions, and lesions from patients with a history of cancer were excluded. We evaluated the location and intensity of bone uptakes suggestive of fracture on bone scintigraphy. 'Non-avid' lesions were determined as lesions with no/mildly increased uptake. The imaging modalities such as X-ray, CT, MRI were used as gold standard for evaluating the location of fracture.

A total of 295 fractures which had available radiography with corresponding changes and had not undergone surgical correction were included in the analysis. The most frequently involved site was the rib (29.8%). The most commonly involved sites according to trauma types (traffic accident by car/motorcycle/bicycle, falling, and slipping) were the spine, rib, scapula, rib, and skull, respectively. Most lesions were avid on bone scintigraphy and the rate of non-avid lesions was 25.4%. Multivariate analysis showed that the fracture location was the most significant factor for non-avidity on bone scintigraphy (P<0.001). Lesions that were located in the skull and the shaft of long bones showed only mild or no uptakes (40/61, 65.6%).

Bone scintigraphy is a useful imaging modality in the mapping of different fracture distributions according to the trauma type. However, lesions located in the skull and the shafts of long bones may show non-avid bone uptakes and require careful attention when interpreting bone scintigraphy.

General Nuclear Medicine_8

Comparison of FDG uptake patterns between activated macrophages and cancer cells according to the difference in glucose-6-phosphatse expression

Youngeun Lee[1,2,3], Mi Jeong Kim[1,3,4], Chul-Hee Lee[1,5], Hyewon Youn[1,3,4,6], Gi Jeong Cheon[1,2,3], Keon Wook Kang[1,3], Abass Alavi[7], June-Key Chung[1,3,4*]

1. Department of Nuclear Medicine and
2. Tumor Biology Program
3. Laboratory of Molecular Imaging and Therapy, Cancer Research Institute
4. Tumor Microenvironment Global Core Research Center
5. Biomedical Sciences
6. Cancer Imaging Center, Seoul National University Cancer Hospital
7. Division of Nuclear Medicine, Department of Radiology, Hospital of the University of Pennsylvania, Philadelphia, Pennsylvania

Purpose: ^{18}F-FDG PET has been widely used in oncologic diagnosis, however, because increased ^{18}F-FDG uptake also shows in inflammation sites, which could be false positive results in cancer diagnosis. This study evaluated ^{18}F-FDG uptake patterns in cancer cells and activated macrophages with expressions of glucose uptake-related proteins including glucose-6-phosphatase (G6Pase).

Methods: Mouse macrophages (RAW264.7) were stimulated with 100 ng/ml lipopolysaccharide (LPS) for 24 h. To confirm the effect by G6Pase expression, G6Pase high-expressing HepG2 and G6Pase low-expressing MDA-MB231 were chosen. For ^{18}F-FDG uptake assay, the cells were incubated with ^{18}F-FDG (5 μCi) for diverse time points (10, 60, 120, 240, 360 min). For ^{18}F-FDG efflux assay, the cells were incubated with ^{18}F-FDG (5 μCi) for 60 min. After replacement of medium, ^{18}F-FDG activity of the cells and the supernatants harvested at 10, 20, 30, 60, 90, 120 min was measured using gamma counter. Expression levels of glucose transport-1 (Glut-1), hexokinase II (HK II) and G6Pase were evaluated by western blot. For inflammatory model, BALB/c nude mouse was injected with turpentine oil (50 μL, 100 μL) or PBS (control) in the thigh muscle. After 3 days, animal PET imaging was performed.

Results: ^{18}F-FDG uptake in activated RAW264.7 cells was increased until 240 min and decreased after then. ^{18}F-FDG uptake in MDA-MB231 cells was gradually increased, whereas that in HepG2 cells was saturated

from 60 min. In efflux analysis, 65%, 54% and 72% of ^{18}F-FDG was released in activated macrophages, MDA-MB231 and HepG2 cells during 120 min. After activation, G6Pase expression in RAW264.7 cells was increased to 1.7 fold although Glut-1 (1.4 fold), HK II (1.7 fold) expression was increased. In inflammatory model, SUV_{max} of ^{18}F-FDG uptake showed a peak as 1.8 at 90 min, which was 2.5-fold higher than control, and decreased after then.

Conclusions: ^{18}F-FDG uptake in activated macrophages was increased and decreased later then. We suggest that G6Ptase expression increased in activated macrophages make to reduce ^{18}F-FDG accumulation as similar result with ^{18}F-FDG uptake saturated in G6Ptase high-expressing HepG2 cells.

Radiochemistry_3

Release-controlled Nano-hydrogels for Diagnosis and Treatment of Ischemia

Hwan-Jeong Jeong, Jeongil Kwon, Chang-Moon Lee, Hwan-Seok Jeong, Hyosook Hwang, Phil-Sun Oh, Eun-Mi Kim, DongHyun Kim, TaiKyoung Lee, Minjoo Kim, HyeonSoo Kim, EunJi Kim, JiHae Choi, Tarique Rajasaheb Bagalkot, SeokTae Lim, Myung-Hee Sohn

Department of Nuclear Medicine, Korea

The vascular endothelial growth factor (VEGF) peptide is a useful angiogenic factor in the treatment of ischemia. Meanwhile, chitosan nano-hydrogel (Nano-CHI) has been established as an affordable vehicle for drug-delivery systems and molecular imaging. However, Nano-CHI is problematic when used as a vehicle, as encapsulated drugs were rapidly released as small molecules before they reach the target site in hydrogel sturcture. For highly effective treatment, chitosan was designed to be used with a biological reducing agent such as glutathione (GSH) in a selective-release structure.

Chitosan was conjugated with N-Succinimidyl 6-(3[2-pyridyldithio]-propionamido) hexanoate (SPDP) and VEGF peptide, CHI-SPDP-VEGF. The chitosan conjugate was gelated with TPP of ATP, and the measured thrbidity and dydrodynamic diameter were evaluated by dynamic light scattering (DLS) and VIS-UV spectrometer. For release testing, the chitosan conjugate was conjugated with Cy 5.5 instead of the VEGF peptide, and the Cy 5.5 was then measured after its release for each of the four environments that it was stored under. Labeling efficiency was used to measure the stability of the technetium-99m (Tc-99m) radio labeling, and the hydrodynamic diameter.

The Nano-CHI formulation with ATP (ATP–Nano–CHI) showed a correlation between size and turbidity. The Cy 5.5-conjugated Nano-CHI (Nano-CHI-Cy 5.5) was not released in 10 mM GSH, but ~ 70 % to 80 % of Nano-CHI-Cy 5.5 was released in a mixture of human serum and 10 mM GSH after 12 h. The result was the same post-gelation. The Tc-99m labeling efficiency was 99 % and the size of the Nano-CHI was unconverted after the previously mentioned method was used.

We developed Nano–CHI as an angiogenic-factor delivery system with selective releasing. The Nano-CHI was used to demonstrate the selective releasing of Cy 5.5 and the improved delivery efficiency of the encapsulation system. Labeling with Tc-99m showed the dignostic potential of this Nano–CHI in a molecular imaging system. Application of this Nano-CHI can be useful as an effective diagnostic and therapeutic vehicle for ischemic lesions.

Oncology_46

The correlation between increased ^{18}F-FDG uptake and adenine nucleotide translocase 2 expression

Chul-Hee Lee[1,2,3,4], Mi Jeong Kim[1,3], Hyewon Youn[1,3,4,5*], Keon Wook Kang[1,2,3], June-Key Chung[1,2,3,4*]

1. Department of Nuclear Medicine
2. Biomedical Sciences
3. Cancer Research Institute
4. Tumor Microenvironment Global Core Research Center, Seoul National University
5. Cancer Imaging Center, Seoul National University Cancer Hospital, Seoul, Korea

Purpose: ^{18}F-FDG, an analogue of glucose, provides valuable functional information based on the increased glucose uptake and glycolysis of cancer cells. Adenine nucleotide translocase 2 (ANT2) imports glycolytic ATP into mitochondria and was shown to be directly associated with glucose metabolisms. Although ANT2 expression has been suggested as a marker of cell proliferation and carcinogenesis, the correlation between ANT2 expression and FDG uptake was not reported.

Methods: Human thyroid carcinoma (TPC-1, FRO), glioma (U87MG, U373), and hepatoma (Hep3B, SK-Hep1) cell lines were used for this research. ANT2 expression was measured by RT-PCR and western blot. 2'-methoxy (2'-OMe) modified siRNAs were used for down-regulation of ANT2, and pcDNA3.1-ANT2 vector was used for up-regulating ANT2. A gamma counter was

used for measuring FDG uptake. Luciferase-expressing FRO cells were subcutaneously grafted in a BALB/c nude mouse, and siRNA was directly injected into the tumor. FDG PET and *in vivo* bioluminescent imaging were obtained using animal PET and IVIS 100 optical imaging system.

Results: FDG uptake rate of FRO was 1.5-fold higher than TPC-1 (P<0.001), U373 was 1.4-fold higher than U87MG (P<0.01), SK-Hep1 was 2.5-fold higher than Hep3B (P<0.001). ANT2 expression of the cell lines with higher FDG uptake was significantly higher than that of the cells with lower FDG uptake. FRO and TPC-1 cells were chosen to investigate the role of ANT2 in FDG uptake. FRO cells treated with 200 nM ANT2 siRNA showed that reduced ANT2 expression, and FDG uptake was significantly decreased in 0.55-fold (P<0.001) compared to the scramble siRNA treatment. TPC-1 cells treated with 12 ug of pcDNA3.1-ANT2 expression vector showed increased ANT2 expression, and FDG uptake was significantly higher (1.7-fold) than that of control. In the xenografted mouse model, 100 uM ANT2 siRNA reduced FDG uptake at 0.8-fold (P<0.001) of the scramble treatment.

Conclusions: We demonstrated that ANT2 expression is related with increased FDG uptake in the various cancer cell lines, and in vivo mouse model by modulating ANT2 expression. Our result suggests that ANT2 expression can be used as a possible biomarker for FDG PET positive tumor.

Molecular Imaging_12

Targeting glucose regulate protein 78 on glioma cells using Cu64-labeled Pep42-R peptide

June-Key Chung, Taemoon Chung, Hyewon Youn, Myung Geun Song, Ji Yong Park, Yun-Sang Lee, Jae-Min Chung, Keon Wook Kang

Seoul National University college of medicine, Korea

Glucose regulated protein 78 (GRP78), a major endoplasmic reticulum chaperone protein, provides a protective cellular response against stress condition in cancer cells. GRP78 targeted therapy could be useful in cancer treatment because GRP78 has an important role in radio- and chemo-resistance of cancer. In this study, we investigated the possible use of radiolabeled-cell penetrating peptide (Pep42, a cyclic 13-mer) as a theranostic probe for targeting GRP78.

RT-PCR and immunoblotting were performed to evaluate GRP78 expression levels in human glioma cell lines (U87MG, U251) and a patient-derived primary glioma cells (GBM28, GBM37; before and after recurrence). Pep42 was identified by phage display. Cells were incubated with red fluorescence labeled Pep42 (Pep42-R) for 2 hours, and visualized by a confocal fluorescence microscope. For in vivo GRP78 targeting, Pep42-R was conjugated with Cu64 labeled human serum albumin (^{64}Cu–HSA-Pep42) to enhance the probe circulation. ^{64}Cu–HSA-Pep42 was intravenously injected into the mice having xenografted U87MG cells, and imaged by an animal PET-BOX.

RT-PCR and immunoblotting assay revealed higher GRP78 expression in U87MG cells than in U251 cells. GRP78 expression was also higher in recurrence tumor GBM37 than in GBM28. Confocal microscope showed the specific binding of Pep42-R at the cytoplasm as well as the membrane of glioma cells. Pep42-R images showed that fluorescent signals from U87MG were 1.98 times more intense than that of U251, and fluorescent signals from GBM37 were 2.04 times more intense than that of GBM28. Labeling efficiency of ^{64}Cu- HSA –Pep42-R was over 95%. Serial PET imaging revealed that GRP78 positive tumor uptake of ^{64}Cu-HAS-Pep42-R was 1.73, 2.03, 4.05 and 4.16 %ID/g at 0, 1, 12, and 20 h post-injection, respectively.

We could determine the expression level of GRP78 on glioma cells using Pep42. ^{64}Cu–HSA-Pep42 imaging probe could significantly accumulate tumor region and specifically visualize GRP78 expression in glioma models. Therefore, this imaging probe might be useful in targeting and treating malignant gliomas.

Molecular Imaging_14

HIV Tat-Derived Peptide Could Be a Prominent And Safe Tool for In Vivo Radio-Imaging of Immune Cells

Cheol Moon[1], Eun Jung Kim[2], Dan Bee Choi[2], Byoung Soo Kim[2], Tae Hyun Choi[2]

1. Department of Clinical Laboratory Science, (Semyung University, Korea)
2. Molecular Imaging Research Center (Korea Institute of Radiological and Medical Sciences (KIRAMS), Korea

Purpose: In vivo tracking of specific immune cells during a pathogenesis is imperative to understand their role in disease development and to devise rational therapeutic strategies. For this purpose, it is important to develop a stable cell-labeling method minimizing cellular physiologic changes. Here, we

report the usefulness of HIV Tat-derived peptide for the radio-labeling immune cells and in vivo imaging.
Methods: ^{131}I was attached to Tat-peptide with the help of an oxidizing agent chloramine T. 2x107 of Balb/c splenocytes were incubated with ^{131}I-Tat-peptides for 30min at 37°C. The splenocytes were introduced into Balb/c mouse and the animal was scanned with γ-camera at various time points. In order to determin organs radioactivity, dissected organs were scanned with γ-counter . For evaluation of Tat-peptides influences on T cell functions, splenic T lymphocytes were activated with anti-CD3/CD28 antibodies. MTS assay and cytokines, IL-2, IFN-γ secretions were mesured in the presence of Tat peptide.
Results: More than 90% of Tat-peptide were successfully radio-labeled. After 10 min of cell injection, the introduced radio-labeled splenocytes were localized and retained in liver, lung, and spleen until the end of observation. Dissected organs' radioactivity was mesured with γ-counter. The most radioactivity are concentrated in spleen. 10μg/ml of Tat-peptide does not influence on the activation and secretion of IL-2, IFN-γ of T lymphocytes.
Conclusions: With these data, HIV Tat-derived peptide, known to deliver a large variety of materials into cells, could be a prominent and safe immune cell labeling tool for in vivo cell tracking.

Radiochemistry_5

Synthesis and Evaluation of Metabolism-resistant Radiolabeled Curcumin Derivatives for Tumor Imaging

Shin Sarah, Koo Hyun-Jung, Choe Yearn Seong*, Choi Joon Young, Lee Kyung-Han, Kim Byung-Tae

Department of Nuclear Medicine, Samsung Medical Center, Sungkyunkwan University School of Medicine

Purpose: Curcumin is known to have anti-cancer, anti-amyloid and anti-inflammatory activity. However, curcumin suffers from poor solubility and rapid metabolism in the liver and intestinal wall. In this study, We designed reductive metabolism-resist curcumin derivatives and synthesized, radiolabeled curcumin derivatives with ^{18}F ([^{18}F]1 and [^{18}F]2), evaluated for tumor imaging agents.
Methods: Radioligands were synthesized by ^{18}F-labeling of the tosylate precursors. For the in vitro metabolism study using alcohol dehydroge nase, which is known to be responsible for the reductive metabolism of curcumin. Cell binding study was performed by incubating the radioligand with HUVE or C6 glioma cells. For the blocking study, the cells were incubated with the radioligand in the presence of non-radioactive ligand 1, 2 and curcumin. C6 glioma tumor-bearing mice were injected with the radioligand and then subjected to microPET imaging.
Results: ^{18}F-labeled ligands were synthesized in relatively good yields. In vitro reductive metabolism study demonstrated that curcumin was mostly converted into THC, whereas curcumin derivatives (1 and 2) remained intact. Cell uptake of radioligand ([^{18}F]1 and [^{18}F]2) increased in a time-dependent manner in two cell lines, and the uptake was reduced in the presence of non-radioactive ligand 1(or 2) and curcumin by 54-64% at 30 min into the incubation. MicroPET imaging of tumor-bearing mice showed high radioactivity accumulation in the intestines, which is similar to the known properties of curcumin. ROI analysis of tumors in mice injected with [^{18}F]1 revealed 1.0 % ID/g at 30 min and 1.1 % ID/g at 60 min. In contrast, higher ROI values were obtained in tumors of mice injected with [^{18}F]2; 3.4% ID/g at 30 min and 3.9% ID/g at 60 min.
Conclusions: Curcumin derivative ([^{18}F]2), does not undergo reductive metabolism and it may be resistant to reductive metabolism in vivo. To the best of our knowledge, this is the first microPET imaging study of radiolabeled curcumin derivatives in tumor-bearing mice. and these results can be widely used in designing metabolism-resistant curcumin derivatives for tumor imaging.

Molecular Imaging_18

[^{18}F]Fluorodeoxysorbitol PET Imaging for Visualization of Tumor-Targeting Salmonella typhimurium in Small Animal Models

Jung-Joon Min, Dong-Yeon Kim, Vu H. Nguyen, Hyeon-sik Kim, Hoon Hyun, Ayoung Pyo, Hee-Seung Bom

Department of Nuclear Medicine, Chonnam National University Hwasun Hospital, Korea

Optical imaging techniques such as bioluminescence or fluorescence were utilized for quantitative and noninvasive imaging of attenuated Salmonella typhimurium (aSL) that have a propensity to naturally accumulate and replicate in a wide range of solid tumors. However, optical imaging techniques have a limitation to apply large animals or human due to shallow penetration depth (<1 cm). Herein, we report a novel PET imaging study to track and visualize intravenously

injected aSL in mouse tumor models using ^{18}F labeled sorbitol (2-[^{18}F]fluorodeoxysorbitol, [^{18}F]FDS), which is a metabolic substrate for Enterobacteriaceae.

[^{18}F]FDS was obtained from commercially available [^{18}F] FDG. [^{18}F]FDG was reduced with sodium borohydride at 35°C for 30 min and the product was passed through an n-alumina Sep-Pak and 0.2-μm filter for in vivo experiments. aSL defective in the synthesis of ppGpp (Δ ppGpp strain) expressing bacterial luciferase (lux) gene were routinely grown overnight in Luria–Bertani (LB) medium. The mice bearing about 300 mm3 s.c. tumors (CT26) were injected intravenously with sterile PBS or 4.5x107 cfu Δ ppGpp strain resuspended in 100μl of sterile PBS. IVIS images were obtained before microPET studies. MicroPET studies were performed at 1h after [^{18}F]FDS injection (7.4 MBq) from 0 to 3 days postinoculum (dpi). Finally, we compared and analyzed IVIS images with microPET images.

[^{18}F]FDS was synthesized easily and non-decay corrected radiochemical yield was around 60 %. Bioluminescence imaging confirmed bacterial targeting and proliferating in tumor tissue between 0 and 3 dpi. [^{18}F]FDS PET also showed tracer accumulation in bacterial colonized tumor. [^{18}F]FDS PET imaging revealed high tumor uptake demonstrating high tumor-to-background ratio (0 dpi: 1.97 ± 0.48, 1 dpi: 2.62 ± 0.59, 2dpi: 2.75 ± 0.33, 3 dpi: 2.38 ± 0.40).

[^{18}F]FDS PET study demonstrated stable uptake in tumor from 1 to 3 dpi and rapid clearance from the blood and other organs within 1 h. It may be a useful tool that allows visualization of injected bacteria for targeted cancer therapy using aSL.

Molecular Imaging_25

Noninvasive imaging of hemoglobin and melanin in tumor using photoacoustic tomography

Jung-Joon Min, Hyeon Sik Kim, Vu H. Nguyen, Hee-Seung Bom

Department of Nuclear Medicine, Chonnam National University Hwasun Hospital, Korea

The photoacoustic imaging (PAI) detects acoustic waves that result from short-pulsed laser-induced transient thermoelastic expansion when the delivered energy is absorbed and converted into heat. In this study, we made melanin producing bacteria and visualized the bacteria using PAI.

We engineered attenuated Salmonella typhimurium expressing tyrosine kinase, key enzyme in the process of melanin synthesis. U87MG human glioma cancer cells were injected subcutaneously into BALB/c nude mice. The melanin was administered by intra-tumoral injection on one mouse. PAI was acquired by Nexus 128, fully 3D photoacoustic computed tomography scanner (ENDRA, Inc). In order to calculate the HbR, HbO2 and melanin in relative values, we modified existing formula as follow: [HbR;HbO2;Melanin](x,y,z)=(MTM)-1MTΦ(x,y,z)

In the phantom experiment, PAI was obtained at 680 nm wavelength every 2 hour during 12 hours. A maximal value was measured and coefficient of determination between max value and time was calculated at the obtained images. In order to detection of melanin, the PAI was acquired at five optical wavelengths which are 680, 750, 850, 900 and 920 nm. HbR, HbO2 and melanin were separated each other from obtained images. In the phantom experiment, correlation between max values and time was evaluated by Spearman correlation analysis. The distribution of vessels and melanin were calculated and compared using the one sample t-test.

In the phantom study, the max value was continuously increased during 12 hours and coefficient of determination (r2) was 0.96 (P<0.01). The distribution of melanin from tumor with or without melanin injection was 31.49 mm3 and 7.58±1.76 mm3, respectively. The distribution of melanin was significantly different (P<0.001).

The melanin was excellently detected by PAI which has shown great potential for imaging molecular signatures of bacterial colonization in tumor.

Neurology_24

Glutamatergic Changes in Parkinson's Disease and Levodopa-induced Dyskinesia: [^{11}C] ABP688 PET/MR Study

Seong A Shin[1,2,3], Jee Young Lee[4,5], Seong Ho Seo[1,6], Yoon Sang Lee[1], Beom S Jeon[4], Jae Sung Lee[1,3], Jae Min Jeong[1], Yu Kyeong Kim[1,2]

1. Department of Nuclear Medicine, Seoul National University College of Medicine, Republic of Korea
2. Department of Nuclear Medicine, Seoul National University Boramae Medical Center, Republic of Korea
3. Department of Biomedical Sciences, Seoul National University, Republic of Korea
4. Department of Neurology, Seoul National University College of Medicine, Republic of Korea
5. Department of Neurology, Seoul National University Boramae Medical Center, Republic of Korea
6. Department of Brain and Cognitive Sciences, Seoul National University, Republic of Korea

Purpose: Glutamate acts as a critical neurotransmitter involved in a multitude of biological functions. Especially,

metabotropic glutamate receptor 5 (mGluR5) is widely distributed in key regions of motor circuits, and its implications in therapeutic modulation of Parkinson's disease (PD) and levodopa-induced dyskinesias (LID) have been evident. In this study, we aim to investigate mGluR5 changes in PD and PD-LID.

Methods: Eleven age-matched normal controls (NC), 12 de novo PD (PD-N), 13 treated PD without dyskinesias (PD-T) and 11 PD with LID (PD-LID) underwent dynamic [^{11}C] ABP688 PET/MR scans for 60-min. Distribution volume ratio (DVR) was estimated by multilinear SRTM. The more affected side of brain was lateralized to the right, and DVRs in subcortical and cortical regions were compared between groups. Correlation analyses were performed between putaminal normalized DVRs and clinical variables.

Results: DVRs in subcortical regions did not significantly differ among the groups. Cortical DVR in whole brain analysis showed increases in bilateral supramarginal gyrus, precentral and postcentral gyrus in PD-T and PD-LID, and the changes were more prominent in PMC. In analysis of DVR relative to putaminal DVR, right precentral and postcentral gyrus, bilateral supplementary motor area and supramarginal gyrus in PD-T and PD-LID displayed abnormally high mGluR5 expression in comparisons to NC. However, the changes were not found significant among PD groups. Furthermore, elevations in mGluR5 expression in right precentral gyrus, supplementary motor area and supramarginal gyrus were positively correlated with UPDRS motor score.

Conclusions: Our results imply that administration of medication in PD disinhibits the downstream cortical areas, although we did not observed any indication of increased striatal outflow. Overexpression of mGluR5 in downstream structures and its high correlations with severity of motor symptoms may explain neuroanatomical enlargements in dyskinetic PD found in previous studies. Increases in cortical glutamatergic expression may provide as future therapeutic targets for medication-induced motor complications in PD.

Physics/Instrument_17

TOF-DOI PET detector using SiPM-LYSO-SiPM module with meantime method

Sung Hyun Song[1], Han Gyu Kang[1], Kyeong Min Kim[2], Seong Jong Hong[1,3]

1. Department of Senior Healthcare, Eulji University, Gyeonggi-do, South Korea
2. Korea Institute of Radiological and Medical Science, Seoul, South Korea
3. Department of Radiological Science, Eulji University, Gyeonggi-do, South Korea

Purpose: Time-of-flight (TOF) information can improve the signal-to-noise ratio (SNR) of positron emission tomography (PET) image. In case of the whole body PET scanner, parallax error caused by an unknown depth-of-interaction (DOI) is occurred not only for radial direction but also for axial direction. The aim of this study is to develop a TOF-DOI PET detector using SiPM-LYSO-SiPM module..

Methods: We used a dual-ended SiPM detector consist of a 2.9 × 2.9 × 20 mm^3 saw-cut LYSO crystal wrapped with the Teflon tape and two SiPMs with sensitive cell of 3 × 3 mm^2. The ^{22}Na point source collimated by 2 mm lead slit was used for DOI resolution measurement. A SiPM–polished Teflon wrapped LYSO (2.9 × 2.9 × 10 mm^3) was used as a reference detector. The coincident events were acquired with NIM module VME QDC, TDC modules The energy resolution, timing resolution and DOI resolution were measured every 2 mm step from source position of 2 mm to 18 mm. To compensate time-walk effect caused by difference DOI, we used meantime method by averaging the photon arrival times of the two SiPMs.

Results: In case of the 2.9 × 2.9 × 30 mm^3 saw-cut LYSO crystal, energy resolution, DOI resolution, and coincidence time resolution were 13.8%, 2.88 ± 0.28 mm, and 615 respectively. In case of the 2.9 × 2.9 × 30 mm^3 medium saw-cut LYSO crystal, the energy resolution, DOI resolution, and coincidence timing resolution were 11.2%, 2.99 ± 0.38 mm, and 453 ps respectively. The coincidence timing resolution can be improved 161 ps when 20 mm long medium saw-cut LYSO crystal was compared to the 30 mm long saw-cut LYSO crystal.

Conclusions: With the proposed dual-ended detector using SiPM, timing and DOI resolution can be improved. The optimal crystal surface roughness and treatment for TOF-DOI PET will be studied in the future work.

Oncology_1

The Deauville 5-point scale improves the prognostic value of interim ^{18}F-FDG-PET/CT in extranodal natural killer/T-cell lymphoma

Russell Oliver Kosik, Chong Jiang, Rong Tian

Stanford University, Santa Clara Valley Medical Center, USA

The prognostic value of ^{18}F-FDG PET/CT in extranodal natural killer/T-cell lymphoma (ENKTL) is still controversial. Further, the utility of the Deauville

5-point scale (DS) in ENKTL is uncertain. Therefore, we designed a prospective study to examine the prognostic value of three methods of PET/CT analysis (International Harmonization Project (IHP) criteria, DS, and SUV-based assessment).

Sixty patients with newly diagnosed, untreated ENKTL were enrolled. PET/CT evaluation was performed prior to initial treatment (pretreatment) and mid-treatment (interim). Interim PET/CT response was determined based on IHP criteria, DS, and change in ^{18}F-FDG uptake (ΔSUV_{max}). IHP criteria, DS, and ΔSUV_{max} were then examined for the ability to predict progression-free survival (PFS) and overall survival (OS).

Over a median follow-up of 23.5 months, interim PET/CT based on DS and ΔSUV_{max} were significant predictors of PFS and OS. After multivariate analysis, DS was an independent predictor of PFS and OS. ΔSUV_{max} was an independent predictor of OS but not of PFS and with a lower accuracy and positive predictive value than DS.

Interim PET/CT analysis with DS predicts unfavorable treatment outcomes in ENKTL patients, whereas interim PET/CT analysis based on IHP criteria and SUV-based assessment have limited prognostic value.

Molecular Imaging_2

The value of 18 flourodeoxyglucose - positron emission tomography / computer tomography (18 FDG - PET/CT) in diagnostic and initial staging of primary colorectal cancer

Mai Hong Son, Le Ngoc Ha, Bui Quang Bieu

Tran Hung Dao hospital, Vietnam

The main purpose of preoperative colorectal cancer staging is emphasis on techniques that might chance the treatment plan. Conventional modalities such as CT, MRI, ultrasound have lower accuracy to detect regional lymph node and distant metastases. This paper is aimed to evaluate important role of ^{18} FDG - PET/CT in the diagnostic and staging of primary colorectal cancer

A total of 60 patients who was diagnosed colorectal tumor by endoscopy. They were scanned with PET/CT and conventional diagnostic imaging (abdominal ultrasound and/or CT and/or pelvic MRI). The reference method selected was pathological histology when possible .

^{18} FDG - PET/CT and conventional CT detected correctly primary colorectal cancer in 55 of 60 patients. According to detection of regional lymph node metastases, PET/CT showed higher sensitivity (78%) and specificity (84%) than CT alone (61% sensitivity and 69% specificity). For distant metastases assessment, the sensitivity and specificity of PET/CT were 100% in all patients who had liver lesions. FDG PET/CT findings were important to change the stage in 50% and modified therapeutic approach in 25% of all patients

FDG-PET CT superior to conventional imaging in pre surgical staging of colorectal cancer and have high impact on treatment‘s management.

Molecular Imaging_4

^{18}Flourodeoxyglucose positron emission tomography/computer tomography (^{18}FDG - PET/CT) in early treatment response assessment in B-cell non Hodgkin lymphoma patients: a preliminary result

Mai Hong Son, Le Ngoc Ha

Nuclear Medicine Department, Tran Hung Dao Hospital, Vietnam

Purpose: The aim of our study to distinguish between responders and non-responders of B-cell non- Hodgkin lymphoma patients to standard treatment based on early ^{18}F-FDG PET/CT.

Methods: In our center, a total of 22 consecutive B-cell non- Hodgkin lymphoma patients were newly diagnosed between July to December 2014. All these patients were underwent ^{18}F-FDG PET/CT scan before treatment, after 3- cycle and 6-cycle chemotherapy using CHOP or R-CHOP. The assessment criteria was followed by modified Ann Aborr for staging and Cheson B. D for treatment response.

Results: After 3-cycle chemotherapy, this results showed 45.5% (10 patients) of those 22 patients with complete response (CR), 50% (11 patients) with partial response who followed the previous regime of chemotherapy (PR). Meanwhile, one patient (4.5%) who had no treatment's response received an alternative chemotherapy. After 6-cycle chemotherapy, all patients in CR group had no evidence of relapse on PET/CT. In PR group, 2/11 (18%) patients became complete response and 7/11 patients (64%) permanently remained partial remission and 2 patients (18%) with relapse afterward. After 6 – cycle chemotherapy, the patient altered treatment strategies was in advanced disease.

Conclusions: ^{18}F-FDG PET/CT has high potential to help oncologist make decision for further treatment of B-cell lymphoma patients.

Oncology_48

Tumor Volume Difference between ^{11}C-methionine PET and Contrast-enhanced MR as a Predictor for Recurrence in Patients with Glioma after Therapy

Jahae Kim[1], Kang-Ho Choi[2], Seong Young Kwon[1], Jung-Joon Min[1], Henry Hee-Seung Bom[1], Ho-Chun Song[1]

1. Department of Nuclear Medicine (Chonnam National University Hospital, Korea)
2. Department of Neurology (Chonnam National University Hwasun Hospital, Korea)

Purpose: The aim of this study was to prediction for evaluation of patients with suspected recurrent cerebral glioma using volumetric analysis of ^{11}C-methionine PET and Gd-DTPA enhanced MRI (MRI).

Methods: A total 48 patients suspected recurrence were evaluated. Recurrence or posttreatment radiation effect was confirmed by radiological follow-up study or surgical biopsy. SUV_{max}, lesion to normal (LN) ratio and metabolic tumor volume (MTV) on PET, and tumor volume of contrast enhancement (MRV) on MRI, and volume difference between PET and MRV (subtract MRV from MTV) were evaluated. Univariate and multiple logistic regression analyses were used for determination of predictor for recurrence of glioma.

Results: Forty-three out of 48 patients (90%) had recurrent glioma. The univariate analysis showed that LN ratio and volume difference were associated with recurrence. According to multiple logistic regression models, volume difference was the significant predictor for recurrence (P=0.031, 95% CI: 1.016 – 1.403, OR: 1.194). The group of MTV larger than MRV (MTV>MRV) showed a higher recurrence risk than that of MRV larger than MTV (MTV<MRV, P=0.028, 95% CI: 1.171 – 115.587, OR: 11.636).

Conclusions: Tumor volume difference between PET and MRI is shown to be a predictor for evaluation of glioma recurrence. Patients with MTV larger than MRV require further work-up for glioma recurrence. Combination of the volumetric analysis from PET and MRI seem to be useful to make treatment decision in patients with suspected glioma recurrence.

Oncology_60

Role of ^{68}Ga-PSMA scan for evaluation of response to docetaxel therapy in metastatic castration resistant prostate cancer

Madhavi Tripathi, Krishan Kant Agarwal, Ranjit Sahoo, Rajiv Kumar, Geetanjali, Chandrashekhar Bal

all india institute of medical sciences, india

Glu-NH-CO-NH-Lys-(Ahx)-[Ga-68(HBED-CC)], abbreviated as ^{68}Ga-PSMA, is a novel radiotracer undergoing evaluation for positron emission tomography/computed tomography (PET/CT) imaging of prostate carcinoma. Its major advantage being sensitive detection of lesions even at low prostate-specific antigen (PSA) and high target to background ratios obtained in metastatic lesions. The objective of this prospective study was to evaluate response to docetaxel chemotherapy (DCT) in metastatic Castration Resistant Prostate Cancer (mCRPC).

A total of 20 male patients (mean age- 59±20) with mCRPC and rising PSA levels that had been planned for DCT were evaluated prospectively. All patients had undergone bilateral orchidectomy. The mean ± SD PSA level was 235±325 ng/mL (median level 130, range 14-1100 ng/mL) and mean Gleason score was 8.0±1. Baseline ^{68}Ga-PSMA PET/CT was done in all patients followed by an interval PET/CT after 4 cycles DCT. Response was graded as partial response (PR), stable (SD) and progressive (PD). In all cases response was correlated to serum PSA levels.

Abnormal tracer accumulation suggestive of metastases was seen in retroperitoneal lymph nodes in 8(40%) patients, pelvic lymph nodes in 14(70%), skeletal sites in 16(80%), internal mammary and supraclavicular lymph nodes in 4(20%) and liver in 4(20%) patients, suggesting Prostate Specific Membrane Antigen (PSMA) expression in baseline scan. PSMA expression was also noted in the primary in prostate in 6(30%) patients. After DCT, 6(30%) PR, 6(30%) SD and 8(40%) patients showed PD in post therapy ^{68}Ga-PSMA scan. In all with PD, PSA levels were also found to rise. PR patients showed decline in PSA levels. Thus ^{68}Ga-PSMA PET/CT is a useful modality for evaluation of response to DCT in mCRPC patients further these patients would also be suitable candidates for ^{177}Lu-PSMA therapy. Further studies in larger populations are needed to confirm these data and to clarify the role of ^{68}Ga-PSMA PET/CT in predicting response to DCT in mCRPC patients.

Molecular Imaging_29

Fluorodeoxyglucose Positron Emission Tomography/Computer Tomography Prediction of Epidermal Growth Factor Receptor Mutation in Non-Small Cell Lung Cancer

Catherine Wong, Frankie Choi, Wai-tat Ngai, Jasmine Yip, Theo Chan

Department of Nuclear Medicine, Pamela Youde Nethersole Eastern Hospital

Purpose: Somatic mutations in tyrosine kinase (TK)

domain of epidermal growth factor receptor (EGFR) of non-small cell lung cancer (NSCLC) predict susceptibility to TK inhibitors and disease prognosis. EGFR-mutant cancers preferentially activate antiapoptotic protein Akt signaling, in turn regulate glucose metabolism hence fluorodeoxyglucose (FDG) avidity. However, there remains controversy regarding the relationship between FDG uptake and EGFR mutation. This study aims to further evaluate their relationship and any predictive value of FDG-PET/CT features for EGFR mutation.

Methods: This study sampled 168 NSCLC patients who underwent pre-treatment FDG-PET/CT and molecular genotyping between January 2013 and May 2015. Clinico-pathological and PET/CT features, viz. maximum standardized uptake value (SUV_{max}), lesion size, ground-glass opacity (GGO) component, lesion margin and multiplicity were analyzed. Predictors for EGFR mutation were determined by multivariate logistic regression and potential predictive SUV_{max} cut-off value was selected by receiver operator characteristic (ROC) curve analysis.

Results: The NSCLC cohort (N=168) was divided into EGFR-mutant (43%) and wild-type (57%) groups. The EGFR-mutant group was comparatively older (71±11 vs 68±11 years, *P*=0.042) with higher rates of female gender (56% vs 25%, *P*<0.001), never-smoking status (74% vs 26%, *P*<0.001), adenocarcinoma histology (97% vs 67%, *P*<0.001) and early clinical stages (46% vs 31%, *P*=0.053). The mutant group was featured with lower SUV_{max} (8.7±5.2 vs 13.9±7.4, *P*<0.001), smaller lesion size (4.3±2.7 vs 5.4±2.5 cm, *P*=0.006) and higher GGO rate (24% vs 11%, *P*=0.036). Multivariate analysis identified independent predictors for EGFR mutations to be never-smoking (odds ratio [OR] 6.20, *P*<0.001), adenocarcinoma (OR 13.31, *P*=0.001) and SUV_{max} (OR 0.92, *P*=0.005). ROC curve analysis selected the optimal cut-off as SUV_{max} ≤8.8 for EGFR mutation (sensitivity 79%, specificity 60%, area under curve [AUC] 0.71), and SUV_{max} ≤7.8 for EGFR mutation in subgroup aged ≤60 years (sensitivity 83%, specificity 83%, AUC 0.84).

Conclusions: FDG SUV_{max} was an independent predictor for EGFR mutation in NSCLC with a higher predictive value in young-age subgroup.

Oncology_64

Role of F-18 FDG PET/CT in restaging hepatocellular carcinoma after curative treatment

Hyoungwoo Kim, Ie Ryung Yoo, Hyukjin Yoon, Sonya Youngju Park, Sae Jung Na, Joo Hyun O, Sung Yong Lee

Seoul St Mary's Hospital, College of Medicine, The Catholic University of Korea, Republic of Korea

Purpose: The goal of this study was to evaluate the role of F-18 FDG PET/CT in hepatocellular carcinoma (HCC) patients following curative treatment.

Methods: This was a retrospective review of 373 F-18 FDG PET/CT scans from 327 HCC patients (244 male and 83 female; age range 27-87 years; mean age 57.6 years), taken between 2009 and 2013, after local or regional treatment. Enrolled patients had received surgical and/or interventional treatment and then underwent F-18 FDG PET/CT scan. Intra-hepatic recurrence and/or extra-hepatic metastases were confirmed by clinical and imaging follow-up or histological confirmation. The diagnostic accuracy of F-18 FDG PET/CT was compared to conventional imaging studies (CIS). Of particular interest was the diagnostic accuracy of F-18 FDG PET/CT in extra-hepatic metastasis.

Results: CIS demonstrated higher sensitivity and lower false-negative error in detecting intra-hepatic recurrence compared to F-18 FDG PET/CT. Extra-hepatic metastasis was reported in 65/373 (17.4%) F-18 FDG PET/CT scans, among which 50/65 (76.9%) were true-positive. 25/50 (50%) of these true-positive cases were reported only by F-18 FDG PET/CT and not by other CIS. 7/25 (28%) of these had elevated tumor markers with false-negative CIS. CIS found no additional cases of extra-hepatic metastasis. Also, another primary malignancy was incidentally detected in 2 cases. The 52 F-18 FDG PET/CT scans that reported true extra-hepatic metastasis or another primary malignancy all resulted in a change in treatment plan.

Conclusions: Restaging F-18 FDG PET/CT has added diagnostic value in the detection of extra-hepatic metastasis following curative treatment of HCC, and provides substantial information for therapeutic planning.

Oncology_72

Metabolic parameters of ^{18}F-FDG PET/CT according to HPV infection, and their prognostic roles in oral cavity and oropharyngeal squamous cell carcinoma patients (OC and OPSCC)

Yeongjoo Lee, Ie Ryung Yoo, Hye Lim Park, Joo Hyun O, Chung Ho Kim, Sung Hoon Kim, Hyung Sun Sohn

Seoul St Mary's Hospital, College of Medicine, The Catholic University of Korea, Republic of Korea

Purpose: The first purpose of this study is to evaluate the relationship between HPV (Human Papilloma Virus) infection status and PET parameters for primary tumor, such as standardized uptake values (SUV_{max}, SUV_{mean}), metabolic tumor volume (MTV), and total lesion glycolysis (TLG) in oral cavity and oropharyngeal

squamous cell carcinoma (OC and OPSCC) patients. The second purpose is to establish the prognostic utility of these PET parameters in relation with progression free survival (PFS).

Methods: We retrospectively reviewed 91 pathologically proven OC and OPSCC patients who had staging PET/CT from Jan 2007 to Nov 2014. SUV_{max}, SUV_{mean}, MTV, and TLG for primary tumor were compared according to HPV infection status. 58 PET/CT scans between Jan 2007 and Dec 2013 were analyzed for association with PFS. Median values of each PET parameters were used to dichotomize PET parameters into high and low. Univariate and multivariate analyses were performed using Cox regression hazard model. Furthermore, subgroup prognosis analysis was performed using Kaplan-Meier survival analysis in combination of HPV infection status and PET parameters.

Results: We retrospectively reviewed 91 pathologically proven OC and OPSCC patients who had staging PET/CT from Jan 2007 to Nov 2014. SUV_{max}, SUV_{mean}, MTV, and TLG for primary tumor were compared according to HPV infection status. 58 PET/CT scans between Jan 2007 and Dec 2013 were analyzed for association with PFS. Median values of each PET parameters were used to dichotomize PET parameters into high and low. Univariate and multivariate analyses were performed using Cox regression hazard model. Furthermore, subgroup prognosis analysis was performed using Kaplan-Meier survival analysis in combination of HPV infection status and PET parameters.

Conclusions: In OC and OPSCC patients, HPV negative primary tumors showed lower SUV_{mean}, MTV, and TLG than HPV positive tumors. Higher PET parameters of MTV and TLG for the primary tumor were significantly associated with poorer progression free survival.

Oncology_73

Potential of ^{18}F-FDG PET/CT for Diagnosis and Staging of IgG4-Related Disease

Won Woo Lee, Seo Young Kang, Yu Kyeong Kim, Sang Eun Kim

Seoul National University Bundang Hospital, Seoul National University College of Medicine, Korea

IgG4-related disease (IgG4-RD) has recently been recognized as a new disease category characterized by IgG4 positive plasma cell infiltration to single or multiple organs. Here, we investigated the usefulness of ^{18}F-FDG PET/CT for diagnosis and staging of IgG4RD.

23 patients (m:f=15:7, age 62±15 yrs) who visited SNUBH or SNUBMC and had clinical suspicions of IgG4-RD were included in this study. Of the 23 potential IgG4-RD, 15 (m:f=10:5, age 58±15.14yrs) were considered as pathology-proven IgG4-RD because the tissue specimens showed more than 10 IgG4 positive plasma cells per high power filed, whereas 8 (m:f=5:2, age 68±12yrs) were suspicious IgG4-RD because the clinical suspicions for IgG4-RD were strong without pathological confirmation (n=8). The number of FDG positive lesions was visually counted and the lesion FDG uptake was quantitatively measured as the maximum standardized uptake value (SUV_{max}).

^{18}F-FDG PET/CT was performed before the initiation of treatment in all the 23 patients. By visual analysis, 59 lesions were found in the proven IgG4-RD (3.93±2.34 lesions per patient, range 1-10) and 10 lesions in the suspicious IgG4-RD (1.50±1.85 lesions per patient, range 0-6) with a significant difference (P<0.05). Furthermore, there was a significant difference in mean SUV_{max} between the proven IgG4-RD (4.08±1.88) vs. the suspicious IgG4-RD (2.80±1.67) (P<0.05). The proven patients showed more severe clinical course because 7 of 15 proven patients needed steroid therapy or additional monoclonal antibody therapy, while no patient in the suspicious IgG4-RD required steroid or additional therapy over 6 months. The 7 proven patients with steroid treatment had higher number of FDG positive lesions (3.86±2.41) and lesion SUV_{max} (6.27±2.41) than steroid-free 16 (8 proven plus 8 suspicious) patients (number of FDG positive lesions=2.81±2.59, and lesion SUV_{max}=4.03±1.92) (P=0.120 and P<0.05, respectively).

FDG uptake was greater in the proven IgG4-RD patients and correlated with disease severity of IgG4-RD. Thus, ^{18}F-FDG PET/CT has a potential role for diagnosis and staging of IgG4-RD.

Oncology_5

Direct comparison of FDG PET/CT, MRI and fused PET/MRI with prone position in primary tumor assessment of patients with invasive ductal breast carcinoma

Soo Hyun Kwon[1*], Bok-Nam Park[1], Joon-Kee Yoon[1], Su Jin Lee[1], Dong Hyun Lee[1], Tae Hee Kim[2], Doo Kyoung Kang[2], Yong Sik Jung[3], Hyunee Yim[4], Young-Sil An[1]

1. Department of Nuclear Medicine and Molecular Imaging
2. Radiology
3. Surgery
4. Pathology, Ajou University School of Medicine, Suwon, Korea

Purpose: The aim of this study was to compare FDG PET/CT, MRI and fused PET/MRI with prone position in primary tumor evaluation of patients with invasive ductal breast carcinoma.

Methods: Preoperative whole-body FDG PET/CT with prone position and a routine breast MRI were performed in 57 female patients with invasive ductal breast carcinoma. The attenuation-corrected prone PET data of chest region and MRI datasets were registered using Analyze software. Mastectomy was performed in all patients, and the diagnostic performance for breast tumor evaluation of each modality was calculated on the basis of pathology reports. McNemar test was performed to measure the concordance among imaging modalities (FDG PET/CT, MRI and fused PET/MRI) and their diagnostic abilities were compared by comparison of ROC curves.

Results: A total of 117 breast lesions were assessed and their size was ranged from 0.8 to 5.0 cm. Of the 117 breast lesions, 92 (78.6%) were invasive ductal carcinoma, of which 25 were found to be benign lesion on pathology. In lesion-by-lesion analysis, the sensitivity, specificity, positive predictive value, negative predictive value, and accuracy for the evaluation of primary breast tumor were 81.5%, 100%, 100%, 59.5%, 85.5% for FDG PET/CT, 100%, 20.0%, 82.1%, 100%, 82.9% for MRI alone, and 89.1%, 96.0%, 98.8%, 70.6%, 90.6% for fused PET/MRI, respectively. There was significant discordance among imaging modalities (FDG PET/CT vs. MRI, $P<0.001$; FDG PET/CT vs. fused PET/MRI, $P=0.008$; MRI vs. fused PET/MRI, $P<0.001$). The diagnostic ability of fused PET/MRI was significantly superior to MRI alone ($P<0.001$). However, there was no significant difference in diagnostic ability between fused PET/MRI and FDG PET/CT ($P=0.459$).

Conclusions: Acquisition of prone PET in breast cancer patients could provide suitable image for fusion with breast MRI. Compared with MRI alone, fused PET and MRI could improve diagnostic ability in primary tumor assessment of patients with invasive ductal breast carcinoma.

Oncology_7

Association between Primary Tumor FDG Avidity and Metastatic Site in Patients with Advanced Breast Cancer

ChaeHong Lim, SeungHwan Moon, YoungSeok Cho, JoonYoung Choi, YearnSeong Choe, ByungTae Kim, KyungHan Lee

Samsung Medical Center, Korea

The prognosis of advanced breast cancer is significantly affected by metastatic site, which in turn is influenced by the "seed and soil". As for the seed, it is possible that the bioenergetics of malignant cells is involved in determining metastatic site. As for the soil, lymph nodes (L/N) and bone have abundant inflammatory components and may be considered more favorable for metastatic growth. We thus tested the hypothesis that primary tumor FDG avidity can influence metastatic site in advanced breast cancer.

Subjects were 271 patients with advanced breast cancer who underwent staging PET/CT and had initial metastasis (n = 185) or metastatic recurrence on f/u (n = 86). Metastatic sites were categorized as either "L/N and/or bone" (favorable microenvironments) or "other visceral organs" (considered less favorable). We investigated the distribution of metastatic sites in patients categorized according to primary tumor FDG avidity. High FDG uptake was defined as primary tumors with SUV_{max} exceeding the median value for each population.

In the "initial-metastasis" population, high and low primary tumor FDG groups showed mild trends for "other visceral organ" (54.8 vs. 45.2%) and "L/N or bone" metastasis (47.5 vs. 52.5%), respectively, although this did not reach statistical significance. In the "f/u-recurrence" population, primary tumors with high FDG uptake had a significantly greater risk of metastasis to "other visceral organs" compared to "L/N or bone"(61.2 vs. 38.8%), whereas those with low FDG uptake had a significantly greater risk of metastasis to "L/N or bone" (64.9 vs. 35.1%; $P= 0.017$). The distribution of "other visceral organs" with metastatic lesions was not significantly different between patients with low and high primary tumor FDG uptake.

Primary tumor FDG avidity significantly influences future metastatic sites in patients with advanced breast cancer. Further investigation is thus warranted to determine the precise clinical implications of this preliminary finding.

Oncology_19

Asphericity of FDG Uptake on ^{18}F FDG PET/CT Provides Independent Prognostic Value in Breast Cancer Patients

Ji-hoon Jung, Choon-Young Kim, Seung Hyun Son, Do-Hoon Kim, Shin Young Jeong, Sang-Woo Lee, Jaetae Lee, Byeong-Cheol Ahn

Department of Nuclear Medicine, Kyungpook National University School of Medicine and Hospital Daegu, Republic of Korea

Purpose: The purpose of this study was to evaluate the prognostic implication of 'asphericity' (ASP); spatial irregularity; of FDG uptake in the primary tumor on pretherapeutic ^{18}F-FDG PET/CT scans in patients with invasive ductal carcinoma (IDC) of the breast.

Methods: One hundred and thirty-one female IDC

patients(mean age= 48.1±10.4 y) with pathological tumor size more than 2cm were retrospectively evaluated. $SUV_{2.5}$ was taken as the cut-off value for the detection of tumor boundaries. ASP was calculated using following formula to characterize the deviation of the tumor's shape from sphere symmetry. Clinicopathologic factors and metabolic PET parameters (maximum standardized uptake value [SUV_{max}], metabolic tumor volume [MTV], and total lesion glycolysis [TLG]) were measured. Univariate and multivariate analyses for the progression free survival (PFS) were performed with these factors and parameters.

Results: The PFS rate among the 131 patients was 890.1%. The mean follow-up times in the entire study cohort and in the recurred patients were 50.0months and 26.2months, respectively. The ASP ranged from 3.44 to 72.48 (mean, 20.13 ± 14.38). T stage, N stage, hormonal receptor(ER/PR) status, SUV_{max} (≤ 5.5), MTV (≤ 4.2 cm3), TLG (≤ 15.1), and ASP (≤ 15.1) affected the PFS on univariate analysis. In multivariate Cox regression, N stage (HR = 17.6), ASP (HR=11.4), and hormonal receptor status (HR =6.9) were independent prognostic factor for PFS. In the subgroup of patients with lymph node metastasis, ASP (HR=10.9), and hormonal receptor status (HR=9.1) were independent prognostic factor for PFS.

Conclusions: ASP on ^{18}F-FDG PET/CT is an independent predictor of outcome in IDC patients, and could improve their prognostic stratification.

Oncology_44

A New Method for Segmentation of FDG PET Metabolic Tumor Volume using the Peritumoral Halo Layer and a 10-Step Color Scale: A Study in Patients with Papillary Thyroid Carcinoma

Sungmin Jun[1], Heeyoung Kim[1], Hyun-Yeol Nam[2]

1. Department of Nuclear Medicine, Kosin University Gospel Hospital, Kosin University College of Medicine, Busan, Korea
2. Department of Nuclear Medicine, Samsung Changwon Hospital, Sungkyunkwan University School of Medicine, Changwon, Korea

Purpose: We observed a layer between tumor activity and background on FDG PET/CT with the 10-step color scale and the window level set properly. We named the layer "*peritumoral halo layer (PHL).*" We performed this study to establish the reliability of metabolic tumor volume (MTV) segmentation using PHL (MTV_{PHL}) in patients with papillary thyroid carcinoma (PTC).

Methods: Of a total of 140 PTC patients, 70 (50.0%) had FDG-avid PTC. In these patients, MTV_{PHL}, MTV segmented according to fixed 50% SUV_{max} ($MTV_{50\%}$), and fixed SUV with 2.5 to 4.0 ($MTV_{2.5}$ to $MTV_{4.0}$) were compared with pathologic tumor volume (PTV). The absolute percentage difference between MTV_{PHL} and PTV was compared in micropapillary carcinoma (MPTC) and non-micropapillary carcinoma (non-MPTC) subgroups. The % SUV_{max} and SUV thresholds of MTV_{PHL} were compared with tumor SUV_{max}.

Results: Among the MTVs, $MTV_{50\%}$ was not correlated with PTV (r = -0.16, P = 0.182) and was not reliable according to the Bland-Altman plot. Although $MTV_{2.5}$, $MTV_{3.0}$, $MTV_{3.5}$, and $MTV_{4.0}$ correlated with PTV (r = 0.85, 0.86, 0.87, and 0.87, respectively; P< 0.001), these MTVs were not reliable on Bland-Altman analyses. MTV_{PHL} was significantly correlated with PTV (r = 0.80, P< 0.001), and the Bland-Altman plot did not show systemic error. The MTV_{PHL} was more accurate in non-MPTC than in MPTC (P< 0.001), and the absolute % difference was smaller as PTV became larger (σ = -0.65, P< 0.001). The MTV_{PHL} thresholds had correlations with SUV_{max} (% SUV_{max} threshold: σ = -0.87, P< 0.001; SUV threshold: r = 0.88, P< 0.001).

Conclusions: MTV_{PHL} was more reliable than $MTV_{\%SUVmax}$ or MTV_{SUV}. The reliability of MTV_{PHL} improved with larger PTVs. The threshold of the MTV_{PHL} was naturally altered by PHL according to SUV_{max}.

Oncology_92

Value of preoperative FDG PET/CT in predicting recurrence and sites of recurrence in patients with resectable pancreatic adenocarcinoma

Narae Lee, Soyoung Kim, Jongtae Cha, Sang Hyun Hwang, Kwanhyeong Jo, Arthur Cho, Won Jun Kang, Mijin Yun

Yonsei Sevrance hospital

To assess the prognostic significance of metabolic parameters on FDG PET/CT at staging in predicting recurrence and sites of recurrence after surgery in pancreatic adenocarcinoma.

From Aug 2006 to Aug 2014, Patients with pancreatic ductal adenocarcinoma who underwent initial FDG PET/CT and subsequent curative surgical resection without neoadjuvant therapy were retrospectively enrolled. Metabolic parameters were measured as SUV_{max} and MTV of primary tumor. MTV_{liver} was defined as total tumor volume with a value of liver SUV_{mean} or greater. SUV_{max}, MTV_{liver}, age, sex, serum CA19-9, tumor location, LN metastasis, histology and overall stage were included as independent variables. And the presence of recurrence and the sites of recurrence were evaluated

as clinical end points.

A total of seventy two patients (mean age 63 ± 8.8, male 43, female 29) were included. Mean follow up was 24.3±18.4 months and mean RFS was 18.6±18.6 months. Among them, 39 patients demonstrated recurrence whereas thirty three patients presented no recurrence on follow up. On univariate analysis, tumor differentiation, LN metastasis, SUV_{max}, MTV_{liver} were significant factors affecting RFS (P<0.05). On multivariate analysis, SUV_{max}, MTV_{liver} were independent prognostic factors for RFS. Sites of the recurrence were locoregional site (n=15) and distant metastases (n=24, liver (n=19), peritoneum (n=3) and lung (n=2)). The distant site recurrence group showed significantly higher SUV_{max} and MTV_{liver} of the primary tumor than the locoregional recurrence group (P<0.05).

SUV_{max} and MTV_{liver}, metabolic parameters on F-18 FDG PET/CT, are independent prognostic factors for recurrence. Also, patients with distant metastasis demonstrated higher FDG uptake or metabolic tumor volume than patients with locoregional recurrence.

Other than initial staging, prognostic implication of FDG PET/CT in predicting recurrence can play an important role in selecting postoperative follow up schedule, risk stratification, and allocation of adjuvant treatment in a high risk group. Additionally, those F-18 FDG PET/CT parameters might be useful clue about prospective recurrence pattern.

Oncology_99

Clinical significance of dual time point ^{18}F-FDG PET/CT for the staging of esophageal cancer

Sohyun Park[1], Jin Chul Paeng[1], Chang Hyun Kang[2], Gi Jeong Cheon[1], Keon Wook Kang[1], June-Key Chung[1], Dong Soo Lee[1]

1. Department of Nuclear medicine, Seoul National University Hospital, Republic of Korea
2. Department of Thoracic and Cardiovascular Surgery, Seoul National University Hospital, Republic of Korea

Purpose: Clinical staging is critical issue for the treatment of esophageal cancer. ^{18}F-FDG PET/CT is widely used for the staging of esophageal cancer. However, its relative low sensitivity to detect regional lymph node metastasis is one of the limitations. The purpose of this study is to investigate the diagnostic ability of dual time point ^{18}F-FDG PET/CT to detect lymph node metastasis.

Methods: A total of 44 patients with pathologically confirmed esophageal squamous cell carcinoma were enrolled, sequentially. Dual time point ^{18}F-FDG PET/CT (scan interval of initial and delayed scan; 60 min) was performed in all patients, pre-operatively. We obtained semi-quantitative parameters of the main mass and regional lymph nodal stations in both initial and delayed scans: SUV_{max}, SUV_{peak} in both time points, Retention index using SUV_{max} (RImax), SUV_{peak} (RIpeak). Node metastases were confirmed on postoperative pathology. ROC curve analysis was done to evaluate the diagnostic performance and cut-off of those semi-quantitative parameters.

Results: For the total 44 esophageal lesions, no parameters showed significant difference according to the location or grade of the tumors (P=ns). For nodal (N) staging, total 257 nodal stations of 28 patients who underwent surgical treatment without neoadjuvant chemotherapy were analyzed. Using ROC analysis, RImax had the largest area under the curve (AUC) to detect metastatic lymphadenopathy (AUC 0.810, cutoff value 0.06, P<0.001), compared to AUC's among investigated parameters after exception of calcified nodal stations (n=230). By dual time point ^{18}F-FDG PET/CT, N staging changed in eleven patients. At the optimal threshold, sensitivity and specificity was 78.9% and 91.9%, respectively.

Conclusions: Dual time point ^{18}F-FDG PET/CT can improve N staging of esophageal cancer. Best diagnostic performance was achieved by exception of calcified lymph node with benign character.

Neurology_27

Comparison of ROI and SPM analysis between 2h and 3h ^{18}F-FP-CIT PET image in non-dopaminergic movement disorders, parkinson's disease and atypical parkinsonism

Hye Joo Son , Young Jin Jeong , Hyun Jin Yoon , Do-Young Kang

Department of Nuclear Medicine, Dong-A University Medical Center, Dong-A University College of Medicine, Busan, Korea

Purpose: In this study, we compared ROI and SPM analysis between 2h and 3h ^{18}F-FP-CIT PET image in non-dopaminergic disorders, parkinson's disease (PD) and atypical parkinsonism.

Methods: 117 patients were divided into three groups: 33 patients with non-dopaminergic disorders (GA), 64 patients with PD (GB), 20 patients with atypical parkinsonism (13 MSA-P, 7 PSP) (GC). Dual time point ^{18}F-FP-CIT PET/CT scans was acquired at 2 h and 3 h and changes between 2h and 3h image were assessed by

both region of interest (ROI) and SPM methods. In ROI method, SUV_{mean} was measured in the both caudate (RC, LC), anterior and posterior putamen (RAP, LAP, RPP, LPP) and occipital as a reference region. The striatooccipital ratio (SOR) between 2 h and 3 h images was compared in each groups using paired t-test.

Results: In GA, mean SOR of 2h (RC: 6.38±0.94, RAP: 7.39±1.06, RPP: 7.09±1.22, LC: 6.58±0.79, LAP: 7.41±1.01, LPP: 7.37±1.17) and 3h image (RC: 7.37±1.26, RAP: 8.77±1.56, RPP: 8.37±1.63, LC: 7.72±1.29, LAP: 8.75±1.44, LPP: 8.59±1.82) were significantly different in all subregions in ROI method (P=0.000). SPM analysis showed significant difference in RC, LC, RAP, RPP, LAP, LPP, claustrum, lentiform nucleus (P< 0.05, k > 100). In GB, mean SOR of 2h (RC : 5.05±1.32, RAP: 4.40±1.17, RPP: 2.66±0.90, LC: 5.08±1.18, LAP: 4.13±1.00, LPP: 2.51±0.81) and 3h (RC: 5.89±1.60, RAP: 4.80±1.54, RPP: 2.62±1.01, LC: 5.94±1.49, LAP: 4.53±1.33, LPP: 2.47±0.98) were different only in RC, LC, RAP, LAP (P = 0.000). SPM analysis showed significant difference in RC, LC, RAP, RPP, LAP, LPP, claustrum, lentiform nucleus (P< 0.05, k > 100). In GC, mean SOR of 2h (RC : 4.04±0.64, RAP: 3.76±0.86, RPP: 2.93±1.05, LC: 4.29±0.68, LAP: 3.70±0.78, LPP: 2.83±1.19) and 3h (RC: 4.70±0.90, RAP: 4.02±1.23, RPP: 2.95±1.32, LC: 4.72±0.66, LAP: 4.01±1.34, LPP: 2.93±1.63) were different only in RC (P=0.000) and LC (P=0.001). SPM analysis showed significant difference in LC, AP, PP, both globus pallidus, claustrum, lentiform nucleus (P< 0.05, k > 100).

Conclusions: ROI and SPM methods correlate well in non-dopaminergic and PD, but showed some discrepancies in atypical parkinsonism. So, further reformation of positional settings in SPM analysis is needed.

Radionuclide Therapy_12

Comparison of ablation success and recurrence between pathological N1a and N1b lymph node metastases in patients with papillary thyroid carcinoma after radioactive iodine ablation

Choon-Young Kim, Sang-Woo Lee, Seung Hyun Son, Ji-hoon Jung, Chang-Hee Lee, Shin Young Jeong, Byeong-Cheol Ahn, and Jaetae Lee

Department of Nuclear Medicine, Kyungpook National University School of Medicine, Hospital, Daegu, Republic of Korea

Purpose: The aim of this study was to determine whether pathologically proven central or lateral lymph node (LN) metastases (pN1a or pN1b) could affect successful radioactive iodine (RAI) ablation and recurrence, and to investigate risk factors for long-term recurrence in patients with node-positive papillary thyroid carcinoma (PTC).

Methods: A total of 277 PTC patients who had pathological N1 (pN1) disease and underwent high-dose RAI ablation (5.55 GBq) after total thyroidectomy with central and/or lateral neck dissections between 2000 and 2006 were retrospectively included. Successful ablation was evaluated during the first 6-12 months after RAI ablation. We compared the ablation success rate and recurrence rate between patients with pN1a and pN1b disease. Univariate and multivariate analyses were performed to investigate risk factors for recurrence in patients with pN1 disease.

Results: Patients were classified as pN1a (n=167/277, 60%) and pN1b (n=110/277, 40%) groups. Median duration of follow-up was 10.2 years (range, 0.8 – 15.2 years). A total of ablation success rate was 64% (n=177/277), and the ablation success rate in pN1b group (49%, n=54/110) was lower than in pN1a group (74%, n=123/167, P<0.001). The overall rate of structural recurrence was 23% (n=63/277). The recurrence rate in pN1b group (30%, n=33/110) was higher than in pN1a group (18%, n=30/167, P=0.028). On univariate and multivariate analyses, higher ratio of metastatic LNs (>0.4, HR=1.77, P=0.031), higher level of pre-ablation thyroglobulin (>10 ng/mL, HR=2.11, P=0.020), and ablation failure (HR=3.12, P<0.001) were significant risk factors for recurrence. Higher pathological N stage was a significant risk factor in univariate analysis, but not in multivariate analysis.

Conclusions: In this study, patients with pN1b disease showed lower ablation success rate and higher recurrence rate than in patients with pN1a disease. However, higher ratio of metastatic LNs, higher level of pre-ablation thyroglobulin, and ablation failure were stronger risk factors than pathological N stage for long term recurrence in patients with node-positive PTC.

Clinical Applications of PET/MR and SPECT/CT_11

Maximum Standardized Uptake Value of Tc-^{99m} HDP Single-Photon Emission Computed Tomography/Computed Tomography for the Evaluation of Temporomandibular Joint Disorder

Min Seok Suh[1], Won Woo Lee[1], Young-Kyun Kim[2], Pil-Young Yun[2], Sang Eun Kim[1]

1. Department of Nuclear Medicine, Seoul National University Bundang Hospital, Seoul National University College of Medicine
2. Department of Oral and Maxillofacial Surgery, Section of Dentistry, Seoul National University Bundang Hospital; 3Institute of Radiation Medicine, Medical Research Center, Seoul National University

Purpose: The purpose of this study was to evaluate the usefulness of a quantitative parameter (standardized uptake value [SUV]) from single-photon emission computed tomography/computed tomography (SPECT/CT) for the evaluation of temporomandibular joint disorder (TMD).

Methods: Forty-four temporomandibular joints (TMJs) of 22 TMD patients (male:female, 5:17; age, 30.0 ± 12.1 years) were evaluated in this study. The patients underwent conventional planar bone scintigraphy and subsequently SPECT/CT 3–4 h after injection of Tc-99m hydroxymethylene diphosphonate (HDP). Planar scintigraphy parameter (relative ratio [RR]) and SPECT/CT parameters (SUV_{mean} and SUV_{max}) were compared for the visual assessment of TMD on the planar bone scintigraphy (normal, mild–moderate, and severe) and the presence of TMJ arthralgia.

Results: On visual assessment, of the 44 TMJs, 19 were classified as normal, 18 as mild–moderate, and 7 as severe. SUV_{max} gradually increased from normal (2.82 ± 0.73) to mild–moderate (3.56 ± 0.76, $P < 0.05$ compared to the normal group) and then to severe (4.86 ± 1.25, $P < 0.05$ compared to the mild–moderate). However, RR and SUV_{mean} did no vary significantly according to visual grade ($P > 0.05$). Of the 44 TMJs, there were 18 arthralgic and 26 were non-arthralgic TMJs. SUV_{max} was significantly greater in arthralgic TMJs (4.15 ± 1.11) than in non-arthralgic TMJs (2.97 ± 0.75, $P = 0.0001$), as was SUV_{mean} (1.63 ± 0.42 versus 1.30 ± 0.31, respectively, $P = 0.0045$). However, there was no significant difference in RR between arthralgic (3.61 ± 0.57) and non-arthralgic TMJs (3.76 ± 0.68, $P = 0.4497$). In receiver-operating characteristic curve analyses for detection of arthralgic TMJ, SUV_{max} had the greatest area-under-the-curve (0.815), followed by SUV_{mean} (0.744), which were both significantly better than that of RR (0.514) ($P = 0.0093$ for SUV_{max}, and $P = 0.0350$ for SUV_{mean}).

Conclusions: SUV_{max} derived from bone SPECT/CT after injection of Tc-99m HDP proved to be useful for the evaluation of TMD. Quantitative bone SPECT/CT is a promising imaging tool for the evaluation of TMD.

Clinical Applications of PET/MR and SPECT/CT_15

Role of ^{99m}Tc-MDP Bone SPECT/CT and ^{99m}Tc-HMPAO-Labeled WBC SPECT/CT in Differential Diagnosis of Clinically Suspicious Post-traumatic Osteomyelitis

Chanwoo Kim, Ji Young Kim, Young Hwan Kim, Yun Young Choi

Hanyang University Medical Center, Korea

Purpose: To compare and analyze the findings on bone SPECT/CT and WBC SPECT/CT in evaluating patients with clinically suspicious post-traumatic osteomyelitis.

Methods: Fourteen patients with clinical suspicion of post-traumatic osteomyelitis underwent three phase bone scan with SPECT/CT and subsequent WBC SPECT/CT within a week. On bone SPECT/CT, osteomyelitis was diagnosed when there was focal increased perfusion and matched bone uptake. In cases with only increased perfusion were considered to be soft tissue inflammation. On WBC SPECT/CT, focal WBC accumulation in area of suspicious osteomyelitis was considered as osteomyelitis, WBC accumulation confined in soft tissue was considered as soft tissue inflammation, and no WBC uptake was considered as negative for inflammation. Confirmative diagnosis was based on pathologic finding or long-term clinical evaluation. Agreement of findings on bone SPECT/CT and WBC SPECT/CT was compared and analyzed with final diagnosis.

Results: Four osteomyelitis, 4 soft tissue inflammation (including 1 incidentally detected skin cancer), 6 negative for inflammation (4 nonunion, and 2 hematoma) were finally diagnosed. Osteomyelitis was correctly diagnosed in 3 of 4 cases on bone SPECT/CT, and in one on WBC SPECT/CT. In soft tissue inflammation, bone SPECT/CT was correct in 2 of 4 cases, WBC SPECT/CT was correct in 3 of 4 cases. In negative cases, bone SPECT/CT was correct in 5 of 6, and WBC SPECT/CT was correct in all 6 cases (NPV : 100 %).

Six of 14 cases made an agreement between bone and WBC SPECT/CT (3 non-union, 2 hematoma, and 1 soft tissue inflammation). WBC SPECT/CT was superior in evaluating extent of inflammation compared to nonspecific uptake on bone SPECT/CT. Bone SPECT/CT showed better results in chronic inflammatory conditions.

Conclusions: Although bone SPECT/CT and WBC SPECT/CT showed disagreements in evaluation of clinically suspected post-traumatic osteomyelitis, WBC SPECT/CT was more correct in distinguishing soft tissue inflammation from osteomyelitis, bone SPECT/CT showed better results in evaluating chronic inflammation, and both studies showed high negative predictive value.

Endocrinology_14

Quantitative Measurement of $^{99m}TcO_4$ Thyroid Uptake using Single-Photon Emission Computed Tomography/Computed Tomography

Hyunjong Lee[1,3], Yeon-koo Kang[1,3], Jae Hoon Moon[2], Won Woo Lee[1]

1. Department of Nuclear Medicine, Seoul National University Bundang Hospital, Seoul National University College of Medicine

2. Department of Internal Medicine, Seoul National University Bundang Hospital, Seoul National University College of Medicine
3. WCU, Department of Molecular Medicine and Biopharmaceutical Science, Graduate School of Convergence Science and Technology, Seoul National University

Purpose: Measurement of technetium pertechnetate ($^{99m}TcO_4$) thyroid uptake is a common nuclear medicine study but there are some drawbacks due to its inaccuracy. Here, we introduced a novel method to measure %thyroid uptake using top-notch quantitative single-photon emission computed tomography/computed tomography (qSPECT/CT) and investigated its feasibility to clinical application.

Methods: We enrolled 36 patients (9 males, 27 females; age, 44.1±14.2 years) who had undergone thyroid uptake tests using conventional thyroid uptake system (TUS) and qSPECT/CT between March and June 2015. Twenty-one were treatment-naïve thyrotoxicosis patients of whom the underlying diseases were not clarified, and fifteen were post-thyroidectomy patients before/after radioactive iodine therapy. Under no specific preparation, they underwent a serial study of thyroid uptake tests (TUS first, and qSPECT/CT next) 20 minutes after a single injection of $^{99m}TcO_4$ (5 mCi). SPECT was performed using a SPECT/CT scanner equipped with 16-channel CT (NM/CT670, GE) for 1 minute and images were reconstructed with CT-based attenuation correction, scatter correction, and resolution recovery. %Thyroid uptake was obtained from CT-based thyroid gland segmentation using dosimetry software (Dosimetry Toolkit, GE). Additionally, %uptake of $^{99m}TcO_4$ for salivary glands and oral cavity saliva were evaluated. Serum free T4 and TSH were also measured.

Results: Patients were classified to Graves' disease (n=10), thyroiditis (n=11), and thyroidectomy (n=15). In all the patients (n=36), TUS %thyroid uptake (6.43±3.69%) was significantly greater than qSPECT/CT %thyroid uptake (1.40±2.63%, P<0.0001 by paired t test) and qSPECT/CT summed %uptake (thyroid, salivary glands, and saliva) (5.36±5.19%, P<0.01 by paired t test), and tended to overestimate the thyroid function as %thyroid uptake increased (Bland-Altman analysis). The conventional TUS %thyroid uptake could not differentiate thyroidectomy (4.44±1.02%) from thyroiditis (4.93±0.82%, P>0.05), but qSPECT/CT %thyroid uptake could discriminate thyroidectomy (0.01±0.01%) from thyroiditis (0.37±0.43%, P<0.05, K-W test). Grave's disease had substantially greater %thyroid uptake by whether qSPECT/CT or TUS (P<0.05, each). In Grave's disease, free T4 showed a significant positive correlation with qSPECT/CT %thyroid uptake (Spearman's r=0.7576, P=0.0149), whereas in thyroiditis, TSH showed a significant positive correlation with qSPECT/CT %thyroid uptake (Spearman's r=0.7988, P=0.0079, n=10).

Conclusions: The accuracy of $^{99m}TcO_4$ %thyroid uptake was improved using the quantitative SPECT/CT compared to the conventional thyroid uptake system.

Endocrinology_19

The relationship between iodine uptake pattern and elevation of serum thyroglobulin level after radioiodine therapy aided by recombinant human TSH

Minchul Song, Geum-Cheol Jeong, Hee Jeong Park, Jung-Joon Min, Ki Seong Park, Sang-Geon Cho, Sae-Ryung Kang, Jahae Kim, Ho-Chun Song, Henry Hee-Seung Bom, Subin Jeon, Seong Young Kwon

Chonnam National University Hwasun Hospital, Korea

The elevation of serum thyroglobulin (Tg) level after radioiodine therapy (RIT) has been known to reflect thyroid tissue injury in previous reports. We investigated whether the elevation of serum Tg level could be affected by other parameters, especially iodine uptake pattern in patients with papillary thyroid cancer. Patients who underwent total or subtotal thyroidectomy and the first RIT aided by recombinant human TSH (rhTSH) were enrolled in this study. They were classified into 2 groups according to the presence of midline uptake in anterior neck on post-therapeutic whole body scan (WBS). Serum Tg level was measured three times; on the day of RIT (D0Tg), day 3 post-RIT (D3Tg) and day 7 post-RIT (D7Tg). We compared serum Tg level at each time point or deltaTg (D7Tg – D0Tg) between the two groups. The patients with anti-Tg antibody ≥ 100 U/mL, distant metastasis, undetectable D0Tg or no iodine uptake in the anterior neck were excluded.

Total 56 patients were enrolled in this study. Midline uptake in anterior neck was observed in 36 patients (64%). They showed significantly higher level of D7Tg (15.67 ± 19.73 vs. 3.27 ± 2.12 ng/mL; P< 0.001) and deltaTg (13.36 ± 19.74 vs. 2.12 ± 2.98 ng/mL; P = 0.002), compared to patients without midline uptake. There was no significantly different in D0Tg (2.31 ± 4.48 vs. 1.15 ± 2.18 ng/mL; P = 0.281), D3Tg (3.85 ± 4.93 vs. 2.07 ± 2.74 ng/mL; P = 0.143) levels between two groups.

The patients with midline uptake in anterior neck on WBS showed the higher level of serum Tg after RIT. Therefore, iodine uptake pattern on WBS has to be considered to evaluate therapeutic effect of remnant thyroid tissue through serum Tg level after RIT.

Endocrinology_20

Surveillance roles of serum thyroglobulin without TSH-stimulation measured by an ultrasensitive kit as a screening tool

Seunggyun Ha[1], Young Joo Park[2], Jin Chul Paeng[1], Keon Wook Kang[1], Dong Soo Lee[1], June-Key Chung[1] and Gi Jeong Cheon[1]

1. Department of Nuclear Medicine
2. Department of Internal Medicine, Seoul National University Hospital, South Korea

Purpose: The purpose of this study was to evaluate possibility of a screening role for ultrasensitive thyroglobulin without TSH-stimulation (unstimulated-uTg).

Methods: Patients (median 44 years, range 20 – 65 years) with DTC were included this analysis by following inclusion criteria: 1) total thyroidectomy, 2) TSH stimulation, and 3) paired serum samples before and after stimulation by T4-withdrawl or rhTSH. Cases of unadequate TSH stimulation were excluded based on 30 uIU/ml. Tg measurements before and after TSH-stimulation were conducted two times by two Tg-kits with different measurable sensitivity as 0.1 ng/ml for conventional kits (Dynotest Tg-plus BRAHMS Gmbh, Germany) and 0.01 ng/ml for ultrasensitive kits (RIAKEY, Shinjin Medics, South Korea). Anti-Tg antibody (anti-TgAb) levels less than 20 U/ml were considered as absence of anti-TgAb.

Results: Two kits had reliable measurements to each other (Pearson correlation coefficient 0.965, $P< 0.001$; intraclass correlation coefficient 0.981, $P< 0.001$). There was a tendency that higher unstimulated-uTg levels induce higher stimulated-Tg levels in less or no Tg-Ab presence ($P< 0.001$). Most cases (94%) with undetectable unstimulated-uTg (<0.01 ng/ml) had results of less than 2 ng/ml of stimulated-Tg levels regardless of anti-TgAb presence. In the cases with undetectable unstimulated-uTg, anti-TgAb levels before TSH-stimulation were directly correlated to those after TSH-stimulation. There were 30 percentages of cases as undetectable uTg and lesser anti-TgAb (< 50 U/ml) before TSH-stimulation, and most of those had restricted anti-TgAb levels less than 50 U/ml in TSH-stimulated condition as well as lesser stimulated-Tg levels (< 2ng/ml).

Conclusions: Unstimulated-uTg levels could predict stimulated-Tg levels in less or no anti-TgAb condition. In the cases that both unstimulated-uTg and Tg-Ab levels without TSH-stimulation were sufficiently low (uTg < 0.01 ng/ml & Tg-Ab < 50 U/ml), TSH-stimulation could be avoided for surveillance because expected Tg and Tg-Ab levels after TSH stimulation were restricted in favorable ranges.

Musculoskeletal System_1

Evaluation of Bone Scan Index Change Over Time on Automated Calculation in Bone Scintigraphy

Rini Shintawati Cahaya, Arifudin Achmad, Tetsuya Higuchi

Ayako Taketomi Takahashi, Takahito Nakajima, Yoshito Tsushima, Gunma University Graduate School of Medicine, Indonesia

to evaluate the efficacy of BONENAVI in determining BSI and hot spots at different time intervals after radioisotope injection.

We evaluated 32 patients, including 22 males and 10 females. Ten patients had breast cancer, 20 patients had prostate cancer, and 2 had malignant phaeochromocytoma. Patients were injected with 20 mCi of ^{99m}Tc-methylene diphosphonate (^{99m}Tc-MDP) and bone scintigraphy was performed at 2, 4, and 6 hours after injection on each patient. The BSI and the number of hot spots were obtained from BONENAVI software. Bone scan images were also visually assessed to exclude false positives due to artifacts. Analyses were performed in all lesions, selected true lesions, segment-based and cancer-type-based. Non-parametric statistical analyses for pairwise multiple group comparison were performed using Friedman test followed with posthoc analysis.

The BSIs and the number of hot spots were significantly increased with time, with significant differences between each of time points ($P< 0.001$). Analysis of regional BSI (rBSI) and hot spot number changes of selected 15 true lesions also showed similar increase ($P<0.001$). In general, the pelvic segment was the most prone to rBSI changes and the chest segment was the most prone to hot spot number changes. on visual assessment showed that BONENAVI diagnosed some typical artifacts as metastases (hot spots).

BONENAVI reading of BSIs and hot spot numbers was highly affected by acquisition time. In serial or follow-up examinations (in particular, for monitoring therapeutic efficacy), acquisition time should be fixed for each patient. Cautious interpretation should be made on segments with high physiological uptake. BONENAVI reading was prone to misinterpretation of artifacts. Visual assessment is necessary to rule out this possibility.

Radiochemistry_6

Consecutive Production of Carbon-11 Labeled Radiopharmaceuticals by Sharing [^{11}C]Methylation Source from One ^{11}C-Automatic Synthetic Module

Byung Chul Lee, Hyun Sik Park, Hong Jin Lee, Byung Seok Moon, Hyun Ho An, Byung Chul Lee, Sang Eun Kim

Department of Nuclear Medicine, Seoul National University Bundang Hospital, Korea

Recently, the production of carbon-11 labeled radiopharmaceuticals require at least two times a day due to their diversity and increase of use in position emission tomography (PET). After first production of the C-11 labeled radiopharmaceutical, however, next production should be delayed at least over 6 h because of radiation exposure and cleaning of module. Thus, there is a need for new methodology giving consecutive production in short time using one ^{11}C-synthetic module without additional purchase. In present study, we describe consecutive production of ^{11}C-PIB and –methionine using one ^{11}C-synthetic module by sharing [^{11}C]methylation source.

To produce ^{11}C-PIB and –methionine, two synthetic modules were used: one is the TRACERlab FX C pro and the other is old and unused ^{18}F-synthetic modules, and each module was connected with 3-way valve to sharing ^{11}C-CH3I or ^{11}C-CH3OTf prepared from ^{11}C-synthetic module. First, ^{11}C-PIB was produced in the TRACERlab FX C pro module and 2nd beam irradiation was carried out during purification process of ^{11}C-PIB. ^{11}C-Methionine was synthesized in the ^{18}F-synthetic module using ^{11}C-CH3I which was resynthesized in the ^{11}C-synthetic module.

The produced radioactivity of ^{11}C-PIB and ^{11}C-methionine were 4.1 ± 0.4 GBq (5.4 ± 0.6%, n.d.c.) and 15.2 ± 1.1 GBq (16.7 ± 0.8%, n.d.c.), respectively, with over 97% of radiochemical purity. The specific activity of ^{11}C-PIB was over 107 GBq/mmol. Total production time of two radiopharmaceuticals needs about 2 h from 1st beam irradiation including quality control test. Final ^{11}C-PIB and ^{11}C-methionine were satisfied all quality control test standards.

We developed a method which can be produced two ^{11}C-radiopharmaceuticals within 2 h in the ^{11}C- and ^{18}F-synthetic module. Studies for the assessment of long term stability of the new developed production system are still undergoing.

Technologist_1

Evaluation of base-free ^{11}C-Raclopride synthesis with various solvents

Yong-Seok Lee, Jae Min Jeong, Yong-Hyun Cho, Jae-Hyung Lee, Hong-Jae Lee, Jin-Eui Kim, Yun-Sang Lee, Keon-Wook Kang

PET center, Department of Nuclear Medicine, Seoul National University Hospital, Korea

Purpose: [^{11}C]Raclopride is usually synthesized using base such as NaH, NaOH or K_2CO_3 in many radiochemistry labs. We evaluated a possibility of six different solvents for [^{11}C]raclopride synthesis without base; DMF, DMSO, EtOH, 2-butanone (MEK), MeCN, or cyclohexanone (c-HXO). We also tried to improve synthesis method using optimal solvent.

Methods: [^{11}C]MeI and [^{11}C]MeOTf were produced by a gas-phase method using TRACERlab FXC Pro. *O*-desmethylraclopride (1 mg, 3 umol) in 100 uL of each solvent, DMF or DMSO for [^{11}C]MeI and MeCN, EtOH ,MEK or c-HXO for [^{11}C]MeOTf, were loaded into HPLC loop. After purging with methylating agents for 3 min at RT, the reaction mixture was purified by HPLC system. To compare the production yield, we performed the vial synthesis method with 200 uL of precursor solution at 80°C, 5 min.

Results: The radiochemical yield of [^{11}C]raclopride was 5.8%, 2.8% or 7.3% with MeCN, MEK or c-HXO as a solvent without decay correction (EOS), respectively, and we could not find the product peak from HPLC using DMF, DMSO or EtOH. Out of MeCN, MEK and c-HXO, c-HXO showed the highest radiolabeling yield for the loop method. The radiolabeling yield of the vial method at 80°C using c-HXO was 30.0% (n=3) without decay correction (EOS).

Conclusions: We confirmed that [^{11}C]raclopride could be synthesized without any base, and c-HXO was the optimal solvent for [^{11}C]raclopride synthesis.

Technologist_2

Evaluation of Perfusion and Image Quality Changes by Reconstruction Methods in ^{13}N-Ammonia Myocardial Perfusion PET/CT

Yong Ho Do[1], Hong Jae Lee[1], Jin Eui Kim[1], Hyung Jun Im[2], Jae Sung Lee[2] and Keon Wook Kang[2]

1. Department of Nuclear Medicine, Seoul National University Hospital, Seoul, Korea
2. Department of Nuclear Medicine, Seoul National University, Seoul, Korea

Purpose: The aim of this study was to evaluate

changes of quantitative and semi-quantitative myocardial perfusion indices and image quality by image reconstruction methods in ^{13}N-ammonia (^{13}N-NH_3) myocardial perfusion PET/CT.

Method: Data of 14 (8 men, 6 women) patients underwent rest and adenosine stress ^{13}N-NH_3PET/CT (Biograph TruePoint 40 with TrueV, Siemens) were collected. Listmode scans were acquired for 10 minutes by injecting 370MBq of ^{13}N-NH_3. Dynamic and static reconstruction was performed by use of FBP, iterative2D (2D), iterative3D (3D) and TrueX. Coronary flow reserve (CFR) of dynamic reconstruction data and extent (%), total perfusion deficit (TPD)(%) measured in sum of 4-10 minutes scan were evaluated compared to 2D method recommended by vendor. And image quality with 5 medical doctor's blind test of each reconstructed data were compared and evaluated.

Results: CFR were lower in TrueX 18.68% (P=0.0002), FBP 4.35% (P=0.1243) and higher in 3D 7.91% (P<0.0001). As semi-quantitative values, extent and TPD of stress were higher in 3D 3.07%p (P=0.001), 2.36%p (P=0.0002), FBP 1.93%p (P=0.4275), 1.57%p (P=0.4595), TrueX 5.43%p (P=0.0003), 3.93%p (P<0.0001). Extent and TPD of rest were lower in FBP 0.86%p (P=0.1953), 0.57%p (P=0.2053) and higher in 3D 3.21%p (P=0.0006), 2.57%p (P=0.0001) and TrueX 5.36%p (P<0.0001), 4.36%p (P<0.0001). Based on image resolution and noise in blind test of snapshot, 3D was obtained the highest score followed by 2D, TrueX and FBP.

Conclusion: Quantitative and semi-quantitative myocardial perfusion values could be under or overestimated according to reconstruction algorithm in ^{13}N-NH_3 PET/CT. Proper dynamic and static reconstruction method should be established to provide accurate myocardial perfusion value.

Technologist_3

Development of Bladder Phantom and Image Evaluation of Lesion in the Vicinity according to Filling and Empty Bladder

Chan Rok Park, Jae Il Kim, Hong Jae Lee, Jin Eui Kim

Department of Nuclear Medicine Seoul National University Hospital, Seoul, Korea

Purpose: There are difficult patients to urinate such as prostate cancer or bladder cancer. In these patients, they get limitation reading around bladder lesion. The purpose of this study was to make bladder phantom and evaluate image quality on the filling bladder and empty bladder.

Methods: Biograph mCT40 (Siemens, Germany) was used. To make bladder phantom, air balloon was used as bladder in the NEMA IEC Body phantom. The 6 inserts was also used by lesion in the vicinity according to bladder. ^{18}F isotope was injected with the ratio 8 : 30 : 1 (insert : bladder : background). Percent Background Variability (% BV) was assessed according to distance from the bladder (0.7, 1.4 cm). We measured distance 6 inserts from the bladder (0.4, 0.6, 1.4, 2.3, 2.7, 3.8 cm) and evaluated SUV difference, average counts, single count, random count and true count according to filling and empty bladder.

Results: At the 1.4 cm, % BV was more decrease than those with 0.7 cm at the filling bladder. When bladder was empty, average counts were increased about 14 % by the 0.4 cm. In addition, true count was decreased by 38 % but, single count and random count were increased by 44 and 61 %. There was no difference greater than 0.4 cm. SUV difference compared with filling and empty bladder was expressed by 7.8 ± 3.8 %.

Conclusions: In this study, we confirmed that there was effect to the lesion in the vicinity according to amount of urine in the bladder. When bladder was full, there were limitation in measuring counts, SUV and image evaluation. Therefore, it is considered to help in the clinical evaluation and accurate scan to urinate prior to scanning.

Technologist_4

The Effect of Different Scan Protocols on Minimizing Misregistration of Lower Extremity PET/CT Scan

Jeoung-Eun Lee, Woo-young Jung, Jae-Kwang Lyu, Sang-ki Shin

Department of Nuclear Medicine, Asan Medical Center, Seoul, Korea

Purpose: Lower extremity PET/CT scan is conducted additionally with ^{18}F-FDG wholebody PET/CT scan when malignancy in lower extremity is suspected. In General lower extremity scan protocol, the scan is continued in Scout-CT-PET order and PET scan direction is craniocaudal (Pelvis to Feet). Using the protocol, however, PET and CT image misregistration resulting from patient movement during the time interval between CT and PET scan poses some problems. The purpose of this study was to validate the effect of different scan protocols of changing the PET/CT scan order or PET scan direction to caudocranial (Feet to Pelvis) on image misregistration reduction.

Materials and Methods: 99 patients (52.95±19.04 years) who had undergone additional lower extremity PET/CT scan were referred. Discovery 690, 710 and 690Elite PET/CT scanners (GE healthcare, USA) were used for the study.

Patients were classified into 3 groups according to PET/CT scan order and PET scan direction (Group 1: Scout-CT-PET/ Craniocaudal, Group 2: Scout-CT-PET/ Caudocranial, Group 3: Scout-PET-CT/ Craniocaudal). The maximum distances (mm) of PET and CT image misregistration were measured from 3 regions (pelvis-thigh, Knee-calf and ankle-foot) and comparatively analyzed in groups.

Results: Pelvis-thigh misregistration distances in Group 1, 2, 3 were 0.96±2.47 mm, 1.92±3.13 mm and 1.12±2.53 mm respectively and there was no significant difference between the groups. Knee-calf misregistration distances in Group 1, 2, 3 were 1.58±3.03 mm, 1.45±3.55 mm and 0.76±2.13 mm respectively and there was no significant difference between the groups. Ankle-foot misregistration distances in Group 1, 2, 3 were 8.53±11.00 mm, 2.95±3.96 mm and 1.69±4.20 mm and there were significant differences Between Group 1 and other groups (P<0.001). But there was no significant difference between Group 2 and 3.

Conclusions: PET and CT image misregistration due to patient movement during lower extremity PET/CT scan was featured prominently on foot. Switching the order of CT and PET scan or changing PET scan direction to caudocranial can minimize the image misregistration and this may be helpful on diagnosis of lower extremity diseases.

Technologist_5

Evaluation about Availability of EKG gated scan on ^{13}N-ammonia PET/CT

Jaeil-Kim. Chanrok-Park. Hongjae-Lee, Jineui-Kim

Nuclear Medicine, Seoul National University Hospital, Seoul, Korea

Purpose: At cardiac nuclear medicine, many kind of pharmaceuticals have been using for evaluation of perfusion or viability of heart. Among those, ^{13}N-ammonia is one of the excellent tracer that evaluate the quantitative for myocardial perfusion. But the spatial resolution of heart PET image is very low because of movement. So in this study, we will evaluate an availability of EKG gated scan about ^{13}N-ammonia myocardial PET.

Methods: We used Biograph True Point (Siemens, Germany) as PET/CT scanner, injected ^{13}N-ammonia (350±53 MBq) to patients (age: 67±11), at same time, acquired PET date as list mode gated EKG trigger during 10 minutes. After then, 2 PET images were reconstructed. The one is 1frame- images summed from 4 minute to 10 minute, the other is 8 frame-image gated by 8 interval gap. We compared and evaluated a FWHM of inferior myocardium.on those 2 reconstructed images. Additionally, the segmented distribution of perfusion(QPS) was compared for quantitative evaluation.

Results: A gated PET image's spatial resolution is better than non-gated image. Especially, FWHM that is calculated a count profile on each PET images is more narrow about 38% than non-gated one. By the way, a score of gated image on QPS did not significantly differ from non-gated image .

Conclusions: As result, the EKG gated scan is useful to minimize a motion artifact of heart with maintain quantitative evaluation. Moreover, in case of PET/CT, PET/MRI that can fuse anatomic and functional image, a gated image will help diagnostic by a high special resolution PET image.

Technologist_6

Clinical usefulness of additional F-18 FDG PET/CT of pelvic prone position in patients with uterine cervix cancer

Gyeong Won Kim, Chan Yong Kim, Sang Min Han, Yong Seok Lee, Jung Jin Roh, Hyeon O Oh, Dong Yeon Kim, Gi Seong Park, Myoung Jun Kim, Seong Young Kwon, Jung-Joon Min, Hee-Seung Bom

Department of Nuclear Medicine, Chonnam National University Hwasun Hospital

Purpose: F-18 FDG (FDG) accumulation in urinary bladder could often lower the quality of PET/CT image especially to evaluate the pelvic lesions. We investigated the clinical usefulness of additional image which was achieved with pelvic prone position in patients with uterine cervix cancer.

Methods: We enrolled 62 patients who underwent PET/CT for staging of uterine cervix cancer. PET/CT images were achieved twice: first images ranged from skull base to middle thigh with supine position and second images in pelvic areas with prone position. We compared the difference of three parameters between 2 serial images: the volume of urinary FDG accumulation, mean SUV in bladder and the length (cm) of abutting plane between uterine cervix cancer and urinary bladder. Visual assessment was performed by two clinicians and image quality was compared between two different positions.

Results: Both volume of urinary FDG accumulation (*P=0.877)* and mean SUV in bladder (*P=0.056)* were not significantly different between two positions. However, the length of abutting plane was significantly

reduced from 2.8 cm in supine position to 2.1 cm in prone position (P<0.001). Image quality was also significantly improved in prone position, compared to supine position (P<0.001).

Conclusions: Our study suggested that image quality achieved with prone position was significantly improved by reducing the length of abutting plane, which could affect the incidence of some artifacts such as spill-over.

Cardiology_4

Liposomal Strategy to Treat Myocardial Ischemia: Increasing Provisions Do Not Necessarily Benefit Myocardial Ischemia

Hwang-Jeong Jeong, Hyosook Hwang, Hwan-Seok Jeong, Eun-Mi Kim, Phil-Sun Oh, Minjoo Kim, Tai-Kyoung Lee, JeongIl Kwon, Hyeon-Soo Kim, Ji-Hae Choi, Min-Ji Kim, SeokTae Lim, Myung-Hee Sohn

Chonbuk National University Medical School & Hospital, Korea

The present study tested the hypothesis that PEGylated nanoliposomes to facilitate targeted delivery can effectively treat myocardial ischemia.

Rats subjected to 30 minutes of myocardial ischemia received ^{99m}Tc-HMPAO or ^{99m}Tc-DTPA labeled liposomes with mean diameters of 100, 300, and 600 nm with or without PEG modification.

The liver and spleen showed the largest capacity for liposome uptakes. This was more pronounced when the sizes of vesicles were increased. Conversely, myocardial liposome uptakes were significantly (P=0.008) greater when the sizes of vesicles were decreased to 100 nm compared to those at 600 nm. Surface modification with PEG significantly (P=0.032) augmented myocardial liposome uptakes at size of 100 nm compared to that with unPEG. However, it did not affect the size dependence (P=0.014 vs. 600 nm). To investigate the efficacy of liposomes, hearts subjected to ischemia received PEGylated nanoliposomes (~100 nm) encapsulated with angiogenic peptides. Treatment effects were examined by studying changes in myocardial perfusion defects by ^{99m}Tc-tetrofosmin autoradiography and vascular density by immunohistochemistry at 7 days post-treatment. Our data demonstrated that PEGylated nanoliposomes loaded with angiogenic peptides improved myocardial perfusion defects (P=0.006 vs. control) and increased vascular density (P=0.004 vs. control). However, such effects only occurred in the group receiving low levels of liposomal provisions.

Our results demonstrated that increasing provisions of liposomal angiogenic formulation with size control and PEG modification did not necessarily benefit myocardial ischemia. These data suggest that optimal liposomal dosage is needed for their therapeutic efficacy.

Cardiology_6

Incidence and effect of right ventricle dysfunction in patients of ischemic heart disease with severely depressed left ventricle

Amitabh Arya, Shantanu Pande

Sanjay Gandhi Post Graduate Institute of Medical Sciences,Lucknow, India

In this study we plan to observe the incidence of RV dysfunction and its effect on long-term follow-up.

This is a pilot study conducted between January 2010 and December 2010. During this period a total of 240 coronary artery bypass procedures were performed of which 22 patients were of severe LV dysfunction (ejection fraction < 40%). Patients undergoing primary coronary artery bypass grafting (CABG) with LV dysfunction of > 6 months were included. Acute MI and acute coronary syndrome patients were excluded. Echocardiography was performed for assessment of LV and its follow-up. Radionuclide ventriculography (MUGA) was performed for assessment of both the ventricles. Patients were divided into 2 groups, I n=13 (RVEF >30%) and II, n=9 (RVEF <30%).

All patients received successful off pump CABG. Echocardiography follow-up is available for a median of 25 months (12-62) and outpatient follow-up of 49 months (12-68). Group I has LVED of 48mm (40-65), LVES of 33mm (28-36) and EF of 40% (20-45). Group II had LVED of 55 mm (52-57), LVES of 42mm (30-45) and EF of 33% (30-35). During follow-up Group I had LVED and EF of 48 (46-56) & 50 (45-60) respectively. Group II in follow-up has LVED and EF of 63 (52-70) and 37 (27-45) respectively. There was significant difference in LVED (P=0.05) and LVEF (P=0.03) of 2 groups in follow up. There was significant improvement of LVEF in group I, P=0.04 while there was no significant effect in group II. There was no correlation between LVEF measured by MUGA and echocardiography.

RV dysfunction is present in 40% of patients with severely depressed LV. This leads to poor recovery of LV in long-term duration when compared to patients with no RV dysfunction. Patients with better RV function show remarkable recovery in their LV function.

Cardiology_12

Factors affecting myocardial FDG uptake by F18-FDG PET/CT for cancer screening in healthy subjects fasted longer relatively

Ji Yeon Kang, Wonsick Choe

Department of Nuclear Medicine (Kangbuk Samsung Hospital, Sungkyunkwan University School of Medicine, Republic of Korea)

Purpose: Myocardial FDG uptake is a limiting factor to image coronary plaque inflammation or to detect cardiac sarcoidosis by F18-FDG PET/CT. This study was designed to evaluate the factors affecting myocardial FDG uptake by F18-FDG PET/CT for cancer screening in healthy subjects who fasted longer relatively than subjects in the previous studies.

Methods: F18-FDG PET/CT was performed on 174 consecutive healthy subjects (mean age 44.5±6.1, male 161). Myocardial FDG uptake was assessed by measuring maximal standardized uptake value (SUV_{max}) and using qualitative visual scale (QVS) (Grade 0; homogeneously minimal, Grade 1; mostly minimal, Grade 2; mostly intense, Grade 3; homogeneously intense). The influences of age, gender, fasting duration, fasting glucose, HbA1c, triglyceride, and insulin were analyzed.

Results: F18-FDG PET/CT was performed on 174 consecutive healthy subjects (mean age 44.5±6.1, male 161). Myocardial FDG uptake was assessed by measuring maximal standardized uptake value (SUV_{max}) and using qualitative visual scale (QVS) (Grade 0; homogeneously minimal, Grade 1; mostly minimal, Grade 2; mostly intense, Grade 3; homogeneously intense). The influences of age, gender, fasting duration, fasting glucose, HbA1c, triglyceride, and insulin were analyzed.

Conclusions: The longer subjects fasted, the less variability and more suppression of myocardial FDG uptake were observed. Besides fasting duration, it is presumed that HbA1c and insulin resistance are the factors related with myocardial FDG uptake. These results may be useful to predict a subject with good suppression of myocardial FDG uptake and to understand the relationship between fasting duration and fatty acid-glucose metabolism in the heart.

Cardiology_17

Relationship of myocardial perfusion, function and dyssynchrony with exercise tolerance of heart failure patients

Chetan D patel, Shambo guha roy, Sandeep seth, Anirban mukherjee

Department of nuclear medicine,AIIMS, New Delhi, India

Heart failure(HF) patients show heterogeneity in their exercise tolerance.Factors contributing to poor exercise tolerance in not well understood.We planned this study to find the relationship of myocardial perfusion,left ventricular function and cardiac mechanical dyssynchrony(CMD) with exercise tolerance in HF patients.

In this single centre observational study we enrolled 50 HF patients(43 male,7 female) aged 53 + 9 years with history of myocardial infarction(MI) or angiographically proved coronary artery disease (CAD). At least 4 weeks after the initial presentation all patients underwent ^{99m}Tc MIBI gated myocardial perfusion SPECT (GMPS). Images were analyzed for perfusion defect using 20 segment model and severity of perfusion defect measured as summed rest score(SRS).Phase standard deviation (PSD) and Phase histogram bandwidth (PHB) were used to assess CMD.LVEF was also evaluated. Exercise tolerance was quantified by 6 minute walk distance (6MWD).6MWD< 300 meters was taken as poor exercise tolerance.Perfusion defects,LVEF and dyssynchrony was compared between two groups with 6MWD<300(group A) and >300 meters(group B).

Twenty nine patients were NYHA class II,rest 21 NYHA class III.Mean LVEF was 29 + 8(range 14 - 41). Mean scar size and SRS were 28+19(range 0-67) and 20+12(range 0-50).Among the dyssynchrony parameters mean PSD was 54+18(range 22-96) and mean PHB was 162+65(range 59-290).In overall study population neither CMD nor perfusion defects showed any correlation with 6MWD,only LVEF showed modest correlation with 6MWD(r = 0.39,*P*=0.005). In group analysis there was no statistically significant difference between the scar size(*P*=0.79),PSD(*P*=0.11) or PHB(*P*=0.36) among the groups.But group A patients showed significantly lower LVEF (*P* = 0.03).Using step wise regression analysis among LVEF,PSD,PHD,scar size;LVEF remained only significant predictor of poor exercise tolerance(<300meters).

The results of our study shows that exercise tolerance of heart failure patients co-relates only with LVEF.Among dyssynchrony,perfusion and functional indices,LVEF is the single most predictor of poor exercise tolerance in heart failure patients.

Cardiology_18

Factors Affecting Fractional Flow Reserve and Thallium-201 Myocardial Perfusion Single Photon Emission Computed Tomography in Patients with Single Vessel Coronary Artery Disease

Soo-Jin Kang, Sangwon Han, Dae Hyuk Moon, Seung-Jung Park

Korea

Myocardial perfusion single photon emission computed tomography(SPECT) measures relative difference in perfusion during the maximal vasodilation generated by stress testing, while fractional flow reserve(FFR) is defined as maximal blood flow in maximal blood flow in a stenotic artery as a ratio to theoretical maximal flow in the same vessel. In a previous study, FFR values has known to be higher in female than in male patients, considering smaller myocardial territory in female may be responsible for the higher FFR. We investigated physiologic factors affecting FFR and thallium SPECT in same patients with single vessel coronary artery disease. We assessed adenosine stress thallium SPECT and FFR in a prospective cohort of 301 patients with single vessel disease with intermediate lesion(angiographic diameter stenosis 30-85%). Patients with previous PCI, acute myocardial infarct, LVEF<40%, significant valve disase, regional wall motion abnormality, left ventricular hypertrophy, left main coronary artery stenosis > 30%, or time interval between performing thallium SPECT and FFR >1 month were excluded.

For diagnosis of positive thallium SPECT, the best cut-off value of FFR was 0.75(area under curve=0.79 [95%CI:0.74-0.83]), with 72.6% sensitivity, 74.6% specificity, 47.4% positive predictive value and 89.5% negative predictive value. Patients with FFR≤0.75 and negative SPECT were seen in 19%(58/301),whereas patients with FFR>0.75 and positive SPECT were seen in only 6%(20/301) of all the patients. In the subgroups of negative SPECT, patients with FFR≤0.75 showed significantly younger age and male sex predominance compared to those with FFR>0.75. On the other hands, in both subgroups of FFR≤0.75 and >0.75, there was no significant age or sexual difference in patients with positive SPECT compared with those with negative SPECT.

Most common discordant finding was normal thallium SPECT but abnormal FFR. Age and sex may influence FFR values without effect on myocardial perfusion assessed by SPECT. Further studies are needed to determine the contribution of age and sex to decision on coronary revascularization, particularly in patients with normal SPECT and abnormal FFR.

Cardiology_19

Accuracy of Left Ventricular Volumes and Ejection Fraction Measured by Quantitative Thallium-201 Gated Single Photon Emission Computed Tomography with Cadmium-Zinc-Telluride detectors: Comparison with Conventional Dual Head Anger-type Camera

Dae Hyuk Moon, Sangwon Han, Duk-Hyun Kang, Jong-Min Song, Jae-Kwan Song

Department of Nuclear Medicine, Asan Medical Center, Korea

Gated single photon emission computed tomography(SPECT) is a valuable tool for analysis of left ventricular(LV) function as well as myocardial perfusion. However, systemic biases in assessing LV volumes and ejection fraction(EF) by gated SPECT have been consistently reported. The new cardiac dedicated camera using cadmium-zinc-telluride(CZT) detector shows improved sensitivity and spatial resolution, so it is likely to provides more accurate assessment of LV volumes and EF. The aim of this study is to compare LV volumes and EF assessment using quantitative gated SPECT between CZT and Anger camera.

We retrospectively assessed 297 patients who underwent adenosine stress gated thallium-201 SPECT using a new cardiac dedicated camera with CZT detectors(n=144; Discovery NM 530c, GE), or a conventional Anger camera(n=153; Ventri, GE). LV end-diastolic(EDV) and end-systolic volumes(ESV) and EF from gated SPECT were calculated by a commercially available software(QGS; Cedars-Sinai). LV volumes and EF from echocardiography were derived by previous validated modified Simpson's biplane disc method. The degree of agreement between SPECT and echocardiography was determined as the mean difference(bias), and the limit of agreement(mean ± 1.96 standard deviation). Both CZT and Anger cameras significantly underestimated EDV and ESV. However, the degree of underestimation were significantly lower with CZT than with Anger SPECT(EDV; CZT: bias=-17.2ml; limits of agreement=-57.8 to +23.4, Anger: bias=-32.0ml; limits of agreement=-72.5 to +8.4, P<0.001) (ESV; CZT: bias=-4.3ml; limits aof agreement=-35.2 to +26.7, Anger: bias=-14.3ml; limits of agreement=-36.7 to +8.2, P<0.001). Gated SPECT with CZT showed good agreement for EF(bias=0.03%; limits of agreement=-18.5 to +18.6), but Anger SPECT showed significant overestimation(bias=6.4%; limits of agreement=-13.8 to +26.3). Bland-Altman plots revealed that EF with CZT was less dependent on

EF magnitude than with Anger SPECT(CZT: R=0.60, *P*<0.001; Anger: R=0.77, *P*<0.001).
CZT SPECT camera can accurately quantify EF. Although it still underestimates LV volumes, CZT camera shows less underestimation of LV volume than Anger-type camera.

Cardiology_27

Comparison the coronary flow reserve using myocardial SPECT/CT in Tl-201 and coronary stenosis

Jung-Min Lee, Young Hwan Kim, Ho-Young Lee

Seoul National University Bundang Hospital, Korea

SPECT/CT is widely used for acquiring tomographic evaluation and quantitative analysis of gamma images. Here, we aimed to evaluate the coronary flow reserve quantitatively and validate its performance using Tl-201 stress/rest myocardial SPECT/CT and compared with coronary angiography (CAG).
To evaluate the diagnostic usefulness of quantitative analysis Tl-201 myocardial SPECT/CT, we compared the quantitative analysis of Tl-201 myocardial stress/rest SPECT/CT with CAG. The patient who underwent CAG within 3 month after Tl-201 stress/rest myocardial SPECT/CT was enrolled and 23 patients were enrolled (M:F= 16:7, mean age). Among 23 patients, 15 patients were one vessel disease, 5 patients were two vessels disease. We used a home-made software to investigate the count of each segments in Bull's eye of myocardial SPECT. Vascular reserve was measured with the ratio of stress to rest mean count.
We compared the vascular reserve of each vascular territory with CAG result. ROC analysis showed sensitivity 89.5% and specificity 87.5% at 1.34. Count of stress ^{201}TI image in the vascular territory with stenosis was 1214.1±545.4 and the Count of rest ^{201}TI image in the vascular territory with stenosis was 614.1±345.4. There was significant difference of mean count between the vascular territory with stenosis and without stenosis (*P*<0.0001).
We have shown that the ratio of image counts from myocardial SPECT could be useful to evaluate coronary flow reserve. Therefore, this study is valuable as the preliminary study to evaluate coronary flow reserve using myocardial SPECT.

Endocrinology_3

Scintigraphic Spectrum of Parathyroid Neoplasms – A Study of 100 Cases from a Single Centre in India

Karuppiah Kumaresan

KK Nuclear Scans, Nava Bharat Chambers, Raj Bhavan Road, Hyderabad, India

A retrospective analysis was carried out on 100 cases in whom Parathyroid Tumor was localized by Planar Scintigraphy between 2009 and 2014.
Dual Phase ^{99m}Tc Sestamibi scan was performed in all patients; In addition ^{99m}Tc Pertechnetate Thyroid Scintigraphy was performed after 24 hours in 25 patients only. The various patterns of the scan findings regarding size, location, degree of uptake of ^{99m}Tc Sestamibi, delayed persistence or washout and the need for ^{99m}Tc Pertechnetate Thyroid scan are presented here. The age of the patients ranged from 14 to 85; Males 44 and Females 56.
The parathyroid tumor was large in 34, medium sized in 48 and small in 18. The ^{99m}Tc Sestamibi uptake by the Parathyroid Tumor was very high in 21, higher than in thyroid gland in 52 and same as or lesser than thyroid activity in 27. The tumor was localized in the Right Superior region in 11, Right Inferior in 34, Left Superior in 14, Left Inferior in 33, Sternal notch in 5 and in the Mediastinum in 3.The Parathyroid Tumor was confidently identified in the early image of ^{99m}Tc Sestamibi scan itself in 56 % patients (located well outside thyroid bed in 12 and seen as a typical protrusion from thyroid margin in 44). The tumor focus could be suspected in the early image and confirmed with confidence in the delayed scan in 31 % patients. Early image was absolutely normal and only the delayed image revealed the lesion in another 5 %..Complete washout of ^{99m}Tc Sestamibi from the Parathyroid Tumor was found in 12 cases including 4 which were clearly identified in the early image. Both early and delayed ^{99m}Tc Sestamibi images were considered negative but comparison with ^{99m}Tc Pertechnetate Thyroid scan revealed the lesion in 8.
Our study shows that when Parathyroid Tumor is localized scintigraphically, Dual Phase ^{99m}Tc Sestamibi scan is adequate in 92% patients and comparison with vPertechnetate Thyroid scan is required only in 8 %.

Radionuclide Therapy_11

SUV_{max} of FDG-avid metastatic lesions could predict prognosis in differentiated thyroid cancer after total thyroidectomy

Yuko Uchiyama[1], Shozo Okamoto[1], Tohru Shiga[1], Florian C. Gaertner[1], Kenji Hirata[1], Osamu

Manabe[1], Yoichi M Ito[2], Keiichirou Yoshinaga[1], Nagara Tamaki[1]

1. Department of Nuclear Medicine, Hokkaido University Graduate School of Medicine
2. Department of Biostatistics, Hokkaido University Graduate School of Medicine, Sapporo, Japan

Purpose: It has been suggested that the patients with positive FDG accumulation in metastases from differentiated thyroid cancer have a poor prognosis. We investigated correlation between quantitative value of FDG-PET before I-131 therapy and prognosis for the patients with FDG-avid metastases from differentiated thyroid cancer.

Methods: A total of 309 patients with FDG-avid metastatic lesions before the first I-131 treatment were retrospectively analyzed. The maximum follow-up period was 57.6±39.1 months. The maximum standardized uptake value (SUV_{max}) in the all metastases was evaluated. We compared SUV_{max} with overall survival after the treatment. We performed survival rate analysis by the Kaplan-Meier method and the single variable and multivariable analysis using Cox regression models with prognostic factors such as SUV_{max}, age, the metastatic sites (lung, bone, neck, mediastinal and others).

Results: The 10-year survival rate was 53.4%. With the cut off value of SUV_{max} 4.6, the Kaplan-Meier curves suggested that the patients with high FDG uptake showed significantly poorer prognosis than the patients with low FDG uptake (P<0.0001). By the univariate analysis, SUV_{max} (P<0.001), sex (P=0.036), age (P=0.002), a metastatic lesion (P<0.001) were significant prognostic factors. In a multivariable analysis, SUV_{max} (P=0.0008), age (P<0.0001), and metastatic sites (P=0.0002) were independent prognostic factors.

Conclusions: These results suggested SUV_{max} of FDG-avid metastasis as a powerful independent prognostic indicator in patients with differentiated thyroid cancer after total thyroidectomy.

Endocrinology_9

The Effect of Salt Iodization on Thyroid Cancer in Oman

Samir Hussein, Alaa Al Hamdani, Nidaa Al Naamani , Asim Al Qureshi, Omayma Taha, Nicholas Woodhouse

Sultan Qaboos University Hospital, Oman

Purpose: To assess the effect of iodized salt on aggressiveness of thyroid cancer in Oman.

Methods: A retrospective cohort case-control study was conducted on 221 thyroid cancer patients referred for radioactive iodine therapy at Sultan Qaboos University Hospital (SQUH). They were divided into two groups depending on their date of presentation. Group 1 as control group (n= 47) from 1991 until 1995 (before salt iodization program), and group 2 as exposure group (n= 174) from 2005 until 2010 (9 years after salt iodization program).

The two groups were compared for age, sex, Tumor size, locality, multifocal, lymph node invasion, extra-thyroid spread and distant metastasis.

Results: Majority of patients were females in both groups, 37 (79%) in Group 1 and 143 (82%) in Group 2, there was no significant difference between the two groups. In group 1 the mean age was 40 years and in group 2 was 38 years there was no significant difference between the two groups. The lymph node invasion and extra-thyroid spread and multifocal tumor were significantly more frequent in group 1 (52%, 26% and 64%, respectively) than in group 2 (21% and 11% and 23%, respectively).

Larger tumors are found mainly in group 1. In particular, tumors of 5 cm or more accounted for 9% of the total patients, with a very significant decrease from 17% of the patient in group 1 to only 7% in group 2.

In this study most thyroid tumors were in stage I, and more advanced stages of thyroid cancer were present in (group 1). Stage I was significantly more common in group 2 (85%) than in group 1 (64%). While the more advanced stage: stage VI was more frequent in group 1 (13%) than in group 2 (9%).

Conclusions: This study showed that the severity of the thyroid cancer decreased significantly after introduction of Iodized Salt in Oman according to the lymph node invasion, extra-thyroid spread, multifocal disease, tumor size and staging.

Clinical Applications of PET/MR and SPECT/CT_20

Total Lesion Uptake Ratio on ^{99m}Tc-MIBI Parathyroid SPECT/CT: a Quantitative Marker Evaluating Disease Burden of Primary Hyperparathyroidism

Zhaoting Cheng[1], Jianhua Yan[2], Sijuan Zou[1], Guopeng Zhang[1], Xiaohua Zhu[1]*

1. Department of Nuclear Medicine, Tongji Hospital, Tongji Medical College, Huazhong University of Science and technology, China
2. A*STAR_NUS Clinical Imaging Research Center for translational Medicine, Singapore

Purpose: Primary hyperparathyroidism (PHPT) is a

disease characterized by hypercalcemia attributable to autonomous overproduction of parathyroid hormone (PTH). In this study, we aimed to investigate the relationship between image features in terms of lesion-to-background (LBR), metabolic volume (MV) and total lesion uptake ratio (TLUR) based on ^{99m}Tc-MIBI parathyroid SPECT/CT and clinical features, including symptoms, preoperative serum intact PTH (iPTH), calcium values and volume of lesion in patients with primary hyperparathyroidism.

Methods: 60 patients with hyperparathyroidism were retrospectively enrolled. A Dual-phase ^{99m}Tc-MIBI planar scintigraphy and a delayed SPECT/CT, an ultrasonography were performed after treatment with calcitonin. The pathologic volume (PV) of each lesion was measured after parathyroidectomy. 38 patients were demonstrated as both positive scintigraphy and no sign of thyroid nodule on ultrasonography. The volumes of lesion were delineated with a thresholding method on the SPECT/CT images. LBR, MV and TLUR were measured for each lesion. In addition, the biochemical features, including preoperative serum iPTH, calcium values before (Ca1) and after (Ca2) calcium-lowering medications were investigated.

Results: 63 lesions were found in 60 patients including 49 single entopic parathyroid adenomas, 3 multiple parathyroid adenomas, 7 parathyroid hyperplasia and 1 parathyroid carcinoma. The symptomatic PHPT patients (SPP) had significantly higher TLUR than the asymptomatic PHPT patients (ASSP). However, there were no significant difference between the SPP and the ASPP in PV, MV and LBR. TLUR was strongly correlated with PV, iPTH and Ca1. LBR, MV and TLUR were all not correlated with Ca2. LBR was significantly correlated with PV and Ca1 (P<0.05), but not correlated with serum iPTH (P>0.05).

Conclusions: TLUR measured on ^{99m}Tc-MIBI parathyroid SPECT/CT, which can reflect both MV and LBR, had a stronger correlation to biochemical markers and clinical features than LBR, and it is less affected by clinical factors due different laboratory error, calcium-lowering medications and other skeletal or renal diseases than biochemical testing methods. TLUR is a better quantitative marker in evaluating disease burden for PHPT patients than other image features, especially for ASPP.

Endocrinology_17

The research of chemotactic factor changes in dedifferentiated thyroid cancer

Dan Li, Zhongwei Lv

Department of Nuclear medicine, Shanghai 10th People's Hospital, Tongji University School of Medicine, 200072, China

Objective: This research aims to determine determine the correlation between chemotactic factor (CF) and dedifferentiation degree in DTC.

Methods:75 DTC patients' venous bloods were collected (25 male and 50 female, average age 41±13) from Shanghai 10th People's Hospital affiliated to Tongji University from April to June, 2014. These blood samples were divided into 2 categories according to metastasis or ^{131}I ablation effects, one category contains non-metastasis group (n=13), only neck lymph node metastasis group (n=47) and distal metastasis group (n=15); the other category contains single ^{131}I effective therapy group (n=62), multiple ^{131}I effective therapy group (n=9) and RAIR group (n=4). The Liquid microbeads floating protein chips (No. 171-AK99MR2, Huaying biochemical Science and Technology Co, Shanghai) were used to detect various CFs in these DTC blood samples through Bio-Plex Validation kit (Bio-Rad, USA).

Results: Eotaxin-3, Fractalkine, GCP-2, Gro-α, IFN-γ, IL-1β, MCP-1, MDC, MIF, TECK and TNF-α were significant lower in metastasis group than non-metastasis group (P<0.05); comparing with neck lymph node metastasis group, MIP-1θ expression was significant higher and SCYB16 expression was significant lower in distal group (P=0.04); comparing with non-metastasis group, lower expression of Eotaxin, Eotaxin-2, Eotaxin-3, Fractalkine, GCP-2, Gro-α, IFN-γ, MCP-4, MDC, MIF, TECK and TNF-α were found in neck lymph node metastasis group (P<0.05), while Eotaxin-3, Fractalkine, IL-16, MDC, SCYB16 and SDF-1α+β showed obviously lower in distal group (P<0.05). In multiple therapy group, MIP-1θshowed a significantly higher expression and SCYB16 expressed significantly lower than single therapy group (P=0.01). In comparison with the single therapy group, CTACK expression was obviously higher in RAIR group (P<0.05), while MPIF-1 and SDF-1α+β were significantly lower (P<0.05); in comparison with the multiple therapy group, CTACK and MIF were significantly higher but MPIF-1 and SDF-1α+β were much lower in RAIR group (P<0.05).

Conclusion: SCYB16 may be associated with distal metastasis of DTC. For the RAIR patients, CTACK, MPIF-1 and SDF-1α+β were the definite CFs which showed significant different expression.

General Nuclear Medicine_6

Utility of F-18 FDG PET/CT for Differential Diagnosis of Patients Suspected of IgG4-related Systemic Disease

Kyung-Han Lee, Joo Hee Lee, Seung Hyup Hyun, Seokhwi Kim, Seung Hwan Moon, Young Seok Cho, Joon Young Choi, Yearn Seong Choe, Byung-Tae Kim

Samsung Medical Center, Korea

Immunoglogulin G4 (IgG4)-related systemic disease

(IgG4-RSD) is a systemic fibro-inflammatory condition characterized by mass forming lesions and specific pathologic features. The precise diagnosis, identification of involved organs, and assessment of disease activity are essential to treatment decision. We thus investigated the ability of FDG PET/CT to diagnose IgG4-RSD in clinically suspected patients.

Study subjects were retrospectively selected from patients who underwent tissue biopsy for suspicion of IgG4-RSD (n = 85) or had elevated serum IgG4 concentrations (>135 mg/dl; n = 9) and underwent FDG PET/CT within 40 days of these tests. Binary logistic regression analysis was performed to select significant variables, and predicted probabilities were calculated for each variable. Variables included SUV_{max} of the main lesion and submandibular glands, FDG uptake pattern, and multi-organ involvement. After adjustment of the logistic model, receiver operating characteristics (ROC) analysis was performed using predicted probabilities.

Of a total of 94 subjects, 28 cases (29.8%) were finally confirmed to have IgG4 RSD, whereas the remaining 66 cases were found to have malignancies or infection/inflammations unrelated to IgG4. Correlation between lesion SUV_{max} and tissue IgG4 counts was weak. Binary logistic regression analysis demonstrated that mild-moderate lesion FDG uptake, high submandibular gland FDG uptake, and multi-organ involvement were significant predictors of IgG4 RSD (P<0.01, P<0.005 and P<0.05). Contrary to previous reports, FDG uptake pattern was not useful for differential diagnosis. Binary logistic regression analyses provided an area under the ROC curve of 0.824 (95% confidence interval, 0.729-0.896). Using optimum criteria, FDG PET/CT had a sensitivity of 85.7% and specificity of 66.1% for correctly diagnosing IgG4 RSD..

FDG PET/CT can help diagnosis IgG4 RSD in clinically suspected patients by using variables of FDG uptake level in the main lesion and submandibular glands, and multi-organ involvement.

General Nuclear Medicine_14

Breast specific gamma imaging in the diagnosis of breast cancer and semi-quantitative index correlation with biologic markers, subtypes and clinicopathologic characteristics

Cheng Hong Shi, Hui Tan

Department of Nuclear Medicine Zhongshan Hospital, Fudan University, China

To determine the sensitivity of BSGI in the diagnosis of breast cancer, and assess the potential correlation between the semi-quantitative index of lesion to non-lesion ratio (L/N) on BSGI and biologic markers, molecular subtypes and clinicopathologic characteristics of breast cancer.

We retrospectively assessed 102 female patients with breast cancer who underwent BSGI 10 days before surgery,and some of them underwent US or MMG. BSGI was evaluated based on the visual interpretation, and semi-quantitative index of L/N which was then analyzed and compared with biologic markers, molecular subtypes and clinicopathologic characteristics. Tumors were analyzed by immunohistochemistry to define ER, PR, Her-2 and Ki-67 status, and gene amplification using FISH was used to determine Her-2 status in cases with a Her-2 score of 2+. The independent t-test and Pearson linear correlation were applied for statistical analysis. The sensitivity of BSGI diagnosing breast cancer by visual analysis was 94.1% (96/102), for cancers size > 2.0cm was 100% (47/47), and for cancers ≤ 2.0cm was 89.1% (49/55), and by semi-quantitative interpretation 79.4% (81/102), compared with US 84.2% (85/101) and MMG 84.5% (11/71). There was no difference between mean L/N values relative to ER, PR, Her-2 or Ki-67, and the same to four subtypes or histologic grade (II versus III) (P > 0.05). However, mean L/N values in non-invasive and infiltrating breast cancer were 2.25 ± 0.14 and 3.15 ± 0.14, respectively (t = 2.89, P = 0.0048) and there was also a significant association with axillary lymph node metastasis (t = 2.22, P = 0.029). When tumors were grouped into those of diameter ≤ 2 cm and >2 cm, the value of L/N correlated with size (t = 3.25, P = 0.0016), and this was confirmed by a positive correlation on linear regression analysis (r = 0.36, P<0.05).

BSGI has a high sensitivity for diagnosing breast cancer by visual analysis. The semi-quantitative index of L/N on BSGI was independently related to infiltration degree, axillary lymph node status and tumor size in breast cancer.

Physics/Instrument_5

Thyroid Volume Determination in Graves' Disease: Comparison Ultrasonography and SUV_Shape

Yangchun Chen, Sipei Xie, Jianwei Chen

Quanzhou First Hospital of Fujian Medical University, China

Thyroid volume measurement based on its Tc-99m pertechnetate single photon emission computed tomography (SPECT) images by the theSUV_Shape

scheme was evaluated.

Twelve consecutive Graves' disease were included in this study. Their thyroid were received both ultrasonography and Tc-99m pertechnetate SPECT imaging within 3 days before iodine-131 therapy. The volume of thyroid lobes were calculated by the ellipsoid equation πabc/6. In this equation, a is the maximum length, b is the maximum width and c is the maximum depth, determinated along the three principal axes of the thyroid lobes. The total volume of thyroid was summed up the volume of both lobes, set as the reference, and recorded as TV_US. By SUV_Shape, the mean counts of voxel on the thyroid boundary, inside the thyroid boundary, in the cervical muscle were recorded as Mb, Mi, and Bg, severally. The initial threshold (Th) for thyroid was set as Bg. Until the Mb was not less than (Mi+Bg)/2, the Th was set as (Mi+Bg)/2 and kept searching the border in the next step. The thyroid volume was defined as the number of voxel inside the border multiplying voxel volume, and labeled as TV_SS. Linear regression analysis, Spearman's rank correlation, and paired-t test would be performed when appropriated.

The TV_SS and TV_US were 51.4±35.6, and 42.8±31.4 mL, they were not significant difference (t=-1.56, *P*=0.15). The Pearson's correlation coefficient between them was 0.845 (*P*<0.01). Their linear regression equation followed as TV_US=0.746×TV_SS+4.476 (R2=0.713). The Pearson's correlation coefficient between Mi/Bg and TV_US/TV_SS ratio was 0.43 (*P*=0.16).

The SUV_Shape had a potential to determinate the thyroid volume with Graves' disease. And the Mi/Bg ratio did not affect the results of SUV_Shape.

Clinical Applications of PET/MR and SPECT/CT_12

Role of ^{18}F-FDG PET/CT Imaging in in patients with adult-onset Still 's disease

Hongcheng Shi, Hui Tan

Department of Nuclear Medicine Zhongshan Hospital, Fudan University, China

To evaluate the imaging characteristics of the ^{18}F-FDG PET/CT in patients with AOSD and to discuss the correlation between the SUV_{max} (spleen, bone and abnormal lymph nodes) of AOSD and its laboratory tests.

^{18}F-FDG PET/CT findings were retrospectively reviewed in 27 patients with ruling out other diseases clinical confirmed AOSD. PET/CT was evaluated based on visual interpretation and semi-quantitative index of SUV_{max} (spleen, bone and abnormal lymph nodes), which were consequently further analyzed and correlated with its clinical features and laboratory tests.

According to the visual analysis, sixteen, twelve, and one of 27 AOSD patients were shown with splenomegaly, lymphadenopathy, and hepatomegaly in PET/CT imaging, separately. And ^{18}F-FDG accumulation by visual analysis was positive mainly in spleen (21/27, 77.9%), bone marrow (24/27, 88. 9%), lymph nodes (12/27, 44.4%) and joints (1/28, 3.6%). In addition, these FDG accumulations in the bone marrow and spleen were diffuse. Whereas there were seven patients with the FDG uptake in multiple whole body lymph nodes, the rest with FDG accumulation mainly bilateral cervical nodes, axillary. The semi-quantitative analysis of PET/CT imaging, mean SUV_{max} in liver was 2.54±0.45 (1.80 ~ 3.50), in spleen was 3.79±1.17 (1.50 ~ 6.70), in bone marrow was 4.32±1.37 (1.30 ~ 6.98), in 12 cases of abnormal lymph nodes was 6.87±3.35 (1.70 ~ 13.90). No significant correlation was found between SUV_{max}(spleen, bone marrow and abnormal lymph nodes) and the laboratory findings (WBC count, CRP, ESR, ferritin, LDH, TNF, IL-2R, IL-6 and IL-8), and all the value of *P* >0.05. However, all 12 cases of abnormal lymph nodes with positive FDG accumulation with the level of ferritin > 1000 ng/ml.

The role of ^{18}F-FDG PET/CT in AOSD patients is just to guide the abnormal lymph node and bone marrow biopsy for ruling out other diseases, and alone is difficult to differentiate AOSD from lymphoma or infectious diseases. In addition, the SUV_{max} (spleen, bone marrow) was not independently related to the laboratory findings, but all 12 cases of abnormal lymph nodes with FDG accumulation with the level of ferritin > 1000 ng/ml.

Musculoskeletal System_9

Clinical correlation of metabolic parameters on F-18 FDG PET/CT in primary frozen shoulder

Kyoung Sook Won, Kyoung Sook Won, Hae Won Kim, Bong-Il Song, Chul-Hyun Cho, Du Hwan Kim

Keimyung University Dongsan Medical Center, Korea

The purpose of this study was to investigate specific uptake pattern on F-18 FDG PET/CT in patients with primary frozen shoulder (FS) and to evaluate correlation between metabolic parameters of F-18 FDG PET/CT and clinical variables.

We prospectively enrolled 35 patients of primary frozen shoulder (M:F=12:23, 53.0±7.0 yrs). All patients were performed F-18 FDG PET after confirmation of primary FS with physical examination and US and/or MRI of the shoulder for exclusion of 2ndary FS. Clinical data such as American Shoulder and Elbow Surgeons (ASES) score, Visual Analogue Scale (VAS) pain score, Subjective shoulder value (SSV) and range of motion of abduction (ABD), forward flexion (FF), external rotation (ER), and internal rotation (IR) were collected. Maximal SUVs (SUV_{max}) were obtained in the region of rotator interval (RI), anterior joint capsule (AJC), axillary recess (AR), and greater tuberosity (GT) of the humerus. $SUV_{max}$and metabolic volume (MV) of the shoulder were also measured.

All patients showed specific uptake pattern on F-18 FDG PET/CT, which is dominant uptake in the RI, AJC, or AR. There was no significant correlation between clinical scores such as ASES score, VAS pain score and SSV and metabolic parameters of FDG PET/CT. However, MV was significantly correlated with ABD, FF, and ER and SUV_{max} of the shoulder was also significantly correlated with ABD, FF and duration of shoulder pain. SUV_{max} of RI was significantly correlated with IR and SUV_{max} of AR was significantly correlated with ABD, FF and duration of shoulder pain. SUV_{max} of AJC was correlated with IR, ER, ABD and FF. There was no significant correlation between SUV_{max} of GT and clinical variables.

Our study demonstrated that anterior-inferior capsular portion including RI and AR is the main pathologic site of primary FS and revealed significant correlations between range of motion and metabolic parameters on F-18 FDG PET/CT. Unlike previous reports, these results support evidence that rotator interval lesion may be associated with internal rotation. Taken together, F-18 FDG PET/CT might be a useful tool for elucidation of pathophysiology of primary FS.

Radionuclide Therapy_16

Risk factors for Persistent Cervical Metastatic Lymph Nodes after I-131 Ablation Therapy in Papillary Thyroid Carcinoma

Byeong-Cheol Ahn, Chang-Hee Lee, Seung Hyun Son, Ji-Hoon Jung, Choon-Young Kim, Ju Hye Jeong, Shin Young Jeong, Sang-Woo Lee, Jaetae Lee

Department of Nuclear Medicine, Kyungpook National University School of Medicine and Hospital, Jung-gu, Daegu 700-721 , Korea

I-131 ablation after thyroidectomy can find and eradicate hidden residual lesions in differentiated thyroid cancer, however the residual lesions can persist after the ablation. Aim of the study is to investigate risk factors for persistent metastatic cervical lymph node(LN)s after first I-131 ablation therapy in papillary thyroid cancer(PTC).

Among 1412 PTC patients who received I-131 ablation, 109 (87 Women, 22 Men; average age: 48±12 years) patients who revealed unsuspected metastatic cervical LNs on postablation whole body scan or SPECT (PaSCAN) and also had appropriate clinical follow-up data were enrolled in this study. Each patient was followed-up at least 6 months after ablation (median: 23 month). Persistent disease was diagnosed by pathologically or clinico-radiologically. Clinical, pathologic, and biochemical factors and imaging findings were reviewed, and their relationships to persistent disease were analyzed.

267 patients (19.1%) had metastatic LNs on PaSCAN, and 158 patients were excluded from the study due to loss of follow-up and, finally, 109 patients was analyzed for the study. 101 (92.7%) among 109 patients (eradication group) revealed no evidence of disease during follow-up study without any further treatment and 8 patients (7.3%) (persistence group) revealed persistent disease. Although there were no significant difference of clinical and pathologic risk factors between persistence and eradication groups, however, persistence group showed high preablation Tg (34.89 ± 59.24 vs. 6.05 ± 20.32 ng/ml, P = 0.002) and high number of metastatic LN on PaSCAN (2.12 ± 0.64 vs. 1.57 ± 0.74, P = 0.0434). Preablation Tg (cut off=2.6, HR: 16.8, P = 0.0108) and number of metastatic LN on PaSCAN (cut off = 1, HR: 9.3, P = 0.0462) were predictors for the persistent disease.

Although, incidence of hidden cervical metastatic LNs was relatively high in thyroidectomized PTC patients, majority of patients with the metastasis was eradicated by I-131 ablation. However, careful follow-up for persistent disease might be needed in cases with high preablation Tg level or multiple LNs metastases.

Radionuclide Therapy_17

A quantitative method to assess leakage of radioactive particles from their disappearance curves during radiosynoviorthesis

Muhammad Sohaib

Pakistan Institute of Engineering and Applied Sciences, Pakistan

Radiosynoviorthesis, the restoration of synovial membrane in diseases like rheumatoid arthritis, osteoarthritis and hemophilic arthropathy is now a

frequently procedure in nuclear medicine. Leakage the labeled particles remains the major concern about this type of therapy. To assess the leakage several methods in clinical and experimental settings have been mentioned in literature. The author here presents a simple radioactive decay method to quantitate the leakage of ^{177}Lu-HA from joints of rabbit models.

Studies were performed after the approval of Ethics Committee of PIEAS and under appropriate guidelines of handling the laboratory animals. The radiopharmaceutical (^{177}Lu-HA) was obtained from PINSTECH (Islamabad, Pakistan). 5 to 10 MBq was injected into the synovial space of right knees of four New Zealand rabbits. Eleven to sixteen images of each rabbit were acquired under gamma camera over a period of 722. A sample of ^{177}LuCl3 from the same batch was also imaged as a control to determine the half-life of ^{177}Lu. Elliptical regions of interest (ROIs) were drawn around the site of activity in the images, and background corrected counts with in the area were computed. They were plotted on semi-log scale and line of best fit was generated with y-intercept at the counts at time point zero. T1/2 of the line-fit was calculated manually at three data points and the average was recorded. T1/2 of ^{177}Lu control vial was also calculated similarly. The leakage was calculated from the difference of theoretical decay and observed decay.

T1/2 of the ^{177}Lu control vial was 158.7 hours (Figure 1). The half-lives of the ^{177}Lu-HA residing in the knees of rabbit 1, 3, 4 and 5 were 140.9, 147.7, 154.4 and 158.1 hours respectively. Their decays curves are compared with decay of the control in Figure 2. The leakage curves over the period of time of all the rabbits is given in Figure 3. They were generated from the difference of two curves at a given time. Cumulative leakage of activity at any time could be calculated from these curves.

The quantitative method of assessment of leakage from the disappearance of the radiopharmaceutical from the intra-articular injection site is a simple method.

Molecular Imaging_49

The findings of Bone SPECT/CT in Rotator Cuff Tear patients of different age group

Jung Min Lee[1,2], So Won Oh[1,2], Ho Young Lee[1,3], Hyungsuk Kim[4], Seo Yong Kang[1,2], Chris Cho[5,6], Yu Kyeong Kim[1,2]

1. Department of Nuclear Medicine, Seoul National University College of Medicine, Seoul, Korea
2. Department of Nuclear Medicine, Seoul National University Boramae Medical Center, Seoul, Korea
3. Department of Nuclear Medicine, Seoul National University Bundang Hospital, Gyeggyi, Korea
4. Department of 3Orthopedics, St. Paul's hospital, The Catholic University of Korea College of Medicine, Seoul, Korea
5. Department of Orthopedics, Seoul National University College of Medicine, Seoul, Korea
6. Department of Orthopedics, Seoul National Seoul National University Boramae Medical Center, Seoul, Korea

Purpose: A rotator cuff tear (RCT) is a common cause of shoulder pain and disability among adults. The overuse or degeneration can act as underlying pathogenesis of the acute and degenerative injury, and the cause of the tearing might differ by age groups. We investigated the differences of bone SPECT finding in RCT according to age groups using shoulder SPECT/CT.

Methods: Among the patients who conducted both shoulder SPECT/CT and MRI for the preoperative evaluation of arthroscopic RCT repair at our institute from March 2011 to February 2015, we retrospectively evaluated 30 patients whose shoulder symptoms developed within 6 months and diagnosed as supraspinatus tendon (SST) tear only. Bone SPECT/CT was obtained from the neck to mid-chest to include the whole shoulder joints.

Firstly, the presences of acromial and greater tubercle uptake were initially evaluated by visually assessment. And, the uptakes in the shoulder region (greater tubercle; GT, glenohumeral joint; GH, acromioclavicular joint: AC, and coracoid process: Cor) were quantitatively measured by relative uptake ratio to the blood pool activity of the aorta. Shoulder SPECT/CT findings were analyzed after dichotomization based on the age of 49; the younger (n=16, 34-49 y) and older group (n=14, 60-65 y), and correlated with arthroscopic and MRI findings.

Results: The increased uptake in GT, an insertion site of the SST, was seen in all the patients. The increase of acromial uptake was frequently found in the older group, compared with the young group (100% vs. 43%, P=0.001). In older patients, the intensity of GT uptake was correlated with the tear size in arthroscopic finding (P=0.013), but not in the younger group.

Conclusions: The radiotracer uptake suggestive of secondary bony change in SST tear was well shown in the acromion as well as GT, and the intensity of GT uptake was related with the tear size in the older group. The differences of shoulder SPECT/CT between the two groups might be explained that RCT result from a wide spectrum of degenerative diseases in the older patients unlike younger patients.

Cardiology_30

Clinical implication of coronary calcium evaluated by low-dose CT of myocardial perfusion SPECT/CT

Sang-Geon Cho, Ki Seong Park, Sae-Ryung Kang, Jong Sang Kim, Seran Min, Jahae Kim, Ho-Chun Song, Minchul Song, Geum-Cheol Jeong, Hee Jeong Park, Seong Young Kwon, Jung-Joon Min, Hee-Seung Bom

Chonnam National University Hwasun Hospital, Korea

We evaluated the clinical implication of coronary calcium evaluated by low-dose attenuation correction CT (AC-CT) of myocardial perfusion SPECT/CT regarding myocardial perfusion.

We retrospectively included 225 patients with low-to-intermediate (≤ 90%) pretest probability, who underwent myocardial perfusion SPECT using NMCT-670 SPECT/CT (GE Healthcare, USA) in 2013. Patients with previous coronary artery disease, clinically suspected heart failure or left ventricular ejection fraction < 45% or wall motion abnormality on echocardiography, heart rate > 75/min, other valvular or myocardial diseases were excluded. Agatston calcium score (ACS) was calculated for each patient's resting AC-CT images. Total perfusion deficit (TPD) was calculated for stress and resting SPECT images, and ischemic TPD was also calculated (stress TPD – resting TPD). Abnormal SPECT was defined as stress TPD ≥ 5% or ischemic TPD ≥ 3%. Clinical implications of ACS by AC-CT were analyzed in terms of its correlation with TPD and its relationship with myocardial perfusion status against other coronary risk factors.

Total ACS by AC-CT showed positive correlations with both stress TPD (r = 0.360, P< 0.001) and resting TPD (r = 0.369, P< 0.001), but not with ischemic TPD (r = 0.065, P< 0.335). SPECT was abnormal in 52 (23%) patients and total ACS by AC-CT was significantly higher in patients with abnormal SPECT, as compared to those with normal SPECT (319.3 ± 681.5 vs 121.2 ± 319.3, P= 0.049). Total ACS ≥ 100 was the only clinical factor related to abnormal SPECT result, after adjustment of the other traditional risk factors of coronary artery disease.

Higher coronary calcium burden on low-dose CT of myocardial perfusion SPECT/CT was indicative of abnormal myocardial perfusion.

Radiochemistry_1

Ex Vivo Autoradiography and Animal PET Imaging Study of [^{18}F]EFQ for Evaluation of mGluR1 Distribution in Rat Brain.

Boeun Lee[1,2], Yu Keong Kim[1], Ji Youn Lee[1,3], Hoyoung Kim[1], Young Joo Kim[1,3], Yun-Sang Lee[1,2], Dong Soo Lee[1,2], June-Key Chung[1,3], Jae Min Jeong[1,3]

1. Department of Nuclear Medicine (Seoul National University, Korea)
2. Department of Molecular Medicine and Biopharmaceutical Sciences (Seoul National University, Korea)
3. Cancer Research Institute (Seoul National University, Korea)

Purpose: Metabotropic glutamate receptor type 1 (mGluR1) in brain is associated with various brain diseases such as Parkinson's disease, motor dysfunction, epilepsy, and stroke. The [^{18}F]EFQ, 3-ethyl-2-[^{18}F]fluoroquinolin-6-yl) *cis*-(4-methoxycyclohexyl) methanone has been developed as a PET ligand for mGluR1 imaging. In this study, we verified the distribution of mGluR1 in rat brain by small animal PET and ex vivo autoradiography using [^{18}F]EFQ.

Methods: We synthesized the precursor of [^{18}F]EFQ according to the previously reported procedure. The precursor was labeled with [^{18}F]fluoride/K222/DMSO at 110 °C for 6 min and the reaction mixture was purified using preparative HPLC. The purified [^{18}F] EFQ was analyzed its radiochemical purity and specific activity by analytical HPLC. The formulated product was injected into rat via tail vein to obtain small animal PET images. Ex vivo autoradiography was performed 10 min after the tail vein injection of [^{18}F]EFQ. The sagittal sections (20 μm) of the rat brain were prepared and autoradiograms were acquired.

Results: We synthesized [^{18}F]EFQ as a mGluR1 PET ligand. The radiochemical yield of [^{18}F]EFQ (EOS) was 29%, the radiochemical purity was over 99%. The specific activity was 81 GBq/mmol. According to PET study, [^{18}F]EFQ showed highest uptake in cerebellum which express high mGluR1, followed by the thalamus, hippocampus, striatum. The time-activity-curve of brain regions showed rapid uptake of [^{18}F]EFQ into brain and washout rate. The autoradiogram also showed similar radioactivity uptake tendency with PET images.

Conclusions: To evaluate the mGluR1 distribution of rat brain, we synthesized a ^{18}F-labeled PET ligand [^{18}F]EFQ, and acquired small animal PET images and autoradiogram. In PET images and autoradiogram, the uptakes of radioactivity showed mGluR1 expressed regions in brain. These results are good correlations with reported mGluR1 distribution.

Oncology_61

Development of $^{99m}Tc(CO)_3$ Labeled 2-(4-chloro)phenylimidazo[1,2-a] pyridine Analog, ^{99m}Tc-CB256, as a SPECT Radiotracer for TSPO-enrich Tumor Imaging

Ji Young Choi[1], Mara Perrone[2], Valentino Laquintana[2], Jae Ho Jung[3], Byung Seok Moon[3], Annalisa Cutrignelli[2], Angela Lopedota[2], Massimo Franco[2], Nunzio Denora[2], Byung Chul Lee[3], Sang Eun Kim[1,3]

1. Seoul National University, Republic of Korea
2. University of Bari "A. Moro", Italy
3. Seoul National University Bundang Hospital, Republic of Korea

Purpose: We herein report the radio-synthesis of $^{99m}Tc(CO)_3$ labeled 2-(8-(2-(bis-(pyridin-2-yl-methyl)amino)acetamido)-2-(4-chlorophenyl)-*H*-imidazo[1,2-a] pyridin-3-yl)-*N*,*N*-dipropylacetamide), ^{99m}Tc-CB256, ([^{99m}Tc]**1**) and its TSPO-positive tumor cell binding assay as a new TSPO SPECT imaging agent.

Methods: The standard compound, $^{185/187}$Re-CB256 ([$^{185/187}$Re]**1**), was synthesized by reacting $(NEt_4)_2[^{185/187}Re(CO)_3Br_3]$ with CB256. The affinity toward TSPO of CB256 was measured on membrane extracts of C6 glioma cells. $^{99m}Tc(CO)_3$ incorporation to CB256 was carried out according to literature [BC Lee et al. RSC adv. **2012**, 3, 782] and the lipophilicity and *in vitro* stability were measured. *In vitro* tumor cell-binding assay of [^{99m}Tc]**1** was performed in C6 rat glioma and U87-MG human glioblastoma cells.

Results: [^{99m}Tc]**1** was synthesized in 75-85% of radiochemical yield (decay corrected) with over 98% of radiochemical purity. The chemical identity of [^{99m}Tc]**1** was confirmed by comparing retention time of [^{99m}Tc]**1** (gamma detection at 22.5 min) with that of [$^{185/187}$Re]**1** (UV detection at 22 min), including $^1H/^{13}C$-NMR and HRMS analysis. The obtained [^{99m}Tc]**1** was shown to be highly stable (>99%) when incubated in human serum for 4 h and had a relatively low lipophilicity (log D = 2.15 ± 0.02). Binding affinities toward TSPO of CB256 and [^{99m}Tc]**1** were 239 ± 43 nM and 364 ± 30 nM, respectively. *In vitro* time dependent tumor cell binding uptake of [^{99m}Tc]**1** was shown 10.26 ± 0.23 and 7.88 ± 0.23 %ID in C6 rat glioma and U87-MG human glioblastoma cells at 60 min, respectively.

Conclusions: Our *in vitro* data indicated that [^{99m}Tc]**1** can be considered as a new TSPO-positive cancer imaging agent and provides the foundation for further *in vivo* biological evaluation in tumor xenograft.

Oncology_66

Preparation and Biological evaluation of ^{64}Cu Labeled Repebody for EGFR-mediated Cancer Imaging in Small Animlas

Ayoung Pyo[1, 2], Misun Yun[1], Hyeon-Sik Kim[1], Dong-Yeon Kim[1], Jung-Joon Min[1]

1. Department of Nuclear Medicine, Chonnam National University Hwasun Hospital, Korea
2. Department of Chemistry, Chonnam National University, Korea

Purpose: The epidermal growth factor receptor(EGFR) is known as a member of the HER family and expressed in many kinds of tumors. Anti-EGFR repebody using this study is a newly designed protein scaffold for tumor targeting that has leucine rich repeat modules. In this study, we performed microPET studies with two kinds of ^{64}Cu labeled complexes (repebody with DOTA and DTPA) and evaluated characteristics in H1650 (human non-small cell lung cancer cell line) bearing nude mice.

Methods: DOTA-NHS ester and ρ-SCN-Bn-DTPA were dissolved in water and pH was adjusted to 9.0 by adding 1M of NaOH. This solutions were added to the repebody in a 1:5 mole ratio (repebody : DOTA-NHS ester, ρ-SCN-Bn-DTPA)[1]. The resulting DOTA-repebody and DTPA-repebody conjugate were purified by HPLC and lyophilized. Purified compounds were radiolabeled with ^{64}Cu by addition of $^{64}CuCl_2$ in 0.1 N NaOAc (pH5.5) buffer followed by incubation for 1 h at 40 °C. The radiolabeled complexes were purified by a PD-10 column. The mircoPET images were obtained at 1,6, and 24h after i.v.injection of ^{64}Cu labeled repebody (7.4MBq) in H1650 (EGFR positive) bearing nude mice. The static images at 1, 6, and 24 h were acquired for 10 min. The ROIs were drawn in the tumor and liver. The tumor-to-liver ratio (T/L) were obtained from max SUV of ROI.

Results: Radiochemical yields of ^{64}Cu-DOTA-repebody and ^{64}Cu-DTPA-repebody were approximately 60∼70%. H1650 tumor was clearly visible after injection of each repebody, with high tumor-to-background ratio for whole time points.^{64}Cu labeled repebody was accumulated specifically at 1 h after i.v. injection and retained in H1650. Uptake of ^{64}Cu-DOTA-repebody(1, 6 h SUV_{max}: 1.80, 2.20) and ^{64}Cu-DTPA-repebody(1, 6 h SUV_{max}: 1.81, 2.19)were increased from 1 h to 6 h. Both ^{64}Cu-DOTA- and ^{64}Cu-DTPA-repebody showed slow clearance from liver as T/Ls were 0.49, 0.59, 0.43 and 0.47, 0.50, 0.41 respectively at 1, 6 and 24 h.

Conclusions: ^{64}Cu-DOTA-repebody and ^{64}Cu-DTPA-repebodydemonstrated specific uptake in H1650 tumor bearing model and might have a potential to be utilized as a novel EGFR targeting agent for PET.

Radionuclide Therapy_19

Cu-64 Labeled Folate Receptor Targeted Nano-Particle Based on Albumin via Strain-Promoted Click Chemistry: A Novel Method for Targeting by Using Albumin Platform

JY Park[1,2], WH Kim[1], [1]MG Song[1], JM Jeong[1,2], YS Lee[1], HW Youn[1], KW Kang[1], DS Lee, [1]JK Chung[1]

1. Department of Nuclear Medicine, Seoul National University College of Medicine, Seoul, Republic of Korea
2. Department of Biomedical Sciences, Seoul National University College of Medicine, Seoul, Republic of Korea

Purpose: Folate receptor (FR) is an attractive molecular target for theranostic approach in oncologic view. Since previous radio-folates has shown intense uptake in kidneys with low tumor-to-kidney ratio (<0.15), its application in the use of therapeutic approach was limited due to renal toxicity. The aim of this study was to synthesize a FR targeting human serum albumin (HSA) which evades renal excretion to enhance tumor-to-kidney ratio and to evaluate its potential as a FR targeted theranostic agent in tumor bearing mouse model.

Methods: HSA was modified with DBCO-NHS under physiologically friendly reaction condition for the preparation of strain promoted azide-alkyne reaction. HSA-DBCO was conjugated with ^{64}Cu labeled NOTA-PEG-azide with or without folate-pentapeptide-azide. Size of the radiolabeled HSAs with or without folate (radiolabeled HSA-Folate or HSA) was determined by dynamic light scattering (DLS). In vivo imaging was acquired after IV injection of ^{64}Cu-HSA and ^{64}Cu-HSA-Folate in mouse model bearing FR positive tumor.

Results: We modified HSA by using DBCO-NHS and found optimized condition for click reaction with azide and DBCO. The number of DBCO conjugated on HSA was checked using MALDI-TOF MS. Labeling with ^{64}Cu-NOTA-PEG-azide and HSA-DBCO or Folate-HSA were shown in excellent labeling efficiency (>99%, Rf=0) with no free ^{64}Cu (Rf=1) and ^{64}Cu-NOTA-PEG-azide (Rf=0.5). We set condition of optimal ratio of DBCO per albumin that showed longer blood pool image than other folic acid conjugated albumin which showed higher liver uptake than tumor. Because of its modification condition (PBS, pH>7.4), actual and longer in vivo half-life than previous study of modified albumin was found in our study. Size of HSA-DBCO and radiolabeled HSA-Folate were 7.80 ± 1.53 nm (mode ± SD) and 8.19 ± 1.13 nm, respectively, which is identical to natural HSA (6.8 ± 1.3 nm). In vivo imaging of radiolabeled HSA-folate has shown intense accumulation on KB tumor suggesting FR specific uptake. But radiolabeled HSA has no accumulation on KB tumor. Kidney uptake of radiolabeled HSA-folate and HSA was neglectable with significant blood pool activity over hours after injection.

Conclusions: Radiolabeled HSA-Folate has shown intense uptake of FR positive tumor with no demonstrable kidney uptake indicating significantly high tumor-to-kidney ratio. FR targeting based on HSA conjugate is a promising and novel method to minimize renal toxicity and to efficiently target FR for theranostic approach of radio-folates.

Molecular Imaging_7

Evaluating the anti-cancer therapeutic efficacy of combination therapy of kinase inhibitors, Sorafenib and 3-bromopyruvate, on the liver cancer

Hyewon Youn, Kyungmin Kim

Department of Nuclear Medicine and Biomedical Sciences, Korea

Hepatocellular carcinoma (HCC) has been treated with surgical resection and chemotherapy. Sorafenib is a multikinase inhibitor which is the first approved drug for the treatment of HCC. However, it only has shown a response rate of about 15-20%. Combination of sorafenib with a hexokinase inhibitor 3- bromopyruvate (3-BrPA) is a good candidate. Therefore, we evaluated therapeutic effect of sorafenib and 3-BrPA in orthotopic liver cancer using mouse xenograft model.

Human HCC cell line, SNU-761 cells were stably transfected with luciferase gene for bioluminescence imaging. Abdominal region of Balb/c-nu mouse was horizontally resected and a lobe of liver was exposed. SNU761-luc cells (2.5x106) were orthotopically injected to the liver. We put the liver into the original site and stitched the resected part. Six days later, mice were randomized into the following 4 groups based on the luciferase signals measured by IVIS 100 (Total flux >1x106 photon/sec/cm2/sr). Drugs (sorafenib: 1.25mg/kg/day, 3-BrPA: 1mg/kg/day) were intraperitoneally injected every 5 days for 4 weeks. Bioluminescence images were taken and the weights of mice were also measured.

Luciferase signal was in concordance with the number of viable cancer cell (R2=0.9978). 3-BrPA, and in combination with sorafenib strongly inhibited primary tumor growth. After 28 days of treatment, bioluminescence signals of sorafenib, 3-BrPA and combination of sorafenib and 3-BrPA treated group were reduced to 63.21%, 23.56% and 5.57% of controls, respectively. Sizes of tumor were measured after autopsy, and they were significantly different among 4 groups similar to the imaging results.

We visualize therapeutic effect of kinase inhibitors after optical assessment. The combination of sorafenib and 3-BrPA has synergistic effect compared with sorafenib-based therapy on HCC. Specially, 3-BrPA enhances therapeutic effect about 40% more than that of sorafenib. Our results demonstrates the possibility of 3-BrPA as an efficient chemo-agent for HCC regression.

Molecular Imaging_42

Synthesis and primary study of fluro[19F] berberine derivative for human hepatocellular carcinoma targetting

Tong Zhang, Xiao-ai Wu, Hua-wei Cai, Chengzhong Fan*

Department of Nuclear Medicine, West China Hospital, Sichuan University, Chengdu, China

Objectives: It was reported that berberine can selectively inhibit human hepatoma cell invasion without cytotoxicity in healthy hepatocytes. This study is to explore the feasibility of fluro [19F] berberine derivative (BBR-F) for human hepatocellular carcinoma targeting.

Methods: The target compound, 9-(3-fluoropropyl) -10-methoxy-5,6-dihydro-[1,3]dioxolo[4,5-g]isoquinolino [3,2-a]isoquinolin-7-ium chloride (BBR-F) was synthesized in one step using berberrubine and 3-fluoropropyl 4-methylbenzenesulfonate. Cellular proliferation Inhibition assay was conducted using a CCK-8 cell proliferation assay kit onwed to SMMC-7721, HepG2 and HL-7702 cells. Cellular uptake and localization of BBR-F were performed by a fluorescence microscope in HepG-2 and HL-7702 cells with increasing concentrations of BBR-F treatment (12.5, 25, 50 and 100 μM) at 37°C for 1h. Semiquantitative analysis on HepG-2 and HL-7702 cell uptake of BBR-F was tested by flow cytometry with 50uM of BBR-F solution incubation at 37°C for 1h.

Results: CCK-8 assay demonstrated that BBR-F leaded to a dose-dependent inhibition on SMMC-7721, HepG2, and HL-7702 proliferation. BBR-F was concentrated in mitochondria and cytoplasm in HCC cells HepG-2 at low dose (12.5μM) and accumulated in nucleus in a concentration-dependent way at higher doses (25 to 100μM) (Figure 1A). In contrast, in normal hepatic HL-7702 cells there was no fluorescent signal seen at low dose (12.5μM). It became faintly visible at higher doses (25 to 50μM), and mitochondria and cytoplasm accumulated BBR-F at 100 μM (Figure 1B). Flowcytometry results indicated that the HepG-2 cells had higher average fluorescence intensity than HL-7702 cells, which were treated with 50 μM BBR-F (Figure 2).

Conclusions: This study shows that fluro[19F] berberine derivative is a potential molecular probe for human hepatocellular carcinoma targeting.

Molecular Imaging_45

Evaluating the efficiency of losartan in pulmonary fibrosis with ^{68}Ga- NOTA-PRGD2

Peilin Wu[1,3], Shaobo Yao[1], Hui Huang[2], Hanping Wang[2], Zhenzhong Zhang[1], uojunXu[2], Zhaohui Zhu[1*],Tong Zhou[3*]

1. Department of Nuclear Medicine, Peking Union Medical College Hospital, Chinese Academy of Medical Science & Peking Union Medical College, Beijing, 100730, China
2. Department of Respiratory Disease, Peking Union Medical College Hospital, Chinese Academy of Medical Science & Peking Union Medical College, Beijing, 100730, China
3. Department of Nuclear Medicine, Dongzhimen hospital, Beijing University of Chinese Medicine,Beijing,100700,China

Objectives: ^{68}Ga-NOTA-PRGD2 can be specifically bonded to the αvβ3-integrin, which is a transmembrane heterodimeric receptor highly express on the surface of fibrocyte, which plays an important role in the overall disease pathology of pulmonary fibrosis .The angiotensin II receptor blocker (ARB) losartan was found to effectively reduce ALI induced by SARS-CoV and avian influenza H5N1virus.This study first apply ^{68}Ga-NOTA-PRGD2 to detect the pulmonary fibrosis, and evaluate the therapy response of losartan in pulmonary fibrosis.

Methods: Six-old C57 mices(n=10) were instilled through endotracheal with 1 unit/kg body weight of bleomycin (Nippon Kayaku Co. Ltd) on day 0 and 7 respectively to induce pulmonary fibrosis, another 10 C57 mices were set as control. After 2 weeks, C57 mice models were intravenous injected with 100 μCi of ^{68}Ga-NOTA-PRGD2 and imaged after 1h by Inveon Micro PET (Siemens).After imaging, C57 mice models were divided to two groups randomly, one group were treated with losartan 2mg/kg body weight for ten consecutive days, the other group was control group. On the 11th day of treatment , all C57 mice models undergone imaging. After imaging, mice were sacrificed by humane euthanasia, cervical dislocation. Lungs were then removed, samples of tissues and cells were collected for further analysis. The tissue radioactivity was calculated and expressed as decay-corrected percentage injected dose per gram of tissue (%ID/g).

Results: The ^{68}Ga- NOTA-PRGD2 accumulated at higher levels in the lung of pulmonary fibrosis models (0.49±0.13 vs. 0.34 ± 0.10 percentage injected dose/gram, $P< 0.05$) than healthy or normal lung at 1 h after injection. The tissue radioactivity of group treated with losartan were lower

than control group (P<0.05).

Conclusions: The^{68}Ga- NOTA-PRGD2 can detect pulmonary fibrosis , losartan was effective in the treatment of pulmonary fibrosis.

Molecular Imaging_52

Tumor-associated macrophage imaging to delineate the margins of glioblastoma using near-infrared fluorescent nanoparticles

Jung Sun Yoo, Chaedong Lee, Juhwan Yoon, Yuanzhe Piao, Sang Eun Kim

Department of Nuclear Medicine, Seoul National University Bundang Hospital, Seoul National University College of Medicine, Korea

Glioblastoma multiforme (GBM) is the most aggressive and lethal type of human brain cancer. Most patients survive no longer than 1 year after diagnosis despite optimal treatment of currently available therapies. One challenge in treating GBM is diffusely infiltrating characteristics of glioma cells that makes complete removal by surgical resection impossible. Complete surgical resection especially for the infiltrative boundary region is pivotal to prevent recurrence and improve survival. Abundant macrophage infiltration is a key feature of GBM margins. Recent studies showed that tumor-associated macrophages (TAMs) actively promote GBM progression in multiple aspects. Therefore, accurate imaging of TAMs which are enriched in GBMs may provide a new option for improved diagnosis and prognosis, related treatment decisions, and intraoperative guidance of GBM resection.

Nanoparticle is a favorite imaging agent for macrophages given their naturally high endocytosis activity. Based on this avidity, we synthesized silica coated iron oxide nanoparticles conjugated with NIR fluorophore for in vivo imaging. In vivo targeting ability for TAMs was confirmed using planar fluorescence imaging and intravital microscopy (custom-built confocal microscope). Immunofluorescence staining with macrophage markers corroborated in vivo results.

The developed nanoparticles showed superior long-term water stability by active introduction of polyethylene glycol MW 600 (PEG). In vivo NIRF imaging with U87-MG GBM xenograft models demonstrated excellent tumoral uptake by nanoparticles and immunofluorescence staining analysis confirmed that the accumulated nanoparticles were exclusively co-localized with F4/80+ TAMs, but not Ki-67+ tumor cells and other stromal cells including CD31+ endothelial cells. Intravital microscopy results showed in vivo stability of nanoparticles in blood circulation and dynamic behaviors of nanoparticles to preferentially accumulate within CD11b+ TAMs.

The presented nanoparticle based approach targeting TAMs may facilitate the development of effective options for GBM treatment to circumvent previous failure of most therapeutics targeting glioma cells.

Radionuclide Therapy_21

Combined use of radioiodine therapy and radiofrequency ablation in treating postsurgical thyroid remnant of differentiated thyroid carcinoma

Bin Long[1], Linfa Li[1], Lifang Yao[1], Shoucong Chen[1], Heqing Yi[1], Xuemei Ye [1], Dong xu[2],Peng Wu[3]

1. Department of Nuclear Medicine, Zhejiang Cancer Hospital, Hangzhou, Zhejiang Province 310022, People's Republic of China
2. Department of Ultrasonography, Zhejiang Cancer Hospital, Hangzhou , Zhejiang Province 310022, People's Republic of China
3. Department of Pathology, Zhejiang Cancer Hospital, Hangzhou, Zhejiang Province 310022, People's Republic of China

Objectives: To determine whether postoperative radioiodine (RAI) combined with radiofrequency ablation (RFA) is an effective, safe and feasible method for elimination of excessive postsurgical thyroid remnant for DTC.

Methods: We took a prospective study and treated 12 DTC patients (4 males, 8 females, age 20-78 years) who underwent thyroidectomy for RFA followed by ^{131}I ablation. The pre-treatment requires Iodine-free diet and thyroid hormone withdrawal for 3-4 week. All the patients showed the level of serum thyroid-stimulating hormone (TSH) <30 mU/L, and obvious thyroid remnant in ^{99m}Tc imaging. Serum TSH level was determined 1 day before RFA and on days 1,7,14 after RFA, and ^{99m}Tc imaging was performed on day 14 after RFA. Subsequently the patients were given oral dosage of 3700MBq ^{131}I for remnant ablation, and RxWBS was performed on day 5 after ablation. Efficacy evaluation was done 4-6 months after treatment. The changes of variants before and after RFA were analyzed by wilcoxon signed rank sum test.

Results: Serum thyroid-stimulating hormone (TSH) was less than 30 μIU/ml (mean value 10.27±6.16 μIU/ml) before RFA, and increased to more than 30μIU/ml (34.73 ± 3.93μIU/ml) two weeks later (P = 0.002, Wilcoxon rank sum test). The ^{99m}Tc uptake ratio on day 14 post-RFA was (0.31±0.12) %, which is significantly lower than before RFA (0.80±0.16) % (P = 0.002, Wilcoxon rank sum test). The success rate of thyroid

remnant ablation was 91.7% (11/12), which was assessed 4 to 6 months after treatment. All patients reported neck discomfort and some are self-limiting, with no hoarseness, choking, or radiation thyroiditis symptoms. Five patients had puncture area pain, among which one patient had neck edema, which was relieved after prednisone treatment.

Conclusion: Combined use of radioiodine therapy and radiofrequency ablation in treating excessive postsurgical thyroid remnant of differentiated thyroid carcinoma can be an effective approach and avoids re-operation. Long-term efficacy monitoring would further determine its feasibility.

Oncology_79

The role of ^{18}F-FDG PET/CT in diagnosis of patients with secondary hemophagocytic lymphohistiocytosis

Zheng Youjing[1], Hu Guilan[2], Li Fang[2], Huo Li[2]

1. Department of Nuclear Medicine, China Japan friendship hospital
2. Department of Nuclear Medicine, Peking Union Medical College Hospital

Objectives: Hemophagocytic lymphohistiocytosis (HLH) is a rare life-threatening disease that could be secondary to various infectious, malignant, and autoimmune triggers. This study was aimed to investigate the significance of ^{18}F-FDG PET/CT (FDG-PET) in determining the underlying causes of secondary HLH.

Methods：43 patients (20 males, median age 48.5 years) who were diagnosed as secondary HLH and received FDG-PET scan before treatment were retrospectively reviewed in this study. Clinical characteristics and PET images were analyzed, and parameters were collected. Statistical analysis was performed with SPSS 19.0.

Results: PET results were helpful in 87.1% (27/31) patients and non-contributory in 12.9% (4/31) for malignancy diagnoses. Focal hypermetabolism, PET parameters SP/M, BM/M, and SUVBM were significantly associated with malignancy with a P value of 0.03, 0.005, 0.001, and 0.024 respectively. At a cutoff of 1.5, the specificity and sensitivity of BM/M were 83.3% and 74.2%, respectively for malignancy diagnosis. Lung hypermetabolism was another indicator for malignancy. C reacting protein (CRP) was found to be a good indicator for the usefulness of PET/CT in HLH patients. Multivariate analysis showed that therapy regimen (Hazard Ratio (HR)=4.99, P=0.026), FBG<1.5g/L (HR=3.87, P=0.049) and SP/M (HR=7.44, P=0.006) were independent prognostic factors for survival.

Conclusions: FDG-PET could be a useful measurement for detecting underlying malignancy for secondary HLH.

Oncology_82

^{68}Ga-NOTA-RGD PET/CT for Preoperative Grading in Gliomas: A Comparison Study with ^{18}F-FDG PET/CT

Wei Zhang[1], Deling Li[2], Xiaobin Zhao[1], Nan Ji[2], Peilin Wu[1], Zhen Qiao[1], Yongji Tian[2], Liwei Zhang[2*], Zhaohui Zhu[1*]

1. Department of Nuclear Medicine, Peking Union Medical College Hospital, Chinese Academy of Medical Sciences and Peking Union Medical College, Beijing 100730, P.R. China
2. Department of Neurosurgery, Beijing Tiantan Hospital, Capital Medical University; China National Clinical Research Center for Neurological Diseases (NCRC-ND); Beijing Key Laboratory of Brian Tumor, Beijing, China

Objectives: Classification and treatment strategy of glioma remain to be optimized. Accumulation of FDG is frequently associated with convulsions due to heterogeneity within gliomas. The Arg-Gly-Asp (RGD) peptide specifically recognizes the integrin which is over expressed on glioma cells. The aim of this study was to compare^{18}F-FDG PET/CT with^{68}Ga-NOTA-RGD PET/CT for glioma grading.

Methods: Twenty-nine patients with gliomas were included in this study. The standardized uptake value (SUV_{max}) and tumor to normal tissue (T/N) ratios were measured. Spearman correlation test was used to calculate the correlation coefficient with pathological grade. Receiver operating characteristic (ROC) curve analyses were performed to assess the value for tumor grading. And the sensitivity, specificity, positive predictive value (PPV), negative predictive value (NPV) and accuracy were compared for ^{18}F-FDG PET/CT and ^{68}Ga-NOTA-RGD PET/CT.

Results: Pathology reports revealed 7 low-grade (WHO grade I or II) gliomas (LGGs) and 22 high-grade (WHO grade III and IV) gliomas (HGGs). All ^{68}Ga-NOTA-RGD PET/CT parameters showed the ability to differentiate between LGGs and HGGs (P=0.04 and P=0.014 for SUV_{max} and T/N ratio separately). The FDG PET/CT parameters cannot differentiate the LGGs and HGGs (P=0.129 and P=0.067 for SUV_{max} and T/N ratio separately). On the ROC analysis, ^{68}Ga-NOTA-RGD PET/CT showed higher area under curve in tumor grade than FDG PET/CT(0.883 vs 0.795,0.812 vs 0.805 for SUV_{max} and T/N ratio separately). According to the cut-off determined from ROC analysis, the sensitivity for FDG PET/CT

(86.4%, 90.9% for SUV_{max} and T/N ratio separately) was higher in predicting tumor grade than the ^{68}Ga-NOTA-RGD PET/CT (77.3%, 72.7%), but FDG PET/CT showed lower specificity (71.4%, 71.4%) than the ^{68}Ga-NOTA-RGD PET/CT (85.7%, 100%). Linear regression analysis revealed significant correlation of SUV_{max} and T/N Ratio both for ^{18}F-FDG (SUV_{max}: r = 0.64, P< 0.001; T/N: r = 0.72, P< 0.001) and ^{68}Ga-NOTA-RGD (SUV_{max}: r = 0.74, P< 0.001; T/N: r = 0.55, P= 0.002) between the WHO grade respectively.

Conclusions: ^{68}Ga-NOTA-RGD PET/CT imaging is a noninvasive modality that is useful in determining a tumor area as well as improving preoperative grading for gliomas.

Oncology_84

Total Lesion Glycolysis Uptake Predict Acquired Resistance of Epidermal Growth Factor Receptor Mutation in Advanced Non-small Cell Carcinoma with Gefitinib Treatment

Hean Ooi, Ching-Yuan Chen, Yu-Chun Hsiao, Bor-Tsung Hsieh, Wen-Sheng Huang

1. Department of Medical Imaging and Radiological Sciences, Central Taiwan University of Science and Technology, Taiwan
2. Departments of Preventive Medicine, Taichung Tzu Chi Hospital, Taiwan
3. School of Medicine, Tzu Chi University, Taiwan
4. Department of Medical Research, China Medical University Hospital, China Medical University, Taiwan

Objectives: It was very difficult for oncologist to predict when resistance will occur during gefitinib treatment. The ^{18}F fluorodeoxyglucose-positron(FDG), is a functional molecular imaging to measure metabolic uptake in cancer. Thus, we hypothesize that there will be exist difference metabolic uptake in between acquired resistance and non-resistance of epidermal growth factor receptor (EGFR) mutation in the non-small cell lung cancer(NSCLC).

Methods: From May 2010 to April 2013, 145 patients with stage IV NSCLC who underwent ^{18}F FDG PET and EGFR mutation analysis before receiving gefitinib treatment were eligible to participate in this study. Standard uptake value(SUV), metabolic tumor volume(MTV) and total lesion glycolysis (TLG) of each malignant lesion were measured. Whole body MTV and whole body TLG were the summation of all the MTV and TLG values in every cancer. The association of wild type, acquired resistance and non-resistance EGFR mutation status with patient characteristics were evaluated

Results: Overall survival (OS) was 12.3 months, and progression-free survival (PFS) was 8.2 months. No difference OS and PFS in non-resistance gefitinib with low or high TLG uptake. However, PFS significantly differed in acquired resistance gefitinib, and high TLG was associated with shorter PFS (6.2 months in high TLG; 10.3 months in low TLG, P< 0.05). Multivariate models adjusted for other factors showed that TLG was an independent predictive factor for PFS in NSCLC with high acquired resistance to gefitinib (P< 0.05).

Conclusions: The quantitative metabolic parameter, TLG, can be used as a tool to predict prognosis of acquired resistance EGFR before the gefitinib treatment. High TLG uptake with (EGFR) mutation in acquired resistance NSCLC should be alert clinicians that resistance will shortly occurred during the gefitnib treatment.

Molecular Imaging_33

Screening Value of ^{99m}Tc-RGD-BBN SPECT for Breast Lesions with BIRADS 4

Tiefeng Ji, Shi Gao, Bin Chen, Qingjie Ma*

Department of Nuclear Medicine,China-Japan Union Hospital of Jilin University, Changchun 130033, China

Objectives: This study aimed to explore the screen performance of single photon emission computed tomography (SPECT) using a new radiotracer ^{99m}Tc-RGD-BBN for breast lesions with BIRADS 4.

Methods: 90 female patients with 94 suspicious breast lesions (BIRADS 4) on traditional methods were included. Breast SPECT was performed at 4h after administration of ^{99m}Tc-RGD-BBN (11.1 MBq/kg). The images were interpreted independently by two experienced nuclear medicine physicians using visual and semi-quantitative analysis. A final diagnosis was made by histopathology of the specimens obtained by the surgical procedure. A fraction of the samples were analyzed immunohistochemically to evaluate integrin $\alpha_v\beta_3$ and GRPR expression.

Results: Among the 94 breast lesions, 22 were diagnosed as malignant and 72 were benign. The mean tumor to non-tumor (T/N) ratio of malignant lesions was significantly higher than benign lesions (3.19 ± 0.82 vs. 1.89 ± 0.71, $P<0.05$). The optimal cutoff values and ROC areas for SPECT visual and semi-quantative analysis were visual score 2 and T/N ratio 2.20. The overall sensitivity and specificity of visual and Semi-quantitative analysis were 95.5% vs. 95.5% (P>0.05) and 66.7% vs. 77.8% (P>0.05), respectively. The empirical

ROC areas of two procedures were 0.811 and 0.866 with no significant difference (P>0.05). The negative predictive value (NPV) of visual and semi-quantitative analysis can reach 97.8% vs. 98.2% (P>0.05). If 1 false-negative case was excluded, their NPV would be 100%. For malignant lesions, 11 were dual $\alpha_v\beta_3$ and gastrin releasing peptide receptor (GRPR) expression (GRPR+/$\alpha_v\beta_3$+), 6 were only GRPR positive expression (GRPR+/$\alpha_v\beta_3$-) and 5 were only integrin $\alpha_v\beta_3$ positive expression (GRPR-/$\alpha_v\beta_3$+). For benign lesions, 5 expressed integrin $\alpha_v\beta_3$ and GRPR simultaneously (GRPR+/$\alpha_v\beta_3$+), 7 expressed GRPR only (GRPR+/$\alpha_v\beta_3$-) and 12 expressed integrin $\alpha_v\beta_3$ only (GRPR-/$\alpha_v\beta_3$+). T/N ratios between receptors positive expression cases and receptor negative expression cases are different (*P<0.05*), but T/N ratios between dual receptors positive expression cases (GRPR+/$\alpha_v\beta_3$+) and single receptor positive expression cases (GRPR+/$\alpha_v\beta_3$- or GRPR-/$\alpha_v\beta_3$+) are not different (*P>0.05*).

Conclusion: ^{99m}Tc-RGD-BBN SPECT showed an excellent ability to identify benign lesions no matter which analysis methods we used. Its high NPV had a possibility of eliminating the necessity of surgical biopsy and histopathologic examination.

Molecular Imaging_35

^{99m}Tc-3PRGD$_2$ SPECT can predict response in stage IIIB and IV Non-Small Cell Lung Cancer patients two weeks after chemotherapy

Bin Ji, Shi Gao, Bin Chen, Tiefeng Ji, Qingjie Ma*

Department of Nuclear Medicine,China-Japan Union Hospital of Jilin University, Changchun 130033, China

Objectives: The aim of this prospective study was to evaluate whether ^{99m}technetium-3P-Arg-Gly-Asp (^{99m}Tc-3PRGD$_2$) single photon emission tomography (SPECT) can useful for the early prediction of clinical response to chemotherapy in Patients with advanced (stage IIIB to IV) non-small cell lung cancer (NSCLC).

Methods: Two ^{99m}Tc-3PRGD$_2$ SPECT scans were acquired after injection of the tracer in 41 patients before and after 2 weeks of therapy. Four patients had extremely low ^{99m}Tc-3PRGD$_2$ uptake at baseline, and were not included in the subsequent studies. Chest CT (baseline versus after 6 weeks of treatment) was performed according to RECIST 1.1 criteria. The images were evaluated by measuring the tumor to non-tumor ratio (T/N) and calculating the percentage change in T/N (ΔT/N) ratio. Receiver operator characteristic (ROC) analysis was used to determine a threshold for percent reduction in T/N ratios. The correlation between ^{99m}Tc-3PRGD$_2$ uptake and clinical response was evaluated in different therapeutic regimens. The predictive ability of ^{99m}Tc-3PRGD$_2$ SPECT response assessment was also evaluated with regard to overall survival (OS).

Results: A total of 37 patients with clearly visible ^{99m}Tc-3PRGD$_2$ uptake at baseline completed all imaging and treatment, which revealed 14 responders and 23 non-responders based on RECIST 1.1 criteria. The mean T/N ratio of baseline scans in responders and non-responders was not statistically different (3.04 ± 0.83 vs. 3.20 ± 0.70, P>0.05). After 2 weeks of treatment, the T/N ratios was lower in the responders compared with the non-responders and had statistical significance (1.85 vs. 2.97, P<0.05). The ΔT/N ratio was larger in responders than non-responders with significant difference (37.4% vs. 7.6%, P<0.05). Using a cut-off value of 24.6% decrease in T/N ratio, the sensitivity, specificity and accuracy of ^{99m}Tc-3PRGD$_2$ SPECT were 85.7%, 87.0% and 86.5%, respectively. Among these patients, the patients treated with chemotherapy plus bevacizumab demonstrated a greater change in T/N ratio than patients treated with chemotherapy alone (27.8% vs. 8.4%, P<0.05). A strong correlation was found between ΔT/N ratios and clinical response in patients treated with chemotherapy plus bevacizumab (P<0.05). Responders based on ^{99m}Tc-3PRGD$_2$ SPECT data survived 1.8 times longer than non-responders (19.2 vs. 10.8 months, P<0.05). Although the OS of patients treated with chemotherapy plus bevacizumab was longer than chemotherapy alone, but there was no statistical significance between them (15.6 vs. 12.1 months, P>0.05).

Conclusion: ^{99m}Tc-3PRGD$_2$ SPECT could identify treatment responders to therapy as early as two weeks after treatment initiation in patient with advanced NSCLC, especially those treated with chemotherapy plus bevacizumab.

Oncology_86

A Comparative analysis of ^{18}F-FDG PET/CT imaging between pancreatic lymphoma and pancreatic carcinoma

Shengnan Ren*, Shengping Hu, Chao Cheng, Changjing Zuo

Department of Nuclear Medicine of Changhai Hospital, Second Military Medical University, 168# Changhai Road, Yangpu District, Shanghai, China, 200433

Objectives: The aim of this study is to evaluate the diagnostic value of ^{18}F-FDG PET/CT in pancreatic

lymphoma and to establish the best means of differential diagnosis between pancreatic lymphoma(PL) and pancreatic carcinoma(PC).

Methods: The clinical features and ^{18}F-FDG PET-CT imaging of sixteen patients who were diagnosed with pancreatic lymphoma from August 2005 to March 2015 were retrospectively reviewed. The location, size, and density of pancreatic lesions, the pancreatic ductal dilatation, the distal pancreatic atrophy, extrapancreatic organs involvement and the maximum standard uptake values (SUV_{max}) of the focus were measured and analysized. All the imaging parameters of patients with pancreatic lymphoma were compared with those of 32 patients with pancreatic cancer.

Results: The mean age of PL patients is younger than PC patients (45.7±17.2 vs 61.3±11.8, P<0.05). The lesion size was larger in PL with a average diameter of 6.3±3.3cm than PC with that of 4.3±1.8cm,P<0.05. Dilated pancreatic duct and distal parenchyma atrophy happened more frequently in patients with PC than PL. The incidence rate of extrapancreatic lesions including kidney infiltration and multiple bone marrow involvement with high FDG uptake was significantly more frequent in patients with PL than PC. The difference of maximum standardized uptake value (SUV_{max}) for routine scanning between the two groups were 12.0±5.5 vs 8.6±3.8, P=0.025. The cutoff value of SUV_{max} was 9.95 with the sensitivity and specificity 68.8%, 71.9% for differentiating PL from PC.

Conclusions: Clinical diagnosis of pancreatic lymphoma should be considered in relatively younger patients, a density of bulky tumoral mass without distinct alteration of pancreatic duct or distal parenchyma atrophy with significant FDG uptake by the pancreas or concomitant extrapancreatic uptake by kidney and bone marrow should suggest the diagnosis.

Physics/Instrument_1

Effective Utilization of VQC Phantom for PET Performance Management

Kazufumi Sasaki, Akihide Sasaki, Shingo Kuribayashi, Mitsuru Taniguchi

Department of Radiology, Jyuzen Memorial Hospital, Hmamatsu Japan

Objectives: According to the NEMA Standard, the PET performance evaluations are generally carried out by sensitivity, spatial resolution, image quality and recovery coefficient. But those operations are not only complicated but needed a high degree of accuracy. For these reason it is difficult to perform frequently from the limitation of time and technology. Generally it is said that sensitivity shows the subtle deterioration of the device. And so the aim of this paper was to investigate the potential for diversion of ^{68}Ga VQC Phantom to the assessment of PET sensitivity and adjustment. This phantom is originally used to coordinate whether the position is correct between PET and CT.

Methods: After acquisition of 9bets setting the center to the VQC Phantom, true counts and NECR were calculated for each bet by total prompts, random and scatter fraction. The proper number of bet was decided by those parameters, and the total counts and the total NECR were compared at 2015/03/19 and 2015/05/12 with the reference on 2014/11/20. And the suitable acquisition time/bet was decided by comparison of the total counts and the total NECR with 10min/bet. The acquisition system was Discovery PET/CT 710 (GE Healthcare) and the phantom was ^{8}Ge-^{68}Ga VQC Phantom-507CE (SANDERS MEDICAL).

Results: Both the total true counts and the total NECR were decreased with the decay of the ^{68}Ge phantom source. Some of them were slipped off near to ±10%, but recovered within ±6% after calibrations. Measurement error were both located within ±1%, so the total true counts and the total NECR were represented the change in sensitivity of the PET equipment. On the other hand, acquisition time was enough in 1min/bet, but if the source decay will progress in future, the extension of the acquisition time is necessary. And the appropriate number of acquisition was more than 5bets.

Conclusions: VQC Phantom-507CE was able to use for judgment of the aging of the sensitivity and of the proper adjustment of the PET system. This was effective in off-subject use, but in the future a research will be needed that until when the present source is usable.

Physics/Instrument_3

Impact of anterior-posterior (AP) and posterior-anterior (PA) scout scans on the CT radiation dose in the whole body PET/CT scan

Guang-Uei Hung, Ching-Ni Lin

Show Chwan Memorial Hospital, Taiwan

CT contributes over 50% of radiation dose to the whole body (WB) PET/CT scan. Tube current modulation (TCM) is a standard technique for reducing CT radiation dose to the patient, and is controlled by a very low-dose scout scan, which assumes the patient is positioned at the center of the CT gantry opening. However, most patients are not positioned at the center due to patient

comfort. We study the impact of the AP and PA scout scans to the patient radiation exposure from CT.
In a retrospective study of 200 patients, each received two WB PET/CT scans: one with the AP scout, and the other one with the PA scout. The helical CT with TCM and PET acquisitions were identical in both scans. Separation of the two scans was about 10 months in average. The scans were performed on the GE PET/CT scanners with the same TCM settings. The 200 patients were selected for the same scan coverage and similar body weight (difference ≤ 3 kg). The tube current in each slice and average exposure to the patient were recorded and compared.
Results: The AP scout caused lower radiation dose on 94% of the patients. Both the tube current, and radiation exposure were reduced by 46±30 mA and 1.6±1.0 mGy, respectively. The effective radiation dose is reduced by 1.7±1.2 mSv. These results were statistically significant (P<0.00001).
The AP scout caused significantly less radiation dose than the PA scout in the CT scan of the whole-body PET/CT scan. Care should be taken to select the orientation of the scout scan to achieve appropriate radiation exposure to the patient when TCM is applied.

Physics/Instrument_4

Increase in cerebral glucose metabolism after non-invasive electrical stimulation of mild cognitive impairment patients

Yong-An Chung, In-Uk Song, Ji-young Ryu, Ikdong Yoo, Eun-Kyoung Choi, Jin-Kyoung Oh

Department of Neurology, Incheon St. Mary's Hospital, College of Medicine, The Catholic University of Korea, korea

We aimed to investigate how regular and relatively long-term (three weeks) treatment with tDCS might affect cerebral metabolism and enhance the cognitive performance of MCI patients.
Using transcranial direct current stimulation (tDCS) and Positron-Emission Tomography (PET), we showed that regular and relatively long-term use of tDCS significantly increased regional cerebral metabolism in MCI patients. Furthermore, subjective memory satisfaction and improvement of the memory strategies of participants were observed only in the real tDCS group after 3 weeks of stimulation.
After three weeks of active tDCS treatment, increased metabolism was observed in the dorsolateral, ventrolateral, and medial prefrontal cortices, parietal cortex, and dorsolateral anterior cingulate, whereas areas of decreased metabolism were observed in both the anterior and posterior insular regions and the hippocampal and parahippocampal regions.
Our findings suggest that neurophysiological intervention at the early stage of MCI could improve transient memory function in MCI patients and even delay the progression to Alzheimer's disease.

Physics/Instrument_14

Harmonizing SUVs from different PET/CT scanners by using Recovery Coefficients

Reeree Lee, Youn Woo Lee, Ji-Yong Kim, Ho-Young Lee

Seoul National University Bundang Hospital, Korea

SUV harmonization is important in case of using multi-scanner or multicenter clinical trial. We evaluated the usefulness of SUVs harmonization methods using recovery coefficients among multi PET/CT scanners of multi-centers. NEMA IEC Body phantom was used to acquired PET/CT image and the recovery coefficients of each scanners. Phantom was prepared by the NEMA protocol. Image acquisition and reconstruction was followed each institutes' protocol. We acquired the recovery coefficient (RC) of each scanner and we used EQ filter to evaluate the value of Gaussian filter for SUV harmonization. 20 PET/CT scanners in 9 institutes were enrolled in this study.
To evaluate the variation of phantom, we acquired RC three times with same scanner in different days. The mean coefficient variation of RC was 10.4%. We acquired the RCs of 20 scanners and the mean RCs was 4.9±0.9. After the application of Gaussian filter, the mean difference of SUVs was 4.8%.
Applying the EQ filter for the purpose of quantification reduces variation in SUVs and enables to increase assurance in quantitative comparing of clinical PET images for monitoring disease course or treatment response in multicenter trials.

Physics/Instrument_16

Reducing Between-scanner Differences in Multicenter Brain PET Studies Using CT-based Tissue Label Map

Hyojeong Moon, Injoo Lee, Jungmin Kim, Jae Seung Kim, Jungsu S. Oh

Department of Nuclear Medicine, Asan Medical Center, University of Ulsan College of Medicine, Korea

Generally, we need to reduce differences (i.e., harmonize) between image qualities of different PET-CT scanners

to use them in same study. The multicenter Alzheimer's Disease Neuroimaging Initiative (ADNI) study proposed the smoothing factor of different scanner models. We devised a new harmonization method by obtaining appropriate smoothing factor using CT-based tissue label map (CTM) for PET scanner harmonization in Korean-ADNI (K-ADNI).
All sites examined Hoffman 3D Brain Phantom images using seven different scanner models of PET-CT scanners. We used the best quality CT data (GE Discovery 690, 690 Elite, and 710) for generating CTM on SPM8 segmentation. The Gray matter (GM) and White matter (WM) in Hoffman phantom were filled with four-to-one FDG activities, respectively. After morphologic image processing, we labelled 4 and 1 for GM and WM, respectively, resulting in the GM/WM CTM for Hoffman phantom.
For the appropriate smoothing kernel, we first cropped the different field-of-view (FOV) of PET-CT images of individual site. All cropped CT images and corresponding CTMs were registered to PET images. Subsequently, we smoothed the CTMs using Gaussian kernel with one-to-ten mm FWHM. Between them, we found the best kernel (one with the highest correlation coefficient with PET images).
As conducted in ADNI study, we found the harmonization smoothing kernel size that makes all PET images from different scanners into the effective resolution of 8 mm.
The harmonization FWHMs for PET image from GE Discovery PET-CT 690/690 Elite/710 were the same, i.e., 5mm; 4mm for Siemens Biograph Truepoint, Philips Gemini TF, and GE Discovery ST(E).
The resulting harmonization FWHMs were similar between ADNI study method and our proposed method. Based on these results, we suggest them to use our devised CTM-based harmonization method instead of using Hoffman phantom bitmap. Moreover, our CTM may be more realistic mask than the bitmap, for instance, our one can describe air bubble contaminated phantom images.

Physics/Instrument_18

Visual and quantitative analysis methods of respiratory patterns for respiratory gated PET/CT

Hye Joo Son, Young Jin Jeong, Hyun Jin Yoon, Do-Young Kang

Department of Nuclear Medicine, Dong-A University Medical Center, Dong-A University College of Medicine, Busan, Korea

Objectives: In this study, we integrated both visual and quantitative methods for analyzing the stability of respiration during respiratory gated PET/CT using four methods : phase space diagrams, Fourier spectra, Poincaré maps, and Lyapunov exponents.

Methods: Respiratory patterns of 139 patients were divided into four groups based on the combination of the regularity of amplitude, period and baseline positions. Visual grading of amplitude, period and baseline position were done by inspecting the shape of phase space diagram, Fourier spectrum and time-amplitude curve and classified into two states: regular and irregular. Then, quantitative evaluation about amplitude, period and baseline was done by measuring standard deviation of x and v coordinates of Poincaré map (SDx, SDv) or the height of the fundamental peak (A1) in Fourier spectrum or calculating the difference between maximal upward drift (MUD) position and maximal downward drift (MDD) position. Quantitative difference between groups was analyzed by ANOVA, MANOVA and ROC analysis.
Results: Each four group revealed characteristic shape and pattern on visual analysis.
There was statistically significant difference of quantitative parameters among four groups in both ANOVA and MANOVA analysis (P = 0.000). In ROC analysis, the cutoff values was 0.11 for SDx (AUC: 0.982, P< 0.0001), 0.062 for SDv (AUC : 0.847, P< 0.0001), 0.117 for A1 (AUC : 0.876, P< 0.0001), 0.349 for MUD-MDD (AUC : 0.948, P< 0.0001). Also, the data for all 139 patients exhibited negative LLEs, ranging from -3.76 to -0.43. (mean : -1.94, standard deviation : 0.46). A visual comparison of the time series with the LLEs suggested that more negative Lyapunov exponents corresponded to faster regularization of initially irregular patterns.
Conclusions: In this study, we integrated both visual and quantitative methods for analyzing the stability of respiration during respiratory gated PET/CT using four methods. Here, we demonstrated that each group revealed characteristic shape and pattern on visual analysis, as well as showing significant difference of the quantitative parameters between groups.

Physics/Instrument_19

Development of a compact and cost-effective PET system for small animals imaging

Hyun-Il Kim, Yong Hyun Chung, kisung Lee, Hakjae Lee, Yongkwon Kim, Jinhun Joung, Kyeong Min Kim

Korea Institute of Radiological Science, Korea

Recently, growing use of small animal Positron Emission Tomography (PET) imaging in treatment of various diseases and development of new drugs make the need to develop compact PET system that can provide cost-effective small animal imaging is increasing. We have

developed a compact and cost effective prototype PET system for imaging small animals.

The system consists of four detector modules and each pair of detectors are faced each other. The distance between the pair of detector module, i.e., inner diameter, is 5 cm. Each detector module is further comprised with a LFS crystal array, 22x22 array with 2x2x10 mm pixel size, optically coupled to a PS-PMT (H8500, Hamamatsu). For data acquisition and processing, a commercially available DAQ system with 64 channels of fast free running 65 MHz ADC (DSGP-DAQ64, Nucare Medical Systems, Inc.) was used.

In system design phase, we used the GATE Monte Carlo simulation tool. And the sensitivity and spatial resolution was simulated to be 5.7% and 2.2 mm, respectively. A prototype system has been built and preliminary studies has been conducted. The flood images of detector modules have been collected using a Na-22 and all 484 pixels per detector were all clearly identified.

Future works include image reconstruction with limited angular samples and extension of axial FOV by adding a ring with four detector modules. Optimization of the first and second ring configuration, i.e., offset angle between rings, is the topic that we are currently conducting.

Physics/Instrument_20

Evaluation of I-131 gamma imaging using new scintillator, GAGG : simulation study

MinHo Kim[1,2], JongGuk KIM[1], WonHo Lee[2], KyeongMin Kim[1,*]

1. Korea Institute Radiological and Medical Science, Molecular Imaging Reasearch Center, Korea
2. Department of Bio-convergence Engineering, Korea University, Korea

Objectives: Imaging of I-131 during radionuclide treatment has been used significantly. Conventional gamma-camera using NaI scintillator has been widely used in nuclear medicine. The characteristics of NaI, however, results in various limitations in the imaging of 364 keV photons of I-131. In this study, we compared the imaging characteristics of both scintillation materials of NaI and GAGG for I-131, using MC simulation.

Methods: GATE package (v6.2) was used in this Monte-Carlo simulation. A clinical SPECT camera (SYMBIA T2, Siemens) with high-energy collimator was modeled. Water-filled cylindrical phantom (10 cm radius, 10 cm height)was placed in the center of FOV of gamma camera detector. The distance of phantom to collimator was set to 10 cm. I-131 line source(1mm diameter, 10cm height, 37 MBq) was placed at the center of phantom. The time of data acquisition time was set 90 sec. Both NaI and GAGG scintillators were applied to the simulation. For the both scintillator, the thickness of 3/8 inch and 1 inch were considered. Triple energy window method using different main energy window sets(364 keV +/- 15% and 20%) was also applied for scatter correction. The values of energy spectrum, main-to-total count ratio, FWHM, Scatter Fraction (SF) were used in comparison.

Results: The shapes of energy spectrum of NaI and GAGG was significantly different, especially in the part of high energy above 400 keV. The changing pattern of energy spectrum between 3/8 and 1 inch scintillator was similar. For increasing main-to-total count ratio, the crystal thickness and the width of main energy window was more significantly for NaI and GAGG, respectively. And this tendency got more cleared after scatter correction. For 3/8 inch thickness, GAGG provided better FWHM and SF, compared to NaI. For 1 inch, however, there is no significant difference of FWHM and SF, before and after scatter correction.

Conclusions: Compared to NaI, GAGG would provide the better performance of I-131 imaging, even no use of thicker scintillator crystal. These simulation results shows that the characteristics of GAGG will need further consideration for optimization and quantitation of I-131 gamma imaging.

Physics/Instrument_21

Clinical significance of dacryoscintigraphy in patients with epiphora: a preliminary study.

Hyo Jung Seo, Jae Seon Eo, Eunsub Lee, Soyeon Park, Seunghong Rhee, Jaehyuk Cho, Sunju Choi, Chulhan Kim, Sungeun Kim, Jae Gol Choe

Department of Nuclear Medicine, Korea University, College of Medicine, Seoul, Korea

Objectives: The aim of this study is to evaluate the diagnostic value of dacryoscintigraphy.

Methods: The inclusion criteria was 180 patients with epiphora and dacryoscintigraphy between August, 2014 and July, 2015. This is a preliminary study of the evaluation of forty eyes in 20 patients with epiphora. Clinical information of underlying disease and endoscopic dacryocystorhinostomy was reviewed. The diagnostic criteria were classified as pre-sac and post-sac obstruction, stasis and no obstruction. Two experience nuclear medicine physicians (8years and 2years) reviewed dacryoscintigraphy and scored the rate. Diagnostic value was compared with between two

nuclear medicine physicians and inter-rater agreement was analyzed sing SPSS. The diagnostic change after stimulation was recorded.

Results: Of 40 eyes, 7 eyes were no obstruction, 9 eyes were pre-sac obstruction, 12 eyes were post-sac obstruction, 5 eyes were pre-sac stasis and 7 eyes were post-sac stasis. After stimulation test, the change from obstruction to stasis was shown in 12 eyes and the change from pre-sac obstruction to post-sac obstruction was shown in 2 eyes. The inter-rater agreement between two nuclear medicine physicians was perfect agreement (K =1.00)

Conclusions: Dacryoscintigraphy is useful to evaluate epiphora and improved diagnostic value after stimulation. The interpretation of diagnosis showed perfect agreement.

Physics/Instrument_22

Dependency of energy width of gamma probe device for quantitative monitoring of patients with I-131 treatment

Se Jong Oh[1,2], Byung Hyun Byun[1], Kwang Sun Woo[1], Wee Sup Chung[1], Sang Moo Lim[1], Kyeong Min Kim[1*]

1. Molecular Imaging Research Center, Korea Institute Radiological and Medical Sciences
2. University of Science and Technology, Daejeon, Korea

Objectives: Iodine-131 has been widely used in nuclear medicine therapy for a long time. Quantification of I-131 remained in the body is significant in monitoring and managing the patient after treatment. Therefore, the selection of suitable radiation detector has been needed in clinical environment. Gamma probe detector has been the one of the instruments used in patient management and monitoring. In this study, we analyzed the detection performance of gamma probe detector depend on the energy window width in the phantom study using high dose of I-131.

Methods: In the phantom study, we used GammaPro 1410 (Nucare Medical Systems) as a digital gamma probe. We used 14 vials containing I-131, and made various activities (10-300mCi) by combining each vial. Activity measurement was conducted at the distance of 3m and 1.5m respectively. We used plastic packs filled water as attenuator. We compared the results based on the five kinds of energy window set around the main photopeak (364 keV ± 5, 10, 15, 20, 30%) and total energy range.

Results: As energy window width is narrowed, overall linearity between activity and counts appeared to increase. There were no significant changes beyond the 20% width. In case of 5% width, some measurement errors were observed, these results are caused by the highly narrow energy window width. However, in all cases, the linearity was better than total energy window width.

Conclusions: For increasing the quantitative accuracy, selecting the proper energy width in the measurement of I-131 radioactivity in patients is important. In this study, 20-30% widths set around the main photopeak showed ideal results. However, in cases of narrow window width, it seems to be important to conduct the proper device calibration.

Radiochemistry_2

The development of PET imaging agent in a mouse model for acute inflammation

Jae Min Jeong, Ji Youn Lee, Hoyoung Kim

Seoul National University, Korea

Human serum albumin (HSA) has potential for diagnosis and therapeutic agent in clinic. Positron emission tomography (PET) is a standard imaging technique for clinic and research. The purpose of experiments was to develop and estimate ^{68}Ga-HSA as a PET agent for acute inflammation.

NOTA-HSA was synthesized by conjugating 2-(p-isothiocyanatobenzyl)-1,4,7-triazacyclononane-1,4,7-triacetic acid to human serum albumin in 0.1 M sodium carbonate buffer (pH 9.5) and then purified using PD-10 size-exclusion column. NOTA-HSA was labeled with ^{68}Ga at room temperature for 10 min. And 8.4% sodium hydrogen carbonate buffer was added for neutralization. ^{68}Ga-NOTA-HSA was purified using alumina N plus light cartridge and 0.22 μm syringe filter. Labeling efficiency and radiochemical purity were determined by ITLC-SG with 0.1 M citric acid. A solution of carrageenan in normal saline was injected subcutaneously in BALB/c mice induce acute inflammation. After 4 hour 1% carrageenan injection, biodistribution study was performed. After 1 hour ^{68}Ga-HSA injection via tail vein, mice were sacrificed. Inflamed footpad, control footpad, blood and other organs were extracted, weighted and counted by gamma counter. Small animal-PET study was performed in acute inflammation mice model after tail vein injection of ^{68}Ga-HSA. PET image were obtained at 70 min after tracer injection.

HSA showed high labeling efficiency (>99%) around pH 7. Biodistribution study showed higher inflamed footpad uptake than control footpad uptake. Small animal-PET study revealed 2 times higher uptake on inflamed footpad compared to control footpad.

In these experiments, we developed ^{68}Ga-HSA for acute inflammation PET imaging agent and evaluate ability of ^{68}Ga-HSA. The results demonstrated that ^{68}Ga-HSA has possibility for PET imaging agents in acute inflammation.

Radiochemistry_8

Optimization Method for Recovering O-18 Enriched Water for Reuse

Suphansa Kijprayoon[1], Ananya Ruangma[2], Suthatip Ngokpol[3], Suwit Khajitkhajonwong[4]

Oncology Imaging & Nuclear Medicine Department, Wattanosoth Hospital, Bangkok Hospital at Headquarter, Thailand

Objectives: To evaluate purification method for recovering O-18 enriched water using solid-phase extraction followed by distillation for reuse in routine production

Methods: 1. Recovering O-18 water purified with solid-phase extraction set of QMA, IC-OH, IC-H and metal scavenger column for removing inorganic ions.

2. After SPE extraction, the recovering enriched water was distilled in evaporator system.

Results: The inorganic ion quantity was reduced after solid-phase extraction method. The metal samples were determined by Inductivity Coupled Plasma-Mass Spectrometry (ICP-MS). The results show that concentrations of all metal are lower than limit values.

The organics impurities were greatly reduced after distillation. The enrich water detected by gas chromatography. The mainly organic solvents are acetonitrile and ethanol.

Conclusions: The amount of impurities after solid-phase extraction method followed by distillation method was considerably reduced. The recovery yield after distillation is at least 94%. Thus this water from this method is suitable for reuse in routine production.

Radiochemistry_9

The importance of unified education in Radiopharmacy and new perspective to pursue a masters degree

Emilija Janevik-Ivanovska[1], Uday Bhonsle [2], Adriano Duatti [3], Zoran Zdravev [4], Osso Júnior João Alberto[2], Meera Venkatesh[2]

1. Faculty of Medical Sciences, Goce Delcev University, Stip, Republic of Macedonia,
2. Radioisotope Products and Radiation Technology Section, Division of Physical and Chemical Sciences, IAEA, Vienna, Austria
3. Laboratory of Radiopharmaceutical Chemistry, Department of Chemical and Pharmaceutical Sciences, University of Ferrara, Italy
4. Faculty of Medical Sciences, Goce Delcev University, Stip, Republic of Macedonia

Purpose: The importance of unified education and recognition in Radiopharmacy became a need all around the world as result of different national regulation and different system of education.

The substantial confusion and challenge in the same time is to define the appropriate and sufficient knowledge, understanding and competences corresponding to their position in the working place

Methods: The goal of the Academic Master program for Radiopharmacy in English, with the recognized accreditation from the National Body and recommended by the Ministry of Education and Science in our country according to the Bologna system with 120 ECTS credits is to give the opportunity for all students that finished academic undergraduate program with at least 240 ECTS (pharmacist, chemist, physicist, biologist, biochemist, physicians and from similar field) to follow it and to receive academic title Master of Radiopharmacy.

The program use all informatics infrastructure from the University including e-learning platform for teaching.

The Radiopharmacy Education Program is according to the General qualifications descriptors and in accordance with the Regulation on the National Framework for Higher Education Qualifications. Its organized according to the University model including Obligatory and Optional Theoretical Courses, Obligatory Practices and Master Thesis on the end of the second year.

Results: The syllabus include knowledge and skills in three categories:

1. Specific knowledge and skills: Design of Radiopharmacy facilities and QA program; Production and synthesis of radionuclides and radiopharmaceuticals; Quality control of radiopharmaceuticals

2. Basic knowledge and skills: Leadership and collaboration; Communication; Negotiations; Analytical and critical thinking skills including creativity and ethical considerations; Pharmaceutical and chemistry knowledge

3. Fundamentals of Radiopharmacy: General models of the area; Key specializations within the field; valuation of performance within the area

Conclusions: The program creates academic staff able to work in all spheres of the modern Radiopharmacy, conventional hospital Radiopharmacy and with the option of continuing their education in some PhD program .

Radiochemistry_10

Implementation of ISO 17025 Standard and accreditation process of Radiopharmacy Laboratory

Apostolova Paulina, Sterjova Marija, Smilkov Katarina, Gorgieva Ackova Darinka, Delipetreva Katarina, Janevik Ivanovska Emilija

Faculty of Medical Sciences, Goce Delcev University – Štip, Republic of Macedonia

Objectives: The Laboratory of Radiopharmacy a part of the Department of Pharmacy in the Faculty of Medical Sciences, at the Goce Delcev University in Stip has a main activity of testing radiopharmaceuticals, but also serves research and educational purposes.

The regulatory body for accreditation of laboratories in our country is The Institute for Accreditation of The Republic of Macedonia, which is responsible for the inspection procedures and the issue of the formal document, The Certificate of Accreditation, upon fulfilling all requirements.

Methods: In order to improve the quality system in the Laboratory of Radiopharmacy, and to fulfill the criteria needed for testing Radiopharmaceuticals, in accordance with the Law for medicines and medicinal products, as well as the Law for ionizing radiation and radiation safety, we have implemented the Standard MKC EN ISO/IEC 17025 - General requirements for the competence of testing and calibration laboratories.

Results: The standard MKC EN ISO/IEC 17025 includes two major clauses, highlighted as Clause 4, that specifies the management requirements, and Clause 5, that specifies the requirements for technical competence for the type of tests the laboratory undertakes. Our organization scheme includes the following staff: Head of Laboratory, responsible for implementation of all standard requirements, management and coordination of the work; Quality Manager, that creates the documentation of the quality system and administrates, maintains, controls and monitors the functionality of the quality system; Laboratory Chief, responsible of control of the laboratory activities, as well as issuance of the reports and result interpretation, Analysts, qualified analysts responsible for performing the analyses and Administrative person, responsible for the administrative work.

Conclusions: The accreditation road that is to be paved by this laboratory will help other similar-type laboratories in country in orienting their activities toward increasing the level of professionalism and organization, thus enabling international recognition.

Radiochemistry_12

Radiopharmacy in Africa: perspective of Ethiopia and Kenya

Aschalew Alemu [2,3], Joel Munene Muchira[1,3], David Mwanza Wanjeh[1,3], Emilija Janevik-Ivanovska[3]

1. Ministry of Health, Kenya
2. Faculty of Medicine, Addis Ababa; Ethiopia
3. Faculty of Medical Sciences, Goce delcev University, Republic of Macedonia

Objectives: The article seeks to describe the current status of Radiopharmacy practice in Eastern Africa using the perspective of Kenya and Ethiopia.

Methods: Non-communicable diseases (NCDs) are a challenge of epidemic proportion and that they will be the commonest cause of mortality in Africa by 2030. Since early detection and treatment is known to significantly improve patient outcomes, radiopharmaceuticals have become of invaluable benefit because they offer the most sensitive tools in the detection, diagnosis and targeted therapy of NCDs and also infectious diseases. In light of the foregoing, therefore, radiopharmacy has a huge role to play in responding to the unfolding new disease trends in sub-Saharan Africa.

Results: The preparation of radiopharmaceuticals for human use requires that it is carried out in well-defined and controlled conditions to avoid the risk contamination with microbes, pyrogens and particulate matter as well as cross contamination with other radiopharmaceuticals.

Accordingly, principles of Good Manufacturing Practices and Good Laboratory Practices should strictly be observed in the production, preparation, testing and the packaging of the final product ready for use. Most radiopharmaceuticals are parenterally administered and must therefore be prepared in such condition, and using such techniques and procedure, that guarantee sterility of the product. Every procedure undertaken should be done according to the clearly defined protocol and under the right conditions so as to build quality into the product. Radiopharmacy professionals should have adequate training in all aspects of sterile production, quality control, GMP , GLP, radiation safety and radiochemistry to ensure that they are competent to handle radioactive materials and that they can take responsibility for their level of practice

Conclusions: The exact information on the number and status of radiopharmacy units, regionally, is still not clearly documented. Important information for the Eastern Africa region that also needs to be documented includes issues of human resource and local demand for the radiopharmacy services. It is the existence of this gap that necessitated the preparation of this article.

Radiochemistry_14

PET/CT Imaging of Brain with the Peripheral Benzodiazepine Receptor (PBR) Imaging Probe, ^{18}F-FEPPA, in Social Deficit Mice Model

Dong Hyun Kim[1,2,3,4,5,7], Minjoo Kim[1,2,3,4,5], Hyeon Soo Kim[1,2,3,4,5], Hwan-Jeong Jeong[1,2,3,4,5], Young Chul Chung[6], In Sun Kim[1,2,3,4,5], JiHae Choi[1,2,3,4,5], Hwan-Seok Jeong[1,2,3,4,5], Eun-Mi Kim[1,2,3,4,5], Phil-Sun Oh[1,2,3,4,5], Tai Kyung Lee[1,2,3,4,5,7], SeokTae Lim[1,2,3,4,5], Myung-Hee Sohn[1,2,3,4,5]

1. Department of Nuclear Medicine
2. Molecular Imaging & Therapeutic Medicine Research Center
3. Cyclotron Research Center
4. Institute for Medical Sciences
5. Biomedical Research Institute
6. Department of Psychiarty, Chonbuk National University Medical School and Hospital, Jeonju, Jeonbuk 561-712, Republic of Korea
7. Kai Bio-Tech. Co. Ltd., Jeonju, Jeonbuk 561-712, Republic of Korea

Objectives: Social deficit is a mental illness which is inability or unwillingness of emotional recognition, mentalizing ability and social communication to act in accordance to age, physical condition and intelligence. It may be involved in regulating the density of peripheral benzodiazepine receptor (PBR) in the brain. Therefore, we synthesized N-2-(2-[^{18}F]fluoroethoxy)benzyl-N-(4-phenoxypyridin-3-yl)acetamide (^{18}F-FEPPA) as a sensitive biomarker for the detection of neuronal damage or inflammation in the brain and evaluated with social deficit mice model.

Methods: Radiochemical synthesis of ^{18}F-FEPPA was carried out by ^{18}F labeling of tosylate precursor with K[^{18}F]F and purified to obtain the desired product. HPLC Purification was performed with reverse phase HPLC (0.1% TFA in water (A) and 0.1% TFA in acetonitrile (B); A:B=90:10 to 60:40 over 30 min, flow rate: 4 mL/min, 254 nm). Animal PET/CT images of ^{18}F-FEPPA were obtained at 30 min post injection using social deficit mice model group and control group. The acquired PET/CT images were evaluated for quantitative analysis using PMOD by mean ROI activity after reconstruction by the OSEM-2D algorithm.

Results: ^{18}F-FEPPA was synthesized in 20% overall radiochemical yield (decay corrected) and high specific acidity (18-23 GBq/mmol). Total synthesis time including HPLC purification and formulation was 90-100 min. Animal PET/CT imaging study for social deficit group and control group showed significant difference brain uptake of ^{18}F-FEPPA. ROI mean activity of ^{18}F-FEPPA was approximately 1.5 times that of the social deficit model group.

Conclusions: The comparison of ^{18}F-FEPPA uptake of the social deficit group and control group showed significant difference PET images. These results demonstrated that ^{18}F-FEPPA may be a potent radioligand for PET imaging study of PBR density of social deficit model in the brain.

MolecularImaging_1

Value of ^{18}flourodeoxyglucose positron emission tomography/computer tomography (^{18}F-FDG PET/CT) in detection of recurrence in colorectal cancer patients

Mai Hong Son, Le Ngoc Ha

Nuclear Medicine Department, Tran Hung Dao Hospital, Vietnam

Objectives: This our study access the role of ^{18}F-FDG PET/CT in detection and management of colorectal cancer patients with suspected recurrence and metastases

Methods: 30 patients suspicious for colorectal cancer recurrence based on clinical symptoms or serum carcinoembryonic antigen (CEA) level were recruited to the study. All patients underwent conventional scan (abdominal CT, ultrasound, chest X-ray) and PET/CT. Sensitivity (SEN), specificity (SPEC), positive predictive value (PPV) and negative predictive value (NPV) were calculated using either histopathology or follow-up imaging as the standard of reference and compared to the ability of CEA level (CEA level higher than 5 ng/ml was considered positive)

Results: Regarding to detection of local recurrence, PET/CT has shown sensitivity of 100%; specificity 67%; PPV 88%; NPV 100%. The SEN, SPEC, PPV, NPV of conventional imaging was 43%, 100%, 100%, 43%, respectively. The value of CEA level was 64%, 67%, 44%, 81% in SEN, SPEC, PPV and NPV, respectively. PET/CT has found 9 of 30 colorectal cancer patients who had positive regional lymph node metastases, however, conventional imaging showed only in 4 of 30 these patients. Similarly, in detection of distant metastases, 4 of 30 cases had liver and lung metastases on PET/CT meanwhile only 2 of 30 cases was shown on CT and chest X-ray

Conclusions: ^{18}F-FDG PET/CT has high accuracy in the assessment of local recurrences and metastases impacting significantly on colorectal cancer patients management.

Molecular Imaging_5

Role of Uncoupling Protein-2 on the Warburg Effect in T47D Breast Cancer Cells

Kyung-Han Lee, Young Seok Cho, Seung Hwan Moon, Jin Won Park, Jin Hee Lee, Kyung-Ho Jung

Samsung Medical Center, Korea

The goal of this study was to investigate the role of UCP2 on the Warburg effect in cancer cells, and to further evaluate the relation of this metabolic effect to changes in ROS production and mitochondrial membrane potential (MMP).

UCP2 protein expression levels were investigated in various cancer cell lines by western blot. Glucose uptake level was measured by incubating cells with FDG for 40 min. UCP2 function was blocked by treating cells with genipin, a specific UCP2 inhibitor. Genetic ablation of UCP2 was achieved by transfection of cells with specific siRNA with experiments performed 48 h later.

Inhibition of UCP2 activity by exposure to genipin caused time- and dose- dependent decrease in FDG uptake. Uptake level was reduced to 49.6% of controls by 2 h exposure of 100 μM genipin, and analysis of the dose-response curve showed a IC50 value of 60.87 μM in T47D cells. Reduced glucose uptake by genipin was accompanied by a decrease of lactate production, indicating suppression of glycolytic flux. Genipin exposure also increased in ROS generation in T47D cells, but a significant influence on MMP level was not detected. Experiments using a XF24 Extracellular Flux Analyzer revealed a significant decrease of the oxygen consumption rate (OCR) to 60.7% of controls by treatment with 100 μM genipin for 24 h. Knock-down of UCP2 protein by siRNA also caused significant reduction of FDG uptake to 65.6% of controls, and significant increase of ROS production to 123.3% of control level. When UCP2 expression was increased by transfection with plasmid DNA, there were significant reductions of ROS production and MMP.

In conclusion, the findings of this study demonstrating that inhibition of UCP2 reduces glycolytic flux as well as mitochondrial oxidative respiration and increases ROS production, suggest that UCP2 may partly contribute to the Warburg effect of cancer cells. Further investigations are warranted to elucidate the precise role of UCP2 in cancer cell metabolism, and to determine whether it could be a potential target for cancer therapy.

Molecular Imaging_16

Effect on Co-culture of Lewis lung cancer cells with Rennila luciferase labelled mMSCs and biodistribution of Rluc MSCs on mouse cancer xenograft model

Senthilkumar Kalimuthu[1] , Prakash Gangadaran[1], Xiu Juan Li[1], Ji Min Oh[1], Shin Young Jeong[1], Sang-Woo Lee[1], Jaetae Lee[1, 2] and Byeong-Cheol Ahn[1]*

1. Department of Nuclear Medicine, Kyungpook National University School of Medicine/Hospital, Daegu-700-721, Republic of Korea
2. Daegu-Gyeongbuk Medical Innovation Foundation (DGMIF), 80 Cheombok-ro, Dong-Gu, Daegu, 701-310, Republic of Korea

Purpose: Mesenchymal stem cells (MSCs), are considered as vehicles for delivery of antitumor agents and recent studies focused on MSC labelling could be useful for molecular imaging study. So the present study elucidate the role of renilla luciferase (Rluc) labeled MSC for assessment of biodistribution of MSCs on lung cancer xenograft animal model.

Methods: Mouse bone marrow derived MSCs are stably transfected with pCMV promoter mCherry-Rluc viral particles and selected with puromycin. Selected cells were analyzed mCherry by flowcytometry and fluorescent image. Further Rluc activity was determined by IVIS imaging. The phenotype markers were analyzed in Rluc MSC by FACS. Lewis lung cancer cells are stably transfected with enhanced firefly luciferase (effluc) gene by retroviral particles. In vitro anticancer effect of MSC to the cancer cell was studied by co-culture. Cell mediated cytotoxicity was assessed by cytotox assay. The migration ability of Rluc labeled MSC cells to tumor was visualized in Lewis lung cancer xenograft bearing mouse model.

Results: Rluc activity was increased with increasing cell numbers in Rluc labeled MSC cells (MSC-Rluc). MSC-Rluc was positive for MSC phenotype markers. In vitro co-culture of Lewis-effluc with MSC-Rluc has significant decreased in viability of Lewis-effluc. After tumor grown $1x10^6$ MSC-Rluc cells injected via the tail vein and successful migration of MSC-Rluc to tumor site was successfully visualized in Lewis lung cancer xenograft mouse model using IVIS imaging system.

Conclusions: The MSC-Rluc has anticancer effect to Lewis lung cancer cells. Also MSC-Rluc migrated to the tumor site after tail vein injection in mouse animal model. So these results suggest that labeling MSC with the reporter gene could be useful as molecular imaging methodology for researching MSC therapy for cancer.

Molecular Imaging_19

Monitoring Immune Response to Hepatitis B Vaccination Using Noninvasive in vivo Imaging

Ha Kim[1,3], Taemoon Chung[1,2,3], Myung Geun Song[1,3], Byung Cheol Ahn[6], Jung Sun Yum[6], Keon Wook Kang[1,2,3], June-Key Chung[1,2,3,4], Hyewon Youn[1,3,4,5*]

1. Department of Nuclear Medicine
2. Biomedical Sciences
3. Cancer Research Institute, Seoul National University College of Medicine
4. Tumor Microenvironment Global Core Research Center, Seoul National University
5. Cancer Imaging Center, Seoul National University Cancer Hospital, Seoul
6. CHA Vaccine Institute, Gyeonggi-do, Korea

Objectives: Bioluminescence imaging (BLI) is among the most powerful tools for noninvasive imaging in small animals. By taking advantage of BLI to non-invasively monitor luciferase expressing splenocytes, we monitored the enhancement of immune response against hepatitis B virus (HBV) vaccine with adjuvants in real time.

Methods: A novel luciferase transgenic mouse model (B6.Luc^{TG}) was generated to monitor the immune response. To visualize vaccinated antigen, large hepatitis B virus antigen (L-HBsAg) was labeled with radioiodine (^{125}I-HBsAg). B6 mice were vaccinated intramusculary with ^{125}I-HBsAg, ^{125}I-HBsAg+adj1 and ^{125}I-HBsAg+adj1+adj2. The localization of vaccinated L-HBsAg was monitored for 5 weeks using animal SPECT/CT. To monitor the immune response, the luciferase expressing splenocytes from the B6.Luc^{TG} were injected intravenously into vaccinated B6 mouse. Bioluminescence signals from splenocytes were measured by IVIS 100 system. The BLI signals from the lymph nodes, organs, and vaccination site were analyzed over time course.

Results: A novel luciferase transgenic mouse model (B6.Luc^{TG}) was generated to monitor the immune response. To visualize vaccinated antigen, large hepatitis B virus antigen (L-HBsAg) was labeled with radioiodine (^{125}I-HBsAg). B6 mice were vaccinated intramusculary with ^{125}I-HBsAg, ^{125}I-HBsAg+adj1 and ^{125}I-HBsAg+adj1+adj2. The localization of vaccinated L-HBsAg was monitored for 5 weeks using animal SPECT/CT. To monitor the immune response, the luciferase expressing splenocytes from the B6.Luc^{TG} were injected intravenously into vaccinated B6 mouse. Bioluminescence signals from splenocytes were measured by IVIS 100 system. The BLI signals from the lymph nodes, organs, and vaccination site were analyzed over time course.

Conclusions: In conclusion, in vivo real-time bioluminescent monitoring of splenocytes homing and proliferation against vaccination successfully provides efficiency of adjuvants. Our system can be used for evaluation of efficacy of vaccination by enhanced the proliferation and activation of splenocytes near the vaccination site.

Molecular Imaging_22

Antibody Mimics, Fibronectin Domain III for EphA2-targeting as a Probe in Murine Tumor Model

Yeongjin Hong, Seung-Hwan Park, Sukho Park, Dong-Geun Lee, Dong-Yeon Kim, Jung-Joon Min

Chonnam National University Hwasun Hospital, Korea

Monobodies are binding scaffold proteins originating from a human fibronectin domain III (Fn3) scaffold that can be easily engineered with specificity and affinity. Human EphA2 (hEphA2) is an early detection marker protein for various tumors including lung, breast, and colon cancer.

We isolated two hEphA2-specific monobodies (E1 and E10) by screening a yeast surface display library. They showed high affinities (Kd~2nM) against recombinant human EphA2 (hEphA2).

In ELISA against EphA2 and their homologs, they only bound hEphA2 and mEphA, although binding to hEphA2 binding is 2-fold higher than mEphA2. Also they showed similar binding to the cells and tumor tissue with EphA expression on the cell surface. In vivo optical imaging showed a strong targeting of Cy5.5-labled E1 in EphA2 over-expressing xenograft models (PC3 cells).

The highly specific monobody E1 is useful as a hEphA2 probe candidate for in vivo diagnosis and therapy.

Molecular Imaging_24

Assessment airway involvement in Relapsing Polychondritis use ^{18}F-FDG PET-CT

Fei Feng, Changjing Zuo

Department of Nuclear Medicine, Changhai Hospital, The Second Military Medical University, China

Objectives: Relapsing polychondritis (RP) is a rare, chronic inflammatory disease. ^{18}F-FDG PET-CT is used

as a powerful tool to evaluate not only the cancer but also inflammation disease, nowadays. To evaluate whether the ^{18}F-FDG PET-CT is useful to assessment of airway involvement of RP.

Methods: We retrospectively reviewed 7 RP patients (6male/1female; average age 56.29±7.83) who went whole body ^{18}F-FDG PET-CT scan in our department and summarized image characters.

Results: Of these 7 patients, 5pts had the history of RP and relapsed, 2pts were newly diagnosed as RP. Clinical symptoms mainly cough, hawking and asthma. C-reactive protein level increased in 5pts and normal in 2pts, 43.53±36.04mg/L. All the patients had bronchoscope and biopsy.The whole body ^{18}F-FDG PET-CT image changes mainly airway changes,include laryngeal cartilages proliferation and calcification in 6pts with FDG uptake increased,SUV_{max}=3.98±1.29. Trachea or bronchus constricted in 7pts with or without the wall thickened (2pts), the FDG uptake increased in 4pts, SUV_{max}=3.71±1.89, while normal in 3pts. Other changes include pulmonary emphysema in 7pts and costal cartilage ossification and high FDG uptake in 3pts,SUV_{max}=5.36.

Conclusions: ^{18}F-FDG PET-CT can well reflected the airway involvement in RP patients according to anatomical changes and metabolic changes.

Molecular Imaging_26

^{18}F-FDG PET/CT Negative But ^{11}C- HED PET/CT Positive In Bladder Paraganglioma: A Case Report

Haonan YU[1], Jiang LI[2], Qiu song CHEN[1]*

1. Department of PET-CT Diagnostic, Tianjin Medical University General Hospital, Tianjin
2. People's Republic of China Department of Urology, Tianjin Medical University General Hospital, Tianjin, People's Republic of China

Objectives: Bladder paraganglioma is a rare neuroendocrine tomour arising from the catecholamine-producing chromaffin cells in extra-adrenal sympathetic paraganglia associated with the urinary bladder wall. A 30-year-old male was referred to the hospital with severe hypertension and palpitation after voiding. A lump was detected in the bladder by ultrasonography. The patient was suspected to paraganglioma, and positron emission tomography with computed tomography (PET/CT) examination was recommended for further investigation.

Methods: ^{11}C-Hydroxyephedrine (^{11}C-HED) is reported as one of the positron-emitting probes of the sympathoadrenal system administered in humans. Similar to ^{131}I- MIBG, it is also a catecholamine substrate analog which targets the cell membrane norepinephrine transporter and vesicular monoamine transporters. The patient was subjected to ^{18}F-FDG PET/CT and ^{11}C-HED PET/CT scans.

Results: The ^{11}C-HED PET/CT scan showed a positive image, while ^{18}F-FDG was negative. THe patient underwent an operation of tomour resection, the pathological diagnosis confirmed the diagnosis of paraganglioma. Shinji et al. studied a cohort of 134 patients suspected pheochromocytoma and paraganglioma using ^{11}C-HED PET/CT for diagnoses, demonstrated 91% sensitivity and 100% specificity. The value of ^{11}C-HED PET for pre- and post-operative clinical management of pheochromocytoma has been investigated in comparison to MIBG scintigraphy, ^{18}F-FDG PET and CT/MRI, especially in detecting recurrent and metastatic disease.

Conclusions: ^{18}F-FDG positive uptake had been reported in ^{131}I-MIBG-negative paraganglioma patients. Our literature search revealed no case report describing the use of ^{11}C-HED to detect metastatic extension or other extra-adrenal locations in bladder paraganglioma. In this case, ^{11}C-HED PET/CT showed its potential clinical value in localizing the tumour arising from sympathetic nerve.

Molecular Imaging_28

Enhancement of expression of sodium/iodide symporter (NIS) in anaplastic thyroid cancer cell by candidate chemicals

Ji Min Oh[1], Senthilkumar Kalimuthu[1], Xiu Juan Li[1], Prakash Gangadaran[1], Shin Young Jeong[1], Sang-Woo Lee[1], Jaetae Lee[1, 2] and Byeong-Cheol Ahn[1]*

1. Department of Nuclear Medicine, Kyungpook National University School of Medicine, Hospital, Daegu-700-721, Republic of Korea
2. Daegu-Gyeongbuk Medical Innovation Foundation (DGMIF), 80 Cheombok-ro, Dong-Gu, Daegu, 701-310, Republic of Korea

Objectives: Among thyroid cancers, anaplastic thyroid cancer (ATC) which does not have Sodium/iodide symporter (NIS) expression, is the most aggressive and resistant cancer to the radioiodine treatment and has poorest prognosis. NIS is the protein which captures iodine in the thyroid cells and can be used for both diagnosis and therapeutic target for the thyroid cancer. Enhancement of NIS expression is able to make the ATC more susceptible

to radioiodine therapy, the aim of this study is search small molecules having ability of enhance NIS expression in ATC cells using NIS promoter reporter gene system.

Methods: 8505C (ATC) was transfected with dual NIS promoter and CMV promoter driven reporter gene system (pNIS-FL2-TurboFP635-pCMV-Rluc plasmid) to make stable cell line (8505C-pNIS-pCMV). The reporter system was confirmed by bioluminescence imaging of 8505C-pNIS-pCMV 8505C-pNIS-pCMV was treated with valproic acid (VPA), sodium butyrate (NaB) and sorafenib tosylate (Soraf) to induce activation of the NIS expression.

Results: 8505C-pNIS-pCMV having dual NIS promoter and CMV promoter driven reporter gene system was stably established confirmed by bioluminescent imaging (BLI). In vitro BLI signals of Fluc (R^2=0.9245, P<0.0001) and Rluc (R^2=0.9820, P. <0.05) increased by increase of cell number. The VPA and Soraf treatments to the 8505C-pNIS-pCMV enhanced NIS promoter activity in dose dependent-manner, but NaB didn't. The VPA and Soraf treatments to the 8505C-pNIS-pCMV increased iodine uptake to the cells.

Conclusions: We developed dual NIS promoter and CMV promoter driven reporter gene system to monitor NIS promoter activity which can be used to screen candidate chemicals of enhancing NIS expression. Results of this study suggest that VPA and Soraf can restore the radioiodine avidity of ATC.

Molecular Imaging_30

Evaluation of migration ability of BMDC stimulated with different cytokine condition with fluorescent optical imaging

Su-Bi Ahn[1], Ho Won Lee[1], Thoudam Debraj Singh[1], Seul-Gi Oh[1], Sang Bong Lee[1,3], Shin Young Jeong[1], Sang-Woo Lee[1,3], Jeoung-Hee Ha[2], Byeong-Cheol Ahn[1], Yong Hyun Jeon[1,3], Jaetae Lee[1,4]

1. Department of Nuclear Medicine, Kyungpook National University, Daegu, Korea
2. Department of Pharmacology, Kyungpook National University, Daegu, Korea
3. Leading-edge Research Center for Drug Discovery and Development for Diabetes and Metabolic Disease, Kyungpook National University Hospital, Daegu, Korea
4. Daegu-Gyeongbuk Medical Innovation Foundation (DGMIF), Daegu, Korea

Objectives: Non-invasive imaging tools with simple and easy labeling have been strongly required to validate the migration levels of DC induced by appropriate cytokines to draining lymph nodes, which facilitate the protocol optimization of DC-based immunotherapy.

Here, the aim of this study is to evaluate the migration ability of BMDC stimulated with different cytokine condition with *in vivo* fluorescent optical imaging in living mice.

Methods: To generate the bone marrow-derived dendritic cells (BMDCs), bone marrow cells from C57BL/6 mice were differentiated with either GM-CSF or with GM-CSF plus IL-4 for 7days. To characterize the differentiated BMDC with different cytokine conditions, phenotype marker analysis ($CD^{11}C$, MHC class I and II, CD54, CD86 and CCR7) and antigen uptake assay and transwell migration test were performed. For in vivo DC tracking, respective BMDCs were labeled with *in vivo* compatible fluorescent dye (DiD, Ex/Em: 644/665, Invitrogen) and labelled cells were subcutaneously injected to footpad of mice. *In vivo* fluorescent imaging (FLI) were conducted from 2h until 72h post-injection of labelled DCs. To further determine the existence of migrated BMDCs, draining popliteal lymph nodes (DPLN) were excised and then both ex vivo BLI and flow cytometry analysis were done.

Results: No significant difference of phenotype expression level, antigen uptake level and migration ability was shown between GM-CSF-induced BMDC and GM-CSF/IL-4-induced BMDCs. *In vivo* FLI imaging revealed that the migration of GM-CSF-induced BMDC to DPLNs was detected at as early as 2h and FLI signals emitted from labeled cells gradually increased at 24h, showing that it reached peak at 72h. Contrary to GM-CSF-induced BMDC, the movement of GM-CSF/IL-4-induced BMDCs was identified at 24h and FLI signals reached peak at 48h. Furthermore, the migration level was approximately two fold higher in GM-CSF- induced BMDC than GM-CSF/IL-4-induced BMDC, which is consistent with *ex vivo* FLI of excised DPLN. Subsequently, using FACS analysis, we can further confirm that DiD-positive population is about two fold higher in the DPLN from mice receiving GM-CSF-induced BMDC than mice receiving GM-CSF/IL-4-induced BMDC.

Conclusions: We successfully visualized DC migration efficacy with fluorescent dye(DID) in different culture conditions and compared the anti-tumor immunity by vaccination of BMDCs(GM-CSF or GM-CSF/ IL-4) in living animal.

Molecular Imaging_31

In vivo optical imaging for detection of macrophage migration to tumor lesion and their promotion of tumor growth in living mice with colon cancer

Seul-Gi Oh[1], Su-Bi Ahn[1], Ho Won Lee[1], Thoudam Debraj Singh[1], Sang Bong Lee, Shin Young Jeong[1], Sang-Woo Lee[1], Jeoung-Hee Ha[2], Byeong-Cheol Ahn[1], Yong Hyun Jeon[1,3] , Jaetae Lee[1,4]

1. Department of Nuclear Medicine, Kyungpook National University, Daegu, Korea
2. Department of Pharmacology, Kyungpook National University, Daegu, Korea
3. Leading-edge Research Center for Drug Discovery and Development for Diabetes and Metabolic Disease, Kyungpook National University Hospital, Daegu, Korea
4. Daegu-Gyeongbuk Medical Innovation Foundation (DGMIF), Daegu, Korea

Purpose: The aim of this study is to not only track the macrophage migration to tumor lesion with an enhanced firefly luciferase but also evaluate the effect of migrated macrophage on tumor growth with mcherry gene as an fluorescent reporter in living mice with colon cancer.

Methods: Murine macrophage Raw264.7 cells expressing an enhanced firefly luciferase (Raw/effluc) and murine colon cancer CT26 cells expressing a mcherry gene (CT26/M) were established. For in vivo tracking of macrophage, subcutaneous tumor model with CT26/M were established. When tumor mass were detected, either PBS or Raw/effluc cells was intravenously transferred to tumor-bearing mice (Group 1: CT26/M alone, Group 2: CT26/M+Raw/effluc). Thereafter, bioluminescence (BLI) was conducted once a day from day 1 to day 4 post-transfer of macrophage. In vivo fluorescent imaging (FLI) was done daily from day 1 to until day 11 post-transfer of macrophage. To evaluate the effect of dexamethasone (DEX) treatment on both macrophage migration and tumor progression, tumor-bearing mice i.p received DEX right after transfer of Raw/effluc cells (Group 1: CT26/M alone, Group 2: CT26/M+Raw/effluc, Group 3: CT26/M+Raw/effluc+DEX) and macrophage migration and tumor growth rate was evaluated by combined FLI and BLI.

Results: The migration of macrophage to tumor lesion was detected at day 1 and BLI signals were distinct at tumor lesion until day 4. The location of macrophage migrated to tumor was well matched with FLI signals from CT26/M tumor. Interestingly, in vivo FLI of tumor progression demonstrated that the rate of tumor growth is significantly more increased in CT26/M+Raw/effluc group than CT26/M alone group, suggesting that Raw/effluc promote the growth of colon cancer (P<0.05). DEX treatment inhibited the migration of Raw/effluc cells to tumor lesion and retardation of tumor growth was detected in DEX-treated group compared with either CT26/M alone group or CT26/M+Raw/effluc group.

Conclusions: We successfully visualized not only the macrophage migration toward tumor lesion but also enhanced tumor growth mediated by macrophage with in vivo optical reporter gene imaging, and furthermore demonstrated the inhibitor effects of DEX on macrophage migration and tumor progression.

Molecular Imaging_34

Radiation dosimetry and biodistribution of ^{99m}Tc-RGD-BBN peptide in patients with breast cancer

Bin Ji, Tiefeng Ji, Shi Gao, Bin Chen, Qingjie Ma*

Department of Nuclear Medicine,China-Japan Union Hospital of Jilin University, Changchun 130033, China

Purpose: Integrin $\alpha_v\beta_3$ and bombesin are well-established targets for developing radiopharmaceuticals for imaging of breast cancer. ^{99m}Tc- Glu-c(RGDyK)-bombesin (^{99m}Tc RGD-BBN), a new dual integrin $\alpha_v\beta_3$ and GRPR targeted peptide, was proved to be a novel radiopharmaceutical for breast cancer imaging. This study reports the first, to our knowledge, human data in female with breast cancer.

Methods: Six female patients with breast cancer were examined. The safety after ^{99m}Tc-RGD-BBN injection were assessed. Serial whole-body scans were acquired at 10min, 30min, 60min, 120min and 1440min after injection of ^{99m}Tc-RGD-BBN. Blood and urine samples for metabolite analysis were taken at 1, 3, 5, 10, 15, 30, 60, 120 min and 0-2, 2-4, 4-8, 8-12 and 12-24 h post-injection. Regions of interest (ROI) were delineated for various source organs and the tumor. Tumor-background (T/B) ratios of all imaging time points were calculated. The OLINDA/EXM 1.0 software was used to estimate the equivalent organ doses and the effective dose.

Results: No serious adverse events or abnormal clinical chemistry were reported by the patients during the study. ^{99m}Tc-RGD-BBN showed rapid clearance from the blood and continuous increasing in urine. Bladder and kidney demonstrated predominant uptake, whilst uptake in heart and brain

was low. The primary tumor was well visualized and the ideal time point was 120min with highest T/B ratio. The highest absorbed radiation dose was in the kidneys ($2.43E\times10^{-2}$ mGy/MBq) and the effective dose was 2.20×10^{-3} mSv/MBq.

Conclusion: ^{99m}Tc-RGD-BBN appears to be safe and to have acceptable dosimetric and biodistribution properties as a diagnostic breast cancer imaging agent.

Molecular Imaging_37

The Relationship between Primary Lesion Glucose Metabolism of NSCLC and Chemotherapy: A Preliminary Study according to PERCIST Criteria

Meijie Chen, Na Li, Bulin Du, Yaming Li*

The First Hospital of China Medical University, Nuclear Medicine Department

Purpose: The aim of this study is to investigate whether metabolic tumor volume (MTV) and total lesion glycolysis (TLG) of primary tumor can give a prediction of the sensitivity in non-small cell lung cancer chemotherapy.

Methods: 18 cases with phase III~IV non-small cell lung cancer patients were reviewed retrospectively, who received platinum-based first-line chemotherapy and had ^{18}F-FDG PET/CT examinations both before and after therapy. MTV and TLG were determined with two thresholds which were 30%SUV_{max} and 50%SUV_{max}, using PERCIST criteria to evaluate outcome. Statistical analysis included rank-sum test and ROC curve

Results: The change rates of indicators including $\Delta TLG_{30\%SUVmax}$ (u=73, P=0.003), $\Delta MTV_{30\%SUVmax}$ (u=73, P=0.003), $\Delta TLG_{50\%SUVmax}$ (u=65, P=0.025), $\Delta MTV_{50\%SUVmax}$ (u=65, P=0.025) and ΔSUV_{max} (u=74, P=0.003) were statistically significant. According to ROC curve, when change rates of TLG and MTV were 62.2% and 56.3% respectively could discriminate sensitivity to chemotherapy with threshold of 30%SUV_{max}, as well as 68.9%, 63.3% with threshold of 50%SUV_{max}.

Conclusions: The change rates of TLG and MTV of primary tumor in non-small cell lung cancer patients can contribute to filtering out chemotherapy sensitivity.

Molecular Imaging_46

Evaluation and analysis of gene expression profiling of metastatic tumors after γ-irradiation

Su Jin Jang, Yong Jin Lee, Kwang Il Kim, Tae Sup Lee, Min-Jung Seo, Kwang Sun Woo, Wee Sup Chung, Jae Gol Choe, Sang Moo Lim, Joo Hyun Kang

Korea Institute of Radiological and Medical Sciences, Korea

Recently, a few reports indicated that a metastatic growth of several human cancer cells could be promoted by radiotherapy. Regular follow-up examinations, such as imaging and tumor marker tests, may be required to detect this metastasis at an early stage.

C6-L cells (5×105) expressing firefly luciferase(fLuc) gene in rat glioma cells (C6) were implanted subcutaneously into right thigh of BALB/c nu/nu mice. γ-irradiation (γ-IR) was locally treated into C6-L xenografted mice with 50 Gy in five 10 Gy fractions. After 1-10 weeks of γ-IR, γ-IR -induced metastasis was evaluated by imaging techniques such as bioluminescence imaging (BLI) and [^{18}F] FDG or [^{18}F]FLT small animal PET/CT. Mice were sacrificed and non-radiated primary tumor (NRPT), radiated primary tumor (RPT) and metastatic lung nodule were removed. Total RNA from NRPT, RPT and metastatic lung nodule was isolated and analyzed with microarray.

After 6-9 weeks of γ-IR, a γ-IR-induced metastasis in lung was detected by BLI and observed in 6 (17.1%) among the 35 mice. A distant metastasis was also detected by [^{18}F]FDG or [^{18}F]FLT small animal PET/CT images and autoradiography with ^{18}F-FLT. The image clearly demonstrated high uptake of [^{18}F]FLT and [^{18}F] FDG in the metastatic nodule of lung. In case of non γ-IR group, there was no occurrence of metastasis at a secondary site. The expression patterns of whole mRNAs were analyzed by microarray to elucidate the changes among NRPT, RPT and metastatic lung nodule after γ-IR. We identified a set of 2,340 genes and 1,296 genes that were differentially expressed between the RPT vs NRPT and metastatic lung nodule vs RPT (fold change ≥ 2).

In this study, we observed γ-IR -induced metastasis in tumor-bearing animal model using molecular imaging methods and analyzed gene expression profiling for elucidation of genetic changes after γ-IR.

Molecular Imaging_47

Heterogeneity of brain metabolism by global and textural feature analysis in ^{18}F FP-CIT images for diagnosis of Parkinson's disease

Hyun Jin Yoon, Young Jin Jeong, Hye Joo Son, Do-Young Kang

Departments of Nuclear Medicine, Dong -A University Medical Center ,Dong-A University, Korea

The quantification of heterogeneity for the region of striatum with ^{18}F FP-CIT PET uptake images will be useful in clinical routine for diagnosis, staging, and response to prediction. The aim of this study was to evaluate various parameters obtained the quantification of heterogeneity for the prediction of stages in patients with Parkinson's disease (PD).

The volume of interest (VOI) was delineated according to equi-contour line around SUV 3.0 g/ml for each region of striatum by PMod 3.6. The values of global and textural feature were analyzed within VOI of 26 patients with and without PD. The global parameters were SUV_{max}, SUV_{mean}, SUV_{SD}, SUV skewness, SUV kurtosis, TLG, tumor volume, entropy and SUV_{peak}. Fifty-nine parameters from textural feature analysis were calculated using co-occurrence, voxel-alignment, neighborhood intensity difference, intensity size-zone, normalized co-occurrence, texture spectrum, texture feature coding, texture feature coding co-occurrence and neighborhood gray-level dependence.

Seventy-two parameters related to heterogeneous were analyzed to distinguish between with and without PD by global and textural feature analysis. The distinction of metastasis in the striatal region of the patients with and without PD was possible by the 13 global parameters (SUV_{max}, SUV_{mean}, SUV_{SD}, SUV variance, SUV kurtosis, SUV_{peak}, etc.) from SUV statistics and the textural feature analysis. Most of the parameters could distinguish between PD and non-PD by the values. Contrast, high-intensity run emphasis, high-intensity short-run emphasis, high-intensity long-run emphasis, size-zone variability, zone percentage, SUV_{max}, SUV_{SD}, SUV skewness, SUV_{peak}, max spectrum, second angular moment, homogeneity, inverse difference moment could distinguished 2 characteristics with PD or not.

The heterogeneous of the striatal region with PD could be distinguished from the patients without PD in most cases from the value of 72 parameters related to the volume and SUV distribution of ^{18}F FP-CIT images. Heterogeneous from local analysis was closely related to monotonous or versatile intensity-histogram pattern, but less related to the volume of striatum.

Molecular Imaging_48

In vivo monitoring of CD44+ cancer stem like cell in breast cancer by gamma irradiation

Mi Hyun Kim, Min Hwan Kim, Ran Ji Yoo, Eun Sang Lee, Gwang Sun Woo, Seung Woo Park, Young Hoon Ji, Kwang Il Kim, Tae Sup Lee, Phil Youl Ryu, Joo Hyun Kang, Yong Jin Lee

Korea Institute of Radiological and Medical Sciences, Korea

This study aimed on noninvasive in vivo monitoring of CD44 positive cancer stem like cells in breast cancer by gamma irradiation using molecular image by fusing the firefly luciferase (fLuc) gene with the CD44 promoter.

Breast cancer cell line was transfected and generated to stably expressed fLuc used recombinant lentiviral vector controlled by CD44 promoter (MCF7-CL). The luciferase activities of MCF7-CL were monitored by bioluminescence assay. Irradiated sphere-formed MCF-CL was observed of CD44 and other CSCs markers, by immunofluorescence, flow-cytometry and RT-PCR. CD44+ cells were sorted by MACs systems. MCF7-CLs were injected into the mice and irradiated by using a cobalt-60 source. A total of 88 mice were used for all in vivo tumor growth and imaging experiments. Then, in vivo monitoring was performed to observe the bioluminescence imaging (BLI). Statistical analyses were performed using GraphPad PRISM.

MCF7-CL grown as irradiated and sphere-formed, which enrich for CSCs, increased bioluminescence activity than non-treated cells and showed up-regulated CD44 and other CSCs markers. When MCF7-CL was treated with siCD44 and irradiated, CD44 expression was inhibited and cell survival ratio was decreased. In vivo BLI, 6 Gy irradiated mice were shown stronger signal (1.2×107 p/s/cm2/sr) than controls (4.4×106 p/s/cm2/sr). CD44+ CSCs showed high BLI signal and tumor growth. In irradiated cancer, relative BLI signal was increased, but tumor volume was decreased.

This system could be useful to evaluating CD44 expressed CSCs in breast cancer by BLI in vivo as well as in vitro during chemo- and radiotherapy.

Cardiology_1

Synthesis and Evaluation of the Tc-^{99m} RRL-containing Hexa-Peptide for Non-Invasive Angiogenesis Imaging in Mice Model of Ischemia

Dae-Weung Kim[1,2], Myoung Hyoun Kim[1], Chang Guhn Kim[1]

1. Department of Nuclear Medicine and Institute of Wonkwang Medical Science, Wonkwang University School of Medicine, Iksan, Jeollabuk-do, Korea
2. Research Unit of Molecular Imaging Agent (RUMIA), Wonkwang University School of Medicine, Iksan, Jeollabuk-do, Korea

Purpose: Arginine-arginine-leucine (RRL) is considered as a tumor endothelial cell-specific binding peptide sequence. RRL-containing peptide could be an excellent candidate for angiogenesis imaging. In this study, we developed RRL-containing hexapeptide, glutamic acid-cysteine-glycine (ECG)-RRL, and evaluated the feasibility of Tc-99m ECG-RRL as a non-invasive angiogenesis imaging in hind limb ischemia mice model.

Methods: Hemi-hind limb ischemia mouse models were prepared by ligating the proximal end of the superficial femoral artery and vein, the origins of the popliteal artery and vein, and the distal portions of the saphenous artery and vein with surgical silk. Hexapeptide, ECG-RRL was synthesized using Fmoc solid-phase peptide synthesis. Radiolabeling efficiency was evaluated using radio-high-performance liquid chromatography (radio-HPLC) and instant thin layer chromatography (ITLC). Gamma imaging with Tc-99m tetrofosmin was performed to observe the changes of perfusion at 7, 14, 21 and 28 days after operation. Gamma imaging with Tc-99m ECG-RRL was also performed at 9, 16, 23 and 30 days after operation.

Results: After radiolabeling procedures with Tc-99m, the complexes of Tc-99m ECG-RRL was prepared in high yield. The ischemic-to-non ischemic limb uptake ratio of Tc-99m tetrofosmin was gradually increased after operation (0.28 ± 0.21, 0.35 ± 0.07, 0.85 ± 0.30 and 0.90 ± 0.05 at 7, 14, 21 and 28 days after operation). On the contrary, Tc-99m ECG-RRL was accumulated substantially in the ischemic limb at 9 days (1 week) after operation, and then gradually decreased. The ischemic-to-non ischemic limb uptake ratio of Tc-99m ECG-RRL was 3.71 ± 0.77, 2.81 ± 0.86, 3.09 ± 0.70 and 1.70 ± 0.14 at 9, 16, 23 and 30 days after operation

Conclusions: This study successfully had developed Tc-99m ECG-RRL and Tc-99m ECG-RRL is a good candidate for the angiogenesis imaging. Further studies correlating Tc-99m ECG-RRL uptake with histologic capillary density and other perfusion measurement methods, were recommended.

Cardiology_2

The Significance of ECG Changes During Adenosine Infusion as a stress agent for Myocardial Perfusion Imaging (MPI) in Predicting Coronary Artery Disease (CAD)

H.Amer[1], K.Niaz[2], Imran Ali[3], A.Jelani[4], M.Sheikh[5]

1. King Abdullah International Medical Research Center
2. King Saud bin Abdulaziz University for Health Sciences, Department of Medical Imaging, Department of Cardiology
3. King Abdulaziz Hospital – NGHA, Al ahasa, Saudi Arabia

Purpose: Selection of the most appropriate stress method is one of the keys to success in myocardial perfusion scintigraphy. Adenosine infusion is not without side effects which may range from minor effects to major consequences. ECG changes are recognized complications of adenosine stress test and their manifestation may range from minor to life threatening changes that urge for stopping the whole procedure. The significance of electrocardiographic ECG changes during adenosine stress test is debatable. This study will further elaborate the significance of these changes in predicting the possibility of CAD.

Methods: This was a retrospective observational registry performed in a single center in the Kingdom of Saudi Arabia. The data were collected from the nuclear medicine database identifying all the reported Gated myocardial perfusion SPECT with adenosine stress tests between January 2013 and January 2014.The adenosine dose were fixed with all patients based on body weight and was given as a continuous infusion of 140 mcg / kg / min over a 6-minute period. Injection of a cardiac radiopharmaceuticals was given at 3 minutes of this 6- minute protocol.

Results: There were 346 patients identified with cardiac nuclear scans in the pre-specified time frame who subjected to adenosine stress scan. 152 of these patients were male accounting for 44% of the total population. Average age at the time of examination was 60.82 ± 11.29 years. Patients were presented with one or more risk factors. Patients with base line abnormalities, past history of CAD with or without PCI or CABG and previous MI were excluded from the study. Ninty eight patients (28%) were reported as positive for CAD, 40 patients were reported with ischemic ECG changes (12%) during adenosine infusion, 23 patients who have ischemic changes were positive on MPI, while 17 patients who have positive ECG had a negative MPI. Odd Ratio (OR) was 4.16 , 95% C.I. was (2.11-8.18). Fisher Exact test was

applied and showed a P value of < 0.01. No reported case of asystole, myocardial infarction or complete heart block in this study period.

Conclusions: The development of ischemic changes during adenosine myocardial perfusion imaging (MPI) has been shown to be a predictor of CAD and consequently subsequent cardiac events and worse outcome. Our study showed that the probability of a positive MPI is 4 times higher with a positive ECG ischemic changes during adenosine stress test and consequently these ECG ischemic changes should be taken in consideration in the final report.

Cardiology_7

Correlation TID With Cardiac Events (Preliminary Study)

Hanif Afkari[1], A. Hussein S Kartamihardja[1]

1. Department of Nuclear Medicine and Molecular Imaging, Faculty of Medicine
2. Universitas Padjadjaran /RSUP Dr. Hasan Sadikin Bandung, Indonesia

Purpose: Myocardial Perfusion Scintigraphy (MPS) provides important information for prognosis, risk stratification, and help make decisions on patient treatment of coronary artery disease (CAD) or CAD suspected. The normal value of MPS has a very low risk of cardiac events exposed in 1-2 years while the MPS results are abnormal increased risk of these events up to 10 times compared to normal. In abnormal results of MPS, Transient Ischemic Dilation (TID) is an independent and incremental prognostic marker of cardiac event. The aim of this study is to find out correlation between TID and cardiac events.

Methods: The retrospective study was collected from medical records of abnormal MPS patients in the nuclear medicine and molecular imaging Hasan Sadikin Hospital. The inclusion criteria are patients abnormal MPS which can monitoring cardiac events. Patients are divided into 2 groups based on the value of TID (Group I: TID abnormal (> 1.12); Group 2 TID normal (≤ 1.12)). Based on defects size (number of abnormal segments), subjects divide into 3 categories (mild, moderate and large).

Results: MPS abnormal values obtained on 118 subjects with only 19 (16%) who met the inclusion criteria. Group 1 as 6 subjects and group 2 were 13 subjects. The range of monitoring was 22-52 months after MPS. There are differences in the incidence of cardiac events in both groups on a hard events (grup1: 21:43% vs 16.67%) and soft events (83.33% vs 78.57%). Subjects with mild category with different TID, incidence of cardiac events twice in group 1 compared to group 2 (33.33% vs 20%). Four subjects got hard events less than six months. Three of them underwent PCA and only one subjects treatment by pass.

Conclusions: There was no correlation between TID and cardiac events in patients with abnormal myocardial perfusion scintigraphy.

Cardiology_9

Transient Ischemic Dilation as a Predictor of Perfusion Improvement in Persistent Perfusion Defects after Coronary Artery Bypass Graft

Hendra Budiawan[1,2], Sohyun Park[1], Gi Jeong Cheon[1], Jin Chul Paeng[1], Keon Wook Kang[1], June-Key Chung[1], Dong Soo Lee[1]

1. Department of Nuclear Medicine, Seoul National University Hospital, Seoul, Korea
2. Department of Nuclear Medicine, Mochtar Riady Comprehensive Cancer Centre, Jakarta, Indonesia

Purpose: It is not uncommon that perfusion improvement were found in cases of irreversible perfusion defects on ^{201}Tl myocardial perfusion scan (MPS) as proved by the presence of normal thallium uptake and better myocardial function after revascularization on the following scans. Transient ischemic dilation (TID) known as the indicator of multivessel disease reflecting the ischemic status were sometimes present in those cases. The objective of this study was to find out the significance of the presence of high TID ratio in detecting perfusion defect area that will show perfusion improvement after coronary artery bypass graft (CABG).

Methods: Subjects of this study were coronary artery disease (CAD) patients who had irreversible perfusion defects on ^{201}Tl rest/dipyridamole stress ^{99m}Tc-methoxyisobutylisonitrile (MIBI) gated myocardial SPECT during 2008-2009. Perfusion improvement of irreversible perfusion defects were determined visually on the following MPS. Besides qualitative analysis using 17-segment cardiac model, TID ratio analysis was performed using Quantitative Gated SPECT (QGS) developed by Cedar-Sinar Medical Center).

Results: During 2008-2009 there were 14 cases of persistent perfusion defects that showed perfusion improvement in some areas (10 males, 4 females; age 64.5+10.8) on the following scans, while the second

group consisting of 38 patients (27 males, 11 females; age 69.8+7.8) still showed irreversible perfusion defects. The mean TID ratio of the first group was significantly higher (1.32+0.08; range: 1.20 – 1.45) than the second group (1.09+0.13; range: 0.78 – 1.32).

Conclusions: Persistent perfusion defects that showed perfusion improvement on the subsequent scans are not uncommon findings. The presence of transient left ventricular enlargement (high TID ratio) in such cases may suggest the possibility of perfusion improvement after CABG.

Cardiology_11

Diagnosis of Coronary Artery Disease: Direct Comparison of Dual-Source CT Angiography, Dual-Energy CT Perfusion, MRI, and SPECT

Hyun Woo Chung

Konkuk University Medical Center, Nuclear Medicine, Korea

We investigated the diagnostic value of dual-source computed tomography angiography (DSCTA), dual-energy computed tomography (DECT), magnetic resonance imaging (MRI), single-photon emission computed tomography (SPECT), and the combined evaluation of DSCTA and myocardial perfusion imaging for coronary artery disease (CAD).

The records of 25 patients who underwent DSCTA, DECT, MRI, and SPECT to evaluate suspected CAD were reviewed retrospectively. Conventional coronary angiography was used as the reference standard.

For per-vascular territory analysis using DSCTA, DECT, MRI, SPECT, DSCTA+DECT, DSCTA+MRI, and DSCTA+SPECT, the sensitivities were 96.7% (29/30), 90.0% (27/30), 93.3% (28/30), 63.3% (19/30), 86.7% (26/30), 90.0% (27/30), and 63.3% (19/30), respectively. The specificities were 75.6% (34/45), 73.3% (33/45), 88.9% (40/45), 88.9% (40/45), 82.2% (37/45), 91.1% (41/45), and 93.3% (42/45), respectively. For per-patient analysis using DSCTA, DECT, MRI, SPECT, DSCTA+DECT, DSCTA+MRI, and DSCTA+SPECT, the sensitivities were 100% (18/18), 100% (18/18), 100% (18/18), 88.9% (16/18), 100% (18/18), 100% (18/18), and 88.9% (16/18), respectively. The specificities were 14.3% (1/7), 42.9% (3/7), 71.4% (5/7), 57.1% (4/7), 42.9% (3/7), 71.4% (5/7), and 57.1% (4/7), respectively. MRI and DSCTA+MRI showed high specificity without a loss of sensitivity. Therefore, MRI may be the most appropriate imaging modality for the detection of CAD.

Cardiology_16

Application of Appropriate Use Criteria for Myocardial Perfusion SPECT Indications in an academic tertiary care teaching hospital - An Audit.

Kavitha Nallapareddy, Rakhi

Nizams Institute of Medical Sciences, India

To audit the clinical indications of MP SPECT by applying AUC in our territory care teaching hospital . This is a small attempt to audit our indications in India where AUC is not very popular.

This is a retrospective analysis of clinical indications of MP SPECT studies requested over a period of three months in a teritiary care academic institution . Indications were categorized according to ACC & ASNC AUC criteria.

Demographic characteristics, symptoms,ECG findings,previous history of coronary procedures and details of the non cardiac surgeries (in setting of pre op evaluation) are all taken into consideration. The data is analysed by a medical officer conducting stress procedures and the NM physician.

The history sheets of the 246 patients referred to the NM department were reviewed. Age range was 37-92 years with 146 (59%) men and 100 (41%) females.

There were 164 (66.7%) appropriate , 36 (14.6%) inappropriate and 46 (18.7%) uncertain indications. The most common inappropriate & uncertain indications are asymptomatic <2yrs after percutaneous coronary intervention , new symptoms in a prior normal CAG ,pre op risk assessment for low risk surgeries and low pretest likelihood of CAD.

In this small attempt to audit the AUC in a teaching hospital majority of indications for MYP SPECT were appropriate. However the sum of inappropriate & uncertain

studies coming up to one third , which is still a substantial proportion in an academic institution.This could be reduced by increasing the awareness of the well said ACC & ASNC laid AUC for Myp scintigraphy in the referring clinician group.

Cardiology_20

Prone versus Supine Position in Detecting Inferior Wall Lesion in Myocardial Perfusion SPECT: A Meta-analysis

Jerry M. Obaldo, Allanbert Gamido Sampana, Deverly T. Tumapon, Herwin John M. Aycocho

Philippine Heart Center, Philippines

To compare the sensitivity and specificity of supine

versus prone position during myocardial perfusion scintigraphy in diagnosis of disease in the inferior wall.

Data Sources: Medline, Embase, bibliographies and references.

Study Selection: Prospective or cross sectional studies that determine the sensitivity and specificity of myocardial perfusion scintigraphy in diagnosing disease in the inferior wall, when the patient is in supine or prone. Coronary angiography was used as standard.

The average sensitivity of supine and prone were 82% (CI 78%-86%) and 80% (CI 73%-84%) respectively, which was not statistically significant. The average specificity of supine and prone were 60% (CI 53%-67%) and 80% (CI 73%-83%) respectively.

For determining if the inferior wall defect in myocardial perfusion scintigraphy is a true defect, prone position can be used since it has a greater diagnostic accuracy, higher specificity and comparable sensitivity with the supine position.

Cardiology_22

ATP Stress MIBI Washout Rate to evaluate Myocardial Ischemia of Patients with Myocardial Bridge

Bulin Du[1], Yaming Li[1*], Bailing Hsu[2]

1. Department of Nuclear Medicine, the First Hospital of China Medical University
2. Nuclear Science and Engineering Institute, University of Missouri-Columbia

Objectives: A myocardial bridge occurs when one of the coronary arteries tunnels through the myocardium. For some patients, myocardial bridge can cause myocardial ischemia with corresponding clinical symptoms. In this study, we aimed to evaluate myocardial ischemia caused by myocardial bridge with ATP stress MIBI myocardial perfusion imaging, and the degree of myocardial injury through the stress MIBI clearance (washout rate, WR).

Methods: a total of 19 patients with mild-to-moderate myocardial bridge in left anterior descending (LAD) confirmed by coronary angiography or coronary CTA were selected (male = 12, age = 55 ± 11 years), all patients had an one day protocol ATP stress/resting MIBI myocardial perfusion imaging, and a delayed imaging 4 h after stress MIBI injection. Stress, stress delay, resting image were reconstructed with quantitative SPECT reconstruction system (QSRS) (including: attenuation, scattering, fuzzy resolution, image noise and other physical correction), to obtain quantitative image format. The perfusion defect scores (SSS, SRS and SDS) and stress MIBI clearance [= (MIBI1.5 h - MIBI4h)/ MIBI4h x 100%] in three vascular territories of LAD, left circumflex coronary artery (LCX) and right coronary artery(RCA) were calculated. The correlation between WR and perfusion defect scores, and the difference of these two indicators between the myocardial bridge area (LAD) and other two vascular areas were analyzed.

Results: six patients with myocardial ischemia were detected by traditional myocardial perfusion imaging (SDS≥2), but all of the patients have a LAD SDS≤1. There was no statistical difference in three vascular areas of SDS, SSS and SRS. MIBI WR, SDS and SSS in three vascular areas had negative correlation (WR=-13.62×SDS–10.56, r=0.51, P<0.001; WR=-12.16×SSS–5.74, r=0.32, P=0.016). Average WR of LAD (19.9%) was higher than LCX (15.5%) and RCA (17.7%) (P= 0.012, P= 0.012).

Conclusions: MIBI myocardial perfusion imaging failed to find significant myocardial ischemia in the myocardial bridge vascular area in patients with mild-to-moderate myocardial bridge. Quantitative stress MIBI clearance can evaluate the degree of myocardial injury caused by myocardial bridge.

Cardiology_24

Bremsstrahlung SPECT-CT for Localization of Inadvertent Extra Articular Injection

Qaisar Hussain Siraj, Noora Bin Essa, Anwar Bana, Michael Masoomi

Farwania Hospital Kuwait

Objectives: Radiosynovectomy (RSO) has now an established place in the management of patients with disabling synovitis. This involves intra articular introduction of colloidal radionuclide which will eventually lead to synovial membrane sclerosis and resolution of symptoms. The knee is the only joint which may be injected without fluoroscopic guidance. However, inadvertent extra-articular injection of radiotracer may lead to complications such as haemorrhage, bruising and even radiation necrosis. Therefore, in order to ascertain correct injection, it is important to image the patient following the Yittrium-90 instillation. This is possible with Bremsstrahlung planar imaging, which is routinely performed. However, the planar images are difficult to interpret at times when extra-articular injection is suspected. We therefore aimed to undertake Bremsstrahlung SPECT-CT for more accurate and précised anatomical localization and distribution of

the intra-articular injection. We report the technique and the importance of Bremsstrahlung SPECT-CT imaging in patients undergoing RSO with an example case report of extra-articular injection of Yttrium-90.
Methods: The radiosynovectomy technique involves insertion of an 18 gauge-needle through the medial aspect of the knee positioned in 45 degrees flexion, aspiration of joint fluid, which is followed by injection of Yttrium-90 citrate. Corticosteroid is next injected and flushed with saline. The knee is then tightly bandaged. Bremsstrahlung planar imaging is performed at 30 minutes post-injection with a Cobalt-57 flood phantom placed beneath the patient to outline the limb silhouette and to delineate the distribution of the radiopharmaceutical. Next, Bremsstrahlung SPECT-CT imaging was performed with the gamma camera set to auto-detect the highest fundamental frequency, which corresponded to xenon-133 window of 81 keV. Bremsstahlung SPECT-CT images were then obtained using Siemens Symbia TruePoint SPECT-CT camera fitted with LEGP and MEGP collimators.
Results: A 45-year-old man with bilateral knee pigmented villonodular synovitis who failed to respond to intra articular anti-inflammatory injections was sent for RSO. A baseline 3-phase bone scan prior to treatment showed evidence of active synovitis in both knees, more pronounced on the right. The procedure was conducted per protocol; however, no joint fluid could be aspirated, but to ensure intra-articular placement of the needle 2 mm of 0.9% saline was injected smoothly. The postinjection planar Bremsstrahlung scan showed only focal activity in the right knee with failure to delineate the synovial cavity. Only with the hybrid SPECT-CT the focal increased activity was correctly localized and was seen to be located to the infra patellar fat pad. Repeat RSO after a few weeks was successful as confirmed by Bremsstrahlung imaging.
Conclusion: This case study illustrates the benefit of Bremsstrahlung PECT-CT imaging in accurately localizing the radioactivity, which helped reveal the non-intended extra-articular injection of the therapeutic agent. On reviewing literature, Shen et al in 1994 depicted the percentages of all recorded photons detected corresponding to different energy ranges for different collimators and concluded that the sensitivity of a medium-energy is 70% greater when compared to a low- energy collimator. We have therefore perfected our Bremsstrahlung SPECT-CT imaging technique to incorporate medium-energy collimators for optimal sensitivity and accuracy.

Cardiology_28

How much radiation dose will be reduced by performing stress-only myocardial perfusion SPECT using Tc-99m-labelled agents?

Sang-Geon Cho[1], Minchul Song[1], Geum-Cheol Jeong[1], Hee Jeong Park[1], Seong Young Kwon[1], Jung-Joon Min[1], Hee-Seung Bom[1], Ki Seong Park[1], Sae-Ryung Kang[2], Seran Min[2], Jahae Kim[2], Ho-Chun Song[2]

1. Department of Nuclear Medicine, Chonnam National University Hwasun Hospital, South Korea
2. Department of Nuclear Medicine, Chonnam National University Hospital, South Korea

Objectives: We evaluated the effective dose estimates (ED) from rest-stress myocardial perfusion SPECT (MPS) using Tc-99m tetrofosmin (TF) or MIBI which were performed in 2013, Korea, and how much dose would be reduced by performing stress-only MPS in selected patients.
Methods: Based on the data from the KSNM protocol survey 2013, ED for rest-stress MPS studies performed at 136 Korean hospitals were calculated based on rest-stress dosing data from each institute and dosimetry calculation on ICRP 120. Eligibility criteria for stress-only MPS and estimated proportion of candidates were assessed from 711 patients who underwent rest-stress MPS in our institution from 2013 to 2014 where those who showed normal stress image without need for resting image were considered eligible for stress-only MPS. The same proportion of patients were considered to be stress-only MPS-eligible in the KSNM survey population, and ED reduction by stress-only MPS [(ED from rest-stress protocol) – (expected ED from stress-only protocol)] was calculated.
Results: Total 4142 MPS studies using Tc-99m-labelled agents (2695 TF and 1447 MIBI) were included. The average EDs for TC-99m TF and MIBI were 9.07 mSv (range: 4.32-16.43 mSv) and 10.74 mSv (range: 5.00-25.01 mSv) and totally 9.66 mSv from rest-stress MPS performed in 2013. Total population dose was 39.99 man-Sv. Eligibility criteria for stress-only MPS were 1) no ECG changes (ST-T changes or abnormal Q) and 2) pretest probability < 66% in multivariate analysis; estimated proportion of stress-only MPS-eligible patients was 10.7%. After application of stress-only protocol for 10.7% of the survey population, the average EDs for TC-99m TF and MIBI were reduced to 8.49 mSv (range: 0.78-12.60 mSv) and 10.06 mSv (range: 2.05-13.15 mSv) and totally 9.03 mSv. Total population dose was reduced to 37.42 man-Sv.
Conclusions: By performing stress-only MPS in 10.7% of patients, their radiation exposure is expected to be reduced by 0.63 mSv per study in average, which correlates to 2.57 man-Sv throughout Korea in a year.

Endocrinology_1

Recent changes in the clinical outcome of papillary thyroid carcinoma with cervical lymph node metastasis

Won Bae Kim, Min Ji Jeon, Young Kee Shong, Won Gu Kim, Dong Eun Song, Suck Joon Hong, Jin-Sook Ryu, Jung Hwan Baek, Jeong Hyun Lee

Department of Medicine, Asan Medical Center, University of Ulsan College of Medicine, Korea

The prognosis of papillary thyroid cancer (PTC) with cervical lymph node (LN) metastasis has changed with increased detection of subclinical metastatic LNs. The number and size of metastatic LNs were proposed as new prognostic factors in PTC with cervical LN metastasis (N1). The aim of study is to evaluate changes in N1 PTC characteristics and clinical outcome over time and to confirm the prognostic value of the number and size of metastatic LNs.

This study included 1,815 N1 PTC patients diagnosed between 1997 and 2011. Patients were classified into three risk groups according to the number and size of metastatic LNs: very low risk, ≤ 5 and < 0.2 cm; low risk, ≤ 5 and ≥ 0.2 cm; and high risk, > 5.

Metastatic LNs became smaller and the ratio of metastatic LNs, which represents the extent of LN involvement and the completeness of surgery, decreased significantly over time. The proportion of patients with excellent response significantly increased from 33% to 67% over time (P< .001). These improvements were more evident in the low- and high-risk groups than in the very low-risk group. The DFS 5 years after initial surgery was also significantly increased from 73% to 91% over time (P< .001). The new LN classification was strongly associated with outcome. Patients in the very low-risk group had longer DFS than those in the low- and high-risk groups during the study period.

The clinical outcome of N1 PTC has significantly improved over time with decreased extent of LN involvement, improved diagnostics and more complete surgical neck dissection. The number and size of metastatic LNs are important prognostic factors of recurrence in N1 PTC.

Endocrinology_6

Association between the dietary items and differentiated thyroid cancer

Seyed Rasoul Zakavi, Zohre Sadat Sangsefidi, Abdoreza Norouzy, Mohammad Safarian, Roxana Kashanifar, Raheleh Pourbaferani, Fateme Ghafouri, Narjess Ayati, Sahar Fallahi, Seyed Rasoul Zakavi

Nutrition Department, Iran

Incidence of differentiated thyroid cancer (DTC) was increasing in the last 20 years throughout the world. Several factors including radiation, improvement in diagnostic modalities and nutritional factors may be responsible for increasing incidence. Effect of nutritional factors on DTC is an important modifiable factor that is not well studied. In this case control study, we assessed the risk of different dietary items in patients with DTC.

Three-hundred patients with DTC and 300 control subjects were investigated regarding nutritional factors using a validated food-frequency questionnaire (FFQ). Information on dietary intake was derived for intake of energy, carbohydrate, fat, protein, low and high-fat dairy, sugars, fruits, vegetables, tea, roasted or fried meat, starchy foods, fish, seafood, fast food and sugar-sweetened drinks. The intake of each dietary item was compared between patients with DTC and control group.

The results showed that there are significant inverse association between the intake of low-fat dairy, fruits, vegetables, tea and DTC (P<0.05). In contrast, consumption of roasted or fried meat and sugars (P<0.05) was directly associated with DTC. Meanwhile we did not find any significant association between DTC and the intake of energy, carbohydrate, fat, protein, high-fat dairy, starchy foods, fish and seafood, fast food and sugar-sweetened drinks (P>0.05).

Higher intake of low fat dairy, fruits, vegetables and tea may be associated with lower risk of DTC, while high intake of roasted and fried meats and sugar (including all sweet foods) may be associated with higher risk of DTC.

Endocrinology_7

Usefulness of thyrotropin receptor antibody titer at the time of withdrawal of antithyroid drug for predicting the relapse of hyperthyroidism in patients with Graves' disease

Won Bae Kim, Hyemi Kwon, Eun Kyung Jang, Won Gu Kim, Yun Mi Choi, Min Ji Jeon, Tae Yong Kim, Young Kee Shong, Jin-Sook Ryu

Department of Internal Medicine, Asan Medical Center, University of Ulsan College of Medicine, Korea

The relapse rate for hyperthyroidism after antithyroid

drug (ATD) withdrawal is approximately 50 - 60% in patients with Graves' disease (GD). Thyrotropin receptor antibody (TRAb) measurement including thyroid stimulatory antibody (TSAb) and thyrotropin binding inhibitory immunoglobulin (TBII) has been known as useful for predicting the relapse of hyperthyroidism. This study was to investigate which assays for TRAb was more useful to predict the relapse of hyperthyroidism after ATD withdrawal in GD patients.

Eighty-two GD patients including 38 of TSAb and 44 of TBII group were enrolled. All patients were followed up with thyroid function tests, TRAb titer (TBII for TBII group, and TSAb for TSAb group) at the time of ATD withdrawal, 3, 9, and 21 months after ATD withdrawal.

The relapse rate was significantly higher in TSAb-positive (60%) than TSAb-negative group (17%, *P*= 0.01). The relapse rate was similar in both TBII positive (40%) and TBII negative groups (38%, = 0.99). The relapse-free interval was also longer in TSAb-negative (36.9 ± 3.2 months) than TSAb-positive group (20.5 ± 3.5 months; *P* = 0.017), but no difference was found in TBII positive (15.0 ± 4.4 months) and negative groups (35.1 ± 3.0 months; *P* = 0.54). TSAb positivity and severe hyperthyroidism at baseline were significant factors in Cox proportional hazard model for predicting the relapse of hyperthyroidism in TSAb group.

TSAb measurement at ATD withdrawal could be useful for predicting the relapse of hyperthyroidism in GD patients.

Endocrinology_8

Early prognostic factors at the time of first radioactive iodine therapy predict survival of patients with bone metastases from differentiated thyroid carcinoma

Tae Yong Kim, Yun Mi Choi, Won Gu Kim, Hyemi Kwon, Min Ji Jeon, Jin-Sook Ryu, Dong Eun Song, Young Kee Shong, Won Bae Kim

Department of Internal Medicine, Asan Medical Center, University of Ulsan College of Medicine, Korea

Bone is the second most common site of distant metastases for differentiated thyroid cancer (DTC) after the lungs. Patients with bone metastases was associated with poor clinical outcomes, however their clinical course was heterogeneous due to recurrent skeletal complications. This study aims to evaluate early prognostic factors associated with survival in patients with bone metastases from DTC.

This retrospective study included 93 patients with bone metastases from DTC in a single center. We evaluated prognostic factors associated with over-all survival (OS) according to the time of initial radioactive iodine therapy (RAIT).

Median age of 93 patients (Male = 30 and F = 63) was 55.4 years and 55 patients (59%) had papillary thyroid cancer. Forty five patients (59%) were dead during median 7.6 years follow-up. Patients who diagnosed bone metastasis before initial RAIT (n = 32) had significantly poor OS (HR 1.86, 95% CI 1.02 – 3.39, *P* = 0.04). There was no significant difference in OS according to the RAI-avidity after initial RAIT in all study subjects (*P* = 0.18). However, RAI-avid bone metastases had better OS in patients who confirmed bone metastases before initial RAIT (HR 0.27, 95% CI 0.10 – 0.76, *P* = 0.01). In patients who detected bone metastasis after initial RAIT, older age (>45 years), elevated serum thyroglobulin level (>250 ng/ml), and presence of skeletal related events (SRE) were significantly associated with poor OS. RAI avidity was not significant prognostic factor in these patients.

Bone metastases detected before initial RAIT was important prognostic factor for patients with bone metastasis from DTC. RAI avidity after initial RAIT was good prognostic indicator only in patients who detected bone metastases before initial RAIT.

Endocrinology_12

The Efficacy of Simplified Low Iodine Diet for Preparation of Radioiodine rhTSH Scanning in Korean Patients

Young Hoon Ryu, Minkyung Lee

Inha University Hospital, Korea

Many physicians in Korea have been recommended a stringent LID for 2 weeks in patient with DTC prior to RAIT or DxWBS because the dietary iodine intake in Korea is higher than all other countries except for Japan and Canada. Considering that seaweeds take up 70% of the dietary iodine intake, body iodine pool may be sufficiently depleted by a simplified LID (seaweeds restriction only) instead of a strict LID. Based on these concepts, we proposed new protocol; a simplified LID and 1 week of thyroid hormone withdrawal for successful LID without intolerable hypothyroidism symptoms and discomfort in diet and applied it to the patients with preparing rhTSH DxWBS. We want to evaluate the efficacy of this compromise plan and compare it with conventional protocol by using spot urine analysis.

Total 80 papillary thyroid cancer patients (62 females, 18 males) preparing for follow-up DxWBS with rhTSH were enrolled. In order to assess the impact of 1 weeks

stringent LID (LID1) on urinary iodine excretion during the preparation of RAIT, morning spot urine specimen was obtained on the final day of LID1 from each patient and the urine iodine excretion (UIE1) was checked to evaluate the efficacy of LID1. For rhTSH DxWBS, they contributed morning spot urine 8 days (LID2) and 10 days (LID3) after a simplified LID prior to DxWBS; on the day of first and second rhTSH injections. The urine iodine excretion on LID2 (UIE2) and LID3 (UIE3) were also evaluated.
The median value of UIE after LID1 was 12.80μg/L. The median value of UIE after LID2 was 109.62μg/L . There was no significant difference in the median UIE values between gender. The median UIE value of LID3 and LID2 was not significantly different. The frequencies of excellent and good iodine deficiency did not differ between 8 and 10days simplified LID .However, the median UIE value of LID1 was significantly lower than that of LID2 and LID3.
From our results, simplified LID protocol is acceptable to achieve an optimal level of iodine restriction for rhTSH DxWBS with simplified LID.

Endocrinology_13

Effectiveness fixed dose ^{131}I for Hypertyroidism to Become Hypothyroidism in 3 months after theraphy

Agus Supriyanto

Department of nuclear medicine, nuclear medicine society of indonesia, Indonesia

Dose of ^{131}I for hyperthyroidism treatment is still controversy. The dose of ^{131}I can be given fixed dose or based on empirical experience dose. The use of radioiodine is well established as safe and effective treatment for hyperthyroidism. However there is no agreement on the regime or the dose of RAI used and succes rate is quite variable. Whilst several large series analysed the number of hypothyroidism patients after radioiodine treatment, there is little published data on the time taken for patients to become hypothyroidism.
Retrospective study was done to 100 patients with hyperthyroidism. Fixed dose of ^{131}I is 8 mCi, and < 8 mCi and > 8 mCi consider as experience dose treated at Hasan Sadikin Hospital between January 2013 and December 2014. All patient were investigated by tyroid scintigraphy and thyroid function test. Patients was designated hypothyroidism when they remain clinically and biochemical hypothyroidism function test.
In this study hypothyroidism was observed on 45.21% of patient using 8 mCi, 25% with < 8 mCi, and 43.48% with > 8 mCi.
Fixed dose of ^{131}I more effective for hyperthyroidism treatment compare to empirical experience dose.

Endocrinology_15

Problematic thyroid cancers

Emerita Andres-Barrenechea, MD, FPCP, FPSNM

St. Luke's Medical center Philippines

Objective: To determine the factors that is involved in problematic thyroid cancers. Despite the good prognosis of DTC, with overall 10-year survival rates of 75-95%, and full remission of more than 40 years, 20% may recur and pose a problem in clinical practice. RAI may no longer be an option in 20-30% of patients whose tumors dedifferentiated. Furthermore the long-term survival in patients with non-avid TC declines to about 10%.
With thyroid cancer, the most important prognostic (outcome) factor is the type of thyroid cancer (TCA) you have, the histopath. Papillary-follicular variant, eosinophilic, oncocytic variety; diffuse sclerosing, tall cell, columnar cell, solid/trabecular and insular variants as well as Hurtle cell have been identified in previous studies as aggressive varieties.
There are several identified prognostic factors that may be predictive of recurrence or death in patients with well-differentiated thyroid cancer. Patient-related factors: Age and Gender, Tumor specific factors: Histology, Size, Extrathyroidal invasion and Treatment related factors: Extent of primary surgery
Methods: A total of 688 thyroid cancer patients were seen in a 5-year study, 28 turned to be iodine refractory thyroid cases; age, sex, histopath and extent of sugery were considered.
Results: There were 18 males and ten females, age range were from 56 to 70;and histopath showed papillary with follicular variant type 11, oncocytic-2, tall cell variant, -7 sclerosing type-4, insular-1, sclerosing-3 .All had near total thyroidectomy but Fifty % did not undergo lymph node dissection. Most of them became resistant to I-131 after 1-131 therapies. They also became non-iodine avid, with increasing thyroglobulin and PET positive.
Conclusion: It has been said that the response of TCA to radioiodine is a more powerful indicator of prognosis than the initial clinic pathological staging. Histopathology, age, gender and extent of surgery were factors to be considered likewise for poor response in this study.

Endocrinology_16

Efficacy of Radioiodine Treatment in Well-differentiated thyroid cancer in Children

Emerita A. Barrenechea

Veterans Memorial Medical Center, St. Luke's Medical Center

Objective: Well-differentiated thyroid cancer in children is the third most common solid tumor malignancy and the most frequent endocrine malignancy in children. They are more aggressive at the time of diagnosis, with metastases and have a higher risk for recurrence. The objective of this paper is to determine the efficacy of radioiodine treatment after five to six years from therapy.

Material and methods: Fifteen (15) pediatric patients with a diagnosis of thyroid carcinoma, aged below 18 years of age were included in a six-year follow-up after treatment. They underwent thyroidectomy, followed by RAI ablation. The predominantly female population (74%) had papillary TCA (13 patients) and (2) had follicular. Nodal metastases were seen in 53% and lung metastases were seen in 20% of the cases.

Results: Of the 13 who underwent RAI ablation, 3 cases of lung metastases while two cases with lymph node metastases needed repeat treatment. On follow-up after an average of six years, all the 13 patients who underwent RAI ablation are doing well with the lifetime thyroid hormone treatment. The remaining two patients who did not undergo therapy succumbed on the 2nd and third year after diagnosis.

Conclusion: WDTCA in children is rare and the biological behavior differs from that of adults. Their presentation is quite aggressive and may be recurrent. Total or near total thyroidectomy with I-131 ablation reduces mortality and hence is efficacious.

Endocrinology_21

Relationship between frequency of high dose radioiodine therapy and pathologic stage in patients with differentiated thyroid cancer

Subin Jeon, Hee-Seung Bom, Jung-Joon Min, Hee Jeong Park, Geum-Cheol Jeong, Seong Young Kwon

Chonnam National University Hwasun Hospital, Korea

Purpose: The radioiodine therapy (RIT) has been used for treatment of residual tissue or metastatic lesions of differentiated thyroid cancer (DTC) after surgery. The purpose of this study was to investigate the relationship between frequency of high dose radioiodine therapy and pathologic stage in patients with DTC.

Methods: The patients who underwent RIT after total or subtotal thyroidectomy from January 2008 to December 2014 were enrolled. We classified these patients into two groups according to the frequency of RIT; patients who underwent RIT once (group 1) and those who underwent RIT twice (group 2). Patients' cancer staging was determined based on pathologic diagnosis after surgery. We analyzed whether pathologic stages were different between two groups, retrospectively.

Results: Total 2,878 patients were enrolled in this study. Number of male or female was 669 (21.7%) or 2209 (71.7%), respectively. Total number of patients in group 1 or 2 was 2,648 (92.0%) or 230 (8.0%), respectively. In group 1, proportions of T and N stage were shown as follows; T1 (1,615, 61%), T2 (114, 4.3%), T3 (778, 29.4%), T4 (141, 5.3%), N0 (506, 19.1%), N1a (1,690, 63.8%), N1b (452, 17.1%). In group 2, proportions of T and N stage were shown as follows; T1 (91, 39.6%), T2 (23, 10%), T3 (90, 39.1%), T4 (26, 11.3%), N0 (26, 11.3%), N1a (98, 42.6%), N1b (106, 46.1%). The proportion of patients with T stage ≥ 2 was significantly higher in group 2 than in group 1 (P<0.001). The proportion of patients with N1b stage was also significantly higher in group 2 than in group 1 (P<0.001).

Conclusions: Patients who underwent RIT twice had the higher proportion in T≥2 or N1b stages, compared to patients who underwent RIT once. Further investigations are necessary to elucidate the correlation among pathologic stages, frequency of RIT and prognosis.

Endocrinology_22

Clinical Outcomes of Patients with Hypercalcitoninemia after Initial Treatment for Medullary Thyroid Cancer and Postoperative Serum Calcitonin Cut-offs for Predicting Structural Recurrence

Yoon Young Cho[1], Dong Ik Cha[2], Ju Young Jang[1], Tae Hyuk Kim[1], Sun Wook Kim[1], Jae Hoon Chung[1]

1. Division of Endocrinology & Metabolism, Department of Medicine, Thyroid Center, Samsung Medical Center, Sungkyunkwan University School of Medicine, Seoul, Korea
2. Department of Radiology, Sungkyunkwan University School of Medicine, Seoul, Korea

Purpose: Biochemical cure after initial treatment has been reported in 40–60% of patients with medullary thyroid cancer (MTC), but clinical outcomes of

patients with persistent hypercalcitoninemia have not been clearly studied. We evaluated the clinical outcomes of MTC patients who had not reached biochemical remission after initial treatment, and assessed the cut-offs of postoperative serum calcitonin for predicting structural recurrence in these patients.

Methods: We enrolled 120 MTC patients who underwent initial thyroid surgery at Samsung Medical Center between 1996 and 2015. Clinical outcomes were evaluated according to the anatomical staging and dynamic risk assessment system, which was originally designed for the follow-up of differentiated thyroid cancer. ROC analysis was performed to calculate the cut-offs of serum calcitonin for predicting structural recurrence.

Results: Thirty patients (25%) had persistent hypercalcitoninemia without evidence of structural disease after initial treatment. Among them, biochemical persistent disease was found in 18 patients (60%), structural identified disease was found in 10 patients (34%), there was no evidence of disease in one patient (3%), and one patient died of the disease (3%). By ROC analysis, 25 pg/mL postoperative serum calcitonin showed 100% sensitivity, 89.7% specificity, and 100% negative predictive value for predicting newly developed structural disease.

Conclusions: Prognosis was variable in MTC patients with a biochemical incomplete response to initial therapy. A postoperative serum calcitonin of 25 pg/mL might be useful for predicting newly developed structural disease.

Endocrinology_23

Childhood thyroid cancer has been increasing in Korea due to natural increase as well as thyroid screening

Yoon Young Cho, Sun Wook Kim, Tae Hyuk Kim, Ju Young Jang, Dong Ik Cha, Jae Hoon Chung

Division of Endocrinology & Metabolism, Department of Medicine, Thyroid Center, Samsung Medical Center, Korea

To characterize the increasing tendency of thyroid cancer in children and adolescents in Korea, and to elucidate whether imaging studies have affected this increase.

Between January 1995 and December 2013, a total of 126 pediatric patients who underwent thyroid surgery for thyroid cancer were eligible for this study.

Among 126 patients, 91 patients (72%) were identified by a palpable neck mass, and the others (n=35, 28%) were diagnosed by imaging studies incidentally or for screening purposes. The proportion of cases found during thyroid screening has increased from 8% in 2000–2004 to 44% in 2010–2013.

The total number of childhood thyroid cancer as well as the rate of thyroid masses noticed during screening has been rising. However, considering that the number of clinically palpable thyroid cancers has also increased steadily, enhanced detection of thyroid nodules could not explain all phenomena.

Musculoskeletal System_2

Altered bone metabolism of the spine in ankylosing spondylitis demonstrated by F-18 fluoride PET/CT:A novel evaluation tool in patients with relatively low modified stoke ankylosing spondylitis spine scores

Yun Young, Ji Young Kim, Seunghun Lee, Young Bin Joo, Tae-Hwan Kim

Hanyang University Medical Center, Korea

To identify alterations of bone metabolism of the spine in patients with ankylosing spondylitis (AS) by F-18 fluoride PET/CT and to consider its potential role in the assessment of spinal involvement in AS.

Thirty-three consecutive AS patients were included in this prospective study. Clinical disease activity was assessed using the Bath AS Disease Activity Index (BASDAI) and the Bath AS Functional Index (BASFI). The presence of altered bone metabolism activity on F-18 fluoride PET/CT was assessed in posterior structures of the spine [cervical, facet joints (FJs), costovertebral joints (CVJs), costotransverse joints (CTJs)] and anterior discovertebral units (DVUs) of vertebral body. Clinical disease activity parameters and F-18 fluoride PET/CT findings were compared in patients with different extents of spinal structural involvement on radiography as assessed by the modified Stoke AS Spinal Score (mSASSS) [low change : mSASSS (≤ 9); high change: mSASSS (> 9)].

Altered bone metabolism in the posterior structures of the spine on F-18 fluoride PET/CT were found in most of the patients (27/33, 81.8%) and there was no difference between the two subgroups of low mSASSS, 10/12, 83.3% vs. high mSASSS, 16/18, 88.9%, respectively]. In the low mSASSS subgroup, the presence of alterations of bone metabolism in posterior structures, especially facet joints, was associated with clinical disease activity scores on the BASDAI and/or BASFI.

F-18 fluoride PET/CT provides additional information about alterations of bone metabolism in the spine compared with

currently used methods of identifying structural changes by mSASSS system. Altered bone metabolism on F-18 fluoride PET/CT is frequently seen in posterior structures of the spine even in the patient with low mSASSS. Moreover, in these patients, metabolic abnormality of the facet joints is associated with daily clinical disease activity scores. We suggest that popularization of F-18 fluoride PET/CT might contribute in the assessment of spinal involvement in AS patients and in the estimation of disease activity, especially in AS patients with low mSASSS.

Musculoskeletal System_4

Quantitative Body Mass Index and Age Influence; As Assessed by SPECT Bone Scintigraphy

Nasim Hosseinifar, Mohammad Hosntalab, Farshid Babapour Mofrad, Mohammad Eftekhari, Parham Geramifar

Islamic Azad University Science and Research Branch, Faculty of Engineering, Tehran, Iran

Bone scintigraphy is a non-invasive diagnostic procedure for investigation of functional disorders of the skeletal system. In addition to quality assurance of the imaging system and the preparation of radiopharmaceutical, there are other factors that could affect the image quality. The aim of this study was to quantitatively analyze the effects of Body Mass Index (BMI) and age (besides post injection time interval factor), in terms of contrast to noise (CNR) as well as bone to soft tissue contrast ratio in SPECT bone images.

Thirty-nine patients (17 male, 22 female), ages 30-78 years (median 60) were entered in the study. Height and weight of patients were used for BMI calculation and age and post injection time interval were recorded for regression analysis. We drew equal regions of interest over the femoral diaphysis and the contralateral adductor area. Furthermore, the total number of counts from bone region of interest (ROI) and soft tissue ROI were used for bone to soft tissue contrast ratio. Pelvic CNR was measured by drawing ROIs over the hip region to determine the number of counts in the bone as well as the soft tissue and background noise. As the rate of bone mass and density loss increase after the ages of 50, patients were divided into two groups (30 - 49 and 50 - 80 years). Regarding the BMI category, patients were divided in three groups (normal weight (18.5<BMI<24.9), overweight (25<BMI<29.9) and obese (BMI>30)).Finally, for post injection time classification, patients were categorized into 2 hours and 3 hours post injection scan time.

There was a strong correlation between age of the patients and post injection time interval with contrast and CNR [P value <0.05]. In addition, linear regression coefficients of -0.408 and -0.119 shows BMI has an inverse correlation with contrast and CNR, respectively. Post injection time interval was the most important factor directly affecting CNR and contrast while BMI and age inversely affect the image quality.

Musculoskeletal System_6

Discordance between Spinal and Hip Bone Mineral Density Values in Patients with Lumbar Scoliosis – Experience of a Single Institute

Shamim M F Begum, Nasreen Sultana, Zeenat Jabin, Rahima Parveen, Azmal Kabir Sarker, Sharmin Reza

National Institute of Nuclear Medicine and Allied Sciences (NINMAS), Dhaka, Bangladesh

Objectives: Osteoporosis and scoliosis are encountered concurrently. It has been suggested that scoliosis predisposes to osteoporosis but degenerative scoliosis could falsely elevate lumbar bone mineral density measurement leading to discordance. This study was conducted to determine the prevalence of discordance between lumbar spines and hip bone mineral density in patients with lumbar scoliosis and to evaluate the other risk factors of discordance.

Methods: This is a prospective study carried out with Norland DEXA- XR 36 machine in National Institute of Nuclear Medicine and Allied Sciences, Dhaka between July 2014 and May 2015. Patients referred for BMD test and having lumbar scoliosis were included in this study. The T scores were recorded for determining osteoporosis in lumbar spines and hip bones (Ward's triangle of femur neck). The prevalence of osteoporosis and discordance of bone density due to overestimation of lumbar spine density was determined as major and minor discordance. Old age, age at menopause, sex and BMI were considered as possible risk factors for discordance and were used in multivariate logistic regression analysis. Patients having history of spine fracture or implants were excluded from this study.

Results: Total 70 patients (M-21, F-49) with a M:F ratio of 2: 2.3 and age ranging between 42 to 88 years (mean ± SD = 64.01± 10.55) were included. Discordance between lumbar spines and hip was found in 55 (78.6 %) patients and among them major and minor discordance of T-scores were seen in 18 (25.7%) and 37 (52.9%) respectively. Concordance of T scores was

seen in 15 (21.4 %). In multivariate logistic regression analysis female sex (P = 0.34, OR 1.95; CI: 0.43-9.99), age older than 60 years (P= 0.23, OR 2.13; CI: 0.53-9.16) and BMI less than 30 kg/m2 (P<0.001, OR 71.56; CI: 7.85-1653.9) was identified as risk factors for T-score discordance.

Conclusions: In lumbar scoliosis DEXA scan might show overestimation of lumbar BMD and may lead to diagnostic dilemma, whereas hip DEXA appears to be more reliable in these cases. However, the physicians should look for the prevalent phenomenon and possible underlying causes of discordance of T score.

Musculoskeletal System_8

Three-dimensional Reformatted PET/CT Application in Musculoskeletal Tumors

Seoung-Oh Yang, Hong Jae Lee

Dongnam Institute for Radiological and Medical Sciences (DIRAMS), Korea

Three-dimensional (3-D) displays for medical imaging is now emerging field and very promising tools for diagnosis, therapy response and detection of tumor recurrence. Morphological criteria for therapy response (CR, PR, SD, PD) have been established with RECIST (Response evaluation criteria in solid tumors). With adoption of metabolic imaging with PET/CT, particularly with F-18-FDG in initial staging and follow up of tumors, there appears to be a need to modify these criteria not only on morphological imaging modalities like CT, but also on tumor metabolism parameters, like SUV (standardized uptake value) as measured by PET. Furthermore, 3-D imaging taken from PET/CT can be an excellent approach to assess the tumor response after appropriate therapy.

In this poster presentation, we will discuss the TrueD (Siemens) application of F-18-FDG PET/CT for both initial staging and post-therapeutic follow-up in patients with musculoskeletal tumors. One-hundred eighty-three patients with musculoskeletal tumors were enrolled in this study.

Seventy-two osteosarcoma, 16 liposarcoma, 16 chondrosarcoma, 10 fibrosarcoma, 10 malignant fibrous histiocytoma (MFH), 8 soft tissue sarcoma, 8 melanoma, 6 leiomyosarcoma, 6 synovial sarcoma, 5 Ewing sarcoma and 16 other tumors are included. Two technologists performed laborious job using TrueD software in patients with more than two PET/CT scans under the supervision of Nuclear Medicine Physician. Among many galleries, the most optimal palette applied according to anatomic location of the tumors (muscle or bone) and other characteristics.

Monitoring of tumor response to therapy is very easy to assess using these TrueD PET/CT images. The recent development of three- and four-dimensional image processing will lead medical imaging to full definition volumetric display for clinician as well as patients themselves. VOIs (volume of interests) of 2 or 3 time points display can be saved and exported as powerful and comprehensive images through the any PACS systems.

Musculoskeletal System_12

Appropriate time point for acquisition of perfusion and blood pool phase images in 3-phase NaF bone PET

Young Jin Jeong[1, 2], Hye Joo Son[1, 2], Hyun Jin Yoon[1, 2], Do-Young Kang[1, 2]

1. Department of Nuclear Medicine, Dong-A University Hospital, Dong-A University College of Medicine, Busan, Korea
2. Institute of Convergence Bio-Health, Dong-A University, Busan, Korea

Objectives: F-18 NaF has a characteristics which is rapid uptake in bone and fast clearance from soft tissue. The aim of this study was to determine an appropriate time point for acquisition of perfusion and blood pool phase image in 3-phase NaF bone PET.

Methods: Thirty-one patients who were performed joint replacement surgery of knee or hip without complication or symptom were enrolled. The patients underwent F-18 NaF PET examinations as following protocol. First, dynamic PET image of an area of interest was obtained for 20 min after injection of F-18 NaF. The data were reconstructed with 30 frames: twelve 10s frames, three 20s frames, six 30s frames and four one min followed by six 2 min frames. Second, delayed static bone phase scanning was performed at around 60 min after injection of radiotracer. Three volume of interest (VOI) were drawn on artery, muscle and bone of dynamic and delayed static PET images, respectively. For each VOI, SUV_{max} and SUV_{mean} were determined and specific bone uptake ratio ((bone SUV_{max} – muscle SUV_{max}) / muscle SUV_{max}) was calculated.

Results: A one average time-activity curve was obtained using the 20 min dynamic PET data of thirty-one patients. We defined the perfusion phase as from the start of acquisition to recovery state to baseline of the arterial uptake from the first peak and the blood pool phase as from the end of perfusion phase to the time point before gradually increased uptake of bone. The duration of perfusion phase is the first 1 min and

blood pool phase is until 4 min 45s from the end of the perfusion phase, respectively.

Conclusions: Our data suggested that an appropriate time point for acquisition of perfusion image was within the first 1 min and blood pool image was within about 5 min after injection of F-18 NaF, respectively.

Musculoskeletal System_13

Preliminary data of the clinical utility of three phase NaF bone PET for evaluation infected prosthesis

Young Jin Jeong[1, 2], Hye Joo Son[1], Hyun Jin Yoon[1], Do-Young Kang[1, 2]

1. Department of Nuclear Medicine, Dong-A University Hospital, Busan, Korea
2. Department of Nuclear Medicine, Dong-A University College of Medicine, Busan, Korea

Objectives: Because F-18 NaF has a rapid kinetics than Tc-99m MDP, F-18 NaF bone PET has many advantages which are clear bone image, short imaging time and ability to quantify bone turn over. However, the usefulness of three phase NaF bone PET to diagnosis bone infection is not well known. In this study, we studied the clinical usefulness of three phase bone PET with F-18 NaF to identify the presence of prosthesis infection of joint.

Methods: Five patients who presented symptoms suggesting infection of joint prosthesis after joint replacement surgery of knee (n=4) or hip (n=1) were enrolled. All patients performed three phase Tc-99m MDP bone scan and F-18 NaF bone PET on the same day. Three patients performed 3-time point PET acquisition (perfusion, blood pool and delayed images). Other two patients underwent F-18 NaF bone PET examinations as following protocol. First, list mode image was obtained for 20 min after injection of F-18 NaF. The list mode data was reconstructed into dynamic curve for 20 min, perfusion and blood pool images. Second, delayed static bone phase scanning was performed at around 60 min after injection of radiotracer. Ten normal controls who underwent joint replace surgery without symptom were also recruited for. Three volume of interest were drawn on artery, muscle, bone marrow and two different site of bone in patients and normal control.

Results: Of five patients, infection of joint prosthesis was confirmed in 4 subjects. Non-infected joint prosthesis was revealed in another one patient and symptom of the patient gradually subsided with symptomatic treatment. As the patients with infected prosthesis, one patient without infection showed increased uptake in the peri-prosthesis area in delayed image. But pattern of tracer uptake was relatively even in patient with non-infected prosthesis. Time-activity curve for 20 min showed markedly different curve pattern between the patients with and without infected prosthesis.

Conclusions: This preliminary data suggested that F-18 NaF bone PET showed clearer three phase images which helped to identify the site and extent of disease. Adding of dynamic curve could improve diagnostic accuracy.

Musculoskeletal System_14

Bone SPECT/CT for Evaluation of Causative Lesion of Low Back Pain

Jeonghun Kim, Seok Tae Lim, Sehun Choi, Chang Ju Na, Yeon-Hee Han, Hwan-Jeong Jeong, Myung-Hee Sohn

Department of Nuclear Medicine, Molecular Imaging & Therapeutic Medicine Research Center, Cyclotron Research Center, Institute for Medical Sciences, Biomedical Research Institute, Chonbuk National University Medical School and Hospital, Jeonju, Republic of Korea

Objectives: We assess the clinical value of bone SPECT/CT for evaluation of causative lesion of low back pain (LBP).

Methods: In retrospective study, patients who underwent bone SPECT/CT for evaluation of LBP were included. Patients with history of recent trauma and who underwent lumbar spine operation within 6 months were excluded. Total 177 bone SPECT/CT were reviewed to find possible causative lesion of LBP . We classified the patients into facet arthritis positive (facet group) vs. facet arthritis negative (non-facet group) groups due to clinical need. Descriptive statistical analysis was performed.

Results: Abnormal findings were noted in 106 of 177 cases (59.9%). Facet arthritis was detected in 76 of 177 cases (42.9%). Total 175 facet joints showed scintigraphically active arthritis. Most commonly involved facet level was L4/5 (60), followed by L3/4 (46), L2/3 (26), L5/S1 (16), L1/2 (10), T12/L1 (9), T11/12 (5) and T10/11 (3). No right vs. left side facet arthritis predominance was found. Thity-eight of 76 patients (50%) were received percutaneous injection therapy following bone SPECT/CT. Estimated concordance rate of percutaneous injection therapy level was 68.4% (26 of 38). Facet group patients were significantly older than non-facet group patients (mean ages: 62.3 yrs vs. 51.2 yrs, $P< 0.0001$). In non-facet group (101 of 177, 57.1%), 70.3% (71 of 101) of cases showed no causative lesion of LBP in bone SPECT/

CT. Other possible causative lesions (30 of 101) were recent compression fracture (5), spondylolysis (4), unusual active degenerative change in patients under the age of 40 (3), intervertebral foramen narrowing (3), active sacroiliitis (3), spinal canal stenosis (3), lumbar spine ligament calcification (2), nonunion of previous pelvic fracture (2), sacral insufficiency fracture (1), active arthritis in lumbosacral transitional vertebra (1), kissing spine syndrome (1), lumbar transverse process fracture (1) and ankylosing spondylitis (1).

Conclusions: Bone SPECT/CT identified about 60% of possible causative lesion in patients with LBP. Facet arthritis was considerable cause of LBP. Bone SPECT/CT accurately localized active facet arthritis and was helpful to target percutaneous injection therapy.

Neurology_3

The Effect of Quantitative Reconstruction Algorithm on the Normal Reference Values of Striatal Uptake in ^{99m}Tc-Trodat-1 SPECT with LEHR Collimation

Wei-Ren Chen[1], Cheng-Yu Wei[2], Bailing Hsu[3], Guang-Uei Hung[1]

1. Department of Nuclear Medicine, Chang Bing Show Chwan Memorial Hospital, Changhua, Taiwan
2. Department of Neurology, Chang Bing Show Chwan Memorial Hospital, Changhua, Taiwan
3. Nuclear Science and Engineering Institute, University of Missouri-Columbia, Missouri, USA

Purpose: ^{99m}Tc-Trodat-1 (TRODAT) SPECT to assess dopamine transporter activity (DTA) has been utilized as a clinical routine to evaluate Parkinson's disease (PD) in Taiwan. However, because of historical development pathway, a systematic research to generate normal reference value (NRV) with LEHR collimation was not yet established.

Methods: Twenty-nine normal subjects (age: 42-82) divided into 4 decade groups were enrolled for TRODAT SPECT and MRI scans. 30 mCi of TRODAT was injected and imaged 4 hours later. SPECT images were reconstructed with FBP and quantitative SPECT reconstruction system (QSRS), including corrections for attenuation, scatter, resolution and noise. SPECT images were fused with MRI images to analyze brain area with the SPM program. A set of region template was applied to obtain absolute uptake in striatum (S), caudate (C) and putamen (P) areas. Mean and SD of specific uptake ratio (SPR) as S/(S-Background) and C-P ratio (CPR) as C/P were calculated, and then compared with the result of fan-beam collimation (Weng, JNM 2004).

Results: From visual inspection, SPECT and MRI images were closely registered perfectly. Among all patients, mean uptake in S, C and P were 20.9±10.8, 17.2±6.2 and 22.4±8.8 kBq/ml. With FBP, the relation of SBR (y) to decade(x) was y=-0.016x+1.55 (R^2=0.93) and y=-0.033x+3.47 (R^2=0.96) for QSRS (P<0.0001). There was two-fold difference among QSRS and FBP corresponding to age effect, and the slope of FBP result matched with fan-beam collimation (Weng, JNM 2004). CPR was y=-0.0019x+0.96 (R^2=0.72) for FBP and y=-0.0005x+0.75 (R^2=0.63) for QSR (P=0.035). FBP presented slightly higher CPR value than QSRS (Δ=0.21).

Conclusions: Dopamine-transporter activity in striatum consistently decreased with elevated ages, but the activity ratio in caudate and putamen stayed unchanged. QSRS provided two-fold more profound SBR scale to separate age effect in normal subjects than FBP, in which it can be positioned as a more sensitive parameter while applied to diagnose PD.

Neurology_6

Assessment of Regional Cerebral Blood Flow before and after Repetitive Transcranial Magnetic Stimulation in Stroke Care

Yong-An Chung, In-Uk Song, Jiyoung Ryu, Ikdong Yoo, Eun Kyoung Choi, Jin Kyoung Oh

Department of Neurology, Incheon St. Mary's Hospital, College of Medicine, The Catholic University of Korea, Korea

Repetitive transcranial magnetic stimulation (rTMS) has recently been clinically applied in the rehabilitation treatment of stroke. Furthermore, the influence of rTMS on the physiology of the brain is not clear. We prospectively evaluated changes of regional cerebral blood flow (rCBF) between pre- and post-rTMS treatment in left MCA infarction patients.

Ten patients with left MCA infarction (6 male, 4 female; age range: 51~77 years; mean age: 61.7±8.4 years) were given rTMS on unaffected brain areas with low frequency (1 Hz), intensity of 100% of resting motor threshold and 20-minute-duration each day for 2 weeks (total 10 session, excluding weekends). Occupational therapy including muscle strengthening, ROM exercise and ADL training (activity of daily living) continued. Tc-99m HMPAO brain perfusion SPECT was obtained before and after rTMS treatment. The changes of cerebral perfusion were analyzed using statistical parametric mapping (SPM12; t=2.71, uncorrected P<0.01, voxel=500).

Following areas showed significant increase in rCBF after 2 weeks rTMS treatment: the frontal pole and the left precentral gyrus. Significant decrement was not noted.

Low-frequency rTMS on the affected brain areas for 2 weeks have increased rCBF in the specific brain regions in left MCA infarction patients. Further analyses correlating clinical characteristics and treatment paradigm with functional imaging data may be helpful in clarifying the pathophysiology of left MCA infarction patients.

Neurology_11

Comparison of the early ^{18}F FP-CIT brain PET to that of brain SPECT in the same patients

Sangdon Kwon, Eunjung Kong, Ihnho Cho, Kyungah Chun

Korea

^{18}F FP-CIT PET, which has recently become available for DAT imaging in clinical practice to evaluate subregional changes in the striatal DAT and dual-phase FP-CIT PET imaging is also studied. There is an assumption that the distribution of radiotracer within the first 15 min would be relative regional cerebral perfusion. If the early phase images reflect regional cerebral perfusion as well as in SPECT, dual-phase ^{18}F FP-CIT PET imaging may be useful for the differential diagnosis of atypical parkinsonism.

The study population comprised patients whom suspected atypical parkinsonian disorders underwent a dual-phase imaging protocol with ^{18}F FP-CIT PET/CT and brain SPECT. PET/CT (Discovery VCT, GE) images were acquired at 10 min (early phase) and 3 h (late phase) after ^{18}F FP-CIT administration (185 MBq). Within 3 days, The SPECT images were obtained 30 minutes after injection of ^{99m}Tc-HMPAO. Regional uptake pattern of cerebral and cerebellar hemispheres was assessed on early phase DAT and SPECT images, using visual and statistical parametric mapping (SPM) analysis (statistical parametric mapping; Institute of Neurology, University of London, UK) and Matlab 6.5(Mathworks, Natick, MA, USA) in 27 patients (male 13, female 14, mean age: 66±11.2 yr).

The visual assessment of the early phase DAT and SPECT images showed slightly different regional uptake in some patients. The group analysis showed that regional uptake of early DAT imaging is decreased in the both cerebellum, both thalamus, both lentiform nucleus and left temporal lobe (Brodmann area 21) and increased in the left limbic area (Brodmann area 36) than the SPECT imaging.

The early phase DAT and SPECT images showed different regional uptake pattern in this study, but further study is needed including more patients and more appropriate comparison methods using ^{18}F FDG PET and early phase ^{18}F FP-CIT PET.

Neurology_20

Improvement of clinical outcome and cerebral perfusion in a patient of artherosclerotic cerebral infarction with repetitive hyperbaric oxygen treatment : A case report and literature review

Shao-Yuan Chen[1,2,4], Chen-Hsu Wang[3,4], Yu-Ming Fan[3,4]

1. Neurological Center
2. Department of Hyperbaric Medicine, Department of Nuclear Medicine, Cardinal Tien Hospital
3. School of Medicine, Fu-Jen Catholic University

Purpose: The most effective treatments for ischemic stroke, such as intravenous or intra-arterial thrombolysis, have a narrow time window and only could be applicable to a limited number of patients. There is an imperative need to develop additional or adjuvant treatment strategies to improve recovery following stroke. Several successful studies in animal models of both focal and global ischemia suggest hyperbaric oxygen therapy (HBOT) may present a possible treatment for acute stroke.

Method: The 56-year-old Chinese man with a history of vascular risk factors. He had an acute ischemic stroke on left corona radiata with right hemiparesis and dysarthria resulting from atherosclerosis. The patient experienced great improvement after repetitive HBOT with lower pressure and shorter duration; this was evidenced by 6 neurological scales and cerebral perfusion images including single-photon emission computed tomography SPECT and brain computed tomography perfusion (CTP).

Conclusions: HBOT should be effective for ischemic stroke patients. However, to date, the benefit of HBOT in acute ischemic strokes could not be demonstrated by a high level of clinical evidence. We highlight the following points:

1. We selected an artherosclerotic stroke patient. (excluding the effect of highly spontaneous
recanalization rate in embolic stroke).
2. Lower pressure (2.0 ATA) and shorter-duration (60 minutes) of HBOT was administered.
3. He was treated with repetitive HBOT for a total of 10 sessions once a day for two weeks.
4. Assessment instruments: 6 neurological scales, 1 for

outcome (mRS), 3 for functional deficit (NIHSS; BI; GCS) and 2 for cognition (MMSE; MoCA); as well as increased regional cerebral blood flow in brain SPECT and decreased penumbra areas in brain CTP.
We proposed the pioneered case with HBOT receiving detailed evaluation and may set up a platform
for future works about adjuvant stroke treatment by HBOT.

Neurology_22

Transient brain ischemia in rats: a study with ^{15}O water PET and digital subtraction angiography

Takashi Kamiya[1,2], Tadashi Watabe[1,4], Genki Horitsugi[1], Keiko Matsunaga[1], Yasukazu Kanai[3,4], Hayato Ikeda[1], Hiroki Kato[1,4], Kayako Isohashi[1,4], Eku Shimosegawa[3,4], Jun Hatazawa[1,4]

1. Department of Nuclear Medicine and Tracer Kinetics (Osaka University Graduate School of Medicine, JAPAN)
2. Department of Medical Technology (Osaka University Hospital, JAPAN)
3. Department of Molecular Imaging in Medicine (Osaka University Graduate School of Medicine, JAPAN)
4. PET Molecular Imaging Center (Osaka University Graduate School of Medicine, JAPAN)

Purpose: To evaluate cerebral blood flow (CBF) by ^{15}O water PET and arterial occlusion/ recanalization by digital subtraction angiography (DSA) with small animal PET/CT in rats.
Methods: In male SD rats (9 weeks old, mean body weight 312g, n=3) under isoflurane anesthesia, transient brain ischemia were created by temporary occlusion (45 min) of the left middle cerebral artery (MCA) by silicone coating suture. Serial dynamic scans of ^{15}O water PET were performed during occlusion and after reperfusion (within 1 hour). DSA was performed just after ^{15}O water PET with iodine contrast medium using the CT of PET/CT scanner. Regions of interest were placed on the ipsilateral and contralateral MCA lesion to measure CBF values (Watabe T, et al., J Nucl Med, 2014).
Results: The CBF ratios of ipsilateral to contralateral lesion were 0.20 ± 0.01 during MCA occlusion and 0.46 ± 0.15 post reperfusion. CBF ratios were significantly increased after reperfusion although ipsilateral CBF remained low level compared to contralateral CBF. DSA revealed the recanalization of ipsilateral MCA vessels.
Conclusions: This study demonstrated the CBF recovery was not sufficient within 1 hours post reperfusion despite recanalization was confirmed by DSA, suggesting recanalization of the artery does not always indicate a full recovery of the CBF.

Neurology_23

Metabolic volumetric analysis for striatum using F-18 FP-CIT PET in patients with Parkinson's disease and normal subjects

Young Jin Jeong[1, 2], Hye Joo Son[1, 2], Hyun Jin Yoon[1, 2], Do-Young Kang[1, 2]

1. Department of Nuclear Medicine, Dong-A University Hospital, Dong-A University College of Medicine, Busan, Korea
2. Institute of Convergence Bio-Health, Dong-A University, Busan, Korea

Purpose: The aim of this study was to compare the difference of volumetric parameters measured by F-18 FP-CIT PET between patients with Parkinson's disease (PD) and normal subjects and to evaluate the correlation between the volumetric parameter's and clinical factors of the PD patients.
Methods: Forty-three PD patients (M = 20, 67.8 ± 5.8 years) and 23 age-matched normal subjects underwent F-18 FP-CIT PET. PET images were acquired at 3 hours after administration of radiotracer. Using dedicated workstation, VOIs for whole striatum were drawn automatically and the velocity method was used to delineate the metabolic margin. Occipital area was used as reference site. Metabolic volume (MV), striatal volume activity (SVA, metabolic volume x SUV_{mean}) and volume specific uptake ratio (VSUR) were calculated in all subjects and the metabolic parameters were compared between PD patients and normal subjects. In PD patients, daily dose of levodopa, H & Y stage, tremor, rigidity and bradykinesia were evaluated and the correlation between the clinical factor and the metabolic parameters was assessed.
Results: MV (14.9 cm^3 vs 19.0 cm^3), SVA (81.7 vs 166.5) and VSUR (6.0 vs 10.7) were significantly lower in PD patients than those of normal subjects ($P < 0.05$). In patients with PD, moderate negative correlation was revealed between SVA and H & Y stage (r = -0.50, P = 0.002), VSUR and H & Y stage (r = -0.51, P = 0.002), and MV and bradykinesia (r = -0.43, P = 0.013), and SVA and bradykinesia (r = -0.45, P = 0.008). Linear regression analysis showed significant correlation between dose of levodopa and metabolic volume parameters (R^2 = 0.10, $P < 0.0001$).
Conclusions: Significant difference in striatal metabolic volume parameter between PD patients and normal subjects and a moderate negative relationship between metabolic and clinical factors was identified. Metabolic volume parameter could be a useful factor to evaluate the striatal function.

Neurology_25

The regions of significant correlation between the scores of Seoul Verbal Learning Test and brain glucose metabolism

Ki Seong Park[1]*, Ho-Chun Song[1], Sae-Ryung Kang[1], Jahae Kim[1], Sang-Geon Cho[1], Minchul Song[2] Geum-Cheol Jeong[2], HeeJeong Park[2], Seong Young Kwon[2], Jung-Joon Min[2], Henry Hee-Seung Bom[2]

1. Department of Nuclear Medicine, Chonnam National University Hospital
2. Department of Nuclear Medicine, Chonnam National University Hwasun Hospital

Purpose: Neuropsychological assessment scores are very useful tool to evaluate the symptoms of dementia patients. The purpose of this study is to demonstrate the regions of significant correlation between the scores of Seoul Verbal Learning Test (SVLT), which is used to evaluate the verbal memory test, and cerebral glucose metabolism using brain ^{18}F-FDG PET (brain PET).

Methods: We enrolled 30 patients who were diagnosed with mild cognitive impairment (MCI) or Alzheimer's disease (AD). They underwent Seoul Verbal Learning Test (SVLT), which is one category of Seoul Neuropsychological Screening Battery-dementia version (SNSB-D) as neuropsychological assessment, and brain PET. The scores of SVLT immediate recall, SVLT delay recall, SVLT discriminability index and brain PET images were analyzed using SPM8 with multiple regression. The voxel threshold for significant differences of FDG uptake was uncorrected $P < 0.001$.

Results: The total score of SVLT immediate recall showed the positive correlation with left mid temporal lobe (X = -58, Y = 36, Z = 6 in Montreal Neurological Institute space (MNI), brodmann area 22), and the score of SVLT delay recall had the positive correlation with left inferior temporal lobe (X = -48, Y = -32, Z = 20 in Montreal Neurological Institute space (MNI), brodmann area 20). The score of SVLT discriminability index showed the positive correlation with the large regions of both temporal lobes and supramarginal gyri (Brodmann 20, 21, 22 and 48).

Conclusions: The impairment of verbal memory is correlated with decreased glucose metabolism of left mid and inferior temporal lobe. This result helps to interpret the hypometabolism of left temporal lobe in brain ^{18}F-FDG PET.

Neurology_26

Quantitative analysis of 2h and 3h ^{18}F-FP-CIT PET in non-dopaminergic movement disorders, parkinson's disease and atypical parkinsonism

Hye Joo Son , Young Jin Jeong , Hyun Jin Yoon , Do-Young Kang

Department of Nuclear Medicine, Dong-A University Medical Center, Dong-A University College of Medicine, Busan, Korea

Purpose: In this study, we evaluated the difference of quantitative value between 2h and 3h ^{18}F- FP-CIT between non-dopaminergic movement disorders, parkinson's disease (PD) and atypical parkinsonism and investigated the possibility of 2h image to substitute 3h image.

Methods: 117 patients were divided into three groups: 33 patients with non-dopaminergic movement disorders (GA), 64 patients with PD (GB), 20 patients with atypical parkinsonism (13 MSA-P, 7 PSP) (GC). Changes of quantitative value between dual time point ^{18}F-FP-CIT PET/CT scans at 2h and 3h were assessed. SUV_{mean} was measured in ROIs of both caudate (RC, LC), anterior and posterior putamen (RAP, LAP, RPP, LPP) and occipital as a reference region. The striatooccipital ratio (SOR) and gradient ratios (AP/C, PP/C) between 2h and 3h images and gradient ratios between disease groups in each 2h and 3h image were compared using paired t-test.

Results: In GA, the mean SOR of 2h and 3h image were different in all subregions in ROI method (P=0.000). In GB, only in RC, LC, RAP, LAP showed difference (P = 0.000). In GC, only RC (P=0.000) and LC (P=0.001) showed difference. In GA, both AP/C and PP/C were not different between 2h and 3h image. In GB, both AP/C and PP/C were different. In GC, both PP/C (Rt : $P < 0.012$, Lt: $P < 0.025$) were different. In 2h image, there was difference in both AP/C and PP/C ($P < 0.00$) between GA (RAP/C: 1.16±0.11, RPP/C: 1.12±0.17, LAP/C: 1.13±0.12, LPP/C:1.12±0.15) and GB (RAP/C: 0.89±0.19, RPP/C: 0.54±0.18, LAP/C: 0.82±0.15, LPP/C: 0.51±0.15). There was difference in both AP/C and PP/C between GA and GC (RAP/C: 0.94±0.19, RPP/C: 0.73±0.27, LAP/C: 0.87±0.16, LPP/C: 0.66±0.26). However, there were difference only in RPP/C ($P < 0.012$) and LPP/C ($P< 0.036$) between GB and GC. In 3h image, difference in gradient ratio between disease groups showed similar pattern as those of 2h image.

Conclusions: Difference of SOR and gradient ratio between 2 h and 3 h image reveals distinctive pattern among disease groups. However, gradient ratio between disease groups at 2h image remained similar pattern with those of 3 h image. Because gradient ratio can be used as clue for differentiating PD with atypical parkinsonism, 2h ^{18}F-FP-CIT can substitute 3h image in visual analysis.

Neurology_29

Experimental Study on Dynamic Changes of DAT and Correlate with Tyrosine Hydroxylase Expression in Striatum of Parkinson's Disease

Chen Wenxin[1], Lin Ling[2], Lin Zhiyi[1], Du Yuequn[2], Ye Jing[2]

1. Department of Nuclear Medicine, Fujian Provincial Hospital, Fuzhou 350001, China.
2. Department of Biochemistry and Molecular Biology, Fujian Medical University, Fuzhou 350108, China

Purpose: To observe dynamic changes in striatal dopamine transporter (DAT) in progression of PD, and to investigate the relationships between changes of DAT and tyrosine hydroxylase (TH) expression in substantia nigra.
Methods: The hemipakinsonium rat model was established by a unilateral injection of 6-OHDA into the right ubstantia nigra pars compacta (SNc) and the right medial forebrain bundle (MFB). Rats were injected with ^{99m}Tc-TRODAT-1 through tail vein at 2,4 and 6 weeks post-lesion, respectively. Both the left and right striata were removed 2h after injection of 7.4 MBq ^{99m}Tc-TRODAT-1.The counts per unit mass of striatum on each side were calculated, then the morphology and distribution of TH in the substantia nigra (SN) were observed, stained with the TH-immunohistochemistry.
Results: The radioactive counts on the lesioned side of SN in PD rats was significantly lower than that of unlesioned side, and it was decreased by 16.8%, 35.9% and 50.1%, respectively when compared with the control side at 2,4 and 6 weeks (P<0.05-0.001,n=5). There existed a positive correlation between radioactive counts and TH immunoreactive positive cells in the denervated substantia nigra. (P<0.01,R=0.9, n=15).
Conclusions: The density of DAT decreases gradually with PD progression, and the distribution of ^{99m}Tc-TRODAT-1 is in consonance with TH gene expression. In a certain extent, ^{99m}Tc-TRODAT-1 imaging can also be used as the objective indicators for the study of transplanted TH gene and genetic therapy.

Oncology_3

F-18 FDG PET/CT in the Detection of Axillary Microcystic Adnexal Carcinoma – a Rare Case Report

Bolormaa Ganbaatar[1,2], Euishin Edmund Kim[3,4], Apichaya Claimon[1,5], Dong Soo Lee[1,3]

1. Department of Nuclear Medicine, Seoul National University Hospital, Seoul, Korea
2. Nuclear Medicine Department of Radiology Center, The First State Central Hospital of Mongolia, Ulaanbaatar, Mongolia
3. Molecular Medicine and Biopharmaceutical Sciences, WCU Graduate School of Convergence Science and Technology, Seoul National University College of Medicine, Seoul, Korea
4. Department of Radiological Sciences, University of California, Irvine, CA, USA
5. Division of Nuclear Medicine, Faculty of Medicine Siriraj Hospital, Mahidol University, Bangkok, Thailand

Purpose: Microcystic adnexal carcinoma (MAC) is a very rare cancer of the skin. Surveillance, epidemiology, and end results (SEER) database analysis identified 223 reported cases. The tumor has locally aggressive behavior and rarely metastasis. Therapy is challenging due to local tumor invasion which may be far beyond visual inspection, and thus imaging is needed to identify tumor extent. The purpose is to demonstrate the first case report of whole-body F-18 FDG PET/CT scan with MAC.
Methods: We report a case of 43-year old man who presented with a painless slow-growing left axillary nodule for 1 year. The nodule was 1 cm in size and excisional biopsy revealed a MAC with positive margin and perineural invasion. One day later, whole-body F-18 FDG PET/CT scan was performed for disease staging.
Results: The PET/CT scan revealed a focal increased activity in the left axillary nodule (1.0 x 2.1 cm. in size) with SUV_{max} of 4.6, consistent with residual tumor. Another faint uptake is seen at subcutaneous lesion in the left upper back with SUV_{max} of 2.6, consistent with post-excisional biopsy change of epidermal After PET/CT study, the wide excision was made, and the pathological report revealed a cluster of atypical epithelial cells involving dermis and subcutis, 0.2 x 0.2 cm in size, consistent with residual MAC. The margin was free from tumor; however, positive perineural invasion was noted.
Conclusions: Our report shows the ability of F-18 FDG PET/CT to detect residual MAC, even though the tumor is very small and has an effect from post-surgical inflammation. Furthermore, PET/CT has a role in evaluation of lymph node and distant metastasis, though it is rare, but affects a clinical management.

Oncology_4

Should Glucoheponate brain SPECT be preferred over FDG PET for evaluation of recurrent high grade brain tumors

Sukanta Barai, Sanjay Gambhir, Shashwat Verma

Department of Nuclear Medicine, SGPGIMS, India

Glucoheptonate is glucose analog with strong affinity for neoplastic brain tissues and until recently was extensively used as a SPECT tracer to differentiate recurrent gliomas from radiation necrosis. However with the wider availability of PET scan facility it is now rarely used in favor of FDG-PET. Though limitation for FDG-PET is well documented in low grade brain tumors, it is considered as tracer of choice for high grade brain tumors. In the present study we report a case where FDG PET failed to detect a high grade multifocal recurrent anaplastic astrocytoma which was nicely detected by a ^{99m}Tc-Glucoheptonate brain SPECT.

A 39 year old female patient who underwent resection of right temporal lobe anaplastic astrocytoma followed by radiotherapy 20 months back was referred to us for evaluation of suspected recurrence. She underwent a FDG-PET/CT scan and subsequently a ^{99m}Tc-Glucoheptonate SPECT of brain using the standard protocols.

Result of Both the FDG-PET and ^{99m}Tc-Glucoheptonate SPECT was reviewed by two nuclear medicine specialist independently and both concurred in their findings. The FDG-PET scan did not reveal any abnormal tracer uptake suggestive of tumor over the entire brain. Since clinical suspicion of tumor recurrence was very high the patient underwent an additional ^{99m}Tc-Glucoheptonate brain SPECT. The study revealed increased tracer uptake in known tumor bed in right temporal lobe and a skip lesion on the contralateral posterior frontal lobe suggestive of viable recurrent tumor.

This study demonstrates that it is possible to have false negative FDG-PET/CT even in high grade brain tumors as well. In presence of high clinical or radiological suspicion of tumor recurrence a normal FDG-PET/CT study should be interpreted with caution and findings may be verified with ^{99m}Tc-Glucoheptonate brain SPECT for proper clinical management.

Oncology_8

The highest metabolic activity on FDG PET is associated with overall survival in limited-stage small-cell lung cancer

Soo Hyun Kwon[1], Seung Hyup Hyun[2], Joon-Kee Yoon[1], Young-Sil An[1], Young-Taek Oh[3], Jin-Hyuck Choi[4], Kwang Joo Park[4] , Su Jin Lee[1]

1. Departments of Nuclear Medicine
2. Department of Nuclear Medicine, Samsung Medical Center, Sungkyunkwan University School of Medicine, Seoul, Korea
3. Radiation Oncology
4. Internal Medicine, Ajou University School of Medicine, Suwon, Korea

Objectives: We evaluated the prognostic value of ^{18}F-fluorodeoxyglucose positron emission tomography (FDG PET) parameters for limited-stage small-cell lung cancer (LS-SCLC).

Methods: We enrolled 59 LS-SCLC patients who underwent pretreatment FDG PET/CT. Various PET parameters were measured in all malignant lesions, and we recorded the highest maximum standardized uptake value (SUV_{max}), and sum of metabolic tumor volume (MTV_{sum}) and total lesion glycolysis (TLG_{sum}). The relationship between SUV_{max} and volumetric PET parameters was evaluated. The prognostic significances of PET parameters and clinical variables were assessed using Cox's proportional hazard regression analysis. Overall survival (OS) and progression-free survival (PFS) were assessed by the Kaplan-Meier method.

Results: The SUV_{max} of the highest metabolic lesion had a significant positive correlation with MTV_{sum} and TLG_{sum} ($P < 0.0001$). Upon multivariate analysis, SUV_{max} was an independent predictor of OS (1 unit increase, hazard ratio [HR]: 1.133, $P = 0.003$) and MTV_{sum} was a significant prognostic factor of PFS after adjusting for age, sex, performance status, tumor stage, and treatment modality. SUV_{max} tended to be a significant prognostic factor for PFS (1 unit increase, HR: 1.078, $P = 0.053$). Patients with higher SUV_{max} (≥ 11) were also characterized by a significantly shorter median OS ($P = 0.0001$) and PFS ($P = 0.0017$) compared with patients with lower SUV_{max}.

Conclusions: The highest SUV_{max} is an independent prognostic factor for survival in LS-SCLC patients.

Oncology_11

Occult tumour thrombosis- Role of F18 FDG PET/CT in Detection

Aditi Khurana[1], Madhavi Tripathi[2], Abhinav Jaimini[3], Anupam Mondal[3] , Rajnish Sharma[3]

1. Department of Nuclear Medicine, VMMC and Safdarjung

Hospital, New Delhi, India
2. All India Institute of Medical Sciences, New Delhi, India
3. Institute of Nuclear Medicine and Allied Sciences, New Delhi, India

Objectives: Tumor thrombus is a rare complication of solid tumors including Renal Cell carcinoma, Wilm's, Testicular tumor, lymphoma, osteosarcoma, pancreatic cancer, adrenal cortical tumors and Ewing's sarcoma. The objective of this study is to evaluate the contribution of ^{18}F FDG positron emission tomography/computed tomography (PET/CT) in the diagnosis of tumor thrombosis.
Methods: We describe 10 cases that harbored occult tumor thrombus detected by fluorine 18 Fluoro-deoxyglucose (^{18}F-FDG) PET/CT imaging as a part of restaging/determination of evaluation of response to treatment. Criteria for positivity of PET/CT included increased focal or linear uptake of ^{18}F-FDG in the involved vessel.
Results: Ten occult tumor thromboses were identified by PET/CT positive scans. Underlying pathologies included choriocarcinoma, lymphoma, renal cell carcinoma, follicular and anaplastic thyroid carcinoma, as well as seminoma.
Conclusions: Cancer related venous thrombus is a rare but significant complication and its recognition by PET/CT can change the management plan and prevent unnecessary long term anticoagulation treatment.

Oncology_12

The Role of Bone Scintigraphy in Newly Diagnosed Prostate Cancer Patients

Padma Savenadia Alam, Johan S. Masjhur

Nuclear Medicine Department of Hasan Sadikin Hospital, universitas Padjajaran, Indonesia

To evaluate the correlation of Gleason score, serum PSA level, and metastatic bone disease in newly diagnosed prostate cancer patients.
This retrospective study was conducted in 59 subjects. Tc-99m methylene-diphosphonate bone scintigraphy, serum PSA level and Gleason score data were collected. Serum PSA levels and Gleason score were compared to bone scintigraphy finding. The data was then analyzed to define the cut-off point by using ROC curve.
Cutt-off point serum PSA level >18 ng/ml, there was only one patient showed bone metastases on bone scitigraphy who had serum PSA level 4 ng/ml and Gleason score 9. Cutt-of point Gleason score 6, there was eight patients showed bone metastases. All of these eight patients had serum PSA level >18 ng/ml.
In newly diagnosed prostate cancer patients with PSA serum level >18 ng/ml or Gleason score >6, bone scintigraphy is recommended to detect bone metastases. PSA serum level is better than Gleason score to predict bone metastases.

Oncology_13

Role of the Baseline Serum Thyroglobulin Levels after Total Thyroidectomy in Patients with Differentiared Thyroid Cancer

Md. Mahbubul Hoque, Ferdous Ara Hussain, Ebnan Ashraf, Nurun Nahar, Sadia Sultana

Institute of Nuclear Medicine and Allied Sciences, Mitford, Dhaka, Bangladesh

Thyroglobulin (Tg) is a well- established biological marker of persistent or recurrent thyroid cancer. The aim of this study was to evaluate the predictive value of the baseline Tg level early after total thyroidectomy, before radioiodine ablation in differentiated Thyroid carcinoma.
A retrospective study was performed on 527 post thyroidectomy patients with differentiated thyroid cancer receiving radioiodine ablation therapy at the institute (in year 2008 and 2009 who had regular follow- ups for 5-6 years. Medical records of these patients were collected and analyzed in December 2014 including clinical characteristics, early post-operative pre-ablation and post ablation Tg (ng/ml) levels , I- 131 whole body scans and ultrasound evaluation of neck.
Patients were classified into 4 groups on basis of baseline Tg level: 0-4, 4.1-10, 10.1-50 and >50 ng/ml. Higher levels of baseline Tg were observed in patients with a larger size of residual tissue (about 12 % cases) and in more extensive disease at the time of presentation, such as neck lymph node metastases (19.8 %) and distant (bone, lung) metastases (about 5%). More than 5% of patients had a baseline Tg level >50 ng/ml. Patients with higher levels of Tg required multiple doses for remission of either persistent or recurrent disease. Lower Tg levels (<4ng/ml) were associated with negligible residual thyroid tissue or a lesser number of metastases. Most of the patients with lower levels of baseline Tg (<2 ng/ml) were found to be in disease-free state at the last follow-up (5-6 years).
In patients with well-differentiated thyroid carcinoma, post-thyroidectomy baseline thyroglobulin level of <4 ng/ml is associated with

a low probability of having persistent disease or metastases. Thus it can be used as a good predictor in disease staging for proper management.

Oncology_14

Clinical Usefulness of F-18 FDG PET/CT for Detection of Synchronous Colorectal Carcinoma in Patients with Gastric Cancer

HaeWon Kim, ByungWook Choi, YoHan Cho, Bong-il Song, KyoungSook Won

Department of Nuclear Medicine, The Armed Forces Capital Hospital, Korea

The purpose of this study was to investigate the diagnostic performance of F-18 fluorodeoxyglucose (FDG) positron emission tomography/computed tomography (PET/CT) for detection of synchronous colorectal carcinoma (CRC) at the time of staging work-up in patients with gastric cancer.

This retrospective study included 256 consecutive patients with gastric cancer who underwent F-18 FDG PET/CT and colonoscopy from May 2008 to July 2014. The diagnosis of focal colonic uptake on F-18 FDG PET/CT was made on the basis of finding of colonoscopy. The histopathologic examinations to confirm diagnosis of colorectal lesions detected by colonoscopy were performed.

The colonoscopy revealed no abnormal lesion in 154 patients and colorectal lesions in 102 patients of 256 patients with gastric cancer. Of the 102 patients, 12 patients had CRC and the incidence of synchronous CRC was 4.7% (12/256) in patients with gastric cancer. The sensitivity, specificity and accuracy of F-18 FDG PET/CT were 83.3%, 92.6% and 92.2%. There was no significant difference of SUV_{max} between true positive and false positive foci on F-18 FDG PET/CT (12.2±7.8 vs. 7.8±2.7, P = 0.116).

F-18 FDG PET/CT showed good performance for detection of synchronous CRC in patients with gastric cancer. F-18 FDG PET/CT is recommended for detection of synchronous CRC in patients with gastric cancer.

Oncology_16

Acrometastasis in Carcinoma Breast- A Case Report

Aditi Khurana[1], Kalpa Jyoti Das[2] , Padma Namgyal[1] ,Ravinder Singh Sethi[1]

1. Department of Nuclear Medicine, VMMC and Safdarjung Hospital, New Delhi, INDIA
2. All India Institute of Medical Sciences, New Delhi, INDIA

Purpose: Bone metastasis to below elbow and below knee is rare. We report two such cases.

Methods: A 30 year old lady presented with complaints of low back ache and inability to move both lower limbs since last 20 days. She had developed difficulty in walking around 6 months back. A trivial trauma 3 months back had led to a fracture neck of left femur for which she was treated conservatively. On questioning further she revealed that she had a right breast mass which was present for almost 2 years now. Clinical examination revealed a 5cmX6cm mass in the upper outer quadrant of right breast. No ulceration or discharge was present. No abnormality was detected in the Left breast on examination. A small right axillary mobile lymph-node was also palpable. She also complained of pain the left wrist since last 1 month. On examination her left wrist and thoracic spine were tender. Biopsy from the breast lesion revealed intra-ductal carcinoma. A whole body radionuclide bone scan and SPECT/CT revealed increased uptake in several bony regions, including the distal end of left radius and the right calcaneum. A CT-guided FNAC of the left radius confirmed metastatic carcinoma.

Results: A diagnosis of multiple skeletal metastases was made and patient was referred back to medical oncology and radiotherapy with reports.

Conclusions: A Whole body MDP planar and SPECT-CT aided the management in a newly diagnosed Stage IV carcinoma breast. These cases are being reported on account of their rarity.

Oncology_20

F-18 FDG PET/CT as a Preoperative Evaluation of Early Gastric Cancer and the Prediction of Lymph Node Metastasis

Sungsoo Kim[1], Ari Chong[2], Jung-Min Ha[2], Min Sung Kim[1], Young Don Min[1]

1. Department of Surgery, Chosun University Hospital, Gwangju, Republic of Korea
2. Department of Nuclear medicine, Chosun University Hospital, Gwangju, Republic of Korea

Purpose: The purpose of this study was to evaluate FDG uptake of early gastric cancer and to evaluate the relationship between lymph node metastasis (nodal metastasis) and FDG uptake of primary tumor in preoperative PET/CT

Methods: This is a retrospective study. We analyzed all patients between 2006 and 2014 who underwent

preoperative PET/CT and whose postoperative diagnosis was T1. If there was not focal FDG uptake compared to adjacent gastric wall, they were categorized as "no uptake group". If there was focal uptake, they were categorized as "uptake group" and SUV_{max} was recored. Other clinical factors including size and depth of tumor, age, sex, differentiation, lauren type and lymphovascular invasion were analyzed between groups.

Results: Total 230 patients were enrolled. The overall incidence of nodal metastasis was 9.6%. Among 230 patients, 39.6% of patients was "no uptake group". In "uptake group", mean SUV_{max} was 4.6±1.7. Tumor size of uptake group was larger (P<0.001, 1.6±0.9 vs 2.6±1.9) and deeper (P=0.004, mucosa vs submucosa) than no uptake group. However, the incidence of differentiation, lauren type, gender, lymphovascular invasion was not significantly different between groups. In addition, there was no statistical difference between incidence of nodal metastasis between groups(P=0.11). In uptake group (n=139), SUV_{max} cut off value for nodal metastasis was 5.75 (sen 52.9%, spe 86.9%). SUV_{max} >5.75 was risk factor for nodal metastasis in uptake group with OR 5.6 (P=0.009).

Conclusions: Larger and deeper tumor showed higher FDG uptake in early gastric cancer. When there is focal uptake of FDG, SUV_{max}>5.75 was risk factor for nodal metastasis in these patients.

Oncology_27

F-18 FDG PET/CT qualitative and quantitative interpretation of mediastinal lymph node in non-small cell lung carcinomapatients with benign mediastinal lymph node hyperplasia

In-Joo Kim, Keunyoung Kim, Seong-Jang Kim, Kyoungjune Pak, Bum Soo Kim, Yun Seong Kim

Department of Nuclear Medicine, Korea

F-18 FDG PET/CT has been reported to be superior to CT imaging alone in identifying metastatic involvement of mediastinal nodes in NSCLC. However, the efficacy of F-18 FDG PET/CT is controversial in regions endemic for granulomatous disease. The accuracy and specificity of F-18 FDG PET/CT are substantially reduced because of falsely increased ^{18}F-FDG uptake in inflammatory nodes. The aim of this study was to evaluate qualitative interpretation of FDG-PET/CT for evaluation of mediastinal nodes to distinguish between malignant and benign lesions compared with objective FDG-PET/CT criterion.

Fifty seven patients with pathologically documented non-small cell lung carcinoma were included in a prospective cohort study and underwent integrated F-18 FDG PET-CT for staging. Forty eight mediastinal nodes were pathologically analyzed through endobronchial ultrasound transbronchial needle aspiration or lymph node dissection. SUV_{max}, $SUV_{max/liver}$, SUV/blood pool and SUV_{max}/contra (lesion uptake adjusted to SUV_{max} of contralateral interlobar LN) were obtained for mediastinal nodes identified with abnormal glucose metabolism.

Qualitative evaluation showed sensitivity, specificity, positive predictive value, and negative predictive value for separating metastatic lymph node benign reactive hyperplasia of 79%, 95%, 95%,and 82%. SUV_{max} and normalized SUV_{max} to liver and blood pool was not significantly different between benign and metastatic lesions. However, SUV_{max}/contra was significantly higher for metastatic lesion than benign leisons. (P<0.05) Receiver-operating-characteristic derived SUV_{max}/contra cutoff was 1.33 (area under the curve, 0.793) and sensitivity and specificity was 71% and 95%.

Qualitative interpretation of F-18 FDG PET/CT was superior to quantitative criterion in discriminating metastatic LNs from benign reactive hyperplasia in patients with benign mediastinal node hyperplasia. SUV_{max}/contra has better sensitivity and specificity than SUV_{max}, $SUV_{max/liver}$ and SUV_{max}/blood pool.

Oncology_30

Value of Interim and Post-therapy ^{18}F-FDG PET/CT for Predicting Outcome of Patients with Angioimmunoblastic T Cell Lymphoma

Ah Young Lee, Seung Hwan Moon, Kyung Han Lee

Samsung Medical Center, Korea

Angioimmunoblastic T cell lymphoma (AITL) is a recently recognized disease entity in Non Hodgkin Lymphoma. ^{18}F-FDG PET/CT (PET/CT) is widely used as a functional image for initial work up, response evaluation, and surveillances of lymphoma. There was no study about the prognostic value of interim and post-therapy PET/CT of AITL which is a kind of T/NK cell lymphoma. Therefore, we studied the prognostic value of the interim and post-therapy PET/CT of AITL patients.

Sixty-three patients who were pathologically diagnosed as AITL were enrolled from March 2007 to

December 2013 in this retrospective study. From the positive and negative results from interim (after 1-4 cycles chemotherapy, n=45) and post-therapy PET/CT (after completion of first line chemotherapy, n=41), the progression free survival and overall survival were analyzed. For 37 patients, Deauville score sum (DSsum) from baseline, interim, and post-therapy was evaluated. In the case of 10 or over DSsum, the progression free survival and overall survival were analyzed, too.

Forty-five patients of 63 patients performed interim PET/CT (71.4%). Thirty-nine patients (86.7 %) were negative while 6 patients (13.3%) were positive. The patients in the positive category showed inferior PFS (P=0.006) and inferior OS (P<0.001). Forty-one patients performed the post-therapy PET/CT. Thirty-five patients (85.4%) were negative while 6 patients (14.6%) were positive. The patients with the positive finding showed inferior PFS and OS, (both P<0.001). Twenty-nine patients (78.4%) were below 10 DSsum and 8 patients (21.6%) were 10 or more DSsum. The patients with 10 or more DSsum showed inferior PFS (P=0.003) and OS (P=0.008). In the multivariable analysis, sex and DSsum were remained as independent predictors.

Both interim PET/CT and post-therapy PET/CT as well as DSsum have significant prognostic values of PFS and OS in AITL.

Oncology_31

Case Series of Pulmonary Lymphoepithelioma-Like Carcinoma (LELC) at Queen Elizabeth Hospital, Hong Kong

BT Kung, KK Ng, TK AuYong, CM Tong

Nuclear Medicine Unit and PDY Clinical PET Centre, Queen Elizabeth Hospital, Hong Kong, China

Purpose: We aim to illustrate the imaging features and role of PET/CT in pulmonary LELC, a rare type of lung cancer associated with Epstein-Barr virus (EBV) infection.

Methods: In this study, the authors reviewed local experience in pulmonary LELC with total of three histologically proven cases of pulmonary LELC where serial FDG-PET/CT imaging was performed at Clinical PET Centre, Queen Elizabeth Hospital, Hong Kong. The clinical, radiological and metabolic features were reviewed.

Results: LELC is a rare type of lung cancer accounting less than 4% of lung cancer and is associated with EBV infection. It is histologically similar to undifferentiated nasopharyngeal carcinoma (NPC), which is also EBV-related and is of particular importance in the Southeast Asia locality. It is crucial to differentiate between primary LELC of the lung versus primary NPC with lung metastases for there are management and prognostic implications. In a case of 65 year-old Chinese woman with incidental finding of left upper lobe lung nodule, PET/CT imaging offered the advantage to review the nasopharyngeal region in the same setting where findings of FDG-avid focus at the nasopharynx alerted the clinician for further endoscopic correlation of the nasopharynx to look for NPC. Furthermore, we have reviewed the radiological and metabolic features of pulmonary LELC in follow-up PET/CT imaging in our case series and compared with primary bronchogenic carcinomas, where the differentiation remain to be challenging. In another case of incidental finding of lung nodule later proven to be LELC, a phenomenon of conversion of metabolic behavior from FDG-negative to –positive was noted in serial FDG PET/CT imaging. The cause remains unclear but other literatures and we postulated that it may be related to the accelerated progression of Epstein-Barr virus infected cell after viral latency.

Conclusions: LELC is a rare but distinct type of pulmonary cancer. This case series serves to review the radiological features and metabolic behaviors of LELC cases and the role of PET/CT imaging from our local experience.

Oncology_32

Ratio of Mediastinal Lymph Node to Primary Tumor FDG Uptake Is Useful in Evaluating Metastatic Lymph Node in Non-Small Cell Lung Cancer

Jaehyuk Cho[1], Sungeun Kim[1], Jae Seon Eo[2], Chulhan Kim[3], Hyo Jung Seo[2], Seunghong Rhee[1], Soyeon Park[2], Eunsub Lee[2], Jukyung Park[1], Sunju Choi[1], Jae Gol Choe[1*]

1. Korea University Anam Hospital, Korea
2. Korea University Guro Hospital, Korea
3. Korea University Ansan Hospital, Korea

Purpose: The aim of our study was to assess diagnostic performance for the ratio of mediastinal lymph node SUV_{max} to primary lung tumor SUV_{max} (LN SUV/primary tumor SUV) and mediastinal lymph node SUV_{max} (LN SUV) compared with visual assessment.

Methods: A total of 154 mediastinal and intrapulmonary lymph nodes from 56 patients (mean age 67.9±8.6) with pathologically confirmed diagnosis of non-small cell lung cancer (NSCLC) between May 2014 and March 2015 were reviewed retrospectively. The pathologic result of lymph nodes were obtained by lymphadenectomy or

endobronchial ultrasonography guided transbronchial needle aspiration (EUBS-TBNA). The LN SUV/primary tumor SUV, the LN SUV and the result of visual assessment were correlated with pathologic findings. Diagnostic performance was assessed by receiver operating characteristic (ROC) analysis and each of methods was worked out optimal cut-off value that would best discriminate between metastatic and benign lymph nodes.

Results: There were significant correlation between all three methods and pathological status of mediastinal lymph nodes (P<0.001). The mean LN SUV/primary tumor SUV of metastatic lymph nodes (0.91±0.5) was significantly higher than that of benign lymph nodes (0.3±0.1, P< 0.001). The mean LN SUV of metastatic lymph nodes (4.9±2.5) was significantly higher than that of benign lymph nodes (1.9±0.6, P< 0.001). As analyze the ROC curve, the area under curve (AUC) of LN SUV/primary tumor SUV (0.903) was significantly higher than that of visual assessment (P=0.03). There were no significant differences between AUC of visual assessment (0.829) and that of LN SUV (0.876, P=0.5). The optimal cut-off value of LN SUV/primary tumor SUV was 0.48 (sensitivity 79.1%, specificity 90.1%).

Conclusions: We found that the LN SUV/primary tumor SUV, LN SUV and visual assessment show statistically significant differences between malignant and benign lymph nodes. The LN SUV/primary tumor SUV might have the best diagnostic performance.

Oncology_33

Unsuspected Embryonal Carcinoma of Testis Diagnosed by ^{18}F-FDG PET/CT

Sunju Choi[1], Jae gol Choe[1], Sungeun Kim[1], Jae Seon Eo[2], Hyo Jung Seo[2], Chulhan Kim[3], Seunghong Rhee[1], Jaehyuk Cho[1], Soyeon Park[2], Eunsub Lee[2]

1. Department of Nuclear medicine in Korea University Anam Hospital, Korea
2. Department of Nuclear medicine in Korea University Guro Hospital, Korea
3. Department of Nuclear medicine in Korea University Ansan Hospital, Korea

Purpose: We report a case of a 32-year-old male affected by embryonal carcinoma of testis which metastasize to lung and supraclavicular, mediastinal, abdominal lymph nodes. The patient admitted for cough and chest pain persisted during three weeks. Chest CT presented that approximately 6.8 cm sized soft tissue mass lesion encircling left upper lobar bronchus with multiple pulmonary parenchymal, pleural nodules in both lungs and extensive retroperitoneal lymphadenopathy. The patient underwent percutaneous needle biopsy from a nodule of left upper lobe. Initially the histologic finding suggested non-small cell carcinoma of lung. To detect other metastatic lesions, patient underwent ^{18}F-FDG PET/CT.

Methods: Maximum intensity projection and cross-sectional views and fusion images of ^{18}F-FDG PET/CT were generated and reviewed.

Results: ^{18}F-FDG PET/CT images showed increased FDG uptake at multiple nodules in both lungs, left supraclavicular, anterior mediastinal, subaortic, retrocrural, left paraaortic, aortocaval, portocaval, and bilateral iliac lymph nodes. Left testis showed intense FDG uptake with maximal standardized uptake value of 7.6. For evaluating unexpected intense FDG uptake in left testis, additional physical examination was done and the patient complained about mild scrotal pain. According to increased FDG uptake of testis and scrotal pain, placental alkaline phosphatase (PLAP) and CD30 immunohistochemistry staining on previous acquired tissue from lung nodule was additionally done. The results of PLAP and CD30 staining were positive. These findings strongly suggested that the lung nodules were originated from embryonal carcinoma of testis.

Conclusions: It was difficult to diagnose metastatic lung lesions from primary testicular germ cell tumor without scrotal symptoms. In this case, systemic evaluation by ^{18}F-FDG PET/CT revealed the testicular lesion without the clinical symptom correlation. In conclusion, this report showed one of the cases that ^{18}F-FDG PET/CT, the principal diagnostic tool to distinguish the primary cancer from other mimicking malignancies which have a high propensity for metastatic spread.

Oncology_35

Influence of Metabolic Health Disorders on the Prognostic Value of Tumor ^{18}F-FDG Uptake in Stage I Non-Small Cell Lung Cancer

Seung Hyup Hyun[1], Kyung-Han Lee[1], Seung Hwan Moon[1], Young Seok Cho[1], Joon Young Choi[1], Yearn Seong Choe[1], Byung-Tae Kim[1], Jhingook Kim[2], Jae Ill Zo[2], Hojoong Kim[3], O Jung Kwon[3], Hee Kyung Ahn[4]

1. Departments of Nuclear Medicine
2. Thoracic Surgery
3. Medicine, Samsung Medical Center, Sungkyunkwan University School of Medicine, Republic of Korea
4. Department of Internal Medicine, Gachon University Gil Medical Center, Republic of Korea

Purpose: Metabolic health disorders such as high body-mass index (BMI), fatty liver disease (FLD), pre-diabetes/

diabetes can influence cancer outcome, but their prognostic impacts on patients with early stage non-small cell lung cancer (NSCLC) have not been fully explored. Furthermore, it is unknown whether they may influence the prognostic value of tumor FDG uptake. We examined prognostic influences of metabolic health disorders and the metabolic health-related prognostic value of tumor FDG uptake in patients with early stage NSCLC.

Methods: The study consisted of a cohort of 1,197 patients with stage I NSCLC, who underwent preoperative FDG PET/CT followed by curative resection without adjuvant therapy. The prognostic associations of tumor FDG uptake, BMI, FLD, and pre-diabetes/diabetes with disease-free survival (DFS) were assessed using Cox regression models and Kaplan–Meier analysis.

Results: High BMI (≥ 23 kg/m^2), pre-diabetes/diabetes, FLD were present in 58.2%, 51.5%, 22.3% of subjects. These metabolic health disorders did not significantly affect tumor FDG uptake level. After adjusting for all potential prognostic factors, high BMI (HR, 0.59; 95% CI, 0.43–0.81; *P* = 0.001) and FLD (HR, 0.60; 95% CI, 0.38–0.94; *P* = 0.027) were associated with better DFS, whereas tumor SUV_{max} (HR, 1.72; 95% CI, 1.43–2.07; *P*< 0.001) and diabetes/pre-diabetes (HR, 1.42; 95% CI, 1.02–1.97; *P* = 0.037) were associated with worse DFS. In addition, when subjects were stratified according to metabolic health disorders, the prognostic value of tumor FDG uptake was preserved in all sub-groups, and its risk stratification was improved by low BMI, no FLD, and pre-diabetes/diabetes.

Conclusions: Metabolic health statuses including lower BMI, absence of FLD, and pre-diabetes/diabetes, as well as higher tumor FDG uptake, are significantly associated with worse DFS in patients with stage I NSCLC following curative resection. In addition, the prognostic value of tumor FDG uptake is strengthened in patients with these metabolic health statuses.

Oncology_41

The Diagnostic Performance of FDG PET/CT for Recurrent Gastric Cancer is Significantly Affected by Primary Tumor FDG Uptake Level

Kyung-Han Lee, Soo Jeong Kim, Young Seok Cho, Seung Hwan Moon, Joon Young Choi, Yearn Seong Choe, Byung-Tae Kim

Department of Nuclear Medicine, Samsung Medical Center, Korea

The outcome of advanced gastric cancer remains poor, and early detection of recurrence is important. FDG PET/CT is known to be useful in detection of recurrent gastric cancer, but the specific indication for surveillance with PET/CT in gastric cancer following curative resection remains unclarified to date. In this study, we evaluated the relation between FDG uptake of primary tumor and the patterns of recurrent disease in advanced gastric cancer. And we investigated whether FDG-avid primary tumors are associated with improved performance of surveillance PET/CT for detecting recurrent gastric cancer.

Subjects were 372 patients (mean age 57.3 ± 11.5 y, male 254) with advanced gastric cancer who underwent curative surgery. All subjects had FDG PET/CT for initial staging and for recurrence surveillance after surgery. Primary tumors were classified as FDG-avid if they displayed focal uptake with SUV_{max} ≥ 4, or were otherwise classified as non-FDG-avid. Follow up FDG PET/CT were evaluated for recurrence. The presence of recurrence was determined by medical records with > 11 mo of follow-up.

Of the 372 subjects, 240 had FDG-avid primary tumors (64.5%; 59.7 y, male 175), whereas 132 had non-FDG-avid primary tumors (35.5%; 52.9 y, male 79). During follow-up, 72 patients (19.6%) were diagnosed to have recurrence. Among 63 cases with eligible follow-up PET/CT, 42 had FDG-avid primary tumors and 21 had non-FDG-avid tumors. For all recurrences, PET/CT sensitivity was 34/42 (81.0%) for the FDG-avid group and 11/21 (52.4%) for the non-FDG-avid group (*P* = 0.018). For recurrences outside the anastomosis site, PET/CT sensitivity was 41/58 (70.7%) for all subjects, 32/39 (82.1%) for the FDG-avid group, and 9/19 (47.4%) for the non-FDG-avid group (*P* = 0.006). PET/CT specificity for recurrence was 97.3%, 97.1%, and 97.5% for respective groups (*P* = n.s.).

In this study, the detection sensitivity of recurrent gastric cancer by FDG PET/CT was superior in patients with FDG avid primary tumors than patients with FDG non-avid tumors. Hence, follow-up FDG PET/CT appears to have greater value for recurrence surveillance in patients with high tumor FDG uptake on initial PET/CT.

Oncology_42

Preoperative breast-specific gamma imaging as an indicator of clinicopathologic features of breast cancer

Jin Kyoung Oh, Eun Kyoung Choi, Jiyoung Ryu, Yong-An Chung, Ikdong Yoo

Department of Radiology, Incheon St. Mary's Hospital, College of Medicine, The Catholic University of Korea, Korea

The purpose of this study is to assess the correlation between breast specific gamma imaging (BSGI)

findings and clinicopathologic features of breast cancer.

Breast cancer patients who performed preoperative BSGI between September 2013 and April 2014 were retrospectively reviewed. All lesions were confirmed by pathology. Clinicopathologic factors were compared with the uptake of masses from BSGI. BSGI was evaluated by visual interpretation, according to 2010 Society of Nuclear Medicine (SNM) guideline. The factors included for analysis were: size of primary tumor, histologic grade, nuclear grade, presence of ductal carcinoma in situ (DCIS), extensive intraductal component (EIC), estrogen receptor (ER), progesterone receptor (PR), human epidermal growth factor receptor 2 (ERBB2, formerly HER2), Ki67 and p53.

A total of 84 lesions from 51 patients were confirmed by surgery or biopsy, with 67 malignant and 17 benign lesions. Among the malignant lesions, BSGI grade was 3 in 10 (15%), 4 in 8 (12%) and 5 in 40 (60%). BSGI grade was higher in cancers with > 1 cm (P < 0.001). In 48 malignant lesions with immunochemical features, higher histologic grade and Ki67 index of primary tumor were significantly associated with high BSGI grade (P = 0.036 and 0.021, respectively). BSGI grade was not significantly associated with nuclear grade, presence of DCIS, EIC, ER, PR, ERBB2 and p53 (P = 0.061, 0.720, 0.815, 0.818, 0.514, 0.405 and 0.066, respectively).

BGGI grade was higher in breast cancers with size larger than 1cm, higher histologic grade and positive Ki67.

Oncology_43

F-18 FDG PET/CT can predict survival of advanced hepatocellular carcinoma patients: a multicenter retrospective cohort study

Mijin Yun, Jin Kyoung Oh, Sae Jung Na, Seung Hyup Hyun, Jeong Won Lee, Il Ki Hong, Bong-Il Song, Tae-Sung Kim, Jae Seon Eo, Yong-An Chung

Department of Nuclear Medicine, Incheon St. Mary's Hospital, College of Medicine, The Catholic University of Korea, Incheon, Korea

We evaluated the prognostic value of pretreatment F-18 flurodeoxyglucose positron emission tomography/computed tomography (F-18 FDG PET/CT) in advanced hepatocellular carcinoma (HCC).

A total of 293 patients with advanced HCC between 2009 and 2010 who underwent staging F-18 FDG PET/CT before treatments were retrospectively enrolled from 7 university hospitals. The metabolic parameters from PET/CT including maximum standardized uptake value (SUV_{max}) and tumor-to-normal liver uptake ratio (TLR) and clinical variables were analyzed with respect to overall survival (OS).

During the median follow-up of 6.6 months, 251 patients died. In the univariate analysis, Child-Pugh classification, distant metastasis, AFP, tumor size, tumor number, $SUV_{max}$and TLR were associated with OS. In multivariate analysis, Child-Pugh classification, distant metastasis, tumor size, SUV_{max} and TLR were significantly correlated with OS. Patients with high F-18 FDG uptake (SUV_{max}≥ 4.5 or TLR ≥ 3.0) showed significantly worse prognosis than those with low F-18 FDG uptake (P < 0.001).

Metabolic parameters from F-18 FDG PET/CT are independent prognostic factors for OS in advanced HCC patients.

Oncology_50

Negative whole body iodine scan with high thyroglobulin during first follow up in differentiated thyroid cancer patients is really a worrisome sign? Five year follow up study in a tertiary care hospital.

Manoj Gupta, P. S. Choudhury, Parul Gupta, Sudipta Nag

Department of Nuclear Medicine, Rajiv Gandhi Cancer Institute and Research Centre, Delhi, India

Objectives: There is a diagnostic and treatment dilemma for patients with high serum thyroglobulin (Tg) with negative imaging during first follow up after optimal primary treatment. Both ATA 2009 and NCCN 2015 suggest cross sectional imaging at sTg more then 5-10ng/ml and empirical high dose treatment for non-localizing disease. we analyzed the long term outcome of these patients with follow up only.

Methods: Retrospective analysis of DTC patients with five years follow-up or till recurrence was done. Patients were divided into group 1 (n-35) with disease free status on first follow-up and group 2 (n-29) with high sTg (> 2µg/l) with normal imaging. Patients were categorized into low, intermediate and high risk based on pathological & diagnostic ^{131}I scan findings.

For statistical analysis, histology, stage & risk-categories of both groups were correlated with p value. Best sTg cut off for predicting recurrence by ROC curve and odd ratio for sTg trend was also analyzed for group 2. Independent T test was used for progression free survival (PFS).

Results: No statistical differences were seen in histology, stage and risk category distributions in groups. Group 2 patients with high sTg (Range 81-2.5 µg/ml, Mean 20.5

μg/l) on first follow-up had higher risk of recurrence (odd ratio 4.304) but p value is insignificant (p value 0.090). 86.2 % of group 2 patients showed decreasing trends and 62.1% patient's sTg become normal in follow up. Indeed, decreasing trends in sTg reduced the risk of recurrence (odd ratio 1.3939, p value 0.7912). No patients with low risk category had recurrence irrespective to sTg value. ROC analysis showed sTg > 11μg/l was the best cutoff in predicting recurrence with sensitivity 100% & specificity 56.52%. High sTg was not associated with lower PFS (p value 0.232), however progressive sTg had significant low PFS (p value <0.005).

Conclusions: High sTg with negative DxWBS doesn't warrant an aggressive diagnostic and therapeutic approach at first encounter. 86.2% of these patients showed decreasing trends with no higher risk of recurrence or bad PFS. Aggressive approach should be reserved for rising trends of sTg patients only.

Oncology_51

The associate factor of the FDG avid lymph node at the time of the gastric cancer staging

Sungmin Jun, Heeyoung Kim

Department of Nuclear Medicine, Kosin University Gospel Hospital, Korea

This study is designed to evaluate the associate factor of the FDG uptake in the metastatic lymph node at the time of the gastric cancer staging.

We retrospectively reviewed medical records of the patients who underwent curative operation from August 2013 to January 2015 for the biopsy proven gastric cancer. Among the patients underwent preoprative PET/CT, the one who showed increased uptake in primary stomach cancer were included the study. Because, without uptake in the primary cancer, there was no case showing hypermetabolic lymph node. The predicting variables are as following: the SUV_{max} of the primary cancer, the location of the primary tumor, gross cancer type, histologic type(tubular adenocarcinoma, signet ring cell carcinoma, others), histologic type by Lauren (indeterminate, diffuse, intestinal and mixed), maximal tumor size, pathologic T stage(1,2,3,4), pathologic N stage(0,1,2,3a,3b), lymphatic invasion, venous invasion, perineural invasion and p53 mutation.

Univariate analysis was done with Chi-square test and ROC curve analysis and multivariate analysis was done with Logistic regression.

Total 95 patients were included and 25 patients showed FDG avid lymph node. There was one false positive lymph node among 95 cases. In the univariate analysis, the SUV_{max} of the primary cancer(>5.4, P<0.0001), tumor size (>4.3cm, P=0.005), gross type (AGC, P=0.005), T stage (P=0.008), N stage (P<0.0001), lymphatic invasion (P=0.009), venous invasion (P=0.003) were statistically significant factor in the prediction of FDG avid lymph node. The Lauren calssification and p53 mutation showed statistically equivocal results (P=0.05 each). The histology, location of the primary tumor or perineural invasion were not statistically correlated with FDG avid lymph node.

In the multivariate analysis except statistically insignificant variables, the SUV_{max} of the primary cancer (>5.4, OR 5.58, P=0.007) and N stage (OR N1 18.93(P=0.013), N2 10.23(P=0.052), N3a 41.66(P=0.003), N3b 104.49(P=0.0001)) remained statistically significant variables.

The associate factor of the FDG avid lymph node at the time of the gastric cancer staging was the SUV_{max} of the primary cancer and N stage.

Oncology_52

Correlation between Proliferation Index and Metabolic Activity at the Biopsy Site in Newly Diagnosed NHL

Vishal Agarwal[1], B Suneetha[2], Surbhi Pande[2], Saroj Sahu[2]

1. SRMS Functional Imaging & Medical Centre, Lucknow, India
2. Medanta the Medicity hospital, Gurgaon, India

Objectives: In recent years, positron emission tomography (PET), particularly with [^{18}F] fluorodeoxyglucose (FDG), has emerged as an alternative to computed tomography (CT) not only in treatment evaluation but also in the staging of lymphomas. In lymphoma, Ki-67 proliferating index (MIB-1 labeling index) indicates the proliferation potential of tumour cells, which often affects the prognosis. Although the correlation between the standardized uptake value (SUV) on PET and the proliferation potential of tumour cells has been reported in several tumours, only few studies have elucidated this in the case of malignant lymphoma, which is one of the most sensitive tumours to therapy.

Methods: We did a retrospective study on 47 patients (45 were aggressive lymphomas and 2 were mantle cell) referred for initial staging of lymphoma to our nuclear medicine department in last 1 year. Inclusion criteria were newly diagnosed biopsy proven lymphoma with complete pre-treatment evaluation including history, physical examination and standard laboratory tests, whole-body FDG PET/CT for pre-treatment staging and biopsy samples evaluation using immunohistochemical staining to look for Ki-67 expression. Recurrent cases of

lymphoma were excluded.
Results: All the cases exhibited high SUVs at the site of biopsy (ranging from 8.8-59.43) and high Ki-67 index, ranging from 40-100%. In 17 of the 47 patients, the biopsy site was discordant with the maximum SUV site. In the remaining 30 patients, biopsy site and the site for maximum SUV were the same. Bx SUV_{max}showed significant positive correlation with the Ki-67 proliferation index (r=0.56; $P < 0.01$). Significant positive correlation was also detected between the Bm $SUV_{max}$and the Ki-67 proliferation index (r=0.52; $P < 0.01$).
Conclusions: The $BxSUV_{max}$ correlated with the Ki-67 proliferation index, and a correlation was detected as well between the maximum SUV of the whole-body ($BmSUV_{max}$) and the Ki-67 proliferation index, indicating that tumour proliferation potential might be predicted in vivo by FDG-PET/CT images and thus, PET/CT may be useful to guide biopsy by selecting sites with the $BmSUV_{max}$ when clinically appropriate.

Oncology_53

Can We Predict Microvascular Invasion in HCC on FDG PET-CT?

Vishal Agarwal[1], Surbhi Pande[2], Saroj Sahu[2], Rashmi Kavindran[2]

1. SRMS Functional Imaging & Medical Centre, Lucknow, India
2. Medanta the Medicity hospital, Gurgaon, India

Objectives: The purpose of this study is to correlate clinicopathologic and PET-CT parameters with the presence of microvascular invasion (MVI) at histopathologic examination (HPE) in patients with hepatocellular carcinoma (HCC) who underwent liver transplantation.
Methods: We assessed 224 patients with HCC undergoing liver transplantion and a pre-transplant PET-CT. Three physicians (two nuclear physicians and one radiologist) analyzed the following tumor parameters in consensus: size, multi-focality, pattern of uptake, quantitative FDG uptake (SUV), pattern of enhancement and distance to closest vessel. The size and number of lesions, tumor differentiation and the presence or absence of microvascular invasion were determined at HPE and these findings were analysed vis-a-vis to the imaging parameters on PET-CT.
Results: None of the clinical parameters was predictive of MVI; however on uni-variate analysis, MVI was significantly associated with multi-focality, uptake pattern and distance to the closest vessel on FDG PET-CT. By applying multiple logistic regression analysis, uptake pattern (heterogeneous and peripheral FDG uptake) was found to be the only independent risk factor for MVI.
Conclusions: Heterogeneous and peripheral FDG uptake on PET-CT was the only parameter that correlated significantly with MVI.

Oncology_54

Cholangiocarcinoma with Metastases to Breast: Rarer Than the Rare Entity

Vishal Agarwal[1], Surbhi Pande[2], Nitin Gangrade[2], Saroj Sahu[2]

1. SRMS Functional Imaging & Medical Centre, Lucknow, India
2. Medanta the Medicity hospital, Gurgaon, India

Objectives: With over 1 million new cases in the world each year, breast cancer is the most common malignancy in women, and accounts for 18% of all female cancers. However, metastatic involvement of the breast is relatively rare, most common causes being contralateral breast cancer, malignant melanoma, lymphoma, lung cancer, ovarian carcinoma, soft tissue sarcoma, gastrointestinal tumors and genitourinary tumors. Autopsy reports indicate an incidence of 1.7% to 6.6% for non-primary breast malignancy. The clinical incidence is only from 0.5% to 1.3%.
Methods: We present a young female of age 35 years, presenting in the hospital for pain abdomen and jaundice. On evaluation, she was found to have a liver mass with altered liver function tests. On FDG PET-CT examination, FDG avid heterogeneously enhancing irregular lesion was noted in the right breast with another FDG avid peripherally enhancing rounded lesion in the left breast. Liver showed a peripherally enhancing FDG avid SOL in segment V, VIII and IV, with ill-defined margins and irregular peripheral enhancement & lobular outline.
Results: In view of hypermetabolic heterogeneously enhancing lesions in B/L breasts and FDG avid peripherally enhancing SOL in liver, diagnoses of metastatic Ca. breast was suggested and pathologic correlation was advised. However, HPE of right breast lesion confirmed it to be metastatic carcinoma rather than the primary of breast.
Conclusions: Cholangiocarcinoma is a slow growing rare, malignant tumor of the bile duct, accounting for less than 1% of all cancers. Mostly, it spreads locally via the lymphatics to regional lymphnodes. Metastatic focus in the breast is a very rare presentation, this being probably the first reported case.

Oncology_65

Assessment of Interobserver Reproducibility in Quantitative F-18 FDG PET Measurements in Non-small cell Lung Cancer

Young Ha Park, Eun Ji Han, Sea Jung Na, Woo Hee Choi

Department of Radiology, College of Medicine, The Catholic University of Korea, Korea

Purpose: The purpose of this study was to evaluate interobserver reproducibility in quantitative fluorine-18 (F-18) fluorodeoxyglucose (FDG) positron emission (PET)/computed tomography (CT) measurements in non-small cell lung cancer (NSCLC) patients.

Methods: Baseline PET/CT scans of 29 NSCLC patients were included. Three blinded nuclear medicine physicians retrospectively assessed the maximal and peak standardized uptake value (SUV_{max} and SUV_{peak}) and metabolic tumor volumes (MTVs) of malignant lesions on PET images. Four cut-off values for MTVs were applied: mean liver SUV + 2 standard deviations (MTV_{liver}), a fixed value of 2.5 ($MTV_{2.5}$), 50% of SUV_{max} (MTV_{max50}), and 50% of SUV_{peak} (MTV_{peak50}). Interobserver reproducibility of parameters was described by intraclass correlation coefficients (ICCs) and estimates of variance.

Results: Mean values of SUV and MTV measurements were not significantly different among the three readers. The SUV measurements were almost perfectly reproducible, with ICCs for SUV_{max} of 0.999 and SUV_{peak} of 1.000. Furthermore, MTV_{max50} and MTV_{peak50} measurements showed excellent reproducibility with ICCs ranging from0.936 to 0.974. The MTV_{liver} and $MTV_{2.5}$ measurements were substantially reproducible, with ICCs ranging from 0.763 to 0.800.

Conclusions: There was almost perfect interobserver reproducibility for SUVs from FDG PET measurements of NSCLC patients. Furthermore, MTV_{max50} or MTV_{peak50} may be appropriate to use for clinical guidance, because they yielded higher ICCs and narrower precision than MTV_{liver} or $MTV_{2.5}$. Although interobserver agreements for MTV_{max50} and MTV_{peak50} were excellent, careful consideration should still be given to determining cut-off points for response criteria or prognosis stratification because some variability does exist.

Oncology_67

Prognostic value of volumetric metabolic parameters measured by ^{18}F-FDG PET/CT in diffuse large B-cell lymphoma patients with extranodal involvement

Shin Young Jeong, Seung Hyun Son, Chang-Hee Lee, Ji-hoon Jung, Choon-Young Kim, Ju Hye Jeong, Sang-Woo Lee, Byeong-Cheol Ahn, Jaetae Lee

Department of Nuclear Medicine, Kyungpook National university, School of Medicine and Hospital, Korea

Extranodal involvement in malignant lymphoma is known as one of the poor prognostic factors. However, prognostic factors in the diffuse large B-cell lymphoma (DLBCL) patients with extranodal involvement are not well known. This study was performed to determine which clinical factor or PET parameter could be the best predictor for prognosis of DLBCL patients with extranodal involvement.

Nineteen DLBCL patients with extranodal involvement who underwent pretreatment ^{18}F-FDG PET/CT were enrolled. Clinical parameters [age, Ann Arbor staging, Eastern Cooperative Oncology Group (ECOG) performance status, serum LDH level, International Prognostic Index (IPI) score, and metabolic complete response (mCR) status] and metabolic PET parameters [nodal metabolic tumor volume (NMTV), extranodal MTV (ENMTV), total MTV (TMTV), and ENMTV/NMTV ratio] were analyzed for their usefulness in predicting disease specific survival (DSS).

Ten of 19 patients (52.6%) died during follow-up period (mean, 40.3 months). Non-survivors had higher TMTV than survivors (768.9±778.8 cm3 vs. 158.1±194.0 cm3, *P*=0.0355). ENMTV was also higher in non-survivors (594.2±738.4 cm3 vs. 83.6±133.1 cm3), but there was no statistical significance (*P*=0.0573). Optimal cutoff values of NMTV, ENMTV, TMTV, and ENMTV/NMTV ratio for DSS were 2.89, 69.63, 73.93 cm3, and 2.83, respectively. On univariate survival analysis, ECOG performance status (≥2, *P*=0.0130), mCR+ status (*P*=0.0033), NMTV (≥2.89, *P*=0.0427), ENMTV (≥69.63, *P*=0.0127), TMTV (≥73.93, *P*=0.0295) were significant prognostic factors for DSS, whereas other clinical factors including IPI score, and ENMTV/NMTV ratio were not. On multivariate survival analysis, TMTV was the best predicting factor for DSS (HR=14.8; *P*=0.0289), followed by mCR+ status and ECOG performance status. The TMTV on pretreatment ^{18}F-FDG PET/CT could be a powerful prognostic factor for DSS in DLBCL patients with extranodal involvement. Patients with high TMTV, mCR- status, high ECOG performance status are at higher risk of shorter survival.

Oncology_69

Elevated CA 125, Ascites and Mass-like Structure on Abdominal CT, and Florid FDG Uptake in Extrapulmonary Tuberculosis

Patricia A. Bautista

St. Luke's Medical Center, Global City, Philippines

Purpose: PET/CT is often utilized to aid in diagnostic challenges. The purpose of this case report is to illustrate a potential interpretive pitfall and serve as a reminder, especially to new PET/CT readers in developing countries, that malignancy, infection and inflammation may present similarly on FDG PET.

Methods: Our patient is a 27-year-old woman who presented with gradual abdominal enlargement, recurrent febrile episodes, elevated CA 125 (1073 U/mL), and massive ascites and a mass-like structure above the mesenteric root found on CT. FDG PET/CT was requested for evaluation of possible malignancy versus infection. Florid FDG uptake was seen in the peritoneum, mesenteric thickening and stranding, and nodular soft tissue foci in both sides of the pelvis. Increased FDG accumulation was also seen in the reticular and nodular densities in the upper lobes of both lungs, subcapsular aspect of the left lobe of the liver, and in lymph nodes in the neck and chest. Mild FDG activity was noted in the left-sided pleural effusion and massive ascites. The patient was eventually diagnosed to have peritoneal tuberculosis upon further laboratory testing.

Results: Its presentations are often not specific and its pattern of uptake, which may be marked accumulation of ^{18}F-FDG, is a mimic of that in peritoneal carcinoma, as reported in several studies. Likewise, the presence of ascites and high levels of CA 125 do not necessarily indicate malignant lesions in reproductive women. After all, tuberculosis is still a global emergency. It is, in fact, still a leading cause of morbidity and mortality in the Philippines, which is ranked eighth among the high-burdened countries in the world. Although PET/CT is useful in the simultaneous assessment of pulmonary and extrapulmonary TB, no characteristic pattern has been identified yet. Standardized uptake values and dual time point imaging are not reliable in distinguishing TB from cancer and nontuberculous inflammatory processes.

Conclusions: Thus, even though the majority of referrals for PET/CT are related to oncology, the possibility of peritoneal tuberculosis should always be entertained in a tuberculosis endemic region.

Oncology_71

Lung cancer versus chronic inflammation: can we differentiate the two on F-18 FDG PET/CT?

Hyoungwoo Kim, Sonya Youngju Park, Hye Lim Park, Eun Ji Han, Woo Hee Choi, Young Ha Park

Seoul St Mary's Hospital, College of Medicine, The Catholic University of Korea, Republic of Korea

Purpose: The aim of this study is to find differentiation points between chronic inflammation and lung cancer of similar findings on F-18 FDG PET/CT.

Methods: FDG PET/CT images from January 2010 to October 2014, performed for evaluation of pulmonary nodule in 180 patients (mean age 62±10 years) who had irregular consolidative nodule/mass greater than 1 cm in diameter with low to moderate FDG avidity were retrospectively reviewed. 174 patients (96.7%) had pathologic confirmation. 6 patients (3.3%) had what were clinically considered benign nodules as they showed decrease in size without treatment. Lesions were analyzed by component (part solid, predominantly solid, and solid only), margin (smooth, partly irregular, and irregular), location (lung lobe), other lung lesion presence, axial diameter and metabolic parameters (SUV_{mean}, SUV_{max} and SUV_{peak}). The Student t test and Pearson's Chi-square test were used to compare continuous variables and categorical variables, respectively.

Results: There were 35 (19%) benign and 155 (81%) malignant cases. The most common type of component in malignant group was part solid (80 cases, 55%) and in benign group was solid only (19 cases, 54%). There was a tendency that malignancy group had more part solid tumors than benign group (80 cases, 55% vs. 11 cases, 31%) with statistically significance (P=0.038). The other parameters showed no significant value in differentiating between chronic inflammation and lung cancer.

Conclusions: The component of nodule provided differentiation value in differentiating chronic inflammation and lung cancer on F-18 FDG PET/CT. The pulmonary nodules with part solid feature showed higher possibility of malignancy than nodules with other component features. However, other parameters including metabolic parameters had no significant value in interpreting ambiguous pulmonary lesions.

Oncology_75

Surveillance F-18 FDG PET/CT in Oral Cavity or Oropharyngeal Cancer Patients

Woo Hee Choi, Eun Ji Han, Ie Ryung Yoo

Department of Radiology, College of Medicine, The Catholic University of Korea, Korea

Purpose: The objective of this study was to evaluate the value of surveillance PET/CT scans in oral cavity or oropharyngeal cancer patients.
Methods: Inclusion criteria were (1) biopsy proven squamous cell carcinoma originating in the oral cavity or oropharynx; (2) completion primary therapy with clinical complete response; (3) 18 years old or over. Patients with non squamos cell carcinoma, distant metastasis during initial staging, history of prior or concurrent second malignancy, history of prior relapse were excluded. A total of 605 follow-up PET/CT scans from 212 patients performed between January 2004 and December 2013 were evaluated retrospectively. The follow-up PET/CT scan results were correlated with clinical assessment. Clinical assessment included conventional physical examination/endoscopy and anatomical imaging (enhanced neck CT or MRI).
Results: The median number of sequential follow-up PET/CT scans per patients was three. During a median follow-up period of 50.3 months, 46 patients out of 212 patients had confirmed relapse. Of these, 22 patients initially had stage IV, 8 had stage III, 6 stage II, 10 stage I. Of these, 21 patients performed FDG PET/CT without clinical suspicion of recurrent disease of metastasis. FDG PET/CT also detected secondary cancers in 10 patients, and recurrence of secondary cancers in 2 patients.
Conclusions: Post-therapy surveillance FDG PET/CT is useful in the early detection of relapse or second primary cancer in patients with oral cavity or oropharyngeal cancers, with significant management implications for effective salvage or definitive therapies.

Oncology_76

Increase in ^{18}F-FDG Uptake of Lesions After Treatment with Angiogenesis Inhibitors for Metastatic Colon Adenocarcinoma: Disease Progression or Expected Response?

Eduardo Erasto Ongkeko, Eduardo Erasto

St. Lukes Medical Center, Philippines

At present, surrogate normal tissue biomarkers for assessment of the responses to antiangiogenic agents are not widely available. FDG PET-CT imaging can correctly predict tissue necrosis of colorectal liver metastases in 70% of patients that showed complete PET response, however it is unclear at present if those that showed high levels of uptake would translate to progressive disease. We then present a case of a patient with rectosigmoid adenocarcinoma metastatic to the liver and treated with Bevacizumab who undergoes follow-up FDG PET-CT study. Baseline and follow-up ^{18}F-FDG PET-CT were done with a 68-day interval between the 2 scans. Contrast CT was simultaneously acquired with slice thickness of 3mm x 1.5mm. Maximum Standard Uptake Value (SUV_{max}) of noted lesions were taken and compared. These were correlated with clinical parameters pre and post treatment.
Post-bevacizumab ^{18}F-FDG PET-CT showed interval increase of SUV_{max} from 6.6 to 8.4 in the metastatic lesions in segments 4, 8 and 5. There was also similar interval increase in the SUV_{max} of lesions in the supraclavicular, mediastinal and retroperitoneal lymph nodes. Clinical symptomatology however was discordant with improvement of VAS and Quality of life index.
It was reported in studies that antiangiogenic drug therapies may have a complex, possibly multiphasic effect on ^{18}F-FDG uptake. An increase in ^{18}F-FDG uptake of metastatic colon cancer lesions on PET-CT after angiogenesis inhibitor treatment does not always translate to disease progression.

Oncology_83

Lung Metastasis Displayed Its Lung Lesion, Pathway of Lymphatic Spreading and Distant Metastasis Similar to Primary Lung Cancer Demonstrated by Serial PET/CT Scans — Report of Two Compared Cases

Chih-Shun Wu[1], Wen-Tsung Huang[2], Wan-Lin Shen[3], Shang-hung Chen[2], Chiang-Hsuan Lee[4]

1. Division of Nuclear Medicine, Department of Medical Imaging, Chi-Mei Medical Center
2. Liouying, Tainan, Taiwan
3. Division of Hematology and Oncology, Department of Internal Medicine, Chi-Mei Medical Center
4. Liouying, Tainan, Taiwan
5. Department of Pathology, Chi-Mei Medical Center, Liouying, Tainan, Taiwan
6. Division of Nuclear Medicine, Department of Medical Imaging, Chi-Mei Medical Center, Tainan, Taiwan

Purpose: PET/CT has been widely used in the diagnosis, and staging of cancer for appropriate treatment. We demonstrate two compared cases but have similar picture. Case I is rectal cancer with synchronous primary lung cancer. Case II is lung metastasis from previous

sigmoid colon cancer. At Case II, the appearance of lung lesion, and pathway of lymphatic spreading to mediastinum and distant metastasis are all similar to primary lung cancer as Case I.

Case Report: Case I is a 68-year-old male. He received PET/CT for staging of rectal cancer. PET/CT revealed rectal cancer with estimated stage T2N2M0 and an incidental finding of an irregular mass, about 4.0 cm in size, in the LLL with FDG uptake and lymphadenopathy in the left pulmonary hilar region. Under the impression of lung cancer with estimated stage T2aN1 or metastasis, wedge resection without lymph node sampling was performed and pathological report revealed primary adenocarinoma of lung.

Case II is a 75-year-old male. He received colectomy for sigmoid colon cancer (pT3N0M0) 6 years ago. A tiny nodule, about 0.5 cm in size, with FDG uptake (SUV: 1.28) in the LUL was noted in the pre-colectomy PET/CT scan. Two to four years after colectomy, CT revealed a cavitary nodule, about 2.2 to 2.8 cm in size, in the LUL with progressively increased wall thickness. From the imaging pattern, primary lung cancer is finally suspected. PET/CT for pre-operative staging revealed increased FDG uptake in the lung nodule with same location as previous PET/CT scan, Lt pulmonary hilum, and Lt para-tracheal region. The patient received lobectomy and dissection of mediastinal lymph nodes. The pathological report revealed the metastatic colorectal adenocarcinoma. Sixteen months later, PET/CT scan demonstrated the recurrence in the Lt para-tracheal lymph nodes, anastomosis site of sigmoid colon, and distant metastasis in the left adrenal gland.

Conclusion: The lung metastasis may act like primary lung cancer as in our cases. Therefore, malignant history and the timing of discovered metastatic lesion may provide an important opportunity to determine the possibility of lung metastasis even it has typical picture of primary lung cancer.

Oncology_85

FDG-PET Evaluating Mediastinal Nodal Metastasis In Patients With Lung Cancer

Po-Ling Chang, Lian-Yuan Wang, Wen-Sheng Huang

Changhua Christian Hospital, Taiwan

Purpose: Lung cancer owns the highest rate of cancer mortality in Taiwan. Accurate staging helps avoid invasive procedures, decide appropriate treatment and increase cure rate. This study was thus to assess the performance of FDG PET in determining mediastinal nodal metastasis in lung cancer patients.

Methods: During 2012-3, a total of 138 patients with tissue proof of lung cancers (91 male, and 47 female, averaged age 66.7 yrs.) were recruited for further staging using the FDG PET. Visual interpretation of PET for possibly mediastinal nodal metastasis was applied using a 5-point scale system, 1-3 is negative and 4-5 is positive. The final pathologic results were served as the golden standard.

Results: 445 lymph node stations with pathologic proof were analyzed, 48 stations are metastatic, 397 stations are negative. PET depicted 24 metastatic stations, but missed the other 24 metastatic stations. PET was negative in 348 stations without metastasis while PET was positive in 49 stations without metastasis. The sensitivity, specificity, positive and negative predict values were 51%, 88.2%, 34% and 94% respectively, yielding an accuracy of 84%. The PET sensitivity and positive predictive value for squamous cell carcinoma appeared better than that of adenocarcinoma.

Conclusions: Our results showing a low sensitivity but high specificity of FDG PET in detecting mediastinal nodal metastasis were in line with the previous reports, and indicated that, for those with CT indeterminate nodal stage, a negative PET is more suitable for the curative surgery.

Oncology_88

Monitoring the therapeutic response with FDG PET/CT in bone metastasis from prostate cancer: comparison with bone scintigraphy

Soyoung Kim, Jongtae Cha, Sang Hyun Hwang, KwanHyeong Jo, Narae Lee, Arthur Cho, Mijin Yun, Won Jun Kang

Department of Nuclear Medicine, Yonsei University College of Medicine, Korea

Objectives: In the evaluation of bone metastasis from prostate cancer(BM form PC), BS is thought to be better than FDG PET-CT(PET) due to its osteoblastic nature of BM. However, it is difficult to differentiate the osteoblastic progression and favorable response of BM form PC in the BS. It has been suggested that PET might be useful in aggressive PC because its FDG uptake is relatively high. We tested the feasibility of PET in the evaluation of therapy response in the BM form PC, and compared the findings with BS.

Methods: The 495 patients diagnosed in PC with bone metastasis between 2007and2014 was retrospectively reviewed. A total of 38 PC patients(median age, 72 years) underwent both FDG PET-CT and BS at baseline and follow up within 3 months were enrolled in this study. 32 patients underwent chemotherapy and 6 patients underwent chemotherapy and radiation therapy.

Average follow-up periods was 18month. Therapeutic responses by BS were graded as progression, stable disease, and favorable response. MaxSUVs of the bone metastastic areas were calculated at baseline and follow-up FDG PET-CT, and its interval change were recorded.

Results: A total of 456 lesions were evaluated. PET-CT showed similar sensitivity to BS for detecting baseline BM form PC (sensitivity: 91.8% in PET-CT, and 91.3% in BS, concordance rate: 93%). A total of 65 metastatic lesions were assessed both by BS and FDG PET-CT for therapeutic monitoring. BS findings were graded as progression in 18 cases, as stable in 27 cases, and as progression in 20 cases. MaxSUVs were changed from 3.1±1.9 to 4.2±2.5 in progression group (71.7% increase), from 3.4±2.0 to 2.2±0.9 in stable group (12.0% decrease), and from 3.3±1.2 to 1.5±0.5 in favorable response group (43.0% decrease).

Conclusions: FDG PET-CT showed comparable sensitivity to detect BM form PC. In monitoring therapeutic response, concordance rate between BS and FDG PET-CT were high in progression/favorable response groups according to BS findings. In stable group by BS, FDG PET-CT could differentiate 67% of the cases into favorable and progression group. FDG PET might be useful to evaluate stable disease by BS in BM form PC work-up.

Oncology_89

Evaluation of prognostic factors to predict the event free survival in DLBCL

Yun Soo Park, Ji Sun Park, Kyung Pyo Jung, Su Jung Choi, Sun Seong Lee, Seok Mo Lee

Department of Nuclear Medicine, Busan Paik Hospital, Inje University College of Medicine, Korea

Diffuse large B-cell lymphoma (DLBCL) represents the most common subtype of non-Hodgkin lymphoma (NHL) and has biological heterogeneity. It is known that there are several prognostic factors related DLBCL such as the revised International Prognostic Index (revised IPI), clinical stage, Cox score risk classification, GCB subtype and SUV_{max}. The purpose of this study is to evaluate the difference of FDG uptake between GCB and non-GCB subtype, and prognostic factors for predicting the event free survival (EFS) of DLBCL patients in the era of RCHOP regimen.

Forty two patients of biopsy proven DLBCL were enrolled in this study. All 42 patients underwent FDG PET/CT scans for staging work up. The malignant lymphoma lesion with the highest FDG uptake were chosen for measuring lesional SUV_{max}. The lesional SUV_{max} between GCB and non GCB subtype were compared. For 32/43 patients who were able to be followed for at least 1 year, we evaluated above prognostic factors (revised IPI, clinical stage, Cox score risk classification, GCB subtype and SUV_{max}) for predicting the EFS.

Although the FDG uptake of GCB subtype was lower than non-GCB subtype, there was no statistical difference (mean SUV_{max} 18.4±4.5 vs. 22.5±4.0, P=0.10). In the univariate analysis, clinical stage (HR of 6.640 [95% CI 1.797-24.537, v=0.001]), revised IPI (HR of 5.163 [95% CI 1.326-20.100, P=0.003]) were significantly associated with EFS, but SUV_{max}(HR of 1.336 [95% CI 0.409-4.362, P=0.629]) and GCB subtype (HR of 1.201 [95% CI 0.369-3.918, P=0.760]) were not significant predictors for event free survival. In the multivariate analysis, clinical stage was only significant prognostic factor (P=0.003).

In our study, GCB subtype showed a tendency of lower FDG uptake than non-GCB subtype, without statistical significance. Among known prognostic factors, clinical stage was only statistically significant prognostic factor to predict EFS. The FDG uptake of DLBCL on baseline study was not significant prognostic factor to predict EFS in the era of RCHOP regimen.

Oncology_91

Pretreatment metabolic tumor volume on FDG PET/CT as a survival predictor in adenoid cystic carcinoma of the head and neck

Narae Lee, Soyoung Kim, Jongtae CHEA, Sang Hyun Hwang, Kwanhyeong Jo, Arthur Cho, Won Jun Kang, Mijin Yun

Yonsei Sevrance hospital

This study was to assess the prognostic value of parameters from FDG uptake on PET/CT in patients with head and neck adenoid cystic carcinoma (ACC).

A total of 51 patients with ACC who underwent staging FDG PET/CT before treatment were retrospectively enrolled. The maximum standardized uptake value (SUV_{max}) of the tumor to mean SUV (SUV_{mean}) of the normal liver (TLR) and metabolic tumor volume using SUV_{mean} of the normal liver+2SD (MTV_{liver}) were measured in each patient. Receiver operating characteristic (ROC) curve analysis was performed to determine optimal cutoff values of TLR and MTV_{liver} and overall survival (OS) was measured by Kaplan-Meier survival analysis. Univariate and multivariate logistic regression analyses were performed using clinicopathologic factors including

age, sex, site of the primary malignancy, overall TNM stage, cervical LN metastasis, perineural invasion, and lymphovascular invasion, TLR and MTV_{liver} on FDG PET/CT for predicting OS.

Of the 51 patients, 10 were died with a medial OS time of 31.5 months in this study. On univariate analysis, stage (I-II vs. III-IV), presence of cervical lymph node (LN) metastasis, TLR, and MTV_{liver} were significant prognostic factors for OS (P<0.05). On multivariate analysis, cervical LN metastasis, TLR, and MTV_{liver} were independent prognostic factors (P<0.05). In the patient groups with high FDG uptake (TLR > 2, MTV_{liver}>15.5) showed significantly worse OS than those with low FDG uptake (TLR ≤2.3, MTV_{liver}≤15.5).

TLR and MTV_{liver} on FDG PET/CT were independent prognostic factors for OS in patients with head and neck ACC.

Oncology_93

Differentiation between Malignant and Inflammatory Ground-Glass Opacity by F-18 FDG PET/CT

Sun Seong Lee, Ji Sun Park

Department of Nuclear Medicine, Inje University College of Medicine, Busan Paik Hospital, Busan

The aim of this study was to assess the ability of F-18 FDG PET/CT for differentiation between malignant and inflammatory ground-glass opacity (GGO).

We searched the clinical records of patients who underwent F-18 FDG PET/CT using the key word "ground-glass opacity" from January 2011 to December 2014. We excluded patients who had GGO less than 1 cm. Total 26 patients were included, and total 26 GGOs were evaluated. Three GGOs were confirmed as adenocarcinoma. One GGO was confirmed as adenocarcinoma in situ. In 3 patients, the GGOs were increased in size on follow up study (follow up period; 12, 35, 36 months), so we considered the GGOs as malignancy. Nineteen GGOs were considered as inflammation because of disappearance or decrease in size on follow up study.

The mean size of malignant GGOs was 18.3 mm (range, 14-23 mm), the mean size of inflammatory GGOs was 28.2 mm (range, 13-47 mm).

We performed the Mann-Whitney U test to compare the SUV_{max} of malignancy and inflammation. We also used a receiver operating characteristic curve to calculate the optimal cut-off value to differentiate SUV_{max} of malignancy and inflammation.

The SUV_{max} was significantly lower in malignancy than in inflammation (P=0.0003). Mean SUV_{max} of malignancy was 0.94 (range, 0.8-1.1), that of inflammation was 3.54 (range, 0.9-10.2). There was moderate correlation between size of GGO and SUV_{max} (r=0.41; P=0.0372). Using the optimal cut-off value of SUV_{max} as 1.1, sensitivity, specificity, area under the curve, and SE were 100%, 94.7%, 0.966, and 0.0347, respectively.

The SUV_{max} of malignant GGO was significantly lower than that of inflammatory GGO. So, GGO that shows SUV_{max} lower than 1.1 could be malignancy rather than inflammation.

Oncology_94

^{18}F-FDG PET parameters predict prognosis of NSCLC patients

Jongtae Cha, So young Kim, Sang Hyun Hwang, Kwanhyeong Jo, Narae Lee, Arthur Cho, Won Jun Kang, Mijin Yun

Department of Nuclear Medicine, Severance Hospital, Yonsei University College of Medicine, Seoul, Korea

Purpose: The aim of this study is to investigate whether ^{18}F-FDG PET parameters of the metastatic lymph nodes have the potential to predict prognosis in patients with non small cell lung cancer.

Methods: A total 61 patients(N stage 1(N=34), stage 2(N=27)) who underwent ^{18}F-FDG PET/CT for initial staging and underwent operation for initial treatment. We determined histologic type, T- stage, and lymph node status from the surgically excised specimens and overall survival from database in hospital. We draw ROI on all pathologic confirmed metastatic lymph nodes in N1 patients and pathologic confirmed metastatic N2 lymph nodes in N2 patients. Variable threshold was used and PET parameters(maximum SUV, mean SUV, total total lesion glycolysis(TLG), metabolic tumor volume(MTV)) of primary tumor and lymph node is estimated.

Results: Among the total 61 patients, 34(55.7%) were N2 stage and 27(44.2%) were N1 stage. 19 (31.1%) died during the follow-up period. In N2 stage patients, OS was significantly shorter in higher MTV(P= 0.006. B = 0.184), TLG(P= 0.008, B=0.037) of metastatic lymph nodes. No other significant PET parameters to predict prognosis in this study.

Conclusions: In N2 stage patients, MTV and TLG of metastatic lymph nodes is significant predictors for poorer OS.

Oncology_96

Interlaced therapy using cell cycle synchronization and 2-deoxyglucose in breast cancer cells

Su Jin Lee, Joon-Kee Yoon, Bok-Nam Park, and Jung Hyun Roh

Department of Nuclear Medicine & Molecular Imaging, Ajou University School of Medicine, Suwon, Korea

Purpose: We assessed how cell cycle synchronization using mibefradil acts on cancer cell glucose uptake, and further investigated the anti-cancer effect of interlaced therapy by 2-deoxyglucose (2-DG).
Methods: MDA-MB-231 breast cancer cells were treated with 0-10 μM mibefradil for 24 h and withdrawn then followed by 1.0 mM 2-DG treatment up to 48 h. Sulforhodamine B colorimetric assay was done for cell viability. Cells were measured for cell cycle by FACS after propidium iodide staining, glucose uptake by 3H-DG, lactate production, and membrane glucose transporter 1 (GLUT1) expression after mibefradil treatment.
Results: Mibefradil and 2-DG suppressed cell survival independently of each other (18.0% and 24.1% of controls, respectively). Interlaced therapy (mibefradil treatment followed by 2-DG treatment) enhanced the killing effect to 31.8% of cells. Mibefradil induced cell cycle arrest at the G0/G1 phase compared with controls (51.5 ± 1.7 vs. 40.5 ± 2.6%, $P < 0.05$). Withdrawal of mibefradil induced the significant increase of cellular 3H-DG uptake (0.39 ± 0.02 vs. 0.19 ± 0.03 %/μg, $P < 0.001$), slight accumulation of lactate in culture media (188.1 ± 7.6 vs. 178.7 ± 11.9 mM/mg, $P = 0.31$), and membrane GLUT1 expression.
Conclusions: Cell cycle synchronization using mibefradil induced the transient increase of cellular glucose uptake, which significantly enhanced the killing effect of 2-DG in the breast cancer cells.

Oncology_97

Comparison of Prognostic Value of Standardized Uptake Value and Tumor-to-Blood Standardized Uptake Ratio in Patients with resectable Non-small-cell Lung Cancer

Seunghyeon Shin, Seong-Jang Kim, Kyoungjune Pak

Pusan National University Hospital, Korea

Purpose: Recent study demonstrated that the standard tumor-to-blood SUV ratio (SUR) was more accurate prognostic method than tumor maximum standardized uptake value (SUV_{max}). The purpose of this study was to evaluate and compare prognostic value of SUV_{max} and SUR in non-small-cell lung cancer (NSCLC) patients who received curative surgery.
Methods: From January 2010 to December 2013, a total of 78 patients who had undergone curative resection for NSCLC were enrolled in this study. Median follow-up was 34.5 months (range: 2.0–64.0 months). Fluorine-18 fluorodeoxyglucose (FDG) positron emission tomography/computed tomography (PET/CT) was performed before surgery. A region of interest was drawn over the entire uptake of lung on axial images semiautomatically. Mean standardized uptake value (SUV_{mean}), SUV_{max}, metabolic tumor volume (MTV) and total lesion glycolysis (TLG) of each lesion was measured on the workstation and mean SUR, maximum SUR and TLGSUR were divided each PET parameters with descending aorta SUV_{mean}.
Results: Median OS and RFS were 34.5 and 32.5 months, respectively. In univariate analysis, N stage predicted for both OS and RFS ($P = .0047$ and $P = .0012$, respectively). N stage was an independent predictor of both OS and RFS ($P = .0042$ and $P = .0027$, respectively). Mean SUR predicted RFS ($P = .0095$), not OS. However, SUV_{max}, SUV_{mean}, MTV 40, TLG 40, maximum SUR and TLGSUR did predict neither OS nor RFS.
Conclusions: SURmean was an independent predictor of recurrence in NSCLC patients who received curative surgery.

Oncology_98

The Role of F-18 FDG PET/CT and Serum CEA in Detection of Recurrent Colorectal Cancer

Sangdon Kwon, Eunjung Kong, Ihnho Cho, Kyungah Chun

Yeung Nam University Hospital, Korea

The surveillance of postoperative colorectal cancer (CRC) is generally followed up by level of the serum carcinoembryonic antigen (CEA). And F-18 positron emission tomography/computerized tomography (PET/CT) is a sensitive imaging tool in the detection of CRC recurrence. The aim of this study was to evaluate the diagnostic performance of F-18 FDG PET/CT in recurrent CRC with different CEA concentration.
We retrospectively recruited patient in prior CRC. A total of 178 patients [82 females and 96 males; age (mean ± SD) 64.5 ± 11.9 years; range 13–87] who had been treated with radical surgery underwent F-18 FDG PET/CT for the detection of recurrence. (The patients

were divided into 2 groups based on whether their serum CEA levels were within normal group (<5 ng/ml, Group 1, n = 158) and elevated CEA level group (>5 ng/ml, Group 2, n = 20). The sensitivity, specificity, positive predictive value (PPV), negative predictive value (NPV) and accuracy of the serum CEA level and F-18 FDG PET/CT scan were estimated.

Thirteen of the 178 consecutive patients had recurrent CRC confirmed by a pathological examination and/or clinical follow up. Overall F-18 FDG scan shows true positive in 12 patients, true negative in 163 patients, false negative in 1 patient and false positive in 2 patients in both groups. The sensitivity, specificity, PPV, NPV and accuracy were 100%, 98.6%, 80%, 100% and 98.7% for group 1; 80%, 100%, 100%, 93.7% and 95% for group 2 in F-18 FDG PET/CT, respectively.

Elevated serum CEA is used as the tumor marker for the recurrent CRC. However, serum CEA do not completely exclude metastasis or recurrence. F-18 FDG PET/CT could accurately find detection of CRC recurrence, regardless of the serum CEA concentration.

Oncology_100

Prognostic value of pretreatment ^{18}F-FDG PET in patients with advanced renal cell carcinoma

Sang Hyun Hwang, Soyoung Kim, Jongtae Cha, Kwanhyeong Jo, Narae Lee, Arthur Cho, Mijin Yun, Won Jun Kang

Department of Nuclear Medicine, Severance Hospital, Yonsei University College of Medicine, Seoul, Korea

To evaluate the prognostic value of pretreatment ^{18}F-FDG PET in patients with advanced renal cell carcinoma (RCC) after anti-VEGF targeted therapy.

From Jan 2007 to Dec 2013, we retrospectively enrolled 56 patients with advanced RCC (44 male, 12 female, median age 60; range 37-88 years old) who underwent ^{18}F-FDG PET/CT for staging and recur evaluation. The highest SUV in the all metastatic RCC lesions of each patient was defined as SUV_{max}. The tumor-to-normal liver standardized uptake value (SUV) ratio (TLR), metabolic tumor volume (MTV) and total lesion glycolysis (TLG) were measured on ^{18}F-FDG PET/CT in all patients. MTV was defined as the sum of above 40% of tumor SUV maximum. TLG was calculated by (MTV) · (mean SUV). The prognostic significances of PET/CT parameters and clinical factors for progression-free survival (PFS) and overall survival (OS) were evaluated by univariate and multivariate analyses.

The most common organ for metastases was lung (35 patients). The remaining metastases were bone (26), lymph node (14), adrenal gland (8), peritoneal seeding (8), brain (2), pancreas (1), and thyroid (1). In univariate analysis, hypercalcemia, time from diagnosis to treatment, TLR, MTV and TLG were significant prognostic factors affecting PFS (P<0.05), and Karnofsky score, hypercalcemia, time from diagnosis to treatment, TLR, MTV and TLG were significant prognostic factors affecting OS (P<0.05). In multivariate analysis, hypercalcemia, MTV and TLG were independent prognostic factors for PFS (P<0.05) and hypercalcemia, time from diagnosis to treatment, MTV and TLG for OS (P<0.05).

MTV and TLG are independent prognostic factors for predicting PFS and OS in patients with advanced RCC. ^{18}F-FDG uptake in the tumor could provide prognostic information for advanced RCC patents who underwent anti-VEGF targeted therapy.

Oncology_101

Prognostic value of pretreatment ^{18}F-FDG PET in patients with hepatocellular carcinoma

Sang Hyun Hwang, Jongtae Cha, Kwanhyeong Jo, Narae Lee, Arthur Cho, Won Jun Kang, Mijin Yun

Department of Nuclear Medicine, Yonsei University College of Medicine, Severance Hospital, Seoul, Korea

To evaluate the prognostic value of metabolic tumor volume (MTV) and total lesion glycolysis (TLG) in patient with hepatocellular carcinoma (HCC) after curative surgical resection

We retrospectively enrolled 133 patients with HCC who underwent preoperative FDG PET/CT before resection with curative intent between January 2007 and December 2013. The volume of interest (VOI) was manually drawn in the HCC lesion and normal liver tissue. The maximum standard uptake values (SUV) to normal liver SUV_{mean} ratio (TLR), MTV which is defined as the sum of the voxels over the value of SUV of 2.5 percentile voxel of the normal liver tissue, and TLG were measured on FDG PET/CT for each patient. The prognostic significance of TLR, MTV, and TLG for intrahepatic metastasis free survival (IHFS), distant metastasis free survival (DMFS), and overall survival (OS) was evaluated and compared with other prognostic factors. Alpha-fetoprotein (AFP) was only significant prognostic factor affecting IHFS (P=0.01). In univariate analysis, MTV (P<0.001), TLG (P<0.001), TLR (P=0.001), AFP (P=0.02), tumor grade (P=0.046), and tumor size (P<0.001) were significant prognostic factors for DMFS, and MTV

(P<0.001), TLG (P<0.001), TLR (P=0.002), and tumor size (P<0.001) were significant prognostic factors for OS. In multivariate analysis, TLG (P=0.013) and MTV (P=0.012) were independent prognostic factors for DMFS and OS.
MTV and TLG were determined to be an independent prognostic factor for DMFS and OS in patients with HCC.

Oncology_102

Outcome and response prediction for primary and oligometastatic spinal sarcoma patients who received stereotactic body radiation therapy (SBRT)

Sang Moo Lim

Department of Nuclear Medicine, Korea Institute of Radiological and Medical Sciences (KIRAMS), Seoul, Republic of Korea

We present the outcome of our primary or oligometastatic spinal sarcoma patients treated with stereotactic body radiotherapy (SBRT). We aimed to evaluate the local recurrence rate and response predictors including ^{18}F-FDG PET/CT for these patients.
A total of 22 spinal lesions in 19 patients with primary (n = 5) or oligometastatic spinal sarcoma (n = 14) were retrospectively analyzed. SBRT was performed for these 22 lesions with the median dose and fractions of 33 Gy and 3 fractions, respectively. The median biological effective dose was 426 Gy and median planning target volume (PTV) was 14.5 cm3. ^{18}F-FDG PET/CT scans before SBRT were available in 14 of 19 patients and the maximum standardized uptake value (SUV_{max}) and metabolic tumor volume at the cut-off SUV of 50% of SUV_{max} (MTV) of spine metastases were calculated on each PET data set.
The local control rate of 22 lesions was 73% at 12 months and 64% at 24 months after SBRT. Lesions with PTV ≤ 17 cm3 (n = 13) showed higher local control rates at 12 months (92% vs. 44%) and 24 months after SBRT (85% vs. 33%) compared to the lesions with PTV > 17 cm3 (n = 9). On patient-based analysis, PTV > 17 cm3 was significantly associated with reduced progression-free survival (P = 0.003) and overall survival (P = 0.026). PTV of deceased patients with oligometastatic spinal sarcoma were larger than that of survived patients (P = 0.198). Among 16 lesions of 14 patients with ^{18}F-FDG PET/CT before SBRT, the 10 lesions with MTV ≤ 6 mL tended to show a higher local control rate at 12 months (90% vs. 50%) and 24 months after SBRT (88% vs. 33%) than 6 lesions with MTV > 6 mL (P = 0.074). The MTV of these 16 lesions were significantly correlated with PTV (P = 0.011).
SBRT is effective for the treatment of spinal oligometastases in patients with sarcoma, especially for patients presenting with small spinal metastasis. Baseline ^{18}F-FDG PET/CT may be useful for prediction of therapeutic response to SBRT.

Oncology_103

Clinicopathologic factors associated with F-18 FDG uptake of early gastric cancer

Joon-Kee Yoon, Kee Myung Lee, Sang-Uk Han, Cheulsu Byun, Dakeun Lee, Young-Bae Kim, Su Jin Lee, Hoon Hur, Seon Kyo Lim, Young-Sil An, Joon-Kee Yoon

Department of Nuclear Medicine and Molecular Imaging, Ajou University School of Medicine, Korea

F-18 fluorodeoxyglucose (FDG) PET/CT is not generally recommended for staging of early gastric cancer (EGC), because of its low detection rate, In this study, we investigated clinicopathologic factors associated with F-18 FDG uptake in EGC.
A total of 229 patients (163 men, 66 women, age = 61 years) who underwent preoperative F-18 FDG
PET/CT were enrolled retrospectively. Pathologic information was obtained through gastrectomy (n = 195) or
endoscopic mucosal dissection (n = 34). Univariate and multivariate analyses were performed to evaluate the
association between clinicopathologic factors (age, sex, multiplicity, location, gross type, WHO classification, Lauren classification, size, depth of invasion, involvement of resection margin and lymphatic/venous/perineural invasion) and F-18 FDG avidity of primary tumors of EGC.
F-18 FDG uptake was observed in 17.5%, 49/223) of patients with EGC. The most common location of primary tumors was lower third (53.3%). The two most common gross types were IIc (43.7%) and IIb (34.1%). The median tumor size was 2.5 cm. On univariate analysis, tumor size, location, gross type, WHO classification, Lauren classification, depth of invasion and lymphatic invasion were significant variables affecting on F-18 FDG uptake. A subsequent multivariate analysis with these factors revealed that tumor size (P = 0.026, exp(B) = 2.527), location (P = 0.035, exp(B) = 1.941), gross type (P < 001, exp(B) = 0.444) and the depth of invasion (P = 0.007, exp(B) = 3.481) were significantly associated with F-18 FDG uptake. Tumors located in the lower third of stomach showed more FDG avidity (23.8%) than those in the upper (11.1%) and the middle third (10.0%). Gross type I (83.3%) and IIa (37.0%) had higher FDG avidity rate. Tumors with submucosal invasion (26.7%) showed FDG uptake more frequently than those limited in mucosa (7.3%). As

expected, larger tumors (≥ 2.5 cm, 29.2%) exhibited more FDG avidity than smaller tumors (10.0%).
F-18 FDG uptake in EGC is dependent on the location, gross type, size and the depth of invasion of primary tumors. This result would help clinicians to decide which patients are eligible for F-18 FDG PET/CT in EGC.

Oncology_104

Correlation between semi-quantitative ^{18}F-FDG PET/CT parameters and Ki-67 expression in small cell lung cancer

Soyeon Park, Eunsub Lee, Seunghong Rhee, Jaehyuk Cho, Sunju Choi, Sinae Lee, Jae Seon Eo, Kisoo Pahk, Jae Gol Choe, Sungeun Kim

Department of Nuclear Medicine, Korea University Anam Hospital, Seoul, Korea

The aim of this study was to evaluate the relationship between semi-quantitative parameters on ^{18}F-FDG PET/CT including maximum standardized uptake value (SUV_{max}), mean standardized uptake value (SUV_{mean}), metabolic tumor volume (MTV), and total lesion glycolysis (TLG) and the expression level of Ki-67 in small cell lung cancer (SCLC).
Ninety four consecutive patients with SCLC were enrolled in this study. They underwent ^{18}F-FDG PET/CT for initial evaluation of SCLC, and we measured SUV_{max}, $avgSUV_{mean}$, MTV_{sum}, and TLG_{total} on ^{18}F-FDG PET/CT images. The protein expression of Ki-67 were examined by immunohistochemical staining.
Significant correlations were found between MTV_{sum} and Ki-67 labeling index (r = 0.254, P = 0.014) and TLG_{total} and Ki-67 labeling index (r = 0.239, P = 0.020). No correlation was found between SUV_{max} and Ki-67 labeling index (r = 0.116, P = 0.264) and $avgSUV_{mean}$ and Ki-67 labeling index (r = 0.031, P = 0.770). Dividing Ki-67 expression level into 3 categories, it was suggested that increasing Ki-67 expression level stepwisely increased MTV_{sum} and TLG_{total}. (P = 0.028 and 0.039, respectively), not SUV_{max} and $avgSUV_{max}$ (P = 0.526 and 0.729, respectively).
In conclusion, the volume based parameters of ^{18}F-FDG PET/CT correlates with immunohistochemical staining of Ki-67 in SCLC. Measurement of MTV_{sum} and TLG_{total} by ^{18}F-FDG PET/CT might be a simple, noninvasive and useful method to determine the proliferative potential of cancer cells.

Oncology_105

Clinical significance of volumetric parameters of ^{18}F-FDG PET/CT correlated with skeletal-related events and survival in patients with bone metastasis

Hyo Jung Seo[1], Jae Seon Eo[1*], Eun Joo Kang[2*], Soyeon Park[1], Seunghong Rhee[1], Jaehyuk Cho[1], Sunju Choi[1], Chulhan Kim[1], Sungeun Kim[1] and Jae Gol Choe[1]

1. Department of Nuclear Medicine, Korea University, College of Medicine, Seoul, Korea
2. Division of Medical Oncology, Department of Internal Medicine, Korea University, Guro Hospital, Seoul, Korea

Purpose: The purpose of this study was to evaluate the clinical significance of volumetric parameters of ^{18}F-FDG PET/CT (PET/CT) in patients with bone metastasis.
Methods: Of 103 cancer patients with bone metastasis, PET/CT, pathology and clinical information including skeletal-related events (SRE), bone pain, and laboratory results were evaluated. Bone metastasis was classified as anatomical regions. Metabolic tumor volume (MTV), tumor lesion glycolysis (TLG), SUV_{max}, SUV_{mean}, lesion to liver ratio, and lesion to muscle ratio were analyzed according to SRE and survival. The free SRE probability and survival rate were estimated using the Kaplan–Meier method. Univariate and multivariate predictors of SRE were determined using the cox proportional-hazards regression. Chi-squared test and independent t-test were used.
Results: Of 103 studied patients, 43% showed bone pain. Cord compression was correlated with bone pain (P < 0.05). SRE was observed in 29 patients. Bone metastases causing SRE were thoracic spines (n=12), lumbar spines (n=12), humerus and femur (n=2), scapula and clavicle (n=1), and cervical spine (n=1). The averages of volumetric parameters and variable ratios in SRE and non-SRE groups were not different. Of univariate analysis, total bone metastasis TLG (> 107.0, P = 0.025), distant metastasis except bone MTV (> 51.2, P = 0.0074), and cord compression (P = 0.047) were significant predictors for SRE. Likewise, total MTV and TLG, total bone metastasis MTV and TLG, primary cancer MTV, SUV_{max} and TLG, LN metastasis MTV and TLG, distant metastasis except bone MTV, SUV_{max}, SUV_{mean} and TLG were significant predictors (P < 0.05) for survival. Of multivariate analysis, total bone metastasis TLG (> 107.0, P = 0.0477) and distant metastasis except bone MTV (> 51.2, P = 0.0069) were significant predictors for SRE. Total bone metastasis TLG (>71.1, P = 0.0316),

primary cancer TLG (>121.9, $P = 0.0102$) and distant metastasis TLG (>441.3, $P < 0.0001$) were significant predictors for survival.

Conclusions: Volumetric parameters were significant predictors for SRE and survival in patients with bone metastasis.

Clinical Applications of PET/MR and SPECT/CT_1

Renal Metastasis from Hurthle Cell Thyroid Cancer Diagnosed with ^{131}I SPECT/CT but Missed with ^{18}F-FDG PET/CT: A Rare Case Report

Apichaya Claimon[1,2], Euishin Edmund Kim[3,4], Bolormaa Ganbaatar[1,5], Gi Jeong Cheon[1], and Dong Soo Lee[1,3]

Department of Nuclear Medicine, Seoul National University Hospital, Seoul, Korea; Division of Nuclear Medicine, Department of Radiology, Faculty of Medicine Siriraj Hospital, Mahidol University, Bangkok, Thailand; Molecular Medicine and Biopharmaceutical Sciences, WCU Graduate School of Convergence Science and Technology, Seoul National University College of Medicine, Seoul, Korea; Department of Radiological Sciences, University of California, Irvine, CA, USA

Nuclear Medicine Department of Radiology Center, The First Central Hospital of Mongolia, Ulaanbaatar, Mongolia

Objectives: To emphasize the potential interpretation pitfall of renal metastasis from differentiated thyroid cancer (DTC) evaluated by ^{131}I scan and ^{18}F-FDG PET/CT. We herein report the first case of renal metastasis from Hurthle cell thyroid cancer that demonstrates positive ^{131}I but negative ^{18}F-FDG uptake.

Methods: We report a case of 62-year old woman with history of left thyroid lobectomy and radiofrequency ablation of right thyroid nodule for 20 and 8 years ago, respectively, without pathological report. She presented with multiple pulmonary metastasis. Biopsy of lung and thyroid nodule revealed Hurthle cell neoplasm. ^{18}F-FDG PET/CT was performed prior to the operation. Hurthle cell adenoma was revealed from completion thyroidectomy, followed by 200 mCi ^{131}I ablation. Her serum level of thyroglobulin (Tg) was 54.92 ng/ml and 224 ng/ml, under TSH suppression and stimulation, respectively.

Results: Preoperative ^{18}F-FDG PET/CT showed hypermetabolic tumor in the right thyroid lobe and bilateral pulmonary metastases. No abnormal uptake or lesion was found in the kidneys from PET/CT scan, whereas ^{131}I scan showed discordant result. Multiple ^{131}I avid foci were seen in both posterior upper abdomen. SPECT/CT imaging localized these lesions in the bilateral renal cortices without hydronephrosis, leading to the conclusion of renal metastasis. Contrast-enhanced CT showed an associated tiny exophytic soft tissue density nodule in the renal cortex, which was too small to characterize. Other ^{131}I avid lesions were consistent with residual thyroid tissue at thyroid bed and metastasis to cervical lymph nodes, lungs and bones. Renal metastasis from DTC is rare, only 46 cases have been reported worldwide. Also, this is the first case report of renal metastasis from Hurthle cell thyroid cancer with positive ^{131}I but negative ^{18}F-FDG uptake. Such discordant findings indicate well-differentiating nature of the renal metastatic lesions that has the ability to utilize iodine.

Conclusions: Renal metastasis from Hurthle cell thyroid cancer is rare. ^{131}I SPECT/CT imaging can contribute to the early detection of renal metastasis while ^{18}F FDG PET/CT exhibits false negative result.

Clinical Applications of PET/MR and SPECT/CT_3

Biodistribution Evaluation of [^{166}Ho]-DTPA-SPION in Normal Rats

Afsaneh Lahooti, Saeed Shanehsazzadeh, Hassan Yousefnia

Cordula Gruettner, Amir Reza Jalilian

Tehran University of Medical Sciences, Iran

Super paramagnetic iron oxide nanoparticles (SPION) with a cross-linked dextran coating can be used as a negative contrast agent in magnetic resonance imaging (MRI) agent. This study describes the preparation, biodistribution of ^{166}Ho-DTPA-SPIONs after intravenous injection in rats.

The chelator diethylenetriamine penta-acetic acid dianhydride was conjugated to SPION using a small modification of the well-known cyclic anhydride method [21,22]. Conjugation was performed at a 1 : 2(SPION : ccDTPA) molar ratio. In brief, SPION (0.8mg, 3.44 μM) and DTPA anhydride (0.84 mg, 6.88 μM) were mixed in 0.3 ml of 0.1 M phosphate buffer solution (pH = 9.0) and 0.3 ml of normal saline and stirred at room temperature under N2 for one hour. Conjugation reaction was purified with Magnetic assorting column (MACs) using high gradient magnetic field Following incubation, the radio labeled conjugate was checked using RTLC method for labeling and purity checked.

The RTLC showed that labeling yield was above 99% after purification and the compound have good in-vitro stabilities until 48 hours post injection in presence of human serum.

The biodistribution of ^{166}Ho-DTPA-SPIONs in rats showed dramatic uptake in reticuloendothelial system (i.e. more than 76 percent of injected dose was in liver and spleen at 30 minutes post injection) and their clearance is so fast in other organs especially in blood.

due to magnificent uptakes of this radiotracer in the liver and spleen and their fast clearance from other tissues especially in blood, it is suggested that this radiotracer would be suitable for RES theranostic purposes.

Clinical Applications of PET/MR and SPECT/CT_13

^{18}F-FDG PET/CT for Diagnosis of Prosthetic Valve Endocarditis

Lucille T. Puracan, Raymund Augustus O. Conlu

Department of Nuclear Medicine and PET Center, St. Luke's Medical Center, Global City, Philippines

Objectives: This case report aims to support the role of ^{18}F-FDG PET-CT as an important tool in diagnosing prosthetic valve endocarditis (PVE).

Accuracy in diagnosing PVE using the traditional diagnostic tools, like transesophageal echocardiograpy and transthoracic echocardiography, decreases in the presence of intracardiac devices, valvular prosthesis, severe pre-existing lesions and a very small or no vegetation. ^{18}F-FDG PET/CT imaging has been reported as an important diagnostic tool in the early diagnosis of PVE, as it has the ability to detect the condition even before the development of structural changes. Few studies emphasize its contribution in increasing the accuracy of Duke's criteria in diagnosing infective endocarditis and moved to include abnormal FDG uptake as a novel major criterion for PVE.

Methods: Here we report a case of a 74-year old female with post transcatheter aortic valvular implantation (TAVI) who presents with fever of unknown origin and persistent leukocytosis and thrombocytopenia. Patient underwent serial blood cultures, ^{99m}Tc-HMPAO-WBC scintigraphy, transesophageal echocardiography, ^{18}F-FDG PET/CT scans (initial scan and two weeks after), and bone marrow aspiration biopsy.

Results: Work-ups showed negative blood cultures, equivocal bone marrow aspiration biopsy, unremarkable ^{99m}Tc-HMPAO-WBC scintigraphy, and negative transesophageal echocardiography. Initial ^{18}F-FDG PET/CT scan showed increased FDG uptake surrounding the aortic valve prosthesis, more intense posteriorly. Follow-up ^{18}F-FDG PET/CT, done 2 weeks after the initial, revealed abnormal FDG uptake surrounding the aortic valve prosthesis, as well as peripheral hypermetabolism in a soft tissue/ fluid collection posterior to the graft. Computed tomography angiography (CTA) done immediately after ^{18}F-FDG PET/CT supported the finding by demonstrating an abscess and peri-graft pseudoaneuryms. This was confirmed by the post-surgical histologic findings of prosthetic valve infective endocarditis, abscess, and pseudoaneurysm of the ascending aorta and aortic root.

Conclusions: ^{18}F-FDG PET-CT can be utilized to diagnose early stages of PVE where conventional diagnostic tools are indeterminate.

Clinical Applications of PET/MR and SPECT/CT_16

The SPECT/CT Characteristic of Increased Bone Metabolic Osteolytic Lesions and Its Correlation with CT Manifestations

Wang Shu[1], Li Yaming[2]

Department of Nuclear Medicine, the First Affiliated Hospital of China Medical University, Shenyang 110001, China

Objectives: To explore the SPECT/CT characteristic of increased bone metabolic lesions and its correlation with CT manifestations.

Methods: A total of 21 cancer patients with osseous metastasis underwent 99Tcm-MDP SPECT/CT (13 males, 8 females, age: (60.52±6.85) years) were enrolled in this study. The relationship between the uptake of 99Tcm-MDP increased bone metabolic lesions (L/B) and CT manifestations were retrospectively analyzed. One-way analysis of variance, two-sample t test and linear correlation analysis were used to process the data.

Results: In 21 patients, a total of 111 lesions were found by 99Tcm-MDP bone scintigraphy ; a total of 125 lesions were found by SPECT/CT, including 111 increased bone metabolic lesions with abnormal CT manifestations and 14 decreased bone metabolic osteolytic lesions. In 111 increased bone metabolic lesions, there were 20.72%(23/111) osteolytic lesions, 48.65%(54/11) osteoblastic lesions and 30.63%(34/111) mixed lesions. The L/B of increased bone metabolic osteolytic lesions (11.82±6.61) was lower than that of osteoblastic lesions (20.03±13.24; F=6.00 P<0.05). The CT value of increased bone metabolic osteolytic lesions ((167.53±79.21) HU) was higher than that of decreased bone metabolic osteolytic lesions ((88.63±49.16) HU;t=3.345, P<0.05). The L/B of increased bone metabolic lesions were positively correlated to CT value (r=0.404, P<0.05).

Conclusions: On SPECT/CT, a part of increased bone

metabolic lesions are osteolytic lesions. The L/B of them is positively correlated to CT value. SPECT/CT can reduce missed diagnosis and misdiagnosis.

Clinical Applications of PET/MR and SPECT/CT_19

^{18}F-FDG PET/CT in the diagnosis and clinical application of lymphoma-associated hemophagocytic syndrome (LAHS)

Dan Peng, Xiaohua Zhu

Department Nuclear Medicine Tongji Hospital, Tongji Medical College, Huazhong University of Science and Technology, Wuhan, Hubei, 430030,P.R. China

Objective The aim of this study was to explore the clinical value of ^{18}F- FDG PET/CT in the diagnosis of lymphoma-associated hemophagocytic syndrome (LAHS).

Methods 4 cases of LAHS were retrospectively analyzed. The ^{18}F-FDG PET/CT image findings and clinical data of the patients with LAHS were compared by using visual inspection and semi-quantitative analysis method.

Results 4 cases of LAHS: 1 case shows that the number of lymph node in the whole body were not increased, without FDG uptake; the spleen was enlarged without FDG uptake; bone marrow have no hypermetabolic image of FDG uptake; 1 case shows that the whole body has more multiple lymph nodes with mild enhancing of FDG uptake; the spleen was enlarged without FDG uptake; bone marrow have no hypermetabolic image of FDG uptake; 1 case shows that the number of lymph node in the whole body were not increased, without FDG uptake; ; the spleen was normal without FDG uptake; bone marrow have no hypermetabolic image of FDG uptake; 1 case shows that the number of lymph node in the whole body were not increased, with high FDG uptake; the spleen was enlarged with FDG uptake; bone marrow have hypermetabolic image of FDG uptake. 4 cases of patients with clinical manifestations: continuous high fever (T > 39.5 ℃, more than 1 week) (100%), splenic enlargement (100%), liver enlargement (75%), laboratory examination (elevated ferritin (SF) and lactate dehydrogenase (LDH), 100%), elevated liver enzyme (100%), active bone marrow hyperplasia, increased lymphocyte percentage (100%) are the most common; Other such as decreased hemocyte (50%), jaundice, skin rash or maculopapule (50%), lung disease (respiratory symptoms 75% pleural effusion and pericardial effusion 75%). The pathological diagnosis was lymphoma-associated hemophagocytic syndrome (LAHS).

Conclusion 18 f - FDG PET/CT lacks specificity for the early diagnosis of LAHS, but combinied with beta 2-MG, SF, LDH, bone marrow hemophagocytic phenomenon and molecular detection (NK cell activity, soluble IL-2 receptor level and perforin gene) has important clinical value. Multi-factor comprehensive analysis and diagnosis, to improve the accuracy in the diagnosis, reduce missed diagnosis.

Clinical Applications of PET/MR and SPECT/CT_22

Metabolism and Diffusion in Various Hepatic Masses: A Preliminary Study

Eunjung Kong, Kyungah Chun, Sangdon Kwon, Ihnho Cho

Yeungnam University Medical School and Hospital, Korea

Glucose metabolism and water diffusion may have a relationship or affect each other in the same tumor. The understanding of their relationship could expand the knowledge of tumor characteristics and contribute to the field of oncologic imaging. The purpose of this study was to evaluate the relationships between metabolism and cellularity of hepatic mass using integrated PET/MRI system with ^{18}F-FDG.

Twenty-six patients with hepatic mass [14 hepatocellular carcinomas, 3 cholangiocarcinomas, 5 metastatic tumors and 4 benign tumors] underwent ^{18}F-FDG PET/MRI before treatment. Maximum standard uptake values (SUV_{max}) from ^{18}F-FDG PET and apparent diffusion coefficient (ADC) from diffusion weighted image were obtained for the tumor and their relationships were examined by Spearman's correlation analysis.

SUV_{max} showed significant negative correlation with ADC (r = -0.48, P = 0.013). Hepatocellular carcinoma showed 5.35 (1.84-16.63) in SUV_{max} and 1023.27 (737-1390) in ADC. Cholangiocarcinoma showed 6.41 (3.71-8.26) in $SUV_{max}$and 1380 (1078-1911) in ADC. Metastatic tumors showed 9.27 (5.1-12.97) in SUV_{max} and 971.6 (875-1352) in ADC. Benign tumors showed 3.83 (1.5-10.18) in SUV_{max} and 1406.5 (1257-1629) in ADC. All cholangiocarcinomas and benign tumors revealed higher than 1000 in ADC.

In this study, the higher the glucose metabolism a tumor had, the higher cellularity it had, and each tumor group might be have some difference in metabolism and cellularity. The evaluation of hepatic mass by PET/MRI could be helpful in understanding tumor characteristics and differential diagnosis.

Clinical Applications of PET/MR and SPECT/CT_23

Comparison of 180° and 360° arc data acquisition to measure scintigraphic parameters from gated SPECT myocardial perfusion imaging: Is there any difference?

Mojtaba Ansari[1*], Hamid Javadi[2], Ali Mahmoud-Pashazadeh[3], Mehdi Mogharrabi[3], Majid Assadi[3]

1. Department of Nuclear Medicine, Imam Hussein Hospital, Shahid Beheshti University of Medical Sciences, Tehran, Iran
2. Golestan Research Center of Gastroenterology and Hepatology (GRCGH), Golestan University of Medical Sciences (GUOMS), Gorgan, Iran
3. The Persian Gulf Nuclear Medicine Research Center, Bushehr University of Medical Sciences, Bushehr, Iran

Aim: The aim of current study was to compare 180° and 360° data collection modes to measure end diastolic volume (EDV), end systolic volume (ESV) and ejection fraction (EF) of cardiac system in gated myocardial perfusion tomography.

Materials and methods: Number of 39 patients underwent gated myocardial perfusion tomography. SPECT data of patients' heart were acquired by 180°(45° left posterior oblique to 45° right anterior oblique), and 360° to obtain EDV, ESV,EF and cardiac volume changes (V1, V2, V3, V4, V5, V6, V7 and V8) throughout each cardiac cycle.

Results: Results of current study indicated that there were no significant difference between 180° and 360° angular sampling to measure EDV, ESV and EF in myocardial perfusion imaging. Pattern of cardiac volume changes during a cardiac cycle measured in by 360° and 180° scans were also the same. We also observed that there is no difference in EDV, ESV and EF of groups that performed exercise to induce stress with the group who experienced stress by dipyridamole.

Conclusion:180°cardiac scan that offers more comfort to patients, better image quality and shorten scanning time, can be used to measure EDV, ESV and EF.

Radionuclide Therapy_3

Paradoxical increase of non-excellent response after I-131 ablation therapy with higher dose for patients with differentiated thyroid carcinoma: A preliminary study

Hee-Seung Bom, Geum-Cheol Jeong, Su bin Jeon, Hee Jeong Park, Sang-Geon Cho, Sae-Ryung Kang, Jahae Kim, Seong Young Kwon, Jung-Joon Min, Ho-Chun Song, Ki Seong Park

Department of Nuclear Medicine, Chonnam National University Hwasun Hospital, Korea

Optimal dose of I-131 ablation therapy (RIT) has been controversial based on previous studies in patients with differentiated thyroid carcinoma (DTC). We compared therapeutic response between two different dose-groups in DTC patients with only central lymph node metastases.

All patients were prepared with thyroid hormone withdrawal before 1st RIT. Patients with pathologic stage of T3N1a and T1N1a were included in this study. We excluded patients with high level of serum thyroglobulin antibody (≥ 60 U/mL), distant metastasis and absence of follow-up data. Dose of I-131 was determined empirically: 6.67 GBq before 2014 (group 1) and 3.70 GBq after 2014 (group 2). Excellent response to RIT was defined as negative finding on imaging studies and either suppressed serum Tg level of <0.2 ng/ml or TSH stimulated serum Tg level of <1 ng/ml on follow-up studies. Remainder of result was defined as non-excellent response. We investigated whether response to RIT was different or not according to dose of I-131 in all patients.

Among 281 patients, 228 patients were included in group 1 and 53 patients in group 2. There was no significant difference of patients' age, distribution of sex, serum Tg and TSH level on the day of RIT between two groups. The prevalence of non-excellent response to RIT was significantly higher in group 1. When patients were divided into two subgroups according to the pathologic T stage (pT1 vs. pT3), the prevalence of non-excellent response to RIT was higher in patients treated with 6.67 GBq of I-131, regardless of subgroup (P = 0.002 in pT1, P =0.018 in pT3). Our study showed that higher dose of I-131 paradoxically resulted in worse response than lower dose in DTC patients. Further studies are mandatory to elucidate the mechanism between I-131 dose and therapeutic failure.

Radionuclide Therapy_4

Long Term Outcome Following Radioiodine Therapy in Differentiated Thyroid Carcinoma

Ferdous Ara Hussain, MD. Mahbubul Hoque, Naureen Mahbub, Nurun Nahar, Sadia Sultana

National Institute of Nuclear Medicine & Allied Sciences, Bangladesh

Management of differentiated thyroid carcinoma by thyroidectomy followed by radioiodine ablation and regular follow up is shown to have better prognosis.

Proper surveillance for possible recurrence in apparently disease-free patients after radioiodine therapy is a major goal of long-term follow-up. Monitoring of thyroxine suppression or replacement therapy is a second goal of long-term follow-up. The aim of this study was to evaluate the outcome and impact of the long-term follow-up.

From total 3827 post thyroidectomy patients with differentiated thyroid carcinoma receiving radioiodine therapy at the institute (1980 to 2014), a retrospective study was performed on 610 patients treated during the period from year 1980 to 2002. The medical records of these patients were analyzed in December 2014 in order to evaluate the follow-up workup for a prolonged period of time of 12-34years. Evaluation of the case files included annual physical examination, serum thyroglobulin (Tg) level on replacement thyroxine, neck ultrasonography, whole body scan and existing status of patients.

Of the 610 patients, majority (> 75 %) had papillary thyroid carcinoma. About 6.5% patients were lost to follow up after the first dose of therapy. About 15.5 %, and 5.7% patients had follow up work up for 1 and 5 years respectively. Around 4% patients showed up for a long term follow up of 10 years or more. A small number of patients (1 -2%) had >20 years of follow up. A large number of patients (70) required multiple doses. Two patients received 9 and 10 doses for persistent disease or recurrence. The patients who showed up for a follow up of 12 years and more in disease free State were considered to be in complete remission.

Regular follow up is mandatory for early discovery and treatment of persistent or recurrent disease after radioiodine ablation of thyroid remnant. Long term follow up can assure a disease-free survival. Proper education and counseling are necessary for the successful management of these patients.

Radionuclide Therapy_8

Enhancing Residualizing Power of Radioiodinated Monoclonal Antibody via Novel Bifunctional Iodination Linker

Eun Jung Kim, Dan Bee Choi, Byoung Soo Kim, Tae Hyun Choi*

Department of Molecular Imaging, Korea Institute of Radiological and Medical Sciences, Seoul, Korea

Purpose: Radioiodine is most commonly employed to prepare radiolabeled proteins (antibodies, peptides) with high specific activity for *in vitro* and *in vivo* applications. However, a major shortcoming of radioiodinated proteins prepared by direct labeling methods is de-iodination *in vivo*. As reported earlier, we have developed a new linker, (N-(4-isothiocyanatobenzyl)-2-(3-(tributyl stannyl) phenyl) acetamide (FCCS12026), for the preparation of more stable radioiodinated antibodies. Herein we present our evaluative studies on using FCCS12026 for the radioiodination of an internalizing antibody (Cetuximab) and its comparison with directly labeled antibody, on the aspect of internalizing characteristics and tumor retentions.

Methods: For direct labeling Cetuximab was labeled with ^{125}I using the Chloramine T method. For indirect labeling FCCS12026 was radioiodinated using chloramine-T to give, N-(4-Isothiocyanatobenzyl)-2-(3-[^{125}I]phenyl) acetamide ([^{125}I]-FCCS12027) which was purified by HPLC, concentrated and conjugated with Cetuximab at pH 8.5. In vitro internalization assays were performed with the LS174T and PC9 cell lines. After i.v. injection of [^{125}I]-Cetuximab or [^{125}I]-FCCS12027-Cetuximab in mice bearing subcutaneous LS174T xenografts, the static images were obtained at 24, 48 and 168 h on a Inveon SPECT scanner equipped with a low energy all purpose collimator.

Results: [^{125}I]-FCCS12027-Cetuximab was shown higher retention of internalized activity compared with [^{125}I]-Cetuximab in the LS174T and PC9 cell lines up to 24 h. The internalized radioactivity from [^{125}I]-Cetuximab was about 4-fold higher than [^{125}I]-Cetuximab at 24 h. In planar images of LS174T xenograft model, radioactivity of [^{125}I]-Cetuximab was shown high level in thyroid glands compared with [^{125}I]-FCCS12027-Cetuximab. Tumor uptake of [^{125}I]-FCCS12027-Cetuximab was shown higher than [^{125}I]-Cetuximab up to 168 h.

Conclusions: All the results indicate that the [^{125}I]-FCCS12027-Cetuximab are considerably more stable and resistant to deiodination *in vivo*. Therefore FCCS12026 is a promising bi-functional linker for radioiodination of internalizing mAbs for *in vivo* application including radioimmunotherapy.

Radionuclide Therapy_20

Assessment of Radioiodine Therapy Efficacy for Treatment of Differentiated Thyroid Cancer Patients with Pulmonary Metastasis Undetected by Chest CT

Bin Long, Mengdi Yang, Zhiwen Yang, Heqing Yi, Linfa Li

Department of Nuclear Medicine, Zhejiang Cancer Hospital, China

Purpose: To assess radioiodine therapy efficacy for treatment of differentiated thyroid cancer patients with

pulmonary metastasis undetected by chest CT.

Methods: We investigated whether Radioiodine therapy is an effective means for treatment of DTC with pulmonary metastases undetected by Computed Tomography (CT) scan. We took a retrospective study analyzing ^{131}I therapy on 21 DTC patients with lung metastasis but undetected by CT scan.

Results: All the 21 patients were first treated with radioiodine ablation of thyroid remnants. Routine chest CT scan was performed before ^{131}I treatment without Diagnostic Radioiodine Whole Body Scan (DxWBS), and post-therapeutic WBS (RxWBS) was performed 3-5 days after oral administration of ^{131}I. The overall effectiveness rate was 95.2% (20/21). Among the patients the rate for complete response (CR), partial response, and no response was 23.8% (5/21), 71.4% (15/21), and 4.7% (1/21), respectively. There were 12 patients with diffusive uptake, and the rest 9 showed focused and low uptake. The difference in CR rate between diffusive uptake and focused uptake patients is not statistically significant (P=0.123 by Fisher's exact test). There was a correlation between Thyroglobulin (Tg) level and extra-pulmonary metastasis. All the patients showed extra-pulmonary metastasis when Tg level > 87.5 ng/ml (Area under ROC curve=1.0, P=0.00).

Conclusions: DTC patients with undetected lung metastasis in CT imaging responded well to ^{131}I radiotherapy and showed good prognosis. The serum Tg level before ^{131}I treatment may correlate with metastasis, and this may suggest DxWBS before radiotherapy.

Radionuclide Therapy_29

Assessment of the number of days of hospitalization of patients I-131 therapy

Chien- hua Lu[1], Chiang-Hsuan Lee[2],Chih- Shun Wu[1]

1. Division of Nuclear Medicine,Chi Mei Medical Center, Liouying,Tainan,Taiwan
2. Division of Nuclear Medicine,Chi Mei Medical Center,Tainan,Taiwan

Objectives: So far the state of iodine-131 (I-131) hospitalized patients outside the hospital conditions of release, the Atomic Energy Commission has not yet set a uniform standard, each hospital will encounter occasionally disable T4, in urgent need of hospitalization of patients discharged, but no body radiation medication exposure rate of the reference data, you can not really grasp the required number of days of hospitalization and scheduling, so statistics on hospital inpatient therapy receiving I-131 radiation exposure rate of the patient's body, in order to provide peer-hospital patients in urgent need of hospital treatment schedule and the number of days of hospitalization reference.

Methods: Statistics from 99.01.01 until 104.6.30 stop of papillary or follicular carcinoma thyroid cancer patients, the post-surgery in hospital receiving I-131 100-200mCi (exclude 100mCi less) high-dose drug therapy,after 24 hours in radiation exposure rate at 1 meter, the patient prior to admission were given appropriate health education of informing two hours after taking the need to drink more water to increase urinary excretion of the body in order to reduce the residual radiation,and flicker investigation ATOMTEX AT1121 inspection device to detect body radiation exposure rate.

Results: 99.01.01.-104.06.30. a total of Prosecution and 423 patients,the radiation exposure rates between: 2.96--99μSv/hr, the average dose rate 36.75μSv/hr.

Conclusions: The standard interpretation discharge of patients outside the hospital is based on the legacy of the atomic energy codification, appendix V, radiation protection II, outside the control of the release time and patient dose levels, based on the standard at 1 meter, radioactivity in the patient exposure ratio is lower then 11 mR / hr , dependents under 45 years old by the majority of people under the control of appropriate guidance can be discharged outside release, according to statistics of the radiation exposure rate, most patients hospitalized 2 days then, if the other hospitals, in case of their own to stop T4 and the urgent need to treat patients, the radiation exposure rate data can also be provided with reference to use.

Radionuclide Therapy_30

Radioimmunotherapy of ^{177}Lu Labeled Anti-HER-1 Antibody in Esophageal Squamous Cell Carcinoma

In Ho Song, Yong Serk Park, Byung Chul Lee, Byung Seok Moon, Wee Sup Chung, Kwang Il Kim, Yong Jin Lee, Joo Hyun Kang, Chang Woon Choi, Sang Moo Lim, Tae Sup Lee

Korea Institute of Radiological and Medical Sciences

Epidermal growth factor receptor (EGFR, HER-1) is a valid target for targeted therapy in several tumors. Due to high frequency of EGFR expression in esophageal squamous cell carcinoma (ESCC), it is clinically expected to treat the ESCC patient with targeted therapy including anti-HER-1 antibody such as cetuximab. We evaluated for feasibility of radioimmunotherapy (RIT) in ESCC xenografts using ^{177}Lu-labeled cetuximab

Cetuximab was conjugated with bifunctional chelating agent, p-SCN-Bn-PCTA and radiolabeled with ^{177}Lu. Serum stability, immunoreactivity, in vitro cell binding assay and in vitro cytotoxicity were performed. Biodistribution, SPECT/CT imaging and digital whole

body autoradiography (DWBA) of ^{177}Lu-cetuximab were performed in TE-8 xenograft. Therapeutic efficacy of ^{177}Lu-cetuximab was evaluated and compared with cold antibody and saline in TE-8 xenografts. Therapeutic response was evaluated using tumor volume measurement, ^{18}F-FDG-PET imaging and immunohistochemical staining.

^{177}Lu labeled antibody showed high radiolabeling yield (> 98%), stability (> 90%) and favorable immunoreactivity. Biodistribution, SPECT/CT imaging and DWBA demonstrated specific uptake in TE-8 tumor. Tumor accumulation of ^{177}Lu-cetuximab was peaked at 120 h. Radioimmunotherapy with ^{177}Lu-cetuximab showed significant inhibition of tumor growth (P < 0.01) and marked reduction of ^{18}F-FDG SUV compared to that of control (P < 0.05). RIT group showed increased TUNEL positivity and decreased Ki-67 staining indices compared to other groups (P < 0.01), respectively.

In this study, we successfully labeled anti-HER-1 antibody with ^{177}Lu and ^{177}Lu-cetuximab radioimmunotherapy showed effective tumor growth inhibition. ^{177}Lu-cetuximab may be useful as a potent RIT agent in EGFR positive ESCC tumor.

General Nuclear Medicine_10

Evaluation of FDG Uptake in Normal Adrenal Gland and Adrenal Mass on PET/CT

Kaoru Maruyama[1], Oku Naohiko [2]

1. Hyogo College of Medicine (Japan)
2. Himedic Osaka (Japan)

Objectives: The aim of this study is assess FDG uptake of normal adrenal glands and adrenal masses.

Methods: Thirteen patients with 16 adrenal lesions detected in FDG-PET/CT were retrospectively evaluated. The study group comprised 9 males and 4 females with a mean age of 65 years (range 37-81 years). Eight lesions of 13 patients were proven to adenoma, 8 lesions were metastasis, and 10 adrenal glands were normal. A PET/CT scanner (Gemini GXL16, Phillips) was used for data acquisition. After one hour of the FDG injection of 4MBq per kilogram of body weight, images ranging from the toe and the top of the skull were acquired. Hounsfield units (HU) and size on non-enhanced CT, adrenal grand and liver SUV_{max} (A and L, respectively) on PET were measured. The A/L ratio was calculated. Correlation analysis was performed between size and the parameters of A, L, A/L with linear regression method.

Results: Adrenal metastases from 5 lung cancer patients and 1 pancreatic cancer patient were found. Bilateral adrenal masses were found in 1 patient of adenoma and 2 patients of metastases. The mean HU in adenoma was lower than those in metastasis. The mean and SD of size was 25±6mm (range 16-33 mm) in adenoma and 25±9mm (range 15-37 mm) in metastasis. There was no significant difference in size between adenoma and metastasis. The mean and SD of A was 1.7±0.5 in normal, 2.0±0.5 in adenoma and 10.3±4.0 in metastasis, respectively. The mean L and SD was similar as background (L=2.7±0.4 in normal, 2.8±0.5 in adenoma and 2.7±0.6 in metastases, respectively). The A/L value was below 1.30 in normal and below 1.4 in adenoma and over 1.8 in metastasis, respectively. The mean A and A/L were significantly higher in metastasis than those in adenoma. There was no correlation between A and size of mass.

Conclusions: FDG-PET/CT may be useful for distinction between metastasis and adenoma in diagnosis, even if those are similar size of adrenal masses.

General Nuclear Medicine_11

Survival in Patients with Bilateral Gross Renal Parenchymal Impairment

Zeenat Jabin, Azmal Kabir Sarker, Sharmin Reza, Shamim Momtaz, Rahima Perveen, Raihan Hussain, Nasreen Sultana

National Institute of Nuclear Medicine and Allied Sciences, Bangladesh

While some cases of bilateral Gross renal Parenchymal Impairement (GPI) improve with appropriate management, few cases progress to renal failure requiring renal replacement therapy or transplant. In the year 2011 renal diseases were responsible for 11th largest number of death cases as reported from secondary and tertiary level hospitals in Bangladesh. This study was carried out to obtain a sketch of survival in patients diagnosed with GPI at our facility.

Tc-99m Diethylene Triamine Penta-acteic acid (DTPA) renogram of 576 patients was performed at National Institute of Nuclear Medicine and Allied Sciences for a period of six months from January to June 2013. Bilateral GPI was diagnosed in patients who had poor perfusion with negligible uptake and washout of tracer resulting in a flat time-activity curve. Over telephone interview was conducted in the year 2015 to obtain the clinical follow up data of patients with bilateral GPI.

Twenty one patients were diagnosed to have bilateral GPI (M/F=15/6) with mean age 45±20.9 (3 months to 71 years). Follow up data of 16 (M/F=12/4) patients with mean age 41.2±22.3 (3 months-65 years) were available. Eleven (68.8%) patients were alive at the time of follow up and five (31.2%) patients were found to be deceased. Deaths in all were reported to be associated with renal

failure and occurred during hospital management. In this patient group, one and two year survival was estimated to be 93.8 and 68.8%. All the patients (n=10) who were alive and were put to 'medical management only' were reported to experience improvement of health (Serum creatinine ≤ 3 mg/dl) except in two who had developed renal failure during two year follow up. One who underwent surgical correction of renal outflow obstruction reported of improving health. Among the five deceased, one who was put to maintenance dialysis after imaging, survived for 13 months. Among the other four patients who were on medical management, two survived for 15 months, one for 12 months and the other one for 25 days.

This study may help assess the disease pattern for future research based on the experience of a single institute.

General Nuclear Medicine_18

The Incidence of Thyroid Malignancy in Patients with Sonographically Benign ppearing Hypofunctioning Nodules.

Kim Xia, Dee Nandurkar

Monash Medical Centre, Australia

A hypofunctioning (cold) nodule on scintigraphy is associated with an increased risk of malignancy. This study assesses if the risk of malignancy in cold nodules can be stratified according to the presence of sonographic features and therefore determine the need for cytopathological correlation.

A retrospective audit correlating the sonographic and histological findings of hypofunctioning nodules on Tc-99m pertechnetate scintigraphy was performed. Patients with cold nodules on scintigraphy carried out at our institution between January 2005 and February 2015 were identified. The presence or absence of specific sonographic features (marked hypoechogenicity, irregular margins, microcalcifications, hypervascularity, taller than wide) was established for each nodule. These findings were correlated with fine needle aspirate cytology results. The sonographic features and histology for benign and malignant nodules were compared using Fischer's exact test.

A total of 53 cold nodules were examined with 21 nodules with suspicious ultrasound findings and 32 nodules with no suspicious ultrasound findings.

In the nodules with no suspicious ultrasound findings, two had malignant histology including papillary carcinoma and follicular with micropapillary carcinoma (2/32) and 30 nodules were benign (30/32). There is a significant association between no suspicious ultrasound features and benign histology (P<0.0001) using an unpaired t-test, with a negative predictive value of 0.94 (0.79 – 0.99).

In the nodules with suspicious ultrasound findings, 3 cancers were detected (3/21), one follicular and two papillary thyroid carcinomas.

There was a strong association between marked hypoechogenicity and malignant histology (P=0.02) but no statistically significant correlation between other sonographic features and malignant histology.

The rate of malignancy in cold nodules is low in the absence of suspicious ultrasound features. There was a statistically significant association between no suspicious sonographic findings and benign histology in our study. This suggests that ultrasound can be used to stratify a cold thyroid nodule before invasive procedures are performed.

General Nuclear Medicine_20

Older age is related to delayed visualization of bile ducts on Tc-99m mebrofenin hepatobiliary scintigraphy

Ho-Chun Song, Seran Min, Seong Young Kwon, Jahae Kim, Geum-Cheol Jeong, Sae-Ryung Kang, Sang-Geon Cho, Henry Hee-Seung Bom, Jung-Joon Min, Ki Seong Park, Hee Jeong Park, Minchul Song

Nuclear Medicine,Chonnam National University Hospital, Korea

The purpose of this study was to evaluate the relationship between image findings on Tc-99m mebrofenin hepatobiliary scintigraphy (HBS) and clinical characteristics of patients with suspected biliary dysfunction.

Total 82 consecutive patients who underwent HBS for evaluation of biliary dysfunction were included. Those who underwent hepatobiliary operation or who did not underwent laboratory test for hepatobiliary function at the time of image acquisition were excluded. Dynamic images were obtained at every minute for the first 60 min, and static images were obtained at 60 min and 120 min, and 240 min if necessary. The time points of the first visualization (in minutes) of the intrahepatic bile duct (t-IHD), common bile duct (t-CBD), gallbladder (t-GB) and small intestine (t-SI) were analyzed on the dynamic and static images. The clinical and laboratory characteristics of patients were analyzed according to different organ visualization time points.

Age and serum gamma glutamyl-transpeptidase (GGT) showed moderate positive correlation with t-CBD and t-GB. Serum GGT also showed a positive correlation with t-IHD. Age and GGT also showed a mutual positive correlation. However, age was the factor best correlating with t-IHD,

t-CBD and t-GB and GGT did not show significant correlation in multiple regression analysis.
Older age was associated with delayed IHD, CBD and GB visualization on HBS. Caution is needed for interpretation of organ visualization time on HBS in older patients.

General Nuclear Medicine_28

The study of $^{99}Tc^{m}$-DTPA Scintigraphic Imaging assess split Renal Function in hydronephrosis

Jingshun Zha[1], Siping Gu[2], Yan Jiang[3], Chunling Huang[1] Yuan Xu[1], Yingrui Shu[1], Tingyin Jiang[1]

1. Department of Nuclear Medicine, the second Affiliated Hospital of Fujian Medical University, Quanzhou, China.
2. Second Department of surgery, Shishi (Overseas Chinese) Hospital, Quanzhou China.
3. Department of Library, the second Affiliated Hospital of Fujian Medical University, Quanzhou, China

Objectives: The aim of this study was assess the value of ^{99m}Tc-DTPA dynamic scintigraphic Imaging that be used to evaluate split renal function in hydronephrosis .
Methods: Retrospective analysis the results of ^{99m}Tc-DTPA dynamic scintigraphic Imaging in 60 inpatients with hydronephrosis. In accordance with unilateral hydronephrosis, bilateral hydronephrosis and mild , moderate and severe packet. The activity - time curve, glomerular filtration rate(GFR) of split kidney and double kidney total GFR was analysised in each group.The double kidney total GFR was compared with the results of clinical evaluation about renal function and blood urea nitrogen(BUN), creatinine(Cr) levels. SPSS.16 statistical software used for statistical analysis.
Results: The incidence of abnormal activity-time curve among various degrees of hydronephrosis were significantly higher than those without hydronephrosis (95.89% vs. 4.2%, X^2=15.93,*P* =0.001). The pattern of activity-time curve presenting mainly high level and extensant line(type Ⅰ) , low level and extensant line(type Ⅱ),and continued ascendant line(type Ⅲ), have 26.02%(19/73), 53.42%(39/73) and 13.69%(10/73) respectively in all of 73 sick kidney with hydronephrosis.Among various patterns of time- activity curve,type I was the most in mild hydronephrosis (14/19) and type II was the most in moderate to severe hydronephrosis (40/51)The GFR of sick kidney be to one after another lower for mild,moderate,severe hydronephrosis with significantly difference generally (*F*=34.56, *P*<0.01).The GFR of each other various degrees of hydronephrosis has significant difference (*t*=3.6758, 5.8975, 3.9391, *P* all<0.005). The double kidney total GFR in bilateral hydronephrosis were lower than unilateral hydronephrosis with significantly difference (*t*=3.5968, *P* <0.01).The incidence of Renal insufficiency in the group of bilateral hydronephrosis was significantly higher than the unilateral hydronephrosis (53.8% vs10.6%,X^2=9.335,*P*<0.005), and serum BUN and Cr levels in bilateral hydronephrosis group were significantly higher than the group of unilateral hydronephrosis with significantly difference (*t*=3.2587,4.5126, *P* All<0.01).
Conclusion: $^{99}Tc^{m}$-DTPA Scintigraphic Imaging be use to assess split renal function and serious degrees of hydronephrosis,which is a simple non-invasive method with a higher sensitivity, but the lack of specificity, the analysis should be combination with clinical situation.

General Nuclear Medicine_29

The Efficacy of F-18 FDG PET/CT and Gallium-67 SPECT/CT in Diagnosing Fever of Unknown Origin: A Preliminary Report

Bor-Tau Hung[1], Pei-Wen Wang[1,2], Shu-Hua Huang[1]

1. Department of Nuclear Medicine, Kaohsiung Chang Gung Memorial Hospital and Chang Gung University College of Medicine, Kaohsiung, Taiwan.
2. Department of Internal Medicine, Kaohsiung Chang Gung Memorial Hospital and Chang Gung University College of Medicine, Kaohsiung, Taiwan

Objectives: The study was to compare the efficacy of F-18 FDG PET/CT and Gallium-67 SPECT/CT in diagnosing fever of unknown origin (FUO) prospectively.
Methods: Forty-three patients with FUO underwent F-18 FDG PET/CT and Gallium-67 SPECT/CT from January 2013 through March 2015. Two patients lost follow-up and were excluded from the investigation. In 17 patients, an infectious underlying disease was found. A malignant disorder was the cause of FUO in 6 patients. A multisystem inflammatory disease was found in 6 patients. Adrenal insufficiency was the cause of FUO in 2 patients. In 10 patients, the cause of FUO was not found. The clinical contribution of both examinations was judged by two clinicians and categorized as helpful in diagnosis or noncontributory to diagnosis.
Results: Twenty (49%) abnormal F-18 FDG PET/CT scans pointed to the source of fever and were judged helpful in diagnosis. Seven (17%) Gallium-67

SPECT/CT scans were judged helpful. All abnormal finding in Gallium-67 SPECT/CT scans were also positive in F-18 FDG PET/CT scans. The clinical contribution of both examinations for diagnosing FUO was significantly different (P<0.05).

Conclusions: On the basis of the preliminary study, F-18 FDG PET/CT is superior to Gallium-67 SPECT/CT in the workup of patients with FUO. Because of the quite result and superior sensitivity, F-18 FDG PET/CT may replace Gallium-67 SPECT/CT where this technique is available.

General Nuclear Medicine_30

Distance Effects on Radio-exposure Measurements In Thyroid Cancer Patients Receiving I-131 Treatment

Wen-Sheng Huang[1], Pei-Yao Lin[2], Chia-Chi Chang[1], Cheng-Yi Cheng[3], Chiang-Hsuan Lee[4]*

1. Department of Nuclear Medicine, Changhua Christian Hospital, Changhua, Taiwan
2. Molecular Imaging Center, National Taiwan University, Taipei, Taiwan
3. Department of Nuclear Medicine, Tri-Service General Hospital, Taipei, Taiwan
4. Department of Nuclear Medicine, Chi Mei Medical Center, Tainan, Taiwan

Objectives: To evaluate effects of distance on the measurements of radiation exposure in thyroid cancer patients after receiving I-131 treatment.

Methods: Twenty-two post- operative differentiated thyroid cancer patients (8 men, 14 women; mean age: 45.5 yrs) who received I-131 treatment (mean 115 mCi) were observed. Measurements of radiation exposure in 1 and 2 meter distances were performed immediately, 3 and 7 days after I-131 administration using a radiodector (SEI Inspector+ EXP; Unit: K CPM). Data expressed as mean±SD. Variation (Var.) and linear correlation(R) between groups were also evaluated.

Results: It appeared underestimate the count rate in 1M compared to that of 2 M at the immediate time point with higher variation (74.6±22.0 vs. 24.4±6.2; Var.= 484.9 vs. 38.7). However, the measured data were compatable at the day 3 and 7 time points (11.6± 6.7 vs. 2.9± 1.7; Var.= 44.8 vs. 3.1 at the day 3 and 0.39± 0.29 vs. 0.12± 0.07; Var.= 0.08 vs. 0.006 at the day 7). Better Rs were aslo noted in the day 3 and 7 than that of the immediate time points (R= 0.994 vs. 0.974 vs. 0.938, respectively).

Conclusions: To evaluate radiation exposure of I-131 treated patients, a 2M measurement might be suggested at the immediated time point while it became comparable between 1 and 2 M measurements at the day 3 and 7 time points.

General Nuclear Medicine_31

Radiation Exposure In I-131 Treated Thyroid Cancer Patients: T4 Withdrawal Versus rhTSH Injection Preparations

Wen-Sheng Huang[1]*, Guang-Hei Hung[2], Pei-Yao Lin[3], Yu-Yeh Kuo[4], Cheng-Yi Cheng[5]

1. Department of Nuclear Medicine, Changhua Christian Hospital, Changhua, Taiwan
2. Department of Nuclear Medicine, Chang Bing Show Chwan Memorial Hospital, Changhua, Taiwan
3. Molecular Imaging Center, National Taiwan University, Taipei, Taiwan
4. Graduate Institute of Medical Sciences, National Defense Medical Center, Taipei, Taiwan
5. Department of Nuclear Medicine, Tri-Service General Hospital, Taipei, Taiwan

Objectives: To observe differences of radiation exposure in I-131 treated thyroid cancer patients preparing with T4 withdrawal and rhTSH injection protocols.

Methods: Twenty-eight differentiated thyroid cancer patients (9 men, 19 women; mean age: 44 yr) who prepared for I-131 treatment were divided into 2 groups (Gp). Gp 1 was prepared with T4 withdrawal (n=22) while Gp 2 was prepared with standard rhTSH injection (n=6). Both groups received a comparable I-131 dosage (averaged 115 vs. 121 mCi). Radiation exposure was measured at immediately, day 3 and 7 after I-131 administration using a radio-detector (SEI Inspector+ EXP; Unit: K CPM). Data expressed as mean±SD.

Results: A comparable radiation exposure was measured from patients immediately after I-131 administration between the 2 groups (74.59±22.02 vs. 74.88±19.47) as measured at 1 meter distance. However, the exposure was significantly decreased in Gp 2 at day 3 (11.62±6.69 vs. 5.62±3.41; P<0.01; or 51.6% decrease) compared to that of Gp. 2. The trend sustained till day 7 after I-131 administration (0.39±0.29 vs. 0.26±0.23; P<0.05; or 33.3% decrease).

Conclusions: While comparable radiation exposure was noted in both T4 withdrawal and rhTSH injection groups immediately after I-131 treatment, preparation with rhTSH injection group showed significantly decreased radiation exposure at day 3 and sustained till day 7 after I-131 treatment.

General Nuclear Medicine_32

Values of Tc-99m Imaging in Thyroidectomized Thyroid Cancer Patients Immediately Before I-131 Treatment

Wen-Sheng Huang[1], Chi-Jung Tsai[2], Yu-Yeh Kuo[3], Cheng-Yi Cheng[2]*

1. Department of Nuclear Medicine, Changhua Christian Hospital, Changhua, Taiwan
2. Department of Nuclear Medicine, Tri-Service General Hospital, Taipei, Taiwan
3. Graduate Institute of Medical Sciences, National Defense Medical Center, Taipei, Taiwan

Objectives: To evaluate the clinical role of technetium-99m pertechnetate (Tc-99m) imaging in thyroidectomized differentiated thyroid cancer (DTC) patients immediately before radioiodine-131 (I-131) treatment (Tx).

Methods: Eighty-six consecutive post-total-thyroidectomy patients (15 men, 71 women; mean age: 46.8 years) with pathologically diagnosed DTC were retrospectively studied. Tc-99m imaging immediately before I-131 Tx using both patient- and lesion-based measurements were analyzed that were further compared with those of post-Tx I-131 whole body scans.

Results: For patients with unequivocally positive Tc-99m uptake, the sensitivity was 77% (patient based) and 59% (site based). The positive predictive value (PPV) was 100% for both patient and site based measurements. If equivocal Tc-99m uptake was counted as positive, the sensitivity was 83% and 67%, and the PPV was 100% and 99% for patient and site based measurements respectively.

Conclusions: 1. To increase sensitivity yet maintaining high PPV, equivocal Tc-99m uptake should be considered a positive finding. 2. The nearly 100% PPV of Tc-99m imaging immediately before I-131 Tx for remnant detection suggests that Tc-99m imaging might provide a clue for the subsequently I-131 therapeutic dosage and the outcome prediction.

General Nuclear Medicine_33

The clinical value of Tc-99m Technegas Ventilation Scan in predicting the severity of airflow limitation in Patients with Chronic Obstructive Lung Disease

Sehun Choi, Chang Ju Na, Jeonghun Kim, Yeon-Hee Han, Hwan-Jeong Jeong, Myung-Hee Sohn, Seoung Ju Park, Seok Tae Lim

Department of Nuclear Medicine, Molecular Imaging & Therapeutic Medicine Research Center, Cyclotron Research Center, Institute, Korea

Chronic obstructive lung disease (COPD) is a major cause of morbidity and mortality throughout the world. This is characterized by persistent airflow limitation that is associated with a chronic inflammatory response in the lungs to noxious particles. Radionuclide ventilation scan using Tc-99m technegas had been reported to be imaged by deposition within airways by their mass median aero-dynamic diameter. The study intends to show the Tc-99m Technegas scan can grade the severity of airflow limitation, and also to correlate with the spirometric parameter (FEV1, FEV1/FVC) in COPD patients.

Retrospectively 107 patients (M:F=81:26, age: 67.0±10.2 yrs) was enrolled, in patients with lung cancer, pulmonary tuberculosis or etc, to measure pre-operative lung function. Of these patients, 54 patients coexist with COPD (with FEV1/FVC<0.7), and 53 patients have no chronic lung disease (with FEV1/FVC>0.7). Ventilation scan is graded by 3 grades; grade1 (n=20, uneven decrease pattern), grade2 (n=21, central deposition), grade3 (n=13, peripheral deposition with decreased uptake). The normal group (n=53) shows homogenous distribution pattern in ventilation scan. This grading system is correlated with FEV1 which was the hallmark of severity of airflow limitation in COPD patients.

The results show the significant difference of FEV1 value in these four groups that are classified by ventilation scan (normal, sub-group of COPD grade 1, 2, 3), (P<0.001). The ranges of FEV1 in the sub-group of COPD patients are as follows; grade1 (70 ± 14.4), grade2 (65 ± 14.3), grade3 (70 ± 14.4). The post-hoc analysis shows there is significant difference in each groups (normal vs. COPD patients (P=0.0001), grade1 vs. grade3 (P=0.001), grade2 vs. grade3 (P=0.012))

In this study, all three sub-groups of COPD patients could not reach the statistically significance (grade1 vs. grade2, P=0.08). However, ventilation scan shows good tendency in correlation with COPD severity. Also, it has many advantages comparing to spirometric analysis, in terms of representing more physiologic status, visualizing airflow obstruction, and not struggling to deep breathing out which is less dependent to patient's effort.

General Nuclear Medicine_34

Post Therapeutic I-131 SPECT/CT in Postoperative Thyroid Cancer Patients : The Relationship Between Anatomical Foci and Follow-Up Serum Thyroglobulin levels

Chang Ju Na, Sehun Choi, Jeonghun Kim, Yeon-Hee Han, Hwan-Jeong Jeong, Myung-Hee Sohn, Seok Tae Lim

Department of Nuclear Medicine, Chonbuk National University Medical School and Hospital, Korea

The relationship between follow-up thyroglobulin (Tg) after total thyroidectomy and visualization of thyroglossal duct & thyroid bed in post therapeutic I-131 scan (I-131 scan) has not yet been determined in differentiated thyroid carcinoma (DTC). The aim of this study was to evaluate the relationship between follow-up Tg levels and anatomic sites of foci in post I-131 ablation therapy SPECT/CT for DTC.

Total of 34 DTC patients (28 papillary & 6 follicular thyroid cancer) who underwent total thyroidectomy followed by I-131 ablation therapy (HD-RIT) were included. The patients with distant metastasis and high level of serum anti-thyroglobulin antibody (≥100 U/mL) were excluded. Stimulated Tg (sTg) levels were measured before HD-RIT and after about 8 months of HD-RIT. All patients underwent post-therapeutic I-131 planar image and SPECT/CT. The anatomic sites (thyroglossal duct & thyroid bed) of abnormal foci in planar image were confirmed through SPECT/CT.

Of the 34 patients, 5 patients showed foci of uptake in only thyroglossal duct, 10 showed the foci in thyroid bed and 15 had foci in both thyroglossal duct and thyroid bed in I-131 SPECT/CT. Thirteen patients showed lower level of sTg (< 1 ng/mL) and 21 had higher level of sTg (≧1) before HD-RIT. After about 8 months of HD-RIT, 11 patients showed incompleted ablation (sTg≧1). Others were completed ablation (sTg<1). Univariate analysis identified visualization of both thyroglossal duct and thyroid bed was an only correlative factor of elevated sTg before HD-RIT (P=0.002). Uptake in either thyroglossal duct or thyroid bed was not statistically related (P=0.413, P=0.719). When compared with sTg after about 8 months of HD-RIT, visualization of both thyroglossal duct & thyroid bed and uptake in only thyroglossal duct or thyroid bed was not statistically related. (P=0.464, P=0.912, P=0.594).

Visualization of both thyroglossal duct and thyroid bed in post-therapeutic I-131 scan was significantly related with sTg levels measured before HD-RIT. But, follow-up sTg levels after HD-RIT were not related with visualization of thyroglossal duct and thyroid bed in post therapeutic I-131 scan.

General Nuclear Medicine_35

Follow-up bone scintigraphy in treated breast cancer patients: The clinical significance of newly appeared rib uptake

Minjung Seo, Seol Hoon Park

Ulsan University Hospital, Korea

The aim of this study is to evaluate the clinical significance of newly appeared rib uptakes on follow-up bone scintigraphy in asymptomatic breast cancer patients after surgery.

Bone scintigraphy which was performed between January 01, 2011 and February 28, 2013 for follow-up in asymptomatic breast cancer patients were retrospectively reviewed. Patients with newly appeared uptake only in the rib were included. A total of 137 lesions in 62 patients were analyzed. The location, intensity, time interval after surgery/radiation therapy, and the final diagnosis of the rib uptake (fracture or metastasis) were evaluated. The bone scintigraphy and concurrent CT were analyzed by two experienced nuclear medicine physicians.

The 137 lesions were more frequently located at the ipsilateral side of breast cancer (66.4%), mid-level ribs (5-8th, 58.4%), anterior arc (67.2%), and presented as single (59.7%), focal (97.1%), moderate to intense (94.9%) uptakes. Rib uptakes were detected at an average of 3.6 and 3.3 years after surgery and radiotherapy, respectively. Most (89.2%) showed fracture lines or callus formations on concurrent CT.

When evaluating ipsilateral uptakes to the cancer site, surgical method (P>0.05) was not a significant factor for rib uptake development. History of radiation bordered on a statistically significant value (P=0.05). In a subgroup analysis of patients who underwent radiotherapy, ipsilateral rib uptake appeared more frequently within 3 years of irradiation (P=0.03).

Among the 137 lesions, 135 turned out to be traumatic fractures (98.5%), while only two lesions in one patient were metastasis. The metastatic lesions were found at the contralateral side of the breast cancer and were located separately (posterior arcs of right 6th and 8th ribs).

New rib uptake detected on follow-up bone scintigraphy without any other new bone lesion in asymptomatic breast cancer patients are frequently located in the anterior arc of mid-level ribs ipsilateral to the cancer site. Metastasis is very rare in such cases. When a new rib uptake is detected on bone scintigraphy in similar circumstances, radiological correlation and follow-up bone scan may be sufficient.

Radiochemistry_4

Fully Automated Radiosynthesis of (R)-[O-methyl-^{11}C] Metomidate: A PET Radiotracer for Adrenal Cortex Imaging

Qiu-Song CHEN, Lei LIU, Yan-sheng LI, Xi-ling XING

Department of PET-CT Diagnostic, Tianjin Medical University General Hospital, China

In the adrenocortex, one of the key enzymes, playing a major role in the biosynthesis, is the 11β-hydroxylase (CYP11B1; P45011β), forming cortisol and aldosterone from the corresponding deoxysteroids. This enzyme can be overexpressed in incidentalomas of the adrenal cortex and was described as a relative excellent target enzyme for adrenocortical imaging. [^{11}C] (R)-1-(1-phenylethyl)-1H-imidazole-5-carboxylic acid methyl ester ((R)-[O-methyl-^{11}C] Metomidate, [^{11}C] MTO), an analogue of Etomidate, well known as a narcotic drug, works as a substrate for this enzyme and therefore was introduced for adrenocortical imaging. With the purpose of developing the PET imaging agent for tumors of adrenal cortex, we researched the radiosynthesis protocol of [^{11}C] MTO, for getting sufficient radiotracers to meet the needs of clinical imaging.

The carboxylate salt of precursor was generated by dissolving 1.0 mg (R)-Desethyl-Etomidate acid in acetone and adding 4-5μl tetrabutyl ammonium hydroxide (25%) for the procedure of labeling reaction. [^{11}C] CO2 was produced via 14N(p, α) ^{11}C nuclear reaction. [^{11}C] CH3OTf, as the [^{11}C] methylation reagent, was obtained online by GE TRACERlab FXc synthesis module, and bubbled into reactor at 0oC until maximum radioactivity accumulated. [^{11}C] MTO was synthesized by direct O-methylation of (R)-Desethyl-Etomidate with [^{11}C]-CH3OTf under 40oC. The product was purified by semi-preparative reversed-phase HPLC with the eluent 0.05 M ammonium acetate (pH 3.5)/ acetonitrile 48/52 (v: v) and formulated with ethanol and saline for intravenous administration.

The total synthesis time of the tracer was approximately 25 min from end-of-bombardment. The radiochemical yield was 47.7% ± 3.4% (40.6%~53.1%) (n=15, corrected to [^{11}C] CH3I). The radiochemical purity of the product was up to 99% and the chemical purity was above 98% (n=15).

The results of our preliminary study illustrated that the radioligands [^{11}C] MTO could be radiosynthesized stably and sufficiently for routine clinical PET imaging of the adrenal cortex and its tumors.

Radiochemistry_7

In vivo biodistribution of ^{64}Cu labeled human serum albumin conjugated with more azide (N3)- or DBCO-functional groups using click chemistry approach

Keon Wook Kang, Myung Geun Song, Ji-Yong Park, Hyewon Youn, Dong Soo Lee, June-Key Chung, Yun-Sang Lee, Jae Min Jeong

Department of Nuclear Medicine, Seoul National University Hospital, Korea

Click chemistry is a powerful chemical reaction with excellent bioorthogonality features. Conjugation methods using click chemistry is a simple and highly efficient strategy to prepare radiolabeled human serum albumin (HSA) with ^{64}Cu preserving the characteristics of HSA. We investigated in vivo biodistribution of ^{64}Cu labeled human serum albumin with the various number of azide (N3)- or DBCO-functional groups.

HSA was conjugated with NHS-DBCO (dibenzyl cyclooctyne) or NHS-N3 (molar ratio of HSA:NHS-DBCO(or -N3) = 1:1, 5, 10 or 20). And DBCO or N3 conjugated with NOTA chelator was synthesized for preparing the pre-radiolabeled alkyne complex with ^{64}Cu in PBS. Radio-TLC, MALDI-TOF-MS and DLS were used for analysis. After injection of ^{64}Cu-HSA to BALB/c nude mice, in vivo biodistribution of ^{64}Cu-HSA were quantitatively evaluated by PET images.

Following incubation with the ^{64}Cu-radiolabeled DBCO or N3 complex (DBCO- or N3-PEG4-NOTA-^{64}Cu), the DBCO or N3-functionalized HSA were radiolabeled successfully with ^{64}Cu, with a high radiolabeling efficiency and yield (>95%). In addition, Size of DBCO or N3-tagged HSA were about 7 - 9.4nm dependent on molar ratio of HSA and NHS-DBCO(or -N3). And zeta-potential of DBCO or N3-functionalized HSA were measured. Serial PET imaging revealed that the ratio of heart-to-liver activity were higher in the condition with one to five ratio of HSA to DBCO or N3 (HSA:DBCO(or N3) = 1:5) than others. However, ^{64}Cu labeled DBCO-HSA was more rapidly cleared than N3-HSA via liver and intestine after 24 h.

Both DBCO- and N3-functionalized HSA showed similar blood circulation time and liver uptake, but DBCO-HSA was more rapidly cleared, suggesting that DBCO-functionalization is more useful for in vivo imaging.

Molecular Imaging_6

In vivo imaging systemically injected exosomes from breast cancer cells using NIR and PET imaging

June-Key Chung, Kyung Oh Jung, Hyewon Youn, Keon Wook Kang

Biomedical Sciences, Korea

Breast cancer cells release exosomes to communicate with tumor microenvironment cells, promoting angiogenesis and metastasis. Physiologic distribution of the exosomes was not clarified until now. To monitor the biodistribution of exosomes, we performed fluorescence and PET imaging in mice.

Exosomes were isolated using ExoQuickTM from cultured medium of 4T1, mouse breast cancer cell line. Exosomes were characterized by western blot, Dynamic Laser Scattering, Nanocyte and TEM. Purified exosomes were labeled with Cy7 and ^{64}Cu. The macrocyclic bifunctional chelator pSCN-NOTA were used to make a bond with amine groups of exosomes, and then ^{64}Cu was labeled in the Exosome-NOTA. These labeled exosomes were systemically injected through tail vein. Fluorescence and PET images were obtained by IVIS and PETBOX, respectively. Radio-activities of organs in ex-vivo were measured with gamma counter, and compared to the numbers from SUV of PET images.

Thin layer chromatography showed that 95% of exosomes were labeled with ^{64}Cu. PET images showed that most of free ^{64}Cu were accumulated in liver, and NOTA-^{64}Cu was mainly accumulated in kidney in PET images, at 4 hr and cleared at 24 hr, whilst radiolabeled-exosomes showed higher uptake in the lung, liver, and spleen at 4 hr. Fluorescence images and the radio-activity of excised organs showed the similar pattern of exosomes bio-distribution with PET images, demonstrating higher uptake in the lung, liver, and spleen.

Tumor exosomes were successfully labeled and visualized by fluorescence and PET imaging, showing that the exosomes initially accumulated in the RES (reticular endothelial system) after i.v. injection. Our results could provide indispensable information of exosome bio-distribution for in vivo application of exosomes as a therapeutic vehicle.

Molecular Imaging_11

PET imaging of activated macrophages using a translocator protein ligand, [^{18}F] FEDAC, in a rheumatoid arthritis model

Gi Jeong Cheon, Seock-Jin Chung, Hai-Jeon Yoon, Hyewon Youn, Mi Jeong Kim, Yun-Sang Lee, Jae Min Jeong, Lin Xie, Ming-Rong Zhang, June-Key Chung, Keon Wook Kang

Department of Nuclear Medicine, Tumor Biology Program, Seoul National University College of Medicine, Seoul, Korea

Activated macrophages congregate at the inflammatory site in the early phase of rheumatoid arthritis (RA) pathogenesis. Translocator protein (TSPO) is abundant in activated macrophages, thus can be used for the target of biomarker of inflammation. [^{18}F]FEDAC (N-Benzyl-N-methyl-2-[7,8-dihydro-7-(2-[^{18}F]fluoroethyl)-8-oxo-2-phenyl-9H-purin-9-yl] acetamide) is a radiolabeled ligand that recognizes TSPO. In this study, we evaluated the efficacy of [^{18}F]FEDAC as a potential PET tracer for TSPO in a mouse RA model.

RAW 264.7 mouse macrophages were activated with lipopolysaccharide (LPS). Expression level of TSPO mRNA and protein measured by quantitative RT-PCR and western blotting. [^{18}F]FEDAC uptake was measured using gamma counter, and a traditional TSPO ligand PK11195 was used for competition assay. We used collagen-induced arthritis (CIA) model as a rheumatoid arthritis animal model for in vivo study. The clinical score of CIA mouse was measured by evaluation of degree of paws swelling. Small animal PET/CT images were acquired using 500 uCi [^{18}F]FEDAC.

mRNA and protein levels of TSPO expression were 3.9 fold and 2.3 fold higher in activated RAW 264.7 than inactivated RAW 264.7. Uptake of [^{18}F]FEDAC in activated RAW 264.7 cells was 1.5 fold higher than that in non-activated cells. In addition, uptake of [^{18}F]FEDAC in activated RAW 264.7 was successfully blocked by a competitor PK11195. Clinical score increased in the CIA model and showed the highest score around at 40 days after modeling. At 1 hr after injection of [^{18}F]FEDAC, radiotracer uptake in arthritic paws were significantly increased at 2 to 3 folds more than that in normal paws. The uptake in arthritic joints from PET imaging showed strong correlation with the clinical severity score.

We demonstrated a specific binding of [^{18}F]FEDAC to activated macrophages which have abundant TSPO. [^{18}F]FEDAC PET/CT showed strong uptake in arthritis areas and correlated with clinical severity score. Our results indicated that [^{18}F]FEDAC PET have a potential to monitor inflammatory activity of rheumatoid arthritis by targeting TSPO.

Molecular Imaging_15

Role for pulmonary macrophage for initiation of lung metastasis in anaplastic thyroid cancer

Byeong-Cheol Ahn, Xiu Juan Li, Prakash Gangadaran, Senthilkumar Kalimuthu, Ji Min Oh, Shin Young Jeong, Sang-Woo Lee, Jaetae Lee

Department of Nuclear Medicine, Kyungpook National University School of Medicine, Korea

Several clinical studies have demonstrated that increased macrophage infiltration into tumor confers metastatic potential and poor prognosis in cancer. Development of lung metastasis worsens the prognosis and complete remission of the metastasis is not achieved frequently in the clinics yet; therefore preclinical studies are needed to develop new strategies for the metastasis. Current study was designed to investigate the impact of pulmonary macrophage on lung metastasis of anaplastic thyroid cancer (ATC).

Human ATC cells (CAL-62) were tagged with enhanced firefly luciferase gene. Expression of effluc gene of CAL-62/effluc was evaluated by RT-PCR analysis, western blotting (WB) and luciferase assay. Co-culture system and migration assay were used to assess the effect of mouse macrophage cells Raw264.7 on the proliferation and migration of CAL-62/effluc cells in vitro. FACS analysis was performed to show the pulmonary macrophage population after intravenous injection of Clodronate using CD11b antibody staining. Clodronate or PBS was injected to nude mice through intravenous route before 24 hours of 1x106 CAL-62/effluc cells injection into nude mice. Effect of Clodronate on the lung metastasis of CAL-62/effluc were assessed by bioluminescence imaging (BLI) with IVIS lumina II imaging system.

RT-PCR and WB revealed effluc expression in CAL-62/effluc cells. BLI signals of CAL-62/effluc increased according to cell numbers. Raw264.7 cells promote CAL-62/effluc proliferation and migration in co-culture system and migration assay. Pulmonary macrophage population decreased 88.38% after Clodronate injection compared to PBS control. Intensity of BLI signal between PBS control and Clodronate groups became different from day 21. Bioluminescence signal was weaker in Clodronate group (1.51E+06) compared to control PBS group (7.49E+06)

Our findings indicated that pulmonary macrophages have an important role in initiation of lung metastasis of anaplastic thyroid cancer.

Molecular Imaging_23

Anticancer effect and biodistribution of extracellular vesicles isolated from Rennila Luciferase labelled mMSCs on lung cancer

Byeong-Cheol Ahn, Senthilkumar Kalimuthu, Prakash Gangadaran, Xiu Juan Li, Ji-Min Oh, Shin Young Jeong, Sang-Woo Lee, Jaetae Lee

Department of Nuclear Medicine, Kyungpook National University School of Medicine and Hospital, Daegu, South Korea

Mesenchymal stem cells (MSCs) can used as a therapeutic armor for cancer and extracellular vesicles (EVs) derived from the MSCs also have been evaluated for immense potential to anticancer effect. For success of the therapy, in vivo targeting of the EVs to the tumor is essential, therefore, non-invasive monitoring of EVs in an animal model is crucial for development of EV for cancer therapy. Recent studies focused on labelling of EVs for non-invasive imaging, but labeling procedures can change characteristics of the EV. So the present study tried to develop self-luminescent emitting EV using Rennila luciferase (Rluc) labeled MSC and to visualize the EV in mouse model with lung cancer xenograft.

Mouse bone marrow derived MSCs were stably transfected with Rluc viral particles and then transfected MSC selected with puromycin (MSC-Rluc). After stable transfection, Rluc activity was determined by IVIS imaging. The phenotype markers for MSC were analyzed in MSC-Rluc. EV (EV-Rluc) from the MSC-Rluc was isolated by ultracentrifugation. Anticancer effect of the EVs to Lewis lung cancer cells (LewisC) was assessed. LewisC was stably transfected with enhanced firefly luciferase (effluc) gene by retroviral particles. The cytotoxicity of LewisC analyzed by CCK8 and IVIS imaging. In vivo migration ability of EV-Rluc to LewisC cancer was tracked by IVIS imaging in a mouse model with tumor xenograft.

Rluc activity of MSC-Rluc and EVs derived from the MSC were confirmed in IVIS imaging. MSC-Rluc cells were positive for MSC phenotype markers. The EV-Rluc showed in vitro cytotoxicity to LewisC. Migration of EVs in mouse model with LewisC xenograft was successfully monitored by IVIS imaging and the EV targeted the tumor effectively.

Self-luminescent EV-Rluc was developed in this study, and results of this study suggested that the EV-Rluc can be used for development EV cancer therapy for both in vitro and in vivo studies.

Molecular Imaging_51

Monitoring of dynamic action of microRNA using transgenic mouse expressing optical reporter transgene with microRNA responsive elements

Yoori Choi, Do Won Hwang, Dong Soo Lee

Seoul National Universtiy, Korea

MicroRNAs (miRNAs) fine-tune target protein synthesis by suppressing gene expression, dynamically in time domain along development and possibly in pathological conditions. A method to quantify the action of miRNAs in vivo will be helpful to understand their dynamic behavior during development and aging.

In this study, we established a transgenic mouse harboring miR-124 responsive element in their luciferase-eGFP reporter transgene which can monitor the action of miR-124 in the brain and other organs in vivo by the bioluminescence imaging.

The mouse model was produced and verified by imaging so that luminescence by luciferase shone and then reduced after injection of lentivirus containing miR-124. We also demonstrated that the bioluminescence dramatically decreased in the brain between embryonic day 13 and 16 as endogenous miR-124 expression increased, and maintained in adulthood. The on-and-off of miR-124 action could also be visualized repeatedly in vivo by bioluminescence imaging.

Taken together, we propose this one can simply use this microRNA-transgenic mouse to investigate the dynamic changes of microRNA action in vivo in the spatial and temporal domains.

Cardiology_26

Stem cell implantation after myocardial infarction in pigs: ^{11}C-acetate PET with dobutamine stress

Genki Horitsugi[1], Masaru Ishida[2], Tadashi Watabe[1,4], Shigeru Miyagawa[2], Yasukazu Kanai[3,4], Hayato Ikeda[1]; Keiko Matsunaga[1], Hiroki Kato[1,4], Kayako Isohashi[1,4], Eku Shimosegawa[3,4], Yoshiki Sawa[2], Jun Hatazawa[1,4]

1. Department of Nuclear Medicine and Tracer Kinetics
2. Department of Cardiovascular Surgery
3. Department of Molecular Imaging in Medicine
4. PET Molecular Imaging Center, Osaka University Graduate School of Medicine

Objectives: To evaluate myocardial oxygen consumption after stem cell sheet therapy for experimental myocardial infarction in pigs.

Methods Myocardial infarction (BW=20.3±1.5 kg, female) were studied at rest and during dobutamine (20 μg/kg/min) stress by means of ^{11}C-acetate PET. Pigs were randomly assigned to two groups: therapy group (n=6) or control group (n=3). In the therapy group, induced pluripotent stem cell-derived cardiomyocytes (iPSC-CMs, n=2), skeletal myoblasts (SKMB, n=2) and mesenchymal stem cells from bone marrow (BM-MSCs, n=2) were transplanted on infarcted areas. Dynamic 15 min PET scan was performed before therapy and 2 months after the therapy. Myocardial clearance rate constants of ^{11}C-acetate (kmono), an index of myocardial oxygen consumption, was obtained from time activity curves and compared by Wilcoxon signed rank test.

Results In the stem cell sheet therapy group, kmono at rest and during stress were 0.136 ± 0.025 min-1 and 0.173 ± 0.047 min-1 before therapy and 0.144 ± 0.027 min-1 and 0.204 ± 0.037 min-1 after therapy, respectively. Kmono after therapy were significantly increased compared to that before therapy in the stress study (P<0.05). In the control group, no significant difference was observed in kmono before and after therapy both at rest and during stress.

Conclusions Stem cell sheet implantation therapy increased myocardial oxygen consumption in the myocardial infarction model, suggesting its promising clinical application as myocardial regenerative therapy using iPS cells.

Clinical Applications of PET/MR and SPECT/CT_14

SPECT/CT imaging for the evaluation of the differentiation efficacy of canine adipose tissue derived MSC (cAD-MSC) into osteogenic lineage

Ana Ivanovska, Stefano Grolli, Virna Conti, Antonio Cacchioli, Francesca Ravanetti, Veronika Haasz-Kovacs, Lajos Balogh

University of Parma, Italy

The purpose of our study was to isolate, amplify and characterize adipose-derived MSC from Beagle dogs, with a particular analysis of their osteogenic differentiation potential. SPECT/CT imaging was performed to observe the ability of cAD-MSC to promote ectopic bone formation on a three-dimensional scaffold.

cAD-MSCs were harvested from subcutaneous and visceral fat of Beagle dogs. Histological and phenotypic

characterization was made before in vivo studies. Cells from young donors with the highest proliferative and osteogenic potential were chosen to evaluate in-vivo behavior of the cAD-MSC towards osteogenic differentiation. Each applied chitosan gelatin scaffold cross-linked with glutaraldehyde contained 2x105 cAD-MSC. After 2 days proliferation in regular medium and one week in osteomedium, scaffolds were implanted in 10 nude mice, 5-6 weeks old divided in 2 groups used for imaging studies. All mice received scaffold containing osteoinduced cells on the right side. The 5 mice from the second group were implanted also with an empty scaffold on the left side. The SPECT/CT whole body images were performed after two months. 80 Bq (100 ml) Tc-99m-MDP were injected into the tail vein of the mice. Two hours later imaging was made by laboratory SPECT/CT hybrid camera (nanoSPECT/CT, Mediso Ltd, Hungary).

SPECT/CT analysis of the dorsal region of mice containing an osteoinduced cAD-MSC-seeded scaffold showed Tc-99m-MDP uptake without exceptions. Bone-like structure was evidenced in the CT slices. On the contrary Tc-99m-MDP accumulation was not present in the empty scaffolds in the control mice. Histological analysis by von Kossa staining showed high mineral concentration in the osteoninduced cAD-MSC scaffolds.

Isolated cAD-MSC have osteogenic potential and have a possible application for the treatment of bone diseases in veterinary medicine. Our results demonstrate that direct in vivo imaging with Tc-99m-MDP is a valid noninvasive method for the evaluation of new bone formation in tissue engineering as it is adsorbed preferentially by newly formed minerals and for clinical studies to determine the bone formation dynamics.

Endocrinology_4

The Impact of Smoking Habit to the Success of Radioactive Iodine Therapy On Hypertiroid

Reza Rinaldy Harahap, Ahmad Hussein Sundawa Kartamihardja

Department of Nuclear Medicine and Molecular Imaging, Society Nuclear Medicine Indonesia, Indonesia

The success of radioactive iodine therapy (RAIT) for hyperthyroidsm, is influenced by many factors, including thyroid gland radioactive iodine absorption. Cigarettes contain thiocyanate, a hydrogen cyanide derivate, can disturb iodine absorption. The aim of the study was to analyze the impact of smoking habit to the success rate of RAIT in hyperthyroid patients.

Retrospective study was conducted in Rumah Sakit Hasan Sadikin Bandung, all male subject were hypertiroid patients treated with I-131. All subject had stopped consuming anti-thyroid medication before RAIT at least 5 day. Subject divided into two groups. Hyperthyroid patients who were actively smoking, were belong to Group I,while patients with no smoking history were belong to Group 2. A successful therapy is defined as the improvement of fT4 level to its normal value in three months follow up.

Sixty subjects age between 20-60 years old divided equally in each group.Only 14 (46.67%) subjects in Group I achieved a successful therapy at the time of follow up, compared to 23 (76.67%) subjects in Group II. Average fT4 level pre- and post-therapy in Group I was 20,83 and 2,39, while in Group II was 18,32 and 1,79 respectively.

Smoking habit may influence the effectiveness of RAIT in hyperthyroid patients atthree months follow up.

Endocrinology_5

^{11}C- Methionine PET CT in Primary Hyperparathyroidism

Nikhil seniaray, Harshul Sharma, Arpana Arbind, Vivek Matthew James, Abhinav Jaimini, Maria D'Souza, Dinesh Kumar, Puja Panwar, AK Mishra, Anupam Mondal, Rajnish Sharma

Department of PET Imaging, Institute of Nuclear Medicine and Allied Sciences, New Delhi, DCRS*, INMAS, Delhi, India, India

In the age of minimally invasive approach for parathyroid adenoma surgery exact pre-operative localization of parathyroid adenoma is essential for a successful minimal accesses surgery. However current imaging modalities are not always successful. The aim of this study was to determine whether ^{11}C- Methionine positron emission tomography-computed tomography (^{11}C Met PET-CT) could accurately localize parathyroid adenomas in patients in comparison to conventional imaging modalities, especially ^{99m}Tc MIBI scintigraphy.

5 patients presenting with hyperparathyroidism were evaluated using PET-CT. Around 740 MBq of ^{11}C Met was injected intravenously and approximately 20 minute later Whole Body PET-CT was done using GE Discovery STE PET-CT camera. Retrospective analysis of other imaging modalities like ultrasonography (USG) neck and ^{99m}Tc MIBI was performed. Patients were followed up with surgical histopathology reports.

All patients had elevated serum parathyroid (PTH) levels and positive scan on ^{11}C Met PET-CT. Out of the 5 patients evaluated 2 patients were negative on parathyroid MIBI scan, 2 had Ectopic parathyroid and

one patient was post parathyroidectomy. ^{11}C Met PET-CT helped in localising parathyroid adenoma in both parathyroid MIBI negative scan. ^{11}C Met PET-CT also showed uptake in ectopic parathyroid adenomas. Surgical histopathology proved adenoma in 5 patients who underwent surgery

^{11}C-Methionine PET is a reliable and highly accurate technique for localizing parathyroid adenomas in patients especially where conventional imaging techniques have failed or are inconclusive in localising parathyroid adenoma

Endocrinology_10

Association between psoas muscle FDG uptake and metabolic syndrome on F-18 FDG PET/CT: May psoas muscle FDG uptake use as a biomarker for metabolic health impairment?

Ji Young Kim, Dae Won Jun, Yun Young Choi

Hanyang University Medical Center, Korea

To identify metabolic characteristics of several organs responsible for the glucose metabolism on F-18 FDG PET/CT according to various clinical metabolic derangements and to evaluate whether it could be used to predict the metabolic syndrome (MS).

We retrospectively analyzed the data from 157 subjects who underwent F-18 FDG PET/CT for health medical examination. Liver function test, total cholesterol, triglyceride, fasting blood glucose (FBG), systolic and diastolic blood pressure, body mass index (BMI) as well as presence of MS were assessed in these subjects. Fixed or flexible spherical volume of interest (VOIs) were used to evaluate maximal and/or mean standardized uptake value (SUV) to assess the metabolism of liver, pancreas, mesenteric visceral fat, psoas muscle, and abdominal subcutaneous fat on F-18 FDG PET/CT. The influences of SUVs of each organ on the metabolic derangement as well as on the presence of MS were analyzed for statistical significance.

Forty subjects (40/157, 25%) had MS and 52 subjects (52/157, 33.1%) were obese with a body mass index (BMI) > 25. SUV_{max} of psoas muscle, mesenteric visceral fat, abdominal subcutaneous fat, and SUV_{mean} of liver were positively correlated with waist, BMI, FBG, and were significantly higher in the subjects with MS. Among them, SUV_{max} of psoas muscle was found to be only risk factor for the presence of MS independent to weight and FBG. With the cutoff value of 1.34, SUV_{max} of psoas muscle accurately predicted MS (sensitivity 72.0%, specificity 87.0%), as well as central obesity, hypertriglyceridemia, impaired fasting glucose and hypertension (AUROC 0.779, 0.810, 0.662, 0.675 and 0.646, respectively, $P < 0.05$).

Metabolism of several organs on F-18 FDG PET/CT were correlated and associated with various clinical metabolic derangements. Among them, SUV_{max} of psoas muscle was only the risk factor for the presence of MS and it could be valuable and convenient tool to predict the MS in clinical circumstances.

Musculoskeletal System_15

Assessing time series changes of osteoblastic reaction after artificial joint replacement surgery using three phase F-18 NaF bone PET

Hye Joo Son, Young Jin Jeong, Hyun Jin Yoon, Do-Young Kang

Department of Nuclear medicine, Dong-A University Medical Center, Dong-A University College of Medicine, Korea

This study is to investigate the serial physiologic changes of osteoblastic reaction with time assessed by three phase F-18 NaF bone PET after artificial joint replacement surgery (AJRS).

Twenty-six patients who presented no complaint and were thought to be well-being state after AJRS were enrolled in this study and classified into four groups according to the period after AJRS, i.e., 6 (GA, n=6), 6-9 (GB, n=6), 10-12 (GC, n =6) and 18-24 (GD, n=8) months. In all patients, three phase F-18 NaF bone PET images were acquired at early dynamic phase for initial 20 min and delayed static phase, and subsequently the early dynamic data was reconstructed into perfusion and blood pool images. SUV_{max} and SUV_{mean} values were measured in 2 VOIs of periprosthetic cortical bone (PB) and 1 VOI of normal bone (NB) at perfusion (1 min), blood pool (5 min), delayed phase (60 min).

Mean SUV_{max} of PB in GA, GB, GC, GD were 3.14, 2.14, 1.88, 2.14 at perfusion phase, 4.39, 3.58. 3.50, 2.89 at blood pool phase, and 11.95, 10.61, 10.23, 9.16 at delayed phase, respectively. Mean SUV_{mean} of PB in GA, GB, GC, GD were 1.90, 1.12, 0.84, 1.17 at perfusion phase, 2.91, 1.98. 1.56, 1.57 at blood pool phase, and 7.94, 6.48, 6.21, 5.1 at delayed phase, respectively. Mean SUV_{max} in NB in GA, GB, GC, GD were 1.16, 1.10, 0.77, 1.03 at perfusion phase, 1.81, 1.70, 1.3, 1.72 at blood pool phase, and 4.07, 4.82, 3.17, 3.71 at delayed phase, respectively. Mean SUV_{mean} in NC in GA, GB, GC, GD were 0.79, 0.77, 0.52, 0.74 at perfusion phase, 1.22, 1.20, 0.91, 1.23 at blood pool phase, and 3.08, 3.49, 2.24. 2.55 at delayed phase, respectively. SUV_{max} and

SUV_{mean} of PB showed serially decreasing tendency with time after AJRS in perfusion, blood pool and delayed phase. However, even at 24 month, $SUV_{max}$and SUV_{mean} values of PB were still higher than those of NB in all three phase.
Using three phase F-18 NaF bone PET, we showed serial osteoblastic changes in patients with no complication after AJRS. Physiologic osteoblastic reaction remained at 2 years after AJRS. Further follow-up is needed.

Neurology_1

Cingulate island sign in Z-score map for brain perfusion SPECT in dementia with Lewy bodies

Etsuko Imabayashi, Hiroshi Matsuda, Masayo Ogawa, Jarek Rokicki, Kota Yokoyama

Integrative Brain Imaging Center, National Center of Neurology and Psychiatry, Japan

Lim et al.[J NuclMed 2009, 50: 1638–1645.] found that reduced glucose metabolism in the medial occipital area and the cingulate island is a highly specific sign of DLB, while the sensitivity of visual inspection ranged from 43% to 50% for the medial occipital and from 62% to 86% for the cingulate island. We aimed to estimate the usefulness of Z-score map for ^{99m}Tc-ethylcysteinate dimer (ECD) brain perfusion SPECT images for discrimination of dementia with Lewy bodies (DLB) from Alzheimer disease (AD).
Eighteen patients with clinical diagnosis of probable DLB (M:F 10:9 73.9±6.8y.o) and age matched18 patients with probable AD(M:F=6:12,73.6±8.9 y.o) were underwent ^{99m}Tc- ECD SPECT scans. Z-score maps for SPECT images were obtained with eZIS® (easy Z-score imaging analysis; Fujifilm RI Pharma Co., Ltd, Tokyo, Japan) software. It includes spatial normalization parameters in SPM2 (http://www.fil.ion.ucl.ac.uk/spm/). Normal databases were included in eZIS and inter-institutional differences were corrected using previously scanned phantom data. The VOIs in the areas where significant perfusion reduction had been assessed in AD by group comparison were originally included in this software. We divided the bilateral posterior cingulate to precunei VOIs into two part of posterior cingulate and precunei using the border of automated anatomical labeling (AAL). Total amount of positive Z-score in posterior cingulate VOI was divided by that in precunei VOI to derive the cingulate island sign (CIS) ratio. With receiver operating characteristic (ROC) curves for CIS ratio, discriminating accuracy of patients with DLB from AD was estimated.
The area under the curve for discriminating patients with DLB from AD with the CIS ratio was 0.855. It demonstrated an accuracy, sensitivity and specificity of 80.6%, 88.9%,and 72.2% respectively.
Z-score ratio of posterior cingulate and precuneus is useful to discriminate demented patients with DLB from AD.

Neurology_2

Differences in regional glucose metabolism of the brain measured with F-18-FDG-PET in patients with essential tremor according to their response to beta-blockers

Yong-An Chung, In-Uk Song, Jiyoung Ryu, Ikdong Yoo, Eunkyoung Choi, Jinkyoung Oh

Department of Neurology, College of Medicine, The Catholic University of Korea, Korea

We investigated whether there is a functional difference in ET according to responses to beta-blockers by evaluating regional changes in cerebral glucose metabolism.
We recruited 17 male patients with ET, 8 that responded to medical therapy(group A) and 9 that did not respond to medical therapy(group B). All subjects underwent F-18 fluorodeoxyglucose(FDG)-PET, and evaluated severity of tremor symptoms was measured as score on the Fahn-Tolosa-Marin rating scale (FTM). FDG-PET images were analyzed using the statistical parametric mapping (SPM) program.
The mean FTM score 6 months after the initiation of propranolol therapy was significantly lower in group A(18.13 > 8.13) compared to group B(14.67 = 14.67). Glucose metabolism in group A in the left basal ganglia was decreased compared with group B. ET showed more significantly decreased glucose metabolism in the both frontotemporooccipital lobes, precuneus of right parietal lobe, and both cerebellums compared to healthy controls.
We hypothesize that ET may have different pathophysiologies in terms of the origin of disease according to response to first-line therapy.

Neurology_9

Evaluation of scatter and attenuation correction methods using a originally designed 3D striatal phantom with 3D printer for quantitative dopamine transporter SPECT

Hiroashi Toyama, Seiichiro Ota, Hiroshi Toyama, Takahiro Natsume, Takashi Ichihara, Akihiro Toyoda, Masanobu Ishiguro, Go Kizawa

Fujita Health University, Japan

Scatter correction (SC) and attenuation correction (AC) are important factors in quantitative brain SPECT. In this study, we evaluated with and w/o SC and AC methods for quantitative dopamine transporter SPECT using phantom.

SPECT imaging of an originally designed 3D striatal (ST) phantom covered with artificial female skull was performed using a triple-head camera with and w/o scatter and 2 AC methods. This phantom was originally designed for ^{123}I SPECT dopamine transporter studies and was manufactured for an anatomically accurate model of ST using 3D printer based on the T1 weighted brain MRI data. It has isolated bilateral caudate nucleus (CN), putamen (PU) and brain shell cavity (background:BG). Each compartment was filled with ^{123}I to obtain different ratios of ST (CN+PU) to BG : right CN; 4.3, right PU; 4.3, left CN; 3.0, left PU; 1.0 to BG; 1.0, respectively, which were considered to be mild Parkinson disease (PD) in right (RT) and severe PD in left (LT) sides. Triple energy window (TEW) method was used as SC. SPECT images were reconstructed with three conditions:(1) w/o SC and AC, (2) with SC and filtered back projection (FBP) with Changs AC, (3) with SC and FBP with AC using an CT image (CTAC). SPECT and CT images were registered using fusion-software. Fused CT based bilateral 3D ROIs were set in ST. SPECT measured ratios of ST-to-BG counts were determined with and w/o SC and 2 AC and were then compared with the true ratios in RT and LT sides, respectively.

W/o SC and AC, measured ST-to-BG ratios were underestimated by 28.3%(RT) and 39.8%(LT) due to effects of scatter and attenuation. SC and FBP with Changs AC underestimated the ratios by 9.0%(RT) and 9.4%(LT) due to skull attenuation showing a significant improvement. SC and FBP with CTAC correction, the ratios were nearly identical to true ratios in RT and LT sides.

SC and CTAC significantly improves the ST-to BG ratios. SC and CTAC for dopamine transporter SPECT would be significant for accurate quantitative measurement.

Neurology_15

Role of early dynamic ^{18}F FP-CIT PET in discriminating Parkinsonism with non-dopaminergic disorders

Do-Young Kang, Hye Joo Son, Young Jin Jeong, Hyun Jin Yoon

Dong-A University Medical Center, Korea

In this study, we investigated the role of kinetic parameters of early dynamic ^{18}F FP-CIT PET in differentiating Parkinsonism with non-dopaminergic disorders.

48 patients were divided into three groups: 23 patients with non-dopaminergic disorders (GA), 27 patients with idiopathic Parkinson disease (GB), 11 patients with atypical parkinsonian disorders (6 MSA-P, 5 PSP) (GC). In 10 minute ^{18}F FP-CIT dynamic PET with 15 frames (6*10 sec, 9*60 sec), relative delivery (R1) and early dynamic binding potential (BP) was estimated by the simplified reference tissue model, with the occipital as a reference region. The VOIs included both caudate (RC, LC), anterior and posterior putamen (RAP, LAP, RPP, LPP), frontal, temporal, parietal, occipital, thalamus, substantia nigra, cerebellum. Delayed static BPnd(max) from 3h static scan was defined as follows: 100 * (SUV_{max} of striatal ROI – SUV_{max} of occipital ROI) / SUV_{max} of occipital ROI. Datas from both scan were compared using ANOVA followed by Tukey post hoc analysis.

Mean early dynamic BP in RC, LC, RAP, LAP, RPP, LPP were 6.01±2.58, 6.55±2.61, 6.80±2.77, 6.71±2.59, 6.55±2.60, 6.20±2.47in GA, 2.72±1.42, 2.35±1.77, 2.67±1.28, 2.81±1.45, 2.35±1.78, 2.43±1.36 in GB, 1.82±0.86, 2.40±1.10, 2.64±1.08, 2.43±1.10, 2.41±1.11, 2.36±1.10 in GC. Mean delayed static BPnd(max) were 4.36±1.23, 4.37±1.31, 4.51±1.18, 4.47±1.34, 4.75±1.40, 4.70±1.62 in GA, 3.30±1.09, 3.36±1.21, 2.65±1.21, 2.42±0.88, 1.52±1.30, 1.27±0.97 in GB, 3.16±0.98, 3.28±0.83, 2.73±1.19, 2.57±1.28, 1.90±1.42, 1.86±1.59 in GC. In ANOVA analysis, R1 was significantly different only between GA and GB in LC ($P < 0.024$), frontal ($P < 0.066$), temporal areas ($P< 0.029$). Both early dynamic BP and delayed static BPnd(max) were significantly different between GA and GB and between GA and GC in all sub-regions. However, there was no significant difference between GB and GC in all sub-regions both in early dynamic and delayed static BP.

Kinetic parameters from early dynamic ^{18}F FP-CIT PET can discriminate Parkinsonism with non-dopaminergic disorders, just as delayed static scan can do. However, it should not be used for differentiating IPD with atypical parkinsonian disease.

Oncology_87

Utility of ^{18}FDG-PET/CT Functional Parameters in Differential Diagnosis Between Focal Autoimmune Pancreatitis and Pancreatic Cancer

Jia Guo-rong, Zhang Jian, liu li, Zuo Chang-jing

Department of Nuclear Medicine, Changhai Hospital, Second Military Medicine University

Objective: Focal autoimmune pancreatitis(focal AIP) is a rare benign disease and manifests as a focal mass in pancreas, an appearance that may mimic that of pancreatic cancer(PC).Few reports were available on PET/CT characteristics of differential diagnose. This study aimed to evaluate the diagnostic value of the metabolic parameters between focal AIP and PC in dual time ^{18}F-FDG PET/CT scan.

Methods: 10 Focal AIP patients and 20 PC patients matched for age and sex were enrolled in this retrospective analysis. In early and delay phase,3D Freeform isocontour tool of Siemens post-processing workstation was performed to delineate volume of interest (VOI) , the parameters extracted included Maximum standardized uptake value (SUV_{max}), mean SUV (SUV_{avg}), metabolic tumor volume (MTV) and total lesion glycolysis(TLG) . 50% SUV_{max} and fixed SUV value 3.0 were set as threshold to fine-tune boundary. The retention indexes(RI) of these parameters was also calculated.Results were assessed by
independent sample T-test and Mann–Whitney U test. Areas under the receiver operating characteristics curves (AUC) were used to evaluate the discriminatory power of metabolic parameters above.

Results: Depending on threshold setting and scan phase, the results included four parts: fixed SUV value 3.0 or 50% SUV_{max} in early phase; fixed SUV value 3.0 or 50% SUV_{max} in delay phase, numbered separately A,B,C,D. The analysis showed that SUV_{max} (A:t=-2.782,*P*=0.010,B:t=-3.983,*P*=0.000,C:t=-1.164,*P*=0.254,D:t=-3.176,*P*=0.004),SUV_{avg} (A,B:t=-3.959,*P*=0.001, C,D:t=-3.350, *P*=0.002) were lower in focal AIP than PC, whereas TLG were not statistically different. There was statistical difference in MTV(B:t=2.374 , *P*=0.036, D:t=2.223, *P*=0.034) using 50 percent SUV_{max} as threshold but no statistical difference in MTV using fixed SUV value 3.0 as threshold .In delay scan, the RI of TLG (t=-2.222,*P*=0.035, AUC 0.745) using 50 percent SUV_{max} as threshold was discriminative.

Conclusion: Dual time ^{18}F-FDG PET/CT scan was useful in discriminating focal AIP and pancreatic cancer .Compared with the fixed SUV 3.0, the 50 percent SUV_{max} used as the threshold could distinguish focal AIP and PC better.

Neurology_28

Quantification of Amyloid-β Deposition Using ^{18}F-FC119S PET in Human Brains: A Phase 0-1 Study

Byung Hyun Byun, Byung Il Kim, Ilhan Lim, Chang Woon Choi, Su Yeon Park, Jung Ho Ha, Kyo Chul Lee, In Ok Ko, Kyeong Min Kim, Sang Moo Lim

Department of Nuclear Medicine, Korea Institute of Radiological & Medical Sciences, Seoul, Republic of Korea

The aim of the present phase 0/1 study was to obtain information about dosimetry, toxicity, pharmacokinetics, optimal dose, and optimal scan time of ^{18}F-FC119S, a new amyloid-β radiotracer.

A total of 19 subjects (M: F = 9: 10) were enrolled. The mean age of control subjects and Alzheimer's disease (AD) patients was 23.0 y and 70.6 y, respectively. In phase 0 study, we acquired a 120 min dynamic brain PET image (3 control subjects and 3 AD patients) or 5 times of whole-body PET images during 4 hr (3 control subjects) after injection of 185 MBq of ^{18}F-FC119S. Dosimetry was evaluated using whole-body PET images. In phase 1 study, we acquired a 60 min dynamic brain PET image in 5 control subjects and 5 AD patients after injection of 370 MBq of ^{18}F-FC119S. Image quality was visually assessed (good/acceptable/poor) and a case with higher or equivocal gray matter uptake compared to the white matter uptake on visual analysis was considered as a PET+. The ratios of cerebral cortical uptake of ^{18}F-FC119S to cerebellar cortical uptake of ^{18}F-FC119S (C/Cbr) were automatically calculated on each PET dataset.

The estimated whole-body dose was 14.7 μSv/MBq and the highest uptake was observed in the liver or gallbladder. No adverse event was observed. C/Cbr continuously increased during the first 30 min after injection of ^{18}F-119S then did not change over 120 min. To determine the optimal scan time, brain PET data acquired during 30-40 min, 30-50 min, and 30-60 min after injection of ^{18}F-FC119S were respectively reconstructed. All the PET images acquired during 30-60 min irrespective of injected dose and all the PET images acquired during 30-50 min after injection of 370 MBq of ^{18}F-FC119S showed good image quality, while others showed poor or acceptable image quality. On visual analysis, 6 of 8 AD patients (75%) and 0 of 8 control subjects (0%) showed PET+. The mean C/Cbr of AD patients and control subjects was 1.57 and 1.11, respectively.

^{18}F-FC119S is safe and its kinetic behavior is suitable for measuring amyloid-β in the brain. PET images acquired during 30-50 min after injection of 370 MBq of ^{18}F-119S showed good image quality.

Oncology_28

Prediction of CNS relapse of diffuse large B-cell lymphoma with ^{18}F-FDG PET/CT

Won Woo Lee, Yoo Sung Song, Sang Eun Kim

Department of Nuclear Medicine, Seoul National University Bundang Hospital, Korea

Relapse of diffuse large B-cell lymphoma (DLBCL) in the central nervous system (CNS) is a rare but serious complication. Numerous reports have suggested various risk factors for high risk of CNS relapse, such as serum lactate dehydrogenase, international prognostic index (IPI), and involvement of specific extranodal organs.Patient selection criteria for CNS prophylaxis in previous studies were based on these risk factors. The effect of CNS prophylaxis with intrathecal methotrexate (IT-MTX) on aggressive lymphoma has been studied in numerous reports. Most studies reveal that IT-MTX does not lower the incidence of CNS relapse. In this study, we evaluated the significance of TLG from pretreatment ^{18}F-FDG PET of DLBCL patients in prediction of CNS relapse.

180 patients newly diagnosed DLBCL patients between March 2009 and January 2015 at Seoul National University Bundang Hospital, Korea, were retrospectively enrolled. The following clinical data were obtained: age, sex, Ann Arbor stage, Eastern Cooperative Oncology Group (ECOG) performance score (PS), International Prognostic Index (IPI), revised IPI (R-IPI), serum lactate dehydrogenase (LDH) level, presence of B symptoms, bulky disease (≥10cm), extranodal involvement, and bone marrow involvement. TLG was calculated as (SUV_{mean} × MTV). MTV with a threshold margin of 50% of SUV_{max} was used, respectively.

The median age was 63 years (average 61.2±13.6), with 104 males and 76 females. Median follow up period was 445 days (average 621.2±507.9), with CNS relapse in 12 patients (6.7%). The site of CNS relapse was intracerebral location in 6 patients, and leptomeningeal seeding in 6 patients. By univariate analysis, high IPI, high R-IPI, presence of bulky lesion, involvement of bone marrow, involvement of any extranodal organs (testis, breast, nasal cavity, orbit), and high TLG50 (>2000) were significant risk factors for CNS relapse (Table 2). High TLG50 (>2000) was the only significant risk factor for CNS relapse by multivariate analysis.

TLG50>2000 is a better prognositic index for CNS relapse than any other previous clinical risk factors.

Oncology_36

Usefulness of Mean Standardized Uptake Value for Liver as a Reference Organ on F-18 FDG PET/CT: Comparison with Standardized Uptake Values Corrected by Various Imaging and Clinical Parameters

Sang Mi Lee, Jiyoun Choi, Jeong Won Lee

Soonchunhyang University Cheonan Hospital, Korea

The use of liver as a reference organ on F-18 FDG positron emission tomographic/computed tomographic (PET/CT) scan is well known. Previous studies about relations between hepatic FDG uptake and various parameters including hepatic fat and blood glucose have been contradictory. The aim of the study is to assess the valid standardized uptake values for liver as a comparator for extrahepatic FDG uptake on F-18 FDG PET/CT scan.

F-18 FDG PET/CT scans were obtained in 186 healthy subjects from October 2012 to November 2014. Mean standard uptake value (SUV_{mean}) and maximum SUV (SUV_{max}) were measured for liver. Other SUVs were also obtained as followings: (1) SUVLBM; SUVs were normalized by lean body mass, (2) fat-adjusted SUV_{mean} (SUVfat); SUV_{mean} was adjusted for hepatic fat using a formula equating percentage fat to CT density, (3) normalized glucose corrected SUV_{max} and SUV_{mean} (SUVglc); SUVs were adjusted for blood glucose level assuming a normal level of 5.55 mmol/L. CT densities (Hounsfield units) were measured in liver and spleen. Fatty liver was defined as CT density of liver was less than that of spleen. The correlation between hepatic FDG uptake and various clinical factors including glucose, liver function test, total cholesterol, triglyceride, erythrocyte sedimentation rate, and high sensitive C-reactive protein were also assessed.

SUVfat and SUVglc of fatty liver were significantly higher than those of non-fatty liver but no difference in SUV_{max}, SUV_{mean}, or SUVLBM. Liver CT density significantly correlated with SUV_{max} before and after correcting by normalized glucose, SUVLBM, and SUVfat. Blood glucose significantly correlated positively with liver SUV_{max}, SUVglc, SUVLBM but not with SUVfat. Liver SUV_{max} also significantly correlated with BMI, AST, ALT, GGT, and TG. Liver SUV_{mean} correlated neither CT density nor blood glucose.

Liver SUV_{mean} correlated neither CT density nor blood glucose while liver SUV_{max} is influenced by blood glucose and fatty liver. On the basis of these data, liver SUV_{mean} is valid as a comparator for extrahepatic foci of increased FDG uptake in patients with abnormal level of blood glucose or fatty liver.

Oncology_40

Kinetics of F-18-Fluofoethylthrosine (F18-FET) in Gliomas using PET-CT

Harshul Sharma, Nikhil Kumar Seniary, Anupam Mondal, Abhinav Jaimini, Rajneesh Sharma, Anil Mishra*, Puja Panwar, Sanjeev Shaw

Institute of Nuclear Medicine and Allied Sciences , New Delhi, India

Role of FDG pet in differentiating low and high grade glioma is limited because of normal FDG uptake in brain. ^{11}C methionine is good to know extent of tumor but can not be used for quantitative evaluation. In this study we are using F-18-fluoroethyltyrosine (F18-FET) for in vivo tumor delineation and grade estimation. F-18-fluoroethyltyrosine (F18-FET) goes inside the tumor but do not get metabolized further like ^{11}C methionine therefore its kinetics can be studied which can lead to change in clinical management.

5 Patients of glioma post operative and post radiotherapy (RT) were taken. All patients had histopathology done prior to PET scan. Patients were made to fast for at least 4 hours before PET study. 185 MBq of F18-FET was injected and dynamic image acquisition was done starting just after injection for 12 frames of 5 minutes each using GE-STE Discovery PET CT. SUV_{max} was noted for each frame and time activity curve was drawn.

Three patients out of five having histopathology showing low grade glioma revealed delayed peaking that is after 15 minutes with a cumulative time activity curve suggestive of low grade glioma while the remaining two with histopathology of high grade gliomas showed peak uptake in less than 15 minutes.

Initial results at our center show that kinetic pattern of FET in patients with glioma can be used to differentiate between different grades of glioma. Further studies are undergoing to obtain statistically significant data.

Oncology_45

The prognostic value of F-18 FDG PET/CT in hepatocellular carcinoma patients treated by TACE: a multicenter retrospective cohort study

Yong-An Chung, Jin Kyoung Oh, Jeong Won Lee, Seung Hyup Hyun, Sae Jung Na, Il Ki Hong, Bong-Il Song, Tae-Sung Kim, Jae Seon Eo, Mijin Yun

Department of Nuclear Medicine, Incheon St. Mary's Hospital, College of Medicine, The Catholic University of Korea, Incheon, Korea

We evaluated the prognostic value of pretreatment F-18 flurodeoxyglucose positron emission tomography/computed tomography (F-18 FDG PET/CT) in hepatocellular carcinoma (HCC) treated by transarterial chemoembolisation (TACE).

A total of 342 patients with HCC treated by TACE between 2009 and 2010 who underwent staging F-18 FDG PET/CT before treatments were retrospectively enrolled from 7 university hospitals. Maximum standardized uptake value (SUV_{max}) and tumor-to-normal liver uptake ratio (TLR) of the primary tumor were measured from F-18 FDG PET/CT. The prognostic significance of the SUV_{max}, TLR and clinical variables were assessed with respect to overall survival (OS).

During the median follow-up of 14.8 months, 222 patients died. In multivariate analysis, stage, Child-Pugh classification, PIVKA-II, SUV_{max} and TLR were significantly correlated with OS. Patients with high F-18 FDG uptake ($SUV_{max} \geq 4.0$ or $TLR \geq 2.0$) showed significantly worse prognosis than those with low F-18 FDG uptake ($P < 0.001$).

Pretreatment SUV_{max} and TNR from F-18 FDG PET/CT are independent prognostic factors for OS in HCC patients treated by TACE.

General Nuclear Medicine_23

Clinical value of F-18 FDG PET/CT in patients with fever of unknown origin (FUO)

Ie Ryung Yoo, Yeongjoo Lee, Hyukjin Yoon, Eun Kyoung Choi, Ik Dong Yoo, Jin Kyoung Oh,Yong An Chung, Sung Hoon Kim

St Mary's Hospital, College of Medicine, The Catholic University of Korea, Korea

The purpose of this study was to evaluate the diagnostic role of F-18 FDG PET/CT in patients with fever of unknown origin (FUO).

We retrospectively reviewed F-18 FDG PET/CT scan data taken for FUO from November 2006 to January 2015. After excluding immnocompromised patients including HIV infection and patients with recent surgery, total of 79 patients' images were analyzed (44 men, 35 women, mean age 49.1, range:1~86). Final diagnosis was made by blood culture, serologic assay, operation, biopsy or at least 6 months of clinical follow-up. F-18 FDG PET/CT scan was interpreted as clinically contributable if it was helpful in final diagnosis or excluding suspicious disease. Performance of F-18 FDG PET/CT scans was evaluated, based on final diagnosis when available.

F-18 FDG PET/CT were clinically contributable in 54.4% (43/79). F-18 FDG PET/CT was helpful

in 18.9% (15/79) of the patients by excluding suspicious disease. Confirmed diagnosis was made in 73.4% (58/79) of the patients – 25 infection, 7 malignancy, 9 non-infectious inflammatory disease, 8 hemophagocytic lymphohistiocytosis, 6 Kikuchi disease and 3 miscellaneous cases. 26.5% (21/79) of the patients could not find the cause of fever, because most of them showed resolution of fever right after empirical therapy. Among 58 patients of confirmed final diagnosis, 74.1% (43/58) F-18 FDG PET/CT scan were considered to be clinically contributable. F-18 FDG PET/CT detected hypermetabolic lymphadenopathy in 20 patients, which led to final diagnosis. The sensitivity, specificity, positive predictive value, and negative predictive value of F-18 FDG PET/CT were 60.3%, 81.0%, 89.7% and 42.5%, respectively.

In FUO patients, overall 54.4% cases of F-18 FDG PET/CT were clinically contributable in finding fever focus or excluding suspicious disease.

General Nuclear Medicine_24

Correlation of Individual Glomerular Filtration Rate Values Determined by In-Vitro technique with Brochner-Mortensen Correction with Renal Cortical Thickness by Ultrasonography

Herwin John M Aycocho, Allanbert Sampana

Philippine Heart Center, Philippines

The objective of this study is to determine the relationship between individual glomerular filtration rates (GFR's) and renal cortical thickness among normal and chronic kidney disease patients

This is a retrospective cross-sectional study where total and individual GFR values were collated from 72 patients who had renal scintigraphy with in-vitro GFR using Technitium-99m Diethyl Triamine Penta-Acetate. Renal cortical thickness measurements were collected from recent (within 90 days) renal and/or whole abdominal ultrasonography of the same patients. Pearson moment correlation (r) was determined in order to establish the relationship between individual GFR values and renal cortical thickness measurements

The correlation between individual GFR values and cortical thicknesses were both strong (left kidney, r = 0.7600; $P<0.0001$, and right kidney, r = 0.6891; $P<0.0001$) A strong correlation was observed between individual GFR values and renal cortical thickness

2015FANMB_1

Is thyroid volume change post iodine therapy an appropriate predictor of treatment response in hyperthyroid patients?(A preliminary report)

Ayati N.[1], Mousavi Z.[2], Davachi B.[3], Zare Namdar S.[1], Sedighi K.[1], Zakavi S.R.[1]

1. Nuclear Medicine Research Center, Mashhad University of Medical Sciences, Mashhad, Iran
2. Endocrinology Research Center, Mashhad University of Medical Sciences, Mashhad, Iran
3. Department of Radiology, Gaem Hospital, Mashhad University of Medical Sciences, Mashhad, Iran

Objectives: This study investigated the relationship between thyroid volume changes and the responsiveness of thyroid tissue to RAI administration.

Methods: 43 consecutive hyperthyroid patients who were referred for radioiodine therapy were included in our study. Administered radio-iodine dose per gram of thyroid tissue ranged from 100-200 uci/gr. Thyroid volume was measured by ultrasonography before and one and three month post RAI administration. Responsiveness was defined as hypothyroidism, subclinical hypothyroidism or euthyroidism and was assessed by clinical and paraclinical parameters evaluation at the end of the first and third month post treatment.

Results: Forty three patients (39 female, 4 male) were studied with mean age of 40.9±16.4 years. Multinodular goiter was seen in 72.1% and diffuse goiter in 27.9%. Mean 24 hours radio-iodine uptake was 55.7%±17.6%. The total iodine dose ranged from 1.5 to 30mCi with a mean activity of 9.0±7.8 mCi. Patients were followed up for a mean of 3.9±2.1 months with a rate of 97.6% at 1 month and 90.7% at 3 months. Thyroid weight (on palpation) was significantly decreased from 44.3±23.2 gr to 35.8±21.1 gr one month after therapy (P=0.002). Using ultrasonography thyroid volume was significantly decreased from 29.8±18.0 to 25.1±20.2 gr at 1 month after therapy (P=0.02) and to 21.6±18.3 gr at 3 months after radio-therapy (P=0.001). Response rate was seen in 66.6% of patients at 1 month and 76.9% of the patients at 3 months. The mean thyroid volume change at 1 month (using ultrasonography) in patients who responded to therapy was 4.9±8.7 ml while it was -0.65 ml ± 3.7 ml in patients who did not responded to therapy(P=0.08). It was significantly higher 3 months after therapy (8.1±9.1 ml) in responded compared to nonresponded patients (-2.4±7.1 ml, P=0.02).

Conclusions: Thyroid volume changes either on palpation or by ultrasonography correlates well with clinical outcome of RAI therapy in hyperthyroidism and can be used as a predictor of treatment efficacy.

2015FANMB_2

Quantitation of Myocardial Blood Flow and Coronary Flow Reserve with ^{99m}Tc-sestamibi Dynamic SPECT: Correlation with ^{13}NH3-PET

Guang-Uei Hung[1], Bailing Hsu[2], Bang-Hung Yang[3], Wen-Sheng Huang[4]

1. Department of Nuclear Medicine, Chang Bing Show Chwan Memorial Hospital, Changhua, Taiwan
2. Nuclear Science and Engineering Institute, University of Missouri-Columbia, Columbia, Missouri, USA
3. Department of Nuclear Medicine, Taipei Veterans General Hospital, Taipei, Taiwan
4. Departments of Medical Research & Nuclear Medicine, Changhua Christian Hospital, Changhua, Taiwan

Objectives: Our previous study has shown that conventional dual-head SPECT/CT systems capable of fast dynamic SPECT (DySPECT) with ^{99m}Tc-sestamibi imaging could perform flow quantitation and enhance the detection of coronary artery disease (CAD). This study compared the myocardial blood flow (MBF) and coronary flow reserve (CFR) quantified by DySPECT and those by ^{13}NH3 PET.

Methods: This study enrolled twelve cases, including 5 normal controls and 7 patients with suspected or known CAD. All received both ^{99m}Tc sestamibi DySPECT and ^{13}NH3 PET within two weeks. The protocols of rest and dipyridamole-stress 3NH3 PET followed the procedure guideline suggested by American Society of Nuclear Cardiology using a PET/CT scanner (GE Discovery VCT PET/CT system), and stress MBF (SMBF), rest MBF (RMBF) and CFR (SMBF/RMBF) were quantified using one-tissue compartment flow model. The DySPECT protocols utilized 12-minutes multiple back-and-forth gantry rotations during injections of ^{99m}Tc-sestamibi at rest or dipyridamole-stress using a dual-head SPECT/CT scanner (Siemens Symbia T2 SPECT/CT system). DySPECT images were reconstructed with full physical corrections and converted to the physical unit of (Bq/ml). Then, MBF and CFR were also quantified one-tissue compartment model using time activity curves derived from DySPECT images. The values of MBF and CFR by DySPECT and PET were compared with Pearson correlation analysis.

Results: The extraction fraction parameters of ^{99m}Tc-sestamibi based on Renkin-Crone model were generated (α=0.756, β=0.151) according to the measured rest/stress K1 values by DySPECT and rest/stress MBF by ^{13}NH3 PET of the 5 normal controls. MBFs (rest or stress) of all studied cases by DySPECT correlated very well with those by ^{13}NH3 PET (r = 0.9446, P < 0.0001). CFRs by DySPECT correlated very well with those by ^{13}NH3 PET (r = 0.9112, P < 0.0001), too.

Conclusions: Our preliminary study suggested that quantitation of MBF and CFR with conventional SPECT/CT correlated very with those with PET and was clinically feasible. Future study with larger case numbers are warranted for further validation.

2015FANMB_3

Evaluation of ^{68}Ga-DOTATATE PET/CT, ^{18}F-FDG PET/CT and ^{131}I-MIBG scintigraphy in metastatic pheochromocytoma/ paraganglioma in relation to genetic mutation: preliminary results.

Teik-Hin Tan[1], Boon-Nang Lee[1], Anilah Abdul Rahim[2], Zanariah Hussein[2]

1. Department of Nuclear Medicine, National Cancer Institute, No 4, Jalan P7, Presint 7, 62250 Putrajaya, Malaysia
2. Department of Endocrinology, Hospital Putrajaya, Presint 7, 62250 Putrajaya, Wilayah Persekutuan, Malaysia

Objectives: To evaluate ^{68}Ga-DOTATATE PET/CT, ^{18}F-FDG PET/CT and ^{131}I-MIBG scintigraphy in mapping of metastatic PCC/ PGL in relation to genetic mutation.

Methods: Eight patients with metastatic pheochromocytoma or paraganglioma (PHEO/PGL) were evaluated with three modalities: ^{131}I-MIBG scintigraphy, ^{68}Ga-DOTATATE PET/ CT and ^{18}F-FDG PET/CT. Lesion sites and the number of lesions were analyzed. Genetic testing was performed on all patients.

Results: Four out of the eight patients with metastatic PHEO/PGL are associated with genetic mutation, in which 2 associated with SDHB mutation and another 2 associated with RET mutation. Both SDHB-mutation patients have extra-adrenal origin, whereas the primary of the remaining patients were from adrenal gland. Surprisingly, one patient with undetected genetic mutation showed extensive metastases including breast and thyroid. Except liver metastasis, which is not present in SDHB-mutation patients, no difference in prevalence of other metastatic sites (regional/ distant lymph node, lung and bone) is observed between patients with and without SDHB mutations. ^{18}F-FDG and ^{68}Ga-DOTATATE were positive in all 8 patients; whereas ^{131}I-MIBG was positive in only 2 patients. Out of the total of 219 lesions detected, ^{68}Ga-DOTATATE demonstrated more lesions than ^{18}F-FDG (197 vs 149 lesions), predominantly in bone metastases. However, 95 discordant lesions were observed between the two modalities. On the contrary, ^{131}I-MIBG only demonstrated 19 lesions, which also can be detected by combined ^{18}F-FDG and ^{68}Ga-DOTATATE. Interestingly, SDHB-related tumour

overall demonstrated higher SUV_{max} on ^{18}F-FDG as compared with non-SDHB-related tumour (mean SUV_{max} 27.63 vs 9.62, P=0.04).

Conclusions: Extensive metastases can occur in any PHEO/PGL even in patient without genetic preponderance. ^{68}Ga-DOTATATE PET/ CT and ^{18}F-FDG PET/ CT may have a complementary role to accurately map the metastatic sites. Discordant lesions demonstrated in ^{68}Ga-DOTATATE PET/ CT and ^{18}F-FDG PET/ CT may suggest the presence of inter-tumoural heterogeneity. Higher SUV in SDHB-related tumour on ^{18}F-FDG suggests more cellular de-differentiation, hence more aggressive behaviour.

2015FANMB_4

Could Normal Renal Ultrasonography Replace the Necessity of DMSA Renal Cortical Scan in the Management of Urinary Tract Infection in Children?

D. K. K. Nanayakkara[1], S.I.Nawaz[2]

1. Nuclear Medicine Unit
2. Faculty of Medicine, University of Peradeniya

Objectives: Ultrasound scan (USS) has replaced the necessity of carrying out the Dimercaptosuccinic acid (DMSA) renal scan in the management of urinary tract infection (UTI) in children. Although initial USS is important to detect structural abnormalities which might need early intervention DMSA scan is needed to assess the renal cortical functional abnormalities. In contrast to DMSA scan as there is no radiation associated with USS clinicians tend to believe that USS is sufficient to detect renal scarring. Aim of this study is to compare the ability of DMSA scan and USS in detecting renal scaring in children following febrile UTI.

Method: A prospective study was conducted between January 2012 and December 2014 for children less than 5years following febrile UTI. USS has been done at the initial stage of UTI and referred them to our institute for DMSA scan in 3-6 months. Children with gross renal anomalies were excluded. Chi-square test was used to compare the 2 imaging methods and p value <0.001was considered as significant. The sensitivity, specificity, positive predictive value (PPV) and negative predictive values (NPV) of USS were calculated considering DMSA scan as the reference imaging method.

Results: A total of 756 kidneys of 378 children were studied. (216 females and 162 males with mean age 23.09±15.5 months). Both USS and DMSA scan showed no abnormalities in 456 kidneys and cortical scars in 62 kidneys. 142 kidneys with normal USS showed scars on DMSA scans. 96 kidneys with abnormal USS were normal on DMSA scans. Detection of renal scars using DMSA scan was significantly higher than using USS (p value < 0.001). USS showed low sensitivity (30.4%) and the PPV of 39.2% and high specificity (82.6%) and NPV of 76.2% for detection of renal scars. Several other studies also have shown that USS does not have sufficient sensitivity to be used as a reliable test to detect renal scarring in children. The USS technique is operator-dependent and relies on the radiologist's skills whereas being a functional study, DMSA scan will not depend on the operator. This study also showed that USS alone is not a good test to find renal scars.

Conclusion: Irrespective of the initial USS results children below 5 years should have a DMSA scan following culture positive febrile UTI to plan the long-term follow up.

2015FANMB_6

Inhibition of growth of Human Ovarian Cancer by Lentivirus-mediated HER2-siRNA and preliminary assessment of the therapeutic efficacy with SPECT

Yang Yi, Shi Yizhen, Liu Zengli, Wu Qiangle, Mao Xingping

Department of Nuclear Medicine, The Second Affiliated Hospital of Soochow University, Suzhou, Jiangsu 215001, People's Republic of China

Objectives: Ovarian cancer is the major cause of cancer mortality in woman. The overexpression of HER2 gene, which is associated with the oncogenesis and progression of ovarian cancers, can be found in about 20-40% ovarian cancers. We investigated the influence of RNAi lentivirus targeting HER2 on the growth of ovarian cancer cells (SKOV-3) and evaluated the potential of SPECT in assessment of RNAi biological treatment.

Methods: Three siRNAs targeting HER2 were designed and siRNA lentiviral vector was constructed. RNAi lentivirus was transfected into SKOV-3 ovarian cancer cells and real-time quantitative PCR was used to detect the expression of mRNA. RNAi lentivirus with the highest interference efficiency was screened out to establish a stably expressing shRNA cell line. Flow cytometry and western blotting were used to analyze the cell surface expression of HER2 protein. The proliferation of SKOV-3 cells was determined by MTT assay and Cell apoptosis was analyzed by FCM. The antitumor effect of RNAi lentivirus was evaluated by establishing xenograft tumor models in nude mice with transfected SKOV-3 cells and observing the growth of tumor. Radioimmunoimaging with ^{131}I-trastuzumab

was also used to evaluate the expression of HER2 protein after treatment with RNAi lentivirus in nude mice bearing SKOV-3 xenografts.

Results: The downregulation of HER2 mRNA and protein expression was confirmed by real-time quantitative PCR and western blotting. In xenograft tumor models of SKOV-3 cells transfected with RNAi lentivirus, the growth of tumor were inhibited and tumor uptake of ^{131}I-trastuzumab was reduced significantly compared with control groups.

Conclusions: RNAi lentivirus targeting HER2 may be a valuable therapeutic method for ovarian cancer over-expressing HER2 gene and radionuclide molecular imaging of HER2 expression in vivo has potential for guiding therapy and evaluating therapeutic response.

2015FANMB_7

Generator Based v/s Cyclotron Based Radiopharmaceuticals- Comparison of Tc-99m Labelled Methionine and C-11 Methionine Radiotracer for Biopsy proven Carcinoma Breast

Aditi Khurana[1], Sonia Mahajan [2], Abhinav Jaimini[2], Maria Souza[2], Anil Mishra[2], Rajnish Sharma[2],Anupam Mondal[2]

1. Department of Nuclear Medicine, VMMC and Safdarjung Hospital, New Delhi-110029
2. Institute of Nuclear Medicine and Allied Sciences (INMAS)

Objectives: Non-availability of Cyclotron and high cost of investigations in underdeveloped & developing countries is a basic problem. Therefore studies were undertaken after labelling Methionine with generator produced Technetium-99m for its possible use in breast cancer imaging.

Methods: 14 patients with biopsy proven carcinoma breast have been included in the study, so far. All patients underwent C-11 MET PET/CT and ^{99m}Tc labelled methionine SPECT-CT scans. Scans were done on two different days. 20mCi of C-11 MET was injected intravenously and images were acquired on PET/CT scanner after 20min. Later 20mCi of ^{99m}Tc MET was injected intravenously and planar/SPECT images were acquired on Dual Head gamma camera after 30min, 1 hour and 2 hours.

Results: Accumulation of C-11 methionine was assessed visually and by calculating SUV values. Assessment of Tc-99m methionine was done visually and by calculating tumour to background ratio and the results were compared. Both ^{99m}Tc methionine and C-11 methionine show increased accumulation at the primary site. Apart from this, increased C-11 MET accumulation is noted in the malignant ipsilateral axillary lymph nodes. However, there is limited concentration of ^{99m}Tc MET in the same anatomical region.

Conclusions: Our preliminary study reveals that ^{99m}Tc methionine is a potential radiotracer to be used as an alternative to C-11 methionine in patients of breast cancer. Further clinical trials shall be conducted to evaluate the role of ^{99m}Tc methionine in patients of breast cancer especially nodal and metastatic involvement.

2015FANMB_8

Impact of PET/CT on the Staging and Restaging of Gynecologic Cancers

Akram Al-ibraheem[1], Abedallatif AlSharif[2], Ramiz Abu-Hijlih[1], Asem Mansour[1], Waleed Mahafza[2], Batool Albalooshi[3], Imad Jaradat[1]

1. King Hussein Cancer Center, Jordan
2. Jordan University Hospital, Jordan
3. Dubai Health Authority, UAE

Objectives: FDG PET/CT has been advocated as adjunct useful modality in the treatment algorithm of gynecologic cancers. The impact of ^{18}F-FDG PET images in gynecologic malignancies still; however, needs further verification, especially in the assessment of suspicious regional and para-aortic lymph nodes. Moreover, clinical outcome in patients with equivocal CT or MRI findings and negative ^{18}F-FDG PET scan has not been adequately evaluated. The purpose of this study is to evaluate the clinical impact of ^{18}F-FDG PET/CT in the treatment of patients with gynecologic cancers.

Methods: Ninety four patients with gynecologic tumors (40 cervical, 37 endometrial and 17 ovarian) were retrospectively evaluated between January 2010 and June 2014, at King Hussein Cancer Center. PET results were compared with MRI and CT findings at time of diagnosis (37 patients) and after treatment, for response evaluation (57 patients). In this study we will investigate the Negative Predictive Value (NPV) of 18-FDG PET in gynecological malignancies with special attention to patients who had equivocal pelvic or extrapelvic lymph nodes on CT or MRI.

Results: FDG PET/CT scan provided additional information in 22 patients; upstaging in 4.2% (4

patients) and down staging in 19.1% (18 patients). As a result, treatment strategy was changed from curative to palliative in three patients, and additional curative therapy was implemented following exclusion of distant metastasis in 11 patients. Median follow up time for the whole cohort was 35 months (range 6-96 months). NPV of ^{18}F-FDG PET/CT was 83.3. PET/CT findings led to modifications in the radiotherapy field and dose, while minimizing treatment-related toxicity.

Conclusions: ^{18}F-FDG PET/CT has a significant influence in management plan of a substantial number of patients with gynecologic malignancies and offers a high negative predictive value in clinical practice.

2015FANMB_9

Patterns of Stress Related Injuries of Lower Limbs on Skeletal Scintigraphy

Ali Jamal, Mujahid Khalid Ali, Tariq Mahmood Mirza, Mehdi Raza, Umer-i-Farooq

Nuclear Medical Centre (NMC), Armed Forces Institute of Pathology (AFIP), Rawalpindi, Pakistan

Objectives: To determine the patterns of stress related injuries of lower limbs on skeletal scintigraphy and ascertain injury prone sites.

Methods: A total of 297 positive cases on 3-phase skeletal scinitigraphy were included in study whereas negative cases were excluded. Radiopharmaceutical, ^{99m}Tc-MDP, in 20 mCi dose was injected intravenously followed immediately by angioscintigraphic and equilibrium blood pool imaging of the involved site with subsequent delayed imaging after 2 hours. Acquisition was done on Siemens E-Cam ® and Scintronix ® Gamma Cameras. Uptake of radiotracer in a more localized focal pattern was labeled as stress fracture and in a linear pattern along the periosteum as sub-periosteal reaction or periostitis. Linear uptake in posteromedial distal tibial aspects was categorized as medial tibial stress syndrome or shin splints. Radiotracer accumulation at insertion sites of major lower limb muscles was labeled as activity induced enthesopathy.

Results: Stress fractures constituted 80.13% cases with bilateral middle third tibiae as the commonest site. Bilateral shin splints were present in 21.88% of cases and sub-periosteal reactive changes in bilateral proximal tibial halves comprised 14.47% of the patients. Activity induced enthesopathy was present in 4.20% of patients with bilateral quadriceps femoris enthesopathy being more prevalent.

Conclusions: Most common overuse injuries are stress fractures followed by shin splints, sub-periosteal reactive changes and activity induced enthesopathy respectively in descending order. Middle third of tibia is commonest site prone to stress fractures and overall right lower limb is frequently involved as compared to left in all stress induced injuries.

2015FANMB_10

Contribution of Abdominal Adiposity to Bone Mineral Density in Healthy Postmenopausal Thai Women

Sirianong Namwongprom[1,2], Sattaya Rojnasatein[3], Chanpen Wongboontan[2], Ampica Mangklabruks[4]

1. Clinical Epidemiology Program, Faculty of Medicine, Chiang Mai University, Thailand
2. Department of Radiology, Faculty of Medicine, Chiang Mai University, Thailand
3. Department of Orthopaedic, Faculty of Medicine, Chiang Mai University
4. Department of Internal Medicine, Faculty of Medicine, Chiang Mai University, Thailand

Objectives: To investigate the relative contribution of abdominal adiposity to bone mineral density (BMD) in healthy postmenopausal Thai women.

Methods: This cross-sectional study enrolled 1,448 healthy Thai women, ages 40-90 without medication history or known disease effecting the BMD. Lumbar spine (LS), total femur (TF), and femoral neck (FN) BMDs, android fat mass (AFM), gynoid fat mass (GFM), and android-to-gynoid fat ratio (AG ratio) were measured by Dual X-ray Absorptiometry (DXA). To evaluate the contribution of abdominal obesity with various measures of BMDs, univariable and multivariable linear regression models were used to estimate the regression coefficients.

Results: AG fat ratio positively correlated with age and menopause duration. GFM had a negative correlation with age and menopause duration. The significant negative correlation was observed only between AFM and menopause duration. The correlation between AFM and age was not significant. In univariable analysis, increased AFM and GFM had a significant positive association with BMD of all measured sites (P<0.001). Significant positive correlation between AG ratio and BMD was found on all measured sites (P<0.001).The strongest association was found between AG ratio and LS BMD (β=0.156, P<0.001). In multivariate linear regression analysis, the results continued to show a positive association between AFM, GFM and

AG ratio at all skeletal sites after adjusting for age, height, and duration of menopause. Among the three abdominal adiposity parameters, the AG ratio had a strongest positive effect to all reference sites for the diagnosis of low bone mass and osteoporosis (LS, TF and FN regions).

Conclusion: Abdominal adiposity has a significant beneficial effect on BMD. AG ratio, rather than AFM and GFM, shows the strongest positive association with BMDs in postmenopausal women and can be considered as one of the determinants of bone mass.

2015FANMB_11

Single Institutional Experience on Yttrium-90 Microspheres Radioembolization of Hepatic Tumours

Senthil Raja[1], Sumati Sundaraiya[1], Uthappa M C[2], Deepashree T[2], Mohammed Rela[3]

1. Department of Nuclear Medicine
2. Department of Radiology
3. Department of Liver surgery
4. Global Health city, 439, Cheran Nagar, Perumbakkam, Chennai, India -600100

Objectives: Aim of this study is to assess the response to Transarterial radioembolisation (TARE) and overall survival in patients with inoperable liver cancer.

Methods: This study included 32 patients (30 males; 2 females; mean age; 55.3 years) with unresectable hepatic tumours which included 29 patients with HCC and 3 patients with colorectal liver metastasis (CRLM). All patients underwent CECT and mapping angiogram with lung shunt assessment. Of 29 patients with HCC, CECT showed bilobar disease in 14 patients whereas single lobe disease in rest (14 patients with right lobe involvement and 1 with left lobe involvement). 28 HCC patients had portal vein thrombosis (PVT). Amongst 3 patients with CRLM, 2 had bilobar disease; one had right lobe metastasis. 2 patients underwent TARE using Y-90 Theraspheres and others had Y-90 SIR spheres.

Results: All patients had an uneventful immediate post therapy period. 23 out of 32 patients had follow up CT (6-8 weeks) and all of them showed partial response to therapy in the form of reduction in the size or arterial enhancement as well as increase in necrotic changes in the target lesions. One patient had complete left lobar ablation with no recurrence. However five patients had new lesions in the liver or lymph nodal and lung metastases. There was significant improvement in the PVT in 5 patients; one of them had recanalisation of portal vein. 4 patients had progression of the PVT. Follow up AFP levels were available in 10 patients, 6 showed reduction in AFP levels and 4 showed increase in AFP levels. One patient with CRLM showed increase in CEA level. 3 patients were lost to follow up and 29/32 patients had an overall mean survival of 9 months (ranging from 2 weeks to 30 months) with 12/29 (41%) survived for more than 1 year.

Conclusion: Our initial experience shows an overall mean survival of 9 months in advanced HCC patients having predominantly PVT, where almost all of them showed partial response of the target lesions on CT with one patient showing complete lobar ablation. TARE is therefore a promising therapeutic modality for advanced inoperable liver tumors, where other loco-regional therapies are not an option.

2015FANMB_12

Obesity Classification: Comparison of Anthropometry vs DXA

Saima Haider

Centre for Nuclear Medicine, Lahore, PAKISTAN

Objectives: Obesity increases risk of chronic diseases &. mortality. Body mass index (BMI) defines overweight & obesity. It is not reliable as weight changes involve not only body fat but lean mass & bone mineral content. DXA can estimate BMD & soft tissue composition with high precision.

Methods: 204 subjects BMI > 18.5kg/m2 underwent whole body DXA scan (WBS) & Body composition analysis (BCA) with Bray classification. ROI drawn within WBS for intra-abdominal fat. Correlation & Pearson's coefficient (r) done with SPSS 16 between BMI vs DXA % Total Body Fat & % Central Abdominal Fat.

Results: BMI classified 12.54% normal vs DXA 6.86% , 37.74% overweight vs 22.54% & 50% obese.vs 70%. BMI correlated % TBF & % CAF, Normal %TBF (r = 0.190, $P > 0.05$) and % CAF (r = 0.602, $P < 0.05$), Overweight %TBF (r = -0.063, $P > 0.05$) & %CAF (r = 0.026, $P > 0.05$) & Obese class-3 %TBF (r = 0.650, $P < 0.05$) and % CAF (r = 0.551, $P > 0.05$).

Conclusion: DXA defines adiposity status accurately with need to consider age & gender for BMI criteria.

2015FANMB_13

Studies of Gastric Emptying Time in Patients with Non-ulcer Dyspepsia

Muhammad Kashif Rahim[1], Durr-e-Sabih[1], Abdul Mateen[1], Najam-Uddin[1] and Muhammad Yousaf[2]

1. Department of Nuclear Medicine, Multan Institute of Nuclear Medicine and Radiotherapy, Multan, Pakistan
2. Department of Medical Sciences, Pakistan Institute of Engineering and Applied Sciences, Islamabad, Pakistan

Objectives: Non-ulcer dyspepsia is characterized by postprandial upper abdominal symptoms in the absence of organic disease. The study was conducted to evaluate gastric emptying time of solid meal in patients having non-ulcer dyspepsia.
Methods: The results of half emptying time for solids (T½) and percent clearance of solid meal at 60 minutes (C60) of patients (N=35) having non-ulcer dyspepsia according to Rome II criteria were compared with age and sex matched controls (N=28). Gastric emptying was studied using ^{99m}Tc-labelled egg omelet. Dynamic study was performed up to 100 minutes and then intermittent study was done up to 3 hours. T½ and C60 were calculated from the computer generated time-activity curve and T½ was also calculated by the curve manually drawn from intermittent study.
Results: Mean T½ of control group was 58.3±14.7 minutes (males = 60.1±18.3 minutes, females = 55.6±5.5 minutes). The normal range of T½ was 28.9 – 87.7 minutes among control group (mean ± 2SD). Mean T½ of patient group was 160.1±96.1 minutes (males = 126.1±75.9 minutes, females = 217.8±101.7 minutes). 12 out of 22 male patients and 11 out of 13 female patients had prolonged T½. Mean C60 of control group was 60.6±16 % (males = 59.5±17.5 %, females = 62.2±14.2 %) and the mean C60 of patient group was 33.1±18.5 % (males = 38.4±16.6 %, females = 23.9 ±18.5 %). While comparing T½ of both groups, *P*-value for male population was 0.001 and <0.001 for female population. Similarly when C60 values were compared, *P*-value was <0.001 both for male and female groups.
Conclusions: Gastric emptying is significantly delayed in both males and females having non-ulcer dyspepsia as T½ is prolonged and C60 is shortened in significant number of these patients.

2015FANMB_14

Outcomes of High-Dose I-131 MIBG Therapy for Refractory Neuroblastoma: The Report from Kanazawa University Hospital, Japan

Daiki Kayano[1], Anri Inaki[1], Hiroshi Wakabayashi[2], Ayane Toratani[1], Seigo Kinuya[1]

1. Department of Nuclear Medicine, Kanazawa University Hospital, Japan
2. Department of Nuclear Medicine, Wuerzburg University , Germany

Objectives: High-dose I-131 MIBG therapy (more than 12mCi/kg I-131 MIBG administration) for refractory neuroblastoma have become common in recent years in Europe and the United states. Kanazawa University Hospital is the only institution which can perform high-dose I-131 MIBG therapy for neuroblastoma in Japan. We investigated the outcomes of high-dose I-131 MIBG therapy in patients with refractory neuroblastoma in Japan.
Methods: This study included 12 patients with refractory neuroblastoma who underwent the first high-dose I-131 MIBG therapy between August 2009 to January 2012 at Kanazawa University Hospital, Japan. Five were males and 7 were females. The mean age at the MIBG therapy was 7.8 years old. The mean dose of I-131 MIBG was 16.3mCi/kg. We investigated the outcomes after MIBG therapy on August 2013.
Results: Following MIBG therapy, all patients were performed chemotherapy and/or stem-cell transplantation. The initial response rate (complete response and partial response) was 67%. Event-free survival (EFS) and overall survival (OS) at 1 year were 67% and 74%. Estimated EFS and estimated OS at 2 years were 38% and 56%. The OS times were significantly longer for patients younger than 10 years old at the MIBG therapy, for patients with less than 3 years for diagnosis to the MIBG therapy, for patients without pain at the MIBG therapy and for patients without elevated urine vanillylmandelic acid and homovanillic acid.
Conclusions: High-dose I-131 MIBG therapy combined with other therapies may provide good response for patients with refractory neuroblastoma. An additional follow-up research is now going on.

2015FANMB_15

Survival Outcome in Patients with Cardiomyopathy Detected by Left Ventricular Quantitative Parameters Derived from Gated SPECT Myocardial Perfusion Imaging

Azmal Kabir Sarker[1], Faria Nasreen[2], Lutfun Nisa[2], Raihan Hussain[2]

1. Institute of Nuclear Medicine and Allied Sciences (INMAS), Cox's Bazar, Bangladesh
2. National Institute of Nuclear Medicine and Allied Sciences (NINMAS), Dhaka, Bangladesh

Objectives: The purpose of this study was to determine the outcome (survival) of patients who were diagnosed with cardiomyopathy (CM) by left ventricular (LV) quantitative parameters derived from gated SPECT myocardial perfusion imaging (GSMPI).
Methods: GSMPI of 879 patients was performed at National Institute of Nuclear Medicine and Allied

Sciences from January 2007 to December 2009. CM was diagnosed in patients who had a LV ejection fraction (EF) of less than 40% with a corresponding end diastolic left ventricular volume (EDV) of more than 130 ml. Telephonic interview was conducted in the year 2015 to obtain the clinical follow up data of patients with CM.

Results: Fifty two patients (M/F=50/2) with mean age 51.6±9.5 (32-75) was diagnosed to have CM with mean EF 27.7±5.5 (18-39) and mean EDV 223±69.7 (135-486). Follow up data of 19 (M/F=18/1) patients with mean age 52.9±7.4 (38-65), EF 29.1±6.6 (18-39), EDV 211±45.4 (135-320) were available. Nine (47.4%) patients were alive at the time of follow up and 10 (52.6%) patients were found to be deceased. Death of two was associated with non cardiac illness; death of four was associated with heart failure and the other four patients died at home. In this patient group one and five year survival were estimated to be 68 and 47%. Among the four patients who underwent immediate revascularization after imaging, two had died within three years (EF 26 and 39%, EDV 193 and 144ml). Among the other 15 patients who were on medical management, eight died within four years. Test of equality of survival distributions for two different treatment strategies revealed no difference (Log Rank significance, $P > 0.05$).

Conclusions: Five year survival in this study group diagnosed with CM by GSMPI was 47% where treatment strategies did not contribute to significant difference of survival.

2015FANMB_16

Gated SPECT Myocardial Perfusion Imaging at Rest in Patients Presenting with Chest Pain

Su Thet Oo[1], Swe Swe Aye[1], Kyin Myint[2]

1. Department of Nuclear Medicine, North Okkalapa General Hospital, Ministry of Health, Yangon, Myanmar
2. Department of Nuclear Medicine, Yangon General Hospital, Ministry of Health, Yangon, Myanmar

Objectives: This study was carried out to assess the prognostic value of rest gated Tc-99m Tetrofosmin SPECT imaging in patients with typical or atypical chest pain and non-diagnostic ECG.

Method: Sixty-one haemodynamically stable patients with chest pain having normal/abnormal or a non-diagnostic (or) abnormal ECG underwent rest gated SPECT imaging using 30mCi of Tc-99m Tetrofosmin. After acquisition, the images are reconstructed by using a Cedar – Sinai Quantitative Gated SPECT processing software. Images were immediately reviewed by four nuclear medicine physicians, with each study read as being normal, abnormal, or equivocal by visual qualitative and analysis.

In this study, the resting ECG was used as a primary diagnosis of coronary artery disease, chest pain and ECG were a presumptive diagnosis of angina (both stable and unstable) and all the cases underwent rest gated SPECT myocardial perfusion scan to detect coronary artery disease. ECG results varied from normal (including RBBB), non-diagnostic to abnormal (ischemia) findings. The patients were grouped into those having normal (or) non diagnostic and abnormal ECG.

Data of selected cases will be collected according to the proforma. SPECT myocardial perfusion scan finding will be correlated with ECG finding in myocardial ischemia. The data will be analyzed with SPSS software, version 13 for accuracy of the test and unvaried analysis in the study.

Results: Rest gated SPECT imaging was highly discriminating, with 75.9% of patients with positive scans but only 24.1% with negative scans having typical chest pain (P = 0.000, χ2test). 18.8% of patients with atypical chest pain had positive scans and 81.35% had negative scans.

29 patients had typical chest pain.16 out of 29 had normal (or) non diagnostic ECG. Case detection rate is 62.5% for normal (or) non diagnostic ECG with typical chest pain. In this study, rest gated SPECT myocardial perfusion scan compared to ECG, was found to have sensitivity of 85.7%, accuracy of 70.49% and negative predictive value of 93.9%.

It is a promising technique for ruling out acute myocardial ischemia in the emergency room and can improve decision making for patients with symptoms suggestive of acute cardiac ischemia without obvious abnormalities on initial ECG.

Conclusion: Abnormal rest Tc-99m Tetrofosmin SPECT imaging accurately predicts acute myocardial infarct in patients with symptoms and non-diagnostic ECG whereas a normal study is associated with very low cardiac event.

If we could compile this service in emergency department, unnecessary hospitalization will be reduced. As it give information regarding risk stratification, it will help in prognostication and appropriate decision can be made for further management.

2015FANMB_17

Effect of Chronic Extreme Hyperglycemia on FDG-PET/CT

Takayoshi Ishimori[1], Yuji Nakamoto[1], Koya Nakatani[2], Kaori Togashi[1]

1. Diagnostic Imaging and Nuclear Medicine, Kyoto University, Japan
2. Diagnostic Radiology, Kurashiki Central Hospital, Japan

Objectives: Hyperglycemia can reduce ^{18}F-fluorodeoxyglucose (FDG) uptake in tumors considerably, but it is also reported that the adverse effects caused by chronic hyperglycemia in interpreting PET images was minimum. The purpose of this study was to evaluate the diagnostic performance of FDG-PET/CT which was performed under chronic extreme hyperglycemic status.

Methods: Among FDG-PET/CT scans between April 2009 and September 2014, 17 scans in 17 patients (pts), who had high plasma glucose level (>300 mg/dl) at FDG injection despite at least 4-h fast, were retrospectively analyzed. Chronic hyperglycemia was derived from uncontrolled diabetes (14 pts) and untreated diabetes (3 pts). Based on the final diagnosis obtained by histopathology or clinical follow-up, the diagnostic performance of visual interpretation of PET/CT was evaluated.

Results: In 10 pts with at least one malignant lesion, PET/CT was true positive in 7 pts, and false negative (FN) in 3 pts. The FN cases were hepatocellular carcinoma in 2 pts and post-chemotherapeutic state of pancreas cancer in 1 pt. Therefore, FN results may not have been caused by hyperglycemia. There were two metastatic lesions detected by CT portion of PET/CT in these 2 FN cases. In the remaining 7 pts who were confirmed to have no malignancy, PET/CT was true negative in 6 pts and false positive in 1 pt (inflammation). Overall, the patient-based sensitivity, specificity, positive predictive value, negative predictive value and diagnostic accuracy were 70%, 86%, 88%, 67% and 76%, respectively.

Conclusions: FDG uptake maintained a sufficiently high level for visual interpretations even under chronic extreme hyperglycemia in most cases, and false negative findings may have been caused by characteristics of lesions. FDG-PET/CT scan can be performed in diabetic patients with chronic hyperglycemia.

2015FANMB_18

Functional Dyspepsia: Impaired Intragastric Distribution or Impaired Gastric Emptying - an Attempted Evaluation by Nuclear Scintigraphy

Vishal Agarwal

Nuclear Medicine Department, SRMS Functional Imaging and Medical Centre, Lucknow, India

Objectives: Functional Dyspepsia (FD) is a heterogeneous disorder and is a diagnoses of exclusion. By definition, presence of symptoms thought to originate in the gastro-duodenal region (post-prandial fullness, early satiation, epigastric pain or burning), in the absence of any organic, systemic or metabolic disorder-should explain the condition. It has been suggested that these patients may respond to gastric pro-kinetic or fundus-relaxing drugs-agents that alter gastric motility. Indeed, some patients do have delayed gastric emptying, but overall, there seems to be little relation between rate of emptying and symptoms.

Methods: We examined 18 patients, having symptoms of bloating and epigastric discomfort but without any identifiable organic cause or acid related disorder; and 08 volunteers. All of them were served Tc-99m DTPA mixed food (consisting of wheat porridge) and were asked to have it over 20 minutes. Soon after finishing their meals, they were asked to stand upright in front of gamma camera, and imaged for 1 minute over the area of upper abdomen, every 10 minutes, for a total of 90 minutes (total 10 images). Then, the images were divided into upper 1/2 (proximal) and lower 1/2 (distal) gastric portions empirically, keeping in mind that stomach otherwise anatomically also consist of proximal: distal in the ratio of 40:60. Being empirical gave us the freedom of being reproducible in every patient. The time-activity curves (TAC) were obtained for upper1/3rd, lower 2/3rd and total stomach region.

Results: TAC of total stomach region between patients and volunteers was not significantly different in its information, meaning that the total emptying in patients was no different from the volunteers except in 2, which showed delayed gastric emptying; but TAC of distal stomach region (lower 2/3rd) was. In the volunteers, food remained predominantly in the proximal half and then moved towards the distal half; however in the patient sub-group, food moved quickly from the fundus to the antrum and showed stasis of food for longer duration (in antrum) as compared to the volunteers.

Conclusions: Our study indicates that the primary cause of FD is the intra-gastric maldistribution of food (stasis in the distal stomach and antrum) rather than the abnormal gastric emptying. This might help in

tailoring better treatment in form of drugs which affect intra- gastric motility rather than drugs which simply enhance gastric emptying.

2015FANMB_19

A Case Report of Diagnosis of Functioning Ectopic Left Kidney by DTPA and DMSA Renogram Failed by Anatomical Imaging

Shamrukh Khan, Molla Abdul Wahab, Mehedi Masud, Forhad Hossain, Prodip Kumar Datta, Rajibul Alam Chowdhury, Liakat Hossain Sardar.

Nuclear Medicine Department, United Hospital Limited, Gulshan-2, Dhaka, Bangladesh

Objectives: Without knowing proper function of an ectopic kidney, unnecessarily it is removed depending on anatomical imaging which may be avoided with help of nuclear imaging. A male baby, born with distention of left side of lower abdomen, was diagnosed as a case of left sided hydronephrosis by abdominal ultrasound. A subsequent intravenous urography showed normal excretion in right kidney with non-functioning or absent left kidney. The patient was scheduled for left sided nephrectomy. Further radionuclide studies revealed ectopic and insufficiently functioning left kidney.

Methods: Tc-99m DMSA renal scan and Tc-99m DTPA renal study was performed in same patient within a span of seven days. DMSA scan was done after 3 hours of intravenous (I.V.) injection of 2.6 mCi of radiotracer. For DTPA renal study 2.6mCi radiotracer was injected I.V. and 20mg of Furosemide I.V. was given at 10 minutes. For both studies standard imaging protocol was followed.

Results: Both DTPA and DMSA scans showed normal size, shape and position of right kidney with uniform tracer uptake and normal washout. Left kidney was irregular bean shaped, not seen in left renal fossa, ectopic, placed in antero-lateral aspect of left pelvic region showing poor uptake of tracer with negligible washout. In DMSA scan, relative renal function of right and left kidney was 76.61% and 23.39%. In DTPA study split renal function and glomerular filtration rate of right and left kidney was 84.64%, 117.61 ml/min and 15.36%, 21.35 ml/min. Based on these findings left sided pyeloplasty was done. Notable increase in patient's body weight with gradual reduction of abdominal distension was observed in subsequent clinical follow up.

Conclusions: Radionuclide scans made a drastic change in patient management. Plan for nephrectomy was replaced by pyeloplasty, saving the patient from losing a kidney and allowing it's functional improvement. This case re-emphasizes necessity of radionuclide scan over any anatomical imaging with nephrotoxic contrast agents in suspected renal agenesis or complete functional impairment that may mislead a surgeon to plan for unnecessary nephrectomy.

2015FANMB_20

Usefulness of texture analysis on FDG PET to differentiate glioblastoma from primary central nervous system lymphoma

Kenji Hirata[1], Kentaro Kobayashi[1], Shigeru Yamaguchi[1,2], Hiroyuki Kobayashi[2], Shunsuke Terasaka[2], Yuki Tomiyama[1], Osamu Manabe[1], Tohru Shiga[1], Sung-Chen Huang[3], Nagara Tamaki[1]

1. Department of Nuclear Medicine, Hokkaido University Graduate School of Medicine, Sapporo, Japan
2. Department of Neurosurgery, Hokkaido University Graduate School of Medicine, Sapporo
3. Department of Molecular and Medical Pharmacology, David Geffen School of Medicine, University of California, Los Angeles, California, USA

Objectives: Glioblastoma and primary central nervous system lymphoma (PCNLS) require different treatment strategies. Although FDG PET is useful to differentiate glioblastoma from PCNLS, highest FDG uptake value in the tumor (e.g., SUV_{max}) is often insufficient for discrimination. Texture analysis is a method to quantify the tumor heterogeneity. Because it is known that glioblastoma is metabolically more heterogeneous than PCNSL, we aimed to investigate whether texture features contribute to the differential diagnosis.

Methods: Twenty-five brain tumor patients, consisting of 12 glioblastoma and 13 PCNSL, underwent FDG PET before surgical intervention. Images were reconstructed with filtered backprojection, and the final voxel size was 2.5 x 2.5 x 2.5 mm. Volumes of interest were defined by manually drawing polygonal regions of interest to enclose the entire tumor. Histogram and four texture matrices (co-occurrence matrix, gray-level run length matrix, gray-level zone length matrix, and neighborhood gray-level different matrix) were generated for each patient to calculate a total of 36 texture features. The final diagnosis was determined by either pathological investigation or clinical follow-up.

Results: Among the 36 parameters, 15 reached statistical significance ($P<0.001$) between glioblastoma and PCNSL. Two features (entropy and energy) from histogram and 9 higher-order features from texture matrices (Homogeneity, SRE, LRE, GLNUr, RLNU, RP, Coarseness, GLNUz, ZLNU) diagnosed with accuracy of 96% (24/25) if the best cut-off values were used, whereas accuracies of SUV_{max} and tumor-

to-normal ratio were 84% for both.

Conclusions: Texture analysis provided useful information to quantify the different levels of metabolic heterogeneity of glioblastoma and PCNSL. Further studies are needed to apply to other brain tumors and to evaluate inter-operator reproducibility of texture analysis.

2015FANMB_21

Relevance of FDG uptake in tonsils in patients with malignant lymphoma

Apolinario M. De Gracia Jr., Takahiro Morita,Kayako Isohashi, Eku Shimosegawa, Jun Hatazawa

Department of Nuclear Medicine and Tracer Kinetics Osaka University Graduate School of Medicine

Objectives: Tonsil is part of an innate immune system important for humoral and cell mediated immunity. Innate immunity can be disturbed by different factors that include chemotherapeutic agents. This study is undertaken to assess changes of FDG activity in tonsil before and after treatment to determine any behavioral pattern of innate immune system relative to treatment response.

Methods: Retrospectively, we reviewed malignant lymphoma cases covering the period of 6 years (2006-2012), who underwent both pre- and post-treatment PET-CT examinations and had chemotherapy. The chemotherapeutic regimen administered to these patients includes CHOP; COPP and THP COP, and ABVD for Hodgkin's disease. The SUV_{max} was taken on the area of both palatine tonsils utilizing 3-D method on fused axial view, with proper adjustment and localization of the volume of interest (VOI) using sagittal and coronal views. The whole body scan is also reviewed to assess the status of the disease. The computed mean pre- and post-therapy SUV_{max} are then compared.

Results: There are 29 cases included in this study- 22 Non Hodgkin's Lymphoma (11-DLBCL; 8-Follicular lymphoma; 1-MALT; 1-Mantle cell lymphoma; 1-ILVCL), and 7-Hodgkin's Disease. There are 19 males and 10 females with mean age of 55, the youngest being 20 years old and the oldest at 79 years old. The mean SUV_{max} of pre-treatment is 3.3 +/- 1.6 while the post-treatment is 2.0 +/- 0.6, - mean difference of 1.2 +/- 1.7, and mean percent change of 26%. Paired t-test p value between pre- and post-treatment SUV_{max} is < 0.001. There are 24 cases that demonstrate lower post-treatment tonsil activity, of which 20 cases (83%) responded well to the treatment, and 4 cases (17%) have persistent disease.

Conclusion: There is an excellent relationship between lower post-treatment FDG tonsil activity and good treatment response in patients with malignant lymphoma. However, it is also observed that as many as 17% may show lower post treatment SUV_{max} in tonsils in spite of persistent disease, and this can be due to reduced innate immune system response that can be attributed to consequential effect of chemotherapeutic drugs and/ or corticosteroid.

2015FANMB_22

Prognostic Value of Metabolic Tumor Burden on Post-chemo (radiation) FDG PET/CT in Patients with Non-small-cell Lung Cancer

Chenpeng Zhang[1], Chuanhong Liao[2], Yonglin Pu[3], Gang Huang[1]

1. Ren Ji Hospital, School of Medicine, Shanghai Jiao Tong University, China
2. Department of Public Health Sciences, University of Chicago, USA 3Department of Radiology , University of Chicago, USA

Objectives: This study is to test our hypothesis that whole-body metabolic tumor burden(MTBWB) can be used for estimating overall survival (OS) in non-small cell lung cancer (NSCLC) patients on post-chemo (radiation) FDG PET/CT.

Methods: 119 cases with NSCLC (65 men, 54 women, median age of 65.3 years) who had post-therapy (chemotherapy with or without radiation) FDG PET/CT scans were retrospectively reviewed. The whole-body metabolic volume (MTVWB), total lesion glycolysis (TLGWB) and whole-body maximum standardized uptake value (SUVWBmax) were measured. OS served as the primary endpoint of the study. Cox regression assessed associations of PET/CT markers with OS.

Results: Compared to those with all negative post-chemo(radiation) FDG PET/CT scans (n=17), presence of FDG-avid tumor was a statistically significant association with OS according to Kaplan-Meier analysis(P=0.002).

For all patients with FDG avid tumor, ln(TLGWB), ln(MTVWB),and ln(SUVWBmax) were significantly associated with OS in univariate analyses (P<0.01). But only ln(TLGWB) was significantly associated with OS in multivariable analyses after adjusting for the patient's age, gender, pathology, re-stage, with or without radiation before post-therapy PET, therapy after PET/CT, and the combine with the therapy before and after PET (P<0.05). The ln(MTVWB) and ln(SUVWBmax) were not significantly associated with OS in multivariable Cox regression model after adjusting others variables.

For sub-group analysis of patients based on with or without co-radiotherapy before PET, ln(TLGWB) and ln(MTVWB) were significantly associated with OS in univariate analyses for both groups(P<0.01). In multivariable survival analysis for sub-group analysis, ln(TLGWB) and ln(MTVWB) were significantly associated with OS only in chemo without radiotherapy group(P<0.05). However, ln(MTVWB) and ln(TLGWB) for patients who had both chemotherapy and radiotherapy before PET were not significantly associated with OS in multivariable Cox regression model (P>0.05).

The OS differences for all patients with FDG avid tumor between the groups correspondingly dichotomized by the median value of MTVWB (50.28 ml) (P=0.001), TLGWB (177.45ml) (P<0.001), and SUVWBmax(8.51) (P=0.012) were statistically significant.

Conclusions: MTBWB in post-chemotherapy FDG PET/CT are related to the patient's overall survival in NSCLC, independent on age, gender, pathology, TNM restage and treatment after PET. But the value of MTBWB in post chemo-radiation FDG PET/CT was needed to be careful.

2015FANMB_23

Added Value of Abdominal I-131 SPECT/CT in Differentiated Thyroid Cancer

Wichana Chamroonrat, Padcha Tunlayadechanont, Chanika Sritara

Ramathibodi Hospital, Mahidol University

Objectives: The purpose of this study is to evaluate value of the abdominal SPECT/CT in post I-131 treatment imaging for differentiated thyroid cancer.

Methods: We included 37 patients with differentiated thyroid cancer who underwent total or complete thyroidectomy, followed by first I-131 ablation and/or treatment (150mCi). Each post I-131 treatment imaging includes planar total body scan and SPECT/CT from neck to abdomen.

Results: Among 37 patients, 25 focal iodine-avid lesions were found in 21 patients. Five of 25 focal iodine-avid lesions (from 5 patient) need further investigation or management including 2 bone metastases in T12 vertebra and right iliac bone, a right kidney metastasis, a fetal thyroid and a left ovarian cyst. The patient with T12 bone metastasis showed low stimulated thyroglobulin (Tg) level and negative diagnostic I-131 imaging (2mCi) a year later. The patient with kidney metastasis had right nephrectomy. Re I-131 treatments were done in the patients with right iliac bone metastasis and kidney metastasis. The pregnant patient had an abortion [1]. Left cystectomy of the left ovarian cyst showed mature cystic teratoma. The rest of the focal lesion turned to be physiologic tracer accumulation in gastrointestinal (GI) and genitourinary (GU) tracts without need for further management. There are 16 gastrointestinal focal activities, 6 at the stomach and 10 at the intestine. Four focal uptakes in the uterus are likely associated with menstruation and nabothian cyst at the uterine cervix.

Dividing focal iodine avid lesions by 9 locations, the 5 aforementioned significant iodine avid lesions include one in the right upper quadrant (RUQ) at the right kidney, one in the mid upper quadrant (MUQ) at T12 vertebra, two in the right lower quadrant (RLQ) at right iliac bone and fetal thyroid and one in the left lower quadrant (LLQ) in the left ovary. Oppositely, there is no focal iodine lesion at GI and GU tract in the RUQ, MUQ and left mid quadrant (LMQ).

Conclusions: Abdominal SPECT/CT in post I-131 treatment imaging of patients with differentiated thyroid cancer shows additional value in identifying accurate location which lead to prompt investigation or management. Significant or suspicious focal iodine-avid lesions tend to be in RUQ and MUQ or upper abdominal zones except LUQ. Equivocal lesions seem to be in all lower abdominal zones.

2015FANMB_24

Effect of Clopidogrel versus Ticagrelor Therapy on Atherosclerotic Plaque Inflammation assessed by Serial [^{18}F]FDG PET/CT: A Prospective Randomized Study

Minyoung Oh[1], Cheol Whan Lee[2], Dae Hyuk Moon[1], Hyo Sang Lee[1], Jung-min Ahn[2]

1. Department of Nuclear Medicine, Asan Medical Center, University of Ulsan, South Korea
2. Heart Institute, Asan Medical Center, University of Ulsan, South Korea

Objectives: Platelet P2Y12 receptor inhibitors has been shown significant cardiovascular benefits in acute coronary syndrome (ACS). We hypothesized that P2Y12 receptor inhibitors may have a direct effect on atherosclerotic plaque inflammation (API). We assessed the effect of clopidogrel versus ticagrelor on API in patients with ACS using serial [^{18}F]FDG PET/CT of carotid artery (CA) and ascending aorta (AA).

Methods: This is a prospective, single center, open-label, randomized trial in patients with ACS. Study inclusion requires a presence of at least one [^{18}F]FDG uptake lesion with ≥ 1.6 target-to-background ratio(TBR) of most diseased segment(MDS) in CA or AA on baseline PET/CT

performed 2 hrs after [^{18}F]FDG injection. MDS was defined 1.5 cm arterial segment, centered on the slice showing the highest FDG uptake. TBR-MDS were calculated as a mean of maximum TBR values of contiguous 6 segments. We planned to enroll 50 patients, randomized 1:1 to clopidogrel (75mg/day) or ticagrelor (90mg twice a day). Follow-up [^{18}F]FDG PET/CT was done at 6 months. We measured TBR-MDS blinded to treatment.

Results: All 50 patients were enrolled. To date, twenty-one of 25 completed the study in each group. There was no statistical difference in baseline characteristics and MDS-TBR between clopidogrel (Age=63.14±11.53, M: F=4:17) and ticagrelor (Age=61.67±8.11, M: F=4:17) group. Among a total 126 vessels (42 AAs and 84 CAs), 61 of clopidogrel and 62 of ticagrelor group had a TBR-MDS of ≥ 1.6. At 6 months, TBR-MDS was significantly reduced in both clopidogrel (2.18±0.41 vs. 1.95±0.30, P<0.001) and ticagrelor (2.41±0.49 vs. 2.01±0.32, P<0.001) group, with a greater reduction in ticagrelor group (P=0.038). Subgroup analysis revealed that TBR-MDS of CA was reduced with ticagrelor (2.23±0.45 vs. 1.90±0.27, P<0.001), but not with clopidogrel (2.01±0.27 vs. 1.90±0.29, P=0.118). That of AA showed a significantly reduction in both without group difference.

Conclusions: Preliminary analysis obtained from patients who completed the study so far showed favorable resolution of API on [^{18}F]FDG PET/CT after clopidogrel- and ticagrelor-treatment. Ticagrelor appears to have a greater effect on API, especially in CA than clopidogrel.

2015FANMB_25

Sirt Experience in Sarawak General Hospital: A Case Series

Chiong Soon Law[1], Ern Tze Reuben Goh[2], Ali Faizal[3], Kong Leong Yu[4], Nik Abdullah Nik Azim[2]

1. Department of Nuclear Medicine, Sarawak General Hospital
2. Department of General Surgery, Sarawak General Hospital
3. Department of Radiology, University Malaysia Sarawak
4. Department of Oncology and Radiotherapy Unit, Sarawak General Hospital

Objectives: Sarawak General Hospital successfully administered Selective Internal Radiation Therapy (SIRT) (Yttrium-90,Y-90) to three patients between December 2014 and April 2015.

Case presentation: Three patients were selected following diagnosis of unresectable Hepatocellular Carcinoma (HCC). First patient had hepatitis B, Child-Pugh's score of 5 and AFP of > 1000. Second patient had hepatitis C, Child-Pugh's score of 6 and AFP of 6.88. Third patient has Hepatitis B with a Child-Pugh score of 5 and AFP of 283. All patients underwent Technetium 99m Macroaggregated Albumin (Tc-99m MAA) study prior to SIRT treatment.

Management and outcome: All patients were scheduled for a re-staging CT at 3 month. First patient developed early recurrence of HCC within three months of SIRT. He then underwent TACE thrice since SIRT. Second and third patient passed away due to rapidly progressive HCC causing liver failure at first and fifth month post SIRT. All three patients had early complications of the treatment like nausea, mild abdominal pain and fever. However, none of them had radiation hepatitis or radiation pneumonitis.

Discussion: SIRT therapy has been studied extensively since its introduction the early 1990s. Currently SIRT is the primary bridging therapy for unresectable HCC before transplant, radiofrequency ablation or resection. Large tumour size and undetectable residual lesions are few of the major risk factors for early tumour recurrence, seen in our first patient who recently underwent his second TACE in mid-June. A high pre-operative AFP and location of tumour near segmental portal branches are risk factors for rapidly progressing tumour.

Conclusion: SIRT has already been proven as a safe and an effective treatment for HCC and liver metastasis in colon cancer worldwide. As the first two centres in Malaysia providing this service, there are still a lot for the teams to learn and improve.

2015FANMB_26

Establishing Nuclear Medicine Facility Guided by IAEA Publication of Nuclear Medicine Resources Manual- Cagayan de Oro Experience

Alvin P. Quinon

Nuclear Medicine Capitol University Medical Center, Philippines

Objectives: The purpose of the study is to relate the experience of establishing Nuclear Medicine (NM) in a city outside Manila using the IAEA NM Resources Manual.

Methods: This is a qualitative research based on ethnographic experience. Literature review of the IAEA manual, interviews of the medical staff and results of the previous survey were incorporated.

In a span of 6 years, there were 2 NM that was fully established in the city. The IAEA NM Resource Manual chapter on establishing a facility was used in providing a blueprint as to the categorization, socioeconomic consideration, need for personnel training and basic infrastructure. Events such as seminars and conferences were made to educate

the clinicians and staff. Attendance was checked and feedback was collected. Marketing and review on the number of referring physicians were done. The patients for treatment were given handouts and asked with regards to the general impression on nuclear medicine.

Results: The first NM section established on 2008 became operational after 8 months of conceptualization, personnel training and acquisition of local license. Following the financial viability of the first center, a second NM section in the city was established. It was observed that during seminars, participants grew in number if foreign or non-local expert were invited. Post event survey shows preference on workshop or case discussions with audience participation versus conventional lecture series. Local endocrinologists' preference for RIA procedures boosts non specialist referral versus ELISA method. The use of radioactive safety precaution handouts based on the IAEA resource manual with vernacular translation helps better understanding but does not lessen the incidence of fear from radiation harm.

Conclusions: Establishing NM in southern Philippines presents hurdle such as infrastructure, staff training, public, referring physician and investors acceptance. IAEA resource manual provides a useful template in starting a facility.

2015FANMB_27

Protein Expression Heterogeneity Between Primary Tumor and Bone Metastasis in Differentiated Thyroid Cancer

Joon Ho Choi[1], ILHAN LIM[1], Jae Kyung Myung[2], Joon Yeun Park[1], Byung Hyun Byun[1],Byung Il Kim[1], Chang Woon Choi[1], Sang Moo Lim[1]

1. Department of Nuclear Medicine
2. Pathology, Korea Cancer Center Hospital, Korea

Objectives: The aim of this study was to investigate the protein expression heterogeneity between primary tumor and bone metastasis in differentiated thyroid cancer (DTC) patients in terms of glucose metabolism and somatostatin receptor (SSTR).

Methods: We retrospectively reviewed 18 DTC patients (M : F = 7 : 11, Age; 56 ± 10) with bone or soft tissue metastases. The protein expressions were assessed as negative, weak positive, strong positive by immunohistochemistry in terms of glucose transporter 1 (GLUT-1), hexokinase 2 (HK-2), and somatostatin receptor 2 (SSTR-2) from surgical specimens. The correlations between protein expression and iodine avidity and FDG avidity were evaluated using radioiodine scan and ^{18}F-FDG PET scan. These parameters were analyzed using Chi-squared test, Mann-Whitney test and spearman correlation.

Results: Metastatic lesions showed higher GLUT-1 expression (65%, 11/17) than primary lesions (50%, 9/18). HK-2 were expressed highly in both primary (17/18) and metastatic (16/17) sites. Primary lesions revealed similar SSTR-2 expression (9/18) to metastatic lesions (7/17). The GLUT-1 expression tended to show positive correlation between primary and bone metastasis (r=0.46, *P*=0.06), but the HK-2 and SSTR-2 did not show the correlation between them respectively (HK-2 r=0.21, *P*=0.42; SSTR-2 r=0.056, *P*=0.83). Of the 8 patients who underwent surgery and PET imaging within 1 year, GLUT-1 positive group showed higher SUV_{max} than GLUT-1 negative group (*P*=0.046), while HK-2 (*P*=0.74) and SSTR-2 (*P*=0.65) did not show significant difference. Regarding iodine avidity and SSTR-2 expression, no significant difference was observed in terms of SSTR-2 expression between iodine avid and iodine non avid patients (*P*=0.57). 4 of 8 patients showed SSTR-2 expression in case of iodine non avid patients.

Conclusion: GLUT-1 expressions showed positive correlation between primary tumor and bone metastatic lesion, which was not observed for HK-2 and SSTR-2. Particularly, SSTR-2 targeted therapy could be applied for some iodide non-avid patients.

2015FANMB_28

Brain metabolic and dopaminergic changes in REM sleep behavior disorders with parkinsonian symptoms

Eun Jin Yoon[1,2,3], Jee Young Lee[4], Hyunwoo Nam[4], Jae Min Jeong[1,2], Yu Kyeong Kim[1,3]

1. Department of Nuclear Medicine, Seoul National University College of Medicine, Seoul, Korea
2. Department of Nuclear Medicine, Seoul National University Boramae Medical Center, Seoul, Korea
3. Institute of Radiation Medicine, Seoul National University Medical Research Center, Seoul National University, Seoul, Republic of Korea
4. Department of Neurology, Seoul National Seoul National University Boramae Medical Center, Seoul, Korea

Objectives: idiopathic rapid eye movement sleep behavior disorder (iRBD) is frequently considered as a prodromal syndrome of alpha-synuclein

neurodegeneration. Recent imaging studies have attempted to identify predictive biomarkers of an evolution toward synucleinopathies from iRBD, but no studies has investigated effect of signs of parkinsonism, one of the hallmarks of the synuclienopathies, yet. In the present study, we examined metabolic and dopaminergic changes in iRBD patients with mild parkinsonian symptoms (MPS) compared to iRBD without MPS.

Methods: Fifteen iRBD patients with MPS (MPS+) and 15 without MPS (MPS-) were enrolled. Regional metabolism and the dopaminergic integrity were respectively measured using FDG PET and FP-CIT PET.

Results: Regardless of MPS, iRBD patients showed significant hypermetabolism in the left primary and supplementary motor cortex in comparison with healthy controls. In patients of MPS+, further metabolic alteration as hypermetabolism was revealed in the bilateral prefrontal, left premotor cortex, insular, and cerebellum. In comparison between patients with/without MPS, MPS+ patients showed hypermetabolism in the right superior frontal gyrus and midbrain, and hypometabolism in the right middle occipital gyrus.

Meanwhile, the nigrostriatal dopaminergic integrity showed the subsequential decreases in iRBD based on MPS. DAT density of the posterior putamen and subthalamic nucleus showed correlation with metabolic alteration in the superior frontal gyrus, middle occipital cortex and midbrain where showed metabolic alteration in MPS+ patients.

Conclusions: We found the metabolic alteration in the occipital, prefrontal cortex and midbrain in iRBD patients with MPS, which regions has been suggested as RBD-related metabolic network. Furthermore, these metabolic alterations are associated with the impairment of nigrostriatal dopaminergic integration. These results suggest that the MPS in iRBD could be possible prodromal stages of synucleinopathies with dopamine degeneration, The metabolic changes in the iRBD with MPS could be use as a predictive biomarkers for future evolution from isolated iRBD to dopaminergic neurodegenerative disease.

2015FANMB_29

The Outcome of Radioiodine 131 Therapy for Differentiated Thyroid Carcinoma at First State Central Hospital

S.Erdenechimeg, B.Enkhtuya, T.Enkh-Amar, G.Erdenebayar

Department of Nuclear Medicine, First State Central Hospital of Mongolia

Objectives: Iodine 131 has been used in the management of patients with differentiated thyroid cancer (DTC) at the First State Central Hospital of Mongolia since 2004. The study is designed to evaluate clinical outcome of Iodine 131 and compare ablation rates obtained with different doses.

Methods: This retrospective study included 128 DTC patients who were treated with Iodine 131 therapy after total or near thyroidectomy from 2009 to the end 2014 in our department. All patients were divided into two groups based to ATA recommendation: low-risk and high risk. In low-risk patients ablation doses were 30 to 50 mCi and for patients with diagnosis high- risk thyroid CA doses varied between 75 to 150 mCi. Patients were followed up 6 -9 months with Iodine-131 whole body scan (WBS), Thyroglobulin (Tg), Anti thyroglobulin antibodies (anti-TgAbs) and neck ultrasound. Successful ablation was defined as minimal or no uptake on Iodine-131 WBS, negative neck ultrasound with Tg level <2ng/ml and anti-TgAbs <20ng/ml when patients in hypothyroid state.

Results: A total of 128 patients (107 female, 21 male, 15-81 years old, with majority being >40 years old (67.1%)) were included in this study. Papillary carcinoma was diagnosed in 75 (58.6%), follicular in 51(39.8%) and mixed types in 2 (1.5%) patients. Iodine 131 doses were 30 mCi, 50 mCi, 75 mCi and 150 mCi in 27(21%), 76(59.3%), 19(14.8%) and 6(4.6%) patients, respectively. The ablation rates at follow up examinations were 27.9%, 62.7%, 61.1%, 74.6%, respectively. Overall treatment response were complete 15.3 %, partial 64.4%, stable 19.1% and progression 1.2%.

Conclusion: Iodine 131 is a safe and effective treatment. Low Iodine 131 activities are acceptable for low-risk patients and activity of 50 mCi seems to be optimal to achieve better success rate. For treatment high-risk patients need more destructive doses.

2015FANMB_30

Myocardial Contractility Assessment as an Additional Parameter in Determining Viability Using Nitrate Augmented MPI Gated SPECT

Ryna Z. Martiana, Basuki Hidayat, A. Hussein S. Kartamihardja

Department of Nuclear Medicine, School of Medicine UniversitasPadjadjaran, Dr. Hasan Sadikin Hospital Bandung, Indonesia

By using myocardial perfusion imaging (MPI) gated SPECT examination with radiopharmaceutical ^{99m}Tc-sestamibi / tetrofosmin, perfusion and myocardial contractility could be examined simultaneusly. Nitrate augmented will improve blood flow in viable myocardial, so that the nitrate administration can be used to

determine myocardial viability by assessing perfusion and myocardial contractility. The purpose of this study was to determine the magnitude of contractility assessment as an additional parameter in determining viability through nitrate augmented MPI gated SPECT.
Method. Patients with myocardial infarction, MPI gated SPECT performed at rest. When the result obtained for perfusion defect was 3 and 4, nitrate augmented MPI gated SPECT examination was conducted. Analysis was performed on 20 segments which were obtained from MPI gated SPECT examinations both at rest and after nitrate augmented. Score for the assessment of perfusion defect is 0-4 according to the ECT software. Contractility score is 0-5 according to G. Germano and D. Berman. Analysis was conducted using Wilcoxon signed rank test, with $P \leq 0.05$.
Results. Twenty two subjects consisting of 20 men and 2 women, aged 47-76 years (mean 58.95). In total, there were 64 segments with perfusion defects score of 3; 42 segments (65.6%) with unchanged perfusion defect score, 22 segments (34.4%) had their scores improved after nitrate augmented (P=0.000); 21segments (21.9%) with contractility score remaining the same, 43 segments (78.1%) with contractility score improved after nitrate augmented (P=0.000). However, there was no correlation between perfusion defect improvement and improvements of contractility (r=0.031;P=0.405). The number of viable segments based on contractility assessment (43segments / 67.2%) is more than the number of viable segments based on assessment of perfusion defects (22 segments / 34.4%).
Conclusion. In gated SPECT MPI examination, nitrate augmented could improve perfusion defects and myocardial contractility. Assessment of myocardial contractility in nitrate augmented MPI gated SPECT can improve the detection of myocardial viability.

2015FANMB_33

Assessment of left ventricular diastolic dysfunction using gated SPECT MPS and its comparison with doppler echocardiography

Nikunj jain[1,*], Harish B[2], Gopinathan Nair[2], Mira Govindrajan[2], Sunil HV, Job Selvakumar[2]

1. Nueclear Healthcare Limited, New Delhi, India
2. Narayana Hrudayalaya, Bangalore, India

Objectives: Diastolic dysfunction is an early manifestation in conditions like HF-PEF and IHD. Although left ventricular diastolic filling patterns can be studied by Doppler echocardiography and gated SPECT, few data exists regarding comparison of these techniques. So comparitive study between two modalities was done with a view to determine congruence between them.
Methods: The prospective study was undertaken on patients who underwent Tc-99m Sestamibi MPI in department of Nuclear Medicine at Narayana Hrudayalaya, Bangalore from July 2010 to 31 st march 2011. 60 patients underwent GSPECT MPS and were evaluated for diastolic function at rest using automated QGS/QPS companion software. PFR and TPFR values were noted. Patients were classified into normal and abnormal diastolic function on the basis of PFR alone, TPFR alone and PFR and TPFR together, taking either abnormal. PFR >1.7EDV/s and TPFR <208ms were taken as normal. Echocardiography (conventional 2D and tissue doppler) was also done the same day. E/A, DT, IVRT were noted on conventional Doppler and e' was noted on TDI to unmask pseudonormalization. E/e' values were calculated. E/A< 1 was considered abnormal and E/e'>15 was considered abnormal. Doppler Echocardiography was taken as standard and various parameters calculated.
Results: The study revealed that combining PFR and TPFR and taking either abnormal had highest sensitivity of 91.6% and highest NPV of 93.3% compared to PFR or TPFR alone. Kappa of 0.667 showed best agreement with TDI. Using PFR gave maximum specificity of 94.4% and PPV of 85.7%. Together PFR and TPFR had best correlation with Doppler echocardiography. It also had best accuracy of 84.7%.
Conclusions: PFR and TPFR are useful diastolic parameters obtained by QGS/QPS companion software. They must be considered for all SPECT MPS (16 gated) studies to allow detection of diastolic dysfunction in presence or absence of CAD.

2015FANMB_34

Preoperative SUV_{max} of primary tumor measured by F-18 FDG PET/CT improves the prediction of lymph node metastasis in invasive ductal breast cancer

Bong-il Song, Hae Won Kim, Kyoung Sook Won

Dongsan Medical Center, Keimyung University School of Medicine, Korea

This study assessed whether preoperative primary tumor SUV_{max} ($pSUV_{max}$) measured by F-18 FDG PET/CT could improve the prediction of lymph node (LN)

metastasis in invasive ductal breast cancer (IDC).
We performed a retrospective review of pretreatment F-18 FDG PET/CT images of 128 female patients (mean age, 53.4±11.2) with IDC who underwent surgical resection of primary tumor with sentinel lymph node biopsy and/or axillary LN dissection without any neoadjuvant treatment between January 2008 and December 2011. All patients were classified as breast cancer subtypes in accordance with the 2011 St. Gallen Consensus Report. The optimal cutoff of $pSUV_{max}$ for the prediction of LN metastasis was determined using receiver operating characteristic (ROC) curve analysis. Further, prognostic accuracy of LN metastasis was assessed using c-statistics.
LN metastasis was found in 52 patients (40.6%). F-18 FDG PET/CT had a sensitivity and specificity of 48.1% and 94.7% for LN metastasis. Immunohistochemical subtypes were classified as follows: 29 (22.7%) as Luminal A, 19 (14.8%) as Luminal B (HER2 negative), 30 (23.4%) as Luminal B-like (HER2 positive), 21 (16.4%) as HER2 positive, and 29 (22.7%) as being a triple-negative subtype. On ROC curve analysis of $pSUV_{max}$ for LN metastasis, optimal cutoff values were 3.9 in entire patients, 2.8 in Luminal A, 3.3 in Luminal B (HER2 negative), 5.3 in Luminal B-like (HER2 positive), 12.7 in HER2 positive, and 11.5 in a triple-negative subtype. A predictive LN metastasis model using nodal FDG uptake finding gave a c-statistic of 0.714 and a model combination of $pSUV_{max}$with nodal FDG uptake finding gave a c-statistic of 0.736 (P = 0.3926). However, a model combination of $pSUV_{max}$considering immunohistochemical subtypes with nodal FDG uptake finding gave a c-statistic of 0.791 (P = 0.0081).
Combining$pSUV_{max}$consideringimmunohistochemical subtypes with nodal FDG uptake finding can improve the prediction precision of LN metastasis in IDC patients.

2015FANMB_35

To assess the role of whole body FDG PET/ CT in the metastatic work up/ staging of Ewing's family of tumors

Sneha Shah, Rashmi Kavindran, Rangarajan

Tata memorial hospital, India

To compare the ability of MDP bone scan and FDG PET/CT in identifying skeletal metastases.
To evaluate the feasibility of utilizing FDG PET/CT as a single modality for metastatic staging of Ewing's family of tumors.
Prospective analysis of 45 histologically proven untreated cases of Ewing's family of tumors. A ^{99m}Tc MDP bone and FDG PET/CT scan as was done in a span of 5 days. A breath hold CT was done at the end of the FDG PET/CT study. Abnormalities in the primary and the metastatic sites were evaluated on both the MDP bone scan and FDG PET/CT scan for all patients. Comparison of skeletal lesions by both modalities was done. An additional site of metastases identified on FDG PET/CT was noted. The lesions identified on either modality will be validated using the morphological characteristic on the CT component of the PET/CT.
MDP bone scan identified in 6% of patients while FDG PET/CT identified skeletal disease in 22% of patients, out of which 85% were purely lytic. It also identified non skeletal metastases (lungs and lymph nodes) in 35% patients.
FDG PET/CT in view of its better sensitivity (incremental value of 22%) in delineating skeletal metastases over MDP bone scan and its ability to detect non skeletal metastases (35%) can be considered as a useful modality for staging. It identified marrow lesions which other modalities could not pick up, thus the incremental value is noted. It can effectively replace the CT thorax and bone scan of the conventional work up and we can detect other metastases which cannot be picked up by any other modality.

2015FANMB_36

The clinical value of PET-guided endobronchial ultrasound-transbronchial needle aspiration (EBUS-TBNA) in regional nodal staging of NSCLC

Sinae Lee[1,2], Daehee Lee[6], Soyeon Park[3], Sungeun Kim[4], Sung Yong Lee[5], Jae Gol Choe[4]

1. Korea University College of Medicine, Korea
2. Department of Nuclear Medicine, G Sam Hospital, Gunpo, Korea
3. Department of Nuclear Medicine, Korea University Guro Hospital, Seoul, Korea
4. Department of Nuclear Medicine, Korea University
5. Anam Hospital, Seoul, Korea, Department of Internal Medicine, Korea University Guro Hospital, Seoul, Korea
6. Department of Internal Medicine, G Sam Hospital, Gunpo, Korea

Objectives: Regional lymph node staging in NSCLC is crucial to set treatment options. But correct nodal staging is also challenging, especially, in regions of endemic for granulomatous diseases. The purpose of the study is to evaluate the value of PET-guided

EBUS-TBNA and the efficacy of PET/CT for prediction of cytopathological results.

Methods: 38 patients who underwent ^{18}F-FDG PET/CT for initial staging of NSCLC and subsequent mediastinal node staging by EBUS-TBNA for clarification of the hilar, mediastinal nodes between Sep.2013 and Jul.2014 were retrospectively reviewed. The clinical nodal staging with PET/CT were correlated with cytopathological results after TBNA. Overall sensitivity, specificity, PPV, NPV, and accuracy were evaluated.

Results: From 38 PET scans, total 112 thoracic lymph node stations had noticeable focal hypermetabolisms. 82 FDG avid stations were suspected to have metastasis,16 stations were considered as inflammatory nodes, and 14 stations were reported as equivocal findings. The majority of the primary lung pathology which showed equivocal nodal PET findings were adenocarcinoma (9/14). Total 58 thoracic lymph nodes (PET positive 38, PET negative 12, and equivocal PET finding in 8 nodes, respectively) were aspirated in 38 patients. Malignancy was detected in 39 (67.2%) out of 58 lymph nodes. 2 patients up-staged from N1 to N2,1 patient up-staged from N2 to N3,and 1 patient down-staged from N3 to N2 after PET-guided EBUS-TBNA. From 8 lymph nodes that showed equivocal PET finding,6 were enlarged and showed heterogenous hypoechogenicity on EBUS. 4 node of those were proved to be cytologically metastatic lymph nodes. The sensitivity, specificity, PPV, NPV and diagnostic accuracy of PET-guided EBUS-TBNA on a node-based analysis was 94.9%, 63.2%, 84.1%, 85.8%,and 84.5%, respectively when we combined EBUS findings with PET.

Conclusions: PET-guide EBUS-TBNA offers an effective, accurate, and minimally invasive strategy for evaluating lymph node staging in NSCLC.

2015FANMB_39

Role of ^{68}Ga-DOTANOC PET-CT in the evaluation of neuroendocrine tumors (NETs)

Abhishek kumar[1], C S Bal[2], Rakesh Kumar[2], Guru P Bandopadhyaya[2]

1. Medanta, India
2. All India institute of Medical sciences, India

Objectives: Identify the role of ^{68}Ga-DOTANOC PET-CT in detection and staging of NETs.

Methods: Retrospective analysis of 126 patients (62 Gasroenteropancreatic neuroendocrine tumors (GEP-NETs), 33 medullary carcinoma thyroid, 31 phaeochromocytoma) with diagnosis of NETs based on histopathology / clinical followup was done. These patients underwent ^{68}Ga-DOTANOC PET-CT for staging and detection of recurrence.

Results: ^{68}Ga – DOTANOC identified more number of lesions in primary and metastatic sites as compared to conventional imaging. In patients with GEP-NETs sensitivity/specificity in primary site was 88/92% and in metastatic sites was 97/100%. In patients with MTC sensitivity/specificity was 80/94%. Higher sensitivity for ^{68}Ga-DOTANOC was noted in detection of metastatic lymph nodes in comparison to conventional imaging. In patients with phaeochromocytomas sensitivity/specificity was 90/85% on a patient basis and 92/85% on a lesion basis. ^{68}Ga-DOTANOC was a better modality for detection in extraadrenal sites. In all these patients ^{68}Ga-DOTANOC was a superior modality in comparison to conventional imaging.

Conclusions: ^{68}Ga-DOTANOC should be used as a preferred modality of choice in detection and staging of neuroendocrine tumors whenever available. ^{68}Ga-DOTANOC PET positivity indicates somatostatin receptor expression, thus guiding further management with octreotide or PRRT and hence providing alternative therapeutic options.

2015FANMB_40

Role of Myocardial FDG PET/ MPI SPECT in predicting post revascularization functional recovery in ischemic left ventricular dysfunction

P Shanmuga Sundaram, S Padma

Department of Nuclear Medicine & PETCT, Amrita Institute of Medical Sciences, Amrita Vishwavidyapeetham University, Cochin, Kerala, India

Objectives: This is a prospective study undertaken to identify roles of myocardial FDG PET & MPI SPECT in predicting functional recovery in ischemic ventricular dysfunction pts undergoing revascularization. Study also tries to predict 'early outcome' i.e mortality in these patients.

Methods: 32 males (mean age 56.81 yrs) with previous MI, ischemic LV dysfunction who underwent separate day MPI gated SPECT and FDG PET myocardial viability study between Sept 2010 -12 were included. Standard procedural guidelines were followed for performing the MPI SPECT and FDG PET studies. Median time post MI was 9 months with 95% CI being +/- 4.09 months. Majority were not lysed (21), 5 were lysed, remaining unclear history. New

York Heart Association functional class was III. Average LVEF was 31.75% in ECHO pre-therapy.

Results: Images were analysed by two experts unbiased by history and clinical findings. Visual interpretation of both SPECT and PET images were performed. A 17 segments polar map was used to evaluate 544 myocardial segments. 393/544 (72.24%) segments were viable (normal & hibernating showing perfusion metabolism mismatch 98 segments) & 151 (27.76%) scarred (perfusion metabolism match defect). Mean viable MIBI segments detected per patient 9.22 (S.D +2.24) & by FDG PET was 12.28 (S.D +1.97). Paired t test was statistically significant (<0.05) for viable segments detected by MIBI & PET. PET detected additional viability in 3.06 segments/ pt. 9 pts (28%) had significant hibernation while 23 pts (72%) had less than significant hibernation. Correlating lysis at time of MI & hibernating myocardium, ANOVA test returned a P value of 0.11 (>0.05, not significant). Bivariate analysis showed P not significant (>0.05) for both pretherapy LVEF, hibernation and for correlating time since MI and hibernation. 15 pts medically managed, 12 had CABG, 5 not treated. On followup 8 pts died (3 revascularized, 5 not treated). Pearsons 'r' test correlating pre and post intervention EF with PET detected hibernation, for revascularized pts: r = 0.51, *P*= 0.16 (*P*> 0.05) & for medically managed pts: r = 0.22, *P*= 0.44 (*P*> 0.05) showing no statistically significant relation between them.

Conclusion: Myocardial FDG PET is superior than MIBI in viability assessment. Baseline, pretreatment LVEF, time since MI, history of lysis and functional class (NYHA) have no statistically relation with PET detected hibernating myocardium and has statistically significant impact on short term mortality in ischemic LV dysfunction pts. Pts with lesser hibernation have significantly higher mortality after revascularization compared to conservative management, in early post intervention period. Extent of hibernating myocardium positively correlates with early post revascularization improvement in EF, however, relation is statistically weak.

2015FANMB_41

Genetic Influence in FDG Uptake in Precuneus and Posterior Cingulate: a Twin Study

Shinichiro Watanabe[1], Hiroki Kato[1], Eku Shimosegawa[2], Jun Hatazawa[1]

1. Department of Nuclear Medicine and Tracer Kinetics, Osaka University Graduate School of Medicine, Suita, Osaka, Japan
2. Department of Molecular Imaging in Medicine, Osaka University Graduate School of Medicine, Suita, Osaka, Japan

Objectives: Previous brain FDG-PET studies using discordant twins reported reduced glucose metabolism characteristic in Alzheimer disease in the non-demented co-twins, suggesting preclinical pathogenesis or genetic contribution. We tried to quantify genetic and environmental influence using clinically non-demented twins.

Methods: 41 mono- and 18 dizygotic twins were included. Mean FDG uptake in precuneus and posterior cingulate was semi-quantified using voxel-based statistical analysis. Structural equation modeling was applied to estimate the influences.

Results: Genetic influence was estimated as 0.39 in left precuneus, 0.28 in right precuneus, and 0.30 in right posterior cingulate, while common environmental rather than genetic influence was indicated in left posterior cingulate.

Conclusion: We demonstrated genetic influence in FDG uptake in precuneus and posterior cingulate.

2015FANMB_42

Can SUV_{max}, a semiquantitative index of ^{18}F FDG uptake be considered as a marker of tissue proliferation in Lymphomas? A correlative study with Ki 67 index

S Padma, P Shanmuga Sundaram

Department of Nuclear Medicine & PETCT, Amrita Institute of Medical Sciences, Amrita Vishwavidyapeetham University, Cochin, Kerala, India

Objectives: Higher cell proliferation rate signifies poor prognosis in cancer. Although various methods of estimating cellular proliferation are available, Ki 67 index, is considered reliable. Studies
have shown varying correlation between FDG uptake and Ki 67 expression among various
cancers. There are few studies correlating Ki index and SUV_{max}, a semi quantitative index of ^{18}F FDG uptake in Lymphomas. This retrospective study examines whether SUV_{max} correlates with Ki 67 index a marker of tissue proliferation in indolent and aggressive lymphomas.

Methods: 30 newly diagnosed lymphomas (NHL & HL) who underwent staging FDG PET-CT between Jan 2011-13 were included. Clinical, histopathological, immunohistochemistry reports were analyzed. Ki-67 nuclear staining was done for all & described as slight, mild, middle, or strong. PET CT images from head to mid thigh were interpreted qualitatively and quantitatitively. Highest SUV_{max} of lymph nodal, extra nodal lesions were noted and compared with Ki67 index of biopsy specimen. Clinical data and imaging findings were separately tabulated and correlated. Correlation coefficient r between FDG uptake

(SUV_{max}) and Ki index was calculated by Spearman's method.

Results: 30 (M:F =11:19, Age range 12-77yrs,mean 47.7yrs) newly diagnosed histopathologically proven lymphomas underwent FDG PETCT imaging. Distribution of pts were NHL : HL, 23 : 7. Of 23 NHL pts, 13 were aggressive (DLBCL: FL-III, 8:5) and 10 non aggressive (FL-I, MZL, MCL, 5:3:2). 10 HL pts were Nodular sclerosis & Mixed cellular types. Positive Ki scores were given when 0-5, 6-20, 21-50 & >50% of cells nuclei showed antigen staining. Mean SUV_{max} & Ki index of nodal and extra nodal lesions in NHL, HL correlated. Aggressive types displayed Ki 2+/ 3+ positivity; non aggressive types mostly very weakly positive (+/−) or weakly positive (+). FDG uptake of aggressive & non aggressive types were 7.0 ± 2.8 & 3.3 ± 1.0 respectively; the difference was statistically significant (t = 6.19, P < 0.01). Positive correlation between FDG uptake & Ki-67 in both lymph nodal lesions (r = 0.750, P< 0.01) and extra-nodal lymphomatous lesions (r = 0.843, P< 0.01). Using the Pearson formula, it was found that there existed correlation between Ki index and SUV_{max}.

Conclusion: SUV_{max} is a reliable indicator of tumour aggressiveness as in other cancers. FDG uptake is found to be higher in aggressive lymphomas than in non aggressive ones. When correlated with Ki-67 values, SUV_{max} can be used as a non invasive marker of proliferative index in lymphomas.

2015FANMB_45

Positron Emission Tomography-Computed Tomography (PET-CT) Guided Transthoracic Lung Biopsy: Evaluation of Diagnostic Yield and Complications.

Abhinav Singhal, Ishita Barat Sen, Vineet Pant

Fortis Memorial Research Institute, India

Objectives: This study evaluated the diagnostic yield of PET-CT guided core biopsies of suspicious lung lesions and identified factors predicting procedure related complications.

Methods: 90 patients (mean age: 52.5 years, range: 7 to 80 years) who underwent PET-CT guided core needle biopsy of suspicious pulmonary lesions were included in this retrospective analysis. All patients first underwent a whole body or limited PET-CT examination of the thorax for metabolic characterisation of their lesions. They then underwent image guided core biopsies under local anaesthesia from the most metabolically active part of the lesions. The diagnostic yield was calculated as the percentage of total samples on which a conclusive pathologic opinion could be given. Correlations between clinico-radiologic factors (lesion's adherence to pleura, number of passes, traversed lung-length and presence of emphysema in surrounding lung) and complications such as pneumothorax, hemothorax and hemoptysis were evaluated.

Results: Biopsy samples were adequate in 85 patients, giving a diagnostic yield of 94.4%. On a subset analysis, the respective diagnostic accuracy for malignant and benign lesions was 95.9% and 87.5%. Pneumothorax occurred in 13 cases (14.4%) of which only 2 patients (2.2%) required insertion of intercostal drain. Mild hemoptysis occurred in 4 patients (4.4%) and small hemothoraces in 3 patients. Using a multi-step regression analysis, the lesion's adherence to the pleura was the only significant factor identified to predict the occurrence of pneumothorax (P = 0.004). The other procedure factors were not significantly associated with any of the complications.

Conclusions: PET-CT guided lung biopsy is a safe procedure with high diagnostic yield and low risk of significant complications. Pleural adherence of the lesion is associated with risk of procedure induced pneumothorax.

2015FANMB_47

Prognostic Value of Follow-up FDG PET/CT in Stomach Cancer

Sonya Youngju Park, Hyelim Park, Sunghoon Kim

Department of Radiology, Seoul St Mary's Hospital, College of Medicine, The Catholic University of Korea, Seoul, Korea

Objectives: The Centers for Medicare and Medicaid Services recently revised coverage of ^{18}F-FDG PET/CT scans to only 3 posttherapy follow-ups for a tumor type per patient. The purpose of this study was to evaluate the added value of a fourth or subsequent follow-up PET/CT scans in clinical assessment and impact on management planning in patients with stomach cancer.

Methods: This was a retrospective study in which a total of 4513 patients with biopsy-proven stomach cancer, who underwent PET/CT between 2010 and 2014 were identified. Among these, 553 patients had taken four or more follow-up PET/CT scans, for a total of 800 fourth and subsequent follow-up scans. Median follow-up from the fourth follow-up PET/CT scan was 23 months, ranging between 4~54 months. The added value of each follow-up PET/CT scan result was determined by correlation with clinical assessment and consequent changes in treatment.

Results: Of the 800 fourth and subsequent follow-up scans, 8 (1%) were interpreted as positive and 792

(99%) were interpreted as negative for local tumor recurrence or metastasis. PET/CT identified recurrent tumors in 4/700 (0.57%) of scan performed without clinical suspicion and ruled out disease in 96/100 (96%) of scan performed with prior clinical suspicion. Treatment changes were made after 5/800 (0.63%) PET/CT scans; new treatment was initiated after 3/800 (0.38%) scans and treatment was changed after 2/800 (0.25%) scans.

Conclusions: Fourth and subsequent follow-up PET/CT scans performed after completion of primary treatment showed limited value in clinical assessment and management. However, they were helpful in excluding disease when performed in the presence of clinical suspicion.

2015FANMB_49

Diagnostic ability of bone metastases in cancer patients: Comparison between whole body bone Scintigraphy and regional CT scan

Pabitra Kumar Bhattacharjee, TU Ahmed, Roquibul Hoque, Sazzad Hossain

^{99m}Tc MDP bone scan is widely available and an important oncological technique especially in developing countries. To evaluate the influence of individual CT scan on detection of bone metastases, we compared the detection ability of individual CT scan with bone scientigraphy in a variety of cancer patients.

Methods: Consecutive twenty eight patients with various cancers, who received both bone scan and CT scan within 02 months, were retrospectively analyzed. A standard whole body bone scan and regional CT scan (Chest & abdomen including upper part of femur and humerus) were performed and those images were interpreted by two experienced nuclear medicine physicians. Each image interpretation was performed according to several different areas (vertebrae, sternum, clavicles, scapula, ribs, pelvis, upper femur & humerus).

Results: In untreated patient, 10 of 28 patients (35.7%), multiple metastases were detected by both bone scan and CT scan. Eight of 28 patients (28.6%), fewer metastases could be detected on CT scan compared to bone scan. Six cases (21.4%) showed false negative in CT possibly due to earlier stage. To see the treatment effect evaluation in post chemotherapy patients, 4 of 28 cases (14.3%), bone scan shows better results because of rapid metabolic response then anatomical change.

There were 04 cases, solitary/ a few lesions located outside the field of view of CT scan in upper cervical vertebrae, skull and knee.

Conclusion: Detection ability of bone metastases was comparable in CT scan and bone scan in the current study. To overcome limited field of view of CT scan as in our cases, whole body CT scan may be performed.

2015FANMB_50

Clinical outcome of postoperative radioiodine therapy with low dose and high dose in intermediate risk differentiated thyroid cancer patients

Ju Hye Jeong[1], Eun Jung Kong[2], Kyung Ah Chun[2], Byeong-Cheol Ahn[1]

1. Department of Nuclear Medicine, Kyungpook National University Hospital, Daegu, Republic of Korea
2. Department of Nuclear medicine, Yeungnam University Hospital, Daegu, Republic of Korea

Objectives: The optimal radioiodine (RAI) dose for postoperative thyroid ablation is not clear to intermediate risk (IR) differentiated thyroid cancer (DTC) patients in countries with consumption of iodine rich foods, such as Korea. We evaluated the response to RAI therapy with low dose (LD) or high dose (HD) and long-term clinical outcomes in Korean DTC patients classified as IR.

Methods: A total of 111 DTC patients who underwent postoperative RAI therapy at two hospitals in 2003 were enrolled in this retrospective study. Eighty-one patients at IR were treated with 3.7 or 5.5GBq in one center and 30 patients with 1.1GBq in another center. Patients were categorized as having excellent response (ER), indeterminate (IDR), biochemical incomplete (BIR), or structural incomplete response (SIR) at during the first 2 years of follow-up after initial RAI therapy using a stimulated or suppressed thyroglobulin (Tg) level, ultrasonography, and ^{123}I or ^{131}I whole body scan. Progression was defined as newly detected biopsy-proven lesion or new structural and biochemical evidence of disease.

Results: ER was observed in 50.6% of patients treated with HD and in 36.7% of those treated with LD, IDR was found in 38.3% of patients treated with HD and in 33.3% of patients treated with LD, BIR was found in 3.7% of HD group and in 20.0% of LD group, SIR was found in 7.4% of HD group and in 10.0% of LD group (P= 0.046). In particular, BIR or SIR rate was lower in

patients treated with HD compared to patients treated with LD (*P*=0.023). At last follow-up (HD, median 11years; LD, median 10 years), no evidence of disease (NED) was observed in 91.3% (73/80) of HD group and in 85.7% (24/28) of LD group. Structural progression was observed in 5% (4/80) of HD group and in 10.7% (3/28) of LD group. There was no significant difference in final outcomes between the two groups (*P*=0.572). However additional RAI therapies were given to 5 patients of HD group and 11 patients of LD group not to progress (*P*=0.001).

Conclusions: Results of this study suggested that LD RAI therapy after thyroidectomy seems to be insufficient to DTC patients classified as IR in countries with consumption of iodine rich foods.

Author Index

INSTRUCTION TO AUTHORS

1- Editorial policy

Asia Oceania Journal of Nuclear Medicine & Biology (AOJNMB) is a peer reviewed biannual journal and serves as the official publication of *Asia Oceania Federation of Nuclear Medicine and Biology (AOFNMB)*. *AOJNMB* publishes material of interest to physicians and scientists working in the fields of nuclear medicine & biology. The journal is an open-access free e-Journal which is sponsored and published by Nuclear Medicine Research Center (NMRC) in Mashhad University of Medical Sciences (MUMS). A limited number of journals in print form is also published. *AOJNMB* publishes a variety of articles including original laboratory and clinical investigations, meta-analyses, short communications, technical notes, case reports and letters to the editor. Also occasionally, invited reviews and continuing education will be published. In preparing manuscripts, authors should follow the *Uniform Requirements for Manuscripts Submitted to Biomedical Journals: Writing and Editing for BiomedicalPublications* (http://www.icmje.org/urm_full.pdf).Manuscripts, including figures and tables, must be original and not under consideration for publication elsewhere. Ethics and malpractice statements of the *Asia Oceania Journal of Nuclear Medicine & Biology*are based on COPE's Best Practice Guidelines for Journal Editors and pertain to all parties involved in the publishing: the editor, the peer reviewer and the author. If there is an allegation of plagiarism, scientific misconduct or fraud, *AOJNMB* shall follow the recommendations of the Uniform Requirements and reserves the right to present the allegations to the author's institution or any other agency.

2- Editorial office

Asia Oceania Journal of Nuclear Medicine & Biology, Nuclear Medicine Research Center, Ghaem Hospital, Ahmadabad Ave, Mashhad, Iran. Post Code: 91766-99199
Tel: +98-51-38400494 (Saturday-Wednesday; 8:00-14:00, Thursday: 8:00-12:00, Local time, GMT+3:30) Fax: +98-51-38419521
E-mail: aojnmb@mums.ac.ir

All manuscript should be submitted and tracked online. All other enquires should be made by E-mail to aojnmb@mums.ac.ir. Other correspondence may be sent to Prof. Seyed Rasoul Zakavi at the address of editorial office.

3- Legal and ethical issues

- Submission of any manuscript to *AOJNMB* signifies that it is original and it has not been published anywhere before (except as a congress abstract of no more than 350 words) nor it is under consideration by another journal. By virtue of the submitted manuscript, the corresponding author acknowledges that all the co-authors have seen and approved the final version of the manuscript. The corresponding author should provide all co-authors with information regarding the manuscript, and obtain their approval as well as approval of their institute before submitting any revisions. The editors consider that all submitted materials including text, figures or tables and any other file are original. If it is not the case, the authors must provide both the print and online permission from the copyright owner. The Asia Oceania Federation of Nuclear Medicine and Biology and the publisher (MUMS) will not be held legally responsible should there be any claims for compensation.The authors are responsible for the whole scientific content as well as the accuracy of the bibliographic information.
- At the time of submission of the manuscript, all authors must disclose any type of conflict of interest including but not limited to financial interests that may influence the submitted manuscript. Any company consultancy, product or stock ownership related to the manuscript must be disclosed. Affiliations of authors should include corporate appointments relating to or in connection with the products or companies mentioned in the article. Authors should declare sources of funding for the work undertaken. If there is no conflict of interest for all of the authors, the phrase 'No potential conflicts of interest were disclosed' should be written in the acknowledgement.
- All manuscripts reporting the results of experimental investigations involving human subjects should include a statement, confirming that informed written consent was obtained from each subject or the subject's guardian. The study must also be approved by local ethics committee and the study must comply with 1964 Declaration of Helsinki and its subsequent revisions.
- For animal studies, it must be in compliance with the regulation(s) of local institution and with generally accepted guideline governing such work.
- All prospective clinical trials must be registered. Registration of prospective clinical trials must be done in one of publicly accessible registries and the registration number must be provided at the end of the abstract.

4- As an open-access journal, *AOJNMB* uses licenses that keep the copyright with the author, but the author transfers all commercial exploitation rights to the publisher (*MUMS*). The

author(s) can post a copy of the published article on his/her own website or his/her institution's website with no permission, provided that full citation of the journal and a link to the *AOJNMB* website are included. Also, it can be used in educational materials by author(s) with citation of the AOJNMB. The author(s) may republish the article in a book written or edited by himself/herself without permission, but with full acknowledgment of the first publisher. All authors must complete and sign the copyright transfer form and submit it with the manuscript to the editorial office.

5- Article types

- Original articles: Manuscripts reporting the results of original researches in preclinical, clinical or technical innovations.
- Meta-analyses: Reporting combined results of individual studies, after a comprehensive search of the available database and using special statistical methods.
- Short communications: A short report from a research work will be published as short communication.
- Case reports: An important and rare presentation of a disease relevant to nuclear medicine or interesting or unusual nuclear medicine images which is either not reported before or infrequently reported.
- Technical notes: A short report on new technical or procedural innovation or modification of established techniques or procedures in nuclear medicine.
- Review articles: Invited reviews and educational materials will be published. The journal prefers systematic reviews. The author(s) of a review article must have at least two published original articles on that subject.
- Letter to the AOJNMB: Letters to the editors on controversial issues which is published in the AOJNMB in the previous issues(no later than 12 months)
- Others: Editorials, History and perspectives, book reviews, upcoming events, meeting reports and news items may be considered for publication.

6- Manuscript submission

All manuscripts should be submitted online using online submission system at http://aojnmb.mums.ac.ir. You need to sign up and log into the system for submission of your manuscript. Please follow the on screen instructions during submission.

After completion of manuscript submission, you can track the status of the manuscript by logging into the system. For any further enquiry you can send an email to aojnmb@mums.ac.ir

7- Manuscript preparation

The manuscript should have the following sections: Title, Abstract, Main document, Acknowledgement, References, Figures and Tables.

7-1: Title page

Title page should include in following order : Title (please keep it short and informative), Full first name and surname (and middle name initials) of all authors, Affiliation (s) and e-mail address(es) of all authors, Corresponding author's Full name, postal address, e-mail address, Telephone and Fax number(s) and a short running title of no more than 40 characters.

7-2: Abstract

It should contain a Maximum of 350 words divided in 4 sections preceded by headings: Objective, Methods, Results and conclusion. For review articles and case reports an unstructured abstract with a maximum of 200 words is required. Three to five keywords are necessary for all abstracts. Word count should be written at the bottom of abstract page.

7-3: Main document

7-3-1: The abstract must be the first page of Main document. For original articles, the following sections should be included: Introduction, Methods, Results, Discussion and Conclusion. For reporting Clinical Trials, please follow reporting requirements published by CONSORT: http://www.consort-statement.org/consort-statement (There is no maximum word limit, but it is preferable to keep Maximum word count at 6000 and Maximum references at 40).

7-3-2: For short communications and technical notes, the following sections should be included: Introduction, Methods, Results, Discussion and Conclusion. (Maximum word count 3000 and Maximum references 20)

7-3-3: For case reports, three sections of Introduction, Case report and Discussion are required. (Maximum word count 3000 and Maximum references 20)

7-3-4: For Meta-analyses, Introduction, Methods, Results, Discussion and Conclusion should be included. Please use PRISMA statement for reporting your work: http://www.prisma-statement.org/statement.htm (There is no maximum word limit, but it is preferable to keep Maximum word count at 6000 and Maximum references at 40)

7-3-5: For review articles; (There is no maximum word limit, but it is preferable to keep Maximum word count at 6000 and Maximum references at 40)

7-4: Formatting

- Use MS Word 97 or later versions.
- Use plain normal fonts (12 Times New Roman) with double space formatting

throughout the document including abstract, manuscript and references.

- Leave 3 cm margin on each side of the page.
- Number pages consecutively, beginning from the Abstract and put it in right upper corner of the page.
- Do not use field function, do not use the space bar, instead use tab stops.
- Cite every reference in the text in parenthesis using Vancouver style in the order they appear in the text. Using Endnote for citation is encouraged.
- Paragraphs should begin with an indentation (One tab of at least five-spaces length).
- Use the equation editor or MathType for inserting equations.
- The abbreviations should be used according to Système Internationale (SI) nomenclature and units and they should be explained the first time they are used in the manuscript. All units of radioactivity should be based on the SI system *i.e.*, Bq, Gy, Sv, *etc.* Chemical formulae should be written according to the recommendations of the American Chemical Society.

7-5: Acknowledgement

Acknowledgements, sponsorship or grants should be written after the main text and before the references.

7-6: References

The references should be listed consecutively in order of citation in the manuscript. All references must be cited either in text, table or figures. Unpublished data and personal communications cannot be cited. The AOJNMB uses Vancouver style for references. For citation of journals, all authors should be listed if the number of authors were 6 or less. If not, please list the first 6 authors followed by *et al.* A paper published online but not in print can be cited using the Digital Object Identifier (DOI). A web document can be cited using the URL address. Using ENDNOTE or similar soft ware and selecting the Vancouver style (parenthesis) in Bibliographic Output Style will facilitate correct reference citation.

Here are samples of citation styles:

a) Journal article (With 6 or less authors)
Palestro CJ. In vivo leukocyte labeling: The quest continues. Journal of Nuclear Medicine. 2007; 48(3):332-4.

b) Journal article (With more than 6 authors)
Intenzo C, Jabbour S, Miller JL, Ahmed I, Furlong K, Kushen M, et al. Subclinical hyperthyroidism: Current concepts and scintigraphic imaging. Clinical Nuclear Medicine. 2011; 36(9):e107-e113.

c) Book
Walsh G. Proteins: biochemistry and biotechnology. 2nd ed. Chichester: John Wiley & Sons; 2002.

d) Book chapter
Moallem SA, Balali Mood K. Opioids and opiates. In: Mozayani A, Raymon LP, editors. Handbook of drug interactions: A clinical and forensic guide. 1st ed. Totowa: Humana Press Inc; 2004. p. 123-149.

e) Epub; Article by DOI:
Daliri M, Shafiei S, Zakavi SR, Dabbagh Kakhki VR, Sadeghi R. Application of (99m)Tc-denatured red blood cells scintigraphy in the evaluation of post-traumatic spleen auto-transplantation. Rev Esp Med Nucl Imagen Mol. 2012 Nov 12. doi:pii: S2253-654X(12)00212-0. 10.1016/j.remn.2012.09.004.

f) Online document:
RCT critical appraisal sheet In: Critical Appraisal Sheets, Center for Evidence Based Medicine 2012. http://www.cebm.net/index.aspx?o=1157. Accessed 3 Dec 2012.

7-7: Figure legends

Figure legends should be written after references, each in a separate sheet preceding with figure number (Figure 1). The figure legends will be published below the figure. The legend should not be included in the figure file. All figures must be cited in the manuscript and numbered consecutively using Arabic numerals.

7-8: Tables

Tables should not be sent as figures or as separate file, they should be inserted at the end of the manuscript, each in a separate sheet. Tables are expected to be self explanatory, should supplement and not duplicate the text and numbered consecutively in order of appearance in the text and using Arabic numerals. Put horizontal line at the top of the table, below column headings and at the bottom of it. Do not use vertical line in the tables.

8- Figures and artworks

Figures and artwork should be submitted as separate files in JPG or TIFF format. Figures should be utilized only if they augment understandability of the text. Drawings and graphs should be professionally prepared in deep black and white with no shading. Professionally designed computer generated graphs with a minimum of 300 DPI laser printer output is preferable. Color photographs are welcomed. Vector graphics containing fonts must have the fonts embedded in the files. For lettering the figures, use 8-12 point (only one size) Helvetica fonts. Name each figure with the word "Fig" followed by figure number without punctuation: "Fig1". If you include a figure from previous

publication, you must provide permission from the copyright owner(s) for both the print and online format.

9- Supplementary materials

Video clips, sound records, excel or SPSS files and other supplementary materials could be sent for electronic linking to the manuscript in the website. MPEG-1 format (.mpg) should be used for video clips. Supplementary documents are encouraged to be sent as .PDF files if possible. Please name each supplementary file beginning with the name of first author (eg. Bom-video.mpg, Sadeghi-data.xls, etc). In text files you should enter the full name of the article and the authors as a header.

10- Cover letter

All manuscripts should be accompanied by a cover letter. In the cover letter signed by corresponding author on behalf of all authors, it must be mentioned that the article is not submitted to any other journal. A sample of cover letter could be found in: http://aojnmb.mums.ac.ir/journal/authors.note

11- Peer review process

All manuscripts will be peer reviewed prior to publication. Authors are encouraged to suggest names of three expert reviewers, but selection remains a prerogative of the Editor. The whole review process depends on receiving referees' comments and revising the manuscripts based on these comments to the author and may take few months. AOJNMB will try to make the time between submission and final decision as short as possible. On receipt of the revised article from the author, and after final approving by the referees, the letter of acceptance is issued to the author.

12- Acceptance/Rejection

You will be notified regarding acceptance or rejection of the article by e-mail. Upon acceptance and after editorial amendments, galley proof will be sent to the corresponding author for final correction. No major change in content or title is accepted at this stage without editor's approval. Any addition or removal of an author from the list of authors must be accompanied with a written and signed agreement of the author(s) to be added or deleted.